

Leonid N. Sindalovskiy

Aquifer Test Solutions

A Practitioner's Guide with Algorithms
Using ANSDIMAT

EXTRAS ONLINE

 Springer

Aquifer Test Solutions

Leonid N. Sindalovskiy

Aquifer Test Solutions

A Practitioner's Guide with Algorithms Using
ANSDIMAT

 Springer

Leonid N. Sindalovskiy
The Russian Academy of Sciences
Institute of Environmental Geology
St. Petersburg
Russia

and

St. Petersburg State University
Institute of Earth Sciences
St. Petersburg
Russia

Additional material to this book can be downloaded from <http://extras.springer.com>.

ISBN 978-3-319-43408-7 ISBN 978-3-319-43409-4 (eBook)
DOI 10.1007/978-3-319-43409-4

Library of Congress Control Number: 2016946627

© Springer International Publishing Switzerland 2017

This work is subject to copyright. All rights are reserved by the Publisher, whether the whole or part of the material is concerned, specifically the rights of translation, reprinting, reuse of illustrations, recitation, broadcasting, reproduction on microfilms or in any other physical way, and transmission or information storage and retrieval, electronic adaptation, computer software, or by similar or dissimilar methodology now known or hereafter developed.

The use of general descriptive names, registered names, trademarks, service marks, etc. in this publication does not imply, even in the absence of a specific statement, that such names are exempt from the relevant protective laws and regulations and therefore free for general use.

The publisher, the authors and the editors are safe to assume that the advice and information in this book are believed to be true and accurate at the date of publication. Neither the publisher nor the authors or the editors give a warranty, express or implied, with respect to the material contained herein or for any errors or omissions that may have been made.

Printed on acid-free paper

This Springer imprint is published by Springer Nature
The registered company is Springer International Publishing AG Switzerland

Preface

This book compiles and systematizes analytical solutions describing groundwater-level changes in aquifers during aquifer tests, carried out under different hydrogeological conditions. The book integrates the majority of known solutions from well hydraulics and subsurface flow theory, starting from the works of the early twentieth century by G. Thiem, P. Forchheimer, C.V. Theis, and M. Muskat up to the most recent publications in periodicals. In this context, special mention should be made of the invaluable contribution to the development of methods for the mathematical analysis of hydrological processes made by M.S. Hantush, H.H. Cooper, C.E. Jacob, N.S. Boulton, S.P. Neuman, and A.F. Moench, whose efforts gave renewed impetus to the theory and methods of aquifer test analysis. The book also contains interesting, though little known, solutions obtained by Russian researchers (e.g., F.M. Bochever, V.M. Shestakov, V.A. Mironenko, etc.), which have not been mentioned in widely distributed scientific publications.

This publication is designed as a handbook. It presents analytical equations for most of conceptual models. Confined, unconfined, confined-unconfined, inhomogeneous, fracture-porous aquifers, as well as leaky aquifers and stratified (multi-layer) aquifer systems are described in the book. A wide range of groundwater-flow equations are given, accounting for complicating factors: anisotropy, flow boundaries in horizontal and vertical planes, partial penetration of the aquifer, wellbore storage, wellbore skin effect, the effect of capillary forces, etc. Considered separately are constant-head tests, pumping tests with horizontal or slanted wells, dipole flow tests, and slug tests.

The book comprises about 300 transient solutions for a single-well test with a constant discharge rate. They create the basis for numerous equations for groundwater-level recovery and drawdown in multi-well pumping tests, with constant or variable discharge rate of the pumping wells.

In addition, quasi-steady-state and steady-state solutions are described, intended for graphical processing of aquifer test results by the straight line method (more than 100 solutions) and the type-curve method (more than 50 varieties of type curves). Formulas for evaluating hydraulic characteristics are proposed for each

graphical method. Many steady-state solutions are given, which can be used for point-wise methods for evaluating hydraulic characteristics by maximal water-level changes in complicated hydrological settings, for which transient relationships acceptable for practical application have not been developed.

A set of both alternative and complementary solutions and methods of data processing are proposed for each combination of conceptual model and test conditions, thus making it possible to evaluate aquifer hydraulic characteristics. The author's own results are given, providing new graphical methods for field data analysis and improving the reliability of parameter estimates.

The book is supplemented with appendices: here a hydrogeologist can find a vast body of useful information. The appendices give mathematical descriptions to the majority of functions used in the book, present their plots and possible approximations, and analyze the algorithms for application of complicated numerical-analytical solutions utilized in rather well-known software developed by S.P. Neuman, A.F. Moench, and others.

The presented analytical solutions have been implemented and tested in a multifunctional software complex ANSDIMAT, developed by the author. The reader is provided with a brief characteristic of the program and, if need be, can run a test module. A trial version of the software and the complete commercial version are available at www.ansdimat.com.

The book comprises three parts, supplemented by appendices. The first two parts contain a systematized set of analytical relationships and methods for aquifer test treatment. The solutions for a pumping test in single vertical wells are described in the first part. The second part is devoted to various types of aquifer tests: pumping from horizontal and slanted wells, pumping with variable discharge rates and multi-wells pumping tests, dipole flow tests, constant-head tests, slug tests, and recovery tests.

The third part gives a brief characteristic of ANSDIMAT software, which incorporates all the potentialities illustrated in this book. The last part of the book gives algorithms for evaluating groundwater-flow parameters by analytical and graphical methods. An alternative approach is proposed to simulate well systems, and additional capabilities of the program are considered, which are intended to solve specific engineering-hydrogeological problems based on groundwater-flow equations, describing liquid flow toward wells.

The author very much appreciates the invaluable help of Dr. Vyacheslav Rumynin in the preparation of the book, including useful hints, comments, and fruitful discussions which enabled the author to improve the quality of the present publication in many respects. The author also appreciates the help of Dr. Gennady Krichevets, who is not only a translator of the book but also a real expert attentive to the works of his colleagues. His remarks regarding the work's contents helped the author to correct deficiencies made apparent during its preparation.

Contents

Part I Basic Analytical Solutions

1	Confined Aquifers	3
1.1	Fully Penetrating Well	3
1.1.1	Aquifer of Infinite Lateral Extent	4
1.1.2	Semi-infinite Aquifer	9
1.1.3	Strip Aquifer	11
1.1.4	Wedge-Shaped Aquifer	17
1.1.5	U-Shaped Aquifer	20
1.1.6	Rectangular Aquifer	23
1.1.7	Circular Aquifer	26
1.2	Partially Penetrating Well: Point Source	29
1.2.1	Aquifer Infinite in the Horizontal Plane and Thickness	30
1.2.2	A Point Source in an Aquifer Semi-infinite in the Horizontal Plane or Thickness	32
1.2.3	A Point Source in an Aquifer Bounded in the Horizontal Plane or Thickness	35
1.3	Partially Penetrating Well: Linear Source	38
1.3.1	Aquifer Infinite in the Horizontal Plane and Thickness	39
1.3.2	A Linear Source in an Aquifer Semi-infinite in the Horizontal Plane or Thickness	41
1.3.3	A Linear Source in an Aquifer Bounded in the Horizontal Plane or Thickness	44
1.4	Confined Aquifer of Nonuniform Thickness	51
	References	53
2	Unconfined Aquifers	55
2.1	Aquifer of Infinite Lateral Extent	55
2.2	Semi-infinite and Bounded Unconfined Aquifers	65

2.3	Sloping Unconfined Aquifer	65
	References.	69
3	Leaky Aquifers	71
3.1	Leaky Aquifer with Steady-State Flow in the Adjacent Aquifers	72
3.1.1	Aquifer of Infinite Lateral Extent	72
3.1.2	Semi-infinite Aquifer	77
3.1.3	Strip Aquifer	78
3.1.4	Wedge-Shaped and U-Shaped Aquifers	82
3.1.5	Circular Aquifer	82
3.2	Leaky Aquifer with Transient Flow in the Adjacent Aquifers	86
3.2.1	Aquifer of Infinite Lateral Extent	87
3.2.2	Circular Aquifer	90
3.3	Leaky Aquifer with Allowance Made for Aquitard Storage	93
3.4	A Partially Penetrating Well in a Leaky Aquifer	98
3.5	Two-Layer Aquifer Systems	100
3.5.1	Two-Layer Unconfined Aquifer System of Infinite Lateral Extent	100
3.5.2	Circular Two-Layer Confined Aquifer System.	103
3.6	Multi-aquifer Systems.	106
3.6.1	Three-Layer System.	106
3.6.2	Two-Layer System	110
	References.	113
4	Horizontally Heterogeneous Aquifers.	115
4.1	Aquifer with Linear Discontinuity	115
4.2	Radial Patchy Aquifer.	119
4.3	Heterogeneous Aquifers with a Constant-Head Boundary.	121
4.3.1	Strip Aquifer	121
4.3.2	Semi-circular Aquifer	122
4.3.3	Wedge-Shaped Aquifer	123
4.3.4	Circular Aquifer	125
	References.	126
5	Pumping Test near a Stream	127
5.1	A Semipervious Stream	127
5.2	Partially Penetrating Stream of Finite Width.	132
5.3	Pumping from a Well under a Stream	136
	References.	137
6	Fractured-Porous Reservoir	139
6.1	Moench Solutions.	139
6.2	Pumping Well Intersecting a Single Vertical Fracture.	142
6.3	Pumping Well Intersecting a Single Horizontal Fracture.	144
	References.	145

Part II Analytical Solutions for a Complex Pumping-Test Setting and Well-System Configurations

7 Horizontal or Slanted Pumping Wells 149

7.1 Confined Aquifer 149

7.2 Unconfined Aquifer 150

7.3 Leaky Aquifer. 152

References. 153

8 Constant-Head Tests 155

8.1 Aquifers of Infinite Lateral Extent 155

8.2 Circular Aquifers 159

8.3 Radial Patchy Aquifer. 164

References. 165

9 Slug Tests. 167

9.1 Cooper and Picking Solutions. 167

9.2 Slug Tests in Tight Formations. 169

9.3 Solutions for Slug Tests with Skin Effect. 170

9.4 Bouwer–Rice Solution 172

9.5 Hvorslev Solutions 175

9.6 Van der Kamp Solution 176

References. 177

10 Multi-well Pumping Tests 179

10.1 Pumping with a Constant Discharge Rate. 179

10.1.1 Fully Penetrating Well in a Confined Aquifer 180

10.1.2 Point Source: Confined Aquifer Infinite in the Horizontal Plane and Thickness. 188

10.2 Pumping with a Variable Discharge Rate 190

10.2.1 Single Pumping Well with a Variable Discharge Rate 191

10.2.2 A System of Pumping Wells with a Variable Discharge Rate 192

10.3 Simultaneous Pumping from Two Aquifers Separated by an Aquitard 193

10.3.1 Aquifers of Infinite Lateral Extent. 193

10.3.2 Circular Aquifers. 195

10.4 Dipole Flow Tests 197

10.4.1 Horizontal Dipole 198

10.4.2 Vertical Dipole 201

References. 204

11 Recovery Tests. 205

11.1 A Single Pumping Well with a Constant Discharge Rate 207

11.1.1 Confined Aquifer. 207

11.1.2 Unconfined Aquifer. 218

11.2 A System of Pumping Wells with Constant Discharge Rates 219

11.3 Variable Discharge Rate 223

References. 224

Part III Solution of Hydrogeological Problems Using ANSDIMAT

12 Aquifer-Test Analytical Methods 227

12.1 Graphical Methods 227

 12.1.1 Straight-Line Method. 228

 12.1.2 Horizontal Straight-Line Method 230

 12.1.3 Type Curve Method 231

12.2 Method of Bisecting Line 233

12.3 Matching Methods 235

 12.3.1 Direct Method: Manual Trial and Error 235

 12.3.2 Inverse Method for Sensitivity Analysis 238

12.4 Diagnostic Curve for Aquifer Tests 241

 12.4.1 Confined Aquifer. 241

 12.4.2 Unconfined Aquifer. 246

 12.4.3 Leaky Aquifer 250

 12.4.4 Horizontally Heterogeneous Aquifer 250

 12.4.5 Pumping Test near a Stream 251

 12.4.6 Pumping Test in a Fractured-Porous Reservoir 252

 12.4.7 Constant-Head Test 254

 12.4.8 Slug Test. 255

 12.4.9 Recovery Test 256

References. 258

13 Analytical Solutions for Complex Engineering Problems 261

13.1 Evaluation of Groundwater Response to Stream-Stage Variation. 262

 13.1.1 Instantaneous Level Change Followed by a Steady-State Period 262

 13.1.2 Multi-stage or Gradual Level Changes 267

13.2 Analytical Modeling 269

13.3 Simplified Analytical Relationships for Assessing Water Inflow into an Open Pit 271

 13.3.1 Effective Open Pit Radius 272

 13.3.2 The Radius of Influence for Infinite Nonleaky Aquifers. 273

 13.3.3 Estimating Water Inflow into an Open Pit. 275

References. 282

Appendix 1: Hydraulic Characteristics 285

Appendix 2: Wellbore Storage, Wellbore Skin, and Shape Factor 289

Appendix 3: Boundary Conditions and Image Wells 293

Appendix 4: Equations for Universal Screening Assessments 305

**Appendix 5: Application of Computer Programs
for Analysis Aquifer Tests 311**

Appendix 6: Application of UCODE_2005 343

**Appendix 7: Special Functions: Analytical Representations,
Graphs, and Approximations 353**

References 387

Index 391

Notations

A	Intercept of the straight line on the ordinate
a	Aquifer hydraulic diffusivity, $a = km/S$ (for an unconfined aquifer, $a = km/S_y$), m^2/d
a_r, a_z	Horizontal and vertical hydraulic diffusivity, $a_r = k_r m/S$, $a_z = k_z m/S$, m^2/d
B	Leakage factor, m
B_p	See L_{Tp} and L_{Bp}
B_w	See L_{Tw} and L_{Bw}
C	Slope of the straight line
C_w	Water compressibility, Pa^{-1}
D	Shift of the plots of the observed and type curves in the vertical direction (see Fig. 12.3)
d	Distance between screen centers in the pumping and observation wells (see Fig. 1.10), m
E	Shift of the plots of the observed and type curves in the horizontal direction (see Fig. 12.3)
F	Shape factor (see Appendix 2), m
F_R	Function of the radius of influence, dimensionless
g	Gravity acceleration, m/s^2
H	Initial head (see Fig. 2.2b), m
k	Aquifer hydraulic conductivity, m/d
k_r, k_z	Hydraulic conductivities in the horizontal and vertical directions, respectively, m/d
k_{skin}	Hydraulic conductivity of the wellbore skin, m/d (see Appendix 2)
k_{skin}^f	Hydraulic conductivity of fracture skin (Fig. 6.1d), m/d
L	Width of the strip aquifer, m
L_{Bp}, L_{Bw}	Vertical distances from screen centers of the observation and pumping wells to the aquifer bottom, respectively (see Fig. 1.19), m

L_f	Fracture length or fracture diameter (see Figs. 6.2 and 6.4), m
L_p	Distance from the observation well to the planar boundary (see Figs. 1.4 and A3.2); for a circular aquifer—the distance from the observation well to the center of the circular aquifer (see Fig. 1.9d); for a fractured–porous reservoir—the horizontal distance from the observation well to the fracture (Fig. 6.2c), m
L_{Tp}, L_{Tw}	Vertical distances from the aquifer top (or from the initial water table of an unconfined aquifer) to the screen centers of the observation and pumping wells (see Figs. 1.19a and 1.22), respectively, m
L_{Up}, L_{Uw}	Distances from the observation and pumping wells to the perpendicular boundary for U-shaped (see Fig. 1.7b) and rectangular (see Fig. 1.8b) aquifers, m
L_w	Distance from the pumping well to the planar boundary (see Figs. 1.4 and A3.2); for a circular aquifer—the distance from the pumping well to the center of the circular aquifer (see Fig. 1.9d), m
L'_p, L'_w	Distances from the observation and image wells to the second boundary of the strip (see Fig. A3.4) or wedge-shaped (see Figs. 1.6b and A3.6) aquifer, $L'_p = L - L_p, L'_w = L - L_w$, m
L'_p	Distance between the observation well and the line passing through the pumping well parallel to x -axis (Fig. 1.26b), m
l_p, l_w	Screen lengths of the observation and pumping wells, respectively, m
m	Thickness of a confined aquifer (see Fig. 1.1) or the initial saturated thickness of an unconfined aquifer (see Fig. 2.1), m
m_b	Average thickness or diameter of blocks (see Fig. 6.1), m
m_f	Average aperture of a fissure (see Figs. 6.1 and 6.4), m
m_{skin}	Thickness of wellbore skin (see Appendix 2), m
m_{skin}^f	Thickness of fracture skin (Fig. 6.1d), m
m_w, m_p	Aquifer thicknesses at the points where the pumping and observation wells are located (Fig. 1.26a), m
N	Number of pumping wells
N_t	Number of pumping wells in operation at moment t
n	Number of image wells, the number of a term in a sum
n	Porosity, dimensionless
n_t	Number of stages in water-level change in a river by moment t
n'_i	Number of steps in the discharge rate of the i th pumping well by moment t
Q	Discharge rate water inflow into open pits, m^3/d
Q_i	Discharge rate of the i th pumping well, m^3/d

Q_i^j	Discharge rate at the j th step in the i th pumping well ($Q_i^0 = 0$) (see Fig. 10.2), m^3/d
R	Radius of a circular aquifer radius of influence, m
R_o	Radius of influence of an open pit, m
r	Radial distance from the pumping to the observation well, m
r_i	Distance from the observation well in which the drawdown is determined to the i th pumping well (Fig. 10.1), m
r_o	Effective pit radius, m
r_c	Casing radius, m
r_p	Radius of the observation well or piezometer, m
r_w	Radius of the pumping well, m
S	Aquifer storage coefficient (elastic), dimensionless
S_R	Storage coefficient at water-level recovery (see Eq. 11.11), dimensionless
S_s	Aquifer specific storage, 1/m
S_{skin}	Storage coefficient of wellbore skin, dimensionless
S_y	Aquifer specific yield, dimensionless
s	Drawdown in an observation well groundwater-level change in an observation well after stream perturbation, m
s_0	Drawdown in the observation well at the moment of pumping cessation, m
s^0	Initial (instantaneous) water-level change in the well (for slug test) an instantaneous initial change in river water level, m
s_j^0	Height of the j th stage of river-level change ($s_0^0 = 0$), m
s_m	Drawdown in the observation well during steady-state period, m
s_{mw}	Drawdown in the pumping well during steady-state period, m
s_o	Drawdown at a pit outline, m
s_r	Recovery in the observation well after the cessation of pumping at moment t_r , $s_r = s_0 - s$, m
s_{skin}	Water-level change in the wellbore zone (in the skin), m
s_w	Drawdown in the pumping well (a constant value in the case of constant-head test), m
$s^{(1)}, s^{(2)}$	Drawdown values in observation wells in the main and the adjacent aquifers (zones), respectively, m
s', s''	Drawdown values in aquitards or the drawdown in the block for fractured-porous reservoir, m
T	Aquifer transmissivity, m^2/d
T_x, T_y	Transmissivities of the aquifer in two perpendicular horizontal directions, m^2/d
t	Time elapsed from the start of aquifer test, d
t_0	Pumping duration, d
t_i	Starting moment of the operation of the i th pumping well, measured from the start of the pumping test, d

t_j	Moment of the start of the j th stage in a river ($t_1 = 0$), d
t_r	Time from the start of recovery, d
t_i^j	Moment of the start of the j th step in the discharge of the i th pumping well ($t_i^1 = 0$) (see Fig. 10.2), d
v	Constant rate of level rise (drop) in a river, m/d
y	Projection of the distance from the observation to the pumping well onto the boundary line (see Fig. A3.2 and Eq. A3.2), m
z	Vertical distance between the screen centers of the pumping and observation wells (Figs. 1.10 and 1.22), m
z_f	Vertical distance from the top of the aquifer to the fracture (Fig. 6.4), m
z_p	Distance from the observation point in the separating aquitard to the top (or bottom) of the main aquifer (Fig. 3.9) for a fractured-porous reservoir (see Figs. 6.1, b)—the distance to block center from the point where water-level changes in the block are measured, m
z_{p1}, z_{p2}	Vertical distances from the confined aquifer top (or from the initial water table of unconfined aquifer) to the bottom and the top of the observation-well screen, respectively (see Figs. 1.22 and 2.1), $z_{p1} = L_{Tp} + l_p/2$, $z_{p2} = L_{Tp} - l_p/2$, m
z_{w1}, z_{w2}	Vertical distances from confined aquifer top (or from the initial water table of an unconfined aquifer) to the bottom and the top of the pumping well screen, respectively (see Figs. 1.22 and 2.1), $z_{w1} = L_{Tw} + l_w/2$, $z_{w2} = L_{Tw} - l_w/2$, m
z_i^j	Vertical distance from the center of the screen of the observation well or the open part of piezometer to the j th image well reflected about the top ($i = 1$) or bottom ($i = 2$) boundary in an aquifer bounded in thickness (see Fig. A3.12a): it is determined by Eqs. A3.22 and A3.23, m
α	Reciprocal of Boulton's delay index (see Eqs. 2.15 and 2.16), 1/d
α	Angle between the abscissa and the direction of anisotropy (see Fig. 1.3c), degrees
ΔL	Retardation coefficient of the semipervious stream bed: depending on the solution, it is determined by Eq. 5.4 or 5.12, m
ε	Recharge rate, m/d
ρ	Distance between the observation and image wells (see Figs. A3.2 and A3.11), m
ρ_j	Distance between the observation well and the j th image well for wedge-shaped aquifers, determined by Eq. A3.6 (see Fig. A3.6 and Eq. A3.6), m

ρ_i^j	Distance between the real observation well and the j th image well reflected from the left ($i = 1$) or right ($i = 2$) boundary (see Fig. A3.4): it is determined by Eqs. A3.3 and A3.4, m
ρ_U	Distance from the pumping to the image well reflected about the perpendicular boundary of U-shaped or rectangular aquifer (see Figs. 1.7 and 1.8): it is determined by Eq. A3.15, m
ρ_{Ui}^j	Distance from the observation well to the j th image well of the second row, reflected about the left ($i = 1$) or right ($i = 2$) boundary of U-shaped aquifer (see Fig. A3.8): it is determined by Eqs. A3.13 and A3.14, m
$\rho_{i,I}^j$	Distance from the observation well to the j th image well: see comment to Eq. 10.16, m
ρ_w	Water density, kg/m^3
θ	For a horizontally anisotropic aquifer (see Fig. 1.3b, c), for an aquifer of nonuniform thickness (see Fig. 1.26b), and sloping unconfined aquifers (see Fig. 2.3c)—the angle between the x -axis and the straight line connecting the pumping and observation wells; for a wedge-shaped aquifer (see Fig. 1.6b)—the angle between two intersecting boundaries; for a circular aquifer—the angle between the vectors from the center of the circular aquifer to the pumping and observation well, respectively (Fig. 1.9d); for a slanted well (see Fig. 7.2c, d)—the angle between the bottom and the well, degrees
θ_s	Slope of the bottom of a sloping unconfined aquifer (see Fig. 2.3), degrees
χ	Coefficient of vertical anisotropy, $\chi = \sqrt{k_z/k_r}$, dimensionless

Superscripts and Subscripts

b	Refers to a block in fractured-porous medium
$I = 1, 2$	Shows the position of an image well in bounded aquifers from the side of its left or right boundary it is used for multi-well, constant-head aquifer tests in bounded aquifers
$i = 1, 2$	Shows the position of an image well in bounded aquifers: from the side of the left (top) or right (bottom) boundary, i is the number of a pumping well in multi-well tests
f	Refers to a fracture

j	For constant-head pumping in bounded aquifers, this is the number of an image well obtained by reflection about a boundary for variable discharge pumping, this is the number of a stage in discharge
o	Refers to an open pit
p	Refers to an observation well or piezometer
w	Refers to a pumping well
1, 2	Refers to the first and second observation wells or the main and adjacent aquifers (zones)
Stroke	Symbols with strokes generally refer to an aquitard, block, or a reduced parameter

Mathematical Constants

π	$\pi = 3.141592653589793$
e	Euler's number: $e = 2.718281828459045$ $e = \sum_{n=0}^{\infty} \frac{1}{n!}$
γ	Euler's constant: $\gamma = 0.577215664901533$ $\gamma = \lim_{n \rightarrow \infty} \left(-\ln n + \sum_{k=1}^n \frac{1}{k} \right)$

Roots of Transcendent Equations (for details, see Appendix 7)

γ_n	Positive roots of equation $\gamma_n \tan \gamma_n = c$; $c = \text{const}$
x_n	Positive roots of equation $J_0(x_n) = 0$
$x_{n,1}$	Positive roots of equation $J_1(x_{n,1}) = 0$
$x_{n,m}$	Positive roots of equation $J_m(x_{n,m}) = 0$
$y_{n,m}$	Positive roots of equation $J'_m(y_{n,m}) = 0$
ζ_n	Positive roots of equation $J_0(\zeta_n)Y_0(\zeta_n c) - J_0(\zeta_n c)Y_0(\zeta_n) = 0$; $c = \text{const}$
ξ_n	Positive roots of equation $J_0(\xi_n)Y_1(\xi_n c) - J_1(\xi_n c)Y_0(\xi_n) = 0$; $c = \text{const}$

List of Functions Used in the Book (for details, see Appendix 7)

$A(u, \beta)$	Flowing well-function for nonleaky aquifers
$\text{erf}(u)$	Error function
$\text{erfc}(u)$	Complementary error function

$F(u, \beta)$	Function for large-diameter wells for nonleaky aquifer
$F(u, \beta_1, \beta_2)$	Function for the drawdown in an observation well located in a nonleaky aquifer in the case of pumping from a large-diameter well
$F_L(u, \beta_2, \beta_3)$	Function for large-diameter wells for leaky aquifer
$F_L(u, \beta_1, \beta_2, \beta_3)$	Function for the drawdown in an observation well located in a leaky aquifer during pumping from a large-diameter pumping well
$F_l(u, \beta_1, \beta_2)$	Linear-source function (see Eq. 1.95)
$F_B(u, \beta)$	Boulton function
$F_s(u, \beta)$	Function for water-level changes in a pumping well during a slug test
$F_{sp}(u, \beta)$	Function for water-level changes in an observation well during slug test
$G(u)$	Flowing well discharge function for nonleaky aquifers
$G(u, \beta)$	Flowing well discharge function for leaky aquifers
$ierfc(u)$	Iterated integral of the complementary error function
$J_0(u)$	Bessel functions of the first kind of the order zero
$J_1(u)$	Bessel functions of the first kind of the order one
$J_m(u)$	Bessel functions of the first kind of the order m
$J^*(u, \beta_1, \beta_2)$	Special function
$H(u, \beta)$	Special function
$I_0(u)$	Modified Bessel functions of the first kind of the order zero
$I_1(u)$	Modified Bessel functions of the first kind of the order one
$I_m(u)$	Modified Bessel functions of the first kind of the order m
$K_0(u)$	Modified Bessel functions of the second kind of the order zero
$K_1(u)$	Modified Bessel functions of the second kind of the order one
$K_m(u)$	Modified Bessel functions of the second kind of the order m
$M(u, \beta)$	Special function
$W(u)$	Well-function
$W(u, \beta)$	Well-function for leaky aquifers
$W_{NW}(u, \beta)$	Special function
$Y_0(u)$	Bessel functions of the second kind of the order zero
$Y_1(u)$	Bessel functions of the second kind of the order one
$Z(u, \beta_1, \beta_2)$	Flowing well-function for leaky aquifers
$\Gamma(u)$	Gamma function
$u, \beta, \beta_1, \beta_2, \beta_3$	Function arguments

Part I

Basic Analytical Solutions

The first part of the book contains basic analytical relationships, describing groundwater-level changes in aquifers during pumping tests. All solutions refer to pumping tests with a single pumping well at a constant discharge rate throughout the test.

This part is divided into chapters, each corresponding to a conceptual model: confined aquifer, unconfined aquifer, leaky aquifer, horizontally heterogeneous aquifer, and fractured-porous medium. The main standard models account for the effect of boundaries in the horizontal or vertical plane. Pumping near a stream is considered separately.

Each model is accompanied by a detail description of the pumping test, and a set of either alternative or complementary solutions, which are used to evaluate the hydraulic characteristics of aquifers. The complementary solutions are those taking into account some complicating factors, such as aquifer anisotropy, wellbore storage, wellbore skin effect, the effect of capillary forces, etc. In the case of deformation of the profile groundwater flow structure, which may be caused by partially penetrating pumping well, the drawdown functions obtained for a piezometer and the drawdown averaged over the length of the pumping well screen can be compared.

Equations for the drawdown are given not only for the pumped aquifer, but also, where possible, for adjacent aquifers and for aquitards. Of interest are the solutions that determine the drawdown in the pumping well itself. Their use is indispensable to obtain accurate and reliable parameter estimates based on the results of pumping from large-diameter wells.

Basic analytical relationships are considered successively for transient, quasi-steady-state, and steady-state groundwater flow regimes. Transient solutions are used in parameter evaluation by the curve-fitting method and the type-curve method (see Chap. 12). Quasi-steady-state and steady-state solutions are used to

derive formulas to evaluate parameters by the straight line method. All possible graphical processing methods are included in tables containing: the name of the method; a plot of drawdown curve, intended for its implementation; and formulas for evaluating the required parameters by the position of the type curve or straight line.

Chapter 1

Confined Aquifers

The top and bottom of a homogeneous aquifer are overlain and underlain by aquicludes, respectively (Fig. 1.1). In the course of testing, the groundwater level never drops below the aquifer top. Aquifer thickness is constant (except for the case considered in Sect. 1.4).

This chapter gives basic analytical solutions for calculating the drawdown in fully penetrating (see Sect. 1.1) and partially penetrating (see Sects. 1.2 and 1.3) pumping and observation wells.

1.1 Fully Penetrating Well

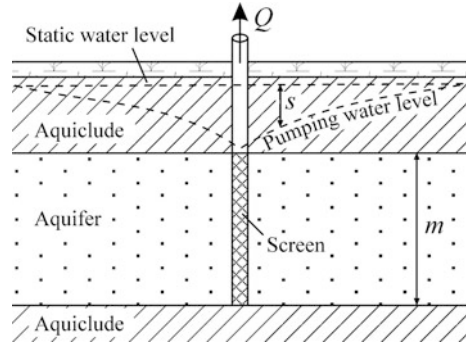
The pumping well is fully penetrating, i.e., its screen length is equal to the thickness of the aquifer (Fig. 1.1).

This section contains transient, quasi-steady-state, and steady-state analytical solutions for calculating drawdown in aquifers with infinite (see Sect. 1.1.1), semi-infinite (see Sect. 1.1.2), and limited (see Sects. 1.1.3–1.1.7) lateral extents. The aquifers with limited lateral extent include strip aquifers, wedge-shaped aquifers, U-shaped aquifers, and aquifers bounded by a closed rectangular or circular contour.

The drawdown in the aquifer is determined at any distance from the pumping well.

Transient solutions can be used to evaluate the transmissivity (T) and the storage coefficient (S) [or hydraulic diffusivity (a)] of an aquifer. For Moench solutions, the hydraulic conductivity and the thickness of the wellbore skin (k_{skin} , m_{skin}) can also be evaluated.

Fig. 1.1 Schematic diagram of a pumping test in a confined aquifer. The pumping well is fully penetrating. Q is the pumping well discharge, s is well drawdown, and m is aquifer thickness



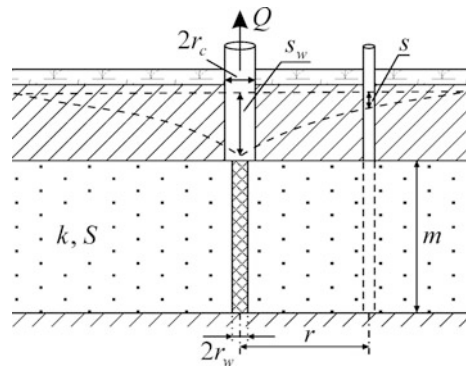
1.1.1 Aquifer of Infinite Lateral Extent

The basic assumptions and conditions (Figs. 1.2 and 1.3) are:

- the aquifer is assumed to be isotropic or horizontally anisotropic with infinite lateral extent;
- the wellbore storage and wellbore skin can be taken into account in evaluating the drawdown.

A typical plot of drawdown in a confined aquifer is given in Fig. 12.9. For the effect of hydraulic parameters, wellbore storage, and wellbore skin on the drawdown in the observation and pumping wells, see Figs. 12.10 and 12.11.

Fig. 1.2 Confined aquifer with infinite lateral extent (cross-section)



Basic Analytical Relationships

Transient Flow Equations

1. The principal solution for drawdown in a confined aquifer is the Theis solution (Carslow and Jaeger 1959; Theis 1935):

$$s = \frac{Q}{4\pi T} W\left(\frac{r^2 S}{4Tt}\right), \quad (1.1)$$

$$W(u) = \int_u^\infty \frac{\exp(-\tau)}{\tau} d\tau, \quad (1.2)$$

where s is the drawdown in an observation well, m; Q is the discharge rate, m³/d; $T = km$ is the transmissivity, m²/d; k , m are the hydraulic conductivity (m/d) and the thickness (m) of the aquifer; S is the storage coefficient, dimensionless; r is the radial distance from the pumping to the observation well, m; t is the time elapsed from the start of pumping, d; $W(u)$ is the well-function (see Appendix 7.1).

For convenience in the subsequent graphic-analytical calculations, we rewrite the solution (Eq. 1.1) as follows:

$$s = \frac{Q}{4\pi T} W\left(\frac{r^2}{4at}\right), \quad (1.3)$$

where $a = T/S$ is hydraulic diffusivity, m²/d.

The Theis solution assumes the wellbore radius is infinitely small, i.e., the wellbore storage is neglected.

2. The Moench solution (Moench 1997) is an extended solution for drawdown in an observation well, taking into account the wellbore storage, skin-effect, and the delayed response of observation piezometer:

$$s = \frac{Q}{4\pi T} f(t, r, r_w, r_c, r_p, T, S, k_{\text{skin}}, m_{\text{skin}}), \quad (1.4)$$

where r_w , r_c , r_p are the radiuses of the pumping well, its casing, and the observation well, respectively, m; and k_{skin} , m_{skin} are the hydraulic conductivity (m/d) and thickness (m) of the wellbore skin (see Appendix 2).

The functional relationship (Eq. 1.4) is treated with the use of an algorithm from the WTAQ3 program (see Appendix 5.3).

3. The Moench solution (Moench 1997) is an extended solution for drawdown in the pumping well, taking into account its storage and skin-effect:

$$s_w = \frac{Q}{4\pi T} f(t, r_w, r_c, T, S, k_{\text{skin}}, m_{\text{skin}}), \quad (1.5)$$

where s_w is drawdown in the pumping well, m.

The functional relationship (1.5) is treated with the use of an algorithm from the WTAQ3 program (see Appendix 5.3).

4. The solution proposed by Papadopoulos and Cooper (1967) is an extended solution, accounting for the wellbore storage and written for the drawdown in the observation well:

$$s = \frac{Q}{4\pi T} F\left(\frac{r_w^2 S}{4Tt}, \frac{r}{r_w}, S \frac{r_w^2}{r_c^2}\right), \quad (1.6)$$

$$F(u, \beta_1, \beta_2) = 8 \frac{\beta_2}{\pi} \int_0^\infty \left\{ \left[1 - \exp\left(-\frac{\tau^2}{4u}\right) \right] \times \right. \\ \left. \times \frac{J_0(\beta_1 \tau) [\tau Y_0(\tau) - 2\beta_2 Y_1(\tau)] - Y_0(\beta_1 \tau) [\tau J_0(\tau) - 2\beta_2 J_1(\tau)]}{[\tau J_0(\tau) - 2\beta_2 J_1(\tau)]^2 + [\tau Y_0(\tau) - 2\beta_2 Y_1(\tau)]^2} \right\} \frac{d\tau}{\tau^2}, \quad (1.7)$$

where $J_0(\cdot)$ and $J_1(\cdot)$ are Bessel functions of the first kind of zero and first order; $Y_0(\cdot)$ and $Y_1(\cdot)$ are Bessel functions of the second kind of zero and first order (see Appendix 7.13).

5. The solution proposed by Papadopoulos and Cooper (1967) is an extended solution accounting for the wellbore storage, written for the drawdown in the pumping well:

$$s_w = \frac{Q}{4\pi T} F\left(\frac{r_w^2 S}{4Tt}, S \frac{r_w^2}{r_c^2}\right), \quad (1.8)$$

$$F(u, \beta) = \frac{32\beta^2}{\pi^2} \int_0^\infty \frac{1 - \exp[-\tau^2/(4u)]}{[\tau J_0(\tau) - 2\beta J_1(\tau)]^2 + [\tau Y_0(\tau) - 2\beta Y_1(\tau)]^2} \frac{d\tau}{\tau^3}, \quad (1.9)$$

where $F(u, \beta)$ is a function for large-diameter wells (see Appendix 7.9).

6. The Hantush solution for a horizontally anisotropic aquifer (Hantush 1966; Hantush and Thomas 1966):

$$s = \frac{Q}{4\pi \sqrt{T_x T_y}} W \left[\frac{r^2 (T_y \cos^2 \theta + T_x \sin^2 \theta) S}{4T_x T_y t} \right], \quad (1.10)$$

where $T_x = k_x m$ and $T_y = k_y m$ are the transmissivities of the aquifer in two perpendicular horizontal directions, m^2/d ; k_x , k_y are hydraulic conductivities in two perpendicular horizontal directions, m/d ; θ is the angle in degrees between the x -axis and the straight line connecting the pumping and observation wells (Fig. 1.3b).

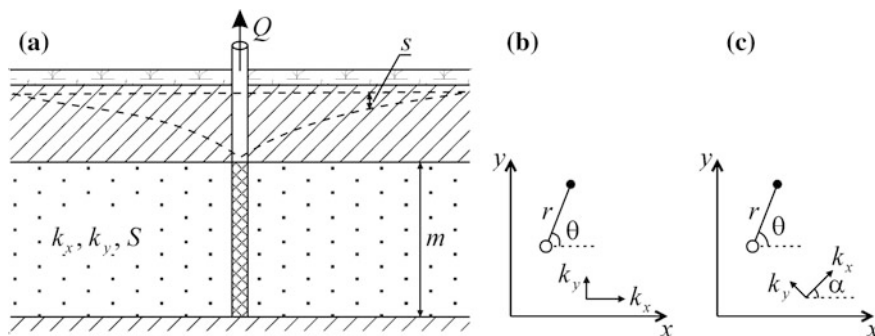


Fig. 1.3 Confined horizontally anisotropic aquifer. **a** Cross-section; **b**, **c** planar views with the anisotropy direction, **b** coinciding and **c** not coinciding with the coordinate axis

Equation 1.10 assumes the anisotropy direction coinciding with the abscissa (Fig. 1.3b). When this is not the case (Fig. 1.3c), the angle θ in (Eq. 1.10) is replaced by the difference $(\theta - \alpha)$, where α is the angle in degrees between the abscissa and the direction of anisotropy.

Unlike all transient solutions given in this section, Eq. 1.10, given angle α , can be used to determine the transmissivities along the anisotropy directions (T_x , T_y) and the storage coefficient (S). The angle θ can be readily derived from the coordinates of the pumping and observation wells.

Quasi-Steady-State Flow Equation

In the plot of observation $s - \lg t$, the quasi-steady-state period is represented by a linear segment. The beginning of this period (see Fig. 12.9) is evaluated via the argument of the well-function $W(u)$ (see Appendix 7.1): for $u \leq 0.05$, Eq. 1.1 is approximated by a straight line (Eq. 1.11).

The Cooper–Jacob solution (Carslow and Jaeger 1959; Jacob 1946; Cooper and Jacob 1946):

$$s = \frac{Q}{4\pi T} \ln \frac{2.25Tt}{r^2 S} = \frac{0.183Q}{T} \lg \frac{2.25Tt}{r^2 S} \quad (1.11)$$

or, expressed in terms of hydraulic diffusivity:

$$s = \frac{Q}{4\pi T} \ln \frac{2.25at}{r^2} = \frac{0.183Q}{T} \lg \frac{2.25at}{r^2}. \quad (1.12)$$

Graphic-Analytical Processing

The procedures of graphic-analytical processing include the method of type curve for the entire testing period, the method of straight line for a quasi-steady-state period, and the method of horizontal straight line for the difference between water-level drawdown in two observation wells in a quasi-steady-state period. The relationships given in Table 1.1 have been derived from Eqs. 1.3 and 1.12.

Table 1.1 Graphic-analytical parameter evaluation

Plot	Method	Relationship
$s - \lg t$	Straight line	$T = \frac{0.183 Q}{C}, \lg a = \frac{A}{C} + \lg \frac{r^2}{2.25}$
$s - \lg r$	The same	$T = \frac{0.366Q}{C}, \lg a = 2 \frac{A}{C} - \lg(2.25 \cdot t)$
$s - \lg \frac{t}{r^2}$	The same	$T = \frac{0.183 Q}{C}, \lg a = \frac{A}{C} - \lg(2.25)$
$\lg s - \lg t$	Type curve: $\lg W(u) - \lg \frac{1}{u}$	$T = \frac{Q}{4\pi 10^D}, a = \frac{r^2 10^E}{4}$
$\lg s - \lg \frac{t}{r^2}$	The same	$T = \frac{Q}{4\pi 10^D}, a = \frac{10^E}{4}$
$\lg s - \lg r$	Type curve: $\lg W(u) - \lg \sqrt{u}$	$T = \frac{Q}{4\pi 10^D}, a = \frac{10^{-2E}}{4t}$
$(s_1 - s_2) - \lg t$	Horizontal straight line	$T = \frac{Q}{2\pi \cdot A} \ln \frac{r_2}{r_1}$

A is the intercept of the straight line on the ordinate (see Sects. 12.1.1 and 12.1.2); C is the slope of the straight line (see Sect. 12.1.1); D, E are the shifts of the plots of the observed and type curves (see Sect. 12.1.3) in the vertical (D) and horizontal (E) directions; s_1, s_2, r_1, r_2 are the values of drawdown (s) and the distances from the pumping well (r) to the first and second observation wells, respectively. In the case of testing in a horizontally anisotropic aquifer, graphic-analytical methods yield effective transmissivity and hydraulic diffusivity, in this case: $T = \sqrt{T_x T_y}, a = T_x/S$ (for $\theta = 0^\circ$), $a = T_y/S$ (for $\theta = 90^\circ$)

In Table 1.1, the values of transmissivity and hydraulic diffusivity are evaluated independently. Given these parameters, the storage coefficient of the aquifer can be readily evaluated: $S = T/a$. In addition, the hydraulic diffusivity and storage coefficient can be evaluated from the intercept on the abscissa (Table 1.2).

Table 1.2 Graphic-analytical parameter evaluation

Plot	Method	Relationship
$s - \lg t$	Straight line	$a = \frac{r^2}{2.25t_x}, S = \frac{2.25Tt_x}{r^2}$
$s - \lg r$	The same	$a = \frac{r_x^2}{2.25t}, S = \frac{2.25Tt}{r_x^2}$
$s - \lg \frac{t}{r^2}$	The same	$a = \frac{1}{2.25(t/r^2)_x}, S = 2.25T(t/r^2)_x$

$t_x, r_x,$ and $(t/r^2)_x$ are intercepts on the abscissas of appropriate plots (see Fig. 12.1)

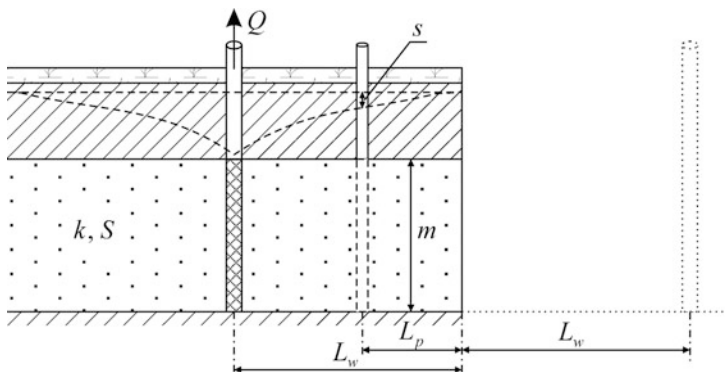


Fig. 1.4 Confined semi-infinite aquifer. The dashed line in the right shows the image well. L_w , L_p are the distances from the pumping and observation wells to the boundary, respectively

1.1.2 Semi-infinite Aquifer

The basic assumptions and conditions (Fig. 1.4) are:

- the aquifer is isotropic and semi-infinite;
- the boundary is linear and infinite.

Two variants of boundary conditions are considered (see Fig. A3.1): (1) constant-head boundary and (2) impermeable boundary.

To solve the problem, the image-well method is used: a single image well is introduced (for the distance to the image well and the sign of its discharge, see Fig. A3.2).

Typical plots of drawdown in the observation well for two variants of boundary conditions are given in Fig. 12.12.

1.1.2.1 Semi-infinite Aquifer: Constant-Head Boundary

Basic Analytical Relationships

Transient Flow Equation

$$s = \frac{Q}{4\pi T} \left[W\left(\frac{r^2}{4at}\right) - W\left(\frac{\rho^2}{4at}\right) \right], \tag{1.13}$$

where ρ is the horizontal distance between the observation and image wells (see Fig. A3.2 and Eq. A3.1), m .

Table 1.3 Graphic-analytical parameter evaluation

Plot	Method	Relationship
$s - \lg t$	Horizontal straight line ^a	$T = \frac{Q}{2\pi \cdot A} \ln \frac{\rho}{r}$
$\lg s - \lg t$	Type curve: $\lg W'(u) - \lg \frac{1}{u}$	$T = \frac{Q}{4\pi 10^D}, a = \frac{r^2 10^E}{4}$
$\lg s - \lg \frac{t}{r^2}$	The same	$T = \frac{Q}{4\pi 10^D}, a = \frac{10^E}{4}$
$s_m - \lg \frac{\rho}{r}$	Straight line	$T = \frac{0.366Q}{C}$
$(s_1 - s_2) - \lg t$	Horizontal straight line ^a	$T = \frac{Q}{2\pi \cdot A} \ln \frac{\rho_1 \rho_2}{\rho_2 r_1}$

^aThe parameters are derived from drawdown values in the steady-state flow period
 ρ_1, ρ_2 are the distances from the first and second observation wells to the image well
 $W'(u) = W(u) - W(ur')$, $r' = (\rho/r)^2$

Steady-State Flow Equations

1. The drawdown in the observation well

$$s_m = \frac{Q}{2\pi T} \ln \frac{\rho}{r} = \frac{0.366Q}{T} \lg \frac{\rho}{r}. \quad (1.14)$$

2. The drawdown in the pumping well (Forchheimer 1914)

$$s_{mw} = \frac{Q}{2\pi T} \ln \frac{2L_w}{r_w}, \quad (1.14a)$$

where s_m, s_{mw} are the drawdowns in the observation and the pumping wells during steady-state period, m; L_w is the distance from the pumping well to the boundary, m.

Graphic-Analytical Processing

The relationships given in Table 1.3 have been derived from Eqs. 1.13 and 1.14.

1.1.2.2 Semi-infinite Aquifer: Impermeable Boundary

Basic Analytical Relationships

Transient Flow Equation

$$s = \frac{Q}{4\pi T} \left[W\left(\frac{r^2}{4at}\right) + W\left(\frac{\rho^2}{4at}\right) \right]. \quad (1.15)$$

Table 1.4 Graphic-analytical parameter evaluation

Plot	Method	Relationship
$s - \lg t$	Straight line	$T = \frac{0.366Q}{C}$, $\lg a = \frac{A}{C} + \lg \frac{r\rho}{2.25}$
$\lg s - \lg t$	Type curve: $\lg W'(u) - \lg \frac{1}{u}$	$T = \frac{Q}{4\pi 10^D}$, $a = \frac{r^2 10^E}{4}$
$\lg s - \lg \frac{t}{r^2}$	The same	$T = \frac{Q}{4\pi 10^D}$, $a = \frac{10^E}{4}$
$s - \lg r\rho$	Straight line	$T = \frac{0.366Q}{C}$, $\lg a = \frac{A}{C} - \lg(2.25 \cdot t)$
$s - \lg \frac{t}{r\rho}$	The same	$T = \frac{0.366Q}{C}$, $\lg a = \frac{A}{C} - \lg 2.25$
$(s_1 - s_2) - \lg t$	Horizontal straight line	$T = \frac{Q}{2\pi \cdot A} \ln \frac{\rho_2 r_2}{\rho_1 r_1}$

$W'(u) = W(u) + W(ur')$, $r' = (\rho/r)^2$

Quasi-Steady-State Flow Equation

$$s = \frac{Q}{2\pi T} \ln \frac{2.25at}{r\rho} = \frac{0.366Q}{T} \lg \frac{2.25at}{r\rho}. \tag{1.16}$$

Graphic-Analytical Processing

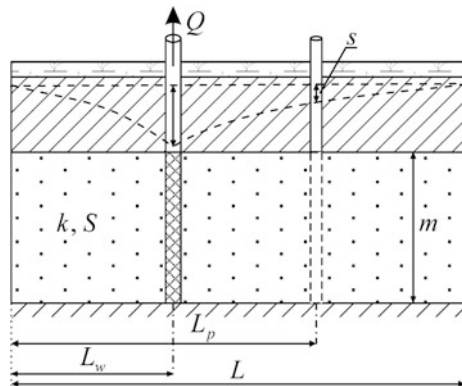
The relationships given in Table 1.4 have been derived from Eqs. 1.15 and 1.16.

1.1.3 Strip Aquifer

The basic assumptions and conditions (Fig. 1.5) are:

- the aquifer is isotropic and bounded in the horizontal plane;
- the boundaries are two infinite parallel straight lines.

Fig. 1.5 Confined bounded aquifer (strip aquifer). L is the width of the strip aquifer



Three variants of boundary conditions are considered (see Fig. A3.3): (1) two constant-head boundaries, (2) two impermeable boundaries, and (3) mixed boundary conditions—constant-head and impermeable boundaries.

To solve the problem, the image-well method is used: image wells form an infinite row (for the distances to the image wells and the signs of their discharges, see in Fig. A3.4).

Typical plots of drawdown in the observation well, taking into account the effects of different types of boundary conditions, are given in Fig. 12.13.

1.1.3.1 Strip Aquifer: Constant-Head Boundaries

Basic Analytical Relationships

Transient Flow Equations

1. Solution based on the superposition principle:

$$s = \frac{Q}{4\pi T} \left\{ W\left(\frac{r^2}{4at}\right) + \sum_{j=1}^n (-1)^j \sum_{i=1}^2 W\left[\frac{(\rho_i^j)^2}{4at}\right] \right\}, \quad (1.17)$$

where ρ_i^j is the distance between the real observation well and the j th image well reflected from the left ($i = 1$) or right ($i = 2$) boundary (see Fig. A3.4): they are determined by Eqs. A3.3 and A3.4, $m; n \rightarrow \infty$ is the number of reflections in the same boundary. In such solutions for bounded aquifers, the infinite number of reflections is replaced by a finite number such that its increase would have no effect on calculation accuracy.

2. Green's function solution (Bochever 1959):

$$s = \frac{Q}{4\pi T} \left\{ \ln \frac{\cosh \frac{\pi y}{L} - \cos \pi \beta_1}{\cosh \frac{\pi y}{L} - \cos \pi \beta_2} + \sum_{n=1}^{\infty} \left[\frac{1}{n} (\cos n\pi \beta_1 - \cos n\pi \beta_2) \times \left(\exp\left(-\frac{n\pi y}{L}\right) \operatorname{erfc}\left(\frac{n\pi\sqrt{at}}{L} - \frac{y}{2\sqrt{at}}\right) + \exp\left(\frac{n\pi y}{L}\right) \operatorname{erfc}\left(\frac{n\pi\sqrt{at}}{L} + \frac{y}{2\sqrt{at}}\right) \right) \right] \right\}, \quad (1.18)$$

where $\beta_1 = (L_p + L_w)/L$; $\beta_2 = (L_p - L_w)/L$; L is the width of the strip aquifer, m ; L_w and L_p are the distances from the pumping well and the observation well to the left boundary, m ; n is summation index; y is the projection of the distance between the observation and pumping wells to the boundary line (see Fig. A3.4 and Eq. A3.2), m .

3. The second Green's function solution, following from the solution (Eq. 3.15) for a leaky aquifer (Hantush and Jacob 1955) at $B \rightarrow \infty$:

$$s = \frac{Q}{2\pi T} \sum_{n=1}^{\infty} \left\{ \frac{1}{n} \sin \frac{n\pi L_p}{L} \sin \frac{n\pi L_w}{L} \times \left[\exp\left(-\frac{n\pi y}{L}\right) \operatorname{erfc}\left(\sqrt{\frac{y^2}{4at}} - \frac{n\pi\sqrt{at}}{L}\right) - \exp\left(\frac{n\pi y}{L}\right) \operatorname{erfc}\left(\sqrt{\frac{y^2}{4at}} + \frac{n\pi\sqrt{at}}{L}\right) \right] \right\}, \quad (1.19)$$

where $\operatorname{erfc}(\cdot)$ is the complementary error function (see Appendix 7.12).

Steady-State Flow Equations

1. Solution based on the superposition principle:

$$s_m = \frac{Q}{2\pi T} \ln r' = \frac{0.366Q}{T} \lg r', \quad (1.20)$$

$$r' = \frac{\rho_1^n}{r} \prod_{j=1,3,\dots}^{n-1} \left(\frac{\rho_1^j \rho_2^j}{\rho_1^{j+1} \rho_2^{j+1}} \right). \quad (1.21)$$

2. Green's function solution (Muskat 1937):

$$s_m = \frac{Q}{4\pi T} \ln r' = \frac{0.183Q}{T} \lg r', \quad (1.22)$$

$$r' = \frac{\cosh \frac{\pi y}{L} - \cos \pi \beta_1}{\cosh \frac{\pi y}{L} - \cos \pi \beta_2}. \quad (1.23)$$

Graphic-Analytical Processing

The relationships given in Table 1.5 have been derived from Eqs. 1.17, 1.20, and 1.22.

Table 1.5 Graphic-analytical parameter evaluation

Plot	Method	Relationship
$s - \lg t$	Horizontal straight line ^a	$T = \frac{Q}{2\pi \cdot A} \ln r'^b$, $T = \frac{Q}{4\pi \cdot A} \ln r'^c$
$\lg s - \lg t$	Type curve: $\lg W'(u) - \lg \frac{1}{u}$	$T = \frac{Q}{4\pi 10^D}$, $a = \frac{r^2 10^E}{4}$
$\lg s - \lg \frac{t}{r^2}$	The same	$T = \frac{Q}{4\pi 10^D}$, $a = \frac{10^E}{4}$
$s_m - \lg r'$	Straight line	$T = \frac{0.366Q_b}{C}$, $T = \frac{0.183Q_c}{C}$
$(s_1 - s_2) - \lg t$	Horizontal straight line ^a	$T = \frac{Q}{2\pi \cdot A} \ln \frac{r'_1}{r'_2}$, $T = \frac{Q}{4\pi \cdot A} \ln \frac{r'_{1c}}{r'_{2c}}$

^aBased on drawdown values for steady-state flow period

^bDerived from solution (Eq. 1.20), r' is determined by Eq. 1.21

^cDerived from solution (Eq. 1.22), r' is determined by Eq. 1.23

$W'(u) = W(u) + \sum_{j=1}^n (-1)^j \sum_{i=1}^2 W(ur_i^j)$, $r_i^j = (\rho_i^j/r)^2$, r'_1 , r'_2 are reduced distances for the first and second observation wells

1.1.3.2 Strip Aquifer: Impermeable Boundaries

Basic Analytical Relationships

Transient Flow Equations

1. Solution based on the superposition principle:

$$s = \frac{Q}{4\pi T} \left\{ W\left(\frac{r^2}{4at}\right) + \sum_{j=1}^n \sum_{i=1}^2 W\left[\frac{(\rho_i^j)^2}{4at}\right] \right\}. \quad (1.24)$$

2. Green's function solution (Bochever 1959):

$$s = \frac{Q}{4\pi T} \left\{ \begin{array}{l} \frac{4\pi\sqrt{at}}{L} i \operatorname{erfc}\left(\frac{y}{2\sqrt{at}}\right) + \ln \frac{\exp\left(2\frac{\pi y}{L}\right)}{4\left(\cosh\frac{\pi y}{L} - \cos\pi\beta_1\right)\left(\cosh\frac{\pi y}{L} - \cos\pi\beta_2\right)} - \\ - \sum_{n=1}^{\infty} \left[\frac{1}{n} (\cos n\pi\beta_1 + \cos n\pi\beta_2) \times \right. \\ \left. \times \left(\exp\left(-\frac{n\pi y}{L}\right) \operatorname{erfc}\left(\frac{n\pi\sqrt{at}}{L} - \frac{y}{2\sqrt{at}}\right) + \right. \right. \\ \left. \left. + \exp\left(\frac{n\pi y}{L}\right) \operatorname{erfc}\left(\frac{n\pi\sqrt{at}}{L} + \frac{y}{2\sqrt{at}}\right) \right) \right] \end{array} \right\}, \quad (1.25)$$

where $\beta_1 = (L_p + L_w)/L$; $\beta_2 = (L_p - L_w)/L$; $i \operatorname{erfc}(\cdot)$ is the iterated integral of the complementary error function (see Appendix 7.12).

For large times, the third term in the curly brackets in (Eq. 1.25) can be omitted, and for $\frac{y}{2\sqrt{at}} < 0.05$, the iterated integral of the complementary error function tends to a constant of 0.56. This allows the hydraulic characteristics to be evaluated by the straight-line method (Borevskiy et al. 1973) on a plot in coordinates $s - \sqrt{t}$ (see Table 1.6 and Fig. 12.14).

3. Second Green's function solution. This solution was derived from solution (Eq. 3.17) for a leaky aquifer (Hantush and Jacob 1955) at $B \rightarrow \infty$:

$$s = \frac{Q}{2\pi T} \left\{ \frac{\sqrt{\pi}}{L} \left[\exp\left(-\frac{y^2}{4at}\right) \sqrt{4at} - \sqrt{\pi}y \operatorname{erfc}\sqrt{\frac{y^2}{4at}} \right] + \sum_{n=1}^{\infty} \left\{ \frac{1}{n} \cos\frac{n\pi L_p}{L} \cos\frac{n\pi L_w}{L} \times \right. \right. \\ \left. \left. \times \left[\exp\left(-\frac{n\pi y}{L}\right) \operatorname{erfc}\left(\sqrt{\frac{y^2}{4at}} - \frac{n\pi\sqrt{at}}{L}\right) - \exp\left(\frac{n\pi y}{L}\right) \operatorname{erfc}\left(\sqrt{\frac{y^2}{4at}} + \frac{n\pi\sqrt{at}}{L}\right) \right] \right\} \right\}. \quad (1.26)$$

Graphic-Analytical Processing

The relationships given in Table 1.6 have been derived from Eqs. 1.24 and 1.25.

Table 1.6 Graphic-analytical parameter evaluation

Plot	Method	Relationship
$\lg s - \lg t$	Type curve: $\lg W'(u) - \lg \frac{1}{u}$	$T = \frac{Q}{4\pi 10^D}, a = \frac{r^2 10^E}{4}$
$\lg s - \lg \frac{t}{r^2}$	The same	$T = \frac{Q}{4\pi 10^D}, a = \frac{10^E}{4}$
$s - \sqrt{t}$	Straight line ^a	$T = \frac{0.56Q\sqrt{a}}{LC}, a = \left(\frac{TLC}{0.56Q}\right)^2$
$(s_1 - s_2) - \lg t$	Horizontal straight line	$T = \frac{(2n+1)Q}{2\pi \cdot A} \ln \frac{r'_2}{r'_1}$

^aSee comment to the solution (Eq. 1.25)

$$W'(u) = W(u) + \sum_{j=1}^n \sum_{i=1}^2 W(ur_i^j), r_i^j = (\rho_i^j/r)^2; r' = \left(r \prod_{j=1}^n \rho_1^j \rho_2^j\right)^{1/(2n+1)}$$

1.1.3.3 Strip Aquifer: Constant-Head and Impermeable Boundaries

Basic Analytical Relationships

Transient Flow Equations

1. Solution based on the superposition principle:

$$s = \frac{Q}{4\pi T} \left\{ \begin{aligned} &W\left(\frac{r^2}{4at}\right) + \sum_{j=1,3,\dots}^n \sum_{i=1}^2 (-1)^{(j+2i-1)/2} W\left(\frac{(\rho_i^j)^2}{4at}\right) + \\ &+ \sum_{j=2,4,\dots}^n (-1)^{j/2} \sum_{i=1}^2 W\left(\frac{(\rho_i^j)^2}{4at}\right) \end{aligned} \right\}. \quad (1.27)$$

2. Green's function solution (Bochever 1959):

$$s = \frac{Q}{4\pi T} \left\{ \begin{aligned} &\ln \frac{\left(\cosh \frac{\pi y}{2L} - \cos \pi \beta_1\right) \left(\cosh \frac{\pi y}{2L} + \cos \pi \beta_2\right)}{\left(\cosh \frac{\pi y}{2L} + \cos \pi \beta_1\right) \left(\cosh \frac{\pi y}{2L} - \cos \pi \beta_2\right)} + \\ &+ \sum_{n=1}^{\infty} \left[\frac{1 - (-1)^n}{n} (\cos n\pi \beta_1 - \cos n\pi \beta_2) \times \right. \\ &\quad \left. \times \left(\exp\left(-\frac{n\pi y}{2L}\right) \operatorname{erfc}\left(\frac{n\pi\sqrt{at}}{2L} - \frac{y}{2\sqrt{at}}\right) + \right. \right. \\ &\quad \left. \left. + \exp\left(\frac{n\pi y}{2L}\right) \operatorname{erfc}\left(\frac{n\pi\sqrt{at}}{2L} + \frac{y}{2\sqrt{at}}\right) \right) \right] \end{aligned} \right\}, \quad (1.28)$$

where $\beta_1 = \frac{L_p + L_w}{2L}$, $\beta_2 = \frac{L_p - L_w}{2L}$. Here, L_p and L_w are the distances from the observation and pumping wells to the constant-head boundary, m.

Steady-State Flow Equations

1. Solution based on the superposition principle:

$$s_m = \frac{Q}{2\pi T} \ln r' = \frac{0.366Q}{T} \lg r', \quad (1.29)$$

$$r' = \frac{\rho_1^n}{r} \prod_{j=1,5,9,\dots}^{n-3} \frac{\rho_1^j \rho_1^{j+1} \rho_2^{j+1} \rho_2^{j+2}}{\rho_1^{j+2} \rho_1^{j+3} \rho_2^j \rho_2^{j+3}}. \quad (1.30)$$

2. Green's function solution (Hantush and Jacob 1954):

$$s_m = \frac{Q}{4\pi T} \ln r' = \frac{0.183Q}{T} \lg r', \quad (1.31)$$

$$r' = \frac{\left(\cosh \frac{\pi y}{2L} - \cos \pi \beta_1\right) \left(\cosh \frac{\pi y}{2L} + \cos \pi \beta_2\right)}{\left(\cosh \frac{\pi y}{2L} + \cos \pi \beta_1\right) \left(\cosh \frac{\pi y}{2L} - \cos \pi \beta_2\right)}. \quad (1.32)$$

Graphic-Analytical Processing

The relationships given in Table 1.7 have been derived from Eqs. 1.27, 1.29, and 1.31.

Table 1.7 Graphic-analytical parameter evaluation

Plot	Method	Relationship
$s - \lg t$	Horizontal straight line ^a	$T = \frac{Q}{2\pi \cdot A} \ln r'^b$, $T = \frac{Q}{4\pi \cdot A} \ln r'^c$
$\lg s - \lg t$	Type curve: $\lg W'(u) - \lg \frac{1}{u}$	$T = \frac{Q}{4\pi 10^D}$, $a = \frac{r^2 10^E}{4}$
$\lg s - \lg \frac{t}{r^2}$	The same	$T = \frac{Q}{4\pi 10^D}$, $a = \frac{10^E}{4}$
$s - \lg r'$	Straight line	$T = \frac{0.366Q_b}{C}$, $T = \frac{0.183Q_c}{C}$
$(s_1 - s_2) - \lg t$	Horizontal straight line ^a	$T = \frac{Q}{2\pi \cdot A} \ln \frac{r'_1}{r'_2}$, $T = \frac{Q}{4\pi \cdot A} \ln \frac{r'_1}{r'_2}$

^aBased on drawdown values for steady-state flow period

^bDerived from solution (Eq. 1.29), r' is determined by Eq. 1.30

^cDerived from solution (Eq. 1.31), r' is determined by Eq. 1.32

$$W'(u) = W(u) + \sum_{j=1,3,\dots}^n \sum_{i=1}^2 (-1)^{(j+2i-1)/2} W(ur_i^j) + \sum_{j=2,4,\dots}^n (-1)^{j/2} \sum_{i=1}^2 W(ur_i^j), \quad r_i^j = (\rho_i^j/r)^2$$

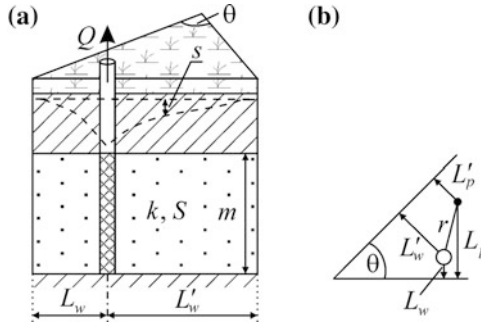


Fig. 1.6 Wedge-shaped confined aquifer: **a** cross-section and **b** planar view. L'_w , L'_p are the distances from the pumping and observation wells to the second boundary, respectively; θ is the angle between two intersecting boundaries

1.1.4 Wedge-Shaped Aquifer

The basic assumptions and conditions (Fig. 1.6) are:

- the aquifer is isotropic and bounded in the horizontal plane;
- the boundaries are two semi-infinite straight half-lines intersecting at an angle between 1° and 90° .

Three variants of boundary conditions are considered (see Fig. A3.5): (1) constant-head boundaries; (2) two impermeable boundaries; (3) mixed boundary conditions—constant-head and impermeable boundaries.

To solve the problem, the image-well method is used: the number of image wells is determined by the angle θ between the intersecting boundaries (Table A3.1); for the signs of the image-well discharges, see Fig. A3.6.

In the case of an aquifer-quadrant (see Fig. A3.6b), where $\theta = 90^\circ$, the image wells number three and the formulas for distances become much simpler (see Eq. A3.11).

The analytical solutions for wedge-shaped aquifers fail to allow an arbitrary angle θ to be specified between the two boundaries. Therefore, the value of θ in the flow equation should be taken in accordance with the rule in Appendix 3 for a wedge-shaped aquifer (see Eq. A3.5).

1.1.4.1 Wedge-Shaped Aquifer: Constant-Head Boundaries

Basic Analytical Relationships

Transient Flow Equation

$$s = \frac{Q}{4\pi T} \left[W\left(\frac{r^2}{4at}\right) + \sum_{j=1}^n (-1)^j W\left(\frac{\rho_j^2}{4at}\right) \right], \quad (1.33)$$

Table 1.8 Graphic-analytical parameter evaluation

Plot	Method	Relationship
$s - \lg t$	Horizontal straight line ^a	$T = \frac{Q}{2\pi \cdot A} \ln r'$
$\lg s - \lg t$	Type curve: $\lg W'(u) - \lg \frac{1}{u}$	$T = \frac{Q}{4\pi 10^D}, a = \frac{r^2 10^E}{4}$
$\lg s - \lg \frac{t}{r^2}$	The same	$T = \frac{Q}{4\pi 10^D}, a = \frac{10^E}{4}$
$(s_1 - s_2) - \lg t$	Horizontal straight line ^a	$T = \frac{Q}{2\pi \cdot A} \ln \frac{r'_1}{r'_2}$

^aBased on drawdown values for steady-state flow period

$$W'(u) = W(u) + \sum_{j=1}^n (-1)^j W(ur'_j), \quad r'_j = (\rho_j/r)^2$$

where ρ_j is the distance between the observation well and the j th image well (see Fig. A3.6a), determined by Eq. A3.6, m ; n is the number of image wells for the given angle θ (see Eq. A3.5 and Table A3.1).

Steady-State Flow Equation

$$s_m = \frac{Q}{2\pi T} \ln r' = \frac{0.366Q}{T} \lg r', \quad (1.34)$$

$$r' = \prod_{j=1,3,\dots}^n \rho_j / r \prod_{j=2,4,\dots}^n \rho_j. \quad (1.35)$$

Graphic-Analytical Processing

The relationships given in Table 1.8 have been derived from Eqs. 1.33 and 1.34.

1.1.4.2 Wedge-Shaped Aquifer: Impermeable Boundaries

Basic Analytical Relationships

Transient Flow Equation

$$s = \frac{Q}{4\pi T} \left[W\left(\frac{r^2}{4at}\right) + \sum_{j=1}^n W\left(\frac{\rho_j^2}{4at}\right) \right], \quad (1.36)$$

Quasi-Steady-State Flow Equation

$$s = \frac{(n+1)Q}{4\pi T} \ln \frac{2.25at}{r^2} = \frac{0.183(n+1)Q}{T} \lg \frac{2.25at}{r^2}, \quad (1.37)$$

$$r' = \left(r \prod_{j=1}^n \rho_j \right)^{1/(n+1)}. \quad (1.38)$$

Table 1.9 Graphic-analytical parameter evaluation

Plot	Method	Relationship
$s - \lg t$	Straight line	$T = \frac{0.183(n+1)Q}{C}$, $\lg a = A/C + \lg \frac{r^2}{2.25}$
$\lg s - \lg t$	Type curve: $\lg W'(u) - \lg \frac{1}{u}$	$T = \frac{Q}{4\pi 10^D}$, $a = \frac{r^2 10^E}{4}$
$\lg s - \lg \frac{t}{r^2}$	The same	$T = \frac{Q}{4\pi 10^D}$, $a = \frac{10^E}{4}$
$(s_1 - s_2) - \lg t$	Horizontal straight line	$T = \frac{Q(n+1)}{2\pi \cdot A} \ln \frac{r'_2}{r'_1}$

$$W'(u) = W(u) + \sum_{j=1}^n W(ur'_j), \quad r'_j = (\rho_j/r)^2$$

Graphic-Analytical Processing

The relationships given in Table 1.9 have been derived from Eqs. 1.36 and 1.37.

1.1.4.3 Wedge-Shaped Aquifer: Constant-Head and Impermeable Boundaries

Basic Analytical Relationships

Transient Flow Equation

$$s = \frac{Q}{4\pi T} \left[\sum_{j=0,2,4,\dots}^n (-1)^{j/2} \left[W\left(\frac{\rho_j^2}{4at}\right) + W\left(\frac{\rho_{j+1}^2}{4at}\right) \right] \right], \quad (1.39)$$

where $\rho_0 = r$.

Steady-State Flow Equation

$$s_m = \frac{Q}{2\pi T} \ln r' = \frac{0.366Q}{T} \lg r', \quad (1.40)$$

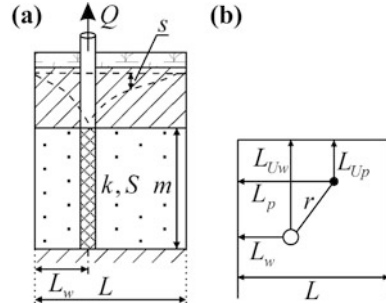
$$r' = \prod_{j=0,4,8,\dots}^n \frac{\rho_{j+2}\rho_{j+3}}{\rho_j\rho_{j+1}}. \quad (1.41)$$

Graphic-Analytical Processing

The graphic-analytical processing is based on Eqs. 1.39 and 1.40 similar to the conditions on the constant-head boundaries (Table 1.8), where the reduced distance is evaluated by Eq. 1.41 and the type curve is constructed taking into account the relationships

$$W'(u) = \sum_{j=0,2,4,\dots}^n (-1)^{j/2} \left[W(ur'_j) + W(ur'_{j+1}) \right], \quad r'_0 = 1.$$

Fig. 1.7 U-shaped confined aquifer: **a** cross-section and **b** planar view. L is distance between parallel boundaries; L_{Uw} , L_{Up} are the distances from the pumping and observation wells to the perpendicular boundary, respectively



1.1.5 U-Shaped Aquifer

The basic assumptions and conditions (Fig. 1.7) are:

- the aquifer is isotropic and bounded in the horizontal plane;
- the boundaries are two parallel semi-infinite linear boundaries and a bounded linear boundary perpendicular to the parallel boundaries.

Six variants of boundary conditions are considered (see Fig. A3.7): (1) all boundaries are of constant-head type; (2) the parallel boundaries are of the constant-head type, and the perpendicular boundary is impermeable; (3) the parallel boundaries are impermeable, and the perpendicular boundary is of constant-head type; (4) all boundaries are impermeable; (5) the parallel boundaries are of the constant-head and impermeable types, and the perpendicular boundary is of the constant-head type; and (6) the parallel boundaries are of the constant-head and impermeable types, and the perpendicular boundary is impermeable.

To solve the problem, the image-well method is used: the image wells form two infinite rows of wells (for the distances to the image wells and the signs of their discharges, see Fig. A3.8).

Basic Analytical Relationships

Transient Flow Equations

1. Parallel constant-head boundaries (see Fig. A3.7a, b):

$$s = \frac{Q}{4\pi T} \left\{ W\left(\frac{r^2}{4at}\right) + \sum_{j=1}^n (-1)^j \sum_{i=1}^2 W\left[\frac{(\rho_i^j)^2}{4at}\right] \pm W\left(\frac{\rho_U^2}{4at}\right) \pm \sum_{j=1}^n (-1)^j \sum_{i=1}^2 W\left[\frac{(\rho_{Ui}^j)^2}{4at}\right] \right\}, \quad (1.42)$$

where ρ_i^j , ρ_{Ui}^j are distances from the observation well to the j th image well of the first (ρ_i^j) and second row (ρ_{Ui}^j), reflected about the left ($i = 1$) or right ($i = 2$) boundary (see Fig. A3.8): they are determined by Eqs. A3.3, A3.4, A3.13 and A3.14, m ; ρ_U is

the distance from the pumping to the image well reflected about the perpendicular boundary: it is determined by Eq. A3.15, m ; n is the number of reflections from the same boundary (see comment to Eq. 1.17); the sign “±”: “+” is assigned to impermeable-boundary conditions on the perpendicular boundary, and “-” to the constant-head boundary.

2. Parallel impermeable boundaries (see Fig. A3.7c, d):

$$s = \frac{Q}{4\pi T} \left[\mathbf{W}\left(\frac{r^2}{4at}\right) + \sum_{j=1}^n \sum_{i=1}^2 \mathbf{W}\left[\frac{(\rho_i^j)^2}{4at}\right] \pm \mathbf{W}\left(\frac{\rho_U^2}{4at}\right) \pm \sum_{j=1}^n \sum_{i=1}^2 \mathbf{W}\left[\frac{(\rho_{Ui}^j)^2}{4at}\right] \right]. \quad (1.43)$$

3. Parallel constant-head and impermeable boundaries (see Fig. A3.7e, f):

$$\begin{aligned} s = \frac{Q}{4\pi T} & \left[\mathbf{W}\left(\frac{r^2}{4at}\right) + \sum_{j=1,3,\dots}^n \sum_{i=1}^2 (-1)^{(j+2i-1)/2} \mathbf{W}\left(\frac{(\rho_i^j)^2}{4at}\right) + \right. \\ & + \sum_{j=2,4,\dots}^n (-1)^{j/2} \sum_{i=1}^2 \mathbf{W}\left(\frac{(\rho_i^j)^2}{4at}\right) \pm \mathbf{W}\left(\frac{\rho_U^2}{4at}\right) \pm \\ & \left. \pm \sum_{j=1,3,\dots}^n \sum_{i=1}^2 (-1)^{(j+2i-1)/2} \mathbf{W}\left(\frac{(\rho_{Ui}^j)^2}{4at}\right) \pm \sum_{j=2,4,\dots}^n (-1)^{j/2} \sum_{i=1}^2 \mathbf{W}\left(\frac{(\rho_{Ui}^j)^2}{4at}\right) \right]. \quad (1.44) \end{aligned}$$

Steady-State Flow Equations

1. Parallel constant-head boundaries (see Fig. A3.7a, b):

(a) the solution based on the superposition principle is:

$$s_m = \frac{Q}{2\pi T} \ln r' = \frac{0.366Q}{T} \lg r', \quad (1.45)$$

where, for the perpendicular constant-head boundary:

$$r' = \frac{\rho_U}{r} \prod_{j=1,3,\dots}^{n-1} \frac{\rho_1^j \rho_2^j \rho_{U1}^{j+1} \rho_{U2}^{j+1}}{\rho_1^{j+1} \rho_2^{j+1} \rho_{U1}^j \rho_{U2}^j}, \quad (1.46)$$

and for the impermeable boundary:

$$r' = \frac{\rho_1^n \rho_{U1}^n}{r \rho_U} \prod_{j=1,3,\dots}^{n-1} \frac{\rho_1^j \rho_2^j \rho_{U1}^j \rho_{U2}^j}{\rho_1^{j+1} \rho_2^{j+1} \rho_{U1}^{j+1} \rho_{U2}^{j+1}}; \quad (1.47)$$

(b) Green's function solution for the constant-head perpendicular boundary (Muskat 1937):

$$s_m = \frac{Q}{4\pi T} \ln \left[\frac{\cosh \frac{\pi(L_{Up} - L_{Uw})}{L} - \cos \frac{\pi(L_p + L_w)}{L}}{\cosh \frac{\pi(L_{Up} - L_{Uw})}{L} - \cos \frac{\pi(L_p - L_w)}{L}} \times \frac{\cosh \frac{\pi(L_{Up} + L_{Uw})}{L} - \cos \frac{\pi(L_p - L_w)}{L}}{\cosh \frac{\pi(L_{Up} + L_{Uw})}{L} - \cos \frac{\pi(L_p + L_w)}{L}} \right], \quad (1.48)$$

where L is the distance between the parallel boundaries, m; L_p , L_w are the distances from the observation and pumping wells to the parallel boundary, respectively, m; L_{Up} , L_{Uw} are the distances from the observation and pumping wells to the perpendicular boundary, respectively, m.

2. Parallel impermeable boundaries (see Fig. A3.7c, d):

(a) for the perpendicular constant-head boundary:

$$s_m = \frac{Q}{2\pi T} \ln r' = \frac{0.366Q}{T} \lg r', \quad (1.49)$$

$$r' = \frac{\rho_U}{r} \prod_{j=1}^n \frac{\rho_{U1}^j \rho_{U2}^j}{\rho_1^j \rho_2^j}, \quad (1.50)$$

(b) for the condition when all three boundaries are impermeable, there is no steady state.

3. Parallel constant-head and impermeable boundaries (see Fig. A3.7e, f):

$$s_m = \frac{Q}{2\pi T} \ln r' = \frac{0.366Q}{T} \lg r', \quad (1.51)$$

where, for a perpendicular constant-head boundary:

$$r' = \frac{\rho_1^n \rho_U}{r \rho_{U1}^n} \prod_{j=1,5,9,\dots}^{n-3} \frac{\rho_1^j \rho_1^{j+1} \rho_2^{j+1} \rho_2^{j+2} \rho_{U1}^{j+2} \rho_{U1}^{j+3} \rho_{U2}^j \rho_{U2}^{j+3}}{\rho_1^{j+2} \rho_1^{j+3} \rho_2^j \rho_2^{j+3} \rho_{U1}^j \rho_{U1}^{j+1} \rho_{U2}^{j+1} \rho_{U2}^{j+2}}, \quad (1.52)$$

and for an impermeable boundary:

$$r' = \frac{\rho_1^n \rho_{U1}^n}{r \rho_U} \prod_{j=1,5,9,\dots}^{n-3} \frac{\rho_1^j \rho_1^{j+1} \rho_2^{j+1} \rho_2^{j+2} \rho_{U1}^j \rho_{U1}^{j+1} \rho_{U2}^{j+1} \rho_{U2}^{j+2}}{\rho_1^{j+2} \rho_1^{j+3} \rho_2^j \rho_2^{j+3} \rho_{U1}^{j+2} \rho_{U1}^{j+3} \rho_{U2}^j \rho_{U2}^{j+3}}. \quad (1.53)$$

Graphic-Analytical Processing

The relationships given in Table 1.10 have been derived from Eqs. 1.42–1.45, 1.49, and 1.51.

Table 1.10 Graphic-analytical parameter evaluation

Plot	Method	Relationship
$s - \lg t$	Horizontal straight line ^a	$T = \frac{Q}{2\pi \cdot A} \ln r'$
$\lg s - \lg t$	Type curve: $\lg W'(u) - \lg \frac{1}{u}$	$T = \frac{Q}{4\pi 10^D}, a = \frac{r^2 10^E}{4}$
$\lg s - \lg \frac{t}{r^2}$	The same	$T = \frac{Q}{4\pi 10^D}, a = \frac{10^E}{4}$
$(s_1 - s_2) - \lg t$	Horizontal straight line ^a	$T = \frac{Q}{2\pi \cdot A} \ln \frac{r'_1}{r'_2}$

^aBased on drawdown values for steady-state flow period

For parallel constant-head boundaries:

$$W'(u) = W(u) + \sum_{j=1}^n (-1)^j \sum_{i=1}^2 W(ur_i^j) \pm W(ur'_U) \pm \sum_{j=1}^n (-1)^j \sum_{i=1}^2 W(ur_{Ui}^j),$$

for impermeable boundaries: $W'(u) = W(u) + \sum_{j=1}^n \sum_{i=1}^2 W(ur_i^j) \pm W(ur'_U) \pm \sum_{j=1}^n \sum_{i=1}^2 W(ur_{Ui}^j)$

for constant-head and impermeable boundaries:

$$W'(u) = \left\{ \begin{aligned} &W(u) + \sum_{j=1,3,\dots}^n \sum_{i=1}^2 (-1)^{(j+2i-1)/2} W(ur_i^j) + \sum_{j=2,4,\dots}^n (-1)^{j/2} \sum_{i=1}^2 W(ur_i^j) \pm \\ &\pm W(ur'_U) \pm \sum_{j=1,3,\dots}^n \sum_{i=1}^2 (-1)^{(j+2i-1)/2} W(ur_{Ui}^j) \pm \sum_{j=2,4,\dots}^n (-1)^{j/2} \sum_{i=1}^2 W(ur_{Ui}^j) \end{aligned} \right\},$$

$r_i^j = (\rho_i^j/r)^2$, $r'_U = (\rho_U/r)^2$, $r_{Ui}^j = (\rho_{Ui}^j/r)^2$, r' is determined with the use of Eqs. 1.46, 1.47, 1.50, 1.52, and 1.53, depending on the type of boundary condition

Plus-minus sign (\pm)—the sign “+” is assigned to impermeable-boundary conditions on the perpendicular boundary and “-” to the constant-head boundary

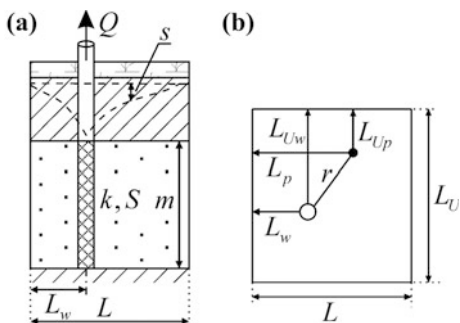
1.1.6 Rectangular Aquifer

The basic assumptions and conditions (Fig. 1.8) are:

- the aquifer is isotropic and bounded in the horizontal plane;
- the boundaries: the domain under consideration is rectangular, bounded by straight-line segments crossing at right angles.

Six variants of boundary conditions are considered (see Fig. A3.9): (1) two parallel constant-head boundaries and two parallel impermeable boundaries; (2) all boundaries are constant-head; (3) all boundaries are impermeable; (4) three constant-head boundaries and one impermeable boundary; (5) two perpendicular

Fig. 1.8 Rectangular confined aquifer: **a** cross-section and **b** planar view. L, L_U are distances between parallel boundaries



constant-head boundaries and two impermeable boundaries; and (6) three impermeable boundaries and one constant-head boundary.

Image wells are not used in the solutions below.

Basic Analytical Relationships

Transient and Steady-State Flow Equations (Chan et al. 1976; Latinopoulos 1982)

1. Two parallel constant-head boundaries and two parallel impermeable boundaries (see Fig. A3.9a):

$$s = s_m - \frac{2Q}{LL_U T} \sum_{i=1}^{\infty} \frac{\exp(-at\alpha_i^2)}{\alpha_i^2} \sin(\alpha_i L_p) \sin(\alpha_i L_w) - \frac{4Q}{LL_U T} \sum_{i=1}^{\infty} \sum_{j=1}^{\infty} \frac{\exp[-at(\alpha_i^2 + \beta_j^2)]}{\alpha_i^2 + \beta_j^2} \sin(\alpha_i L_p) \sin(\alpha_i L_w) \cos(\beta_j L_{Up}) \cos(\beta_j L_{Uw}), \quad (1.54)$$

where s_m is drawdown in the steady-state flow period:

$$s_m = \frac{Q}{LT} \sum_{i=1}^{\infty} \frac{\sin(\alpha_i L_p) \sin(\alpha_i L_w)}{\alpha_i \sinh(\alpha_i L_U)} \times \{ \cosh[\alpha_i(L_U - |L_{Uw} - L_{Up}|)] + \cosh[\alpha_i(L_U - L_{Uw} - L_{Up})] \}. \quad (1.55)$$

2. All boundaries are constant-head (see Fig. A3.9b):

$$s = s_m - \frac{4Q}{LL_U T} \sum_{i=1}^{\infty} \sum_{j=1}^{\infty} \frac{\exp[-at(\alpha_i^2 + \beta_j^2)]}{\alpha_i^2 + \beta_j^2} \sin(\alpha_i L_p) \sin(\alpha_i L_w) \sin(\beta_j L_{Up}) \sin(\beta_j L_{Uw}), \quad (1.56)$$

where s_m is the drawdown in the steady-state flow period:

$$s_m = \frac{Q}{LT} \sum_{i=1}^{\infty} \frac{\sin(\alpha_i L_p) \sin(\alpha_i L_w)}{\alpha_i \sinh(\alpha_i L_U)} \times \{ \cosh[\alpha_i(L_U - |L_{Uw} - L_{Up}|)] - \cosh[\alpha_i(L_U - L_{Uw} - L_{Up})] \}. \quad (1.57)$$

3. All boundaries are impermeable (see Fig. A3.9c):

$$s = s_m - \frac{2Q}{LL_U T} \sum_{i=1}^{\infty} \frac{\exp(-at\alpha_i^2)}{\alpha_i^2} \cos(\alpha_i L_p) \cos(\alpha_i L_w) - \frac{2Q}{LL_U T} \sum_{j=1}^{\infty} \frac{\exp(-at\beta_j^2)}{\beta_j^2} \cos(\beta_j L_{Up}) \cos(\beta_j L_{Uw}) - \frac{4Q}{LL_U T} \sum_{i=1}^{\infty} \sum_{j=1}^{\infty} \frac{\exp[-at(\alpha_i^2 + \beta_j^2)]}{\alpha_i^2 + \beta_j^2} \cos(\alpha_i L_p) \cos(\alpha_i L_w) \times \cos(\beta_j L_{Up}) \cos(\beta_j L_{Uw}), \quad (1.58)$$

where s_m is the drawdown in the quasi-steady-state flow period:

$$s_m = \frac{Qat}{LL_U T} + \frac{QL_U}{2LT} \left(\frac{2}{3} - \frac{|L_{Uw} - L_{Up}| + L_{Uw} + L_{Up}}{L_U} + \frac{L_{Uw}^2 + L_{Up}^2}{L_U^2} \right) + \frac{Q}{LT} \sum_{i=1}^{\infty} \frac{\cos(\alpha_i L_p) \cos(\alpha_i L_w)}{\alpha_i \sinh(\alpha_i L_U)} \times \{ \cosh[\alpha_i(L_U - |L_{Uw} - L_{Up}|)] + \cosh[\alpha_i(L_U - L_{Uw} - L_{Up})] \}. \quad (1.59)$$

4. Three constant-head boundaries and one impermeable boundary (see Fig. A3.9d):

$$s = s_m - \frac{4Q}{LL_U T} \sum_{i=0}^{\infty} \sum_{j=1}^{\infty} \frac{\exp[-at(\alpha_i'^2 + \beta_j^2)]}{\alpha_i'^2 + \beta_j^2} \times \cos(\alpha_i'(L - L_p)) \cos(\alpha_i'(L - L_w)) \sin(\beta_j L_{Up}) \sin(\beta_j L_{Uw}), \quad (1.60)$$

where s_m is the drawdown in the steady-state flow period:

$$s_m = \frac{Q}{L_U T} \sum_{j=1}^{\infty} \frac{\sin(\beta_j L_{Up}) \sin(\beta_j L_{Uw})}{\beta_j \cosh(\beta_j L)} \times \{ \sinh[\beta_j(L - |L_w - L_p|)] - \sinh[\beta_j(L - L_w - L_p)] \}. \quad (1.61)$$

5. Two perpendicular constant-head boundaries and two impermeable boundaries (see Fig. A3.9e):

$$s = s_m - \frac{4Q}{LL_U T} \sum_{i=0}^{\infty} \sum_{j=0}^{\infty} \frac{\exp[-at(\alpha_i'^2 + \beta_j^2)]}{\alpha_i'^2 + \beta_j^2} \cos(\alpha_i'(L - L_p)) \cos(\alpha_i'(L - L_w)) \times \cos(\beta_j'(L_U - L_{Up})) \cos(\beta_j'(L_U - L_{Uw})), \quad (1.62)$$

where s_m is the drawdown in the steady-state flow period:

$$s_m = \frac{Q}{LT} \sum_{i=0}^{\infty} \frac{\cos(\alpha_i'(L - L_p)) \cos(\alpha_i'(L - L_w))}{\alpha_i' \cosh(\alpha_i' L_U)} \times \{ \sinh[\alpha_i'(L_U - |L_{Uw} - L_{Up}|)] - \sinh[\alpha_i'(L_U - L_{Uw} - L_{Up})] \}. \quad (1.63)$$

6. Three impermeable boundaries and one constant-head boundary (see Fig. A3.9f):

$$\begin{aligned}
 s = s_m - \frac{2Q}{LL_U T} \sum_{i=0}^{\infty} \frac{\exp[-at\alpha_i'^2]}{\alpha_i'^2} \cos(\alpha_i'(L - L_p)) \cos(\alpha_i'(L - L_w)) - \\
 - \frac{4Q}{LL_U T} \sum_{i=0}^{\infty} \sum_{j=1}^{\infty} \frac{\exp[-at(\alpha_i'^2 + \beta_j'^2)]}{\alpha_i'^2 + \beta_j'^2} \times \\
 \times \cos(\alpha_i'(L - L_p)) \cos(\alpha_i'(L - L_w)) \cos(\beta_j' L_{Up}) \cos(\beta_j' L_{Uw}), \quad (1.64)
 \end{aligned}$$

where s_m is the drawdown in the steady-state flow period:

$$\begin{aligned}
 s_m = \frac{Q}{LT} \sum_{i=0}^{\infty} \frac{\cos(\alpha_i'(L - L_p)) \cos(\alpha_i'(L - L_w))}{\alpha_i' \sinh(\alpha_i' L_U)} \times \\
 \times \{ \cosh[\alpha_i'(L_U - |L_{Uw} - L_{Up}|)] + \cosh[\alpha_i'(L_U - L_{Uw} - L_{Up})] \}. \quad (1.65)
 \end{aligned}$$

In all solutions (Eqs. 1.54–1.65):

$\alpha_i = i\pi/L$, $\beta_j = j\pi/L_U$, $\alpha_i' = (i + 0.5)\pi/L$, $\beta_j' = (j + 0.5)\pi/L_U$, L , L_U are the distances between parallel boundaries, m ; L_w , L_p and L_{Uw} , L_{Up} are the distances from the pumping and observation wells to the boundaries of the rectangular aquifer (see Fig. 1.8), m . In the case of combined boundary conditions, incorporating constant-head and impermeable parallel boundaries (see Fig. A3.9d–f), the distances from wells to the boundary are taken to be those to the constant-head boundary.

The relationships for the drawdown in a rectangular aquifer can also be constructed with the use of Eq. (1.1) by summing the values of the drawdown due to image wells (Ferris et al. 1962).

1.1.7 Circular Aquifer

The basic assumptions and conditions (Fig. 1.9) are:

- the aquifer is isotropic and bounded in the horizontal plane;
- the aquifer has a circular boundary of groundwater flow along its outer contour;
- the pumping well is located either in the center of the circular aquifer (concentric) or off-center.

One of two boundary conditions is specified on the outer contour of the aquifer (see Fig. A3.10): (1) constant-head boundary or (2) impermeable boundary.

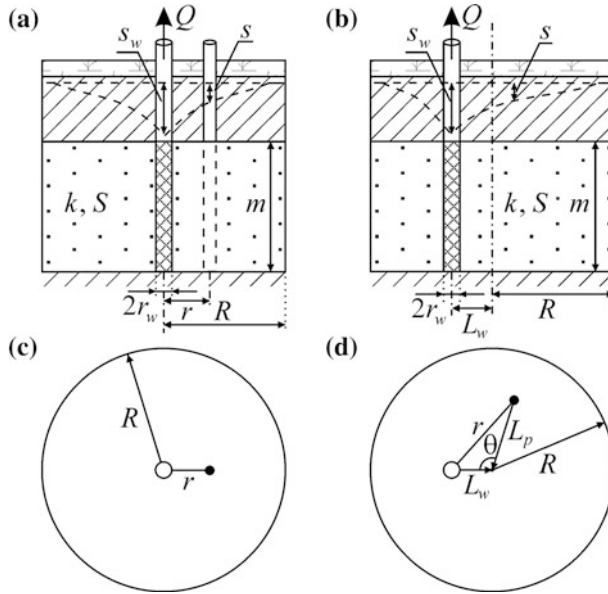


Fig. 1.9 Circular confined aquifer. **a, b** Cross-sections, **c, d** planar views; **a, c** the pumping well is in the center or **b, d** shifted with respect to the center. R is the radius of the circle

Basic Analytical Relationships

Transient Flow Equations

1. The pumping well is located in the center of a circular aquifer (Fig. 1.9a, c)

1.1. The outer contour of the aquifer is a constant-head boundary (Bochever and Verigin 1961):

$$s = \frac{Q}{2\pi T} \left[\ln \frac{R}{r} - 2 \sum_{n=1}^{\infty} \frac{1}{x_n^2 J_1^2(x_n)} J_0 \left(x_n \frac{r}{R} \right) \exp \left(-x_n^2 \frac{at}{R^2} \right) \right], \quad (1.66)$$

where x_n are positive roots of equation $J_0(x_n) = 0$ (see Appendix 7.15); R is the radius of a circular aquifer, m .

1.2. Impermeable contour of the aquifer (Bochever and Verigin 1961)

$$s = \frac{Q}{2\pi T} \left[2 \frac{at}{R^2} + \frac{r^2}{2R^2} + \ln \frac{R}{r} - \frac{2}{3} - 2 \sum_{n=1}^{\infty} \frac{1}{x_{n,1}^2 J_0^2(x_{n,1})} J_0 \left(x_{n,1} \frac{r}{R} \right) \exp \left(-x_{n,1}^2 \frac{at}{R^2} \right) \right] \quad (1.67)$$

where $x_{n,1}$ are positive roots of equation $J_1(x_{n,1}) = 0$ (see Appendix 7.15).

2. The pumping well is located off-center in a circular aquifer (Fig. 1.9b, d)

2.1. The outer contour of the aquifer is a constant-head boundary (Hantush and Jacob 1960):

$$s = \frac{Q}{2\pi T} \left\{ \ln \frac{R}{r} - 2 \sum_{n=1}^{\infty} \frac{\exp(-x_n^2 at/R^2)}{x_n^2 J_1^2(x_n)} J_0\left(x_n \frac{L_w}{R}\right) J_0\left(x_n \frac{L_p}{R}\right) - 4 \sum_{m=1}^{\infty} \sum_{n=1}^{\infty} \frac{\exp(-x_{n,m}^2 at/R^2)}{x_{n,m}^2 J_{m+1}^2(x_{n,m})} \cos(m\theta) J_m\left(x_{n,m} \frac{L_w}{R}\right) J_m\left(x_{n,m} \frac{L_p}{R}\right) \right\}, \quad (1.68)$$

$$\cos \theta = \frac{L_w^2 + L_p^2 - r^2}{2L_w L_p}, \quad (1.69)$$

where L_w and L_p are the distances from the pumping well and the observation well to the center of the circular aquifer, m ; $x_{n,m}$ are positive roots of equation $J_m(x_{n,m}) = 0$ (see Appendix 7.15); $J_m(\cdot)$ is Bessel functions of the first kind of the order m (see Appendix 7.13); θ is the angle between the vectors from the center of the circular aquifer to the pumping and observation well, respectively (Fig. 1.9d), degree: this angle is found from (Eq. 1.69).

The solution (Eq. 1.68) was derived from solution (Eq. 3.29) for a leaky aquifer at $B \rightarrow \infty$.

2.2. Impermeable contour of the aquifer (Bochever 1968):

$$s = \frac{Q}{2\pi T} \left[2 \frac{at}{R^2} + \ln \frac{R}{r^*} - 2 \sum_{n=1}^{\infty} J_0\left(y_{n,0} \frac{L_p}{R}\right) J_0\left(y_{n,0} \frac{L_w}{R}\right) \frac{\exp(-y_{n,0}^2 at/R^2)}{y_{n,0}^2 J_0^2(y_{n,0})} - 4 \sum_{m=1}^{\infty} \sum_{n=1}^{\infty} J_m\left(y_{n,m} \frac{L_p}{R}\right) J_m\left(y_{n,m} \frac{L_w}{R}\right) \frac{\exp(-y_{n,m}^2 at/R^2)}{(y_{n,m}^2 - m^2) J_m^2(y_{n,m})} \cos(m\theta) \right], \quad (1.70)$$

$$r^* = r \sqrt{1 - \frac{L_p^2 R^2 - L_w^2}{R^2} - \frac{L_w^2}{R^2} + \frac{r^2}{R^2} \exp\left(\frac{3}{4} - \frac{L_p^2 - L_w^2}{2R^2}\right)}, \quad (1.71)$$

where $y_{n,m}$ are positive roots of equation $J'_m(y_{n,m}) = 0$ (see Appendix 7.15).

Steady-State Flow Equations

The steady-state flow period occurs in the presence of a constant-head boundary on the outer contour of the circular aquifer.

1. The pumping well is located in the center of the circular aquifer (Fig. 1.9a, c).
 - 1.1. The drawdown in the observation well (Jacob 1949; Hantush and Jacob 1960)

$$s_m = \frac{Q}{2\pi T} \ln \frac{R}{r}. \quad (1.72)$$

1.2. The drawdown in the pumping well (Muskat 1937; Jacob 1949)

$$s_{mw} = \frac{Q}{2\pi T} \ln \frac{R}{r_w}. \quad (1.73)$$

2. The pumping well is located off-center in a circular aquifer (Fig. 1.9b, d).

2.1. The drawdown in the observation well (Hantush and Jacob 1960)

$$\begin{aligned} s_m &= \frac{Q}{4\pi T} \ln \left[\left(\frac{L_w}{rR} \right)^2 \left(\frac{R^4}{L_w^2} + L_p^2 - 2 \frac{L_p R^2}{L_w} \cos \theta \right) \right] = \\ &= \frac{Q}{4\pi T} \ln \left(\frac{R^2}{r^2} + \frac{L_w^2 L_p^2}{r^2 R^2} - \frac{L_w^2 + L_p^2 - r^2}{r^2} \right), \end{aligned} \quad (1.74)$$

where the angle θ (Fig. 1.9d) can be readily found from the cosine theorem given the distances r , L_w , L_p (Eq. 1.69). The solution (Eq. 1.74) has been derived from the equation (Hantush and Jacob 1960)

$$s_m = \frac{Q}{2\pi T} \left[\ln \frac{R}{r} - \sum_{n=1}^{\infty} \frac{1}{n} (L_w L_p / R^2)^n \cos n\theta \right], \quad (1.75)$$

which has a more complex form, but can also be applied to this case. An alternative solution with the distance to the image well taken into account is given in (Shchelkachev and Lapuk 1949):

$$s_m = \frac{Q}{2\pi km} \ln \frac{L_w \rho}{Rr}, \quad (1.76)$$

$$\rho = \sqrt{(\rho_w + L_w)^2 + L_p^2} - (\rho_w + L_w) \frac{L_w^2 + L_p^2 - r^2}{L_w}, \quad \rho_w = \frac{R^2 - L_w^2}{L_w}. \quad (1.77)$$

2.2. The drawdown in the pumping well (Hantush and Jacob 1960)

$$s_{mw} = \frac{Q}{2\pi T} \ln \frac{R^2 - L_w^2}{r_w R}. \quad (1.78)$$

1.2 Partially Penetrating Well: Point Source

The pumping and observation wells are partially penetrating. The screen length of the pumping well is much less than the thickness of the aquifer.

This section gives transient, quasi-steady-state, and steady-state analytical solutions for isotropic aquifers that are infinite, semi-infinite, and bounded in the

horizontal plane or thickness. To take into account the vertical anisotropy, the flow equations are to be transformed:

- the hydraulic conductivity k is to be changed to the horizontal hydraulic conductivity k_r ;
- the hydraulic diffusivity a is to be changed to the vertical hydraulic diffusivity a_z , where $a_z = k_z/S_s$ (S_s is specific storage, 1/m);
- the distance from the pumping well r is to be replaced by a corrected distance χr (where $\chi = \sqrt{k_z/k_r}$ is the coefficient of vertical anisotropy, dimensionless; k_r , k_z are hydraulic conductivities in the horizontal and vertical directions, respectively, m/d; the same change is to be made for all horizontal distances characterizing the position of wells relative to boundaries in aquifers semi-infinite or bounded in horizontal plane).

For example, the solution (Eq. 1.81) for an aquifer with vertical anisotropy will be written as

$$s = \frac{Q}{4\pi k_r d_a} \operatorname{erfc} \frac{d_a}{2\sqrt{a_z t}}, \quad (1.79)$$

where $d_a = \sqrt{(\chi r)^2 + z^2}$; r is the horizontal distance between the pumping and observation wells, m; z is the vertical distance between the screen centers of the pumping and observation wells (Fig. 1.10), m. When the vertical displacement is zero ($z = 0$), Eq. 1.79 becomes simpler

$$s = \frac{Q}{4\pi\sqrt{k_r k_z} r} \operatorname{erfc} \frac{\chi r}{2\sqrt{a_z t}}. \quad (1.80)$$

The transient solutions given in this section can be used to evaluate the hydraulic conductivity (k) and hydraulic diffusivity (a) of an isotropic aquifer or the horizontal hydraulic conductivity (k_r), vertical hydraulic conductivity (k_z), and vertical hydraulic diffusivity (a_z) of an anisotropic aquifer. Tables 1.11, 1.12, 1.13, and 1.14 give relationships for evaluating the hydraulic characteristics of an isotropic aquifer by graphic-analytical methods.

The drawdown can be evaluated at any point of the aquifer.

1.2.1 Aquifer Infinite in the Horizontal Plane and Thickness

The basic assumptions and conditions (Fig. 1.10) are:

- the aquifer is anisotropic in the vertical plane;
- there are no boundaries in the vertical (aquifer with an infinite thickness) and horizontal (aquifer of infinite lateral extent) planes.

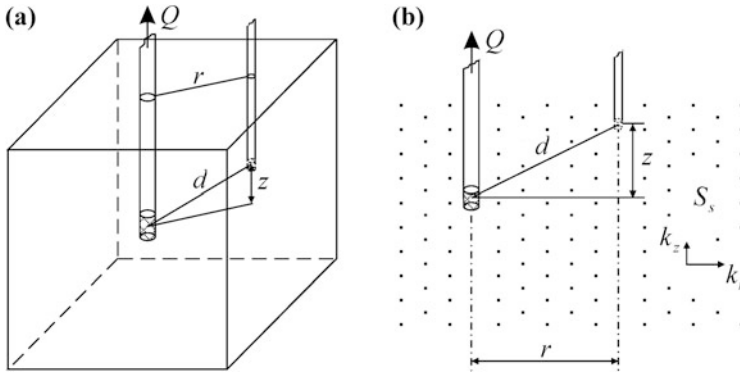


Fig. 1.10 A point source in a confined aquifer infinite in the horizontal plane and thickness. **a** Three-dimensional representation; **b** cross-section

Typical plots of drawdown in an observation well in a horizontally isotropic and vertically anisotropic aquifer are given in Fig. 12.15.

Basic Analytical Relationships

Transient Flow Equation (Carslow and Jaeger 1959)

$$s = \frac{Q}{4\pi kd} \operatorname{erfc} \frac{d}{2\sqrt{at}}, \tag{1.81}$$

where $d = \sqrt{r^2 + z^2}$ is the distance between screen centers in the pumping and observation wells (Fig. 1.10), m.

Quasi-Steady-State Flow Equation

$$s = \frac{Q}{4\pi k} \left(\frac{1}{d} - \frac{1}{\sqrt{\pi at}} \right). \tag{1.82}$$

In the plot of observation $s - 1/\sqrt{t}$ (see Fig. 12.15b), the quasi-steady-state period is represented by a linear segment. The beginning of this period is evaluated via the argument of the complementary error function $\operatorname{erfc}(u)$ (see Appendix 7.12): for $u \leq 0.1$, Eq. 1.81 is approximated by a straight line (Eq. 1.82).

Steady-State Flow Equation

$$s_m = \frac{Q}{4\pi kd}. \tag{1.83}$$

Graphic-Analytical Processing

The relationships given in Table 1.11 have been derived from Eqs. 1.81–1.83.

Table 1.11 Graphic-analytical parameter evaluation

Plot	Method	Relationship
$s - \lg t$	Horizontal straight line ^a	$k = \frac{Q_b}{4\pi \cdot d \cdot A}$
$\lg s - \lg t$	Type curve: $\lg \operatorname{erfc}(u) - \lg \frac{1}{u^2}$	$k = \frac{Q}{4\pi \cdot d \cdot 10^{D^2}}, a = \frac{d^2 10^E}{4}$
$s - \frac{1}{\sqrt{t}}$	Straight line	$k = \frac{Q}{4\pi \cdot d \cdot A}, a = \frac{(A/C)^2}{\pi} d^2$
$s - \frac{1}{d}$	The same	$k = \frac{Q}{4\pi \cdot C}, a = \frac{(C/A)^2}{\pi \cdot t}$
$ds - \frac{d}{\sqrt{t}}$	The same	$k = \frac{Q}{4\pi \cdot A}, a = \frac{(A/C)^2}{\pi}$
$\lg(ds) - \lg \frac{t}{d^2}$	Type curve: $\lg \operatorname{erfc}(u) - \lg \frac{1}{u^2}$	$k = \frac{Q}{4\pi \cdot 10^{D^2}}, a = \frac{10^E}{4}$
$(s_1 - s_2) - \lg t$	Horizontal straight line	$k = \frac{Q}{4\pi \cdot A} \left(\frac{1}{d_1} - \frac{1}{d_2} \right)_b$

^aBased on drawdown values for a steady-state flow period

^bIn the case of a vertically anisotropic aquifer, at $z = 0$, the hydraulic conductivity is replaced by an integral parameter $\sqrt{k_r k_z}$ (see Eq. 1.80)

1.2.2 A Point Source in an Aquifer Semi-infinite in the Horizontal Plane or Thickness

The basic assumptions and conditions are:

- the aquifer is vertically anisotropic and semi-infinite in the vertical or horizontal plane;
- the boundary is an infinite straight line in either the vertical or horizontal plane.

Two variants of boundary conditions are considered (Fig. 1.11): (1) a constant-head boundary in the horizontal plane and (2) an impermeable boundary in the vertical or horizontal plane.

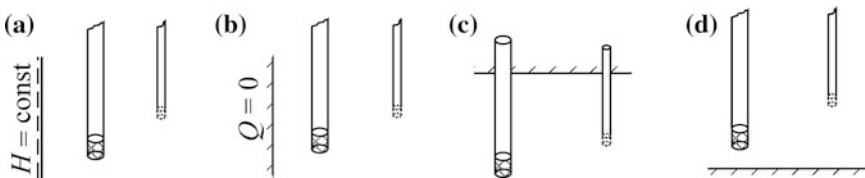
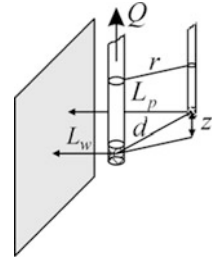


Fig. 1.11 Schematic cross-sections of a semi-infinite aquifer. **a** Constant-head boundary in the horizontal plane; **b** impermeable boundary in the horizontal plane; **c** top of the aquifer as a boundary in the vertical plane; **d** bottom of the aquifer as a boundary in the vertical plane

Fig. 1.12 A point source in a confined aquifer of infinite thickness with a constant-head boundary in the horizontal plane: a three-dimensional view



1.2.2.1 Aquifer Semi-infinite in the Horizontal Plane: Constant-Head Boundary

The basic assumptions and conditions (Figs. 1.11a and 1.12) are:

- the general conditions for a semi-infinite aquifer (see the beginning of Sect. 1.2.2);
- a constant-head boundary lies in the horizontal plane left or right of the pumping and observation wells;
- the aquifer is infinite in thickness.

To solve the problem, the image-well method is used: a single image well with a discharge equal to that of the pumping well with an opposite sign (see Fig. A3.11a).

Basic Analytical Relationships

Transient Flow Equation

$$s = \frac{Q}{4\pi k} \left(\frac{1}{d} \operatorname{erfc} \frac{d}{2\sqrt{at}} - \frac{1}{\rho} \operatorname{erfc} \frac{\rho}{2\sqrt{at}} \right), \quad (1.84)$$

where ρ is the distance between the observation and image wells (see Fig. A3.11a and Eq. A3.16), m.

Steady-State Flow Equation

$$s_m = \frac{Q}{4\pi k} \frac{(\rho - d)}{d\rho}. \quad (1.85)$$

Graphic-Analytical Processing

The relationships given in Table 1.12 have been derived from Eqs. 1.84 and 1.85.

Table 1.12 Graphic-analytical parameter evaluation

Plot	Method	Relationship
$s - \lg t$	Horizontal straight line ^a	$k = \frac{Q}{4\pi \cdot A} r'$
$\lg s - \lg t$	Type curve: $\lg \operatorname{erfc}'(u) - \lg \frac{1}{u^2}$	$k = \frac{Q}{4\pi d 10^D}, a = \frac{d^2 10^E}{4}$
$\lg(ds) - \lg \frac{t}{d^2}$	The same	$k = \frac{Q}{4\pi \cdot 10^D}, a = \frac{10^E}{4}$
$(s_1 - s_2) - \lg t$	Horizontal straight line	$k = \frac{Q}{4\pi \cdot A} (r'_1 - r'_2)$

^aBased on the drawdown values for steady-state flow period

$$\operatorname{erfc}'(u) = \operatorname{erfc}(u) - \frac{1}{r'} \operatorname{erfc}(ur''), \quad r'' = \rho/d, \quad r' = \frac{\rho - d}{d\rho}$$

1.2.2.2 Aquifer Semi-infinite in the Horizontal Plane or Thickness: Impermeable Boundary

The basic assumptions and conditions (Figs. 1.11b–d and 1.13) are:

- the general conditions for a semi-infinite aquifer (see the beginning of Sect. 1.2.2);
- an impermeable boundary may lie in the cross-section (the top or the bottom of the aquifer) or in the horizontal plane (to the left or right of the wells);
- the aquifer is semi-infinite in thickness for a boundary in the vertical plane and unlimited in thickness for a boundary in the horizontal plane.

To solve the problem, the image-well method is used: an image well with a discharge equal to that of the pumping well (see Fig. A3.11).

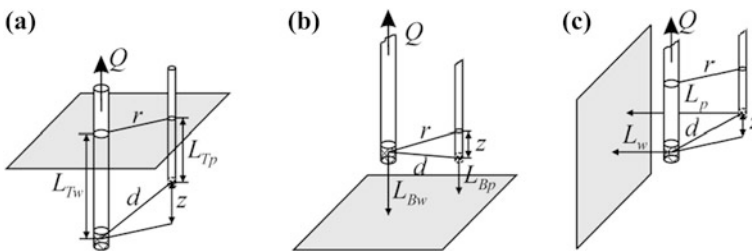


Fig. 1.13 A point source in a confined aquifer with an impermeable boundary in the vertical or horizontal plane: three-dimensional views. **a** The boundary is the top of the aquifer; **b** the boundary is the bottom of the aquifer; **c** the boundary is in the horizontal plane

Basic Analytical Relationships

Transient Flow Equation

$$s = \frac{Q}{4\pi k} \left(\frac{1}{d} \operatorname{erfc} \frac{d}{2\sqrt{at}} + \frac{1}{\rho} \operatorname{erfc} \frac{\rho}{2\sqrt{at}} \right), \tag{1.86}$$

where ρ is the distance between the observation well and an image well reflected about the boundary in the vertical (see Eq. A3.17) or the horizontal (see Eq. A3.16) plane (see Fig. A3.11), m.

Quasi-Steady-State Flow Equation

$$s = \frac{Q}{4\pi k} \left(\frac{d + \rho}{d\rho} - \frac{2}{\sqrt{\pi at}} \right). \tag{1.87}$$

Steady-State Flow Equation

$$s_m = \frac{Q}{4\pi k} \frac{d + \rho}{d\rho}. \tag{1.88}$$

Graphic-Analytical Processing

The relationships given in Table 1.13 have been derived from Eqs. 1.86–1.88.

1.2.3 A Point Source in an Aquifer Bounded in the Horizontal Plane or Thickness

The basic assumptions and conditions (Fig. 1.14) are:

- the aquifer is vertically anisotropic, bounded in thickness or in the horizontal plane;
- the boundaries are two parallel linear, infinite, in the vertical or horizontal plane.

Table 1.13 Graphic-analytical parameter evaluation

Plot	Method	Relationship
$s - \lg t$	Horizontal straight line ^a	$k = \frac{Q}{4\pi \cdot A} r'$
$s - \frac{1}{\sqrt{t}}$	Straight line	$k = \frac{Q}{4\pi \cdot A} r', a = \frac{4}{\pi} \left(\frac{A}{Cr'} \right)$
$\lg s - \lg t$	Type curve: $\lg \operatorname{erfc}'(u) - \lg \frac{1}{u^2}$	$k = \frac{Q}{4\pi \cdot d \cdot 10^D}, a = \frac{d^2 10^E}{4}$
$\lg(ds) - \lg \frac{t}{d^2}$	The same	$k = \frac{Q}{4\pi \cdot 10^D}, a = \frac{10^E}{4}$
$(s_1 - s_2) - \lg t$	Horizontal straight line	$k = \frac{Q}{4\pi \cdot A} (r'_1 - r'_2)$

^abased on the drawdown values for a steady-state flow period

$$\operatorname{erfc}'(u) = \operatorname{erfc}(u) + \frac{1}{r'} \operatorname{erfc}(ur''), r'' = \rho/d, r' = \frac{\rho + d}{d\rho}$$

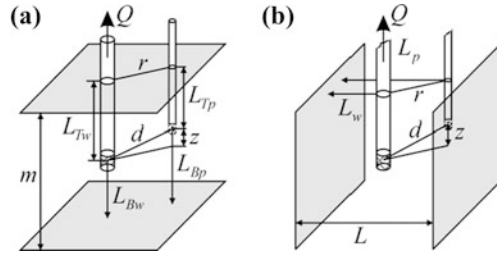


Fig. 1.14 A three-dimensional view of a point source in a confined **a** aquifer bounded in thickness and **b** a strip aquifer of infinite thickness

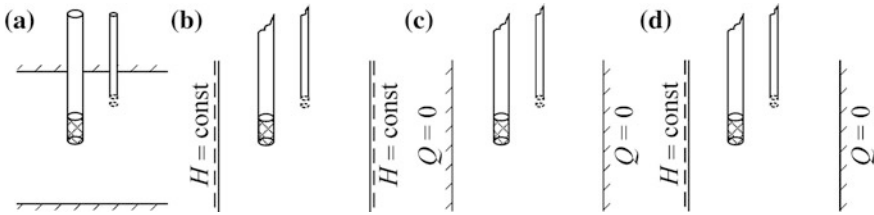


Fig. 1.15 Schematic cross-section of a bounded aquifer. **a** Impermeable boundaries in the vertical plane; **b** constant-head boundaries in the horizontal plane; **c** impermeable boundaries in the horizontal plane; and **d** mixed boundary conditions in the horizontal plane

Four variants of boundary conditions are considered (Fig. 1.15): (1) two impermeable boundaries in the vertical plane; (2) two constant-head boundaries in the horizontal plane; (3) two impermeable boundaries in the horizontal plane; and (4) two boundaries in the horizontal plane with mixed boundary conditions: constant-head and impermeable boundaries.

To solve the problem, the image-well method is used: image wells form an infinite row (for the signs of discharges and the distances to the image wells, see Fig. A3.12b, c).

Basic Analytical Relationships

Transient Flow Equations

1. Two constant-head boundaries (Fig. 1.15b):

$$s = \frac{Q}{4\pi k} \left[\frac{1}{d} \operatorname{erfc} \frac{d}{2\sqrt{at}} + \sum_{j=1}^n (-1)^j \sum_{i=1}^2 \frac{1}{\rho_i^j} \operatorname{erfc} \frac{\rho_i^j}{2\sqrt{at}} \right]. \tag{1.89}$$

2. Two impermeable boundaries (Fig. 1.15a, c):

$$s = \frac{Q}{4\pi k} \left[\frac{1}{d} \operatorname{erfc} \frac{d}{2\sqrt{at}} + \sum_{j=1}^n \sum_{i=1}^2 \frac{1}{\rho_i^j} \operatorname{erfc} \frac{\rho_i^j}{2\sqrt{at}} \right]. \quad (1.90)$$

3. Mixed boundary conditions—constant-head and impermeable boundaries (Fig. 1.15d):

$$s = \frac{Q}{4\pi k} \left[\frac{1}{d} \operatorname{erfc} \frac{d}{2\sqrt{at}} + \sum_{j=1,3,\dots}^n \sum_{i=1}^2 \frac{(-1)^{(j+2i-1)/2}}{\rho_i^j} \operatorname{erfc} \frac{\rho_i^j}{2\sqrt{at}} + \sum_{j=2,4,\dots}^n (-1)^{j/2} \sum_{i=1}^2 \frac{1}{\rho_i^j} \operatorname{erfc} \frac{\rho_i^j}{2\sqrt{at}} \right], \quad (1.91)$$

where ρ_i^j is the distance from the observation well to the j th image well reflected from the left/top ($i = 1$) or the right/bottom ($i = 2$) boundary (see Fig. A3.12), are determined by Eqs. A3.18 and A3.20, and Eqs. A3.19 and A3.21, m.

Steady-State Flow Equations

1. Two constant-head boundaries (Fig. 1.15b):

$$s_m = \frac{Q}{4\pi k} \left[\frac{1}{d} + \sum_{j=1}^n (-1)^j \sum_{i=1}^2 \frac{1}{\rho_i^j} \right]. \quad (1.92)$$

2. Mixed boundary conditions—constant-head and impermeable boundaries (Fig. 1.15d):

$$s_m = \frac{Q}{4\pi k} \left[\frac{1}{d} + \sum_{j=1,3,\dots}^n \sum_{i=1}^2 \frac{(-1)^{(j+2i-1)/2}}{\rho_i^j} + \sum_{j=2,4,\dots}^n (-1)^{j/2} \sum_{i=1}^2 \frac{1}{\rho_i^j} \right]. \quad (1.93)$$

Graphic-Analytical Processing

The relationships given in Table 1.14 have been derived from Eqs. 1.89–1.93.

Table 1.14 Graphic-analytical parameter evaluation

Plot	Method	Relationship
$s - \lg t$	Horizontal straight line ^a	$k = \frac{Q}{4\pi \cdot A} r'$ (2)
$\lg s - \lg t$	Type curve: $\lg \operatorname{erfc}'(u) - \lg \frac{1}{u^2}$	$k = \frac{Q}{4\pi \cdot d \cdot 10^D}$, $a = \frac{d^2 10^E}{4}$
$\lg(ds) - \lg \frac{t}{d^2}$	The same	$k = \frac{Q}{4\pi \cdot 10^D}$, $a = \frac{10^E}{4}$
$(s_1 - s_2) - \lg t$	Horizontal straight line	$k = \frac{Q}{4\pi \cdot A} (r'_1 - r'_2)$

^aBased on the drawdown values for steady-state flow period (this method will not work for aquifers with impermeable boundaries)

Two constant-head boundaries:

$$\operatorname{erfc}'(u) = \operatorname{erfc}(u) + \sum_{j=1}^n (-1)^j \sum_{i=1}^2 \frac{1}{r_i^j} \operatorname{erfc}(ur_i^j), \quad r' = \frac{1}{d} + \sum_{j=1}^n (-1)^j \sum_{i=1}^2 \frac{1}{\rho_i^j}$$

Two impermeable boundaries:

$$\operatorname{erfc}'(u) = \operatorname{erfc}(u) + \sum_{j=1}^n \sum_{i=1}^2 \frac{1}{r_i^j} \operatorname{erfc}(ur_i^j), \quad r' = \frac{1}{d} + \sum_{j=1}^n \sum_{i=1}^2 \frac{1}{\rho_i^j}$$

Mixed boundary conditions—constant-head and impermeable boundaries:

$$\operatorname{erfc}'(u) = \operatorname{erfc}(u) + \sum_{j=1,3,\dots}^n \sum_{i=1}^2 \frac{(-1)^{(j+2i-1)/2}}{r_i^j} \operatorname{erfc}(ur_i^j) + \sum_{j=2,4,\dots}^n (-1)^{j/2} \sum_{i=1}^2 \frac{1}{r_i^j} \operatorname{erfc}(ur_i^j),$$

$$r' = \frac{1}{d} + \sum_{j=1,3,\dots}^n \sum_{i=1}^2 \frac{(-1)^{(j+2i-1)/2}}{\rho_i^j} + \sum_{j=2,4,\dots}^n (-1)^{j/2} \sum_{i=1}^2 \frac{1}{\rho_i^j}, \quad r_i^j = \rho_i^j / d$$

1.3 Partially Penetrating Well: Linear Source

The pumping and observation wells are partially penetrating. The screen length of the pumping well is less than the aquifer thickness.

Here we consider drawdown values obtained during pumping tests in an observation well and a piezometer (a small-diameter tube, receiving water through its bottom hole). The drawdown in the observation well is averaged over its screen length. It is generally less than that in the piezometer.

This section gives transient, quasi-steady-state, and steady-state analytical solutions for isotropic aquifers that are infinite, semi-infinite, and bounded in the horizontal plane or thickness. To take into account the vertical anisotropy of the aquifer requires some changes in the flow equations (see the beginning of Sect. 1.2). Of greatest practical interest are solutions for a linear source in an aquifer bounded in the vertical plane (see Sect. 1.3.3.1).

Transient solutions are used to determine the hydraulic conductivity (k) and hydraulic diffusivity (a) of an isotropic aquifer or the horizontal (k_r) and vertical (k_z) hydraulic conductivities and, depending on the solution, the vertical or horizontal hydraulic diffusivity of an anisotropic aquifer. For Moench solutions (see Sect. 1.3.3), the hydraulic conductivity and the thickness of the wellbore skin (k_{skin} , m_{skin}) can also be evaluated.

1.3.1 Aquifer Infinite in the Horizontal Plane and Thickness

The basic assumptions and conditions (Fig. 1.16) are:

- the aquifer is anisotropic in the vertical plane;
- there are no boundaries in the vertical (aquifer with an infinite thickness) and horizontal (aquifer of infinite lateral extent) planes.

The drawdown is determined in an observation well or in a piezometer, both located at any point of the aquifer.

Basic Analytical Relationships

Transient Flow Equations

1. The average drawdown in an observation well (Hantush 1961b):

$$s = \frac{Qr}{8\pi kl_w l_p} \left[F_l \left(\frac{r^2}{4at}, \frac{z_{w1} + z_{p1}}{r}, \frac{z_{w1} - z_{p1}}{r} \right) - F_l \left(\frac{r^2}{4at}, \frac{z_{w2} + z_{p1}}{r}, \frac{z_{w2} - z_{p1}}{r} \right) + F_l \left(\frac{r^2}{4at}, \frac{z_{w2} + z_{p2}}{r}, \frac{z_{w2} - z_{p2}}{r} \right) - F_l \left(\frac{r^2}{4at}, \frac{z_{w1} + z_{p2}}{r}, \frac{z_{w1} - z_{p2}}{r} \right) \right], \quad (1.94)$$

$$F_l(u, \beta_1, \beta_2) = \beta_1 M(u, \beta_1) - \beta_2 M(u, \beta_2) + 2\sqrt{1 + \beta_2^2} \operatorname{erfc} \sqrt{(1 + \beta_2^2)u} - 2\sqrt{1 + \beta_1^2} \operatorname{erfc} \sqrt{(1 + \beta_1^2)u} + 2 \frac{\exp[-(1 + \beta_1^2)u] - \exp[-(1 + \beta_2^2)u]}{\sqrt{\pi u}}, \quad (1.95)$$

where l_p, l_w are the screen lengths of the observation and pumping wells, respectively, m ; $z_{p1}, z_{p2}, z_{w1}, z_{w2}$ are vertical distances, which determine the positions of the observation and pumping wells relative to the aquifer top (see Fig. 1.22b), m ; $M(u, \beta)$ is a special function (see Appendix 7.3).

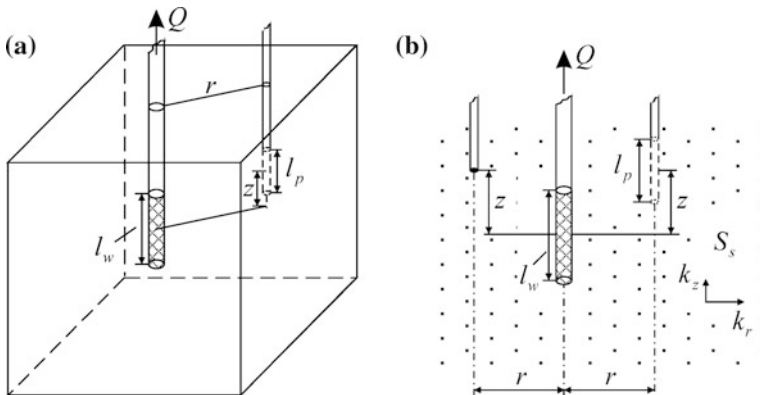


Fig. 1.16 Linear source in a confined aquifer infinite in the horizontal plane and thickness. **a** A three-dimensional view; **b** a cross-section with an observation well and a piezometer

2. The drawdown in the piezometer (Hantush 1961a, b):

$$s = \frac{Q}{8\pi kl_w} \left[\begin{aligned} & \text{M}\left(\frac{r^2}{4at}, \frac{z_{w1} + L_{Tp}}{r}\right) - \text{M}\left(\frac{r^2}{4at}, \frac{z_{w2} + L_{Tp}}{r}\right) + \\ & + \text{M}\left(\frac{r^2}{4at}, \frac{z_{w1} - L_{Tp}}{r}\right) - \text{M}\left(\frac{r^2}{4at}, \frac{z_{w2} - L_{Tp}}{r}\right) \end{aligned} \right], \quad (1.96)$$

where L_{Tp} is the vertical distance from aquifer top to the open part of the piezometer (see Fig. 1.22b), m.

3. The drawdown in the piezometer (simplified solution) (Mironenko and Shestakov 1978):

$$s = \frac{Q}{8\pi kl_w} \left[\text{M}\left(\frac{r^2}{4at}, \frac{0.5l_w + z}{r}\right) + \text{M}\left(\frac{r^2}{4at}, \frac{0.5l_w - z}{r}\right) \right], \quad (1.97)$$

where z is the vertical distance between the screen centers of the pumping and observation wells (Fig. 1.16), m

Steady-State Flow Equation (Girinskiy 1950; Babushkin 1954)

$$\begin{aligned} s_m &= \frac{Q}{4\pi kl_w} \left[\text{arcsinh} \frac{0.5l_w - z}{r} + \text{arcsinh} \frac{0.5l_w + z}{r} \right] = \\ &= \frac{Q}{4\pi kl_w} \ln \frac{\sqrt{(z + 0.5l_w)^2 + r^2} + (z + 0.5l_w)}{\sqrt{(z - 0.5l_w)^2 + r^2} + (z - 0.5l_w)}. \end{aligned} \quad (1.98)$$

Graphic-Analytical Processing

The relationships given in Table 1.15, have been derived from Eqs. 1.94, 1.96–1.98.

Table 1.15 Graphic-analytical parameter evaluation

Plot	Method	Relationship
$s - \lg t$	Horizontal straight line ^a	$k = \frac{Q}{4\pi \cdot l_w \cdot A} r'$
$\lg s - \lg t$	Type curve ^b : $\lg f - \lg \frac{1}{u}$	$k = \frac{Q}{8\pi \cdot l_w \cdot 10^D}, a = \frac{r^2 10^E}{4}$
$(s_1 - s_2) - \lg t$	Horizontal straight line	$k = \frac{Q}{4\pi \cdot A} (r'_1 - r'_2)$

^aBased on drawdown values for steady-state flow period

^bIn the construction of a type curve for the average drawdown in the observation well (Eq. 1.94), the hydraulic conductivity is $k = Qr / (8\pi l_w l_p 10^D)$

f is one of the functional expressions in square brackets in Eqs. 1.94, 1.96, or 1.97

$$r' = \ln \frac{\sqrt{(z + 0.5l_w)^2 + r^2} + (z + 0.5l_w)}{\sqrt{(z - 0.5l_w)^2 + r^2} + (z - 0.5l_w)} \text{ or } r' = \text{arcsinh} \frac{0.5l_w - z}{r} + \text{arcsinh} \frac{0.5l_w + z}{r}$$

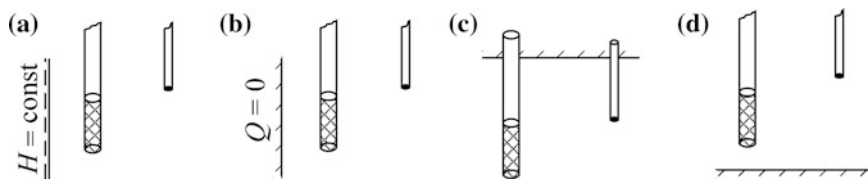


Fig. 1.17 Schematic cross-sections of a semi-infinite aquifer. **a** Constant-head boundary in the horizontal plane; **b** impermeable boundary in the horizontal plane; **c** profile boundary—aquifer top; **d** profile boundary—aquifer bottom

1.3.2 A Linear Source in an Aquifer Semi-infinite in the Horizontal Plane or Thickness

The basic assumptions and conditions are:

- the aquifer is vertically anisotropic, semi-infinite in the horizontal plane or thickness;
- the boundary is straight and infinite in the vertical or horizontal plane.

The drawdown is determined in a piezometer situated at any point in the aquifer.

Three variants of boundary conditions are considered (Fig. 1.17): (1) a planar constant-head boundary, (2) an impermeable planar boundary, and (3) an impermeable boundary in the vertical plane.

The relationships described in this section are based on the superposition principle. The flow equation is constructed using solution (Eq. 1.97) for the drawdown in a piezometer, located in an aquifer infinite in the horizontal plane and thickness.

1.3.2.1 Aquifer Semi-infinite in the Horizontal Plane: Constant-Head or Impermeable Boundary

The basic assumptions and conditions (Figs. 1.17a, b and 1.18) are:

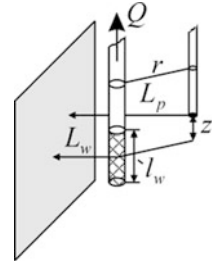
- general conditions for a linear source in a semi-infinite aquifer (see the beginning of Sect. 1.3.2);
- a constant-head boundary or an impermeable boundary is located in the horizontal plane left or right of the pumping and observation wells;
- the aquifer is infinite in thickness and semi-infinite in the horizontal plane.

To solve the problem, the image-well method is used: there is a single image well (for the imaginary discharge, see Fig. A3.2).

Basic Analytical Relationships

Transient Flow Equation

Fig. 1.18 A linear source in a confined aquifer of infinite thickness semi-infinite in the horizontal plane



$$s = \frac{Q}{8\pi kl_w} \left[\begin{matrix} M\left(\frac{r^2}{4at}, \frac{0.5l_w + z}{r}\right) + M\left(\frac{r^2}{4at}, \frac{0.5l_w - z}{r}\right) \pm \\ \pm M\left(\frac{\rho^2}{4at}, \frac{0.5l_w + z}{\rho}\right) \pm M\left(\frac{\rho^2}{4at}, \frac{0.5l_w - z}{\rho}\right) \end{matrix} \right], \quad (1.99)$$

the “+” sign corresponds to an impermeable boundary; and the “-” to constant-head boundary.

Steady-State Flow Equation

$$\begin{aligned} s_m &= \frac{Q}{4\pi kl_w} \left[\begin{matrix} \operatorname{arcsinh} \frac{0.5l_w - z}{r} + \operatorname{arcsinh} \frac{0.5l_w + z}{r} \pm \\ \pm \operatorname{arcsinh} \frac{0.5l_w - z}{\rho} \pm \operatorname{arcsinh} \frac{0.5l_w + z}{\rho} \end{matrix} \right] = \\ &= \frac{Q}{4\pi kl_w} \left[\begin{matrix} \ln \frac{\sqrt{(z + 0.5l_w)^2 + r^2} + (z + 0.5l_w)}{\sqrt{(z - 0.5l_w)^2 + r^2} + (z - 0.5l_w)} \pm \ln \frac{\sqrt{(z + 0.5l_w)^2 + \rho^2} + (z + 0.5l_w)}{\sqrt{(z - 0.5l_w)^2 + \rho^2} + (z - 0.5l_w)} \end{matrix} \right]. \end{aligned} \quad (1.100)$$

Graphic-Analytical Processing

The relationships given in Table 1.16 have been derived from Eqs. 1.99 and 1.100.

Table 1.16 Graphic-analytical parameter evaluation

Plot	Method	Relationship
$s - \lg t$	Horizontal straight line ^a	$k = \frac{Q}{4\pi \cdot l_w \cdot A} r'$
$\lg s - \lg t$	Type curve: $\lg M'(u, \beta) - \lg \frac{1}{u}$	$k = \frac{Q}{8\pi l_w 10^D}, a = \frac{r^2 10^E}{4}$
$(s_1 - s_2) - \lg t$	Horizontal straight line	$k = \frac{Q}{4\pi \cdot A} (r'_1 - r'_2)$

^aBased on drawdown values for steady-state flow period

$$\begin{aligned} M'(u, \beta) &= M\left(u, \frac{0.5l_w + z}{r}\right) + M\left(u, \frac{0.5l_w - z}{r}\right) \pm M\left(ur'', \frac{0.5l_w + z}{\rho}\right) \pm M\left(ur'', \frac{0.5l_w - z}{\rho}\right), \\ r'' &= (\rho/r)^2, r' = \ln \frac{\sqrt{(z + 0.5l_w)^2 + r^2} + (z + 0.5l_w)}{\sqrt{(z - 0.5l_w)^2 + r^2} + (z - 0.5l_w)} \pm \ln \frac{\sqrt{(z + 0.5l_w)^2 + \rho^2} + (z + 0.5l_w)}{\sqrt{(z - 0.5l_w)^2 + \rho^2} + (z - 0.5l_w)} \end{aligned}$$

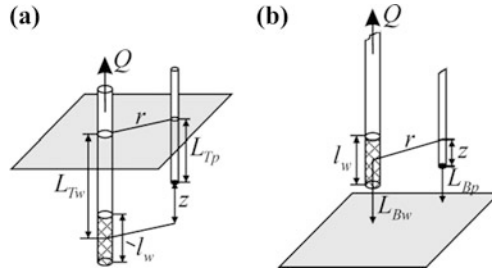


Fig. 1.19 A linear source in a confined aquifer with an impermeable profile boundary. **a** The boundary is the aquifer top; **b** the boundary is the aquifer bottom

1.3.2.2 Aquifer Semi-infinite in Thickness: Impermeable Boundary

The basic assumptions and conditions (Figs. 1.17c, d and 1.19) are:

- general conditions for a linear source in a semi-infinite aquifer (see the beginning of Sect. 1.3.2);
- impermeable boundary in the cross-section (the top or bottom of the aquifer);
- the aquifer is semi-infinite in thickness and infinite in the horizontal plane.

To solve the problem, the image-well method is used: an image well with a discharge equal to that of the pumping well.

Basic Analytical Relationships

Transient Flow Equation

$$s = \frac{Q}{8\pi kl_w} \left[\begin{aligned} &M\left(\frac{r^2}{4at}, \frac{0.5l_w + z}{r}\right) + M\left(\frac{r^2}{4at}, \frac{0.5l_w - z}{r}\right) + \\ &+ M\left(\frac{r^2}{4at}, \frac{0.5l_w + B_w + B_p}{r}\right) + M\left(\frac{r^2}{4at}, \frac{0.5l_w - B_w - B_p}{r}\right) \end{aligned} \right], \tag{1.101}$$

where $B_p = L_{Tp}$ or $B_p = L_{Bp}$ is the vertical distance from the open part of piezometer to the top (L_{Tp}) or bottom (L_{Bp}) of the aquifer, m; $B_w = L_{Tw}$ or $B_w = L_{Bw}$ is the vertical distance from the center of pumping well screen to the top (L_{Tw}) or bottom (L_{Bw}) of the aquifer, m.

Table 1.17 Graphic-analytical parameter evaluation

Plot	Method	Relationship
$s - \lg t$	Horizontal straight line ^a	$k = \frac{Q}{4\pi \cdot l_w \cdot A} r'$
$\lg s - \lg t$	Type curve: $\lg M'(u, \beta) - \lg \frac{1}{u}$	$k = \frac{Q}{8\pi l_w 10^D}$, $a = \frac{r^2 10^E}{4}$
$(s_1 - s_2) - \lg t$	Horizontal straight line	$k = \frac{Q}{4\pi \cdot A} (r'_1 - r'_2)$

^aBased on drawdown values for steady-state flow period

$$M'(u, \beta) = M\left(u, \frac{0.5l_w + z}{r}\right) + M\left(u, \frac{0.5l_w - z}{r}\right) + M\left(u, \frac{0.5l_w + B_w + B_p}{r}\right) + M\left(u, \frac{0.5l_w - B_w - B_p}{r}\right)$$

$$r' = \ln \frac{\sqrt{(z + 0.5l_w)^2 + r^2} + (z + 0.5l_w)}{\sqrt{(z - 0.5l_w)^2 + r^2} + (z - 0.5l_w)} + \ln \frac{\sqrt{(B_w + B_p + 0.5l_w)^2 + r^2} + (B_w + B_p + 0.5l_w)}{\sqrt{(B_w + B_p - 0.5l_w)^2 + r^2} + (B_w + B_p - 0.5l_w)}$$

Steady-State Flow Equation

$$s_m = \frac{Q}{4\pi k l_w} \left[\begin{aligned} &\operatorname{arcsinh} \frac{0.5l_w - z}{r} + \operatorname{arcsinh} \frac{0.5l_w + z}{r} + \\ &+ \operatorname{arcsinh} \frac{0.5l_w - B_w - B_p}{r} + \operatorname{arcsinh} \frac{0.5l_w + B_w + B_p}{r} \end{aligned} \right] =$$

$$= \frac{Q}{4\pi k l_w} \left[\begin{aligned} &\ln \frac{\sqrt{(z + 0.5l_w)^2 + r^2} + (z + 0.5l_w)}{\sqrt{(z - 0.5l_w)^2 + r^2} + (z - 0.5l_w)} + \\ &+ \ln \frac{\sqrt{(B_w + B_p + 0.5l_w)^2 + r^2} + (B_w + B_p + 0.5l_w)}{\sqrt{(B_w + B_p - 0.5l_w)^2 + r^2} + (B_w + B_p - 0.5l_w)} \end{aligned} \right]. \quad (1.102)$$

Graphic-Analytical Processing

The relationships given in Table 1.17 have been derived from Eqs. 1.101 and 1.102.

1.3.3 A Linear Source in an Aquifer Bounded in the Horizontal Plane or Thickness

The basic assumptions and conditions (Figs. 1.20 and 1.21) are:

- the aquifer is vertically anisotropic, bounded in the horizontal plane or thickness;
- the boundary consists of two parallel infinite straight lines, in either the vertical or horizontal plane.

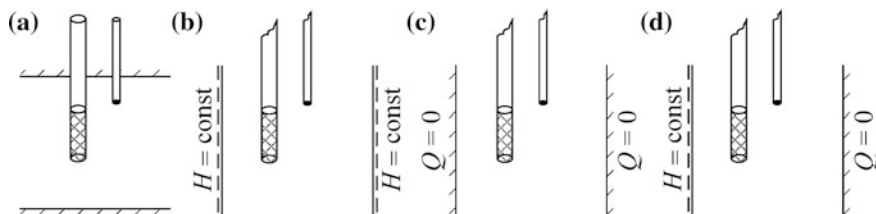


Fig. 1.20 Schematic cross-sections of a bounded aquifer. **a** Profile impermeable boundaries; **b** constant-head boundaries in the horizontal plane; **c** impermeable boundaries in the horizontal plane; **d** mixed boundary conditions in the horizontal plane

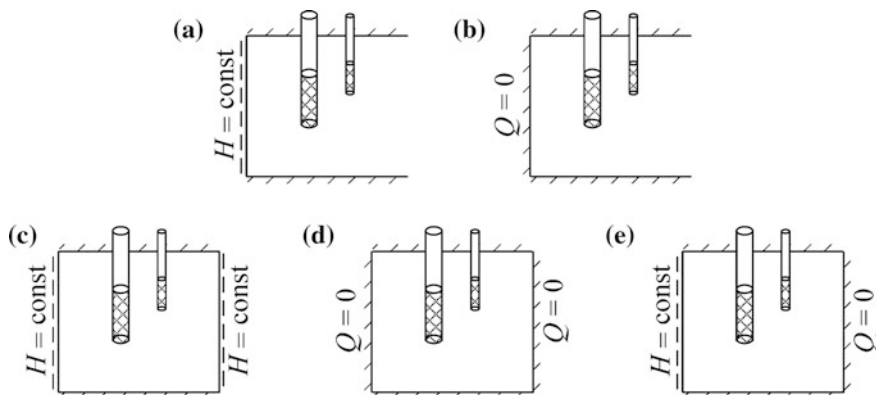


Fig. 1.21 Schematic cross-sections of an aquifer bounded in the horizontal plane and thickness: **a, b** aquifers semi-infinite in the horizontal plane; **c, d, e** aquifers bounded in the horizontal plane

Four variants of boundary conditions are considered (Fig. 1.20): (1) two impermeable boundaries in the vertical plane; (2) two planar constant-head conditions; (3) two planar impermeable boundaries; and (4) two planar boundaries with mixed boundary conditions—constant head and impermeable boundaries.

In addition, planar boundaries of groundwater flow (Fig. 1.21) are also considered for the aquifer bounded in thickness (Fig. 1.20a). This enables the partial penetration of wells to be taken into account in semi-infinite aquifers (see Sect. 1.1.2) and strip aquifers (see Sect. 1.1.3).

1.3.3.1 Aquifer Bounded in Thickness

The basic assumptions and conditions (Figs. 1.22, 1.23, and 1.24) are:

- general conditions for a bounded aquifer (see the beginning of Sect. 1.3.3);
- two impermeable boundaries in the vertical plane;

where z_i^j is the vertical distance from the center of the screen of the observation well or the open part of piezometer to the j th image well reflected about the top ($i = 1$) or bottom ($i = 2$) boundary in an aquifer bounded in thickness (see Fig. A3.12a), m ; it is determined by formulas (Eq. A3.22) and (Eq. A3.23).

2. The Hantush solution for the drawdown in a piezometer and for the average drawdown in an observation well (Hantush 1961b, 1964):

$$s = \frac{Q}{4\pi k_r m} f(r). \quad (1.104)$$

Here, for the drawdown in a piezometer, we have:

$$f(r) = W\left(\frac{r^2}{4a_r t}\right) + \frac{2m}{\pi l_w} \sum_{n=1}^{\infty} \left[\frac{1}{n} W\left(\frac{r^2}{4a_r t}, \chi \frac{n\pi r}{m}\right) \left(\sin \frac{n\pi z_{w1}}{m} - \sin \frac{n\pi z_{w2}}{m} \right) \cos \frac{n\pi L_{Tp}}{m} \right], \quad (1.105)$$

and for the average drawdown in an observation well:

$$f(r) = W\left(\frac{r^2}{4a_r t}\right) + \frac{2m^2}{\pi^2 l_w l_p} \sum_{n=1}^{\infty} \left[\frac{1}{n^2} W\left(\frac{r^2}{4a_r t}, \chi \frac{n\pi r}{m}\right) \times \left(\sin \frac{n\pi z_{w1}}{m} - \sin \frac{n\pi z_{w2}}{m} \right) \left(\sin \frac{n\pi z_{p1}}{m} - \sin \frac{n\pi z_{p2}}{m} \right) \right], \quad (1.106)$$

where z_{w1} and z_{w2} are the vertical distances from the aquifer top to the bottom and the top of the pumping well screen, respectively, m (Fig. 1.22); z_{p1} and z_{p2} are the same for the observation well; $a_r = k_r m / S$ is the horizontal hydraulic diffusivity, m^2/d .

3. The Moench solution for the drawdown in a partially penetrating observation well or piezometer (Moench 1993, 1996):

$$s = \frac{Q}{4\pi k_r m} f(t, r, m, l_w, l_p, L_{Tw}, L_{Tp}, k_r, k_z, S). \quad (1.107)$$

The functional relationship (Eq. 1.107) is treated with the use of an algorithm from WTAQ2 program (see Appendix 5.2).

4. The Moench solution for the drawdown in a partially penetrating observation well or piezometer, with the wellbore storage and skin, as well as the delayed response of observation piezometer taken into account (Moench 1997):

$$s = \frac{Q}{4\pi k_r m} f(t, r, r_w, r_c, r_p, m, l_w, l_p, L_{Tw}, L_{Tp}, k_r, k_z, S, k_{skin}, m_{skin}). \quad (1.108)$$

The functional relationship (Eq. 1.108) is treated with the use of an algorithm from WTAQ3 program (see Appendix 5.3).

5. Moench solution for drawdown in a partially penetrating pumping well takes into account the wellbore storage and skin (Moench 1997):

Table 1.18 Graphic-analytical parameter evaluation

Plot	Method	Relationship
$\lg s - \lg t$	Type curve: $\lg M'(u, \beta) - \lg \frac{1}{u}$	$k = \frac{Q}{8\pi \cdot l_w \cdot 10^D}, a = \frac{r^2 10^E}{4}$
$M'(u, \beta) = M\left(u, \frac{0.5l_w + z}{r}\right) + M\left(u, \frac{0.5l_w - z}{r}\right) + \sum_{j=1}^n \sum_{i=1}^2 \left[M\left(u, \frac{0.5l_w + z_i^j}{r}\right) + M\left(u, \frac{0.5l_w - z_i^j}{r}\right) \right]$		

$$s_w = \frac{Q}{4\pi k_r m} f(t, r_w, r_c, m, l_w, L_{Tw}, k_r, k_z, S, k_{skin}, m_{skin}). \tag{1.109}$$

The functional relationship (Eq. 1.109) is treated with the use of an algorithm from WTAQ3 program (see Appendix 5.3).

In solutions (Eqs. 1.107 and 1.108) for the drawdown in the piezometer, the length of the screen of the observation well (l_p) is excluded from the function.

Graphic-Analytical Processing

The relationships given in Table 1.18 have been derived from Eq. 1.103.

Semi-infinite Aquifer

The test scheme is given in Fig. 1.21a, b and Fig. 1.23. The general form of the Hantush and Moench solutions (see Sect. “Aquifer Infinite in the Horizontal Plane”) for the average drawdown in an observation well or the drawdown in a piezometer is

$$s = \frac{Q}{4\pi k_r m} [f(r) \pm f(\rho)], \tag{1.110}$$

where f is taken from Eq. 1.104 or 1.107, depending on the solution; the sign “+” corresponds to a constant-head boundary condition and “-” to an impermeable boundary.

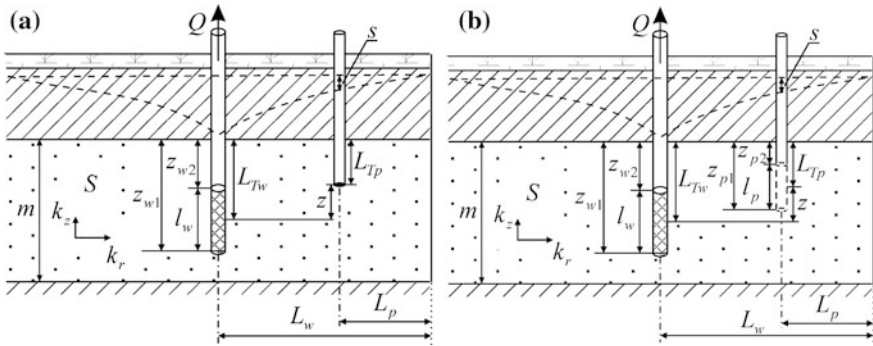


Fig. 1.23 A linear source in a confined semi-infinite in the horizontal plane aquifer. Schematic cross-sections: **a** with a piezometer, **b** with an observation well

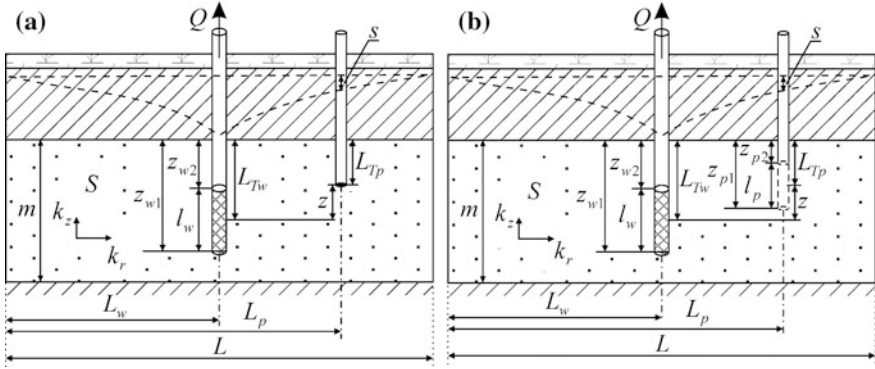


Fig. 1.24 A linear source in a confined aquifer bounded in the horizontal plane (strip aquifer). Schematic cross-sections **a** with a piezometer, **b** with an observation well

Aquifer Bounded in the Horizontal Plane

The test scheme is given in Fig. 1.24. The general form of the Hantush and Moench solutions (see Sect. “Aquifer Infinite in the Horizontal Plane”) for the average drawdown in an observation well or the drawdown in a piezometer is for constant-head boundaries (Fig. 1.21c):

$$s = \frac{Q}{4\pi k_r m} \left[f(r) + \sum_{j=1}^n (-1)^j \sum_{i=1}^2 f(\rho_i^j) \right], \tag{1.111}$$

for impermeable boundaries (Fig. 1.21d):

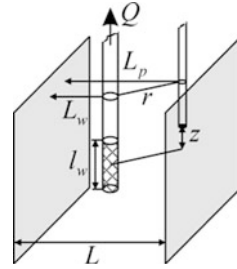
$$s = \frac{Q}{4\pi k_r m} \left[f(r) + \sum_{j=1}^n \sum_{i=1}^2 f(\rho_i^j) \right], \tag{1.112}$$

for constant-head and impermeable boundaries (Fig. 1.21e):

$$s = \frac{Q}{4\pi k_r m} \left\{ f(r) + \sum_{j=1,3,\dots}^n \sum_{i=1}^2 (-1)^{(j+2i-1)/2} f(\rho_i^j) + \sum_{j=2,4,\dots}^n (-1)^{j/2} f(\rho_i^j) \right\}, \tag{1.113}$$

where f is taken from Eq. 1.104 or 1.107, depending on the solution.

Fig. 1.25 A linear source in a confined aquifer bounded in the horizontal plane and infinite in thickness



1.3.3.2 Strip Aquifer

The basic assumptions and conditions (Figs. 1.20b–d and 1.25) are:

- general conditions for a strip aquifer (see the beginning of Sect. 1.3.3);
- the aquifer is infinite in thickness and bounded in the horizontal plane;
- the boundaries are two parallel straight lines in the horizontal plane.

Three variants of boundary conditions are considered (Fig. 1.20b–d): (1) two constant-head boundaries; (2) two impermeable boundaries; and (3) mixed boundary conditions—constant-head and impermeable boundaries.

The drawdown is determined in a piezometer located at any point of the aquifer.

To solve the problem, the image-well method is used: image wells form an infinite row (for the distances to the image wells and the signs of discharges, see Figs. A3.4 and A3.12c).

Basic Analytical Relationships

Transient Flow Equations

1. Two constant-head boundaries (Fig. 1.20b):

$$s = \frac{Q}{8\pi kl_w} \left\{ M_1 + M_2 + \sum_{j=1}^n (-1)^j \sum_{i=1}^2 (M_3 + M_4) \right\}, \quad (1.114)$$

where $M_1 = M\left(\frac{r^2}{4at}, \frac{0.5l_w + z}{r}\right)$, $M_2 = M\left(\frac{r^2}{4at}, \frac{0.5l_w - z}{r}\right)$,

$$M_3 = M\left(\frac{(\rho_i^j)^2}{4at}, \frac{0.5l_w + z}{\rho_i^j}\right), \quad M_4 = M\left(\frac{(\rho_i^j)^2}{4at}, \frac{0.5l_w - z}{\rho_i^j}\right).$$

2. Two impermeable boundaries (Fig. 1.20c):

$$s = \frac{Q}{8\pi kl_w} \left\{ M_1 + M_2 + \sum_{j=1}^n \sum_{i=1}^2 (M_3 + M_4) \right\}. \quad (1.115)$$

Table 1.19 Graphic-analytical parameter evaluation

Plot	Method	Relationship
$\lg s - \lg t$	Type curve: $\lg M'(u, \beta) - \lg \frac{1}{u}$	$k = \frac{Q}{8\pi \cdot l_w \cdot 10^D}, a = \frac{r^2 10^E}{4}$

Two constant-head boundaries: $M'(u, \beta) = M_{u1} + M_{u2} + \sum_{j=1}^n (-1)^j \sum_{i=1}^2 [M_{u3} + M_{u4}]$

Two impermeable boundaries: $M'(u, \beta) = M_{u1} + M_{u2} + \sum_{j=1}^n \sum_{i=1}^2 [M_{u3} + M_{u4}]$

Constant-head and impermeable boundaries

$$M'(u, \beta) = \left\{ M_{u1} + M_{u2} + \sum_{j=1,3,\dots}^n \sum_{i=1}^2 (-1)^{(j+2i-1)/2} [M_{u3} + M_{u4}] + \sum_{j=2,4,\dots}^n (-1)^{j/2} \sum_{i=1}^2 [M_{u3} + M_{u4}] \right\}$$

$$M_{u1} = M\left(u, \frac{0.5l_w + z}{r}\right), M_{u2} = M\left(u, \frac{0.5l_w - z}{r}\right), M_{u3} = M\left(ur_i^j, \frac{0.5l_w + z}{\rho_i^j}\right),$$

$$M_{u4} = M\left(ur_i^j, \frac{0.5l_w - z}{\rho_i^j}\right), r_i^j = \rho_i^j / r$$

3. Constant-head and impermeable boundaries (Fig. 1.20d):

$$s = \frac{Q}{8\pi k l_w} \left\{ M_1 + M_2 + \sum_{j=1,3,\dots}^n \sum_{i=1}^2 (-1)^{(j+2i-1)/2} (M_3 + M_4) + \sum_{j=2,4,\dots}^n (-1)^{j/2} \sum_{i=1}^2 (M_3 + M_4) \right\}. \tag{1.116}$$

The solutions (Eqs. 1.114–1.116) have been derived from the superposition principle.

Graphic-Analytical Processing

The relationships given in Table 1.19 have been derived from Eqs. 1.114–1.116.

1.4 Confined Aquifer of Nonuniform Thickness

The basic assumptions and conditions (Fig. 1.26) are:

- the aquifer has a variable thickness along the x axis and constant thickness along the y axis (though varying along the abscissa);
- the thickness decreases exponentially along the x axis;
- the aquifer is assumed isotropic with infinite lateral extent;
- the pumping and observation wells are fully penetrating.

The drawdown is determined in an observation well located at any distance from the pumping well in the direction of decreasing aquifer thickness. The only restriction in the direction of thickness increase is that the rate of increase in the aquifer thickness is less than 0.2 (i.e., the ratio of an increase in aquifer thickness within some distance to this distance is less than 0.2): $\Delta m / \Delta x < 0.2$.

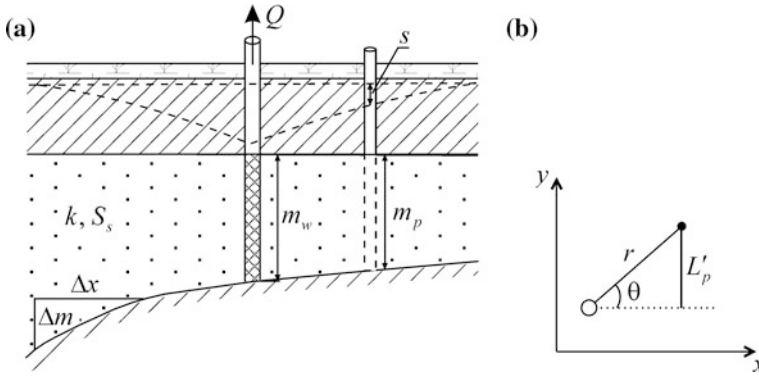


Fig. 1.26 Schematic diagram of a confined aquifer of nonuniform thickness: **a** cross-section and **b** planar view

Basic Analytical Relationships

Transient Flow Equations

The Hantush solution (Hantush 1962):

$$s = \frac{Q}{4\pi km_w} \exp\left(\frac{r}{a_s} \cos \theta\right) W\left(\frac{r^2 S_s}{4kt}, \frac{r}{a_s}\right), \quad (1.117)$$

$$a_s = 2 \frac{\sqrt{r^2 - L_p'^2}}{\ln(m_w/m_p)}, \quad (1.118)$$

where a_s is a geometric parameter, determining the exponential increase in aquifer thickness, m ; θ is the angle between the x axis and the line passing through the pumping and observation wells (Fig. 1.26b), in degrees; the cosine of the angle can be written as:

$$\cos \theta = \frac{1}{r} \sqrt{r^2 - L_p'^2}, \quad (1.119)$$

where L_p' is the distance between the observation well and the line passing through the pumping well parallel to the x axis (Fig. 1.26b), m ; m_w , m_p are aquifer thicknesses at the points where the pumping and observation wells are located (Fig. 1.26a), m .

The Eq. 1.117 can be simplified by substituting expressions (Eqs. 1.118 and 1.119):

$$s = \frac{Q}{4\pi km_w} \sqrt{\frac{m_w}{m_p}} W\left(\frac{r^2 S_s}{4kt}, \frac{r}{a_s}\right). \quad (1.120)$$

Under ideal conditions for a nonuniform thickness aquifer, the drawdown in an observation well located some distance toward a decrease in aquifer thickness (see Fig. 1.26a) should be greater than that in a well located the same distance in the direction of increasing thickness.

The solution (Eq. 1.120) can be used to evaluate the hydraulic conductivity (k) and the specific storage (S_s) of an aquifer of nonuniform thickness.

References

- Babushkin VD (1954) Evaluating permeability of anisotropic rocks from pumping tests data. Prospect Prot Mineral Res 6:50–53 (In Russian)
- Bochever FM (1959) Unsteady-state groundwater flow towards the well in a river valley. Izvestia AN SSSR OTN 5:115–118 (In Russian)
- Bochever FM (1968) Theory and practical methods of groundwater yield evaluation. Nedra, Moscow (In Russian)
- Bochever FM, Verigin NN (1961) Guidance manual for design calculations of groundwater resources and water-supply systems. Gosstroyizdat, Moscow (In Russian)
- Borevskiy BV, Samsonov BG, Yazvin LS (1973) Methods for aquifer parameters estimation from pumping test data. Nedra, Moscow (In Russian)
- Carslow HS, Jaeger JC (1959) Conduction of heat in solids. Oxford at the Clarendon Press, London
- Chan YK, Mullineux N, Reed JR (1976) Analytic solutions for drawdowns in rectangular artesian aquifers. J Hydrol 31(1/2):151–160
- Cooper HH, Jacob CE (1946) A generalized graphical method for evaluating formation constants and summarizing well-field history. EOS T Am Geophys Un 27(4):526–534
- Ferris JG, Knowles DB, Brown RN, Stallman RW (1962) Theory of aquifer test. U.S. Geological Survey Water-Supply, paper 1536-E
- Forchheimer P (1914) Hydraulik. Teubner, Leipzig und Berlin
- Girinskiy NK (1950) Hydraulic conductivity evaluation from pumping tests at variable discharge rate. Gosgeolizdat, Moscow (In Russian)
- Hantush MS (1961a) Aquifer tests on partially penetrating wells. J Hydr Eng Div-ASCE 87 (HY5):171–195
- Hantush MS (1961b) Drawdown around a partially penetrating well. J Hydr Eng Div-ASCE 87 (HY4):83–98
- Hantush MS (1962) Flow of ground water in sands of nonuniform thickness. Part 3. Flow to wells. J Geophys Res 67(4):1527–1534
- Hantush MS (1964) Hydraulics of wells. In: Chow VT (ed) Advances in hydroscience, vol 1. Academic Press, New York, London, pp 281–432
- Hantush MS (1966) Analysis of data from pumping tests in anisotropic aquifers. J Geophys Res 71 (2):421–426
- Hantush MS, Jacob CE (1954) Plane potential flow of ground water with linear leakage. EOS T Am Geophys Un 35(6):917–936
- Hantush MS, Jacob CE (1955) Non-steady green's functions for an infinite strip of leaky aquifer. EOS T Am Geophys Un 36(1):101–112
- Hantush MS, Jacob CE (1960) Flow to an eccentric well in a leaky circular aquifer. J Geophys Res 65(10):3425–3431
- Hantush MS, Thomas RG (1966) A method for analyzing a drawdown test in anisotropic aquifers. Water Resour Res 2(2):281–285

- Jacob CE (1946) Effective radius of drawdown test to determine artesian well. *J Hydr Eng Div-ASCE* 72(5):629–646
- Jacob CE (1949) Flow of ground water. In: Rouse H (ed) *Engineering hydraulics*, chap 5. Wiley, New York, London, pp 321–386
- Latinopoulos P (1982) Well recharge in idealized rectangular aquifers. *Adv Water Resour* 5:233–235
- Mironenko VA, Shestakov VM (1978) Theory and methods of pumping test analysis and interpretation. Nedra, Moscow (In Russian)
- Moench AF (1993) Computation of type curves for flow to partially penetrating wells in water-table aquifers 31(6):966–971
- Moench AF (1996) Flow to a well in a water-table aquifer: an improved Laplace transform solution. *Ground Water* 34(4):593–596
- Moench AF (1997) Flow to a well of finite diameter in a homogeneous, anisotropic water table aquifer. *Water Resour Res* 33(6):1397–1407
- Muskat M (1937) *The flow of homogeneous fluids in porous media*. McGraw-Hill Book Co., New York and London
- Papadopoulos IS, Cooper HH (1967) Drawdown in a well of large diameter. *Water Resour Res* 3(1):241–244
- Shchelkachev VN, Lapuk BB (1949) *Groundwater hydraulics*. Gostoptehizdat, Moscow (In Russian)
- Theis CV (1935) The relation between the lowering of the piezometric surface and the rate and duration of discharge of a well using ground-water storage. *EOS T Am Geophys Un* 16(2):519–524

Chapter 2

Unconfined Aquifers

The chapter considers analytical solutions and analytical methods used in pumping tests in an unconfined aquifer with infinite lateral extent. The construction of groundwater flow equations for unconfined aquifers, semi-infinite or bounded in the horizontal plane, is briefly described in Sect. 2.2. Section 2.3 focuses on pumping tests in unconfined aquifers with sloped bottoms.

The basic assumptions and conditions (Fig. 2.1) are:

- the aquifer is unconfined, homogeneous, isotropic or vertically anisotropic, infinite in the horizontal plane, and underlain by an aquiclude; the case of leakage from an underlying layer and pumping in a confined–unconfined aquifer is considered (Fig. 2.2);
- the initial saturated aquifer thickness is constant;
- the pumping well is fully or partially penetrating;
- wellbore storage, wellbore skin, and delayed response of observation piezometer can be taken into account in the evaluation of the drawdown.

The drawdown is determined in a fully or partially penetrating observation well or a piezometer at any point of the aquifer.

Typical plots of drawdown in the observation well are given in Figs. 12.17 and 12.18. For the effect of the storage coefficient and specific yield on the drawdown in an unconfined aquifer, see Fig. 12.20.

2.1 Aquifer of Infinite Lateral Extent

This section gives transient and quasi-steady-state analytical solutions for calculating the drawdown in an unconfined aquifer infinite in the horizontal plane. The hydraulic characteristics to be determined are listed for each case, depending on the chosen solution.

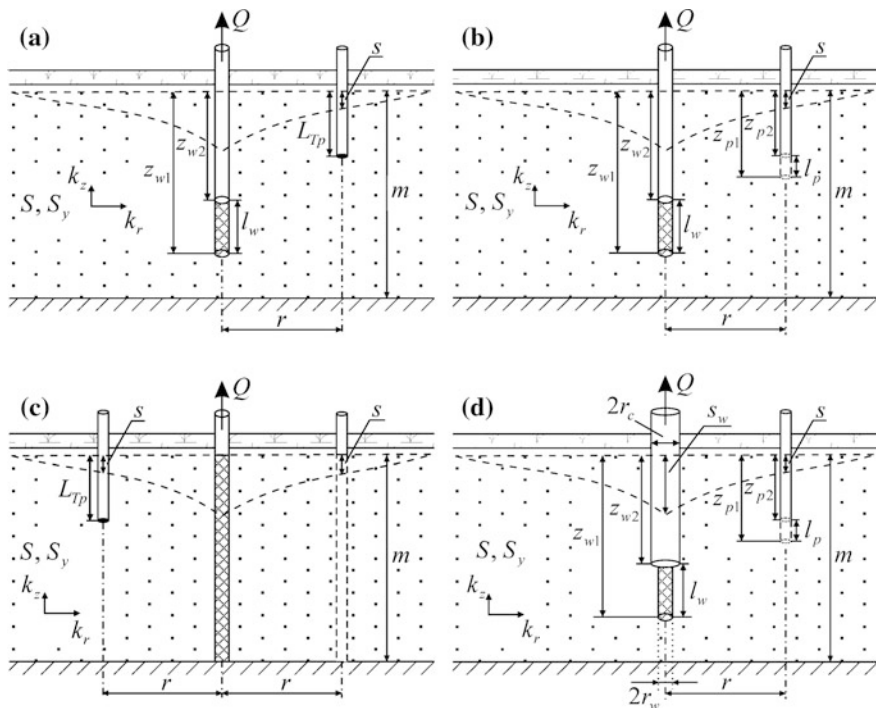


Fig. 2.1 Vertically anisotropic unconfined aquifer. **a** Partially penetrating pumping well and piezometer; **b** partially penetrating pumping and observation wells; **c** fully penetrating pumping well with a piezometer and fully penetrating observation well; **d** an example of unconfined aquifer scheme for Moench solution

Basic Analytical Relationships

Transient Flow Equations

1. Neuman solution (see Appendix 7.6) for the average drawdown in an observation well and the drawdown in a piezometer for a fully or partially penetrating pumping well in an anisotropic aquifer (Neuman 1972–1975) is:

$$s = \frac{Q}{4\pi k_r m} \int_0^\infty 4\tau J_0\left(\tau\chi\frac{r}{m}\right) \left[u_0(\tau) + \sum_{n=1}^\infty u_n(\tau) \right] d\tau, \tag{2.1}$$

where s is the drawdown in the observation well (or piezometer), m ; Q is the discharge rate, m^3/d ; $\chi = \sqrt{k_z/k_r}$ is anisotropy factor; k_r , k_z are the horizontal and

vertical hydraulic conductivities, respectively, m/d ; m is the initial saturated thickness of an unconfined aquifer (see Fig. 2.1), m ; r is the radial distance from the pumping to the observation well (or to a piezometer), m ; $J_0(\cdot)$ is Bessel function of the first kind of the zero order (see Appendix 7.13).

Depending on the degree of penetration (full or partial) of the pumping and observation wells, the functional expressions for $u_0(\tau)$ and $u_n(\tau)$ can be written as follows.

1.1. For a partially penetrating pumping well and piezometer (Neuman 1974) (see Fig. 2.1a):

$$u_0(\tau) = \beta_0 \cosh\left(\gamma_0 \frac{m - L_{Tp}}{m}\right) \frac{\sinh\left(\gamma_0 \frac{m - z_{w2}}{m}\right) - \sinh\left(\gamma_0 \frac{m - z_{w1}}{m}\right)}{\frac{l_w}{m} \sinh \gamma_0}, \quad (2.2)$$

$$u_n(\tau) = \beta_n \cos\left(\gamma_n \frac{m - L_{Tp}}{m}\right) \frac{\sin\left(\gamma_n \frac{m - z_{w2}}{m}\right) - \sin\left(\gamma_n \frac{m - z_{w1}}{m}\right)}{\frac{l_w}{m} \sin \gamma_n}, \quad (2.3)$$

where z_{w1} and z_{w2} are the vertical distances from the initial water table to the bottom and the top of the pumping well screen, respectively (Fig. 2.1a, b), m ; L_{Tp} is the vertical distance from the initial water table to the open part of the piezometer, m ; l_w is pumping-well screen length, m .

1.2. For partially penetrating pumping and observation wells (Neuman 1974) (see Fig. 2.1b):

$$u_0(\tau) = \beta_0 \left[\sinh\left(\gamma_0 \frac{m - z_{p2}}{m}\right) - \sinh\left(\gamma_0 \frac{m - z_{p1}}{m}\right) \right] \frac{\sinh\left(\gamma_0 \frac{m - z_{w2}}{m}\right) - \sinh\left(\gamma_0 \frac{m - z_{w1}}{m}\right)}{\frac{l_w l_p}{m m} \gamma_0 \sinh \gamma_0}, \quad (2.4)$$

$$u_n(\tau) = \beta_n \left[\sin\left(\gamma_n \frac{m - z_{p2}}{m}\right) - \sin\left(\gamma_n \frac{m - z_{p1}}{m}\right) \right] \frac{\sin\left(\gamma_n \frac{m - z_{w2}}{m}\right) - \sin\left(\gamma_n \frac{m - z_{w1}}{m}\right)}{\frac{l_w l_p}{m m} \gamma_n \sin \gamma_n}, \quad (2.5)$$

where z_{p1} and z_{p2} are the vertical distances from the initial water table to the bottom and top of the observation well screen, respectively (Fig. 2.1b), m ; l_p is the observation-well screen length, m .

1.3. For a fully penetrating pumping well and piezometer (Neuman 1972, 1973) (see Fig. 2.1c):

$$u_0(\tau) = \beta_0 \cosh\left(\gamma_0 \frac{m - L_{Tp}}{m}\right), \quad (2.6)$$

$$u_n(\tau) = \beta_n \cos\left(\gamma_n \frac{m - L_{Tp}}{m}\right). \quad (2.7)$$

1.4. For fully penetrating pumping and observation wells (Neuman 1973, 1975) (see Fig. 2.1c):

$$u_0(\tau) = \beta_0 \frac{\sinh \gamma_0}{\gamma_0}, \quad (2.8)$$

$$u_n(\tau) = \beta_n \frac{\sin \gamma_n}{\gamma_n}. \quad (2.9)$$

In expressions (Eqs. 2.2–2.9), γ_0 and γ_n are the roots of the equations

$$\sigma \gamma_0 \sinh \gamma_0 = (\tau^2 - \gamma_0^2) \cosh \gamma_0, \quad \gamma_0^2 < \tau^2;$$

$$\sigma \gamma_n \sin \gamma_n = -(\tau^2 + \gamma_n^2) \cos \gamma_n, \quad (2n - 1) \frac{\pi}{2} < \gamma_n < n\pi, \quad n \geq 1;$$

$$u = \frac{k_z t}{Sm}, \quad \sigma = S/S_y,$$

$$\beta_0 = \frac{1 - \exp(-u(\tau^2 - \gamma_0^2))}{\tau^2 + (1 + \sigma)\gamma_0^2 - (\tau^2 - \gamma_0^2)^2/\sigma} \times \frac{1}{\cosh \gamma_0},$$

$$\beta_n = \frac{1 - \exp(-u(\tau^2 + \gamma_n^2))}{\tau^2 - (1 + \sigma)\gamma_n^2 - (\tau^2 + \gamma_n^2)^2/\sigma} \times \frac{1}{\cos \gamma_n},$$

where S is the storage coefficient, dimensionless; S_y is the specific yield, dimensionless; t is the time elapsed from the start of pumping, d.

Equation 2.1 is solved by using the algorithm of DELAY2 code (see Appendix 5.1). The Neuman solution (Eq. 2.1) is used to determine the hydraulic conductivities in the vertical and horizontal directions (k_r , k_z), storage coefficient (S) and specific yield (S_y) of an unconfined aquifer.

2. For the Boulton solutions (Boulton 1963) for the drawdown in a fully penetrating observation well in an isotropic aquifer (the pumping well is fully penetrating), two such solutions are used, yielding nearly the same drawdown:

$$s = \frac{Q}{2\pi km} \int_0^\infty \frac{1}{\tau} J_0\left(r\sqrt{\frac{\alpha S_y}{km}}\tau\right) \left\{ 1 - \frac{1}{\tau^2 + 1} \exp\left(-\frac{\alpha t}{\tau^2 + 1} \tau^2\right) - \frac{\tau^2}{\tau^2 + 1} \exp\left[-\alpha \frac{S + S_y}{S} t(\tau^2 + 1)\right] \right\} d\tau, \quad (2.10)$$

$$s = \frac{Q}{2\pi km} \int_0^{\infty} \frac{1}{\tau} \left\{ \frac{1 - \exp(-\mu_1) \times}{\cosh \mu_2 + \frac{\alpha t \eta (1 - \tau^2)}{2\mu_2} \sinh \mu_2} \right\} J_0 \left(r \sqrt{\frac{\alpha(S + S_y)}{T}} \tau \right) d\tau, \quad (2.11)$$

where

$$\mu_1 = \frac{\alpha t \eta (1 + \tau^2)}{2}, \quad (2.12)$$

$$\mu_2 = \frac{\alpha t \sqrt{\eta^2 (1 + \tau^2)^2 - 4\eta \tau^2}}{2}, \quad (2.13)$$

$$\eta = \frac{S + S_y}{S}, \quad (2.14)$$

k is the hydraulic conductivity of an isotropic unconfined aquifer, m/d.

The empirical parameter α (so-called reciprocal of Boulton's delay index) (1/d) can be defined as

$$\alpha = \frac{3k}{S_y m}. \quad (2.15)$$

For a vertically anisotropic aquifer, $k = k_z$ in formula (2.15). Neuman (1975, 1979) proposed another relationship for α :

$$\alpha = \frac{k_z}{S_y m} \left[3.063 - 0.567 \lg \left(\frac{\chi r}{m} \right)^2 \right], \quad (2.16)$$

which suggests that the further the observation well is from the pumping well, the less the value of α .

Boulton solutions (Eqs. 2.10 and 2.11) are used to determine the hydraulic conductivity, the storage coefficient, and specific yield (k , S , S_y) of an unconfined aquifer.

3. The Boulton solution (Boulton 1954) for the drawdown of the water table (corresponds to the gravity-drainage period) in a fully penetrating observation well in an isotropic aquifer (the pumping well is fully penetrating) is:

$$s = \frac{Q}{2\pi km} F_B \left(\frac{kt}{S_y m}, \frac{r}{m} \right), \quad (2.17)$$

$$F_B(u, \beta) = \int_0^{\infty} \frac{1}{\tau} J_0(\beta \tau) [1 - \exp(-u \tau \tanh \tau)] d\tau, \quad (2.18)$$

where $F_B(u, \beta)$ is the Boulton function (see Appendix 7.5).

The Boulton solution (Eq. 2.17) with drawdown values corresponding to a gravity-drainage period (see Fig. 12.17) is used to determine the hydraulic conductivity (k) and the specific yield (S_y) of the unconfined aquifer.

4. The Moench solution (Moench 1993, 1996) for the drawdown in a fully or partially penetrating observation well or a piezometer is:

$$s = \frac{Q}{4\pi k_r m} f(t, r, m, l_w, l_p, L_{Tw}, L_{Tp}, k_r, k_z, S, S_y), \quad (2.19)$$

where L_{Tp} is the vertical distance from the initial water table to the open part of the piezometer or the center of observation well screen (for the observation well, $L_{Tp} = z_{p2} + l_p/2$), m; $L_{Tw} = z_{w2} + l_w/2$ is the vertical distance from the initial water table to the center of the pumping well screen, m.

The functional relationship (Eq. 2.19) is treated using the algorithm of WTAQ2 code (see Appendix 5.2). The Moench solution (Eq. 2.19) is used to evaluate the vertical and horizontal hydraulic conductivities (k_r , k_z), as well as the storage coefficient (S) and specific yield (S_y) of an unconfined aquifer.

5. The Moench solution (Moench 1997) for the drawdown in a fully or partially penetrating observation well or a piezometer with the storages of the pumping and observation wells taken into account is:

$$s = \frac{Q}{4\pi k_r m} f(t, r, r_w, r_c, r_p, m, l_w, l_p, L_{Tw}, L_{Tp}, k_r, k_z, S, S_y, k_{skin}, m_{skin}), \quad (2.20)$$

where r_w , r_c , r_p are the radiuses of the pumping well, its casing, and the observation well, m; k_{skin} , m_{skin} are the hydraulic conductivity (m/d) and the thickness (m) of the wellbore skin (see Appendix 2).

The functional relationship (Eq. 2.20) takes into account the wellbore storage, the delayed response of the observation piezometer, and the wellbore skin. The algorithm of WTAQ3 code is used for its treatment (see Appendix 5.3). The Moench solution (Eq. 2.20) is used to determine the horizontal and vertical hydraulic conductivities (k_r , k_z), the storage coefficient (S), the specific yield (S_y) of the unconfined aquifer and, additionally, to evaluate the hydraulic conductivity and the thickness of the wellbore skin (k_{skin} , m_{skin}).

In addition, the functional relationships (Eqs. 2.20 and 2.21) enable one to take into account the effect of the delayed drainage from the unsaturated zone on the drawdown in the wells during pumping. In this case, the code WTAQ version 2 (see Appendix 5.4) is used for calculations (Barlow and Moench 2011).

6. Moench's solution (Moench 1997) for the drawdown in a fully or partially penetrating pumping well:

$$s_w = \frac{Q}{4\pi k_r m} f(t, r_w, r_c, m, l_w, L_{Tw}, k_r, k_z, S, S_y, k_{skin}, m_{skin}). \quad (2.21)$$

The functional relationship (Eq. 2.21) takes into account the wellbore storage and the wellbore skin. The algorithm of WTAQ3 code is used for its calculation (see Appendix 5.3). The parameters being determined are similar to the Moench relationship (Eq. 2.20). Here, as well as in (Eq. 2.20), the effect of the capillary fringe is evaluated.

7. A simplified solution for the drawdown during the gravity-drainage period (see Fig. 12.17) in a fully penetrating observation well in an isotropic unconfined aquifer (the pumping well is fully penetrating) (Jacob 1963) is:

$$s = m - \sqrt{m^2 - \frac{Q}{2\pi k} W\left(\frac{r^2}{4at}\right)}, \quad (2.22)$$

where a is the hydraulic diffusivity of the unconfined aquifer, m^2/d ; $W(u)$ is a well-function (see Appendix 7.1).

Solution (Eq. 2.22) is used to evaluate the hydraulic conductivity (k) and the hydraulic diffusivity ($a = km/(S + S_y) \approx km/S_y$) of the unconfined aquifer.

8. A simplified solution for the drawdown in a fully penetrating observation well in an isotropic unconfined aquifer (the pumping well is fully penetrating) during gravity-drainage period with the leakage through aquifer bottom taken into account (Fig. 2.2a) is:

$$s = m - \sqrt{m^2 - \frac{Q}{2\pi k} W\left(\frac{r^2}{4at}, \frac{r}{B}\right)}, \quad (2.23)$$

$$B = \sqrt{\frac{k\bar{m}m'}{k'}}, \quad (2.24)$$

where B is the leakage factor, m ; $\bar{m} = m$ is the initial saturated thickness of the unconfined aquifer, m ; k' , m' are the hydraulic conductivity (m/d) and thickness (m) of the aquitard; $W(u, \beta)$ is the well-function for leaky aquifers (see Appendix 7.2).

The solution (Eq. 2.23) is used to evaluate the hydraulic conductivity (k) and hydraulic diffusivity ($a = km/S_y$) of the unconfined aquifer, as well as the leakage factor (B).

9. The Moench–Prickett solution (Moench and Prickett 1972) for a confined–unconfined aquifer (Fig. 2.2b) is:

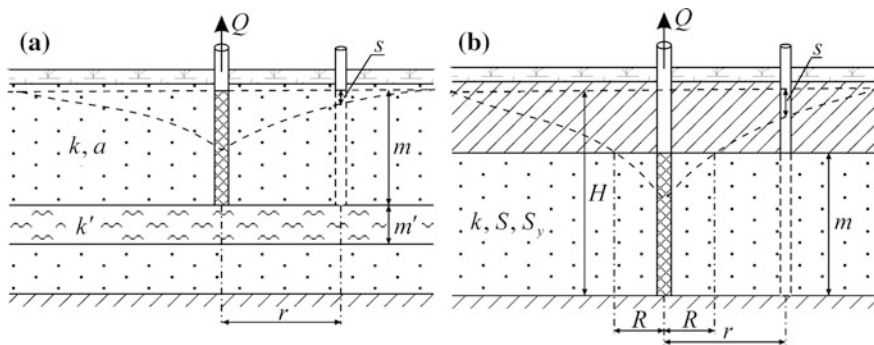


Fig. 2.2 a Unconfined leaky aquifer and b confined-unconfined aquifer

$$\begin{cases} s = \frac{Q}{4\pi km} \left[W\left(\frac{r^2 S_y}{4kmt}\right) - W\left(\frac{R^2 S_y}{4kmt}\right) \right] + H - m & \rightarrow r < R \\ s = \frac{Q}{4\pi km} \exp\left(-\frac{R^2 (S_y - S)}{4kmt}\right) W\left(\frac{r^2 S}{4kmt}\right) & \rightarrow r > R, \end{cases} \quad (2.25)$$

where H is the initial head, m ; m is confined-aquifer thickness, m ; R is the horizontal distance from the pumping well to the point where the confined aquifer becomes unconfined (Fig. 2.2b).

The distance R is calculated from a transcendental equation for any moment t :

$$\frac{Q}{4\pi km(H - m)} \exp\left(-\frac{R^2 S_y}{4kmt}\right) - \exp\left(-\frac{R^2 S}{4kmt}\right) / W\left(\frac{R^2 S}{4kmt}\right) = 0. \quad (2.26)$$

Depending on the radius, a solution from the system of Eq. 2.25 is chosen, in which the top equation accounts for the drawdown for the periods when the observation well is located in the unconfined flow zone, and the bottom equation accounts for the same for the confined zone. When the initial head is below the top of the aquifer, the system of Eq. 2.25 transforms into an equation for gravity-drainage conditions

$$s = \frac{Q}{4\pi km} W\left(\frac{r^2 S_y}{4kmt}\right), \quad (2.27)$$

which is an analog of the solution (Eq. 2.22). The Moench–Prickett solution (Eq. 2.25) is used to determine the hydraulic conductivity of the aquifer (k), the storage coefficient of the confined flow zone (S), and the specific yield for the zone of unconfined flow (S_y).

When evaluating drawdown in an unconfined aquifer with the use of transient flow relationships, one should keep in mind that: (1) the screen length of the observation well (l_p) is eliminated in solutions (Eq. 2.19) and (Eq. 2.20) in the calculation of the drawdown in the piezometer; and (2) the drawdown in the

observation well derived from solutions (Eqs. 2.1, 2.19, and 2.20) is averaged over its screen length.

The solutions (Eqs. 2.1, 2.10, 2.11, 2.17, and 2.19–2.21) imply a slight decline in the water table in the course of testing, relative to the initial saturated thickness of the aquifer. Otherwise, it is recommended to introduce a correction (Jacob 1963) to the drawdown evaluated by these relationships, i.e.

$$s_c = m - \sqrt{m^2 - 2ms}, \tag{2.28}$$

where s_c is the corrected drawdown, m ; s is the drawdown derived from formulas without correction, m .

The need to introduce corrections to the drawdown (see Fig. 12.19) in the solutions given above, depending on the degree of penetration (full or partial) of the pumping well and the magnitude of drawdown, is classified in Table 2.1.

Quasi-Steady-State Flow Equation (corresponds to the gravity-drainage period)

$$s(2m - s) = \frac{Q}{2\pi k} \ln \frac{2.25kmt}{r^2 S_y} = \frac{0.366Q}{k} \lg \frac{2.25kmt}{r^2 S_y} \tag{2.29}$$

or, in terms of hydraulic diffusivity:

$$s(2m - s) = \frac{Q}{2\pi k} \ln \frac{2.25at}{r^2} = \frac{0.366Q}{k} \lg \frac{2.25at}{r^2}. \tag{2.30}$$

The equation for quasi-steady-state period implies the full penetration of the pumping and observation wells and the isotropy of the unconfined aquifer.

Table 2.1 Application of analytical solutions for different degrees of penetration of the pumping well and the magnitude of drawdown

Pumping well penetration	Condition	Solution	Correction
Full	Small drawdown ^a	2.1, 2.10, 2.11, 2.17, 2.19–2.21	Not required
Full	Large drawdown ^a	2.1, 2.10, 2.11, 2.17, 2.19–2.21	Obligatory
Partial	Water table lies above the screen top ^b	2.1, 2.19–2.21	Not applied
Partial	Water table lies below the screen top ^c	The solutions are inapplicable	Not applied

^aThe drawdown can be considered small when it is less than 20 % of the initial saturated thickness of an unconfined aquifer, i.e., $s < 0.2m$ (Borevskiy et al. 1973)

^bThe screen of the pumping well during the pumping test remains fully within the saturated zone

^cWater table can drop below the top of the pumping well screen during the test: the length of the part of the screen within the saturated zone varies during the pumping test

Graphic-Analytical Processing

The relationships given in Table 2.2 have been derived from simplified solutions (Eqs. 2.22 and 2.30), which assume the pumping and observation wells are fully penetrating. The graphic-analytical processing involves only drawdown values corresponding to the gravity-drainage period in an isotropic aquifer.

In Table 2.2, the values of the hydraulic conductivity and hydraulic diffusivity are determined independently. Given these characteristics, the specific yield of the unconfined aquifer can be readily evaluated: $S_y = km/a$. In addition, the hydraulic diffusivity and the specific yield can be evaluated based on the intercept of the straight line on the abscissa (Table 2.3).

Table 2.2 Graphic-analytical parameter evaluation

Plot	Method	Relationship
$s(2m - s) - \lg t$	Straight line	$k = \frac{0.366Q}{C}, \lg a = \frac{A}{C} + \lg \frac{r^2}{2.25}$
$s(2m - s) - \lg r$	The same	$k = \frac{0.732Q}{C}, \lg a = 2\frac{A}{C} - \lg(2.25 \cdot t)$
$s(2m - s) - \lg \frac{t}{r^2}$	The same	$k = \frac{0.366Q}{C}, \lg a = \frac{A}{C} - \lg 2.25$
$\lg[s(2m - s)] - \lg t$	Type curve: $\lg W(u) - \lg \frac{1}{u}$	$k = \frac{Q}{2\pi \cdot 10^D}, a = \frac{r^2 \cdot 10^E}{4}$
$\lg[s(2m - s)] - \lg \frac{t}{r^2}$	The same	$k = \frac{Q}{2\pi \cdot 10^D}, a = \frac{10^E}{4}$
$\left[\begin{matrix} s_1(2m - s_1) - \\ -s_2(2m - s_2) \end{matrix} \right] - \lg t$	Horizontal straight line	$k = \frac{Q}{\pi \cdot A} \ln \frac{r_2}{r_1}$

A is the intercept on the ordinate axis (see Sects. 12.1.1 and 12.1.2); C is the slope of the straight line (see Sect. 12.1.1); D, E are the shifts of the plot of the actual and reference curves (see Sect. 12.1.3) in the vertical (D) and horizontal (E) directions, respectively;

s_1, s_2, r_1, r_2 is the drawdown (s) in and the distance to the pumping well (r) for the first and second observation wells, respectively. In the case of vertical anisotropy, horizontal hydraulic conductivity is determined: $k = k_r$

Table 2.3 Graphic-analytical parameter evaluation

Plot	Method	Relationship
$s(2m - s) - \lg t$	Straight line	$a = \frac{r^2}{2.25t_x}, S_y = \frac{2.25kmt_x}{r^2}$
$s(2m - s) - \lg r$	The same	$a = \frac{r_x^2}{2.25t}, S_y = \frac{2.25kmt}{r_x^2}$
$s(2m - s) - \lg \frac{t}{r^2}$	The same	$a = \frac{1}{2.25(t/r^2)_x}, S_y = 2.25km(t/r^2)_x$

t_x, r_x and $(t/r^2)_x$ are the intercepts on the abscissas of appropriate plots (see Fig. 12.1)

2.2 Semi-infinite and Bounded Unconfined Aquifers

To solve the boundary problem for unconfined aquifers, one may use the same approach as for confined aquifers (see Sects. 1.1.2–1.1.5). The solutions for the drawdown are derived from basic solutions (Eqs. 2.1, 2.10, 2.11, 2.17, and 2.19) with the effect of image wells taken into account through the superposition principle.

For example, the Boulton solution (Eq. 2.17) for a semi-infinite aquifer with a constant-head boundary can be written as:

$$s = \frac{Q}{2\pi km} \left[F_B \left(\frac{kt}{S_y m}, \frac{r}{m} \right) - F_B \left(\frac{kt}{S_y m}, \frac{\rho}{m} \right) \right], \quad (2.31)$$

and the solution (Eq. 2.22) for an impermeable boundary as:

$$s = m - \sqrt{m^2 - \frac{Q}{2\pi k} \left[W \left(\frac{r^2}{4at} \right) + W \left(\frac{\rho^2}{4at} \right) \right]}, \quad (2.32)$$

where ρ is the horizontal distance from the observation to the image well (see Fig. A3.2 and Eq. A3.1), m .

2.3 Sloping Unconfined Aquifer

The basic assumptions and conditions (Figs. 2.3 and 2.4) are:

- the aquifer is unconfined, isotropic, sloped, and underlain by an aquiclude (Fig. 2.3a) or an aquitard (Fig. 2.3b), through which water leaks during the test;
- the initial saturated thickness of the aquifer does not change over the space;
- the slopes of the aquiclude and groundwater table are the same; the presented solutions are applicable to aquicludes with a slope less than 0.2;
- the drawdown in the pumping well must not exceed half the initial saturated thickness of the main aquifer;
- in the case of a leaky aquifer, the storage of the aquiclude is neglected;
- the aquifer is infinite in the horizontal plane (Fig. 2.3) or semi-infinite with a constant-head boundary (Fig. 2.4).

The drawdown is determined in the aquifer at any distance from the pumping well for the gravity-drainage period. The drawdown for sloped aquifers depends on both the distance to the pumping well and the angle θ (Fig. 2.3c), as well as the relative positions of the observation and pumping wells: whether the former lies upstream or downstream of the latter. Ideally, the drawdown in the observation well upstream of the pumping well is less than that downstream of it.

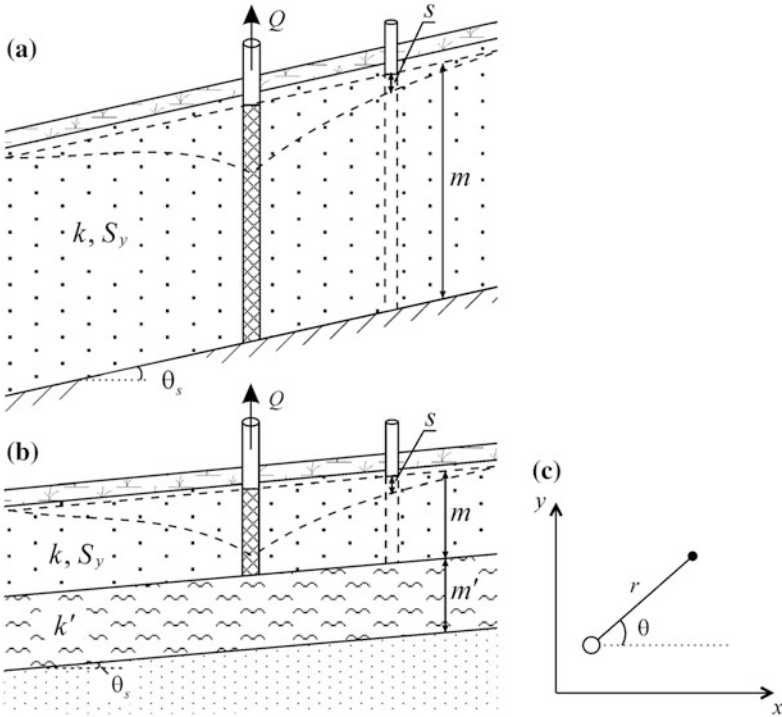


Fig. 2.3 Sloped unconfined aquifer of infinite lateral extent: **a** nonleaky aquifer; **b** leaky aquifer. **c** Planar view

The analytical relationships are used to determine the hydraulic conductivity (k) and specific yield (S_y) of the unconfined aquifer. In the case where leakage is taken into account, the leakage factor (B) is also evaluated.

Basic Analytic Relationships

Transient Flow Equations

1. Solutions for unconfined nonleaky aquifer (Hantush 1962)

1.1. Aquifer of infinite lateral extent (Fig. 2.3a):

$$s = m - \sqrt{m^2 - \frac{Q}{2\pi k} \exp\left(-\frac{r}{\gamma} \cos \theta\right) W\left(\frac{r^2 S_y}{4kmt}, \frac{r}{\gamma}\right)}, \tag{2.33}$$

$$\gamma \approx (1.75 \div 2) \frac{m}{\tan \theta_s}, \tag{2.34}$$

where m is the initial saturated thickness of the sloped unconfined aquifer, m; θ_s is the slope of the bottom of the aquifer, degree; θ is the angle between the x axis and

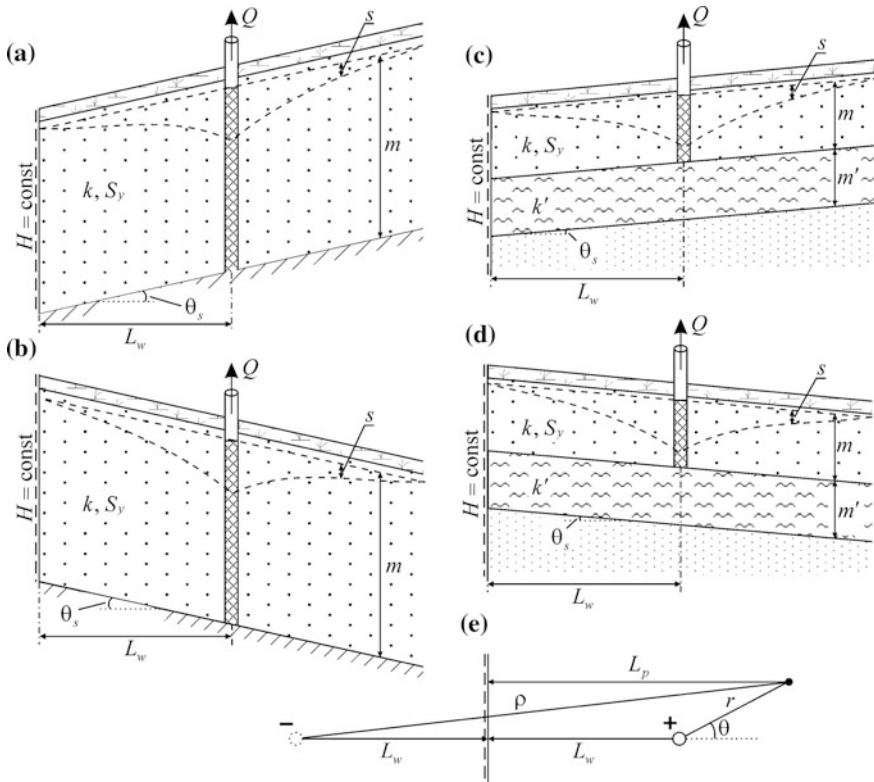


Fig. 2.4 Sloped unconfined aquifer semi-infinite in the horizontal plane: **a, b** nonleaky aquifers; **c, d** leaky aquifers. **e** A planar view with the distances to the boundary and an image well (the signs of actual and image flow rates are given near the wells); **a, c** wells are located upstream of the boundary; **b, d** wells are located downstream of the boundary. L_w, L_p are the distances from the pumping and observation wells to the boundary, respectively

the line connecting the pumping and observation wells (see Figs. 2.3c and 2.4e); the cosine in degrees can be expressed in terms of the distances (Eq. 1.119).

1.2. Semi-infinite aquifer (Fig. 2.4a, b):

$$s = m - \sqrt{m^2 - \frac{Q}{2\pi k} \exp\left(n \frac{r}{\gamma} \cos \theta\right) \left[W\left(\frac{r^2 S_y}{4kmt}, \frac{r}{\gamma}\right) - W\left(\frac{\rho^2 S_y}{4kmt}, \frac{\rho}{\gamma}\right) \right]}, \quad (2.35)$$

where $n = -1$ for a well upstream from the boundary (Fig. 2.4a, c) and $n = 1$ for a well downstream from the boundary (Fig. 2.4b, d); ρ is the horizontal distance from the observation well to the image well (Eq. A3.1), m.

2. Solutions for unconfined leaky aquifer (Hantush 1964)

2.1. Aquifer infinite in the horizontal plane (Fig. 2.3b):

$$s = m - \sqrt{m^2 - \frac{Q}{2\pi k} \exp\left(-\frac{r}{\gamma} \cos \theta\right) \mathbf{W}\left(\frac{r^2 S_y}{4kmt}, r\gamma'\right)}, \quad (2.36)$$

$$\gamma' = \sqrt{\frac{1}{\gamma^2} + \frac{1}{B^2}}, \quad (2.37)$$

where B is the leakage factor (Eq. 2.24), m .

2.2. Aquifer semi-infinite in the horizontal plane (Fig. 2.4c, d):

$$s = m - \sqrt{m^2 - \frac{Q}{2\pi k} \exp\left(n\frac{r}{\gamma} \cos \theta\right) \left[\mathbf{W}\left(\frac{r^2 S_y}{4kmt}, r\gamma'\right) - \mathbf{W}\left(\frac{\rho^2 S_y}{4kmt}, \rho\gamma'\right)\right]}. \quad (2.38)$$

Steady-State Flow Equations

1. Solutions for an unconfined nonleaky aquifer (Hantush 1962)

1.1. Aquifer infinite in the horizontal plane (Fig. 2.3a):

$$s = m - \sqrt{m^2 - \frac{Q}{\pi k} \exp\left(-\frac{r}{\gamma} \cos \theta\right) \mathbf{K}_0\left(\frac{r}{\gamma}\right)}, \quad (2.39)$$

where $\mathbf{K}_0(\cdot)$ is a modified Bessel function of the second kind of the zero order (see Appendix 7.13).

1.2. Semi-infinite aquifer (Fig. 2.4a, b):

$$s = m - \sqrt{m^2 - \frac{Q}{\pi k} \exp\left(n\frac{r}{\gamma} \cos \theta\right) \left[\mathbf{K}_0\left(\frac{r}{\gamma}\right) - \mathbf{K}_0\left(\frac{\rho}{\gamma}\right)\right]}. \quad (2.40)$$

2. Solutions for unconfined leaky aquifer (Hantush 1964)

2.1. Aquifer infinite in the horizontal plane (Fig. 2.3b):

$$s = m - \sqrt{m^2 - \frac{Q}{\pi k} \exp\left(-\frac{r}{\gamma} \cos \theta\right) \mathbf{K}_0(r\gamma')}. \quad (2.41)$$

2.2. Aquifer semi-infinite in the horizontal plane (Fig. 2.4c, d):

$$s = m - \sqrt{m^2 - \frac{Q}{\pi k} \exp\left(n\frac{r}{\gamma} \cos \theta\right) [\mathbf{K}_0(r\gamma') - \mathbf{K}_0(\rho\gamma')]}. \quad (2.42)$$

References

- Barlow PM, Moench AF (2011) WTAQ version 2—a computer program for analysis of aquifer tests in confined and water-table aquifers with alternative representations of drainage from the unsaturated zone. U.S. Geological Survey. Techniques and Methods 3-B9
- Borevskiy BV, Samsonov BG, Yazvin LS (1973) Methods for aquifer parameters estimation from pumping test data. Nedra, Moscow (In Russian)
- Boulton NS (1954) The drawdown of the water-table under non-steady conditions near a pumped well in an unconfined formation. *P I Civil Eng* 3(4):564–579
- Boulton NS (1963) Analysis of data from non-equilibrium pumping tests allowing for delayed yield from storage. *P I Civil Eng* 26(3):469–482
- Hantush MS (1962) Hydraulics of gravity wells in sloping sands. *J Hydr Eng Div-ASCE* 88 (HY4):1–15
- Hantush MS (1964) Hydraulics of wells. In: Te Chow Ven (ed) *Advances in hydroscience*, vol 1. Academic Press, New York and London, pp 281–432
- Jacob CE (1963) Determining the permeability of water-table aquifer. In: Bentall R (ed) *Methods of determining permeability, transmissibility and drawdown*. Geological Survey Water-Supply, paper 1536-I, Washington, pp 245–271
- Moench AF (1993) Computation of type curves for flow to partially penetrating wells in water-table aquifers. *Ground Water* 31(6):966–971
- Moench AF (1996) Flow to a well in a water-table aquifer: an improved Laplace transform solution. *Ground Water* 34(4):593–596
- Moench AF (1997) Flow to a well of finite diameter in a homogeneous, anisotropic water table aquifer. *Water Resour Res* 33(6):1397–1407
- Moench AF, Prickett TA (1972) Radial flow in an infinite aquifer undergoing conversion from artesian to water table conditions. *Water Resour Res* 8(2):494–499
- Neuman SP (1972) Theory of flow in unconfined aquifers considering delayed gravity response. *Water Resour Res* 8(4):1031–1045
- Neuman SP (1973) Supplementary comments on theory of flow in unconfined aquifers considering delayed gravity response. *Water Resour Res* 9(4):1102–1103
- Neuman SP (1974) Effect of partial penetration on flow in unconfined aquifers considering delayed gravity response. *Water Resour Res* 10(2):303–312
- Neuman SP (1975) Analysis of pumping test data from anisotropic unconfined aquifers. *Water Resour Res* 11(2):329–345
- Neuman SP (1979) Perspective on delayed yield. *Water Resour Res* 15(4):899–908

Chapter 3

Leaky Aquifers

A complex of water-saturated rocks, consisting of aquifers separated by aquitards (low-permeability layers), is considered in this chapter (Fig. 3.1). The pumping well penetrates only one (the main) aquifer. The head in the adjacent aquifer is either constant throughout the pumping-test period or varies over time due to pumping. The storage of the aquitards can be taken into account.

The initial formulation of the problem takes into account the processes of interlayer hydrodynamic interaction, which can be accounted for in several limit models (schemes), based on the following assumptions:

- the water level in the adjacent aquifer (where steady-state flow occurs) remains constant during the pumping test; the effect of the lateral flow boundaries can be taken into account; the storage of the aquitard is neglected;
- the water level in the adjacent aquifer (where transient flow occurs) changes during the pumping test; the storage of the aquitard is neglected;
- the water level in the adjacent aquifer either remains constant or varies and the storage of the separating aquitard is taken into account.

The basic solutions are used to construct relationships, which take into account the planar boundaries of the flow.

In addition, this chapter presents flow equations, describing the drawdown in complex stratified systems with various profile boundary conditions.

All solutions for leaky aquifers imply vertical flow in the aquitards and horizontal flow in the main isotropic aquifer. Some analytical solutions have been obtained for the partially penetrating well in an aquifer characterized by anisotropy in the vertical plane.

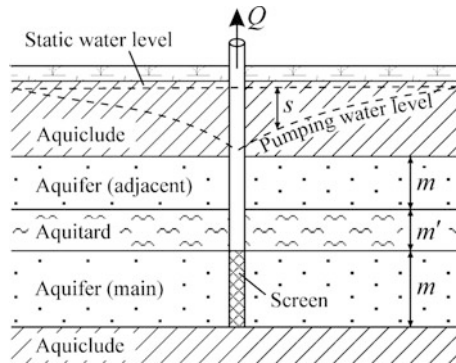


Fig. 3.1 Schematic diagram of a pumping test in a leaky aquifer system. Q is pumping-well discharge, s is the drawdown, m is aquifer thickness, m' is the aquitard thickness

3.1 Leaky Aquifer with Steady-State Flow in the Adjacent Aquifers

This section gives transient and steady-state analytical solutions for leaky aquifers with infinite, semi-infinite, and limited lateral extent assuming a constant head in the adjacent aquifers. The transient solutions are used to evaluate the transmissivity (T), storage coefficient (S) and hydraulic diffusivity (a) of the main aquifer, as well as the leakage factor (B). The hydraulic characteristics are derived from data on the drawdown in the main aquifer.

3.1.1 Aquifer of Infinite Lateral Extent

The basic assumptions and conditions (Fig. 3.2) are:

- the leaky aquifer system consists of two or three aquifers separated by aquitards;
- the main aquifer, penetrated by the pumping well, is isotropic or anisotropic in the horizontal plane;
- the water level in the adjacent aquifers remains unchanged during the pumping test;
- the initial water levels in the aquifers can be either the same or different;
- the aquifer has no lateral boundaries (infinite in the horizontal plane);
- the pumping well fully penetrates the main aquifer; the storage of the well can be taken into account;
- the aquitard has negligible storage.

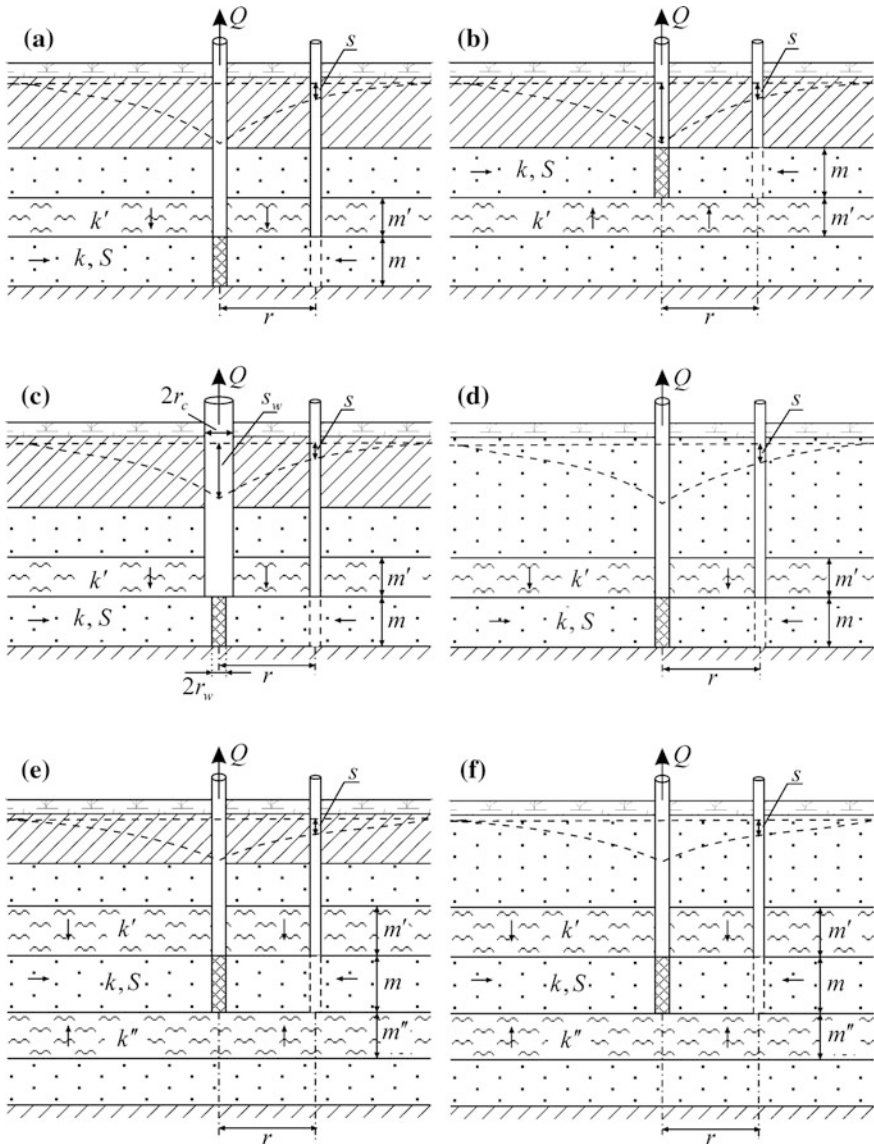


Fig. 3.2 A leaky aquifer with the level in adjacent aquifers remaining unchanged during the pumping test (cross-section view): **a** a two-aquifer system with downward leakage; **b** the same with upward leakage; **c** an example of a scheme of a leaky aquifer system for solutions taking into account pumping-well storage; **d** a leaky confined aquifer with an adjacent unconfined aquifer; three-aquifer; **e** confined and **f** unconfined systems. The arrows show flow direction in the layers

The drawdown is determined at any distance from the pumping well in the main aquifer. Typical plots of the drawdown in an observation well and the effect of hydraulic parameters on the drawdown are given in Fig. 12.21.

Basic Analytical Relationships

Transient Flow Equations

1. The principal solution for a leaky aquifer is the Hantush–Jacob solution (Hantush and Jacob 1955b):

$$s = \frac{Q}{4\pi T} W\left(\frac{r^2 S}{4Tt}, \frac{r}{B}\right) = \frac{Q}{4\pi T} W\left(\frac{r^2}{4at}, \frac{r}{B}\right), \quad (3.1)$$

$$W(u, \beta) = \int_u^\infty \frac{1}{\tau} \exp\left(-\tau - \frac{\beta^2}{4\tau}\right) d\tau, \quad (3.2)$$

where, for a single adjacent aquifer (Fig. 3.1a–d):

$$B = \sqrt{\frac{Tm'}{k'}}, \quad (3.3)$$

and for two adjacent aquifers (Fig. 3.1e, f):

$$B = \sqrt{\frac{Tm'm''}{k'm'' + k''m'}}, \quad (3.4)$$

where s is the drawdown in the observation well, m ; Q is the discharge rate, m^3/d ; $T = km$ is the transmissivity of the main aquifer, m^2/d ; k , m are the hydraulic conductivity (m/d) and thickness (m) of the aquifer; S is the aquifer storage coefficient, dimensionless; $a = T/S$ is the hydraulic diffusivity of the aquifer, m^2/d ; B is the leakage factor, depending on the number of adjacent aquifers (see Appendix 1), m ; k' , m' and k'' , m'' are the hydraulic conductivities (m/d) and thicknesses (m) of the aquitards; r is the radial distance from the pumping to the observation well, m ; t is the time elapsed from the start of pumping, d ; $W(u, \beta)$ is the well-function for leaky aquifers (see Appendix 7.2).

The Hantush–Jacob solution assumes an infinitely small wellbore radius, i.e., the wellbore storage is neglected.

2. The extended solution, accounting for the wellbore storage, written for the drawdown in the observation well (Lai and Su 1974), is:

$$s = \frac{Q}{4\pi T} F_L\left(\frac{r_w^2 S}{4Tt}, \frac{r}{r_w}, \frac{r_w}{B}, S \frac{r_w^2}{r_c^2}\right), \quad (3.5)$$

$$F_L(u, \beta_1, \beta_2, \beta_3) = 8 \frac{\beta_3}{\pi} \int_0^\infty \left\{ \left[1 - \exp\left(-\frac{\tau^2 + \beta_2^2}{4u}\right) \right] \frac{\tau}{\tau^2 + \beta_2^2} \times \right. \\ \left. \times \frac{J_0(\beta_1 \tau) [(\tau^2 + \beta_2^2) Y_0(\tau) - 2\beta_3 \tau Y_1(\tau)] - Y_0(\beta_1 \tau) [(\tau^2 + \beta_2^2) J_0(\tau) - 2\beta_3 \tau J_1(\tau)]}{[(\tau^2 + \beta_2^2) J_0(\tau) - 2\beta_3 \tau J_1(\tau)]^2 + [(\tau^2 + \beta_2^2) Y_0(\tau) - 2\beta_3 \tau Y_1(\tau)]^2} \right\} d\tau, \quad (3.6)$$

where r_w is pumping well radius, m; r_c is the casing radius, m; $J_0(\cdot)$ and $J_1(\cdot)$ are Bessel functions of the first kind of the zero and the first order; $Y_0(\cdot)$ and $Y_1(\cdot)$ are Bessel functions of the second kind of the zero and the first order (see Appendix 7.13).

3. The extended solution accounting for the wellbore storage, written for the drawdown in the pumping well (Lai and Cheh-Wu Su 1974), is:

$$s_w = \frac{Q}{4\pi T} F_L\left(\frac{r_w^2 S}{4Tt}, \frac{r_w}{B}, S \frac{r_w^2}{r_c^2}\right), \quad (3.7)$$

$$F_L(u, \beta_2, \beta_3) = 32 \frac{\beta_3^2}{\pi^2} \int_0^\infty \left\{ \left[1 - \exp\left(-\frac{\tau^2 + \beta_2^2}{4u}\right) \right] \frac{\tau}{\tau^2 + \beta_2^2} \times \right. \\ \left. \times \frac{1}{[(\tau^2 + \beta_2^2) J_0(\tau) - 2\beta_3 \tau J_1(\tau)]^2 + [(\tau^2 + \beta_2^2) Y_0(\tau) - 2\beta_3 \tau Y_1(\tau)]^2} \right\} d\tau, \quad (3.8)$$

where s_w is the drawdown in the pumping well, m.

4. Hantush solution for a horizontally anisotropic aquifer (Hantush 1966; Hantush and Thomas 1966) is:

$$s = \frac{Q}{4\pi \sqrt{T_x T_y}} W\left[\frac{r^2 (T_y \cos^2 \theta + T_x \sin^2 \theta) S}{4T_x T_y t}, \frac{r}{B}\right], \quad (3.9)$$

with the leakage factor for the horizontally anisotropic aquifer of:

$$B = \sqrt{\frac{T_x m'}{k'}}, \quad (3.10)$$

where $T_x = k_x m$ and $T_y = k_y m$ are the transmissivities of the aquifer in two perpendicular horizontal directions, m²/d; k_x , k_y are the hydraulic conductivities in two perpendicular directions, m/d; θ is the angle in degrees between the x axis and the line connecting the pumping and observation wells (Fig. 3.3b).

The Eq. 3.9 implies that the abscissa coincides with the direction of anisotropy (Fig. 3.3b). For the case where the coordinate axes do not coincide (Fig. 3.3c), see comments to the analogous solution (Eq. 1.10) in a nonleaky aquifer.

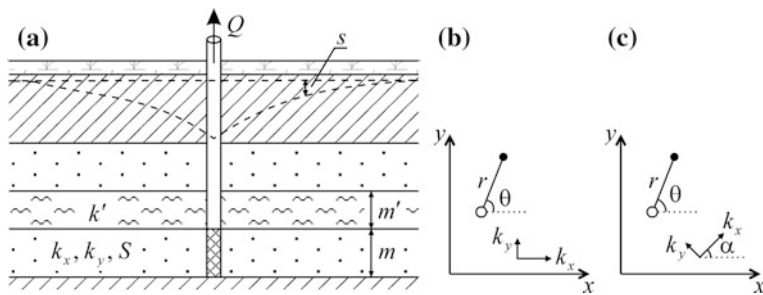


Fig. 3.3 A horizontally anisotropic leaky aquifer: **a** cross-section, **b**, **c** planar view: for the coordinate axis **b** coinciding and **c** not coinciding with the direction of anisotropy

Unlike all transient solutions given in this section, Eq. 3.9 is used to determine the transmissivities (T_x, T_y), the storage coefficient of the main aquifer (S), and the leakage factor (B), which can be evaluated from (Eq. 3.10).

Steady-State Flow Equations

1. The drawdown in the observation well (De Glee 1930; Jacob 1946)

$$s_m = \frac{Q}{2\pi T} K_0\left(\frac{r}{B}\right). \tag{3.11}$$

2. The drawdown in the pumping well

$$s_{mw} = \frac{Q}{2\pi T} \ln \frac{1.12B}{r_w}, \tag{3.11a}$$

where s_m, s_{mw} are the drawdowns in the observation and the pumping wells during steady-state period, m; $K_0(\cdot)$ is modified Bessel function of the second kind of the zero order (see Appendix 7.13).

Equation 3.11a follows from an approximation of function $K_0(\cdot)$ for small arguments (see Table A7.24).

In the case of a horizontally anisotropic layer, the transmissivity T in the solutions (Eqs. 3.11 and 3.11a) is replaced by the effective transmissivity $\sqrt{T_x T_y}$, and the leakage factor B is calculated by Eq. 3.10.

Graphic-Analytical Processing

The relationships given in Table 3.1 have been derived from Eqs. 3.1 and 3.11.

To evaluate the parameters of a horizontally anisotropic aquifer using the graphic-analytical methods, it is necessary: (1) to change the obtained transmissivity, T , to an effective transmissivity, $\sqrt{T_x T_y}$; (2) to use formula Eq. 3.10 for specification of the leakage factor, B ; (3) to change the obtained hydraulic diffusivity, a , to: $a = T_x/S$ (for $\theta = 0^\circ$), $a = T_y/S$ (for $\theta = 90^\circ$).

Table 3.1 Graphic-analytical parameter evaluation

Plot	Method	Relationship
$s - \lg t$	Horizontal straight line ^{a, b}	$T = \frac{Q}{2\pi \cdot A} K_0\left(\frac{r}{B}\right)$
$\lg s - \lg t$	Type curve ^b : $\lg W\left(u, \frac{r}{B}\right) - \lg \frac{1}{u}$	$T = \frac{Q}{4\pi \cdot 10^D}, a = \frac{r^2 10^E}{4}$
$\lg s - \lg \frac{t}{r^2}$	The same	$T = \frac{Q}{4\pi \cdot 10^D}, a = \frac{10^E}{4}$
$\lg s - \lg r$	Type curve ^a : $\lg K_0(\beta) - \lg \beta$	$T = \frac{Q}{2\pi \cdot 10^D}, B = 10^{-E}$
$(s_1 - s_2) - \lg t$	Horizontal straight line ^b	$T = \frac{Q}{2\pi \cdot A} \left[K_0\left(\frac{r_1}{B}\right) - K_0\left(\frac{r_2}{B}\right) \right]$

A is the intercept of the straight line on the ordinate axis (see Sect. 12.1.2); D, E are the shifts of the plots of the actual and type curves (see Sect. 12.1.3) in the vertical (D) and horizontal (E) directions; s_1, s_2, r_1, r_2 are the drawdown (s) and distance to the pumping well (r) for the first and second observation wells, respectively

^aBased on drawdown values for steady-state flow period

^bGiven the leakage factor B

3.1.2 Semi-infinite Aquifer

The basic assumptions and test conditions (Fig. 3.4) are:

- the main assumptions for an infinite leaky aquifer are given in Sect. 3.1.1;
- the boundary is linear and infinite.

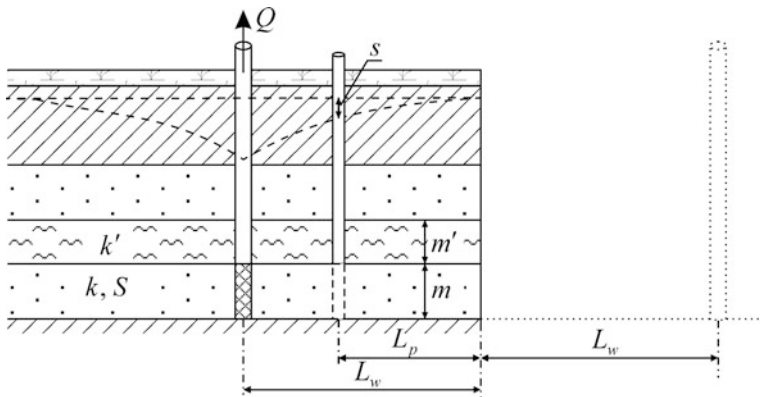


Fig. 3.4 A semi-infinite leaky aquifer. The *dashed line* on the right shows the image well. L_w, L_p are the distances from the pumping and observation wells to the boundary, respectively

Two variants of boundary conditions are considered (see Fig. A3.1): (1) constant-head boundary and (2) impermeable boundary.

To solve the problem, the image-well method is used: a single image well is introduced (for the distance to the image well and the sign of its discharge, see Fig. A3.2).

Basic Analytical Relationships

Transient-Flow Equation

$$s = \frac{Q}{4\pi T} \left[W\left(\frac{r^2}{4at}, \frac{r}{B}\right) \pm W\left(\frac{\rho^2}{4at}, \frac{\rho}{B}\right) \right], \quad (3.12)$$

where the signs “+” and “-” correspond to constant-head and impermeable boundary conditions, respectively; ρ is the distance between the real observation well and the image well (see Fig. A3.2 and Eq. A3.1), m.

Steady-State Flow Equation

$$s_m = \frac{Q}{2\pi T} \left[K_0\left(\frac{r}{B}\right) \pm K_0\left(\frac{\rho}{B}\right) \right]. \quad (3.13)$$

Graphic-Analytical Processing

The relationship given in Table 3.2 has been derived from Eq. 3.13.

3.1.3 Strip Aquifer

The basic assumptions and test conditions (Fig. 3.5) are:

- the main assumptions for an infinite leaky aquifer are given in Sect. 3.1.1;
- the two aquifer boundaries are approximated by two infinite parallel straight lines.

Three variants of boundary conditions are considered (see Fig. A3.3): (1) two constant-head boundaries, (2) two impermeable boundaries, and (3) mixed boundary conditions—constant-head and impermeable boundaries.

To solve the problem, the image-well method is used: image wells form an infinite row (for the distances to the image wells and the signs of their discharges, see Fig. A3.4).

Table 3.2 Graphic-analytical parameter evaluation

Plot	Method	Relationship
$s - \lg t$	Horizontal straight line ^a	$T = \frac{Q}{2\pi \cdot A} \left[K_0\left(\frac{r}{B}\right) \pm K_0\left(\frac{\rho}{B}\right) \right]$

^aBased on drawdown values for steady-state flow period given the leakage factor B

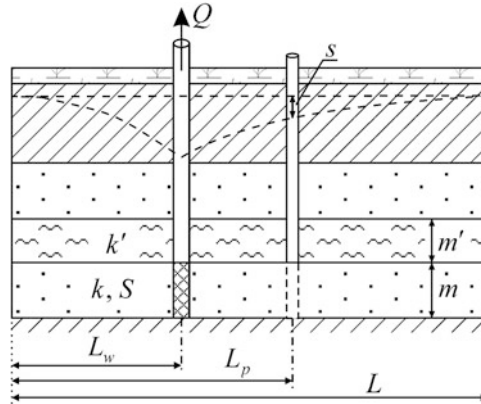


Fig. 3.5 A leaky aquifer, bounded by two parallel boundaries (strip aquifer). L is the width of the strip aquifer

Basic Analytical Relationships

Transient-Flow Equations

Constant-head boundary conditions

1. Solution based on the superposition principle:

$$s = \frac{Q}{4\pi T} \left\{ W\left(\frac{r^2}{4at}, \frac{r}{B}\right) + \sum_{j=1}^n (-1)^j \sum_{i=1}^2 W\left(\frac{(\rho_i^j)^2}{4at}, \frac{\rho_i^j}{B}\right) \right\}. \tag{3.14}$$

where $n \rightarrow \infty$ is the number of reflections from a boundary; ρ_i^j is the distance between the real observation well and the j -th image well reflected from the left ($i = 1$) or right ($i = 2$) boundary (see Fig. A3.4): determined by Eqs. A3.3 and A3.4, m.

2. Green’s function solution (Hantush and Jacob 1955a):

$$s = \frac{Q}{2\pi T} \sum_{n=1}^{\infty} \left\{ \frac{1}{\beta_n} \sin \frac{n\pi L_p}{L} \sin \frac{n\pi L_w}{L} \times \left(\exp\left(-\frac{\pi y}{L} \beta_n\right) \operatorname{erfc}\left(\sqrt{\frac{y^2}{4at}} - \frac{\pi\sqrt{at}}{L} \beta_n\right) - \exp\left(\frac{\pi y}{L} \beta_n\right) \operatorname{erfc}\left(\sqrt{\frac{y^2}{4at}} + \frac{\pi\sqrt{at}}{L} \beta_n\right) \right) \right\}, \tag{3.15}$$

where $\beta_n = \sqrt{n^2 + \left(\frac{L}{\pi B}\right)^2}$; L is the width of the strip aquifer, m; L_w and L_p are the distances from the pumping well and the observation well to the left boundary, m; y —see Eq. A3.2, m; $\operatorname{erfc}(\cdot)$ is the complementary error function (see Appendix 7.12).

Impermeable boundary conditions

1. Solution based on the superposition principle:

$$s = \frac{Q}{4\pi T} \left\{ W\left(\frac{r^2}{4at}, \frac{r}{B}\right) + \sum_{j=1}^n \sum_{i=1}^2 W\left(\frac{(\rho_i^j)^2}{4at}, \frac{\rho_i^j}{B}\right) \right\}. \quad (3.16)$$

2. Green's function solution (Hantush and Jacob 1955a):

$$s = \frac{Q}{2\pi T} \left\{ \frac{\pi B}{2L} \left[\exp\left(-\frac{y}{B}\right) \operatorname{erfc}\left(\sqrt{\frac{y^2}{4at}} - \frac{\sqrt{at}}{B}\right) - \exp\left(\frac{y}{B}\right) \operatorname{erfc}\left(\sqrt{\frac{y^2}{4at}} + \frac{\sqrt{at}}{B}\right) \right] + \sum_{n=1}^{\infty} \left[\frac{1}{\beta_n} \cos \frac{n\pi L_p}{L} \cos \frac{n\pi L_w}{L} \times \left(\exp\left(-\frac{\pi y}{L} \beta_n\right) \operatorname{erfc}\left(\sqrt{\frac{y^2}{4at}} - \frac{\pi\sqrt{at}}{L} \beta_n\right) - \exp\left(\frac{\pi y}{L} \beta_n\right) \operatorname{erfc}\left(\sqrt{\frac{y^2}{4at}} + \frac{\pi\sqrt{at}}{L} \beta_n\right) \right) \right] \right\}. \quad (3.17)$$

Combined boundary condition: constant-head at one aquifer boundary and impermeable at the other

Solution based on the superposition principle:

$$s = \frac{Q}{4\pi T} \left\{ W\left(\frac{r^2}{4at}, \frac{r}{B}\right) + \sum_{j=2,4,\dots}^n (-1)^{j/2} \sum_{i=1}^2 W\left(\frac{(\rho_i^j)^2}{4at}, \frac{\rho_i^j}{B}\right) + \sum_{j=1,3,\dots}^n \left[(-1)^{(j+1)/2} W\left(\frac{(\rho_1^j)^2}{4at}, \frac{\rho_1^j}{B}\right) + (-1)^{(j+3)/2} W\left(\frac{(\rho_2^j)^2}{4at}, \frac{\rho_2^j}{B}\right) \right] \right\}. \quad (3.18)$$

Steady-State Flow Equations

Constant-head boundary conditions

1. Solution based on superposition principle:

$$s_m = \frac{Q}{2\pi T} \left\{ K_0\left(\frac{r}{B}\right) + \sum_{j=1}^n (-1)^j \sum_{i=1}^2 K_0\left(\frac{\rho_i^j}{B}\right) \right\}. \quad (3.19)$$

2. Green's function solution (Hantush and Jacob 1954):

$$s_m = \frac{Q}{2\pi T} \sum_{n=1}^{\infty} 2 \left\{ \frac{1}{\beta_n} \exp\left(-\frac{\pi y}{L} \beta_n\right) \sin \frac{n\pi L_p}{L} \sin \frac{n\pi L_w}{L} \right\}. \quad (3.20)$$

Impermeable boundary conditions

1. Solution based on the superposition principle:

$$s_m = \frac{Q}{2\pi T} \left\{ K_0\left(\frac{r}{B}\right) + \sum_{j=1}^n \sum_{i=1}^2 K_0\left(\frac{\rho_i^j}{B}\right) \right\}. \quad (3.21)$$

2. Green's function solution (Hantush and Jacob 1954):

$$s_m = \frac{Q}{2\pi T} \left\{ \frac{\pi B}{L} \exp\left(-\frac{y}{B}\right) + 2 \sum_{n=1}^{\infty} \left[\frac{1}{\beta_n} \exp\left(-\frac{\pi y}{L} \beta_n\right) \cos \frac{n\pi L_p}{L} \cos \frac{n\pi L_w}{L} \right] \right\}. \quad (3.22)$$

Combined boundary condition: constant-head at one aquifer boundary and impermeable at the other

1. Solution based on superposition principle:

$$s_m = \frac{Q}{2\pi T} \left\{ K_0\left(\frac{r}{B}\right) + \sum_{j=1,3,\dots}^n \left[(-1)^{(j+1)/2} K_0\left(\frac{\rho_1^j}{B}\right) + (-1)^{(j+3)/2} K_0\left(\frac{\rho_2^j}{B}\right) \right] + \sum_{j=2,4,\dots}^n (-1)^{j/2} \sum_{i=1}^2 K_0\left(\frac{\rho_i^j}{B}\right) \right\}. \quad (3.23)$$

2. Green's function solution (Hantush and Jacob 1954):

$$s_m = \frac{Q}{2\pi T} \sum_{n=1}^{\infty} 4 \left\{ \frac{(-1)^n}{\beta_{2n}} \exp\left(-\frac{\pi y}{2L} \beta_{2n}\right) \sin \frac{(2n-1)\pi(L_p-2L)}{2L} \cos \frac{(2n-1)\pi(L_w-L)}{2L} \right\}, \quad (3.24)$$

where $\beta_{2n} = \sqrt{(2n-1)^2 + \left(\frac{2L}{\pi B}\right)^2}$. Here, L_p and L_w are the distances from the observation and pumping wells to the constant-head boundary, m.

Graphic-Analytical Processing

The relationship given in Table 3.3 has been derived from Eqs. 3.19–3.24.

Table 3.3 Graphic-analytical parameter evaluation

Plot	Method	Relationship
$s - \lg t$	Horizontal straight line ^a	$T = \frac{Q}{2\pi \cdot A} f$

f is the expression in Eqs. 3.19–3.24, following the ratio $Q/(2\pi T)$

^aBased on the drawdown values for steady-state flow period given the leakage factor B

3.1.4 Wedge-Shaped and U-Shaped Aquifers

Solutions for the drawdown in leaky aquifers with boundaries of those types are constructed with the use of superposition principle, similarly to the solutions for nonleaky aquifers (see Sects. 1.1.4 and 1.1.5). Here, instead of the well-function $W(u)$, a well-function for leaky aquifers $W(u, \beta)$ is used. For example, for a leaky aquifer with two intersecting constant-head boundaries, the transient solution (see Eq. 1.33) can be written as

$$s = \frac{Q}{4\pi T} \left[W\left(\frac{r^2}{4at}, \frac{r}{B}\right) + \sum_{j=1}^n (-1)^j W\left(\frac{\rho_j^2}{4at}, \frac{\rho_j}{B}\right) \right], \quad (3.25)$$

whereas for the drawdown during a steady-state flow period under such conditions:

$$s_m = \frac{Q}{2\pi T} \left[K_0\left(\frac{r}{B}\right) + \sum_{j=1}^n (-1)^j K_0\left(\frac{\rho_j}{B}\right) \right], \quad (3.26)$$

where ρ_j and n in Eqs. 3.25 and 3.26 see in Sect. 1.1.4.1.

3.1.5 Circular Aquifer

The basic assumptions and conditions (Fig. 3.6) are:

- the main assumptions for an infinite leaky aquifer are given in Sect. 3.1.1;
- the boundary is a circular boundary of groundwater flow passing along the outer contour of the aquifer;
- the pumping well is located in the center of the circular aquifer (concentrically) or shifted from the center (eccentrically).

One of two boundary conditions is specified on the outer contour of the aquifer system (see Fig. A3.10): (1) constant-head boundary or (2) impermeable boundary.

Basic Analytical Relationships

Transient Flow Equations

1. The pumping well is located in the center of the circular aquifer (Fig. 3.6a, c).

1.1. A constant-head boundary is specified on the outer contour of the aquifer (Jacob 1946; Hantush and Jacob 1960):

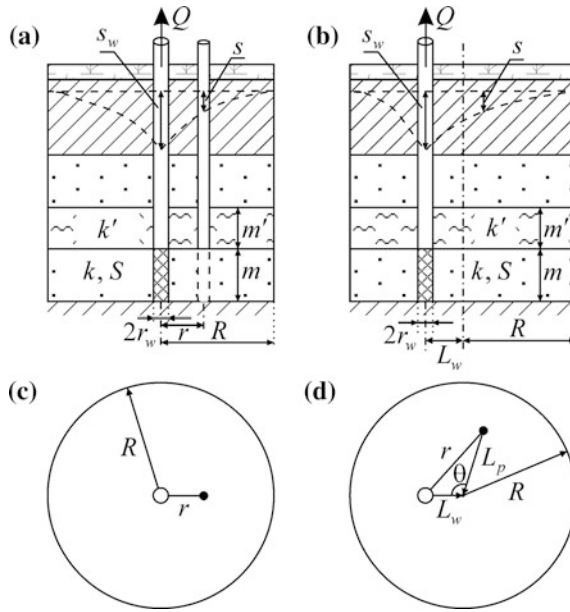


Fig. 3.6 Circular leaky aquifer system. **a, b** Cross-sections, **c, d** planar views; **a, c** the pumping well is located in the center of the aquifer or **b, d** is shifted from the center. L_w, L_p are the distances from the pumping and observation wells to the center of the circular aquifer; R is the radius of the circle

$$s = \frac{Q}{2\pi T} \left[K_0\left(\frac{r}{B}\right) - \frac{K_0\left(\frac{R}{B}\right)I_0\left(\frac{r}{B}\right)}{I_0\left(\frac{R}{B}\right)} - 2 \sum_{n=1}^{\infty} \frac{J_0\left(x_n \frac{r}{R}\right) \exp\left[-\left(x_n^2 + \frac{R^2}{B^2}\right) \frac{at}{R^2}\right]}{J_1^2(x_n) \left(x_n^2 + \frac{R^2}{B^2}\right)} \right], \quad (3.27)$$

where x_n are positive roots of the equation $J_0(x_n) = 0$ (see Appendix 7.15); R is the radius of a circular aquifer, m.

1.2. The aquifer contour is an impermeable boundary (Hantush and Jacob 1960):

$$s = \frac{Q}{2\pi T} \left[\frac{K_0\left(\frac{r}{B}\right) + I_0\left(\frac{r}{B}\right)K_1\left(\frac{R}{B}\right) / I_1\left(\frac{R}{B}\right) - 2 \frac{R^2}{B^2} \exp\left(-\frac{at}{B^2}\right)}{-2 \sum_{n=1}^{\infty} \frac{J_0\left(x_{n,1} \frac{r}{R}\right) \exp\left[-\left(x_{n,1}^2 + \frac{R^2}{B^2}\right) \frac{at}{R^2}\right]}{J_0^2(x_{n,1}) \left(x_{n,1}^2 + \frac{R^2}{B^2}\right)}} \right], \quad (3.28)$$

where $x_{n,1}$ are positive roots of the equation $J_1(x_{n,1}) = 0$ (see Appendix 7.15); $I_0(\cdot)$ and $I_1(\cdot)$ are modified Bessel functions of the first kind of the zero and the first order; $K_0(\cdot)$ and $K_1(\cdot)$ are modified Bessel functions of the second kind of the zero and the first order (see Appendix 7.13).

2. The pumping well is located off-centered in a circular aquifer (Fig. 3.6b, d).

2.1. The aquifer contour is a constant-head boundary (Hantush and Jacob 1960):

$$\begin{aligned}
 s = & \frac{Q}{2\pi T} \left\{ K_0\left(\frac{r}{B}\right) - K_0\left(\frac{R}{B}\right) I_0\left(\frac{L_w}{B}\right) I_0\left(\frac{L_p}{B}\right) / I_0\left(\frac{R}{B}\right) - \right. \\
 & - 2 \sum_{m=1}^{\infty} K_m\left(\frac{R}{B}\right) I_m\left(\frac{L_w}{B}\right) I_m\left(\frac{L_p}{B}\right) / I_m\left(\frac{R}{B}\right) \cos(m\theta) - \\
 & - 2 \sum_{n=1}^{\infty} \frac{J_0\left(x_n \frac{L_w}{R}\right) J_0\left(x_n \frac{L_p}{R}\right)}{\left(x_n^2 + \frac{R^2}{B^2}\right) J_1^2(x_n)} \exp\left[-\left(x_n^2 + \frac{R^2}{B^2}\right) \frac{at}{R^2}\right] - \\
 & \left. - 4 \sum_{m=1}^{\infty} \sum_{n=1}^{\infty} \frac{J_m\left(x_{n,m} \frac{L_w}{R}\right) J_m\left(x_{n,m} \frac{L_p}{R}\right)}{\left(x_{n,m}^2 + \frac{R^2}{B^2}\right) J_{m+1}^2(x_{n,m})} \cos(m\theta) \exp\left[-\left(x_{n,m}^2 + \frac{R^2}{B^2}\right) \frac{at}{R^2}\right] \right\}, \quad (3.29)
 \end{aligned}$$

where $x_{n,m}$ are positive roots of equation $J_m(x_{n,m}) = 0$ (see Appendix 7.15); $J_m(\cdot)$ is Bessel function of the first kind of the m order; $I_m(\cdot)$ and $K_m(\cdot)$ are modified Bessel functions of the first and the second kind of the m order (see Appendix 7.13); θ is the angle between vectors from the center of the circular aquifer to the pumping and observation wells, respectively (Fig. 3.6d), degree: it is determined from Eq. 1.69; L_w , L_p are the distances from the pumping and observation wells to the center of the circular aquifer, m .

2.2. The aquifer contour is an impermeable boundary (Hantush and Jacob 1960):

$$\begin{aligned}
 s = & \frac{Q}{2\pi T} \left\{ K_0\left(\frac{r}{B}\right) + K_1\left(\frac{R}{B}\right) I_0\left(\frac{L_w}{B}\right) I_0\left(\frac{L_p}{B}\right) / I_1\left(\frac{R}{B}\right) + \right. \\
 & + 2 \sum_{m=1}^{\infty} \frac{\left[K_{m+1}\left(\frac{R}{B}\right) + K_{m-1}\left(\frac{R}{B}\right) \right] I_m\left(\frac{L_w}{B}\right) I_m\left(\frac{L_p}{B}\right)}{I_{m+1}\left(\frac{R}{B}\right) + I_{m-1}\left(\frac{R}{B}\right)} \cos(m\theta) - 2 \frac{R^2}{B^2} \exp\left[-\frac{at}{B^2}\right] - \\
 & - 2 \sum_{n=1}^{\infty} \frac{J_0\left(y_{n,0} \frac{L_w}{R}\right) J_0\left(y_{n,0} \frac{L_p}{R}\right)}{\left(y_{n,0}^2 + \frac{R^2}{B^2}\right) J_0^2(y_{n,0})} \exp\left[-\left(y_{n,0}^2 + \frac{R^2}{B^2}\right) \frac{at}{R^2}\right] - \\
 & \left. - 4 \sum_{m=1}^{\infty} \sum_{n=1}^{\infty} \frac{J_m\left(y_{n,m} \frac{L_w}{R}\right) J_m\left(y_{n,m} \frac{L_p}{R}\right)}{\left(y_{n,m}^2 - m^2\right) \left(1 + \frac{R^2}{B^2 y_{n,m}^2}\right) J_m^2(y_{n,m})} \cos(m\theta) \exp\left[-\left(y_{n,m}^2 + \frac{R^2}{B^2}\right) \frac{at}{R^2}\right] \right\}, \quad (3.30)
 \end{aligned}$$

where $y_{n,m}$ are positive roots of equation $J'_m(y_{n,m}) = 0$ (see Appendix 7.15).

Steady-State Flow Equations

1. The pumping well is located in the center of a circular aquifer (Fig. 3.6a, c).

1.1. The outer contour of the aquifer is a constant-head boundary.

1.1.1. The drawdown in the observation well (Jacob 1946) is:

$$s_m = \frac{Q}{2\pi T} \left[K_0\left(\frac{r}{B}\right) - K_0\left(\frac{R}{B}\right) I_0\left(\frac{r}{B}\right) / I_0\left(\frac{R}{B}\right) \right]. \quad (3.31)$$

1.1.2. The solution for the drawdown in the pumping well is:

$$s_{mw} = \frac{Q}{2\pi T} \left[K_0\left(\frac{r_w}{B}\right) - K_0\left(\frac{R}{B}\right) / I_0\left(\frac{R}{B}\right) \right]. \quad (3.32)$$

The solution (Eq. 3.32) has been derived from Eq. 3.31. For practical calculations, $K_0(r_w/B)$ can be replaced by $\ln(1.12B/r_w)$.

1.2. The aquifer contour is an impermeable boundary.

1.2.1. The drawdown in the observation well (Bochever 1963) is:

$$s_m = \frac{Q}{2\pi T} \frac{B}{r_w} \frac{K_0\left(\frac{r}{B}\right) I_1\left(\frac{R}{B}\right) + K_1\left(\frac{R}{B}\right) I_0\left(\frac{r}{B}\right)}{K_1\left(\frac{r_w}{B}\right) I_1\left(\frac{R}{B}\right) - K_1\left(\frac{R}{B}\right) I_1\left(\frac{r_w}{B}\right)}. \quad (3.33)$$

Equation 3.33, which takes into account the wellbore storage, can be applied to aquifers of arbitrary radius (R); however, the simplified solution below is quite enough for practical calculations when $R/r_w > 5$ (Hantush and Jacob 1960):

$$s_m = \frac{Q}{2\pi T} \left[K_0\left(\frac{r}{B}\right) + I_0\left(\frac{r}{B}\right) K_1\left(\frac{R}{B}\right) / I_1\left(\frac{R}{B}\right) \right]. \quad (3.34)$$

1.2.2. The solution for the drawdown in the pumping well (Bochever 1968) is:

$$s_{mw} \approx \frac{Q}{2\pi T} \left[\ln \frac{1.123B}{r_w} + K_1\left(\frac{R}{B}\right) / I_1\left(\frac{R}{B}\right) \right]. \quad (3.35)$$

The solution (Eq. 3.35) follows from Eq. 3.34.

2. The pumping well is located off-center in a circular aquifer (Fig. 3.6b, d).

2.1. The outer contour of the aquifer is a constant-head boundary.

2.1.1. The drawdown in the observation well (Hantush and Jacob 1960) is:

$$s_m = \frac{Q}{2\pi T} \left[\begin{aligned} & \left[\text{K}_0\left(\frac{r}{B}\right) - \text{K}_0\left(\frac{R}{B}\right) \text{I}_0\left(\frac{L_w}{B}\right) \text{I}_0\left(\frac{L_p}{B}\right) / \text{I}_0\left(\frac{R}{B}\right) - \right. \\ & \left. - 2 \sum_{m=1}^{\infty} \cos(m\theta) \text{K}_m\left(\frac{R}{B}\right) \text{I}_m\left(\frac{L_w}{B}\right) \text{I}_m\left(\frac{L_p}{B}\right) / \text{I}_m\left(\frac{R}{B}\right) \right] \end{aligned} \right]. \quad (3.36)$$

2.1.2. The drawdown in the pumping well (Hantush and Jacob 1960) is:

$$s_{mw} = \frac{Q}{2\pi T} \left[\text{K}_0\left(\frac{r_w}{B}\right) - \frac{\text{K}_0\left(\frac{R}{B}\right) \text{I}_0^2\left(\frac{L_w}{B}\right)}{\text{I}_0\left(\frac{R}{B}\right)} - 2 \sum_{m=1}^{\infty} \frac{\text{K}_m\left(\frac{R}{B}\right) \text{I}_m^2\left(\frac{L_w}{B}\right)}{\text{I}_m\left(\frac{R}{B}\right)} \right]. \quad (3.37)$$

2.2. The aquifer contour is an impermeable boundary.

2.2.1. The drawdown in the observation well (Hantush and Jacob 1960) is:

$$s_m = \frac{Q}{2\pi T} \left[\begin{aligned} & \left[\text{K}_0\left(\frac{r}{B}\right) + \text{K}_1\left(\frac{R}{B}\right) \text{I}_0\left(\frac{L_w}{B}\right) \text{I}_0\left(\frac{L_p}{B}\right) / \text{I}_1\left(\frac{R}{B}\right) + \right. \\ & \left. + 2 \sum_{m=1}^{\infty} \frac{\left[\text{K}_{m+1}\left(\frac{R}{B}\right) + \text{K}_{m-1}\left(\frac{R}{B}\right) \right] \text{I}_m\left(\frac{L_w}{B}\right) \text{I}_m\left(\frac{L_p}{B}\right)}{\text{I}_{m+1}\left(\frac{R}{B}\right) + \text{I}_{m-1}\left(\frac{R}{B}\right)} \cos(m\theta) \right] \end{aligned} \right]. \quad (3.38)$$

2.2.2. The drawdown in the pumping well is:

$$s_{mw} = \frac{Q}{2\pi T} \left[\text{K}_0\left(\frac{r_w}{B}\right) + \frac{\text{K}_1\left(\frac{R}{B}\right) \text{I}_0^2\left(\frac{L_w}{B}\right)}{\text{I}_1\left(\frac{R}{B}\right)} + 2 \sum_{m=1}^{\infty} \frac{\left[\text{K}_{m+1}\left(\frac{R}{B}\right) + \text{K}_{m-1}\left(\frac{R}{B}\right) \right] \text{I}_m^2\left(\frac{L_w}{B}\right)}{\text{I}_{m+1}\left(\frac{R}{B}\right) + \text{I}_{m-1}\left(\frac{R}{B}\right)} \right]. \quad (3.39)$$

The solution (Eq. 3.39) has been derived from solution Eq. 3.38.

3.2 Leaky Aquifer with Transient Flow in the Adjacent Aquifers

This section gives transient analytical solutions for a leaky aquifer with the hydraulic head in the adjacent aquifer varying because of pumping. Two configurations of flow domain are considered: an aquifer of infinite lateral extent (Sect. 3.2.1) and a circular aquifer (Sect. 3.2.2). The solutions are used to determine the transmissivity and hydraulic diffusivity of the main and adjacent aquifers (T_1 , a_1 , T_2 , a_2) and the

leakage factor for the main aquifer (B_1). The hydraulic parameters are derived from the data on the drawdown in the main and adjacent aquifers.

3.2.1 Aquifer of Infinite Lateral Extent

The basic assumptions and conditions (Fig. 3.7) are:

- the leaky aquifer system consists of two confined isotropic aquifers separated by an aquitard;
- the main aquifer (1) is penetrated by the pumping well;
- the adjacent aquifer (2) is an unpumped aquifer; the water level in this aquifer changes during the pumping test because of pumping;
- the initial water levels in the aquifers can be either the same or different;
- the aquifer has no lateral boundaries (infinite in the horizontal plane);
- the pumping well fully penetrates the main aquifer; the wellbore storage is not taken into account;
- the aquitard storage is neglected.

The drawdown is determined at any distance from the pumping well in the main and adjacent aquifers. A characteristic plot of drawdown in the observation well located in the main aquifer is given in Fig. 12.22 (curve 3). For solutions for the drawdown in the case of simultaneous water withdrawal from two aquifers, see Sect. 10.3.

Basic Analytical Relationships

Transient Flow Equations (Hantush 1967):

1. The drawdown in the main aquifer is

$$s^{(1)} = \frac{Q}{2\pi(T_1 + T_2)} (\psi_1 - \psi_2 + \psi_3 + \psi_4). \tag{3.40}$$

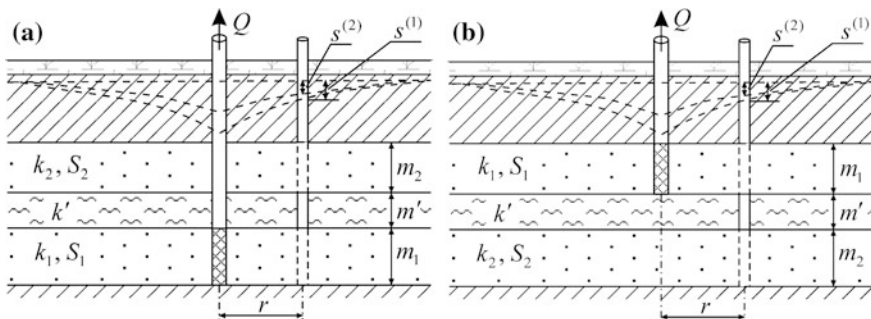


Fig. 3.7 A leaky aquifer with transient flow in the adjacent aquifer. The main aquifer is located in different parts of the cross-section: **a** in the lower part, and **b** in the upper part

2. The drawdown in the adjacent aquifer is:

$$s^{(2)} = \frac{Q}{2\pi(T_1 + T_2)} (\psi_1 - \psi_2), \quad (3.41)$$

$$\psi_1 = \frac{a_1 r^2}{a_2 B^{*2}} \int_0^\infty \left[1 - \exp\left(-\varphi_3 \frac{a_2 t}{r^2}\right) \right] \frac{\tau}{\varphi_1 \varphi_3} J_0(\tau) d\tau, \quad (3.42)$$

$$\psi_2 = \frac{a_1 r^2}{a_2 B^{*2}} \int_0^\infty \left[1 - \exp\left(-\varphi_2 \frac{a_2 t}{r^2}\right) \right] \frac{\tau}{\varphi_1 \varphi_2} J_0(\tau) d\tau, \quad (3.43)$$

$$\psi_3 = \frac{a_1}{a_2} \left(1 + \frac{T_2}{T_1} \right) \int_0^\infty \left[(\varphi_3 - \tau^2) \exp\left(-\varphi_3 \frac{a_2 t}{r^2}\right) \right] \frac{\tau}{\varphi_1 \varphi_3} J_0(\tau) d\tau, \quad (3.44)$$

$$\psi_4 = \frac{a_1}{a_2} \left(1 + \frac{T_2}{T_1} \right) \int_0^\infty \left[\frac{\varphi_1 \tau^2}{\varphi_3} - (\varphi_2 - \tau^2) \exp\left(-\varphi_2 \frac{a_2 t}{r^2}\right) \right] \frac{\tau}{\varphi_1 \varphi_2} J_0(\tau) d\tau, \quad (3.45)$$

$$\varphi_1 = \sqrt{\left[\left(1 - \frac{a_1}{a_2} \right) \tau^2 + \left(\frac{r}{B_2} \right)^2 - \frac{a_1}{a_2} \left(\frac{r}{B_1} \right)^2 \right]^2 + 4 \frac{a_1}{a_2} \left(\frac{r^2}{B_1 B_2} \right)^2}, \quad (3.46)$$

$$\varphi_2 = 0.5 \left[\left(1 + \frac{a_1}{a_2} \right) \tau^2 + \left(\frac{r}{B_2} \right)^2 + \frac{a_1}{a_2} \left(\frac{r}{B_1} \right)^2 + \varphi_1 \right], \quad (3.47)$$

$$\varphi_3 = 0.5 \left[\left(1 + \frac{a_1}{a_2} \right) \tau^2 + \left(\frac{r}{B_2} \right)^2 + \frac{a_1}{a_2} \left(\frac{r}{B_1} \right)^2 - \varphi_1 \right]; \quad (3.48)$$

$$\frac{1}{B^{*2}} = \frac{1}{B_1^2} + \frac{1}{B_2^2} \quad (3.49)$$

or in another form:

$$B^* = \sqrt{T^* \frac{m'}{k'}}, \quad (3.50)$$

$$T^* = \frac{T_1 T_2}{T_1 + T_2}, \quad (3.51)$$

$$B_1 = \sqrt{T_1 \frac{m'}{k'}}, \quad (3.52)$$

$$B_2 = \sqrt{T_2 \frac{m'}{k'}} = B_1 \sqrt{\frac{T_2}{T_1}}, \quad (3.53)$$

where $s^{(1)}$, $s^{(2)}$ are the drawdown values in the observation wells in the main and the adjacent aquifer, respectively, m; $T_1 = k_1 m_1$ and $T_2 = k_2 m_2$ are the transmissivities of the main and adjacent aquifers, respectively, m^2/d ; k_1 , m_1 and k_2 , m_2 are the hydraulic conductivities (m/d) and thicknesses (m) of the main and adjacent aquifers; $a_1 = T_1/S_1$ and $a_2 = T_2/S_2$ are the hydraulic diffusivities of the main and adjacent aquifers, respectively, m^2/d ; S_1 and S_2 are specific storages of the main and adjacent aquifers, respectively, dimensionless; k' and m' are the hydraulic conductivity (m/d) and thickness (m) of the aquitard, respectively.

3. The drawdown in the main aquifer, when the main and adjacent aquifers have the same hydraulic diffusivity:

$$s^{(1)} = \frac{Q}{4\pi(T_1 + T_2)} \left[W\left(\frac{r^2}{4at}\right) + \frac{T_2}{T_1} W\left(\frac{r^2}{4at}, \frac{r}{B^*}\right) \right], \quad (3.54)$$

where $a = a_1 = a_2$ is the hydraulic diffusivity of the main and adjacent aquifers, m^2/d ; $W(\cdot)$ is the well-function (see Appendix 7.1).

4. The drawdown in the adjacent aquifer, when the main and adjacent aquifers have the same hydraulic diffusivity is:

$$s^{(2)} = \frac{Q}{4\pi(T_1 + T_2)} \left[W\left(\frac{r^2}{4at}\right) - W\left(\frac{r^2}{4at}, \frac{r}{B^*}\right) \right]. \quad (3.55)$$

Quasi-Steady-State Flow Equations (Hantush 1967)

1. The drawdown in the main aquifer is:

$$s^{(1)} = \frac{Q}{4\pi(T_1 + T_2)} \left[\ln \frac{2.25a^*t}{r^2} + 2 \frac{T_2}{T_1} K_0\left(\frac{r}{B^*}\right) \right], \quad (3.56)$$

$$a^* = \frac{2a_1a_2}{a_1 + a_2}. \quad (3.57)$$

2. The drawdown in the adjacent aquifer is:

$$s^{(2)} = \frac{Q}{4\pi(T_1 + T_2)} \left[\ln \frac{2.25a^*t}{r^2} - 2K_0\left(\frac{r}{B^*}\right) \right]. \quad (3.58)$$

Graphic-Analytical Processing

The relationship given in Table 3.4 has been derived from Eq. 3.56 or 3.58. Although those solutions have been derived from transient-flow as in Eq. 3.54 or Eq. 3.55 for equal hydraulic diffusivities in the main and adjacent aquifers, the straight-line method still can be used when this condition is not satisfied.

Table 3.4 Graphic-analytical parameter evaluation

Plot	Method	Relationship
$s \text{---} \lg t$	Straight line	$T_1 + T_2 = \frac{0.183Q}{C}$

C is the slope of the straight line (see Sect. 12.1.1)

3.2.2 Circular Aquifer

The basic assumptions and conditions (Fig. 3.8) are:

- the main assumptions for infinite leaky aquifer are given in Sect. 3.2.1;
- the outer contour of the aquifer is a circular boundary of groundwater flow;
- the pumping well is located in the center of the circular aquifer system, in either its top or bottom aquifer.

The outer contour of the aquifer system (Fig. A3.10a, c) is either (1) constant-head boundary or (2) impermeable boundary.

Basic Analytical Relationships

Transient Flow Equations

1. The outer contour of the aquifer is a constant-head boundary (Hantush 1967).
 - 1.1. The drawdown in the main aquifer is:

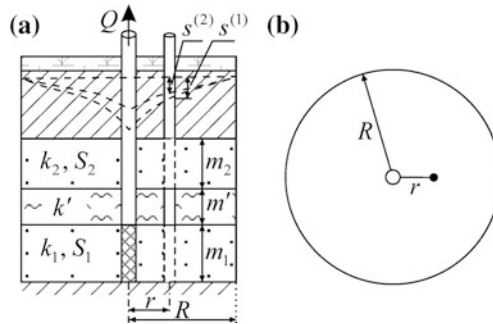


Fig. 3.8 Circular leaky aquifer system with transient flow in the adjacent aquifer: **a** cross-section and **b** planar view. R is the radius of the circle

$$\begin{aligned}
s^{(1)} = & \frac{Q}{2\pi(T_1 + T_2)} \left\{ \ln \frac{R}{r} + \frac{T_2}{T_1} \left[K_0 \left(\frac{r}{B^*} \right) - K_0 \left(\frac{R}{B^*} \right) I_0 \left(\frac{r}{B^*} \right) / I_0 \left(\frac{R}{B^*} \right) \right] - \right. \\
& - \frac{2a_1 R^2}{a_2 B^{*2}} \sum_{n=1}^{\infty} \left[\frac{1}{\lambda_n} \left(\frac{1}{\varepsilon_n} \exp \left(-\varepsilon_n \frac{a_2 t}{R^2} \right) - \right) \frac{J_0 \left(x_n \frac{r}{R} \right)}{J_1^2(x_n)} \right] - \\
& \left. - \frac{2a_1 B_2^2}{a_2 B^{*2}} \sum_{n=1}^{\infty} \left[\frac{1}{\lambda_n} \left(\left(1 - \frac{x_n^2}{\delta_n} \right) \exp \left(-\delta_n \frac{a_2 t}{R^2} \right) - \right) \frac{J_0 \left(x_n \frac{r}{R} \right)}{J_1^2(x_n)} \right] \right\}, \tag{3.59}
\end{aligned}$$

$$\lambda_n = \sqrt{\left[\left(1 - \frac{a_1}{a_2} \right) x_n^2 + \frac{R^2}{B_2^2} - \frac{a_1 R^2}{a_2 B_1^2} \right]^2 + 4 \frac{a_1 R^4}{a_2 B_2^2 B_1^2}}, \tag{3.60}$$

$$\delta_n = 0.5 \left[\left(1 + \frac{a_1}{a_2} \right) x_n^2 + \frac{R^2}{B_2^2} + \frac{a_1 R^2}{a_2 B_1^2} + \lambda_n \right], \tag{3.61}$$

$$\varepsilon_n = 0.5 \left[\left(1 + \frac{a_1}{a_2} \right) x_n^2 + \frac{R^2}{B_2^2} + \frac{a_1 R^2}{a_2 B_1^2} - \lambda_n \right], \tag{3.62}$$

where B^* , B_1 , B_2 are determined by Eqs. 3.49–3.53.

1.1. The drawdown in the adjacent aquifer is:

$$s^{(2)} = \frac{Q}{2\pi(T_1 + T_2)} \left\{ \ln \frac{R}{r} - K_0 \left(\frac{r}{B^*} \right) + K_0 \left(\frac{R}{B^*} \right) I_0 \left(\frac{r}{B^*} \right) / I_0 \left(\frac{R}{B^*} \right) - \right. \\
\left. - 2 \frac{a_1 R^2}{a_2 B^{*2}} \sum_{n=1}^{\infty} \left[\frac{1}{\lambda_n} \left(\frac{1}{\varepsilon_n} \exp \left(-\varepsilon_n \frac{a_2 t}{R^2} \right) - \right) \frac{J_0 \left(x_n \frac{r}{R} \right)}{J_1^2(x_n)} \right] \right\}. \tag{3.63}$$

2. The contour of the aquifer is an impermeable boundary. The drawdown in the main and adjacent aquifers (Bochever 1968) is:

$$s = \frac{Q}{4\pi T} \left\{ \pm \left[\begin{aligned} & \left[2 \frac{at}{R^2} + \ln \frac{R}{r} - \frac{2}{3} + \frac{r^2}{2R^2} - 2 \sum_{n=1}^{\infty} \frac{J_0 \left(x_{n,1} \frac{r}{R} \right) \exp \left(-x_{n,1}^2 \frac{at}{R^2} \right)}{x_{n,1}^2 J_0^2(x_{n,1})} \right] \pm \\ & \left[K_0 \left(\frac{r}{B} \right) + I_0 \left(\frac{r}{B} \right) \frac{K_1 \left(\frac{R}{B} \right)}{I_1 \left(\frac{R}{B} \right)} - 2 \frac{B^2}{R^2} \exp \left(-\frac{R^2}{B^2} \frac{at}{R^2} \right) - \right. \\ & \left. - 2 \sum_{n=1}^{\infty} \frac{J_0 \left(x_{n,1} \frac{r}{R} \right) \exp \left[-\left(x_{n,1}^2 + \frac{R^2}{B^2} \right) \frac{at}{R^2} \right]}{J_0^2(x_{n,1}) \left(x_{n,1}^2 + \frac{R^2}{B^2} \right)} \right] \right\}, \end{aligned} \right. \quad (3.64)$$

where “ \pm ” denotes the sign “+” corresponding to the drawdown determined in the observation well in the main aquifer ($s = s^{(1)}$), and “-” is the drawdown determined in the observation well in the adjacent aquifer ($s = s^{(2)}$).

Steady-State Flow Equations (Hantush 1967)

The steady-state flow regime will be reached when the outer contour of the circular aquifer is a constant-head boundary.

1. The drawdown in the main aquifer is:

$$s_m^{(1)} = \frac{Q}{2\pi(T_1 + T_2)} \left\{ \ln \frac{R}{r} + \frac{T_2}{T_1} \left[K_0 \left(\frac{r}{B^*} \right) - K_0 \left(\frac{R}{B^*} \right) I_0 \left(\frac{r}{B^*} \right) / I_0 \left(\frac{R}{B^*} \right) \right] \right\}. \quad (3.65)$$

2. The drawdown in the adjacent aquifer is:

$$s_m^{(2)} = \frac{Q}{2\pi(T_1 + T_2)} \left\{ \ln \frac{R}{r} - \left[K_0 \left(\frac{r}{B^*} \right) - K_0 \left(\frac{R}{B^*} \right) I_0 \left(\frac{r}{B^*} \right) / I_0 \left(\frac{R}{B^*} \right) \right] \right\}. \quad (3.66)$$

During the steady-state flow period, the drawdown values in the interacting aquifers are nearly the same. The comparison of solutions (Eqs. 3.65 and 3.66) with solutions for an aquifer of infinite lateral extent (Eqs. 3.56 and 3.58) shows them to differ in the second term in the square brackets, which tends to zero with increasing radius R and becomes significant when the aquifer radius is small.

3.3 Leaky Aquifer with Allowance Made for Aquitard Storage

This section gives transient analytical solutions for a leaky aquifer with infinite lateral extent, taking into account the aquitard storage, and the formation of a depression cone in the adjacent aquifer under the influence of the pumping test. The solutions are used to evaluate the hydraulic parameters of this system based on data on the drawdown in the main aquifer, the adjacent aquifer, and the aquitard.

Some particular solutions for a slightly leaky aquitard (Neuman and Witherspoon 1968) are also presented: the drawdown in the aquitard can be measured and used for data analysis, but the leakage itself can be neglected in the evaluation of parameters of the main aquifer, i.e., the aquifer being tested is considered as an isolated confined layer (see Sect. 1.1.1).

The basic assumptions and conditions (Fig. 3.9) are:

- the leaky aquifer system is a confined system comprising two isotropic aquifers separated by an aquitard; a particular case is an aquifer in contact with a semi-infinite compressible aquitard underlying or overlying it (Fig. 3.10);
- the main aquifer (1) is penetrated by the pumping well;
- the adjacent aquifer (2) is an unpumped aquifer; the water level in the adjacent aquifer remains constant or varies as a result of pumping;
- the aquitard storage is taken into account;
- the aquifer has no lateral boundaries (infinite in the horizontal plane);
- the pumping well fully penetrates the main aquifer; the storage of the well is not taken into account.

The drawdown is determined at any distance from the pumping well in the main and adjacent aquifers, as well as in any point of the aquitard. Typical drawdown plots in an observation well in the main aquifer are given in Fig. 12.22 (curves 2, 4).

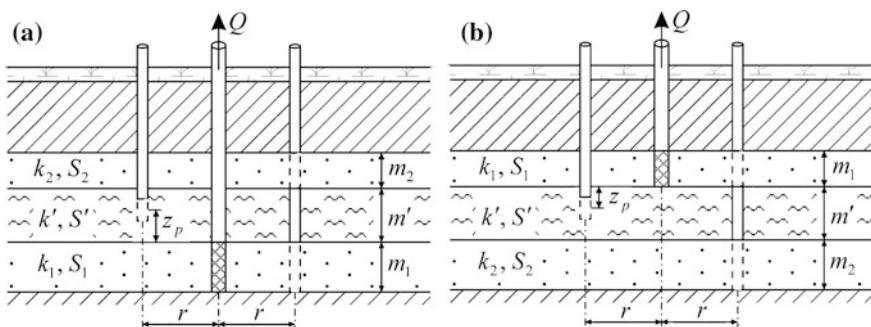


Fig. 3.9 A leaky aquifer with allowance made for aquitard storage. The main aquifer is located in different parts of the cross-section: **a** in the lower part, and **b** in the upper part

Basic Analytical Relationships

Transient Flow Equations (Neuman and Witherspoon 1969a, b)

1. Solutions for the drawdown in the main aquifer (1) and the separating aquitard at a constant water level in the adjacent aquifer (2) during the pumping test are considered.

1.1. The drawdown in the main aquifer is:

$$s^{(1)} = \frac{Q}{2\pi T_1} \int_0^{\infty} [1 - \exp(-\tau^2 u_\lambda)] J_0(\omega_1) \frac{d\tau}{\tau}, \quad (3.67)$$

$$u_\lambda = \frac{T_1 t}{S_1 r^2} \lambda_1. \quad (3.68)$$

1.2. The drawdown in the aquitard is:

$$s' = \frac{Q}{4\pi T_1} \frac{4}{\pi} \sum_{n=1}^{\infty} \left\{ \frac{1}{n} \sin \frac{n\pi z_p}{m'} \int_0^{\infty} \left[\frac{1 - \exp(-n^2 \pi^2 u_\lambda) + \frac{\exp(-n^2 \pi^2 u_\lambda) - \exp(-\tau^2 u_\lambda)}{1 - \tau^2 / (n^2 \pi^2)}}{J_0(\omega_1)} \frac{d\tau}{\tau} \right] \right\}, \quad (3.69)$$

where s' is the drawdown values in the observation wells in the aquitard, m ; ω_1 in (Eqs. 3.67 and 3.69) is calculated as

$$\omega_1 = \sqrt{\lambda_1 \tau^2 - (r/B_1)^2 \tau \cotan \tau}; \quad (3.70)$$

B_1 —see formula (Eq. 3.52); S_1 is the storage coefficient of the main aquifer, dimensionless; z_p is the distance from the observation point in the separating aquitard to the top (or bottom) of the main aquifer (Fig. 3.9), m ; λ_1 —see formula (Eq. 3.81).

1.3. The drawdown in the aquitard for a slightly leaky aquifer (Neuman and Witherspoon 1968) is:

$$s' = \frac{Q}{4\pi T_1} \frac{4}{\pi} \sum_{n=1}^{\infty} \left[\frac{1}{n} \sin \frac{n\pi z_p}{m'} \int_0^u \mathbf{W} \left(\frac{n^2 \pi^2 r^2 a'}{4(n^2 \pi^2 a' t - m'^2 \tau^2) a_1} \right) \tau \exp(-\tau^2) d\tau \right], \quad (3.71)$$

where

$$u = \frac{n\pi \sqrt{a' t}}{m'}, \quad (3.72)$$

or an approximation for long time periods:

$$s' = \frac{Q}{4\pi T_1} \left(1 - \frac{z_p}{m'}\right) W\left(\frac{r^2}{4a_1 t}\right), \quad (3.73)$$

where $a_1 = T_1/S_1$ and $a' = k'm'/S'$ are the hydraulic diffusivities of the main aquifer and the aquitard, respectively, m^2/d ; S' is the storage coefficient of the aquitard, dimensionless; $W(\cdot)$ is the well-function (see Appendix 7.1).

For a leaky aquifer with steady-state flow in the adjacent aquifer, the hydraulic parameters will be calculated based on data on the drawdown in the main aquifer and the aquitard. Equations 3.67 and 3.69 are used to evaluate the transmissivity and the storage coefficient of the main aquifer (T_1 , S_1), the leakage factor (B_1), and the storage coefficient of the aquitard (S'). The parameters determined by the solution neglecting the leakage (Eq. 3.71) are the transmissivity and the hydraulic diffusivity of the main aquifer (T_1 , a_1), as well as the hydraulic diffusivity of the aquitard (a').

2. Solutions for the drawdown in the main aquifer (1), the adjacent aquifer (2), and the aquitard at a varying hydraulic head in the adjacent aquifer during the pumping test are considered.

2.1. The drawdown in the main aquifer (1) is:

$$s^{(1)} = \frac{Q}{4\pi T_1} \int_0^\infty [1 - \exp(-\tau^2 u_\lambda)] \left[\left(1 + \frac{M(\tau)}{F(\tau)}\right) J_0(\omega_1) + \left(1 - \frac{M(\tau)}{F(\tau)}\right) J_0(\omega_2) \right] \frac{d\tau}{\tau}. \quad (3.74)$$

2.2. The drawdown in the adjacent aquifer (2) is:

$$s^{(2)} = \frac{Q}{4\pi T_1} \int_0^\infty [1 - \exp(-\tau^2 u_\lambda)] \frac{2(r/B_2)^2}{F(\tau)} [J_0(\omega_1) - J_0(\omega_2)] \frac{d\tau}{\sin \tau}. \quad (3.75)$$

2.3. The drawdown in the aquitard is:

$$s' = \frac{Q}{4\pi T_1} \frac{2}{\pi} \sum_{n=1}^\infty \left\{ \frac{1}{n} \sin \frac{n\pi z_p}{m'} \times \left[-1 + \exp(-n^2 \pi^2 u_\lambda) - \frac{\exp(-n^2 \pi^2 u_\lambda) - \exp(-\tau^2 u_\lambda)}{1 - \tau^2 / (n^2 \pi^2)} \right] \times \int_0^\infty \left[\left(\frac{2(r/B_2)^2 (-1)^n \tau}{F(\tau) \sin \tau} - \frac{M(\tau)}{F(\tau)} - 1 \right) J_0(\omega_1) - \left(\frac{2(r/B_2)^2 (-1)^n \tau}{F(\tau) \sin \tau} - \frac{M(\tau)}{F(\tau)} + 1 \right) J_0(\omega_2) \right] \frac{d\tau}{\tau} \right\}, \quad (3.76)$$

where

$$\omega_1 = \sqrt{\frac{N(\tau) + F(\tau)}{2}}, \quad \omega_2 = \sqrt{\frac{N(\tau) - F(\tau)}{2}}, \quad (3.77)$$

$$F(\tau) = \sqrt{M^2(\tau) + \left[\frac{2(r/B_1)(r/B_2)\tau}{\sin \tau} \right]^2}, \quad (3.78)$$

$$M(\tau) = (\lambda_1 - \lambda_2)\tau^2 - \left[\left(\frac{r}{B_1} \right)^2 - \left(\frac{r}{B_2} \right)^2 \right] \tau \cotan \tau, \quad (3.79)$$

$$N(\tau) = (\lambda_1 + \lambda_2)\tau^2 - \left[\left(\frac{r}{B_1} \right)^2 + \left(\frac{r}{B_2} \right)^2 \right] \tau \cotan \tau, \quad (3.80)$$

$$\lambda_1 = \frac{r^2 S_1}{B_1^2 S'}, \quad (3.81)$$

$$\lambda_2 = \frac{r^2 S_2}{B_2^2 S'}, \quad (3.82)$$

B_1 —see Eq. 3.52, B_2 —see Eq. 3.53.

If the expression under the square root in the right-hand part of the equalities (Eq. 3.77) is negative, then, for $\omega_1^2 < 0$, we assign $J_0(\omega_1) = 0$, and for $\omega_2^2 < 0$, accordingly, $J_0(\omega_2) = 0$.

For a leaky aquifer with transient flow in the adjacent aquifer, the hydraulic parameters will be calculated based on data on the drawdown in both aquifers and the aquitard. Equations 3.74–3.76 are used to evaluate the transmissivity of the main and adjacent aquifers (T_1 , T_2), the storage coefficients of the main and adjacent aquifers (S_1 , S_2), the leakage factor for the main aquifer (B_1), and the storage coefficient of the aquitard (S').

3. Solutions for the drawdown in the semi-infinite aquitard in the vertical plane (Fig. 3.7).

3.1. The drawdown in the semi-infinite aquitard is:

$$s' = \frac{Q}{4\pi T_1} \int_u^\infty \frac{e^{-\tau}}{\tau} \operatorname{erfc} \left(\frac{\sqrt{u}}{\sqrt{\tau(\tau - u)}} \left(\frac{r}{4} \sqrt{\frac{k'}{k_1 m_1}} + \tau \frac{z_p}{r} \sqrt{\frac{k_1 m_1}{k'}} \right) \sqrt{\frac{S'_s}{S_1}} \right) d\tau, \quad (3.83)$$

$$u = \frac{r^2}{4a_1 t} = \frac{r^2 S_1}{4T_1 t}, \quad (3.84)$$

where k' and S'_s are the hydraulic conductivity (m/d) and the specific storage (1/m) of the aquitard.

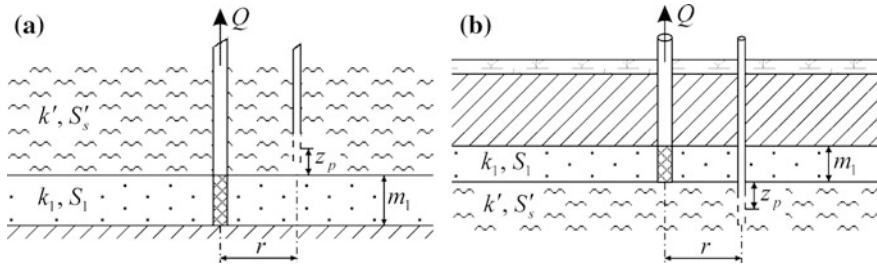


Fig. 3.10 An aquifer in contact with **a** an overlying and **b** an underlying semi-infinite compressible aquitard

3.2. The drawdown in the semi-infinite aquitard for a slightly leaky aquifer (Neuman and Witherspoon 1968) is:

$$s' = \frac{Q}{4\pi T_1} W_{NW} \left(\frac{r^2}{4a_1 t}, \frac{z_p^2}{4a' t} \right), \tag{3.85}$$

$$W_{NW}(u, u') = \frac{2}{\sqrt{\pi}} \int_0^\infty \frac{W \left(\frac{u\tau^2}{\tau^2 - u'} \right) \exp(-\tau^2) d\tau}{\sqrt{u'}}, \tag{3.86}$$

$$u' = \frac{z_p^2}{4a' t} = \frac{z_p^2 S'_s}{4k' t}, \tag{3.87}$$

or an approximation for a long time periods:

$$s' = \frac{Q}{4\pi T_1} W \left(\frac{r^2}{4a_1 t} \right), \tag{3.88}$$

where $W_{NW}(u, u')$ is a special function (see Appendix 7.8).

Data on the drawdown in the semi-infinite aquitard along with Eq. 3.83 are used to evaluate the transmissivity and the storage coefficient of the main aquifer (T_1, S_1), as well as the hydraulic conductivity and the specific storage of the aquitard (k', S'_s). In the case of pumping from a slightly leaky aquifer (Eq. 3.85), the parameters to be determined are the transmissivity and hydraulic diffusivity of the main aquifer (T_1, a_1) and the hydraulic diffusivity of the aquitard (a').

3.4 A Partially Penetrating Well in a Leaky Aquifer

This section gives transient and steady-state analytical solutions for the drawdown in a leaky aquifer of infinite lateral extent at a constant head in the adjacent aquifer. The transient solution takes into account the vertical anisotropy of the leaky aquifer and partially penetrating pumping and observation wells. The drawdown in the leaky aquifer (Eqs. 3.89 and 3.90) can be used to evaluate the hydraulic parameters of the aquifer: the horizontal and vertical hydraulic conductivity (k_r, k_z), the storage coefficient of the leaky aquifer (S), and the leakage factor, depending on the horizontal hydraulic conductivity (Eq. 3.91).

The basic assumptions and conditions (Fig. 3.11) are:

- the main assumptions for infinite leaky aquifer are given in Sect. 3.1.1;
- the main aquifer is vertically anisotropic;
- the pumping well partially penetrates the aquifer.

The drawdown is determined at any point of the main aquifer. The solutions given in this section can be applied to any combination of the aquifers and aquitards shown in Fig. 3.2.

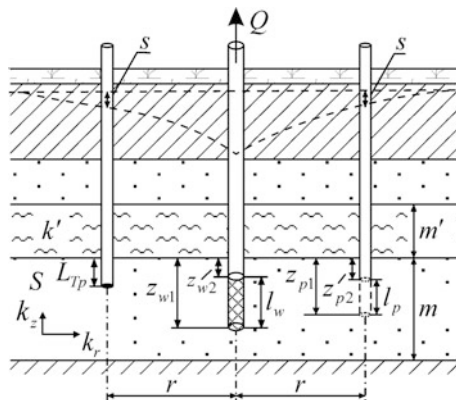
Basic Analytical Relationships (Hantush 1964)

Transient Flow Equations

The drawdown in the piezometer is:

$$s = \frac{Q}{4\pi k_r m} \left\{ W\left(\frac{r^2 S}{4k_r m t}, \frac{r}{B_r}\right) + \frac{2m}{\pi l_w} \sum_{n=1}^{\infty} \left[\frac{1}{n} W\left(\frac{r^2 S}{4k_r m t}, \beta\right) \left(\sin \frac{n\pi z_{w1}}{m} - \sin \frac{n\pi z_{w2}}{m} \right) \cos \frac{n\pi L_{Tp}}{m} \right] \right\} \quad (3.89)$$

Fig. 3.11 A partially penetrating pumping well in a leaky aquifer with a piezometer and a partially penetrating observation well



and the average drawdown in the observation well is:

$$s = \frac{Q}{4\pi k_r m} \left\{ W\left(\frac{r^2 S}{4k_r m t}, \frac{r}{B_r}\right) + \frac{2m^2}{\pi^2 l_w l_p} \sum_{n=1}^{\infty} \left[\frac{1}{n^2} W\left(\frac{r^2 S}{4k_r m t}, \beta\right) \left(\sin \frac{n\pi z_{w1}}{m} - \sin \frac{n\pi z_{w2}}{m} \right) \times \left[\sin \frac{n\pi z_{p1}}{m} - \sin \frac{n\pi z_{p2}}{m} \right] \right] \right\}, \quad (3.90)$$

$$B_r = \sqrt{\frac{k_r m m'}{k'}}, \quad (3.91)$$

where $\beta = \sqrt{\left(\frac{r}{B_r}\right)^2 + \chi^2 \left(\frac{n\pi r}{m}\right)^2}$; z_{w1} and z_{w2} are the vertical distances from the leaky aquifer top to the bottom of the pumping-well screen and to the pumping-well screen top, m (Fig. 3.11); z_{p1} and z_{p2} are the same characteristics for the observation well; L_{Tp} is the vertical distance from the leaky aquifer top to the open part of the piezometer, m ; $\chi = \sqrt{k_r/k_z}$ is anisotropy factor, dimensionless; k_r and k_z are the horizontal and vertical hydraulic conductivities, respectively, m/d ; l_p and l_w are the screen lengths of the observation and pumping wells, respectively, m .

Steady-State Flow Equations

The drawdown in the piezometer is:

$$s_m = \frac{Q}{2\pi k_r m} \left\{ K_0\left(\frac{r}{B_r}\right) + \frac{2m}{\pi l_w} \sum_{n=1}^{\infty} \left[\frac{1}{n} K_0(\beta) \left(\sin \frac{n\pi z_{w1}}{m} - \sin \frac{n\pi z_{w2}}{m} \right) \cos \frac{n\pi L_{Tp}}{m} \right] \right\}, \quad (3.92)$$

and the averaged drawdown in the observation well is:

$$s = \frac{Q}{2\pi k_r m} \left\{ K_0\left(\frac{r}{B_r}\right) + \frac{2m^2}{\pi^2 l_w l_p} \sum_{n=1}^{\infty} \left[\frac{1}{n^2} K_0(\beta) \left(\sin \frac{n\pi z_{w1}}{m} - \sin \frac{n\pi z_{w2}}{m} \right) \times \left[\sin \frac{n\pi z_{p1}}{m} - \sin \frac{n\pi z_{p2}}{m} \right] \right] \right\}. \quad (3.93)$$

Graphic-Analytical Processing

The relationship given in Table 3.5, has been derived from Eqs. 3.92 and 3.93 with no allowance made for the anisotropy of the leaky aquifer: $k_r = k$, $B_r = B$.

Table 3.5 Graphic-analytical evaluation of parameters

Plot	Method	Relationship
$s-\lg t$	Horizontal straight line ^a	$k = \frac{Q}{2\pi m \cdot A} f$

f is the expression in curly brackets in Eq. 3.92 or Eq. 3.93

^aBased on the drawdown value for the steady-state flow period given the leakage factor B

3.5 Two-Layer Aquifer Systems

The section considers:

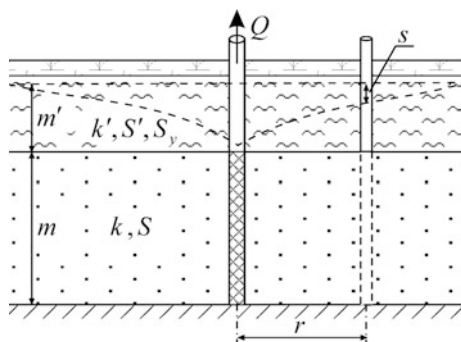
- (1) an unconfined aquifer system of infinite lateral extent (Sect. 3.5.1);
- (2) a confined aquifer system with a circular constant-head boundary (Sect. 3.5.2).

3.5.1 Two-Layer Unconfined Aquifer System of Infinite Lateral Extent

The basic assumptions and conditions (Fig. 3.12) are:

- the aquifer system consists of two isotropic aquifers with different hydraulic characteristics;
- the aquifer system is of infinite lateral extent;
- the top is an unconfined aquifer with a relatively low permeability;
- the bottom is a confined main aquifer with a relatively high permeability;
- the pumping well is fully penetrating and located in the main aquifer; its storage is neglected;
- the flow is vertical in the top aquifer and horizontal in the bottom aquifer.

Fig. 3.12 Two-layer unconfined aquifer system



The drawdown is determined at any distance from the pumping well in the main aquifer. A typical plot of drawdown in the observation well in the main aquifer is given in Fig. 12.23.

Basic Analytical Relationships

Transient Flow Equations

1. The Mironenko solution (Mironenko and Serdyukov 1968) is:

$$s = \frac{Q}{2\pi T} \left(\ln \frac{R(t)}{r} + \frac{r}{R(t)} - 1 \right), \quad (3.94)$$

$$R(t) = \sqrt{\frac{12T}{S_y + S} \left\{ t + \frac{m'S_y^2}{k'(S_y + S)} \left[1 - \exp\left(-\frac{(S_y + S)k't}{S_y S m'} t\right) \right] \right\}}, \quad (3.95)$$

where k' , S_y , m' are the hydraulic conductivity (m/d), the specific yield (dimensionless), and the initial saturated thickness (m) of the unconfined aquifer, respectively.

The solution (Eq. 3.94) is used for observation wells at distances less than the conventional radius of influence: $r \leq R(t)$. Otherwise, the drawdown is assumed zero.

Data on the drawdown in the main aquifer are used to derive from Eq. 3.94 the transmissivity and the storage coefficient of the confined aquifer (T , S), as well as the specific yield and the hydraulic conductivity of the unconfined aquifer (S_y , k').

2. Cooley–Case solution (Cooley and Case 1973). The solution is given for short and long time periods.

- 2.1. For short time periods, $t \leq 0.1 \cdot m'S'/k'$:

$$s = \frac{Q}{4\pi T} H \left[\frac{r^2 S}{4Tt}, \frac{r}{4B} \sqrt{\frac{S'}{S}} \right], \quad (3.96)$$

where $B = \sqrt{Tm'/k'}$ is the leakage factor, m; $H(u, \beta)$ is a special function (see Appendix 7.4).

- 2.2. For long time periods, $t \geq 10 \cdot m'S'/k'$:

$$s = \frac{Q}{4\pi T} \int_{\mu}^{\infty} \left\{ \left[1 - \exp\left(-\frac{\tau^2}{u_y}\right) \left(\cosh \mu_2 + \frac{\beta^2 \eta - 4\eta_2 \tau^2}{\mu_2 4u_y \eta_2} \sinh \mu_2 \right) \right] \times \right. \\ \left. \times J_0 \left(\sqrt{\frac{8\tau^2}{\eta} - \frac{\beta^2}{\eta_2}} \right) \frac{16\eta_2 \tau}{8\eta_2 \tau^2 - \eta \beta^2} \right\} d\tau, \quad (3.97)$$

where

$$u_y = r^2 \frac{S + S' + S_y}{4Tt}, \quad (3.98)$$

$$\beta = \frac{r}{B}, \quad (3.99)$$

$$\mu = \beta \sqrt{\frac{\eta}{8\eta_2}}, \quad (3.100)$$

$$\mu_2 = \frac{\sqrt{16\eta_2^2\tau^4 - 8\eta_2\tau^2\beta^2 + \eta\beta^4}}{4u_y\eta_2}, \quad (3.101)$$

$$\eta = \frac{S + S' + S_y}{S}, \quad (3.102)$$

$$\eta_2 = \frac{S_y}{S + S' + S_y}. \quad (3.103)$$

3. A simplified solution of Eq. 3.97, neglecting the storage coefficient of the main aquifer ($\eta \rightarrow \infty$) is:

$$s = \frac{Q}{4\pi T} \int_0^\infty \frac{2J_0(2\tau)}{\tau} \left[1 - \frac{\beta^2}{\beta^2 + 4\tau^2} \exp\left(-\frac{\beta^2\tau^2}{u\beta^2 + 4u\tau^2}\right) \right] d\tau, \quad (3.104)$$

where

$$u = \frac{r^2 S_y}{4Tt}. \quad (3.105)$$

Data on the drawdown in the main aquifer are used to evaluate, from Eqs. 3.96 and 3.97, the transmissivity and the storage coefficient of the confined main aquifer (T , S), as well as the hydraulic conductivity, storage coefficient, and specific yield of the unconfined low-permeability aquifer (S' , S_y , k'). The parameters determined from Eq. 3.104 are T , S_y , k' .

Equations 3.96 and 3.97 can be written with the effect of capillary fringe taken into account (Cooley and Case 1973).

3.5.2 Circular Two-Layer Confined Aquifer System

The basic assumptions and conditions (Figs. 3.13 and A3.10a) are:

- the aquifer system comprises two confined isotropic aquifers: an aquifer with a relatively high permeability (main) and an aquifer with a relatively low permeability (adjacent); the main aquifer can lie either in the bottom of the two-layer system (Fig. 3.13a, c), or in its top (Fig. 3.13b, d);
- the boundary is circular, constant-head, and running along the outer contour of the aquifer (see Fig. A3.10a);
- the pumping well is fully penetrating; it is located in the center of the circle in the main aquifer.

The drawdown is determined for the period of steady-state flow at any point in the main and adjacent aquifers given the hydraulic conductivities of these aquifers.

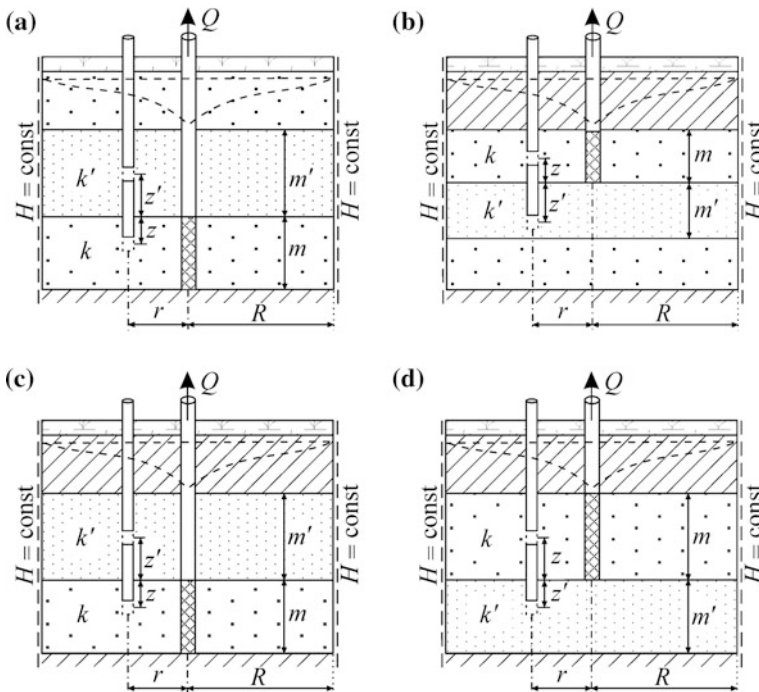


Fig. 3.13 Two-layer aquifer system with a circular constant-head boundary: **a, b** the low-permeability aquifer adjoins, **a** at the top and **b** at the bottom, an aquifer, the water level in which remains constant during the pumping test; **c, d** an isolated two-layer aquifer system. R is the radius of the circle

Two variants are considered:

variant 1—the adjacent aquifer adjoins the main (pumped) aquifer from one side and from the other side, the aquifer, the water level of which remains constant throughout the pumping-test period (Fig. 3.13a, b);

variant 2—aquicludes overlay and underlie the two-layer aquifer system (Fig. 3.13c, d).

Basic Analytical Relationships

Steady-State Flow Equations (Hantush and Jacob 1955c)

1. Solutions for the first variant (Fig. 3.13a, b)

1.1. The drawdown in the main aquifer is:

$$s_m = \frac{Q}{2\pi km} \left[\ln \frac{R}{r} - \frac{k'}{k} \sum_{n=1}^{\infty} \cosh \left(x_n \frac{m'}{R} \right) \cosh \left(x_n \frac{m-z}{R} \right) \frac{\lambda_n}{\delta_n} \right], \quad (3.106)$$

$$\lambda_n = J_0 \left(x_n \frac{r}{R} \right) \frac{4}{x_n^2 J_1^2(x_n)}, \quad (3.107)$$

$$\delta_n = \left(1 + \frac{k'}{k} \right) \cosh \left(x_n \frac{m+m'}{R} \right) - \left(1 - \frac{k'}{k} \right) \cosh \left(x_n \frac{m-m'}{R} \right), \quad (3.108)$$

where x_n are positive roots of equation $J_0(x_n) = 0$ (see Appendix 7.15); k, k' are the hydraulic conductivities of the main and adjacent aquifers, m/d ; m, m' are the thicknesses of the main and adjacent aquifers, m ; R is the radius of a circular aquifer, m ; z is the distance from the observation point in the main aquifer to the top (or bottom) of the same (Fig. 3.13), m .

1.2. The drawdown in the adjacent aquifer is:

$$s'_m = \frac{Q}{2\pi km} \sum_{n=1}^{\infty} \sinh \left(x_n \frac{m}{R} \right) \sinh \left(x_n \frac{m'-z'}{R} \right) \frac{\lambda_n}{\delta_n}, \quad (3.109)$$

where z' is the distance from the observation point in the adjacent aquifer to the top (or bottom) of the main aquifer (Fig. 3.13), m .

2. Solutions for the second variant (Fig. 3.13c, d)

2.1. The drawdown in the main aquifer is:

$$s_m = \frac{Q}{2\pi km} \left[\ln \frac{R}{r} - \frac{k'}{k} \sum_{n=1}^{\infty} \sinh \left(x_n \frac{m'}{R} \right) \cosh \left(x_n \frac{m-z}{R} \right) \frac{\lambda_n}{\varepsilon_n} \right], \quad (3.110)$$

$$\varepsilon_n = \left(\frac{k'}{k} + 1 \right) \sinh \left(x_n \frac{m+m'}{R} \right) + \left(\frac{k'}{k} - 1 \right) \sinh \left(x_n \frac{m'-m}{R} \right). \quad (3.111)$$

2.2. The drawdown in the adjacent aquifer is:

$$s'_m = \frac{Q}{2\pi km} \sum_{n=1}^{\infty} \sinh\left(x_n \frac{m}{R}\right) \cosh\left(x_n \frac{m' - z'}{R}\right) \frac{\lambda_n}{\varepsilon_n}. \tag{3.112}$$

When the hydraulic parameters of the main and adjacent aquifers are equal, the two-layer aquifer system can be regarded as a single-layer aquifer with a partially penetrating pumping well, adjoining its bottom or top (Hantush and Jacob 1955c).

A steady-state solution for the case of a fully penetrating pumping well intersecting two aquifers (Fig. 3.14), is considered in (Shchelkachev and Lapuk 1949):

$$s_{mw} = \frac{Q}{2\pi(k_1 m_1 + k_2 m_2)} \ln \frac{R}{r_w}, \tag{3.113}$$

where s_{mw} is the drawdown in the pumping well during a steady-state period, m.

The mean hydraulic conductivity of the aquifer system can be calculated as:

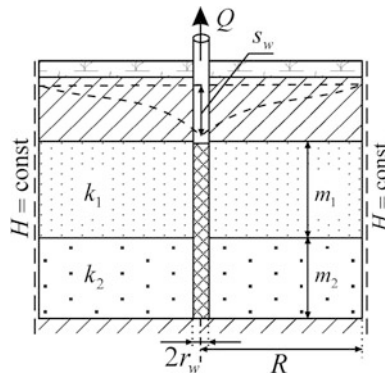
$$\bar{k} = \frac{k_1 m_1 + k_2 m_2}{m_1 + m_2}. \tag{3.114}$$

The solution (Eq. 3.113) is used to evaluate the averaged drawdown in the pumping well, located in the center of a two-layer aquifer system. This relationship will hold for a many-layer stratum as well:

$$s_{mw} = \frac{Q}{2\pi T_{\Sigma}} \ln \frac{R}{r_w}, \tag{3.115}$$

here T_{Σ} is the total transmissivity of the multilayer stratum, defined by the formula (see Eq. A1.8), m^2/d .

Fig. 3.14 Two-layer aquifer system with a circular constant-head boundary: the pumping well intersects two aquifers



3.6 Multi-aquifer Systems

This section considers aquifer systems with alternation of aquifers and aquitards. Such systems can be divided into three- and two-layer systems, depending on the number of aquitards that are in contact with the main pumped aquifer. The three-layer system consists of a main aquifer, underlain and overlain by aquitards (see Sect. 3.6.1), while the two-layer system is a main aquifer underlain or overlain by an aquitard (see Sect. 3.6.2). For each system, several models can be suggested, depending on the boundary conditions above and below this system (Figs. 3.15 and 3.17).

Two sets of transient solutions are available for stratified systems: Hantush solutions (Hantush 1960) and Moench solutions (Moench 1985). The solutions of those two authors differ by their potentialities.

Hantush solutions are easy-to-use and based on well-known hydrogeological functions; however, they have some limitations: they describe the drawdown only in the pumped aquifer, and they are applicable to certain time intervals (for short and long time periods). The behavior of the drawdown function in the intermediate time can be described by a linear function (Hantush 1960).

Moench solutions are more universal: the model curve is being constructed for the entire time interval and the drawdown is calculated in the aquitards as well; the solutions can account for the wellbore storage and the skin, which is evaluated from the hydraulic conductivity and the thickness of the wellbore skin (see Appendix 2).

For the multi-aquifer systems, it is assumed that:

- the flow is of infinite lateral extent;
- the flow is vertical in aquitards and horizontal in the main (pumped) aquifer;
- the flow regime in the aquitards is assumed elastic;
- the fully penetrating pumping well is in the main aquifer;
- the water level in the adjacent aquifers remains constant during the pumping test.

The drawdown is determined at any distance from the pumping well in the main aquifer; for Moench solutions, it is also determined in the aquitards.

Typical plots of the drawdown in an observation well in the main aquifer of a three-flow system are given in Fig. 12.24.

3.6.1 Three-Layer System

The basic assumptions and conditions (Fig. 3.15) are:

- the aquifer system consists of an isotropic aquifer with a relatively high permeability, overlain and underlain by aquitards;
- the main is a high-permeability aquifer containing the pumping well;
- adjacent high-permeability aquifers may lie in the top or bottom of the aquifer system;
- aquitard storages are taken into account.

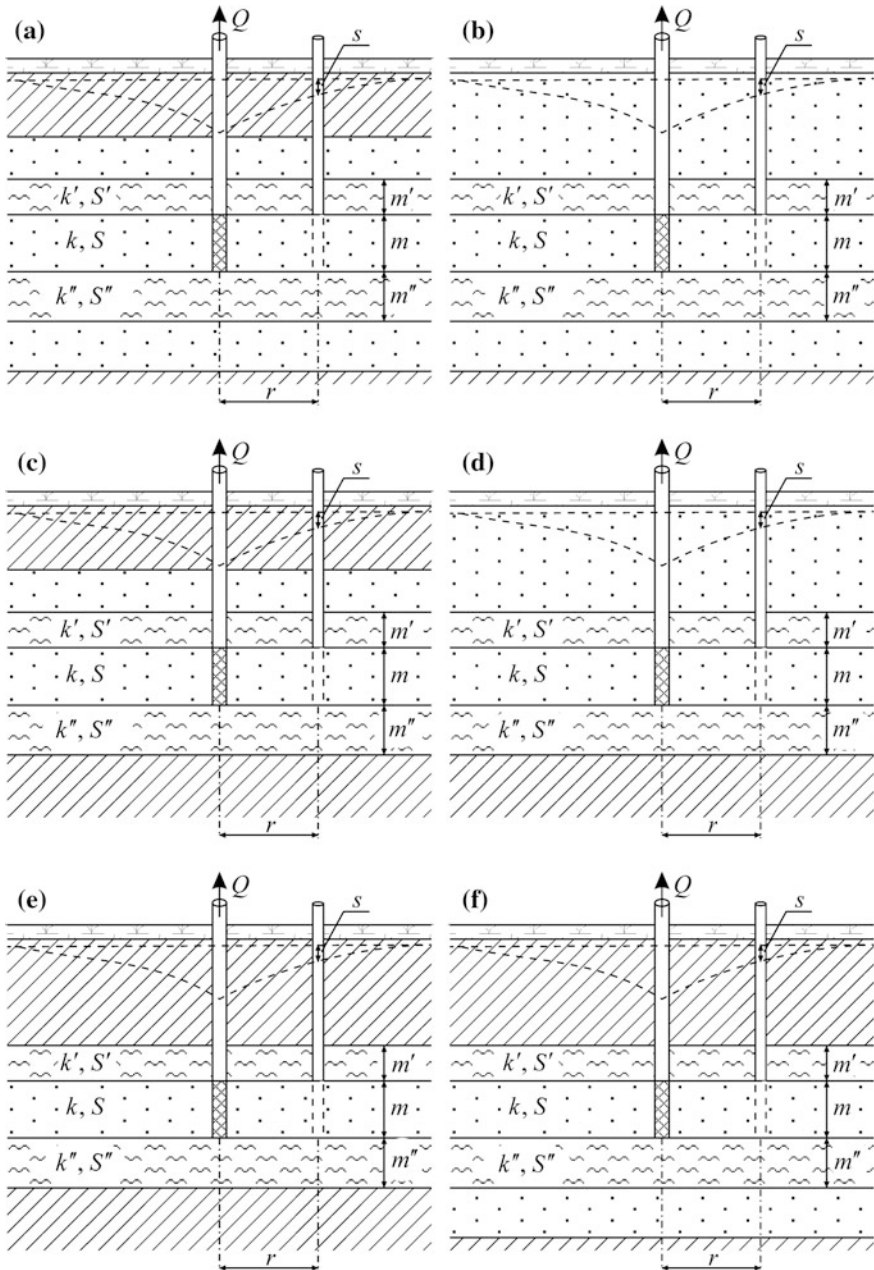


Fig. 3.15 Three-layer systems: **a, b** the top and bottom are constant-head aquifers—**a** a confined aquifer in the top, **b** an unconfined aquifer in the top; **c, d** the top is a constant-head aquifer (**c** confined, **d** unconfined), the bottom is an aquiclude; **e** the top and bottom are aquicludes; **f** an aquiclude in the top, a constant head aquifer in the bottom

Three variants are considered:

variant 1—the top and bottom of the aquifer system are adjacent aquifers with a constant head (Fig. 3.15a, b);

variant 2—the top and bottom of the aquifer system are aquicludes (Fig. 3.15e);

variant 3—the bottom of the aquifer system is underlain by an aquiclude, while its top is overlain by an adjacent aquifer (Fig. 3.15c, d), or, conversely, the bottom of the aquifer system is underlain by an adjacent aquifer, while its top is overlain by an aquiclude (Fig. 3.15f).

Basic Analytical Relationships

Transient Flow Equations

Hantush solutions (Hantush 1960)

The solutions are given for the drawdown in the main aquifer, separately for short and long time periods and depending on the chosen variant of the calculation model.

1. For short time periods, $t < 0.1 m' S' / k'$ and $t < 0.1 m'' S'' / k''$ (or $t < 0.1 B_1^2 S' / T$ and $t < 0.1 B_2^2 S'' / T$):

$$s = \frac{Q}{4\pi T} \text{H} \left[\frac{r^2 S}{4Tt}, r \left(\frac{1}{B_1} \sqrt{\frac{S'}{S}} + \frac{1}{B_2} \sqrt{\frac{S''}{S}} \right) \right], \quad (3.116)$$

$$B_1 = \sqrt{T \frac{m'}{k'}}, \quad (3.117)$$

$$B_2 = \sqrt{T \frac{m''}{k''}}, \quad (3.118)$$

where k' , k'' are the hydraulic conductivities of aquitards, m/d; S' , S'' are storage coefficients of the aquitards, dimensionless; m' , m'' are the thicknesses of the aquitards, m; $\text{H}(u, \beta)$ is a special function (see Appendix 7.4).

Equation 3.116 is applicable to all three variants.

2. For long time periods:

variant 1 (Fig. 3.15a, b)—for $t > 5 m' S' / k'$ and $t > 5 m'' S'' / k''$ (or $t > 5 B_1^2 S' / T$ and $t > 5 B_2^2 S'' / T$):

$$s = \frac{Q}{4\pi T} \text{W} \left[\frac{r^2 S}{4Tt} \left(1 + \frac{S' + S''}{3S} \right), r \sqrt{\left(\frac{1}{B_1} \right)^2 + \left(\frac{1}{B_2} \right)^2} \right]; \quad (3.119)$$

variant 2 (Fig. 3.15e)—for $t > 10 m' S' / k'$ and $t > 10 m'' S'' / k''$ (or $t > 10 B_1^2 S' / T$ and $t > 10 B_2^2 S'' / T$):

$$s = \frac{Q}{4\pi T} W \left[\frac{r^2 S}{4Tt} \left(1 + \frac{S' + S''}{S} \right) \right]; \tag{3.120}$$

variant 3 (Fig. 3.15c, d, f)—for $t > 5m'S'/k'$ and $t > 10m''S''/k''$ (or $t > 5B_1^2S'/T$ and $t > 10B_2^2S''/T$):

$$s = \frac{Q}{4\pi T} W \left[\frac{r^2 S}{4Tt} \left(1 + \frac{S'' + S'/3}{S} \right), \frac{r}{B_1} \right]. \tag{3.121}$$

Moench solutions (Moench 1985)

The solutions are given as drawdown values in the main aquifer and in the aquitards. The drawdown in the aquitards is determined taking into account the depth to the piezometer or the screen of the observation well (see z_p in Fig. 3.16). For an aquitard in the top of the main aquifer, this is the distance from the observation point to the layer bottom; and for an aquitard in the bottom of the main aquifer, the distance from the observation point to the top of the layer.

1. The drawdown in the main aquifer is:

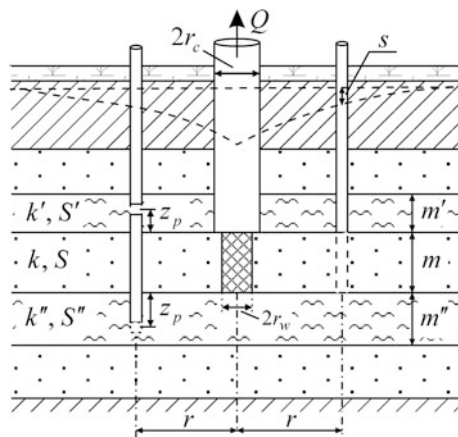
$$s = \frac{Q}{4\pi T} f(t, r, r_w, r_c, T, S, S', S'', B_1, B_2, k_{\text{skin}}, m_{\text{skin}}), \tag{3.122}$$

where $k_{\text{skin}}, m_{\text{skin}}$ are the hydraulic conductivity (m/d) and thickness (m) of the wellbore skin (see Appendix 2).

2. The drawdown in the top or bottom aquitard is:

$$s' = \frac{Q}{4\pi T} f(t, r, r_w, r_c, T, S, S', S'', B_1, B_2, z_p, k_{\text{skin}}, m_{\text{skin}}), \tag{3.123}$$

Fig. 3.16 An example of a three-layer system for Moench solutions. All variants of aquifer positions can be treated (see Fig. 3.15)



where the distance z_p depends on the position of the aquitard relative to the main aquifer.

The relationships (Eqs. 3.122 and 3.123) are treated by the algorithm of the program DP_LAQ (see Appendix 5.5).

For a three-layer system, data on the drawdown in the main aquifer (Eqs. 3.116, 3.119–3.122) or in aquitards (Eq. 3.123) are used to evaluate the transmissivity and storage coefficient of the main aquifer (T, S), the storage coefficients of the aquitards (S', S''), and the leakage factors through the top and bottom aquitards (B_1, B_2).

3.6.2 Two-Layer System

The basic assumptions and conditions (Fig. 3.17) are:

- the aquifer system consists of an isotropic aquifer with a relatively high permeability, overlain or underlain by aquitard;
- the main is a high-permeability aquifer containing the pumping well;
- adjacent high-permeability aquifer may lie in the top or bottom of the aquifer system;
- aquitard storage is taken into account.

Two variants are considered:

variant 1—the top or bottom of the aquifer system is adjacent aquifer with a constant head (Fig. 3.17a–c);

variant 2—aquitards lie in the top and bottom of the aquifer system (Fig. 3.17d, e).

Basic Analytical Relationships

Transient Flow Equations

Hantush solutions (Hantush 1960)

The solutions are given for the drawdown in the main aquifer, separately for short and long time periods and depending on the chosen variant of the calculation model.

1. For short time periods $t \leq 0.1 m'S'/k'$ (or $t \leq 0.1 B^2 S'/T$):

$$s = \frac{Q}{4\pi T} \text{H} \left[\frac{r^2 S}{4Tt}, \frac{r}{4B} \sqrt{\frac{S'}{S}} \right], \quad (3.124)$$

where the leakage factor is evaluated as $B = \sqrt{Tm'/k'}$.

Equation 3.124 is applicable to two variants.

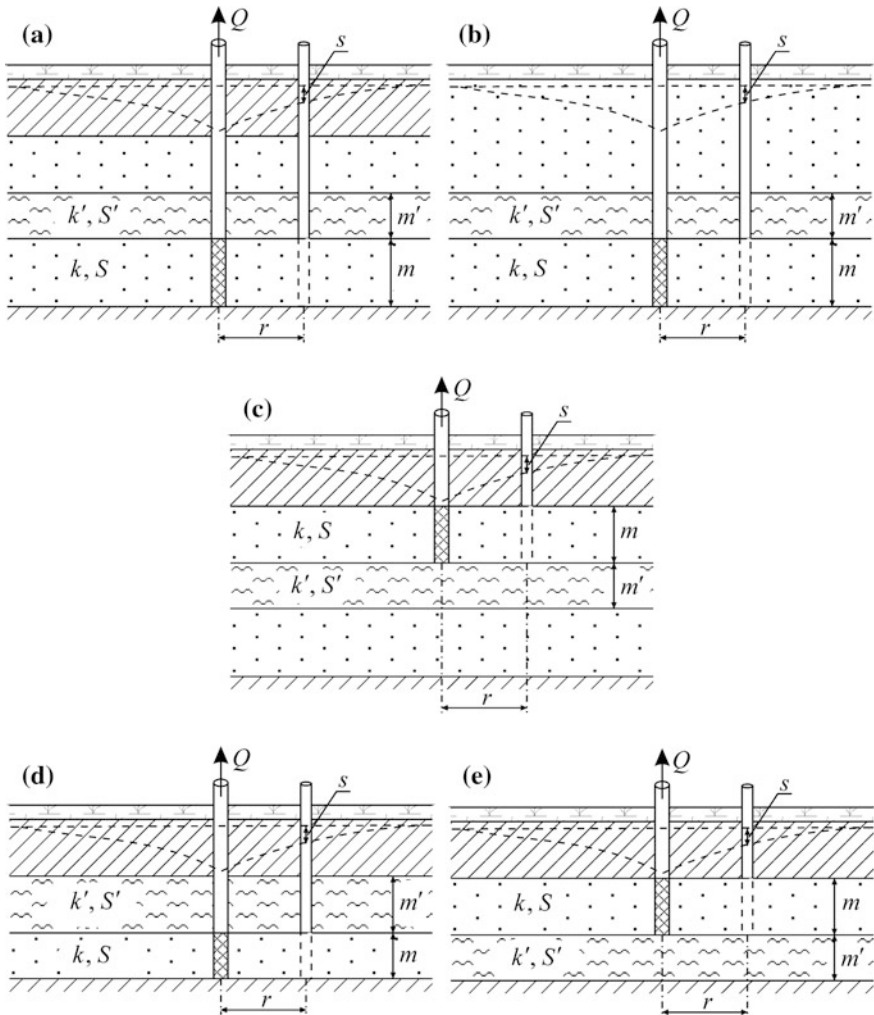


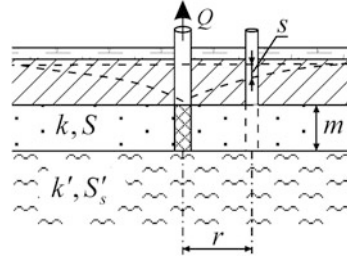
Fig. 3.17 Two-aquifer systems: **a, b** the adjacent aquifer with constant head in the top of the aquifer system is **a** confined or **b** unconfined; **c** the adjacent aquifer with constant head is in the bottom of the aquifer system; **d, e** aquicludes in the top and bottom of the aquifer system, an aquitard **d** overlays or **e** underlies the main aquifer

2. For long time periods:

variant 1 (Fig. 3.17a-c)—for $t \geq 5m'S'/k'$ (or $t \geq 5B^2S'/T$):

$$s = \frac{Q}{4\pi T} W \left[\frac{r^2 S}{4Tt} \left(1 + \frac{S'}{3S} \right), \frac{r}{B} \right]; \quad (3.125)$$

Fig. 3.18 Aquifer system with an aquitard semi-infinite in thickness



variant 2 (Fig. 3.17d, e)—for $t \geq 10m'S'/k'$ (or $t \geq 10B^2S'/T$):

$$s = \frac{Q}{4\pi T} W \left[\frac{r^2 S}{4Tt} \left(1 + \frac{S'}{S} \right) \right]. \quad (3.126)$$

For a two-layer system, in which the aquitard is semi-infinite in thickness (Fig. 3.18), the drawdown in the main aquifer for all time measurements can be written as

$$s = \frac{Q}{4\pi T} H \left[\frac{r^2 S}{4Tt}, \frac{r}{4} \sqrt{\frac{k'S'_s}{TS}} \right]. \quad (3.127)$$

The drawdown in the aquitard for such conditions can be derived from solution (Eq. 3.83).

In the case of a semi-infinite aquitard, Eq. 3.127 is used to evaluate the transmissivity and the storage coefficient (T, S) of the main aquifer and the hydraulic conductivity and specific storage (k', S'_s) of the aquitard.

Moench solution (Moench 1985)

Moench solutions are used to determine the drawdown in the main aquifer and in the aquitard. In the aquitard, the depth at which the piezometer or the screen of the observation well is installed is taken into account (see z_p in Fig. 3.19).

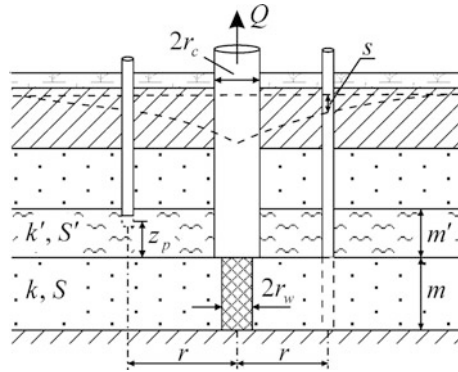
1. The drawdown in the main aquifer is:

$$s = \frac{Q}{4\pi T} f(t, r, r_w, r_c, T, S, S', B, k_{\text{skin}}, m_{\text{skin}}). \quad (3.128)$$

2. The drawdown in the aquitard is:

$$s' = \frac{Q}{4\pi T} f(t, r, r_w, r_c, T, S, S', B, z_p, k_{\text{skin}}, m_{\text{skin}}). \quad (3.129)$$

Fig. 3.19 An example of a two-layer system for Moench solutions. All variants of layer positions can be treated (see Fig. 3.17)



The relationships (Eqs. 3.128 and 3.129) were treated using the algorithm of the program DP_LAQ (see Appendix 5.5).

For a two-layer system, data on the drawdown in the main aquifer (Eqs. 3.124–3.126, 3.128) or in the aquitard (Eq. 3.129) are used to evaluate the transmissivity and the storage coefficient of the main aquifer (T, S), the storage coefficient of the aquitard (S'), and the leakage factor ($B = \sqrt{Tm'/k'}$).

References

- Bochever FM (1963) Design calculations for water intake and drainage wells in bounded aquifers. In: Issues of hydrological design calculations for water intake and drainage systems, vol. 5. VODGEO, Moscow, pp 65–94 (In Russian)
- Bochever FM (1968) Theory and practical methods of groundwater yield evaluation. Nedra, Moscow (In Russian)
- Cooley RL, Case CM (1973) Effect of a water table aquitard on drawdown in an underlying pumped aquifer. *Water Resour Res* 9(2):434–447
- De Glee GJ (1930) Over grondwaterstromingen bij wateronttrekking door middel van putten. Waltman, Delft
- Hantush MS (1960) Modification of the theory of leaky aquifers. *J Geophys Res* 65(11):3713–3725
- Hantush MS (1964) Hydraulics of wells. In: Chow VT (ed) *Advances in hydroscience*, vol 1. Academic Press, New York and London, pp 281–432
- Hantush MS (1966) Analysis of data from pumping tests in anisotropic aquifers. *J Geophys Res* 71(2):421–426
- Hantush MS (1967) Flow to wells in aquifers separated by a semipervious layer. *J Geophys Res* 72(6):1709–1720
- Hantush MS, Jacob CE (1954) Plane potential flow of ground water with linear leakage. *EOS Trans Am Geophys Union* 35(6):917–936
- Hantush MS, Jacob CE (1955a) Non-steady Green's functions for an infinite strip of leaky aquifer. *EOS Trans Am Geophys Union* 36(1):101–112

- Hantush MS, Jacob CE (1955b) Non-steady radial flow in an infinite leaky aquifer. *EOS Trans Am Geophys Union* 36(1):95–100
- Hantush MS, Jacob CE (1955c) Steady three-dimensional flow to a well in a two-layered aquifer. *EOS Trans Am Geophys Union* 36(2):286–292
- Hantush MS, Jacob CE (1960) Flow to an eccentric well in a leaky circular aquifer. *J Geophys Res* 65(10):3425–3431
- Hantush MS, Thomas RG (1966) A method for analyzing a drawdown test in anisotropic aquifers. *Water Resour Res* 2(2):281–285
- Jacob CE (1946) Radial flow in a leaky artesian aquifer. *EOS Trans Am Geophys Union* 27(2):198–205
- Lai RYS, Cheh-Wu Su (1974) Nonsteady flow to a large well in a leaky aquifer. *J Hydrol* 22(3/4):333–345
- Mironenko VA, Serdyukov LI (1968) Analysis of pumping test results from two-layer aquifer. *Prospect Prot Miner Resour* 10:34–38 (In Russian)
- Moench AF (1985) Transient flow to a large-diameter well in an aquifer with storative semiconfining layers. *Water Resour Res* 21(8):1121–1131
- Neuman SP, Witherspoon PA (1968) Theory of flow in aquicludes adjacent to slightly leaky aquifers. *Water Resour Res* 4(1):103–112
- Neuman SP, Witherspoon PA (1969a) Applicability of current theories of flow in leaky aquifers. *Water Resour Res* 5(4):817–829
- Neuman SP, Witherspoon PA (1969b) Theory of flow in a confined two aquifer system. *Water Resour Res* 5(4):803–816
- Shchelkachev VN, Lapuk BB (1949) *Groundwater hydraulics*. Gostoptehizdat, Moscow (In Russian)

Chapter 4

Horizontally Heterogeneous Aquifers

A confined isotropic aquifer comprises two or more horizontally adjacent zones with different hydraulic properties. The aquifer is of constant thickness. The pumping and observation wells are fully penetrating.

This chapter considers analytical solutions for calculating the drawdown in the following horizontally heterogeneous aquifers:

- (1) an aquifer comprising two zones separated by a linear boundary (Sect. 4.1);
- (2) an aquifer comprising two zones with a common circular boundary (Sect. 4.2);
- (3) heterogeneous aquifers with a constant-head boundary (Sect. 4.3).

Transient solutions are used to evaluate the transmissivity and storage coefficient (or hydraulic diffusivity) of the main and adjacent zones. Steady-state solutions are used to determine the transmissivities of the two zones. For the majority of solutions, the hydraulic parameters are evaluated based on the drawdown values in both the main and the adjacent zones.

4.1 Aquifer with Linear Discontinuity

This section gives transient and quasi-steady-state analytical solutions, which are used to evaluate the drawdown in a horizontally heterogeneous aquifer with a linear boundary between the two zones.

The basic assumptions and conditions (Fig. 4.1) are:

- the aquifer consists of two zones that are semi-infinite in the horizontal plane with a common linear boundary;
- the pumping well is located in the main zone;
- the observation well is located in the main or the adjacent zone.

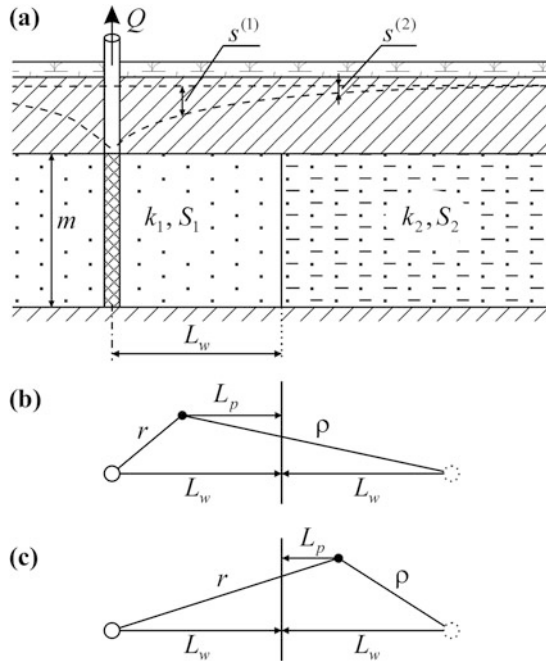


Fig. 4.1 Horizontally heterogeneous aquifer with two zones. **a** Cross-section; **b, c** planar view with the distance to image wells: the observation well is located in **b** the main and **c** the adjacent zone

The drawdown is evaluated in two zones at any distance from the pumping well. Typical plots of the drawdown in observation wells in the main and adjacent zones are given in Fig. 12.25a.

The distance (ρ) from the observation well lying in the main zone (Fig. 4.1b) to the image well is determined in the same manner as in the case of a semi-infinite aquifer (see Sect. 1.1.2 and Eq. A3.1), and that for the observation well in the adjacent zone (Fig. 4.2c), as

$$\rho = \sqrt{r^2 - 4L_w L_p}, \tag{4.1}$$

where r is the radial distance from the pumping to the observation well, m ; L_w and L_p are the distances from the pumping well and the observation well to the boundary between the zones, m .

Basic Analytical Relationships

Transient Flow Equation

For these conditions, the solutions of two authors—Maksimov (1962) and Fenske (1984)—are considered. The solutions yield similar results, though the relationships given by Fenske have a simpler mathematical representation and introduce no limitations to the choice of the hydraulic parameters of an aquifer.

1. The Maksimov solution (Maksimov 1962): the drawdown in the main zone is:

$$s^{(1)} = \frac{Q}{4\pi T_1} \left[\mathbf{W} \left(\frac{r^2}{4a_1 t} \right) + \frac{T_1 - T_2}{T_1 + T_2} \mathbf{W} \left(\frac{\rho^2}{4a_1 t} \right) - \delta_1 \right], \quad (4.2)$$

$$\delta_1 \approx \delta_{1\infty} \left[\exp \left(-\frac{\rho^2}{4a_1 t} \right) - \frac{\sqrt{\pi}(L_w + L_p)}{2\sqrt{a_1 t}} \exp \left(-\frac{r^2 - (L_w - L_p)^2}{4a_1 t} \right) \operatorname{erfc} \frac{L_w + L_p}{2\sqrt{a_1 t}} \right], \quad (4.3)$$

$$\delta_{1\infty} = \begin{cases} \frac{2T_1 T_2}{T_1^2 - T_2^2} \left[\ln \frac{a_2}{a_1} + 4T_1 \sqrt{\frac{a_1 - a_2}{T_1^2 a_2 - T_2^2 a_1}} \times \right. \\ \left. \times \arctan \sqrt{\frac{(\sqrt{a_1} - \sqrt{a_2})(T_1 \sqrt{a_2} - T_2 \sqrt{a_1})}{(\sqrt{a_1} + \sqrt{a_2})(T_1 \sqrt{a_2} + T_2 \sqrt{a_1})}} \right] \rightarrow T_1 \neq T_2; \\ \frac{a_1}{a_2 - a_1} \ln \frac{a_1}{a_2} + 1 \rightarrow T_1 = T_2; \end{cases} \quad (4.4)$$

and the drawdown in the adjacent zone is:

$$s^{(2)} = \frac{Q}{4\pi T_2} \left[\frac{2T_2}{T_1 + T_2} \mathbf{W} \left(\frac{r^2}{4a_2 t} \right) - \delta_2 \right], \quad (4.5)$$

$$\delta_2 \approx \delta_{2\infty} \left[\exp \left(-\frac{r^2}{4a_2 t} \right) - \frac{\sqrt{\pi}(L_w + L_p)}{2\sqrt{a_2 t}} \exp \left(-\frac{r^2 - (L_w + L_p)^2}{4a_2 t} \right) \operatorname{erfc} \frac{L_w + L_p}{2\sqrt{a_2 t}} \right], \quad (4.6)$$

$$\delta_{2\infty} = \frac{T_2}{T_1} \delta_{1\infty} - \frac{2T_2}{T_1 + T_2} \ln \frac{a_1}{a_2}, \quad (4.7)$$

where $s^{(1)}$, $s^{(2)}$ are the drawdown values in the observation wells in the main and the adjacent zone, respectively, m ; Q is the discharge rate, m^3/d ; $T_1 = k_1 m$ and

$T_2 = k_2 m$ are the transmissivities of the main and adjacent zones, respectively, m^2/d ; k_1, k_2 are the hydraulic conductivities of the main and adjacent zones, respectively, m/d ; m is aquifer thickness, m ; $a_1 = T_1/S_1$ and $a_2 = T_2/S_2$ are the hydraulic diffusivities of the main and adjacent zones, respectively, m^2/d ; S_1 and S_2 are storage coefficients of the main and adjacent zones, respectively, dimensionless; t is the time elapsed from the start of pumping, d ; $W(\cdot)$ is well-function (see Appendix 7.1).

2. The Fenske solution (Fenske 1984) for the drawdown in the main zone is:

$$s^{(1)} = \frac{Q}{4\pi T_1} \left[W\left(\frac{r^2}{4a_1 t}\right) + \frac{\varepsilon T_1 - \omega T_2}{\varepsilon T_1 + \omega T_2} W\left(\frac{\rho^2}{4a_1 t}\right) \right], \quad (4.8)$$

for the drawdown in the adjacent zone is:

$$s^{(2)} = \frac{Q}{4\pi T_2} \frac{2\varepsilon\omega T_2}{\varepsilon T_1 + \omega T_2} W\left(\frac{r^2}{4a_2 t}\right), \quad (4.9)$$

$$\omega = W\left(\frac{L_w^2 + r^2 - (L_w \pm L_p)^2}{4a_1 t}\right) / W\left(\frac{L_w^2 + r^2 - (L_w \pm L_p)^2}{4a_2 t}\right), \quad (4.10)$$

$$\varepsilon = \exp\left(-\frac{L_w^2 + r^2 - (L_w \pm L_p)^2}{4a_1 t}\right) / \exp\left(-\frac{L_w^2 + r^2 - (L_w \pm L_p)^2}{4a_2 t}\right), \quad (4.11)$$

where sign “+” is used for the drawdown evaluated in the adjacent zone and “-” for the main zone.

Steady-State Flow Equations

Equations 4.2 and 4.5, along with the assumption that for long time periods, δ_1 (Eq. 4.3) and δ_2 (Eq. 4.6) are approximately equal to $\delta_{1\infty}$ (Eq. 4.1) and $\delta_{2\infty}$ (Eq. 4.7), respectively, the solution for a period of quasi-steady-state flow can be written as (Maksimov 1962):

$$s^{(1)} = \frac{Q}{4\pi \bar{T}} \left(\ln \frac{2.25a_1 t}{r\rho} + \frac{T_2}{T_1} \ln \frac{\rho}{r} - \frac{\bar{T}}{T_1} \delta_{1\infty} \right), \quad (4.12)$$

$$s^{(2)} = \frac{Q}{4\pi \bar{T}} \left(\ln \frac{2.25a_2 t}{r^2} - \frac{\bar{T}}{T_2} \delta_{2\infty} \right), \quad (4.13)$$

$$\bar{T} = \frac{T_1 + T_2}{2}. \quad (4.14)$$

Table 4.1 Graphic-analytical parameter evaluation

Plot	Method	Relationship
$s^{(1)} - \lg t$	Straight line	$\bar{T} = \frac{0.183Q}{C}$
$s^{(2)} - \lg t$	The same	$\bar{T} = \frac{0.183Q}{C}, \lg a_2 \approx \frac{A}{C} + \lg \frac{r^2}{2.25}$
$s^{(2)} - \lg r$	The same	$\bar{T} = \frac{0.366Q}{C}, \lg a_2 \approx 2 \frac{A}{C} - \lg(2.25 \cdot t)$
$s^{(2)} - \lg \frac{t}{r^2}$	The same	$\bar{T} = \frac{0.183Q}{C}, \lg a_2 \approx \frac{A}{C} - \lg(2.25)$

A is the intercept of the straight line on the ordinate axis (see Sect. 12.1.1); C is the slope of the straight line (see Sect. 12.1.1); \bar{T} is the mean transmissivity (see Eq. 4.14), m^2/d

Graphic-Analytical Processing

The relationships given in Table 4.1 have been derived from Eqs. 4.12 and 4.13.

The hydraulic diffusivity (a_2) of the adjacent zone, as determined in Table 4.1, is an overestimate, because the value of $\delta_{2\infty}$ is neglected in the calculations.

4.2 Radial Patchy Aquifer

The basic assumptions and conditions (Fig. 4.2) are:

- the aquifer horizontally comprises two zones with different hydraulic parameters and with a common circular boundary;
- the pumping well is located in the center of the circular zone (wellbore zone), surrounded by the main zone;
- the observation well is located in the main or wellbore zone;
- the wellbore storage is taken into account in the drawdown estimation.

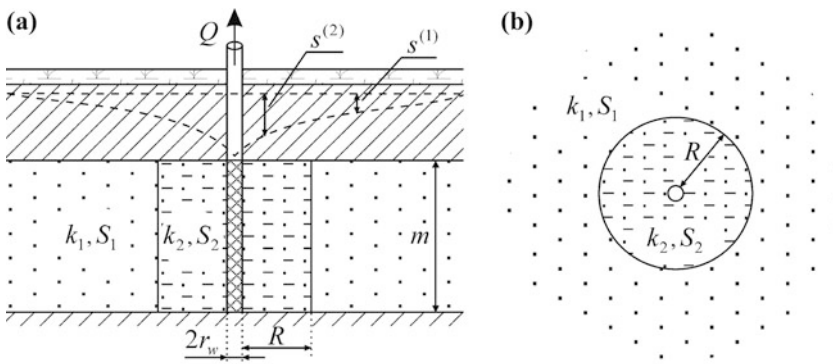


Fig. 4.2 Radially heterogeneous aquifer with two zones: **a** cross-section; **b** planar view

The drawdown is determined in two zones at any distance from the pumping well. A typical plot of the drawdown in an observation well located in the main zone is given in Fig. 12.25b.

This configuration can be regarded as a homogeneous confined aquifer with a pumping well surrounded by an area that plays a role of wellbore skin. In this formulation, analytical solutions enable the estimation of the thickness and the hydraulic conductivity of the skin, as well as its storage coefficient.

Basic Analytical Relationships

Transient Flow Equation (Yeh et al. 2003)

1. The drawdown in the main zone is:

$$s^{(1)} = \frac{Q}{4\pi T_2} \frac{8}{\pi^2 r_w R^+} \int_0^\infty [1 - \exp(-u\tau^2)] \frac{Y_0(rc_1\tau)B_1 - J_0(rc_1\tau)B_2}{B_1^2 + B_2^2} \frac{d\tau}{\tau^3}, \quad (4.15)$$

$$B_1 = J_0(R^+ c_1\tau)[J_1(R^+\tau)Y_1(r_w\tau) - Y_1(R^+\tau)J_1(r_w\tau)] - c_2 J_1(R^+ c_1\tau)[J_0(R^+\tau)Y_1(r_w\tau) - Y_0(R^+\tau)J_1(r_w\tau)], \quad (4.16)$$

$$B_2 = Y_0(R^+ c_1\tau)[J_1(R^+\tau)Y_1(r_w\tau) - Y_1(R^+\tau)J_1(r_w\tau)] - c_2 Y_1(R^+ c_1\tau)[J_0(R^+\tau)Y_1(r_w\tau) - Y_0(R^+\tau)J_1(r_w\tau)], \quad (4.17)$$

$$u = a_2 t, \quad c_1 = \sqrt{a_2/a_1}, \quad c_2 = \frac{T_1}{T_2} \sqrt{a_2/a_1}, \quad R^+ = R + r_w, \quad (4.18)$$

where R is the radius of the wellbore zone less the well radius (i.e., skin thickness), m; r_w is pumping well radius, m; $J_0(\cdot)$ and $J_1(\cdot)$ are Bessel functions of the first kind of the zero and the first order; $Y_0(\cdot)$ and $Y_1(\cdot)$ are Bessel functions of the second kind of the zero and the first order (see Appendix 7.13).

2. The drawdown in the wellbore zone:

$$s^{(2)} = \frac{Q}{4\pi T_2} \frac{4}{\pi r_w} \int_0^\infty [1 - \exp(-u\tau^2)] \frac{A_1 B_1 + A_2 B_2}{B_1^2 + B_2^2} \frac{d\tau}{\tau^2}, \quad (4.19)$$

$$A_1 = Y_0(R^+ c_1\tau)[J_1(R^+\tau)Y_0(r\tau) - Y_1(R^+\tau)J_0(r\tau)] - c_2 Y_1(R^+ c_1\tau)[J_0(R^+\tau)Y_0(r\tau) - Y_0(R^+\tau)J_0(r\tau)], \quad (4.20)$$

$$A_2 = J_0(R^+ c_1\tau)[Y_1(R^+\tau)J_0(r\tau) - J_1(R^+\tau)Y_0(r\tau)] - c_2 J_1(R^+ c_1\tau)[Y_0(R^+\tau)J_0(r\tau) - J_0(R^+\tau)Y_0(r\tau)]. \quad (4.21)$$

4.3 Heterogeneous Aquifers with a Constant-Head Boundary

4.3.1 Strip Aquifer

The basic assumptions and conditions (Fig. 4.3) are:

- general conditions for a horizontally heterogeneous aquifer with a linear interface (see the beginning of Sect. 4.1);
- the main zone is a strip aquifer, which is limited by a constant-head boundary from one side and by the interface between the two zones from the other side.

Basic Analytical Relationships

Steady-State Flow Equations (Bochever et al. 1979)

1. The drawdown in the main zone is:

$$s_m^{(1)} = \frac{Q}{2\pi T_1} \left\{ \ln \frac{\rho}{r} + \frac{1}{2} \sum_{n=1}^{\infty} \left(\frac{T_2 - T_1}{T_2 + T_1} \right)^n \left[\begin{aligned} & \ln \frac{(2nL + L_p + L_w)^2 + y^2}{(2nL + L_p - L_w)^2 + y^2} + \\ & + \ln \frac{(2nL - L_p - L_w)^2 + y^2}{(2nL - L_p + L_w)^2 + y^2} \end{aligned} \right] \right\}. \quad (4.22)$$

2. The drawdown in the adjacent zone is:

$$s_m^{(2)} = \frac{Q}{\pi(T_1 + T_2)} \left\{ \ln \frac{\rho}{r} + \frac{1}{2} \sum_{n=1}^{\infty} \left(\frac{T_2 - T_1}{T_2 + T_1} \right)^n \ln \frac{(2nL + L_p + L_w)^2 + y^2}{(2nL + L_p - L_w)^2 + y^2} \right\}, \quad (4.23)$$

where $s_m^{(1)}$, $s_m^{(2)}$ are the drawdown values in the period of steady-state flow in observation wells in the main and adjacent zones, respectively, m ; L is the width of the strip aquifer, m ; L_p and L_w are the distances from the observation and pumping wells to the constant-head boundary, m ; ρ is the distance between the observation and the image wells (Fig. 4.3b, c), which is determined in the same manner as in aquifers semi-infinite in the horizontal plane, i.e., by formula (Eq. A3.1), m ; for y , see Eq. A3.2, m .

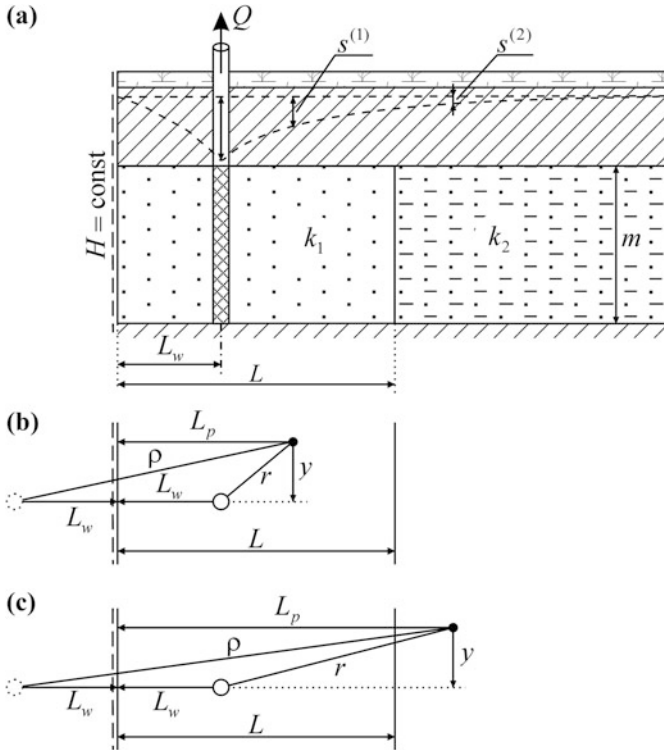


Fig. 4.3 Semi-infinite horizontally heterogeneous aquifer with two zones. **a** Cross-section; **b, c** a planar view with an observation well in **b** the main and **c** adjacent zone

4.3.2 Semi-circular Aquifer

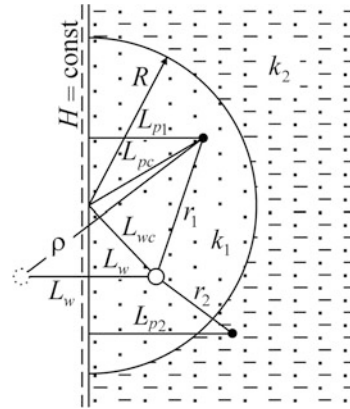
The basic assumptions and conditions (Fig. 4.4) are:

- general conditions for a horizontally heterogeneous aquifer with a linear interface (see the beginning of Sect. 4.1);
- in the horizontal plane, the main zone is limited by a linear constant-head boundary and a circular interface between the two zones;
- the adjacent zone is limited in the horizontal plane by a linear constant-head boundary and a circular interface between the two zones.

Basic Analytical Relationships

Steady-State Flow Equations (Bochever et al. 1979)

Fig. 4.4 Horizontally heterogeneous aquifer with a semicircle interface between the two zones (a planar view). The figure shows the image well and the distance to it



1. The drawdown in the main zone is:

$$s_m^{(1)} = \frac{Q}{2\pi T_1} \left\{ \ln \frac{\rho}{r} + \frac{1}{2} \left(\frac{T_1 - T_2}{T_1 + T_2} \right) \ln \frac{(L_{wc}^2 - R^2)(L_{pc}^2 - R^2) + \rho^2 R^2}{(L_{wc}^2 - R^2)(L_{pc}^2 - R^2) + r^2 R^2} \right\}, \quad (4.24)$$

where R is the radius of the semicircle, m ; L_{wc} is the distance from the pumping well to the center, m ; L_{pc} is the distance from the observation well to the center, which is evaluated based on specified distances:

$$L_{pc} = \sqrt{\left(\sqrt{r^2 - (L_w - L_{p1})^2} - \sqrt{L_{wc}^2 - L_w^2} \right)^2 + L_{p1}^2}. \quad (4.25)$$

For the calculation of the distance to the image well (ρ), see Eq. A3.1.

2. The drawdown in the adjacent zone is:

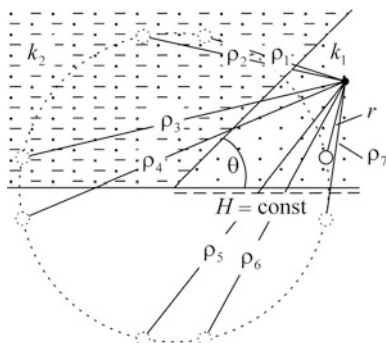
$$s_m^{(2)} = \frac{Q}{\pi(T_1 + T_2)} \ln \frac{\rho}{r}. \quad (4.26)$$

4.3.3 Wedge-Shaped Aquifer

The basic assumptions and conditions (Fig. 4.5) are:

- general conditions for a horizontally heterogeneous aquifer with a linear interface (see the beginning of Sect. 4.1);

Fig. 4.5 Horizontally heterogeneous aquifer with two intersecting rectilinear boundaries (planar view). Image wells and the distances to them are shown in the figure



- the main zone is limited by two semi-infinite crossing boundaries (a wedge-shaped aquifer), of which one is a constant-head boundary and the other is the interface between the two zones;
- the adjacent zone is semi-limited in the horizontal plane by a linear impermeable boundary and the interface between the two zones;
- an observation well, fully penetrating, is located in the main zone.

The drawdown is determined in the main zone.

As was the case with a wedge-shaped aquifer (see Sect. 1.1.4), the angle between the two boundaries cannot be arbitrary. The list of angle sizes acceptable for processing is the same as that for a pumping test in a wedge-shaped aquifer with mixed boundary conditions (see Appendix 3).

With an increase in the hydraulic conductivity of the adjacent zone, the problem setting transforms to a setting of a wedge-shaped aquifer with a constant-head boundaries (see Sect. 1.1.4.1); while a decrease in the hydraulic conductivity results in mixed boundary conditions (see Sect. 1.1.4.3).

The drawdown in the main zone in the steady-state flow period is described by the following equation (Bochever et al. 1979):

$$s_m^{(1)} = \frac{Q}{2\pi T_1} \left\{ \ln \frac{\rho_{4n-1}}{r} + \left(\frac{T_2 - T_1}{T_2 + T_1} \right)^n \ln \frac{\rho_{2n-1}}{\rho_{2n}} + \ln \sum_{j=1}^{n-1} \left(\frac{T_2 - T_1}{T_2 + T_1} \right)^j \ln \frac{\rho_{2j-1} \rho_{4n-2j-1}}{\rho_{2j} \rho_{4n-2j}} \right\}, \quad (4.27)$$

$$n = \frac{\pi}{2\theta} = \frac{90}{\theta}, \quad (4.28)$$

where θ is the angle between the intersecting boundaries (Fig. 4.5), in degrees; ρ_j are the distances to the image wells, which are evaluated similarly to the scheme of a wedge-shaped aquifer (see Eq. A3.6), m.

4.3.4 Circular Aquifer

Concentric planar zones with different hydraulic conductivity are considered (Fig. 4.6). The outer zone has a circular constant-head boundary. The drawdown in the steady-state flow period is determined in the pumping well located in the center of the first zone.

The maximal drawdown in the pumping well (Pykhachov and Isayev 1973) is:

$$s_{mw} = \frac{Q}{2\pi m} \left(\frac{1}{k_1} \ln \frac{R_1}{r_w} + \sum_{i=2}^N \frac{1}{k_i} \ln \frac{R_i}{R_{i-1}} \right), \quad (4.29)$$

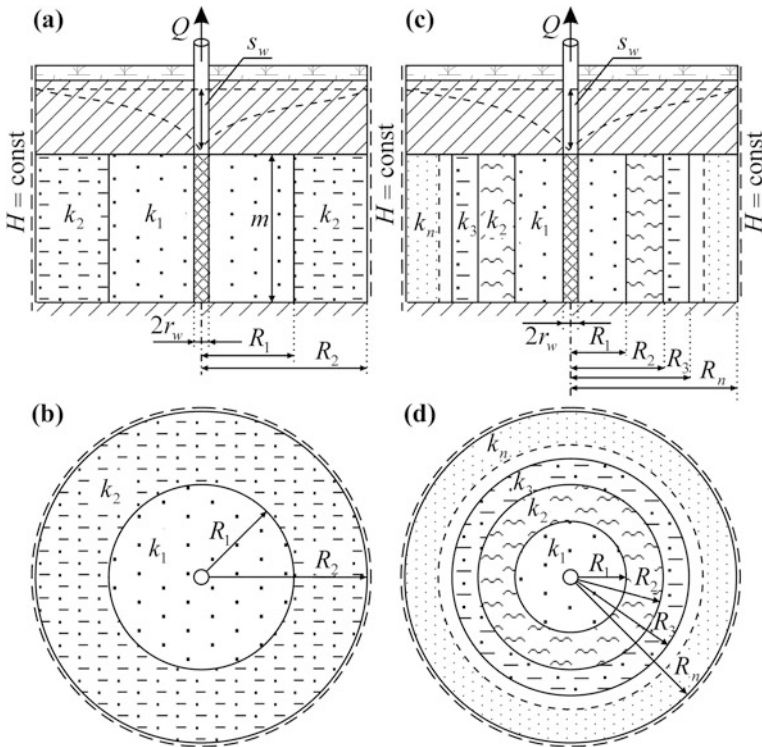


Fig. 4.6 Horizontally heterogeneous aquifer limited by a circular constant-head boundary. The section and plan for **a, b** two and **c, d** several circular zones

where k_i is the hydraulic conductivity of the i -th zone, m/d; N is the number of circular zones; R_i is the radius of the i -th zone, m.

In the case of two circular zones, the solution (Eq. 4.29) becomes simpler (Shchelkachev and Lapuk 1949):

$$s_{mw} = \frac{Q}{2\pi m} \left(\frac{1}{k_1} \ln \frac{R_1}{r_w} + \frac{1}{k_2} \ln \frac{R_2}{R_1} \right). \quad (4.30)$$

References

- Bochever FM, Lapshin NN, Oradovskaya AE (1979) Design calculations for wellhead protection areas. Nedra, Moscow (In Russian)
- Fenske PR (1984) Unsteady drawdown in the presence of a linear discontinuity. In: Rosenshein JS, Bennett GD (eds) Groundwater hydraulics. Water Resources Monograph Series 9. American Geophysical Union, Washington, pp 125–145
- Maksimov VA (1962) On unsteady-state flow of elastic fluid to a well in heterogeneous media. J Appl Mech Tech Phys 3:109–112 (In Russian)
- Pykhachov GB, Isayev RG (1973) Groundwater hydraulics. Nedra, Moscow (In Russian)
- Shchelkachev VN, Lapuk BB (1949) Groundwater hydraulics. Gostoptehizdat, Moscow (In Russian)
- Yeh HD, Yang SY, Peng HY (2003) A new closed-form solution for a radial two-layer drawdown equation for groundwater under constant-flux pumping in a finite-radius well. Adv Water Resour 26(7):747–757

Chapter 5

Pumping Test near a Stream

An isotropic aquifer is crossed by a river. The pumping and observation wells are fully penetrating. The chapter considers analytical solutions for calculating the drawdown depending on river geometry and hydrodynamic conditions: (1) the stream is a boundary of the flow (Sect. 5.1) and (2) the stream is a boundary that does not limit the cone depletion (Sect. 5.2). Steady-state solutions for pumping from a well under the stream are considered separately (Sect. 5.3).

5.1 A Semipervious Stream

The basic assumptions and conditions (Figs. 5.1 and 5.3) are:

- the aquifer is semi-infinite, confined or unconfined;
- a Cauchy boundary condition is considered.

To solve the problem, the image-well method is used: a single image well is introduced.

The drawdown is determined within the aquifer at any distance from the pumping well to the river. A typical plot of the drawdown in the observation well is given in Fig. 12.26.

Basic Analytical Relationships

Transient Flow Equations

1. The Shestakov solution (Zeegofer and Shestakov 1968) (Fig. 5.1) is:

$$s = \frac{Q}{4\pi T} \left[W\left(\frac{r^2}{4at}\right) - W\left(\frac{\rho_L^2}{4at}\right) \right], \quad (5.1)$$

$$\rho_L = \rho \cdot f_L\left(\frac{\Delta L}{\rho}\right), \quad (5.2)$$

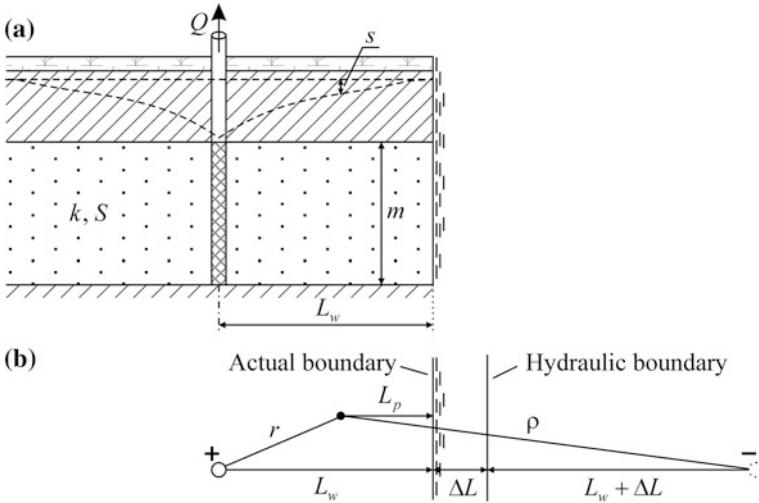


Fig. 5.1 Schematic diagram of a pumping test near a stream. A scheme for the Shestakov solution. **a** Cross-section; **b** planar view (the signs of actual and image discharge are given at the wells)

$$\rho = \sqrt{(L_p + L_w + 2\Delta L)^2 + r^2 - (L_w - L_p)^2}, \tag{5.3}$$

where s is the drawdown in an observation well, m ; Q is the discharge rate, m^3/d ; t is the time elapsed from the start of pumping, d ; $T = km$ is aquifer transmissivity, m^2/d ; k , m are the hydraulic conductivity (m/d) and thickness (m); $a = T/S$ is aquifer hydraulic diffusivity, m^2/d ; S is the aquifer storage coefficient, dimensionless; r is the radial distance from the pumping to the observation well, m ; L_w and L_p are the distances from the pumping well and the observation well to the boundary, m ; ΔL here, is the retardation coefficient of the semipervious stream bed (Eq. 5.4), m ; ρ is the distance from the observation to the image well with the stream bed resistance taken into account (Eq. 5.3), m ; $W(\cdot)$ is the well-function (see Appendix 7.1); $f_L(\cdot)$ is a special function (Fig. 5.2, Table 5.1).

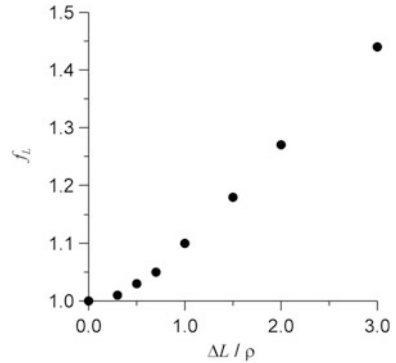
The retardation coefficient of the semipervious stream bed is calculated using the theoretical relationship (Mironenko and Shestakov 1978):

$$\Delta L = \sqrt{Tm'/k'} \cotanh\left(\frac{nb}{\sqrt{Tm'/k'}}\right), \tag{5.4}$$

Table 5.1 Table of f_L and $\Delta L/\rho$

$\Delta L/\rho$	0.0	0.3	0.5	0.7	1.0	1.5	2.0	3.0
f_L	1.00	1.01	1.03	1.05	1.10	1.18	1.27	1.44

Fig. 5.2 Dependence of f_L on the ratio $\Delta L/\rho$



where m' is the thickness of the semipervious layer of the stream bed, m ; k' the hydraulic conductivity of the semipervious layer of the stream bed, m/d ; b is river width, m ; $n = 0.5, 1$, depending on river width.

Zeegofer and Shestakov (1968) tabulated the function f_L depending on the ratio of ΔL to ρ (Table 5.1).

Function f_L is plotted in Fig. 5.2.

For $\beta = \Delta L/\rho > 2$, we have an approximation (Zeegofer and Shestakov 1968):

$$f_L(\beta) = 0.96 + 0.16 \beta. \tag{5.5}$$

For $\beta = \Delta L/\rho \leq 2$, the following polynomial approximation can be used (Sindalovskiy 2006):

$$f_L(\beta) = 1 - 0.00259435 \beta + 0.1424847 \beta^2 - 0.04896219 \beta^3 + 0.0060177989 \beta^4. \tag{5.6}$$

According to Shestakov's estimates (1973), Eq. 5.1 can be used in calculations with acceptable accuracy (from 1 to 2 %), for time $t \geq (5 \cdot \Delta L)^2/a$.

The Shestakov solution (Eq. 5.1) yields the transmissivity (T) and storage coefficient (S) of the aquifer and estimates the retardation coefficient of the semipervious stream bed (ΔL), calculated by (Eq. 5.4).

2. The Hantush solution (Hantush 1965) (Fig. 5.3) is:

$$s = m - \sqrt{m^2 - \frac{Q}{2\pi k} \left[W\left(\frac{r^2}{4at}\right) - W\left(\frac{\rho^2}{4at}\right) + 2J^*(u, \beta_1, \beta_2) \right]}, \tag{5.7}$$

$$J^*(u, \beta_1, \beta_2) = 2 \int_1^{\infty} \exp[-\beta_1(\tau - 1) - u(\tau^2 + \beta_2^2)] \frac{\tau}{\tau^2 + \beta_2^2} d\tau, \quad (5.8)$$

$$u = \frac{(L_w + L_p)^2}{4at}, \quad (5.9)$$

$$\beta_1 = \frac{L_w + L_p}{\Delta L}, \quad (5.10)$$

$$\beta_2 = \frac{\sqrt{r^2 - (L_w - L_p)^2}}{L_w + L_p}, \quad (5.11)$$

$$\Delta L = \frac{k}{k'} m', \quad (5.12)$$

where $a = km/S_y$ is the hydraulic diffusivity of the unconfined aquifer, m^2/d ; S_y is the specific yield, dimensionless; m is the initial saturated thickness of unconfined aquifer, m; ΔL is the retardation coefficient of the semipervious stream bed (Eq. 5.12), m; k' , m' is the hydraulic conductivity (m/d) and thickness (m) of the semipervious stream bed; ρ is the distance between the observation and image wells (Eq. A3.1), m; $J^*(u, \beta_1, \beta_2)$ is a special function (see Appendix 7.7).

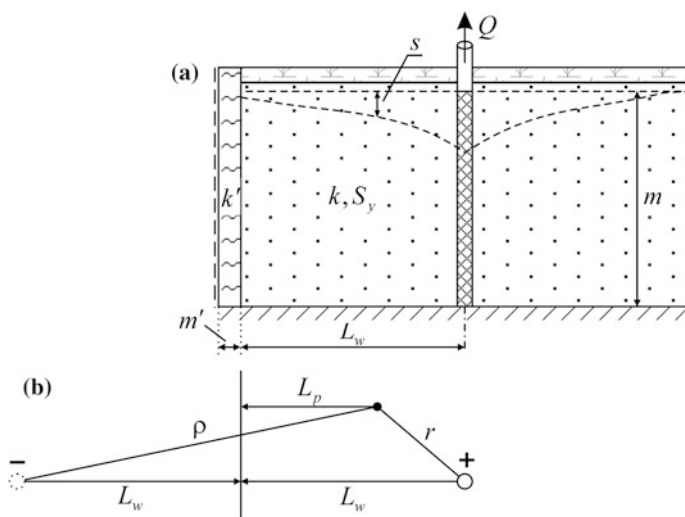


Fig. 5.3 Schematic diagram of a pumping test near a stream. Scheme to apply the Hantush solution. **a** Cross-section; **b** planar view (the signs of the actual and image discharges are given at the wells)

Table 5.2 Transformation of Eq. 5.7

k'	ΔL	$J^*(\cdot)$	Equation 5.7
$k' \rightarrow \infty$	$\Delta L \rightarrow 0$	$J^*(u, \infty, \beta_2) = 0$	Constant-head boundary ^a
$k' \rightarrow 0$	$\Delta L \rightarrow \infty$	$J^*(u, 0, \beta_2) = W(u + u\beta_2^2) = W\left(\frac{\rho^2}{4at}\right)$ ^b	Impermeable boundary ^c

$$^a s = m - \sqrt{m^2 - \frac{Q}{2\pi k} \left[W\left(\frac{r^2}{4at}\right) - W\left(\frac{\rho^2}{4at}\right) \right]}$$
—solution for a constant-head boundary

$$^b u + u\beta_2^2 = \frac{(L_w + L_p)^2}{4at} + \frac{(L_w + L_p)^2}{4at} \left(\frac{\sqrt{r^2 - (L_w - L_p)^2}}{L_w + L_p} \right)^2 = \frac{r^2 + 4L_w L_p}{4at} = \frac{\rho^2}{4at}$$

$$^c s = m - \sqrt{m^2 - \frac{Q}{2\pi k} \left[W\left(\frac{r^2}{4at}\right) + W\left(\frac{\rho^2}{4at}\right) \right]}$$
—solution for an impermeable boundary

Solution (Eq. 5.7) is given for a gravity-drainage period. At the limiting values of hydraulic conductivity of the stream bed k' , Eq. 5.7 tends to the equation for a constant-head or impermeable boundary (Table 5.2).

The Hantush solution (Eq. 5.7) is determined by the following hydraulic parameters: hydraulic conductivity (k), specific yield (S_y), and the retardation coefficient of the semipervious stream bed (ΔL), calculated by (Eq. 5.12).

Steady-State Flow Equation

$$s_m = \frac{Q}{2\pi T} \ln \frac{\rho_L}{r}, \tag{5.13}$$

where s_m is the drawdown in the observation well during steady-state period, m.

Equation 5.13, derived from Shestakov solution (Eq. 5.1), is applied to the scheme given in Fig. 5.1.

Graphic-Analytical Processing

The relationship given in Table 5.3 has been derived from Eq. 5.13.

Table 5.3 Graphic-analytical parameter evaluation

Plot	Method	Relationship
$s - \lg t$	Horizontal straight line ^a	$T = \frac{Q}{2\pi \cdot A} \ln \frac{\rho_L}{r}$

^aThe plot is constructed by the drawdown values for a steady-state flow period, given the retardation coefficient of the semipervious stream bed ΔL , which is evaluated by Eq. 5.4

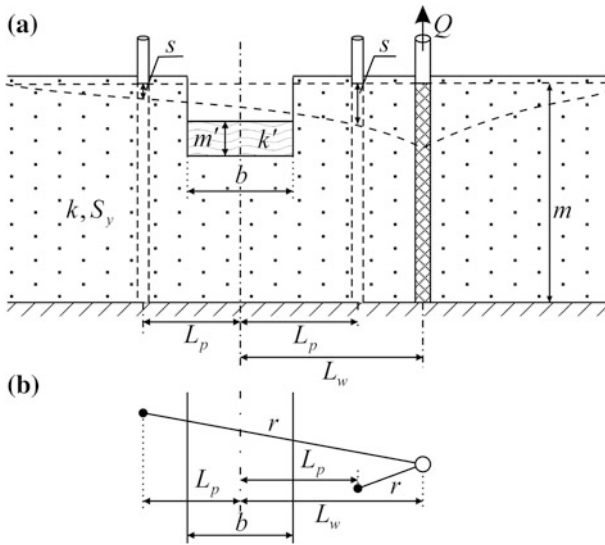


Fig. 5.4 Schematic diagram of a pumping test in an aquifer near a partially penetrating stream of finite width. **a** Cross-section; **b** planar view

5.2 Partially Penetrating Stream of Finite Width

The basic assumptions and conditions (Figs. 5.4, 5.5, and 5.6) are:

- the aquifer is unconfined; the case of leakage from the underlying aquifer is considered (Fig. 5.5);
- the boundary is partially penetrating river of a finite width.

The drawdown is determined within the aquifer at any distance from the pumping well.

Basic Analytical Relationships

Transient Flow Equations

1. Nonleaky aquifer (Hunt 1999) (Fig. 5.4):

$$s = \frac{Q}{4\pi km} \left[W\left(\frac{r^2}{4at}\right) - \int_0^{\infty} e^{-\tau} W\left(\frac{\rho_0^2}{4at}\right) d\tau \right], \quad (5.14)$$

$$\rho_0^2 = \left(L_w + L_p + 2\Delta L \frac{m}{b} \tau\right)^2 + y^2, \quad (5.15)$$

where b is river width, m ; ΔL is retardation coefficient of the semipervious stream bed (Eq. 5.12), m ; L_w, L_p are the distances from the pumping and observation wells to the middle of the river, respectively, m.

The value of y is calculated depending on the position of the observation well with respect to the river: in front of the river (on the same side as the pumping well):

$$y^2 = r^2 - (L_w - L_p)^2 \tag{5.16}$$

or over the river:

$$y^2 = r^2 - (L_w + L_p)^2. \tag{5.17}$$

2. A leaky aquifer (Zlotnik and Tartakovsky 2008) (Fig. 5.5):

$$s = \frac{Q}{4\pi km} \left[W\left(\frac{r^2}{4at}, \frac{r}{B}\right) - \int_0^\infty e^{-\tau} W\left(\frac{\rho_0^2}{4at}, \frac{\rho_0}{B}\right) d\tau \right]; \tag{5.18}$$

here:

$$B = \sqrt{km m''/k''}, \tag{5.19}$$

k'', m'' are aquitard hydraulic conductivity (m/d) and thickness (m); $W(u, \beta)$ is the well-function for leaky aquifers (see Appendix 7.2).

With a correction of the drawdown (see Sect. 2.1), solutions (Eqs. 5.14 and 5.18) become:

$$s = m - \sqrt{m^2 - \frac{Q}{2\pi k} f}, \tag{5.20}$$

where f is the expression in square brackets in Eqs. 5.14 and 5.18.

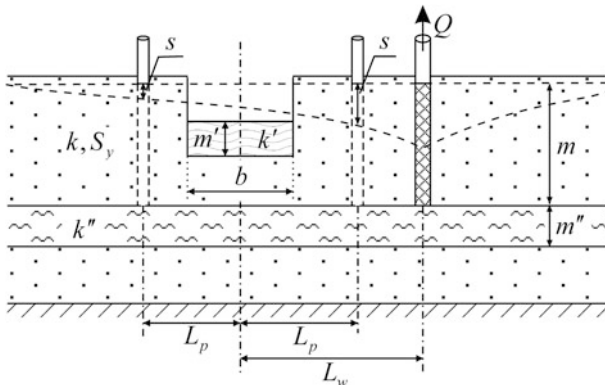


Fig. 5.5 Schematic diagram of a pumping test in a leaky aquifer near a partially penetrating stream of finite width: cross-section; for a planar view, see Fig. 5.4b

Solutions (Eqs. 5.14 and 5.18) are given for a gravity-drainage period. As was the case with Hantush solution (Eq. 5.7), the hydraulic parameters to be determined in this case are the hydraulic conductivity (k), specific yield (S_y), and retardation coefficient of the semipervious stream bed (ΔL), calculated by Eq. 5.12. In addition, solution (Eq. 5.18) takes into account the leakage factor (B), which, in notations of Fig. 5.5, corresponds to formula (Eq. 5.19).

Steady-State Flow Equations (Zlotnik and Tartakovsky 2008)

1. Nonleaky aquifer (Fig. 5.4):

$$s_m = \frac{Q}{4\pi km} \left[\ln \frac{(L_w + L_p)^2 + y^2}{r^2} + 2 \int_{1+L_p/L_w}^{\infty} \frac{\tau}{\tau^2 + (y/L_w)^2} \exp\left(-L_w \frac{\tau - 1 - L_p/L_w}{2\Delta L} \frac{b}{m}\right) d\tau \right]. \quad (5.21)$$

2. Leaky aquifer (Fig. 5.5):

$$s_m = \frac{Q}{2\pi km} \left[K_0\left(\frac{r}{B}\right) - \int_0^{\infty} e^{-\tau} K_0\left(\frac{\rho_0}{B}\right) d\tau \right], \quad (5.22)$$

where ρ_0 see Eq. 5.15; B see Eq. 5.19; $K_0(\cdot)$ is modified Bessel function of the second kind of the zero order (see Appendix 7.13).

3. The drawdown in observation wells in the period of steady-state flow is determined in three zones (Fig. 5.6): (1) in front of the river—the zone of location of the pumping well, (2) over the river, and (3) under the riverbed. All zones have the same values of hydraulic conductivity. The thickness of the third zone is generally less than the thickness of the first two. Riverbed hydraulic conductivity differs from that of the aquifer.

The maximal drawdown in each of the three zones is calculated by the following equations (Bochever and Gylybov 1966; Bochever et al. 1968):

$$s_m^{(1)} = \frac{Q}{2\pi km} \left(\ln \frac{\rho}{r} + f_1 + f_2 \right), \quad (5.23)$$

$$s_m^{(2)} = \frac{Q}{2\pi km} (f_2 - f_1), \quad (5.24)$$

$$s_m^{(3)} = \frac{Q}{2\pi km} \frac{1}{\sinh(b/B)} \left[\sinh \frac{b - L_{p3}}{B} (f_1 + f_2) + \sinh \frac{L_{p3}}{B} (f_2 - f_1) \right]. \quad (5.25)$$

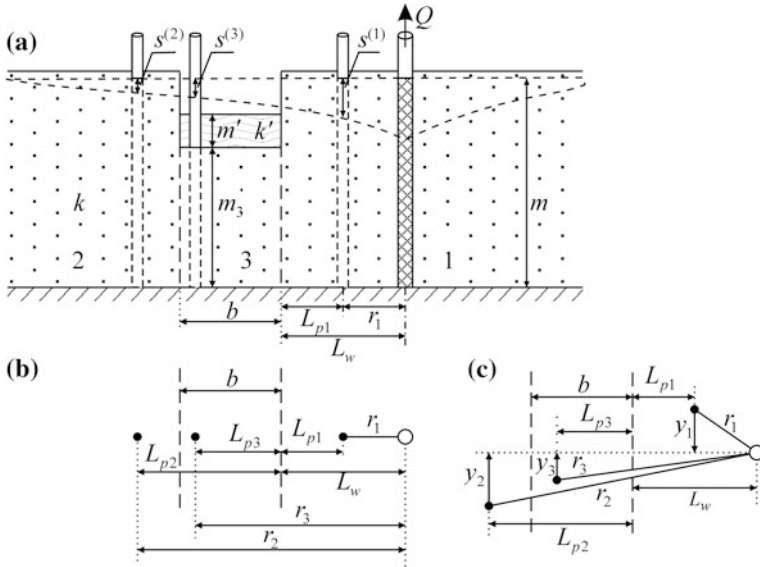


Fig. 5.6 Pumping near a stream. Scheme for determining drawdown in three zones. **a** Cross-section; **b, c** a planar view for wells **b** located along a straight line perpendicular to the river and **c** arbitrarily distributed. The numbers show the zones in which the drawdown is evaluated

Table 5.4 The values of functions f_1 and f_2 for different well locations

Wells are located along a straight line (Fig. 5.6b)	Arbitrary location of wells (Fig. 5.6c)
$f_1 = \exp(\alpha_i \beta_1) W(\alpha_i \beta_1)$	$f_1 = F_r(\alpha_i \beta_1, \alpha y \beta_1)$
$f_2 = \exp(\alpha_i \beta_2) W(\alpha_i \beta_2)$	$f_2 = F_r(\alpha_i \beta_2, \alpha y \beta_2)$

Table 5.5 Formulas for calculating α_i and y_i for three zones

	Zone 1	Zone 2	Zone 3
α_i	$\alpha_1 = \alpha(L_w + L_{p1})$	$\alpha_2 = \alpha(L_w + L_{p2} - b)$	$\alpha_3 = \alpha L_w$
y_i	$y_1 = \sqrt{r_1^2 - (L_w - L_{p1})^2}$	$y_2 = \sqrt{r_2^2 - (L_w + L_{p2})^2}$	$y_3 = \sqrt{r_3^2 - (L_w + L_{p3})^2}$

To solve Eqs. 5.23–5.25, Tables 5.4 and 5.5 are to be used along with the relationships:

$$F_r(\gamma_1, \gamma_2) = \int_0^{\infty} \frac{\exp(-\tau \gamma_1)}{1 + \tau} \cos(\tau \gamma_2) d\tau, \quad (5.26)$$

$$\beta_1 = 1 + \frac{1}{\cosh(b/B)}, \quad \beta_2 = 1 - \frac{1}{\cosh(b/B)}, \quad (5.27)$$

$$\alpha = \frac{m_3 \Delta L}{m B^2}, \quad (5.28)$$

$$B = \sqrt{km_3 m' / k'}, \quad (5.29)$$

where B is leakage factor: formula (Eq. 5.29), m ; $F_r(\gamma_1, \gamma_2)$ is a special function; α is a combined characteristic of the river-channel penetration and low-permeability of the river bed: formula (Eq. 5.28), $1/m$; m_3 is aquifer thickness under the river, m ; L_w is the distance from the pumping well to the boundary, m ; L_{pi} , y_i ($i = 1, 2, 3$) are the distances from the observation wells to the boundary and projections of the distances from the observation wells to the pumping well onto the boundary line (see Table 5.5 and Fig. 5.6), m ; α_i —see Table 5.5; ρ is the distance from the observation well, located in the first zone, to the image well (m), which is determined in the same manner as for the semi-infinite aquifers, and, in the denotations of this problem is:

$$\rho = \sqrt{r^2 + 4L_w L_{p1}}; \quad (5.30)$$

ΔL is the retardation coefficient of the semipervious stream bed (m), which is calculated similar to Eq. 5.4, and in the denotations of this problem so:

$$\Delta L = B \cotanh(b/B). \quad (5.31)$$

When all wells are located on a straight line (Fig. 5.6b), we have $y_i = 0$, and the distances between the wells can be expressed in terms of the distances to the river: $r_1 = L_w - L_{p1}$, $r_2 = L_w + L_{p2}$, $r_3 = L_w + L_{p3}$.

5.3 Pumping from a Well under a Stream

The pumping well is located under river bed (Fig. 5.7). The drawdown during the steady-state flow period depends on whether there is a semipervious stream bed.

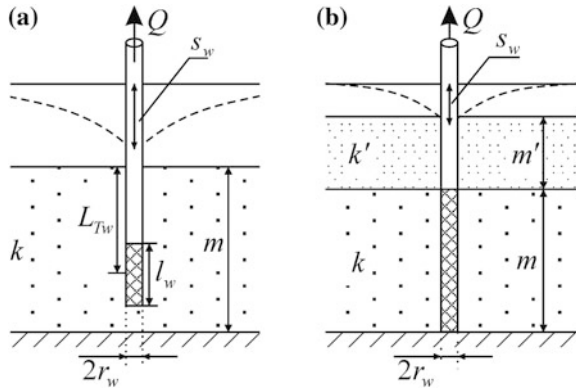
Basic Analytical Relationships

Steady-State Flow Equations

1. Pumping from a partially penetrating well (Fig. 5.7a), directly interacting aquifer and river. The drawdown in the pumping well (Babushkin 1954) is:

$$s_{mw} = \frac{Q}{2\pi k l_w} \left[\ln \frac{0.75l_w \sqrt{m - L_{Tw} + 0.25l_w}}{r_w \sqrt{m - L_{Tw} - 0.25l_w}} - \frac{1}{2} \ln \frac{(L_{Tw} + 0.25l_w)(m + 0.25l_w)}{(L_{Tw} - 0.25l_w)(m - 0.25l_w)} \right], \quad (5.32)$$

Fig. 5.7 Pumping under a river: **a** direct interaction between the aquifer and the river and **b** there is a semipervious stream bed



where s_{mw} is the drawdown in the pumping well during a steady-state period, m ; L_{Tw} is the vertical distance from the river bed to the center of pumping well screen, m ; l_w is screen length, m ; r_w pumping well radius, m .

2. Pumping from a fully penetrating well (Fig. 5.7b) in the presence of a low-permeability bed. The drawdown in the pumping well (Bindeman 1951) is:

$$s_{mw} = \frac{Q}{2\pi km} \ln \left(\frac{1.12}{r_w} \sqrt{\frac{km m'}{k'}} \right). \quad (5.33)$$

References

Babushkin VD (1954) Evaluating permeability of rocks under the river bed. Prospect Prot Miner Resour 4:45–53 (In Russian)

Bindeman NN (1951) Methods for water flow properties evaluation from pumping, injection and recharge test data. Ugltehizdat, Moscow (In Russian)

Bochever FM, Gylybov MM (1966) Evaluation of silting and heterogeneity of river bed deposits from pumping test data. Prospect Prot Miner Resour 2:44–49 (In Russian)

Bochever FM, Lapshin NN, Khohlatov EM (1968) Evaluation of groundwater inflow to wells in river valleys. Prospect Prot Miner Resour 9:44–49 (In Russian)

Hantush MS (1965) Wells near streams with semipervious beds. J Geophys Res 70(12):2829–2838

Hunt B (1999) Unsteady stream depletion from ground water pumping. Ground Water 37(1): 98–102

Mironenko VA, Shestakov VM (1978) Theory and methods of pumping test analysis and interpretation. Nedra, Moscow (In Russian)

Sindalovskiy LN (2006) Handbook of analytical solutions for aquifer test analysis. SpBSU, Sankt-Petersburg (In Russian)

Zeehofer YO, Shestakov VM (1968) Methods for analysis of data from pumping test near a river. Prospect Prot Miner Resour 9:38–44 (In Russian)

Zlotnik VA, Tartakovsky DM (2008) Stream depletion by groundwater pumping in leaky aquifers. J Hydrol Eng 13(2):43–50

Chapter 6

Fractured-Porous Reservoir

This chapter considers solutions for pumping tests in different types of fractured–porous media (Moench solutions) and in aquifers where the pumping well crosses a single vertical or horizontal fracture (fissure) of a finite size.

6.1 Moench Solutions

Pumping tests in fractured–porous media can be described by Moench solutions (Moench 1984). Such solutions are available for: (1) slab-shaped blocks (Fig. 6.1a), (2) sphere-shaped blocks (Fig. 6.1b), and (3) an orthogonal fracture system, Warren–Root model (Warren and Root 1963) (Fig. 6.1c).

A typical drawdown plot in a fractured-porous medium is given in Fig. 12.27.

Basic Analytical Relationships

The basic flow equations are too complicated for practical application, because they depend on many parameters and require special software. Graphic-analytical processing methods are not given here; however, simplified relationships can be used in some cases (see Eqs. 6.7–6.9).

Transient Flow Equations

1. The drawdown in a fracture (s) and a block (s') for a layered system of fractures and blocks (Fig. 6.1a, d) and for spherical blocks (Fig. 6.1b) is:

$$s = \frac{Q}{4\pi km} f\left(t, r, r_w, r_c, k, k', S_s, S'_s, m_b, k_{skin}, m_{skin}, k_{skin}^f, m_{skin}^f\right), \quad (6.1)$$

$$s' = \frac{Q}{4\pi km} f\left(t, r, r_w, r_c, k, k', S_s, S'_s, m_b, z_p, k_{skin}, m_{skin}, k_{skin}^f, m_{skin}^f\right), \quad (6.2)$$

where Q is the discharge rate, m^3/d ; m is aquifer thickness, m ; r is the radial distance from the pumping to the observation well, m ; r_w , r_c are the radiuses of the pumping well and its casing, m ; t is the time elapsed from the start of pumping, d .

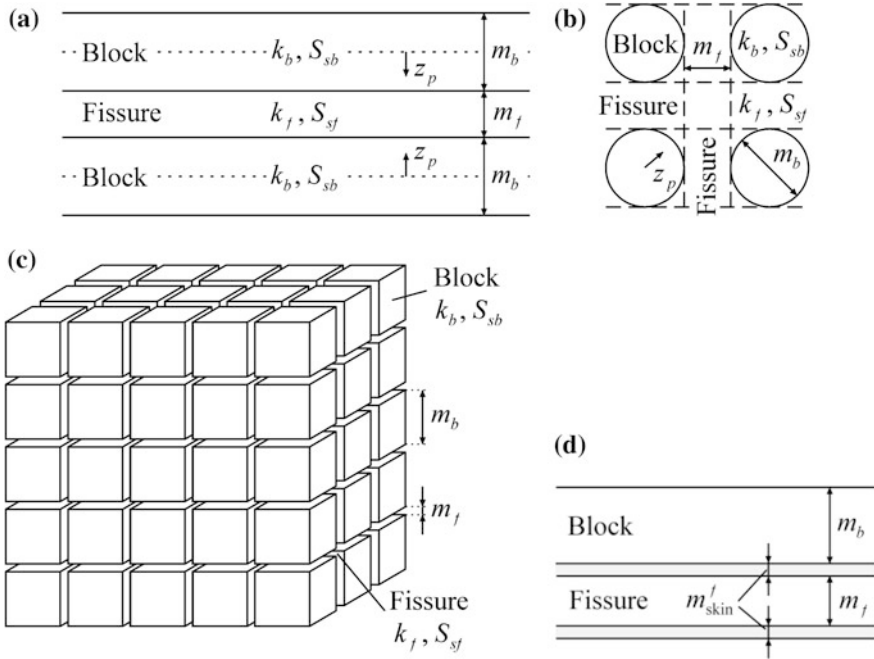


Fig. 6.1 Schematic diagrams of fracture–porous media. **a** Slab-shaped blocks; **b** sphere-shaped blocks; **c** an orthogonal fracture system (Warren–Root model); **d** a scheme of a fracture and a block with a fracture skin

2. The drawdown in an aquifer with an orthogonal fracture system (Fig. 6.1c) is:

$$s = \frac{Q}{4\pi km} f(t, r, r_w, r_c, k, k', S_s, S'_s, m_b, k_{skin}, m_{skin}). \quad (6.3)$$

The algorithm of the program DP_LAQ (see Appendix 5.5) is used to process the functional relationships (Eqs. 6.1–6.3).

Given below are parameter denotations for the solutions under consideration: k_{skin} , m_{skin} are the hydraulic conductivity (m/d) and the thickness (m) of wellbore skin, respectively (see Appendix 2); k_{skin}^f , m_{skin}^f are the hydraulic conductivity (m/d) and the thickness (m) of fracture skin, respectively (Fig. 6.1d); $k = k_f V_f / V$ is the hydraulic conductivity of the fissure system, m/d; $k' = k_b V_b / V$ is the hydraulic conductivity of the block system, m/d; k_f is the hydraulic conductivity of an average fissure, m/d; k_b is the hydraulic conductivity of an average block, m/d; m_b is the average thickness or diameter of blocks, m; m_f is the average aperture of a fissure, m; $S_s = S_{sf} V_f / V$ is the specific storage of the fracture system, 1/m; $S'_s = S_{sb} V_b / V$ is the specific storage of the block system, 1/m; S_{sf} is the specific storage of an average fissure, 1/m; S_{sb} is the specific storage of an average block, 1/m; V_f is the

volume of fissures, m^3 ; V_b is the volume of blocks, m^3 ; V is the bulk volume, m^3 ; z_p is the distance to block center, i.e., the point where level variations in the block are measured (see Fig. 6.1a, b), m.

Moench solutions are used to evaluate the hydraulic conductivity and the specific storage of fractured (k , S_s) and block (k' , S'_s) systems. The solutions can take into account the wellbore storage and the skin effect, which is derived from the hydraulic conductivity and thickness of the wellbore skin k_{skin} , m_{skin} ; for solutions (Eqs. 6.1 and 6.2), in addition, the hydraulic conductivity and the thickness of fracture skin (k_{skin}^f , m_{skin}^f) are also determined. For all solutions, the block size (m_b) is to be specified: the block thickness for a layered fracture system, the radius for spherical blocks, and the edge length of a cubic block for an orthogonal system.

The wellbore storage of a fully penetrating pumping well in a fractured-porous medium is calculated as (Moench 1984):

$$W_D = \frac{r_c^2}{2r_w^2 S_s m}. \quad (6.4)$$

The effect of wellbore skin can be written by analogy with Eq. A2.2 as:

$$W_{\text{skin}} = \frac{km_{\text{skin}}}{r_w k_{\text{skin}}}. \quad (6.5)$$

The estimation of dimensionless parameters (Eqs. 6.4 and 6.5) involves the hydraulic parameters of the fractured system (see comments above).

The skin effect of the fracture (Fig. 6.1d) is accounted for by the following dimensionless parameter (dimensionless fracture skin) (Moench 1984):

$$W_{\text{skin}}^f = \frac{k' m_{\text{skin}}^f}{k_{\text{skin}}^f m_b / 2}. \quad (6.6)$$

3. Simplified solutions. De Smedt (2011) gives some approximations that can be applied at some limiting values of block storage.

3.1. In the case of no storage in the blocks $S' \rightarrow 0$ or no fluid exchange between fissures and blocks, $C \rightarrow 0$:

$$s = \frac{Q}{4\pi km} W\left(\frac{r^2 S}{4kmt}\right), \quad (6.7)$$

where $C = \alpha k' m$ is the leakage coefficient between fissures and blocks, $1/d$; α is a geometric parameter (see the description of the program DP_LAQ in Appendix 5.5), $1/m^2$; $W(u)$ is the well-function (see Appendix 7.1).

3.2. The response of block storage is instantaneous $C \rightarrow \infty$:

$$s = \frac{Q}{4\pi km} W\left(\frac{r^2(S+S')}{4kmt}\right). \quad (6.8)$$

3.3. The storage of blocks is infinite $S' \rightarrow \infty$:

$$s = \frac{Q}{4\pi km} W\left(\frac{r^2 S}{4kmt}, r\sqrt{\frac{C}{km}}\right), \quad (6.9)$$

where $W(u, \beta)$ is the well-function for leaky aquifers (see Appendix 7.2).

6.2 Pumping Well Intersecting a Single Vertical Fracture

The basic assumptions and conditions (Fig. 6.2) are:

- the aquifer is confined and isotropic, with infinite lateral extent;
- the fracture is of limited length and a height equal to the aquifer thickness;
- the pumping well is fully penetrating, located in the center of the fracture;
- the observation well is fully penetrating;
- the flow to the well is pseudoradial (Fig. 6.3a) or linear (Fig. 6.3b);
- fracture storage is ignored.

The drawdown is determined at any distance from the pumping well.

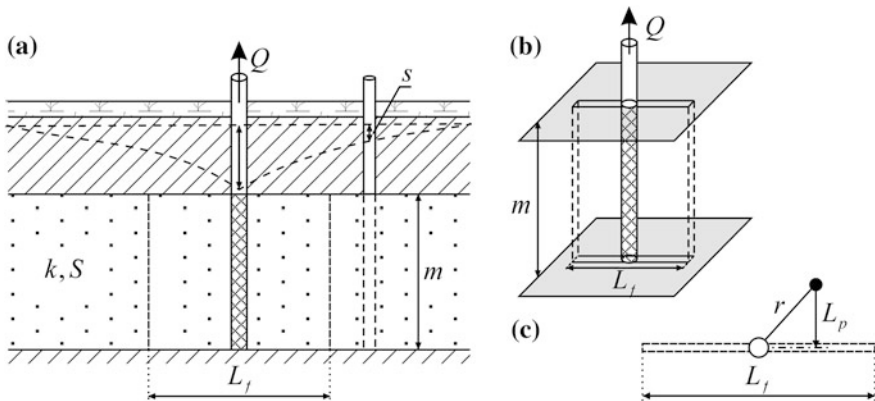


Fig. 6.2 Schematic diagram of a well in a vertical fracture of limited length. **a** Cross-section; **b** three-dimensional representation; **c** planar view

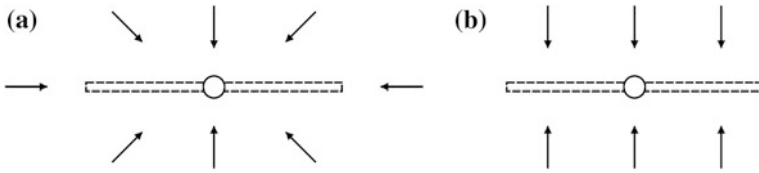


Fig. 6.3 Schemes (planar view) of **a** pseudo-radial and **b** linear flow toward a vertical fracture

Basic Analytical Relationships

Transient Flow Equations

1. Pseudo-radial flow toward a fracture (Fig. 6.3a) (Gringarten et al. 1974) is:

$$s = \frac{Q}{8\sqrt{\pi}T} \int_0^u \exp\left(\frac{-L_p^2/L_f^2}{\tau}\right) \left(\operatorname{erf} \frac{1-\beta}{2\sqrt{\tau}} + \operatorname{erf} \frac{1+\beta}{2\sqrt{\tau}} \right) \frac{d\tau}{\sqrt{\tau}}, \quad (6.10)$$

$$u = \frac{4Tt}{L_f^2 S}, \quad (6.11)$$

$$\beta = 2 \frac{\sqrt{r^2 - L_p^2}}{L_f}, \quad (6.12)$$

where T , S is the transmissivity (m^2/d) and the storage coefficient (dimensionless) of the aquifer; L_f is fracture length, m; L_p is the horizontal distance from the observation well to the fracture (Fig. 6.2c), m; $\operatorname{erf}(\cdot)$ is error function (see Appendix 7.12).

2. Linear (parallel) flow to a fracture (Fig. 6.3b) (Jenkins and Prentice 1982) is:

$$s = \frac{Q}{2L_f T} \left\{ \sqrt{\frac{4Tt}{\pi S}} \exp\left[-\frac{L_p^2 S}{4Tt}\right] + L_p \left[\operatorname{erf} \sqrt{\frac{L_p^2 S}{4Tt}} - 1 \right] \right\}. \quad (6.13)$$

The relationship for linear flow (Eq. 6.10) is recommended for use in the case of pumping from a well located in a fracture of great length or for initial moments in time.

Solutions (Eqs. 6.10 and 6.13) are used to determine the transmissivity (T) and the storage coefficient (S) of a confined aquifer with known fracture length (L_f).

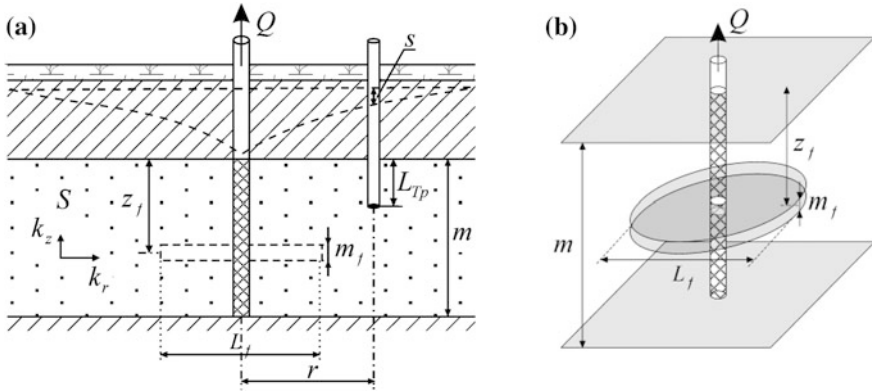


Fig. 6.4 A well in a horizontal fracture. **a** Cross-section; **b** three-dimensional representation

6.3 Pumping Well Intersecting a Single Horizontal Fracture

The basic assumptions and conditions (Fig. 6.4) are:

- the aquifer is confined and anisotropic in the vertical plane, of infinite lateral extent;
- the fracture is of limited radius and parallel to aquifer bottom;
- the pumping well is fully penetrating, located in the center of the circular fracture;
- the average aperture of the fracture can be taken into account.

The drawdown is determined at any point in the aquifer.

Basic Analytical Relationships

Transient Flow Equations (Gringarten and Ramey 1974)

1. The drawdown in a piezometer with the average aperture of the fracture taken into account is:

$$\begin{aligned}
 s = & \frac{Q}{2\pi k_r m} \int_0^u \left\{ \exp\left(-\frac{r^2/L_f^2}{\tau}\right) \left[\int_0^1 I_0\left(\frac{r/L_f}{\tau} \tau'\right) \exp\left(-\frac{\tau'^2}{4\tau}\right) \tau' d\tau'\right] \times \right. \\
 & \times \left[1 + \frac{4m}{\pi m_f} \sum_{n=1}^{\infty} \frac{1}{n} \exp\left[-\tau \left(\frac{n\pi L_f}{2m\sqrt{k_r/k_z}}\right)^2\right] \times \right. \\
 & \left. \left. \times \sin\frac{n\pi m_f}{2m} \cos\frac{n\pi(m-z_f)}{m} \cos\frac{n\pi(m-L_{Tp})}{m} \right] \right\} \frac{d\tau}{\tau}, \quad (6.14)
 \end{aligned}$$

where k_r , k_z are the horizontal and vertical hydraulic conductivities, m/d; L_{Tp} is the vertical distance from the aquifer top to the open part of the piezometer, m; L_f is fracture diameter, m; m_f is the average aperture of the fracture, m; z_f is the vertical distance from the top of the aquifer to the fracture (Fig. 6.4), m; $I_0(\cdot)$ is modified Bessel function of the first kind of the zero order (see Appendix 7.13).

2. The drawdown in the piezometer with fracture thickness not taken into account is:

$$s = \frac{Q}{2\pi k_r m} \int_0^u \left\{ \exp\left(-\frac{r^2/L_f^2}{\tau}\right) \left[\int_0^1 I_0\left(\frac{r/L_f}{\tau} \tau'\right) \exp\left(-\frac{\tau'^2}{4\tau}\right) \tau' d\tau' \right] \times \right. \\ \left. \times \left[1 + 2 \sum_{n=1}^{\infty} \exp\left[-\tau \left(\frac{n\pi L_f}{2m\sqrt{k_r/k_z}}\right)^2\right] \cos\frac{n\pi(m-z_f)}{m} \cos\frac{n\pi(m-L_{Tp})}{m} \right] \right\} \frac{d\tau}{\tau}. \quad (6.15)$$

In the solutions (6.14) and (6.15),

$$u = \frac{4k_r t}{S_s L_f^2}. \quad (6.16)$$

Solutions (Eqs. 6.11 and 6.12) are used to determine the horizontal and vertical hydraulic conductivities (k_r , k_z) and the specific storage (S_s) of a confined aquifer. The parameters to be specified also include fracture diameter, the vertical distance to the fracture, and, if the average aperture of the fracture is to be taken into account, m_f .

References

- De Smedt F (2011) Analytical solution for constant-rate pumping test in fissured porous media with double-porosity behavior. *Transport Porous Med* 88(3):479–489
- Gringarten AC, Ramey HJ Jr (1974) Unsteady-state pressure distributions created by a well with a single horizontal fracture, partial penetration, or restricted entry. *Soc Petrol Eng J* 14(4): 413–426
- Gringarten AC, Ramey HJ Jr, Raghavan R (1974) Unsteady-state pressure distributions created by a well with a single infinite-conductivity vertical fracture. *Soc Petrol Eng J* 14(4):347–360
- Jenkins DN, Prentice JK (1982) Theory for aquifer test analysis in fractured rocks under linear (nonradial) flow conditions. *Ground Water* 20(1):12–21
- Moench AF (1984) Double-porosity models for a fissured groundwater reservoir with fracture skin. *Water Resour Res* 20(7):831–846
- Warren JE, Root PJ (1963) The behavior of naturally fractured reservoirs. *Soc Petrol Eng J* 3(3):245–255

Part II

Analytical Solutions for a Complex Pumping-Test Setting and Well-System Configurations

This part, which is a continuation of the first part, considers analytical relationships to describe water-level changes in aquifers under different scenarios of aquifer testing.

The second part considers: tests with pumping from a horizontal or inclined well, constant-head tests, slug tests, multi-well constant-discharge tests, variable discharge tests, simultaneous pumping from adjacent aquifers, and dipole flow tests. Detailed description is provided for functions of water-level recovery.

Also treated are rules for constructing analytical solutions with the use of the superposition principle. This principle is widely used in calculating the drawdown during multi-well tests, tests with variable discharge rate, and recovery tests. The superposition principle is extended to tests in bounded aquifers.

Graphical methods are proposed for most aquifer tests, including recovery tests and multi-well pumping tests.

Chapter 7

Horizontal or Slanted Pumping Wells

This chapter considers several basic solutions for calculating the drawdown in observation wells and piezometers during constant-discharge pumping tests from horizontal and slanted wells in a confined aquifer (Sect. 7.1), an unconfined aquifer (Sect. 7.2), or a leaky aquifer (Sect. 7.3). All solutions are given for aquifers of infinite lateral extent with vertical anisotropy taken into account.

7.1 Confined Aquifer

The basic assumptions and conditions (Fig. 7.1) are:

- the aquifer is confined and vertically anisotropic;
- the pumping well is horizontal, parallel to the aquifer bottom.

The drawdown is determined in a piezometer located at any point within the aquifer.

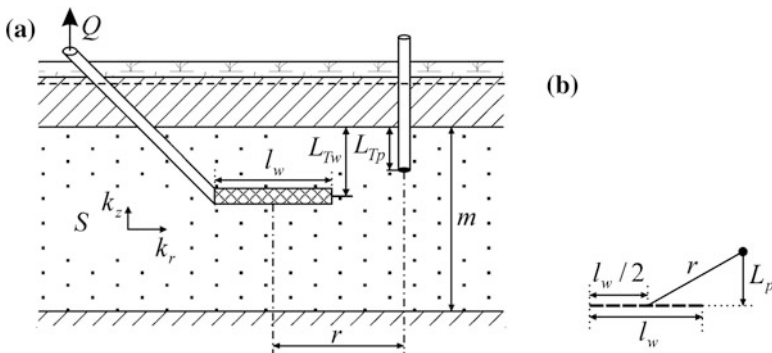


Fig. 7.1 Horizontal pumping well in a confined aquifer. **a** Cross-section; **b** planar view

Basic Analytical Relationships

Transient Flow Equation (Zhan et al. 2001):

$$s = \frac{Q}{4l_w\sqrt{\pi k_r k_z}} \int_0^u \left\{ \left[\operatorname{erf} \left(\chi \frac{l_w + 2\sqrt{r^2 - L_p^2}}{4m\sqrt{\tau}} \right) + \operatorname{erf} \left(\chi \frac{l_w - 2\sqrt{r^2 - L_p^2}}{4m\sqrt{\tau}} \right) \right] \exp \left(-\frac{\chi^2 L_p^2}{4m^2\tau} \right) \times \left[1 + 2 \sum_{n=1}^{\infty} \left(\cos \left(n\pi \frac{m - L_{Tp}}{m} \right) \cos \left(n\pi \frac{m - L_{Tw}}{m} \right) \exp(-n^2\pi^2\tau) \right) \right] \right\} \frac{d\tau}{\sqrt{\tau}} \quad (7.1)$$

$$u = \frac{k_z}{Sm} t, \quad (7.2)$$

where s is the drawdown in a piezometer, m; Q is the discharge rate, m³/d; $\chi = \sqrt{k_z/k_r}$ is the coefficient of vertical anisotropy; k_r , k_z are the horizontal and vertical hydraulic conductivities, m/d; m is aquifer thickness, m; S is the storage coefficient, dimensionless; L_p is the distance in the plan from the observation well to the line on which the pumping well is located (Fig. 7.1b), m; L_{Tw} , L_{Tp} are the vertical distances from the aquifer top to the horizontal screen of the pumping well, and the open part of the piezometer (Fig. 7.1a), respectively, m; l_w is the length of pumping well screen, m; r is the horizontal distance from the center of the screen to the piezometer, m; t is the time elapsed from the start of pumping, d; $\operatorname{erf}(\cdot)$ is error function (see Appendix 7.12).

Equation 7.1 is used to evaluate the horizontal (k_r) and vertical (k_z) hydraulic conductivities and the storage coefficient (S) of a confined aquifer.

7.2 Unconfined Aquifer

The basic assumptions and conditions (Fig. 7.2) are:

- the aquifer is unconfined and vertically and horizontally anisotropic;
- the pumping well is horizontal or slanted.

The drawdown is determined at any point within the aquifer in an observation well or a piezometer.

Basic Analytical Relationships

Transient Flow Equation (Zhan and Zlotnik 2002)

The drawdown in a piezometer or a fully/partially penetrating observation well is:

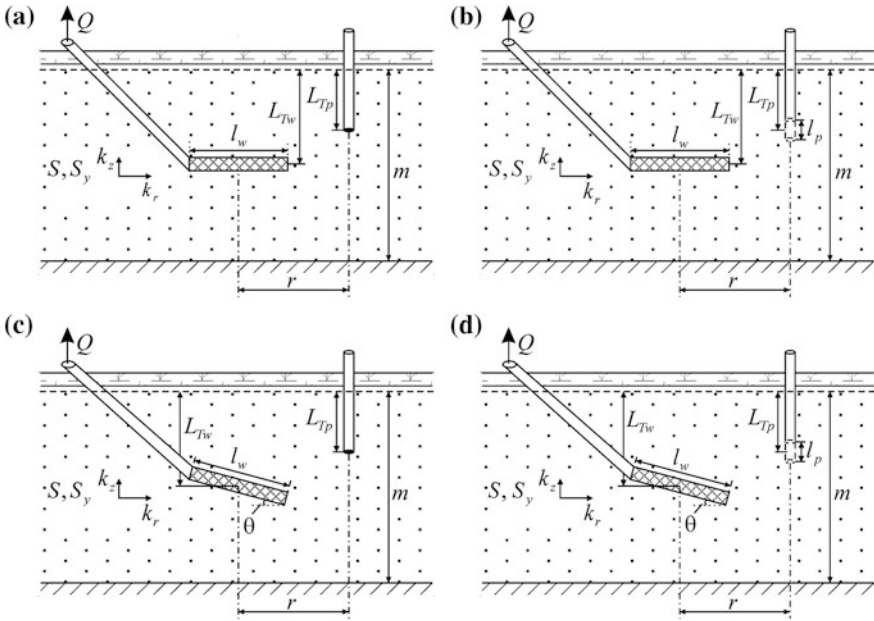


Fig. 7.2 a, b Horizontal and c, d slanted pumping wells in an unconfined aquifer. The drawdown is monitored in (a, c) a piezometer or (b, d) an observation well. A planar view is given in Fig. 7.1b

$$s = \frac{Q}{2\pi m \sqrt[3]{k_x k_y k_z}} f(t, r, L_p, l_p, l_w, \theta, L_{Tw}, L_{Tp}, k_x, k_y, k_z, S, S_y), \quad (7.3)$$

where $k_x = k_r$, k_y , k_z are the hydraulic conductivities of the aquifer along the abscissa, ordinate, and applicate, respectively, m/d; S_y is the specific yield, dimensionless; L_{Tp} is the vertical distance from the initial water table to the open part of the piezometer or the center of observation well screen, m; L_{Tw} is the vertical distance from the initial water table to the screen center of the horizontal or slanted pumping well (Fig. 7.2), m; l_p is the length of observation well screen, m; θ is the angle between the bottom and the well (Fig. 7.2c, d), in degrees.

In the calculation of drawdown in the piezometer, the length of the observation-well screen (l_p) is excluded from the function (Eq. 7.3). For a horizontal pumping well, the angle (θ) is zero. In a fully-penetrating observation well, the screen length is equal to the initial water-saturated thickness of the unconfined aquifer.

Equation 7.3 estimates the hydraulic conductivities along three directions (k_x , k_y , k_z), the storage coefficient (S), and the specific yield (S_y) of the unconfined aquifer. Solution (Eq. 7.3) can take into account the effect of the delayed drainage, the calculation of which involves the reciprocal of Boulton’s delay index (α) (see Eqs. 2.15 and 2.16). In the case of slanted pumping well, the drawdown in the aquifer depends not only on the distance to the pumping well, but also on the

position of the observation well relative to the screen center of the pumping well (to the right or to the left).

The relationship (Eq. 7.3) is treated by the algorithm of WHI program (see Appendix 5.6).

7.3 Leaky Aquifer

The basic assumptions and conditions (Fig. 7.3) are:

- a leaky aquifer system consists of two aquifers (the main and an adjacent), separated by an aquitard; the bottom boundary is impermeable, the top boundary is either impermeable or constant-head (the leaky aquifer is located under a water reservoir);
- the pumping well is horizontal, located in the main aquifer;
- the level in the adjacent aquifer does not change during the pumping test;
- aquitard storage is ignored.

The drawdown is determined in a piezometer located at any point within the main aquifer.

Basic Analytical Relationships

Transient Flow Equation (Zhan and Park 2003)

$$s = \frac{Q}{4l_w\sqrt{\pi k_r k_z}} \int_0^u \left\{ \begin{aligned} & \exp\left(-\frac{\chi^2 L_p^2}{4m^2\tau}\right) \sum_{n=1}^2 \operatorname{erf}\left(\chi \frac{l_w + (-1)^n 2\sqrt{r^2 - L_p^2}}{4m\sqrt{\tau}}\right) \times \\ & \times \left[\exp\left(-\frac{m^2}{B^2}\tau\right) + 2 \sum_{n=1}^{\infty} \left(\cos\left(\beta \frac{m - L_{Tp}}{m}\right) \cos\left(\beta \frac{m - L_{Tw}}{m}\right) \times \right. \right. \\ & \left. \left. \times \exp\left(-\left[\beta^2 + \frac{m^2}{B^2}\right]\tau\right) \right) \right] \end{aligned} \right\} \frac{d\tau}{\sqrt{\tau}} \tag{7.4}$$

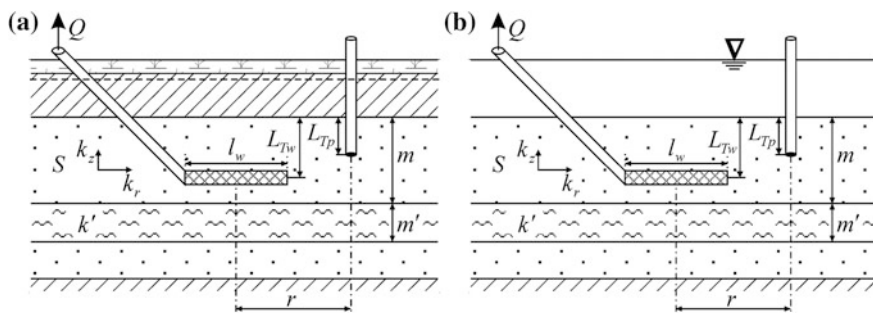


Fig. 7.3 Horizontal pumping well in a leaky aquifer. **a** Leaky confined aquifer; **b** a leaky aquifer underlying a water reservoir

$$B = \sqrt{k_z m m' / k'}, \quad (7.5)$$

where $i = 1$, $\beta = n\pi$; B is the leakage factor, m ; k' , m' are the hydraulic conductivity (m/d) and thickness (m) of the aquitard; for u see Eq. 7.2.

For a leaky aquifer underlying a water reservoir (Fig. 7.3b), $i = 0$, $\beta = n\pi + \pi/2$.

Equation 7.4 is used to determine the horizontal (k_r) and vertical (k_z) hydraulic conductivities and the storage coefficient (S) of the main aquifer, as well as the leakage factor (B).

References

- Zhan H, Park E (2003) Horizontal well in leaky aquifers. *J Hydrol* 281:129–146
- Zhan H, Wang LV, Park E (2001) On the horizontal-well pumping tests in anisotropic confined aquifers. *J Hydrol* 252:37–50
- Zhan H, Zlotnik VA (2002) Groundwater flow to a horizontal or slanted well in an unconfined aquifer. *Water Resour Res* 38(7). doi:[10.1029/2001WR000401](https://doi.org/10.1029/2001WR000401)

Chapter 8

Constant-Head Tests

This chapter provides analytical solutions describing the drawdown in isotropic confined nonleaky and leaky aquifers during a constant-head pumping test. The aquifer is of a constant thickness. The pumping and observation wells are fully penetrating. Three configurations of flow domains are considered: an aquifer of infinite lateral extent (Sect. 8.1), a circular aquifer (Sect. 8.2), and a radially heterogeneous aquifer (Sect. 8.3).

For this type of testing, the drawdown in the observation well depends only on the aquifer hydraulic diffusivity and, in the case of leakage, on the leakage factor.

With the drawdown in the pumping well kept constant, the well discharge will be decreasing over time. The changes in the discharge under such conditions will depend on aquifer transmissivity, hydraulic diffusivity (or storage coefficient), and, in the case of leakage, on the leakage factor.

The analytical relationships given in this chapter can be used to calculate the drawdown in an observation well, located at any distance from the pumping well, and the pumping well discharge.

8.1 Aquifers of Infinite Lateral Extent

The basic assumptions and conditions (Fig. 8.1) are:

- the aquifer is of infinite lateral extent, either nonleaky or leaky;
- the drawdown in the pumping well is kept constant during the test;
- wellbore storage is taken into account.

Typical plots of drawdown in an observation well and discharge in the pumping well in a confined aquifer and a leaky aquifer system are depicted in Fig. 12.28. For the effect of hydraulic characteristics on the drawdown and discharge, see Fig. 12.29.

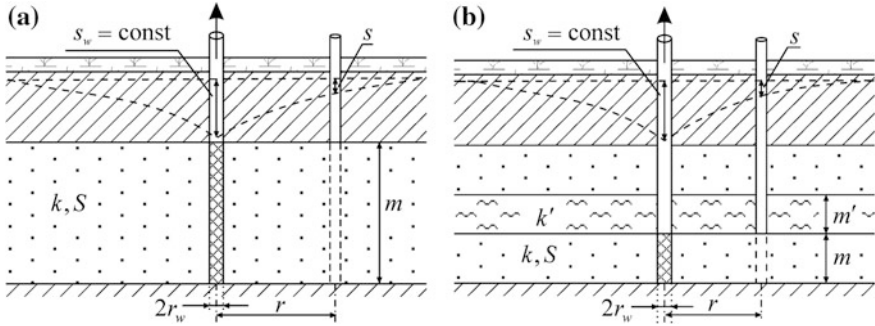


Fig. 8.1 Constant-head test. **a** Confined aquifer; **b** leaky aquifer system: any combination of aquifers and aquitards shown in Fig. 3.2 can be considered

Basic Analytical Relationships

Transient Flow Equations

1. Nonleaky aquifer (Fig. 8.1a)

1.1a. The solution for drawdown in an observation well (Jaeger 1956; Hantush 1964) is:

$$s = s_w A\left(\frac{at}{r_w^2}, \frac{r}{r_w}\right), \quad (8.1)$$

$$A(u, \beta) = 1 - \frac{2}{\pi} \int_0^{\infty} \frac{J_0(\tau) Y_0(\tau\beta) - Y_0(\tau) J_0(\tau\beta) \exp(-u\tau^2)}{J_0^2(\tau) + Y_0^2(\tau)} \frac{d\tau}{\tau}, \quad (8.2)$$

where s is the drawdown in the observation well, m ; s_w is the constant drawdown in the pumping well, m ; $a = T/S$ is the hydraulic diffusivity, m^2/d ; $T = km$ is the transmissivity, m^2/d ; k , m are the hydraulic conductivity (m/d) and thickness (m) of the aquifer; r is the radial distance from the pumping to the observation well, m ; t is the time elapsed from the start of pumping, d ; r_w is well radius, m ; $A(u, \beta)$ is the flowing well function for nonleaky aquifers (see Appendix 7.11); $J_0(\cdot)$ and $Y_0(\cdot)$ are Bessel functions of the first kind and the second kind of the zero order (see Appendix 7.13).

1.1b. A solution for pumping well discharge (Jacob and Lohman 1952) is:

$$Q = 2\pi T s_w G\left(\frac{at}{r_w^2}\right), \quad (8.3)$$

$$G(u) = \frac{4u}{\pi} \int_0^{\infty} \tau \exp(-u\tau^2) \left[\frac{\pi}{2} + \arctan \frac{Y_0(\tau)}{J_0(\tau)} \right] d\tau, \quad (8.4)$$

where Q is the discharge rate (varying over time), m^3/d ; $G(u)$ is the flowing well discharge function for nonleaky aquifers (see Appendix 7.11).

1.2a. An alternative form of solution for the drawdown (Sternberg 1969) is:

$$s \approx s_w K_0 \left(r \sqrt{\frac{1}{2at}} \right) / K_0 \left(r_w \sqrt{\frac{1}{2at}} \right). \quad (8.5)$$

1.2b. An alternative form of solution for the discharge rate (Sternberg 1969) is:

$$Q \approx 2\pi T s_w r_w \sqrt{\frac{1}{2at}} K_1 \left(r_w \sqrt{\frac{1}{2at}} \right) / K_0 \left(r_w \sqrt{\frac{1}{2at}} \right), \quad (8.6)$$

where $K_0(\cdot)$ and $K_1(\cdot)$ are modified Bessel functions of the second kind of the zero and the first order, respectively (see Appendix 7.13).

Equations 8.5 and 8.6 have been derived from Eqs. 8.15 and 8.17 for a leaky aquifer at $B \rightarrow \infty$.

Another simplified solution is given in Mishra and Guyonnet (1992) for the drawdown in an observation well:

$$s \approx s_w W \left(\frac{r^2}{4at} \right) / W \left(\frac{r_w^2}{4at} \right) \quad (8.7)$$

with an approximation for $t > 5r^2/a$:

$$s \approx s_w \ln(2.25at/r^2) / \ln(2.25at/r_w^2), \quad (8.8)$$

and for the discharge of the pumping well:

$$Q \approx 4\pi T s_w \exp \left(\frac{r_w^2}{4at} \right) / W \left(\frac{r_w^2}{4at} \right) \quad (8.9)$$

with an approximation for $t > 5r_w^2/a$:

$$Q \approx 4\pi T s_w / \ln(2.25at/r_w^2), \quad (8.10)$$

where $W(\cdot)$ is the well-function (see Appendix 7.1).

2. Leaky aquifer (Fig. 8.1b)

2.1a. A solution for the drawdown in an observation well (Hantush 1959, 1964) is:

$$s = s_w Z \left(\frac{at}{r_w^2}, \frac{r}{r_w}, \frac{r_w}{B} \right), \quad (8.11)$$

$$Z(u, \beta_1, \beta_2) = \frac{K_0(\beta_1\beta_2)}{K_0(\beta_2)} + \exp(-u\beta_2^2) \frac{2}{\pi} \int_0^\infty \frac{J_0(\tau\beta_1)Y_0(\tau) - Y_0(\tau\beta_1)J_0(\tau) \exp(-u\tau^2)}{J_0^2(\tau) + Y_0^2(\tau)} \frac{\tau \exp(-u\tau^2)}{\tau^2 + \beta_2^2} \tau d\tau, \quad (8.12)$$

where B is the leakage factor (m), which is determined depending on the number of adjacent aquifers (see Appendix 1); $Z(u, \beta_1, \beta_2)$ is flowing well function for leaky aquifers (see Appendix 7.11).

2.1b. A solution for the pumping-well discharge (Hantush 1959) is:

$$Q = 2\pi T s_w G\left(\frac{at}{r_w^2}, \frac{r_w}{B}\right), \quad (8.13)$$

$$G(u, \beta) = \frac{\beta K_1(\beta)}{K_0(\beta)} + \frac{4}{\pi^2} \exp(-u\beta^2) \int_0^\infty \frac{1}{J_0^2(\tau) + Y_0^2(\tau)} \frac{\tau \exp(-u\tau^2)}{\tau^2 + \beta^2} d\tau, \quad (8.14)$$

where $G(u, \beta)$ is the flowing well discharge function for leaky aquifers (see Appendix 7.11).

2.2a. An alternative form of solution for the drawdown (Sternberg 1969) is:

$$s \approx s_w K_0\left(r\sqrt{\frac{1}{2at} + \frac{1}{B^2}}\right) / K_0\left(r_w\sqrt{\frac{1}{2at} + \frac{1}{B^2}}\right) \quad (8.15)$$

or, for tentative calculations, by analogy with (Eq. 8.7):

$$s \approx s_w W\left(\frac{r^2}{4at}, \frac{r}{B}\right) / W\left(\frac{r_w^2}{4at}, \frac{r_w}{B}\right), \quad (8.16)$$

where $W(u, \beta)$ is the well-function for leaky aquifers (see Appendix 7.2).

2.2b. An alternative form of solution for the discharge rate (Sternberg 1969) is:

$$Q \approx 2\pi T s_w r_w \sqrt{\frac{1}{2at} + \frac{1}{B^2}} K_1\left(r_w\sqrt{\frac{1}{2at} + \frac{1}{B^2}}\right) / K_0\left(r_w\sqrt{\frac{1}{2at} + \frac{1}{B^2}}\right). \quad (8.17)$$

Equations 8.5–8.10 and 8.15–8.17 are approximate.

Steady-State Flow Equations

Steady-state estimates in a leaky aquifer can be based on the following solutions (Hantush 1959):

Table 8.1 Graphic-analytical parameter evaluation

Plot	Method	Relationship
$\frac{s_w}{Q} \lg t$	Straight line	$T = \frac{0.183}{C}, \lg a = \frac{A}{C} + \lg \frac{r_w^2}{2.25}$ or $a = \frac{r_w^2}{2.25t_x}, S = \frac{2.25Tt_x}{r_w^2}$
$Q - \lg t$	Horizontal straight line ^a	$T \approx \frac{A}{2\pi T s_w} \left(\frac{B}{r_w} \right) \frac{K_0(r_w/B)}{K_1(r_w/B)}$

A is straight line intercept on the ordinate (see Sects. 12.1.1 and 12.1.2); C is straight line slope (see Sect. 12.1.1); t_x is the intercept of the straight line on the abscissa

^aThe parameters are evaluated based on discharge rates in the period of steady-state flow, given the leakage factor B

- for maximal drawdown in an observation well:

$$s_m \approx s_w \frac{K_0(r/B)}{K_0(r_w/B)}; \tag{8.18}$$

- for minimal discharge in the pumping well:

$$Q \approx 2\pi T s_w \left(\frac{r_w}{B} \right) \frac{K_1(r_w/B)}{K_0(r_w/B)}. \tag{8.19}$$

Graphic-Analytical Processing

The relationships given in Table 8.1 have been derived from Eqs. 8.10 and 8.19.

8.2 Circular Aquifers

The basic assumptions and conditions (Fig. 8.2) are:

- general conditions for constant-head tests in nonleaky and leaky aquifers of infinite lateral extent (see the beginning of Sect. 8.1);
- a circular boundary along the external contour of the aquifer;
- the pumping well is located in the center of the circular aquifer.

The boundary condition on the external contour of the aquifer specifies either (1) a constant-head or (2) a impermeable boundary (see Fig. A3.10a, c).

Basic Analytical Relationships

Transient Flow Equations (Hantush 1959)

1. Nonleaky aquifer

1.1. Constant-head boundary on the outer contour

A solution for the drawdown in an observation well is:

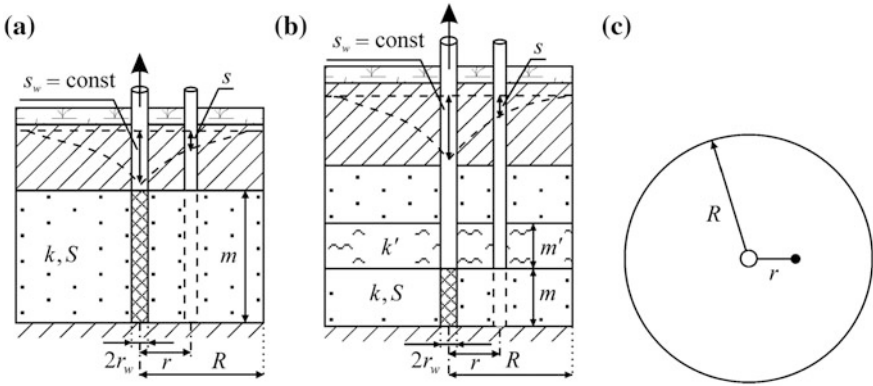


Fig. 8.2 Circular aquifer: constant-head test. **a, b** Cross-sections for **a** nonleaky aquifer and **b** leaky aquifer; **c** a planer view. R is the radius of the circle

$$s = s_w \left\{ \frac{\ln \frac{R}{r}}{\ln \frac{R}{r_w}} + \pi \sum_{n=1}^{\infty} \left[\frac{J_0(\zeta_n) J_0\left(\zeta_n \frac{R}{r_w}\right) \exp\left(-\zeta_n^2 \frac{at}{r_w^2}\right)}{J_0^2(\zeta_n) - J_0^2\left(\zeta_n \frac{R}{r_w}\right)} \times \right. \right. \\ \left. \left. \times \left[J_0\left(\zeta_n \frac{r}{r_w}\right) Y_0\left(\zeta_n \frac{R}{r_w}\right) - J_0\left(\zeta_n \frac{R}{r_w}\right) Y_0\left(\zeta_n \frac{r}{r_w}\right) \right] \right] \right\} \quad (8.20)$$

and for discharge rate:

$$Q = 2\pi T s_w \left\{ \frac{1}{\ln(R/r_w)} + 2 \sum_{n=1}^{\infty} \frac{J_0^2\left(\zeta_n \frac{R}{r_w}\right) \exp\left(-\zeta_n^2 \frac{at}{r_w^2}\right)}{J_0^2(\zeta_n) - J_0^2\left(\zeta_n \frac{R}{r_w}\right)} \right\}, \quad (8.21)$$

where R is the radius of the circular aquifer, m ; ζ_n are positive roots of equation $J_0(\zeta_n) Y_0(\zeta_n R/r_w) - J_0(\zeta_n R/r_w) Y_0(\zeta_n) = 0$ (see Appendix 7.15).

1.2. The aquifer contour is an impermeable boundary

A solution for the drawdown in an observation well is:

$$s = s_w \left\{ 1 + \pi \sum_{n=1}^{\infty} \left[\frac{J_1^2\left(\xi_n \frac{R}{r_w}\right) \exp\left(-\xi_n^2 \frac{at}{r_w^2}\right)}{J_0^2(\xi_n) - J_1^2\left(\xi_n \frac{R}{r_w}\right)} \times \right. \right. \\ \left. \left. \times \left[J_0\left(\xi_n \frac{r}{r_w}\right) Y_0(\xi_n) - J_0(\xi_n) Y_0\left(\xi_n \frac{r}{r_w}\right) \right] \right] \right\} \quad (8.22)$$

and for the discharge rate:

$$Q = 4\pi T s_w \sum_{n=1}^{\infty} \frac{J_1^2\left(\xi_n \frac{R}{r_w}\right) \exp\left(-\xi_n^2 \frac{at}{r_w^2}\right)}{J_0^2(\xi_n) - J_1^2\left(\xi_n \frac{R}{r_w}\right)}, \quad (8.23)$$

where $J_1(\cdot)$, $Y_1(u)$ are Bessel functions of the first kind and the second kind of the first order (see Appendix 7.13); ξ_n are positive roots of the equation $J_0(\xi_n)Y_1(\xi_n R/r_w) - J_1(\xi_n R/r_w)Y_0(\xi_n) = 0$ (see Appendix 7.15).

The solutions (Eqs. 8.20–8.23) have been derived from solutions (Eqs. 8.24–8.27) at $B \rightarrow \infty$.

2. Leaky aquifer

2.1. The external contour of the aquifer is a constant-head boundary

A solution for the drawdown in an observation well is:

$$s = s_w \left\{ \frac{K_0\left(\frac{r}{B}\right) - K_0\left(\frac{R}{B}\right) I_0\left(\frac{r}{B}\right) / I_0\left(\frac{R}{B}\right)}{K_0\left(\frac{r_w}{B}\right) - K_0\left(\frac{R}{B}\right) I_0\left(\frac{r_w}{B}\right) / I_0\left(\frac{R}{B}\right)} + \right. \\ \left. + \pi \sum_{n=1}^{\infty} \left[\frac{\zeta_n^2 J_0(\zeta_n) J_0\left(\zeta_n \frac{R}{r_w}\right) \exp\left[-\left(\zeta_n^2 + \left(\frac{r_w}{B}\right)^2\right) \frac{at}{r_w^2}\right]}{\left[\zeta_n^2 + \left(\frac{r_w}{B}\right)^2\right] \left[J_0^2(\zeta_n) - J_0^2\left(\zeta_n \frac{R}{r_w}\right)\right]} \times \right. \right. \\ \left. \left. \times \left[J_0\left(\zeta_n \frac{r}{r_w}\right) Y_0\left(\zeta_n \frac{R}{r_w}\right) - J_0\left(\zeta_n \frac{R}{r_w}\right) Y_0\left(\zeta_n \frac{r}{r_w}\right) \right] \right] \right\} \quad (8.24)$$

and for the discharge rate:

$$Q = 2\pi T s_w \left\{ \frac{\frac{r_w}{B} K_1\left(\frac{r_w}{B}\right) + K_0\left(\frac{R}{B}\right) I_1\left(\frac{r_w}{B}\right) / I_0\left(\frac{R}{B}\right)}{K_0\left(\frac{r_w}{B}\right) - K_0\left(\frac{R}{B}\right) I_0\left(\frac{r_w}{B}\right) / I_0\left(\frac{R}{B}\right)} + \right. \\ \left. + 2 \sum_{n=1}^{\infty} \frac{\zeta_n^2 J_0^2\left(\zeta_n \frac{R}{r_w}\right) \exp\left[-\left(\zeta_n^2 + \left(\frac{r_w}{B}\right)^2\right) \frac{at}{r_w^2}\right]}{\left[\zeta_n^2 + \left(\frac{r_w}{B}\right)^2\right] \left[J_0^2(\zeta_n) - J_0^2\left(\zeta_n \frac{R}{r_w}\right)\right]} \right\}, \quad (8.25)$$

where $I_0(\cdot)$ and $I_1(\cdot)$ are modified Bessel functions of the first kind of the zero and the first order.

2.2. The aquifer contour is an impermeable boundary

A solution for the drawdown in an observation well:

$$s = s_w \left\{ \frac{K_0\left(\frac{r}{B}\right) + K_1\left(\frac{R}{B}\right) I_0\left(\frac{r}{B}\right) / I_1\left(\frac{R}{B}\right)}{K_0\left(\frac{r_w}{B}\right) + K_1\left(\frac{R}{B}\right) I_0\left(\frac{r_w}{B}\right) / I_1\left(\frac{R}{B}\right)} + \right. \\ \left. + \pi \sum_{n=1}^{\infty} \frac{\frac{\xi_n^2 J_1^2\left(\xi_n \frac{R}{r_w}\right) \exp\left[-\left(\xi_n^2 + \left(\frac{r_w}{B}\right)^2\right) \frac{at}{r_w^2}\right]}{\left[\xi_n^2 + \left(\frac{r_w}{B}\right)^2\right] \left[J_0^2(\xi_n) - J_1^2\left(\xi_n \frac{R}{r_w}\right)\right]} \times \right. \\ \left. \times \left[J_0\left(\xi_n \frac{r}{r_w}\right) Y_0(\xi_n) - J_0(\xi_n) Y_0\left(\xi_n \frac{r}{r_w}\right) \right] \right\} \quad (8.26)$$

and for the discharge rate:

$$Q = 2\pi T s_w \left\{ \frac{\frac{r_w}{B} K_1\left(\frac{r_w}{B}\right) - K_1\left(\frac{R}{B}\right) I_1\left(\frac{r_w}{B}\right) / I_1\left(\frac{R}{B}\right)}{K_0\left(\frac{r_w}{B}\right) + K_1\left(\frac{R}{B}\right) I_0\left(\frac{r_w}{B}\right) / I_1\left(\frac{R}{B}\right)} + \right. \\ \left. + 2 \sum_{n=1}^{\infty} \frac{\xi_n^2 J_1^2\left(\xi_n \frac{R}{r_w}\right) \exp\left[-\left(\xi_n^2 + \left(\frac{r_w}{B}\right)^2\right) \frac{at}{r_w^2}\right]}{\left[\xi_n^2 + \left(\frac{r_w}{B}\right)^2\right] \left[J_0^2(\xi_n) - J_1^2\left(\xi_n \frac{R}{r_w}\right)\right]} \right\}. \quad (8.27)$$

Steady-State Flow Equations (Hantush 1959)

1. Nonleaky aquifer. The external contour of the aquifer is a constant-head boundary. The maximal drawdown in the observation well is:

$$s_m = s_w \ln\left(\frac{R}{r}\right) / \ln\left(\frac{R}{r_w}\right) \quad (8.28)$$

and the minimal discharge rate is:

$$Q = 2\pi T s_w / \ln\left(\frac{R}{r_w}\right). \quad (8.29)$$

2. Leaky aquifer

2.1. The external contour of the aquifer is a constant-head boundary

The maximal drawdown in the observation well is:

$$s_m = s_w \frac{K_0\left(\frac{r}{B}\right) - K_0\left(\frac{R}{B}\right) I_0\left(\frac{r}{B}\right) / I_0\left(\frac{R}{B}\right)}{K_0\left(\frac{r_w}{B}\right) - K_0\left(\frac{R}{B}\right) I_0\left(\frac{r_w}{B}\right) / I_0\left(\frac{R}{B}\right)} \quad (8.30)$$

and the minimal discharge rate is:

$$Q = 2\pi T s_w \frac{r_w}{B} \frac{K_1\left(\frac{r_w}{B}\right) + K_0\left(\frac{R}{B}\right) I_1\left(\frac{r_w}{B}\right) / I_0\left(\frac{R}{B}\right)}{K_0\left(\frac{r_w}{B}\right) - K_0\left(\frac{R}{B}\right) I_0\left(\frac{r_w}{B}\right) / I_0\left(\frac{R}{B}\right)}. \quad (8.31)$$

2.2. The aquifer contour is an impermeable boundary

The maximal drawdown in the observation well is:

$$s_m = s_w \frac{K_0\left(\frac{r}{B}\right) + K_1\left(\frac{R}{B}\right) I_0\left(\frac{r}{B}\right) / I_1\left(\frac{R}{B}\right)}{K_0\left(\frac{r_w}{B}\right) + K_1\left(\frac{R}{B}\right) I_0\left(\frac{r_w}{B}\right) / I_1\left(\frac{R}{B}\right)} \quad (8.32)$$

and the minimal discharge rate is:

$$Q = 2\pi T s_w \frac{r_w}{B} \frac{K_1\left(\frac{r_w}{B}\right) - K_1\left(\frac{R}{B}\right) I_1\left(\frac{r_w}{B}\right) / I_1\left(\frac{R}{B}\right)}{K_0\left(\frac{r_w}{B}\right) + K_1\left(\frac{R}{B}\right) I_0\left(\frac{r_w}{B}\right) / I_1\left(\frac{R}{B}\right)}. \quad (8.33)$$

The solution for a nonleaky aquifer (Eq. 8.28) was derived from the solution for a leaky aquifer (Eq. 8.30) at $B \rightarrow \infty$. Steady-state solutions for the discharge rates (Eqs. 8.29, 8.31, and 8.33) follow from the appropriate transient Eqs. 8.21, 8.25, and 8.27 when extended by approximation to longer time periods (Hantush 1959).

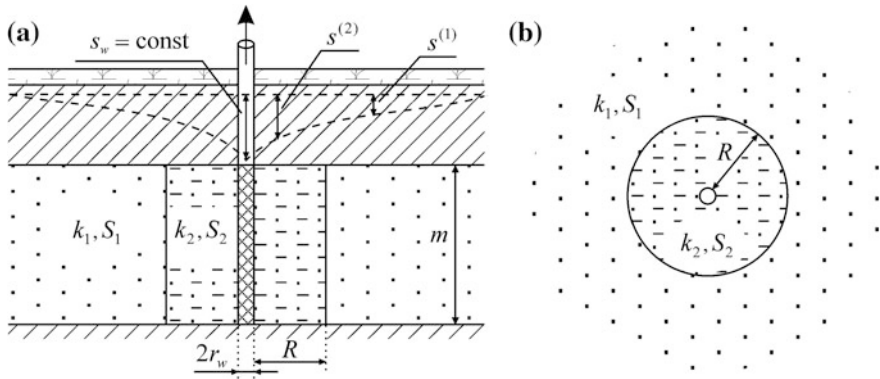


Fig. 8.3 Radially heterogeneous aquifer: constant-head test. **a** Cross-section; **b** planar view

8.3 Radial Patchy Aquifer

The basic assumptions and conditions (Fig. 8.3) are:

- general conditions for constant-head test in a nonleaky aquifer of infinite lateral extent (see the beginning of Sect. 8.1);
- in the planar view, the aquifer consists of two zones of heterogeneity with a common circular boundary;
- the pumping well is located in the center of a circular zone (wellbore zone), surrounded by the main zone;
- the observation well is located in the main or wellbore zone.

This configuration can be regarded as a homogeneous confined aquifer with a pumping well surrounded by an area that plays a role of wellbore skin. In this formulation, analytical solutions enable the estimation of the thickness and the hydraulic conductivity of the skin, as well as its storage coefficient.

Basic Analytical Relationships

Transient Flow Equations (Yang and Yeh 2006)

1. Solution for the drawdown in the main zone is:

$$s^{(1)} = s_w \left(1 - \frac{4}{\pi^2 R^+} \int_0^\infty \exp(-u\tau^2) \frac{J_0(rc_1\tau)B_1 + Y_0(rc_1\tau)B_2}{B_1^2 + B_2^2} \frac{d\tau}{\tau^2} \right), \quad (8.34)$$

$$u = a_2 t, \quad c_1 = \sqrt{a_2/a_1}, \quad c_2 = \frac{T_1}{T_2} \sqrt{a_2/a_1}, \quad R^+ = R + r_w, \quad (8.35)$$

$$B_1 = \left\{ \begin{array}{l} c_2 Y_1(R^+ c_1 \tau) [J_0(R^+ \tau) Y_0(r_w \tau) - Y_0(R^+ \tau) J_0(r_w \tau)] - \\ - Y_0(R^+ c_1 \tau) [J_1(R^+ \tau) Y_0(r_w \tau) - Y_1(R^+ \tau) J_0(r_w \tau)] \end{array} \right\}, \quad (8.36)$$

$$B_2 = \left\{ \begin{array}{l} c_2 J_1(R^+ c_1 \tau) [Y_0(R^+ \tau) J_0(r_w \tau) - J_0(R^+ \tau) Y_0(r_w \tau)] - \\ - J_0(R^+ c_1 \tau) [Y_1(R^+ \tau) J_0(r_w \tau) - J_1(R^+ \tau) Y_0(r_w \tau)] \end{array} \right\}. \quad (8.37)$$

2. Solution for the drawdown in the wellbore zone is:

$$s^{(2)} = s_w \left(1 + \frac{2}{\pi} \int_0^\infty \exp(-u\tau^2) \frac{A_1 B_2 - A_2 B_1}{B_1^2 + B_2^2} \frac{d\tau}{\tau} \right), \quad (8.38)$$

$$A_1 = \left\{ \begin{array}{l} c_2 Y_1(R^+ c_1 \tau) [J_0(R^+ \tau) Y_0(r\tau) - Y_0(R^+ \tau) J_0(r\tau)] - \\ - Y_0(R^+ c_1 \tau) [J_1(R^+ \tau) Y_0(r\tau) - Y_1(R^+ \tau) J_0(r\tau)] \end{array} \right\}, \quad (8.39)$$

$$A_2 = \left\{ \begin{array}{l} c_2 J_1(R^+ c_1 \tau) [Y_0(R^+ \tau) J_0(r\tau) - J_0(R^+ \tau) Y_0(r\tau)] - \\ - J_0(R^+ c_1 \tau) [Y_1(R^+ \tau) J_0(r\tau) - J_1(R^+ \tau) Y_0(r\tau)] \end{array} \right\}, \quad (8.40)$$

where $s^{(1)}$, $s^{(2)}$ are the drawdown values in observation wells located in the main and wellbore zones, m; $T_1 = k_1 m$ and $T_2 = k_2 m$ are the transmissivities of the main and wellbore zones, respectively, m^2/d ; k_1 , k_2 are the hydraulic conductivities of the main and wellbore zones, m/day; m is aquifer thickness, m; $a_1 = T_1/S_1$ and $a_2 = T_2/S_2$ are the hydraulic diffusivities of the main and wellbore zones, respectively, m^2/d ; R is the radius of the wellbore zone less the well radius (i.e., skin thickness), m; r_w is the pumping-well radius, m.

The transient solutions (Eqs. 8.34 and 8.38) are used to evaluate the transmissivities and hydraulic diffusivities (or storage coefficients) of the two zones.

References

- Hantush MS (1959) Nonsteady flow to flowing wells of leaky aquifers. *J Geophys Res* 64 (8):1043–1052
- Hantush MS (1964) Hydraulics of wells. In: Chow VT (ed) *Advances in hydroscience*, vol 1. Academic Press, New York and London, pp 281–432
- Jacob CE, Lohman SW (1952) Nonsteady flow to a well of constant drawdown in an extensive aquifer. *EOS T Am Geophys Un* 33(4):559–569
- Jaeger JC (1956) Numerical values for the temperature in radial heat flow. *J Math Phys Camb* 34 (4):316–321
- Mishra S, Guyonnet D (1992) Analysis of observation-well response during constant-head testing. *Ground Water* 30(4):523–528
- Sternberg YM (1969) Some approximate solutions of radial flow problems. *J Hydrol* 33(2):158–166
- Yang SY, Yeh HD (2006) A novel analytical solution for constant-head test in a patchy aquifer. *Int J Numer Anal Met* 30(12):1213–1230

Chapter 9

Slug Tests

This type of aquifer testing consists of an instantaneous injection or withdrawal of a known volume of water into or from the tested well, followed by monitoring the water-level recovery in the same well until its original value is attained. Basic analytical relationships for slug tests are given for different experimental conditions. All such relationships take into account the wellbore storage.

9.1 Cooper and Picking Solutions

The basic assumptions and conditions (Fig. 9.1) are:

- a confined and isotropic aquifer with infinite lateral extent;
- a fully penetrating tested well.

Examples of recovery curves in the tested and observation wells during a slug test are shown in Fig. 12.30. For the effect of hydraulic parameters on the recovery regime, see Fig. 12.31.

Basic Analytical Relationships

Transient Flow Equations

1. The principal solution for slug tests is associated with a Cooper solution for a tested well as a response to instantaneous change in the water-level in the same well (Carslow and Jaeger 1959; Cooper et al. 1967):

$$s_w = s^0 F_s \left(\frac{Tt}{r_c^2}, \frac{r_w^2}{r_c^2} S \right), \tag{9.1}$$

$$F_s(u, \beta) = \frac{8\beta}{\pi^2} \int_0^\infty \frac{\exp(-u\tau^2/\beta)}{[\tau J_0(\tau) - 2\beta J_1(\tau)]^2 + [\tau Y_0(\tau) - 2\beta Y_1(\tau)]^2} \frac{d\tau}{\tau}, \tag{9.2}$$

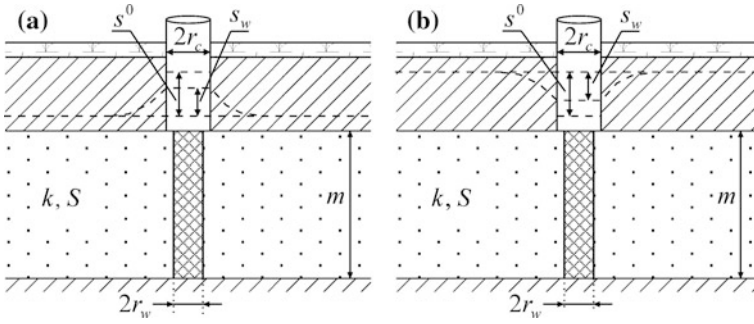


Fig. 9.1 Slug test in a confined isotropic aquifer. **a** Instantaneous water injection into the well; **b** instantaneous water withdrawal from the well

where s^0 is the initial (instantaneous) water-level change in the tested well, m ; s_w is water-level recovery in the tested well, m ; $T = km$ is the transmissivity, m^2/d ; k , m are the hydraulic conductivity (m/d) and the thickness (m) of the aquifer; S is the storage coefficient, dimensionless; r_w , r_c are the radiuses of the tested well and its casing, respectively, m ; t is the time elapsed from the start of slug test, d ; $F_s(u, \beta)$ is a slug test function (see Appendix 7.10); $J_0(\cdot)$ and $J_1(\cdot)$ are Bessel functions of the first kind of the zero and the first order; $Y_0(\cdot)$ and $Y_1(\cdot)$ are Bessel functions of the second kind of the zero and the first order (see Appendix 7.13).

2. A Cooper solution for an observation well (Carslow and Jaeger 1959; Cooper et al. 1967) is:

$$s = s^0 F_{sp} \left(\frac{Tt}{r_c^2}, \frac{r_w^2}{r_c^2} S, \frac{r}{r_w} \right), \quad (9.3)$$

$$F_{sp}(u, \beta_1, \beta_2) = \frac{2}{\pi} \int_0^{\infty} \exp(-u\tau^2/\beta_1) \times \\ \times \frac{J_0(\tau\beta_2)[\tau Y_0(\tau) - 2\beta_1 Y_1(\tau)] - Y_0(\tau\beta_2)[\tau J_0(\tau) - 2\beta_1 J_1(\tau)]}{[\tau J_0(\tau) - 2\beta_1 J_1(\tau)]^2 + [\tau Y_0(\tau) - 2\beta_1 Y_1(\tau)]^2} d\tau, \quad (9.4)$$

where s is water-level change in the observation well, m ; r is the radial distance from the tested to the observation well, m ; $F_{sp}(u, \beta_1, \beta_2)$ is a special function for water-level change in an observation well during a slug test.

3. Picking solution (Picking 1994) treats a noninstantaneous change in the initial level (before level recovery, water was being withdrawn from or injected into the well with a constant discharge within time t_0):

$$s_w = s_0 \frac{F\left(\frac{r_w^2 S}{4T(t_0 + t_r)}, \frac{r_w^2}{r_c^2} S\right) - F\left(\frac{r_w^2 S}{4T t_r}, \frac{r_w^2}{r_c^2} S\right)}{F\left(\frac{r_w^2 S}{4T t_0}, \frac{r_w^2}{r_c^2} S\right)}, \tag{9.5}$$

where $F(u, \beta)$ is a function for large-diameter wells (see Appendix 7.9); s_0 , here, is the water-level change in the tested well at the moment when water withdrawal (injection) was stopped, m ; t_0 is the duration of water withdrawal (injection), d ; t_r is the time since the beginning of level recovery, d .

Equation 9.5 can be conveniently used when data on level recovery after a short-time constant-discharge withdrawal are available.

Cooper and Picking solutions (Eqs. 9.1, 9.3, and 9.5) are used to evaluate aquifer transmissivity (T) and storage coefficient (S). Cooper solutions enable the parameters to be evaluated by the water-level change in both the tested well (Eq. 9.1) and the observation well (Eq. 9.3).

9.2 Slug Tests in Tight Formations

The performance of slug tests in tight formations can be complicated by the unacceptable duration of the experiment and the lack of data on the initial head distribution. Bredehoeft and Papadopoulos (1980) proposed an alternative procedure, i.e., the pressure pulse method, for carrying out slug tests in tight formations and processing their results.

The essence of the procedure is as follows. A shut-in well is filled with water up to a certain level. As the rocks are tight, the water level will remain nearly constant after that. This implies that knowledge of the initial groundwater level is not required. The newly reached level is taken as the initial head distribution. Next, the pressure in the well is to be abruptly raised through injection of some volume of water, which is equivalent to the value s^0 for an ordinary slug test (Fig. 9.2b). After

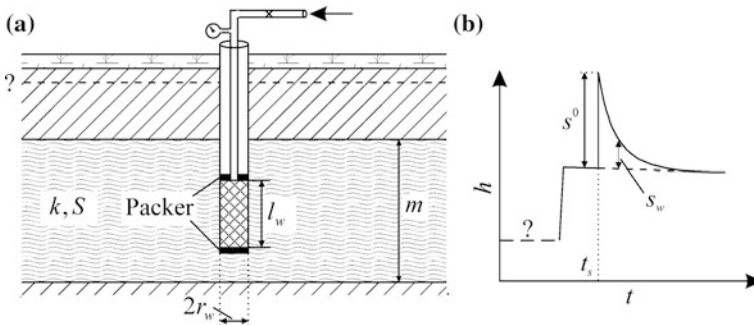


Fig. 9.2 Scheme for the slug-test procedure in tight formations: **a** cross-section and **b** a schematic plot of water-level change in a well during the test

that, the procedure described above is followed, and data on level recovery are recorded.

In the case of an unconsolidated formation, the test interval is taken to be the length of the well screen, while for consolidated formations, this is the distance between packers (Fig. 9.2a). Data processing is based on a Cooper solution (Eq. 9.1). The difference is that the values of the arguments of function $F_s(u, \beta)$ are somewhat different: the actual casing radius is replaced by an effective radius:

$$r_c = \sqrt{V_w C_w \rho_w g / \pi}, \quad (9.6)$$

where V_w is the volume of water injected into the well, m^3 ; C_w is water compressibility, Pa^{-1} ; ρ_w is water density, kg/m^3 ; g is gravity acceleration, m/s^2 .

Under normal conditions, the effective radius calculated by (Eq. 9.6) is less than 1 mm. The volume of injected water can be calculated as:

$$V_w = \pi r_w^2 l_w + \pi r_t^2 l_t, \quad (9.7)$$

where r_t is the radius of the pipe used for water injection from the pump, l_w is the length of tested well screen, m; l_t is pipe length from the top packer to the manometer.

With this taken into account, the solution (Eq. 9.1) becomes:

$$s_w = s^0 F_s \left(\frac{\pi T t}{V_w C_w \rho_w g}, \frac{\pi r_w^2}{V_w C_w \rho_w g} S \right). \quad (9.8)$$

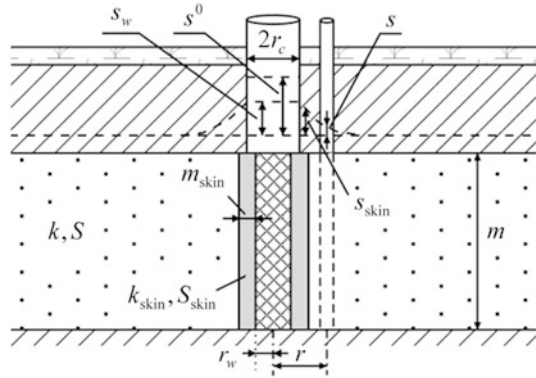
First changes in the head during the standard slug test in tight formations will take place tens or even hundreds of days after the perturbation, and reaching a steady-state may require several decades (Bredehoeft and Papadopoulos 1980), while the major portion of recovery in the proposed method will take place within a few hours.

This method is recommended for use in rocks with a permeability below 1 milidarcy ($\approx 1 \times 10^{-15} \text{ m}^2$), which, under normal conditions, is equivalent to a hydraulic conductivity of 0.001 m/d.

9.3 Solutions for Slug Tests with Skin Effect

In addition to the conditions described in Sect. 9.1, the hydraulic characteristics of the wellbore zone are taken into account in this case. Its effect can be regarded as wellbore skin (Fig. 9.3). The water-level change is monitored in the tested well and the observation wells, located in the aquifer and wellbore zone.

Fig. 9.3 Slug test with wellbore skin. s_{skin} is water-level change in the wellbore skin



Basic Analytical Relationships

Transient Flow Equations (Yeh and Yang 2006)

1. A solution for the water-level change in the tested well is:

$$s_w = s^0 \frac{2\eta r_w}{\pi} \int_0^\infty \exp(-u\tau^2) \frac{A_1 B_1 + A_2 B_2}{B_1^2 + B_2^2} d\tau, \tag{9.9}$$

$$u = \frac{k_{skin} m}{S_{skin}} t, \quad \alpha = S \left(\frac{r_w}{r_c} \right)^2, \quad \zeta = \frac{k}{k_{skin}}, \quad \eta = \frac{S}{S_{skin}}, \tag{9.10}$$

$$c_1 = \sqrt{\eta/\zeta}, \quad c_2 = \sqrt{\eta\zeta}, \quad R^+ = m_{skin} + r_w, \tag{9.11}$$

$$A_1 = Y_0(R^+ c_1 \tau) [Y_1(R^+ \tau) J_0(r_w \tau) - J_1(R^+ \tau) Y_0(r_w \tau)] - c_2 Y_1(R^+ c_1 \tau) [Y_0(R^+ \tau) J_0(r_w \tau) - J_0(R^+ \tau) Y_0(r_w \tau)], \tag{9.12}$$

$$A_2 = J_0(R^+ c_1 \tau) [J_1(R^+ \tau) Y_0(r_w \tau) - Y_1(R^+ \tau) J_0(r_w \tau)] - c_2 J_1(R^+ c_1 \tau) [J_0(R^+ \tau) Y_0(r_w \tau) - Y_0(R^+ \tau) J_0(r_w \tau)], \tag{9.13}$$

$$B_1 = A_2 \eta r_w u - 2\alpha \left\{ J_0(R^+ c_1 \tau) [J_1(R^+ \tau) Y_1(r_w \tau) - Y_1(R^+ \tau) J_1(r_w \tau)] - c_2 J_1(R^+ c_1 \tau) [J_0(R^+ \tau) Y_1(r_w \tau) - Y_0(R^+ \tau) J_1(r_w \tau)] \right\}, \tag{9.14}$$

$$B_2 = -A_1 \eta r_w u - 2\alpha \left\{ Y_0(R^+ c_1 \tau) [J_1(R^+ \tau) Y_1(r_w \tau) - Y_1(R^+ \tau) J_1(r_w \tau)] - c_2 Y_1(R^+ c_1 \tau) [J_0(R^+ \tau) Y_1(r_w \tau) - Y_0(R^+ \tau) J_1(r_w \tau)] \right\}, \tag{9.15}$$

where k_{skin} , S_{skin} , m_{skin} are the hydraulic conductivity (m/d), storage coefficient (dimensionless), and thickness (m) of the wellbore skin.

2. A solution for the water-level change in an observation well located in the aquifer is:

$$s = s^0 \frac{4\eta r_w}{\pi^2 r_s} \int_0^{\infty} \exp(-u\tau^2) \frac{J_0(rc_1\tau)B_2 - Y_0(rc_1\tau)B_1}{B_1^2 + B_2^2} \frac{d\tau}{\tau}. \quad (9.16)$$

3. A solution for the water-level change in an observation well located in the wellbore zone (in the skin) is:

$$s_{\text{skin}} = s^0 \frac{2\eta r_w}{\pi} \int_0^{\infty} \exp(-u\tau^2) \frac{A_1^{\text{skin}}B_1 + A_2^{\text{skin}}B_2}{B_1^2 + B_2^2} d\tau, \quad (9.17)$$

$$A_1^{\text{skin}} = Y_0(R^+ c_1\tau)[Y_1(R^+\tau)J_0(r\tau) - J_1(R^+\tau)Y_0(r\tau)] - c_2 Y_1(R^+ c_1\tau)[Y_0(R^+\tau)J_0(r\tau) - J_0(r_s\tau)Y_0(r\tau)], \quad (9.18)$$

$$A_2^{\text{skin}} = J_0(R^+ c_1\tau)[J_1(R^+\tau)Y_0(r\tau) - Y_1(R^+\tau)J_0(r\tau)] - c_2 J_1(R^+ c_1\tau)[J_0(R^+\tau)Y_0(r\tau) - Y_0(R^+\tau)J_0(r\tau)], \quad (9.19)$$

where s_{skin} is water-level change in the wellbore skin, m.

The measured water-level change in the tested well (Eq. 9.9) or in an observation well, located in the aquifer (Eq. 9.16) or wellbore zone (Eq. 9.17), are used to evaluate the hydraulic conductivities (k , k_{skin}), and the storage coefficients (S , S_{skin}) of the aquifer and wellbore zone.

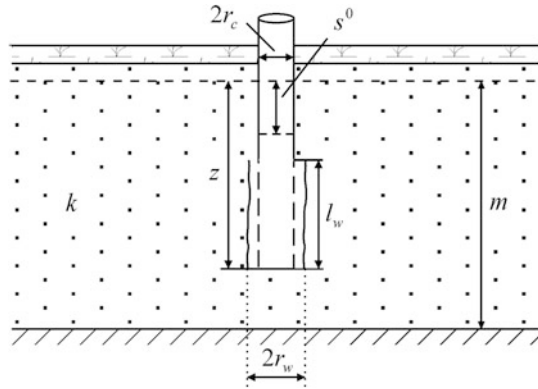
9.4 Bouwer–Rice Solution

This section gives a solution for treating slug tests carried out in a partially penetrating well. The Bouwer–Rice solution uses a straight-line method to evaluate the hydraulic conductivity (k) of an aquifer.

The basic assumptions and conditions (Fig. 9.4) are:

- an unconfined and isotropic aquifer of infinite lateral extent;
- a partially penetrating tested well.

Fig. 9.4 Scheme for Bouwer–Rice solution. Slug test in an isotropic unconfined aquifer with a partially penetrating tested well



Transient flow equation (Bouwer and Rice 1976):

$$\ln \frac{s^0}{s_w} = \frac{2kl_w}{r_c^2 \ln(R/r_w)} t, \tag{9.20}$$

where the radius of influence R for a partially penetrating well is evaluated as:

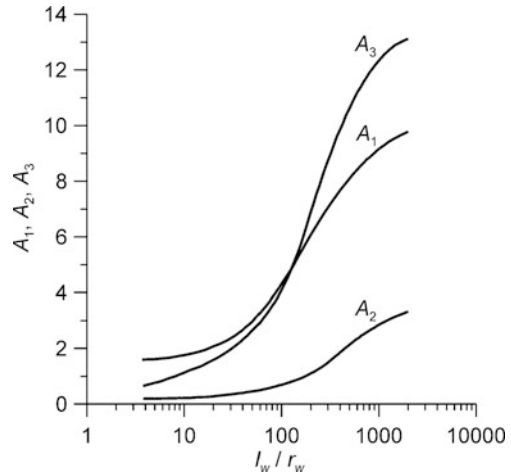
$$\ln \frac{R}{r_w} = \left(\frac{1.1}{\ln(z/r_w)} + \frac{r_w}{l_w} \left[A_1 + A_2 \ln \frac{m-z}{r_w} \right] \right)^{-1}. \tag{9.21}$$

In Eq. 9.21, the allowable upper limit of the expression $\ln[(m-z)/r_w]$ is six. Therefore, in the case of testing aquifers with greater thickness, the expression $\ln[(m-z)/r_w]$ is replaced by 6. This equation also cannot be used when $m = z$, i.e., when the partially penetrating well reaches the aquifer bottom. In the case of a fully penetrating well or when $m = z$, the radius of influence is calculated as:

$$\ln \frac{R}{r_w} = \left(\frac{1.1}{\ln(z/r_w)} + \frac{r_w}{l_w} A_3 \right)^{-1}. \tag{9.22}$$

Here, z is the distance from the water table to the bottom of well screen, m ; A_1, A_2, A_3 are dimensionless parameters, depending on the screen length and the radius of the tested well; these parameters are to be obtained empirically (Fig. 9.5) (Bouwer and Rice 1976).

Fig. 9.5 Plot for determining dimensionless empirical coefficients in Eqs. 9.21 and 9.22



For practical calculations, dimensionless parameters can be evaluated with the use of the following approximation (Sindalovskiy 2006):

- for the range $1 \leq \beta \leq 200$ ($\beta = l_w/r_w$):

$$A_1 = \left[\begin{array}{l} 1.4773306 + 0.02741954\beta + 8.0340006 \cdot 10^{-5}\beta^2 - 2.5045234 \cdot 10^{-7}\beta^3 - \\ -1.2204508 \cdot 10^{-8}\beta^4 + 9.7196356 \cdot 10^{-11}\beta^5 - 2.1463808 \cdot 10^{-13}\beta^6 \end{array} \right],$$

$$A_2 = \left[\begin{array}{l} 0.166753 + 0.004970107\beta + 5.4654427 \cdot 10^{-5}\beta^2 - 1.278645 \cdot 10^{-6}\beta^3 + \\ + 1.1887909 \cdot 10^{-8}\beta^4 - 5.1785833 \cdot 10^{-11}\beta^5 + 8.6501211 \cdot 10^{-14}\beta^6 \end{array} \right],$$

$$A_3 = \left[\begin{array}{l} 0.3905696 + 0.08310949\beta - 0.001515863\beta^2 + 2.1736242 \cdot 10^{-5}\beta^3 - \\ -1.653479 \cdot 10^{-7}\beta^4 + 6.3107187 \cdot 10^{-10}\beta^5 - 9.4937404 \cdot 10^{-13}\beta^6 \end{array} \right];$$

- for the range $200 < \beta < 2000$:

$$A_1 = \left[\begin{array}{l} 2.510366 + 0.0260556\beta - 5.08597807 \cdot 10^{-5}\beta^2 + 5.8230884 \cdot 10^{-8}\beta^3 - \\ -3.7929349 \cdot 10^{-11}\beta^4 + 1.2935074 \cdot 10^{-14}\beta^5 - 1.7859607 \cdot 10^{-18}\beta^6 \end{array} \right],$$

$$A_2 = \left[\begin{array}{l} -0.0651429 + 0.006547392\beta - 4.1237584 \cdot 10^{-6}\beta^2 - 2.1340524 \cdot 10^{-9}\beta^3 + \\ + 4.5603083 \cdot 10^{-12}\beta^4 - 2.3529733 \cdot 10^{-15}\beta^5 + 4.0923695 \cdot 10^{-19}\beta^6 \end{array} \right],$$

$$A_3 = \left[\begin{array}{l} 0.2593157 + 0.04869992\beta - 9.4552972 \cdot 10^{-5}\beta^2 + 1.05714921 \cdot 10^{-7}\beta^3 - \\ -6.7058679 \cdot 10^{-11}\beta^4 + 2.2286538 \cdot 10^{-14}\beta^5 - 3.004312102 \cdot 10^{-18}\beta^6 \end{array} \right].$$

Graphic-Analytical Processing

The relationship given in Table 9.1 has been derived from Eq. 9.20.

Table 9.1 Graphic-analytical parameter evaluation

Plot	Method	Relationship
$\lg \frac{s^0}{s_w} - t$	Straight line	$k = 2.3 \frac{r_c^2}{2l_w} C \ln \frac{R}{r_w}$

C is the slope of the straight line (see Sect. 13.1.1)

The straight line is to pass through the origin of coordinates; when the plot contains two linear segments, the treatment is to be based on the second one, because the first accounts for a disturbed zone around the well or suggests leakage; the plot may also contain a third segment (not straight), which corresponds to the final stage of the test and shows small increments of the water level

9.5 Hvorslev Solutions

This section gives solutions for processing slug tests in wells with different designs. Hvorslev solutions allow the straight-line method to be used to evaluate the horizontal hydraulic conductivity (k_r) and the coefficient of vertical anisotropy (χ) of the aquifer.

The basic assumptions and conditions (Fig. 9.6) are:

- the aquifer is confined or unconfined and vertically anisotropic and has infinite lateral extent;
- the tested well is partially penetrating.

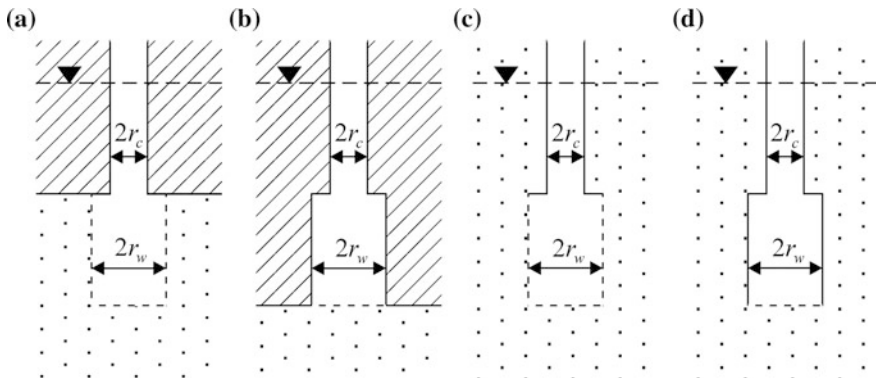


Fig. 9.6 Layout of the tested well in an aquifer for processing slug-test data by the Hvorslev method. **a** Partially penetrating well in a confined aquifer; **b** a well in an aquiclude reaching a confined aquifer at its bottom; **c, d** unconfined aquifer: **c** partially penetrating well and **d** piezometer

Table 9.2 Graphic-analytical parameter evaluation

Scheme	Relationship
Partially penetrating well in a confined aquifer with a screen reaching the aquifer top (Fig. 9.6a)	$k_r = \frac{2.3r_c^2}{2l_w} C \ln \left(\frac{l_w}{\chi r_w} + \sqrt{1 + \left(\frac{l_w}{\chi r_w} \right)^2} \right)$ for $\frac{l_w}{\chi r_w} > 4 - k_r = \frac{2.3r_c^2}{2l_w} C \ln \frac{2l_w}{\chi r_w}$
Well in an aquiclude reaching a confined aquifer at its bottom (Fig. 9.6b)	$k_r = \frac{2.3\pi r_c^2}{4\chi r_w} C$
Partially penetrating well in an unconfined aquifer (Fig. 9.6c)	$k_r = \frac{2.3r_c^2}{2l_w} C \ln \left(\frac{l_w}{\chi 2r_w} + \sqrt{1 + \left(\frac{l_w}{\chi 2r_w} \right)^2} \right)$ for $\frac{l_w}{\chi r_w} > 8 - k_r = \frac{2.3r_c^2}{2l_w} C \ln \frac{l_w}{\chi r_w}$
Piezometer in an unconfined aquifer (Fig. 9.6d)	$k_r = \frac{2.3\pi 2r_c^2}{11\chi r_w} C$

$\chi = \sqrt{k_z/k_r}$ is the dimensionless coefficient of vertical anisotropy; k_r, k_z are hydraulic conductivities in the horizontal and vertical directions, respectively, m/d

Graphic-Analytical Processing

Table 9.2 gives Hvorslev solutions (Hvorslev 1951) for evaluating the horizontal hydraulic conductivity for each of the four typical models (Fig. 9.6). The evaluation is made by straight-line method on the plot $\lg(s^0/s_w) - t$.

The straight line is to pass through the origin of coordinates. The vertical hydraulic conductivity is evaluated given the vertical-anisotropy coefficient.

9.6 Van der Kamp Solution

In highly permeable aquifers, water-level oscillations may appear during slug tests.

The solutions for this type of effects is based on the concept of attenuating sinusoidal motion (Van der Kamp 1976):

$$s_w = s^0 \exp(-\beta\lambda t) \cos\left(t\beta\sqrt{(1-\lambda^2)}\right), \quad (9.23)$$

$$\beta = \sqrt{\frac{g}{L'}}, \quad \lambda = -\frac{r_c^2}{8T} \beta \ln\left(0.79r_w^2 \frac{S}{T} \beta\right), \quad |\lambda| \leq 1, \quad (9.24)$$

where L' is an effective length of water column (m): $L' = L_c + r_c^2/r_w^2 \frac{m}{2}$ (Kipp 1985); in the case of close values of the radiuses of the screen and casing: $L' = L_c + 0.375l_f$ (Cooper et al. 1965), l_f is the well-screen length (in this case, equal to

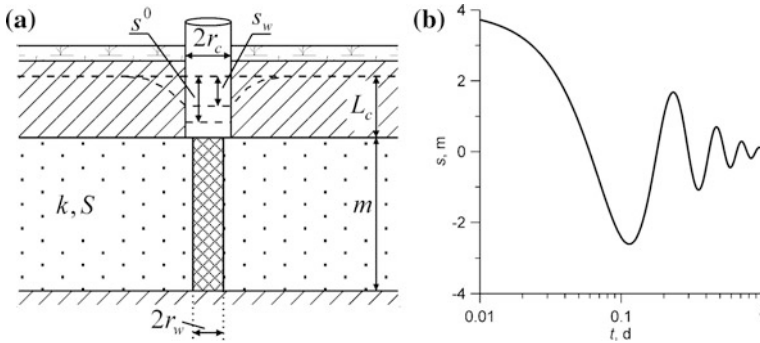


Fig. 9.7 Scheme for processing slug-test data by the Van der Kamp method: **a** cross-section and **b** a characteristic plot of water-level change in the tested well

aquifer thickness), m ; L_c is the initial height of water column in the casing (Fig. 9.7a), m .

Equation 9.23 is used to evaluate aquifer storage coefficient (S) and transmissivity (T).

References

Bouwer H, Rice RC (1976) A slug test for determining conductivity of unconfined aquifers with completely or partially penetrating wells. *Water Resour Res* 12(3):423–428

Bredehoeft JD, Papadopoulos IS (1980) A method for determining the hydraulic properties of tight formations. *Water Resour Res* 16(1):233–238

Carslow HS, Jaeger JC (1959) *Conduction of heat in solids*. Oxford at the Clarendon Press, London

Cooper HH, Bredehoeft JD, Papadopoulos IS (1965) The response of well-aquifer systems to seismic waves. *J Geophys Res* 70(16):3917–3926

Cooper HH, Bredehoeft JD, Papadopoulos IS (1967) Response of a finite diameter well to an instantaneous charge of water. *Water Resour Res* 3(1):263–269

Hvorslev MJ (1951) Time lag and soil permeability in groundwater observations. U.S. Army Corps Engineers, Waterways Experiment Station, Bulletin 36, Vicksburg, MS

Kipp KL (1985) Type curve analysis of inertial effects in the response of a well to a slug test. *Water Resour Res* 21(9):1397–1408

Picking LW (1994) Analyzing the recovery of a finite-diameter well after purging at an unknown rate—a substitute for slug-testing. *Ground Water* 32(1):91–95

Sindalovskiy LN (2006) *Handbook of analytical solutions for aquifer test analysis*. SpBSU, Sankt-Petersburg (In Russian)

Van der Kamp G (1976) Determining aquifer transmissivity by means of well response tests: the underdamped case. *Water Resour Res* 12(1):71–77

Yeh HD, Yang SY (2006) A novel analytical solution for a slug test conducted in a well with a finite-thickness skin. *Adv Water Resour* 29(10):1479–1489

Chapter 10

Multi-well Pumping Tests

The analytical solutions given in the first chapters (see Chaps. 1–6) described pumping tests, involving a single pumping well with a constant discharge rate. This chapter gives basic relationships for calculating the drawdown in aquifers at (1) multi-well pumping tests with constant or variable discharge rates (Sects. 10.1 and 10.2) (2) simultaneous pumping from two adjacent aquifers (Sect. 10.3), and (3) dipole flow tests (Sect. 10.4).

The solutions for the first two sections are provided by graphic-analytical procedures for processing input data.

10.1 Pumping with a Constant Discharge Rate

This section focuses on analytical solutions for calculating the drawdown during pumping tests involving several wells with constant discharge rates. The discharge rates of the wells may differ in both their magnitudes and signs. All solutions considered here are based on the superposition principle, which determines the drawdown in an observation well as the sum of drawdown values induced by each pumping well separately.

The general equation for the drawdown for a system of pumping wells in the case of a confined aquifer of infinite lateral extent (see Sect. 1.1.1) can be written as:

$$s = \frac{1}{4\pi T} \left[Q_1 W\left(\frac{r_1^2}{4at}\right) + Q_2 W\left(\frac{r_2^2}{4at}\right) + \dots + Q_N W\left(\frac{r_N^2}{4at}\right) \right], \quad (10.1)$$

where s is the drawdown in an observation well, m; T is the transmissivity, m^2/d ; t is the time elapsed from the start of pumping, d; a is the hydraulic diffusivity, m^2/d ; N is the number of pumping wells; Q_1, Q_2, \dots, Q_N are the constant discharge rates in the 1st, 2nd, ..., N th pumping wells, respectively, m^3/d ; r_1, r_2, \dots, r_N are the distances from the observation well in which the drawdown is determined to the 1st, 2nd, ..., N th pumping wells, respectively, m; $W(\cdot)$ is well-function (see Appendix 7.1).

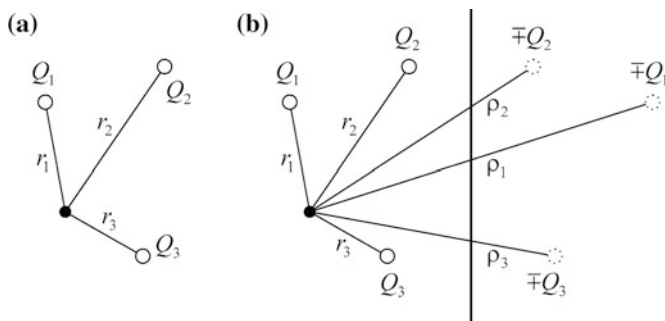


Fig. 10.1 Example of layout of three pumping wells for a multi-well constant-discharge test in an aquifer with **a** infinite and **b** semi-infinite lateral extent. The signs of the discharge rates of the image wells are minus for a constant-head boundary and plus for an impermeable boundary

The equation for any other aquifer types (see Chaps. 1–6) can be written similarly to formula (Eq. 10.1) with the well-function $W(\cdot)$ replaced by another basic drawdown function. In the case of a flow limited by some boundaries, the formula (Eq. 10.1) is supplemented with terms (with signs corresponding to the boundary condition) that account for image wells. In such case, the number N increases by the number of image wells.

Figure 10.1 shows examples with the layout of three pumping wells and one observation well in an aquifer of infinite (Fig. 10.1a) and semi-infinite (Fig. 10.1b) lateral extent.

10.1.1 Fully Penetrating Well in a Confined Aquifer

Graphic-analytical methods for processing multi-well, constant-discharge tests are best developed for confined aquifers. The procedure for constructing a solution takes into account the effect of the planar boundaries of the groundwater flow. For the analytical relationships in a single-well, constant-discharge pumping test under such conditions, see Sect. 1.1.

10.1.1.1 Aquifer of Infinite Lateral Extent

The solutions given in this section are arranged depending on the synchronicity of the start of the pumping-well operation.

Simultaneous Start of Pumping Wells

Basic Analytical Relationships

Transient Flow Equation

$$s = \frac{1}{4\pi T} \sum_{i=1}^N Q_i W\left(\frac{r_i^2}{4at}\right), \tag{10.2}$$

where Q_i is the constant discharge rate of the i th pumping well, m^3/d ; r_i is the distance from the observation well in which the drawdown is determined to the i th pumping well (Fig. 10.1), m.

Quasi-Steady-State Flow Equation

$$s = \frac{Q_t}{4\pi T} \ln \frac{2.25at}{r'^2}, \tag{10.3}$$

$$\ln r' = \frac{1}{Q_t} \sum_{i=1}^N Q_i \ln r_i, \tag{10.4}$$

$$Q_t = \sum_{i=1}^N Q_i. \tag{10.5}$$

Graphic-Analytical Processing

The relationships given in Table 10.1 have been derived from Eqs. 10.2 and 10.3.

Table 10.1 Graphic-analytical parameter evaluation

Plot	Method	Relationship
$s - \lg t$	Straight line	$T = \frac{0.183Q_t}{C}$, $\lg a = \frac{A}{C} + \lg \frac{r'^2}{2.25}$
$\lg s - \lg t$	Type curve: $\lg W'(u) - \lg \frac{1}{u}$	$T = \frac{1}{4\pi 10^D}$, $a = \frac{r_1^2 10^E}{4}$
$s - \lg r'$	Straight line	$T = \frac{0.366Q_t}{C}$, $\lg a = 2\frac{A}{C} - \lg(2.25 \cdot t)$
$s - \lg \frac{t}{r'^2}$	The same	$T = \frac{0.183Q_t}{C}$, $\lg a = \frac{A}{C} - \lg(2.25)$
$(s_1 - s_2) - \lg t$	Horizontal straight line	$T = \frac{Q_t}{2\pi \cdot A} \ln \frac{r'_2}{r'_1}$

A is the intercept of the straight line on the ordinate (see Sects. 12.1.1 and 12.1.2); C is the slope of the straight line (see Sect. 12.1.1); D, E are the shifts of the plots of the factual and type curves (see Sect. 12.1.3) in the vertical (D) and horizontal (E) directions. s_1, s_2, r'_1, r'_2 are the drawdown (s) and reduced distances from the pumping well (r') to the first and second observation wells. r' is calculated by (10.4). $W'(u) = \sum_{i=1}^N Q_i W(ur'_i), r'_i = (r_i/r_1)^2$. The value of r'_i can be normalized to the distance to any pumping well (the distance to this well is also used when determining the hydraulic diffusivity by a type curve)

Asynchronous Start of Pumping Wells

Basic Analytical Relationships*Transient Flow Equation*

$$s = \frac{1}{4\pi T} \sum_{i=1}^{N_t} Q_i W\left(\frac{r_i^2}{4a(t-t_i)}\right); \quad (10.6)$$

here, N_t is the number of pumping wells in operation at moment t ; t_i is the starting moment of the operation of the i th pumping well, measured from the start of the pumping test, d.

Quasi-Steady-State Flow Equation

$$s = \frac{Q_t}{4\pi T} \ln \frac{2.25at'_A}{r'^2}, \quad (10.7)$$

$$\ln t'_A = \frac{1}{Q_t} \sum_{i=1}^{N_t} Q_i \ln(t-t_i), \quad (10.8)$$

$$\ln r' = \frac{1}{Q_t} \sum_{i=1}^{N_t} Q_i \ln r_i, \quad (10.9)$$

where Q_t is determined by (Eq. 10.5) with N replaced by N_t .

Graphic-Analytical Processing

The relationships in Table 10.2 have been derived from Eq. 10.7.

Table 10.2 Graphic-analytical parameter evaluation

Plot	Method	Relationship
$\frac{s}{Q_t} - \lg t'_A$	Straight line ^a	$T = \frac{0.183}{C}$, $\lg a = \frac{A}{C} + \lg \frac{r'^2}{2.25}$
$\frac{s}{Q_t} - \lg r'$	Straight line	$T = \frac{0.366}{C}$, $\lg a = 2\frac{A}{C} - \lg(2.25 \cdot t'_A)$
$\frac{s}{Q_t} - \lg \frac{t'_A}{r'^2}$	Straight line ^b	$T = \frac{0.183}{C}$, $\lg a = \frac{A}{C} - \lg(2.25)$

^aThe number of linear segments corresponds to the number of activations of pumping wells

^bAll measured values fall onto a single linear segment

r' is determined by Eq. 10.9

10.1.1.2 Aquifer Semi-infinite in the Horizontal Plane: Constant-Head Boundary

Basic Analytical Relationships

Transient Flow Equation

$$s = \frac{1}{4\pi T} \sum_{i=1}^N Q_i \left[W\left(\frac{r_i^2}{4at}\right) - W\left(\frac{\rho_i^2}{4at}\right) \right]; \tag{10.10}$$

here, ρ_i is the distance from the observation well in which the drawdown is measured to an image well (see Eq. A3.1) obtained as a mirror reflection of the i th pumping well (Fig. 10.1b), m.

Steady-State Flow Equation

$$s_m = \frac{1}{2\pi T} \ln r', \tag{10.11}$$

$$\ln r' = \sum_{i=1}^N Q_i \ln \frac{\rho_i}{r_i}, \tag{10.12}$$

where s_m is the drawdown in the observation well during the steady-state flow period, m.

Graphic-Analytical Processing

The relationships given in Table 10.3 have been derived from Eqs. 10.10 and 10.11.

Table 10.3 Graphic-analytical parameter evaluation

Plot	Method	Relationship
$s - \lg t$	Horizontal straight line	$T = \frac{1}{2\pi \cdot A} \ln r'$
$\lg s - \lg t$	Type curve: $\lg W'(u) - \lg \frac{1}{u}$	$T = \frac{1}{4\pi 10^D}, a = \frac{r_1^2 10^E}{4}$
$s - \lg r'$	Straight line	$T = \frac{0.366}{C}$
$(s_1 - s_2) - \lg t$	Horizontal straight line	$T = \frac{1}{2\pi \cdot A} \ln \frac{r'_1}{r'_2}$

$W'(u) = \sum_{i=1}^N Q_i [W(ur'_i) - W(u\rho'_i)]$, $r'_i = (r_i/r_1)^2$, $\rho'_i = (\rho_i/r_1)^2$. The values of r'_i and ρ'_i can be normalized to the distance to any pumping well (see note to Table 10.1). r' is determined by formula (Eq. 10.12)

10.1.1.3 Aquifer Semi-infinite in the Horizontal Plane: Impermeable Boundary

Basic Analytical Relationships

Transient Flow Equation

$$s = \frac{1}{4\pi T} \sum_{i=1}^N Q_i \left[W\left(\frac{r_i^2}{4at}\right) + W\left(\frac{\rho_i^2}{4at}\right) \right]. \quad (10.13)$$

Quasi-Steady-State Flow Equation

$$s = \frac{Q_t}{2\pi T} \ln \frac{2.25at}{r'}, \quad (10.14)$$

$$\ln r' = \frac{1}{Q_t} \sum_{i=1}^N Q_i \ln r_i \cdot \rho_i. \quad (10.15)$$

Graphic-Analytical Processing

The relationships given in Table 10.4 have been derived from Eqs. 10.13 and 10.14.

Table 10.4 Graphic-analytical parameter evaluation

Plot	Method	Relationship
$s - \lg t$	Straight line	$T = \frac{0.366Q_t}{C}$, $\lg a = \frac{A}{C} + \lg \frac{r'}{2.25}$
$\lg s - \lg t$	Type curve: $\lg W'(u) - \lg \frac{1}{u}$	$T = \frac{1}{4\pi 10^D}$, $a = \frac{r_1^2 10^E}{4}$
$s - \lg r'$	Straight line	$T = \frac{0.366Q_t}{C}$, $\lg a = \frac{A}{C} - \lg(2.25 \cdot t)$
$s - \lg \frac{t}{r'}$	The same	$T = \frac{0.366Q_t}{C}$, $\lg a = \frac{A}{C} - \lg(2.25)$
$(s_1 - s_2) - \lg t$	Horizontal straight line	$T = \frac{1}{2\pi \cdot A} \ln \frac{r'_1}{r'_2}$

$W'(u) = \sum_{i=1}^N Q_i [W(ur'_i) + W(ur'_i)]$; see note to Table 10.3. r' is determined by formula (Eq. 10.15)

10.1.1.4 Strip Aquifer: Constant-Head Boundaries

Basic Analytical Relationships

Transient Flow Equation

$$s = \frac{1}{4\pi T} \sum_{i=1}^N Q_i \left[W\left(\frac{r_i^2}{4at}\right) + \sum_{j=1}^n (-1)^j \sum_{l=1}^2 W\left(\frac{(\rho_{i,l}^j)^2}{4at}\right) \right], \tag{10.16}$$

where $n \rightarrow \infty$ is the number of reflections at a single boundary; $\rho_{i,l}^j$ is the distance from the observation well in which the drawdown is measured to the j th image well, reflected from the left ($l = 1$) or right ($l = 2$) boundary and obtained by reflection of the i th pumping well, m.

The solution (Eq. 10.16) was derived from Eq. 1.17. Similarly, relationships can be derived from Eqs. 1.18 and 1.19.

Steady-State Flow Equations

1. A solution based on the superposition principle is:

$$s_m = \frac{1}{2\pi T} \ln r' = \frac{0.366}{T} \lg r', \tag{10.17}$$

$$\lg r' = \sum_{i=1}^N Q_i \lg \left(\frac{1}{r_i \rho_{i,1}^n} \prod_{j=1,3,5,\dots}^n \frac{\rho_{i,1}^j \rho_{i,2}^j}{\rho_{i,1}^j \rho_{i,2}^j} \right) = \sum_{i=1}^N Q_i \lg \left(\frac{\rho_{i,1}^1 \rho_{i,2}^1}{r_i \rho_{i,1}^n} \prod_{j=2}^{n-1} \frac{\rho_{i,1}^{j+1} \rho_{i,2}^{j+1}}{\rho_{i,1}^j \rho_{i,2}^j} \right). \tag{10.18}$$

2. Green’s function solution is:

$$s_m = \frac{1}{4\pi T} \ln r' = \frac{0.183}{T} \lg r', \tag{10.19}$$

$$\ln r' = \sum_{i=1}^N Q_i \ln \frac{\cosh \frac{\pi y_i}{L} - \cos \frac{\pi(L_p + L_{w,i})}{L}}{\cosh \frac{\pi y_i}{L} - \cos \frac{\pi(L_p - L_{w,i})}{L}}, \tag{10.20}$$

$$y_i = \sqrt{r_i^2 - (L_{w,i} - L_p)^2}, \tag{10.21}$$

where L is the width of the strip aquifer, m; $L_{w,i}$ is the distance from the left boundary to the i th pumping well, m; L_p is the distance from the observation well to the left boundary, m.

Table 10.5 Graphic-analytical parameter evaluation

Plot	Method	Relationship
$s-\lg t$	Horizontal straight line	$T = \frac{1}{2\pi \cdot A} \ln r'^a, T = \frac{1}{4\pi \cdot A} \ln r'^b$
$\lg s-\lg t$	Type curve: $\lg W'(u)-\lg \frac{1}{u}$	$T = \frac{1}{4\pi 10^D}; a = \frac{r_1^2 10^E}{4}$
$s_m-\lg r'$	Straight line	$T = \frac{0.366_a}{C}, T = \frac{0.183_b}{C}$
$(s_1 - s_2)-\lg t$	Horizontal straight line	$T = \frac{1}{2\pi \cdot A} \ln \frac{r'_1}{r'_2}, T = \frac{1}{4\pi \cdot A} \ln \frac{r'_1}{r'_2}$

^aWith the use of superposition principle

^bBased on Green’s function

$W'(u) = \sum_{i=1}^N Q_i \left[W(ur'_i) + \sum_{j=1}^n (-1)^j \sum_{l=1}^2 W(ur'_{i,l}{}^j) \right], r'_i = \left(\frac{r_i}{r_1} \right)^2, r'_{i,l}{}^j = \left(\frac{\rho_{i,l}^j}{r_1} \right)^2$. The values of r'_i and $r'_{i,l}{}^j$ can be normalized to the distance to any pumping well (see note to Table 10.1). r' is determined by Eq. 10.18 or Eq. 10.20

Graphic-Analytical Processing

The relationships given in Table 10.5 have been derived from Eqs. 10.16, 10.17, and 10.19.

10.1.1.5 Strip Aquifer: Impermeable Boundaries

Basic Analytical Relationships

Transient Flow Equation

$$s = \frac{1}{4\pi T} \sum_{i=1}^N Q_i \left[W\left(\frac{r_i^2}{4at}\right) + \sum_{j=1}^n \sum_{l=1}^2 W\left(\frac{\left(\rho_{i,l}^j\right)^2}{4at}\right) \right]. \tag{10.22}$$

The solution (Eq. 10.22) was derived from Eq. 1.24. Similarly, relationships can be derived from Eqs. 1.25 and 1.26.

Graphic-Analytical Processing

The relationships given in Table 10.6 have been derived from Eq. 10.22.

Table 10.6 Graphic-analytical parameter evaluation

Plot	Method	Relationship
$\lg s - \lg t$	Type curve: $\lg W'(u) - \lg \frac{1}{u}$	$T = \frac{1}{4\pi 10^D}, a = \frac{r_1^2 10^E}{4}$
$(s_1 - s_2) - \lg t$	Horizontal straight line	$T = \frac{(2n+1)Q_t}{2\pi \cdot A} \ln \frac{r_2'}{r_1'}$

$W'(u) = \sum_{i=1}^N Q_i \left[W(ur_i') + \sum_{j=1}^n \sum_{l=1}^2 W(ur_{i,l}^{j,l}) \right]$; the determination of r_i' and $r_{i,l}^{j,l}$ see in the note to Table 10.5; $\ln r' = \frac{1}{Q_t} \sum_{i=1}^N \left[Q_i \ln \left(r_i \prod_{j=1}^n \rho_{i,1}^j \rho_{i,2}^j \right)^{1/(2n+1)} \right]$; $Q_t = \sum_{i=1}^N Q_i$

10.1.1.6 Strip Aquifer: Constant-Head and Impermeable Boundaries

Basic Analytical Relationships

Transient Flow Equation

$$s = \frac{1}{4\pi T} \sum_{i=1}^N Q_i \left[W\left(\frac{r_i^2}{4at}\right) + \sum_{j=1,3,\dots}^n \sum_{l=1}^2 (-1)^{(j+2l-1)/2} W\left(\frac{(\rho_{i,l}^j)^2}{4at}\right) + \sum_{j=2,4,\dots}^n (-1)^{j/2} \sum_{l=1}^2 W\left(\frac{(\rho_{i,l}^j)^2}{4at}\right) \right]. \tag{10.23}$$

The solution (Eq. 10.23) was derived from Eq. 1.27. Similar relationships can be derived from Eq. 1.28.

Steady-State Flow Equations

1. Solution based on the superposition principle:

$$s_m = \frac{1}{2\pi T} \ln r' = \frac{0.366}{T} \lg r', \tag{10.24}$$

$$\lg r' = \sum_{i=1}^N Q_i \lg \left(\frac{\rho_{i,1}^n}{r_i} \prod_{j=1,5,9,\dots}^{n-3} \frac{\rho_{i,1}^j \rho_{i,1}^{j+1} \rho_{i,2}^{j+1} \rho_{i,2}^{j+2}}{\rho_{i,1}^{j+2} \rho_{i,1}^{j+3} \rho_{i,2}^j \rho_{i,2}^{j+3}} \right). \tag{10.25}$$

2. Green’s function solution:

$$s_m = \frac{1}{4\pi T} \ln r', \tag{10.26}$$

Table 10.7 Graphic-analytical parameter evaluation

Plot	Method	Relationship
$s - \lg t$	Horizontal straight line	$T = \frac{1}{2\pi \cdot A} \ln r'^a, T = \frac{1}{4\pi \cdot A} \ln r'^b$
$\lg s - \lg t$	Type curve: $\lg W'(u) - \lg \frac{1}{u}$	$T = \frac{1}{4\pi 10^D}, a = \frac{r_1^2 10^E}{4}$
$s_m - \lg r'$	Straight line	$T = \frac{0.366_a}{C}, T = \frac{0.183_b}{C}$
$(s_1 - s_2) - \lg t$	Horizontal straight line	$T = \frac{1}{2\pi \cdot A} \ln \frac{r'_{1a}}{r'_2}, T = \frac{1}{4\pi \cdot A} \ln \frac{r'_{1b}}{r'_2}$

^aWith the use of superposition principles

^bBased on Green’s function

$$W'(u) = \sum_{i=1}^N Q_i \left[W(ur'_i) + \sum_{j=1,3,\dots}^2 \sum_{l=1}^2 (-1)^{(j+2l-1)/2} w(ur'^j_{i,l}) + \sum_{j=2,4,\dots}^n (-1)^{j/2} \sum_{l=1}^2 w(ur'^j_{i,l}) \right].$$

Determining r'_i and $r'^j_{i,l}$ see in the note to Table 10.5. r' is determined by Eqs. 10.25 or 10.27

$$\ln r' = \sum_{i=1}^N Q_i \ln \frac{\left[\cosh \frac{\pi y_i}{2L} - \cos \frac{\pi(L_p + L_{w,i})}{2L} \right] \left[\cosh \frac{\pi y_i}{2L} + \cos \frac{\pi(L_p - L_{w,i})}{2L} \right]}{\left[\cosh \frac{\pi y_i}{2L} + \cos \frac{\pi(L_p + L_{w,i})}{2L} \right] \left[\cosh \frac{\pi y_i}{2L} - \cos \frac{\pi(L_p - L_{w,i})}{2L} \right]} \tag{10.27}$$

Here, L_p and $L_{w,i}$ are the distances from the observation well and i th pumping well to the constant-head boundary, m.

Graphic-Analytical Processing

The relationships given in Table 10.7 have been derived from Eqs. 10.23, 10.24, and 10.26.

10.1.2 Point Source: Confined Aquifer Infinite in the Horizontal Plane and Thickness

For analytical relationships for a single-well pumping test with constant discharge rate, see Sect. 1.2.1.

Basic Analytical Relationships

Transient Flow Equation

$$s = \frac{1}{4\pi k} \sum_{i=1}^N \frac{Q_i}{d_i} \operatorname{erfc} \frac{d_i}{2\sqrt{at}}, \tag{10.28}$$

$$d_i = \sqrt{r_i^2 + z_i^2}; \tag{10.29}$$

here z_i is the vertical distance between the center of the filter of the i th pumping well and the observation well (see Fig. 1.10), m.

Quasi-Steady-State Flow Equation

$$s = \frac{Q_t}{4\pi k} \left(\frac{1}{Q_t} \sum_{i=1}^N \frac{Q_i}{d_i} - \frac{1}{\sqrt{\pi at}} \right). \tag{10.30}$$

Steady-State Flow Equation

$$s_m = \frac{1}{4\pi k} \sum_{i=1}^N \frac{Q_i}{d_i}. \tag{10.31}$$

Graphic-Analytical Processing

The relationships given in Table 10.8 have been derived from Eqs. 10.28, 10.30, and 10.31.

Table 10.8 Graphic-analytical parameter evaluation

Plot	Method	Relationship
$s - \lg t$	Horizontal straight line	$k = \frac{1}{4\pi \cdot A} \sum_{i=1}^N \frac{Q_i}{d_i}$
$\lg s - \lg t$	Type curve: $\lg \operatorname{erfc}'(u) - \lg \frac{1}{u^2}$	$k = \frac{1}{4\pi 10^D}, a = \frac{d_1^2 10^E}{4}$
$s \frac{1}{\sqrt{t}}$	Straight line	$k = \frac{1}{4\pi \cdot A} \sum_{i=1}^N \frac{Q_i}{d_i}, a = \frac{(A/C)^2}{\pi} \left(Q_t / \sum_{i=1}^N \frac{Q_i}{d_i} \right)^2$
$(s_1 - s_2) - \lg t$	Horizontal straight line	$k = \frac{1}{4\pi \cdot A} \left(\sum_{i=1}^N \frac{Q_i}{d_{i,1}} - \sum_{i=1}^N \frac{Q_i}{d_{i,2}} \right)$

$\operatorname{erfc}'(u) = \sum_{i=1}^N \frac{Q_i}{d_i} \operatorname{erfc}'(ud'_i), d'_i = (d_i/d_1)^2$. The value of d'_i can be normalized to the distance to any pumping well (the distance to this well is used in evaluating the hydraulic diffusivity by type-curve method)

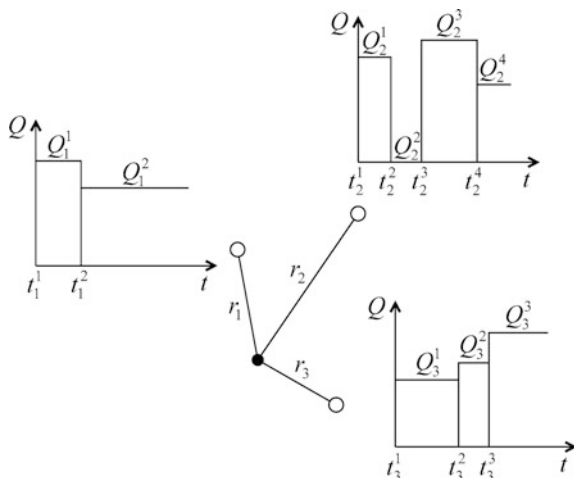


Fig. 10.2 An example of layout of three pumping wells with arbitrary step-wise variations of their discharge rates

10.2 Pumping with a Variable Discharge Rate

The construction of analytical relationships for calculating the drawdown in aquifers during pumping tests involving one or several pumping wells with discharge rates arbitrarily varying over time is based on the principle of superposition.

Figure 10.2 shows an example of the layout with three pumping wells and one observation well. A plot of discharge rate vs. time is given for each pumping well.

The drawdown in an aquifer under the effect of a pumping test is calculated as the sum of the drawdowns induced by each pumping well separately. Each increment of the pumping-well discharge rate creates an additional term in the sum of drawdown values. In this case, the discharge rate is assumed constant during each interval between its changes (Fig. 10.2), i.e., it is described by a step-function. In the case of aquifers bounded in the horizontal plane and/or thickness, a water-level change caused by image wells, obtained by the reflection of pumping wells in planar or vertical boundaries, will be superimposed on the overall flow pattern.

The general equation for the water-level drawdown in an observation well during a multi-well test with variable discharge rate can be written as:

$$s = P \sum_{i=1}^{N+M} \sum_{j=1}^{n_i^i} (Q_i^j - Q_i^{j-1}) f[r_i, (t - t_i^j)], \quad (10.32)$$

where f is a drawdown function accounting for aquifer type; M is the number of image wells for bounded aquifers (in the case of aquifers of infinite extent, $M = 0$); N is the number of pumping wells; n_i^j is the number of steps in the discharge rate of the i th pumping well by moment t ; P is a constant value, depending on the conceptual model; Q_i^j is the discharge rate at the j th step in the i th pumping well ($Q_i^0 = 0$), m^3/d ; r_i is the distance from the observation well to the i th pumping well (either real or image), m ; t is the time elapsed since the pumping began, d ; t_i^j is the moment of the start of the j th step in the discharge of the i th pumping well ($t_i^1 = 0$), d .

The basic analytical relationships given below exemplify a test of a confined aquifer of infinite extent (see Sect. 1.1.1).

10.2.1 Single Pumping Well with a Variable Discharge Rate

Basic Analytical Relationships

Transient Flow Equation

$$s = \frac{1}{4\pi T} \sum_{j=1}^{n_1^1} (Q_1^j - Q_1^{j-1}) W\left(\frac{r^2}{4a(t - t_1^j)}\right). \quad (10.33)$$

Quasi-Steady-State Flow Equation

$$s = \frac{Q_t}{4\pi T} \ln \frac{2.25at'}{r^2}, \quad (10.34)$$

$$\ln t' = \frac{1}{Q_t} \sum_{j=1}^{n_1^1} (Q_1^j - Q_1^{j-1}) \ln(t - t_1^j), \quad (10.35)$$

$$Q_t = \sum_{j=1}^{n_1^1} (Q_1^j - Q_1^{j-1}). \quad (10.36)$$

Graphic-Analytical Processing

The relationships given in Table 10.9 have been derived from Eq. 10.34.

Table 10.9 Graphic-analytical parameter evaluation

Plot	Method	Relationship
$\frac{s}{Q_t} - \lg t'$	Straight line	$T = \frac{0.183}{C}, \lg a = \frac{A}{C} + \lg \frac{r^2}{2.25}$
$\frac{s}{Q_t} - \lg r$	Straight line	$T = \frac{0.366}{C}, \lg a = 2 \frac{A}{C} - \lg(2.25 \cdot t')$
$\frac{s}{Q_t} - \lg \frac{t'}{r^2}$	Straight line ^a	$T = \frac{0.183}{C}, \lg a = \frac{A}{C} - \lg(2.25)$

^aAll measurements fall on the same straight line

The measurements made during a stop of pumping are ignored in the construction of the plot. r' is evaluated by Eq. 10.40

10.2.2 A System of Pumping Wells with a Variable Discharge Rate

Basic Analytical Relationships

Transient Flow Equation

$$s = \frac{1}{4\pi T} \sum_{i=1}^N \sum_{j=1}^{n'_i} (Q_i^j - Q_i^{j-1}) W\left(\frac{r_i^2}{4a(t-t_i^j)}\right). \quad (10.37)$$

Quasi-Steady-State Flow Equation

$$s = \frac{Q_t}{4\pi T} \ln \frac{2.25at'}{r'^2}, \quad (10.38)$$

$$\ln t' = \frac{1}{Q_t} \sum_{i=1}^N \sum_{j=1}^{n'_i} (Q_i^j - Q_i^{j-1}) \ln(t-t_i^j), \quad (10.39)$$

$$\ln r' = \frac{1}{Q_t} \sum_{i=1}^N \ln r_i \sum_{j=1}^{n'_i} (Q_i^j - Q_i^{j-1}), \quad (10.40)$$

$$Q_t = \sum_{i=1}^N \sum_{j=1}^{n'_i} (Q_i^j - Q_i^{j-1}). \quad (10.41)$$

Graphic-Analytical Processing

The relationships given in Table 10.10 have been derived from Eq. 10.38.

Table 10.10 Graphic-analytical parameter evaluation

Plot	Method	Relationship
$\frac{s}{Q_t} - \lg t'$	Straight line ^a	$T = \frac{0.183}{C}, \lg a = \frac{A}{C} + \lg \frac{r'^2}{2.25}$
$\frac{s}{Q_t} - \lg r'$	Straight line	$T = \frac{0.366}{C}, \lg a = 2 \frac{A}{C} - \lg(2.25t')$
$\frac{s}{Q_t} - \lg \frac{t'}{r'^2}$	Straight line ^b	$T = \frac{0.183}{C}, \lg a = \frac{A}{C} - \lg(2.25)$

^aThe number of linear segments corresponds to the number of discharge steps

^bAll measured values fall onto a single linear segment

The measurements made during a stop of pumping are ignored in the construction of the plot

10.3 Simultaneous Pumping from Two Aquifers Separated by an Aquitard

The pumping test is carried out in a leaky aquifer system, as described in Sect. 3.2, except that the wells are pumping both adjacent aquifers. This section considers leaky aquifers of infinite lateral extent (Sect. 10.3.1) and those limited by a circular boundary (Sect. 10.3.2).

10.3.1 Aquifers of Infinite Lateral Extent

The basic assumptions and conditions (Fig. 10.3):

- the general conditions for a leaky aquifer of infinite lateral extent are considered (see the beginning of Sect. 3.2.1);
- two pumping wells are located in two adjacent aquifers (1) and (2).

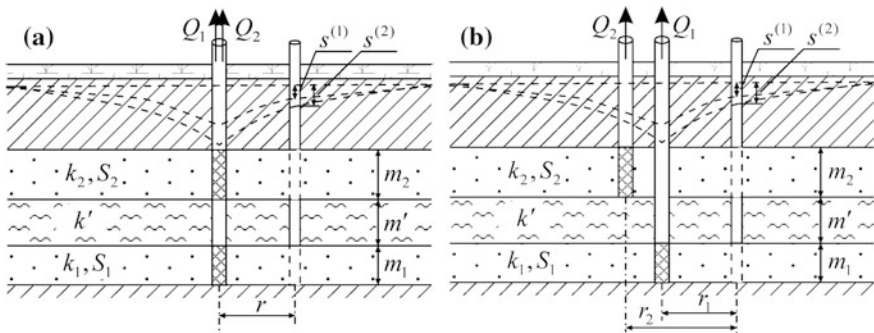


Fig. 10.3 Leaky aquifers with pumping from two aquifers through **a** a single pumping well with two screens and **b** two wells

Solutions are given for calculating the drawdown in two aquifers during pumping (1) from a single well (or two close wells), pumping both aquifers (Fig. 10.3a) and (2) two pumping wells located at some distance from one another (Fig. 10.3b). The second solution admits asynchronous starts of the operation of pumping wells.

Basic Analytical Relationships

Transient Flow Equations

1. The drawdown in observation wells (Fig. 10.3a) located in the first and second aquifers during pumping from a single well can be written as (Babushkin et al. 1974):

$$s^{(1)} \approx \frac{1}{4\pi(T_1 + T_2)} \left[(Q_1 + Q_2)W\left(\frac{r^2}{4a^*t}\right) + \left(Q_1 \frac{T_2}{T_1} - Q_2\right)W\left(\frac{r^2}{4a^*t}, \frac{r}{B^*}\right) \right], \quad (10.42)$$

$$s^{(2)} \approx \frac{1}{4\pi(T_1 + T_2)} \left[(Q_1 + Q_2)W\left(\frac{r^2}{4a^*t}\right) + \left(Q_2 \frac{T_1}{T_2} - Q_1\right)W\left(\frac{r^2}{4a^*t}, \frac{r}{B^*}\right) \right], \quad (10.43)$$

$$a^* = \frac{2a_1a_2}{a_1 + a_2}, \quad (10.44)$$

where $s^{(1)}$, $s^{(2)}$ are the drawdown values for the first and second aquifers, m; Q_1 , Q_2 are the discharge rates for the first and second aquifers, respectively, m³/d; r is the distance from the observation well located in one of the aquifers to the pumping well, m; $T_1 = k_1m$ and $T_2 = k_2m$ are the transmissivities of the first and second aquifers, respectively, m²/d; $a_1 = T_1/S_1$ and $a_2 = T_2/S_2$ are the hydraulic diffusivities of the first and second aquifers, respectively, m²/d; S_1 , k_1 , m_1 and S_2 , k_2 , m_2 are storage coefficients (dimensionless), the hydraulic conductivities (m/d) and thicknesses (m) of the first and second aquifers, respectively; $W(u)$ and $W(u, \beta)$ are the well-function and the well-function for a leaky aquifer, respectively (see Appendixes 7.1 and 7.2). For the formulas for calculating B^* , see Eqs. 3.49–3.53.

Equations 10.42 and 10.43 are applicable to time $t > 5m^2/a'$, where a' , m' are the hydraulic diffusivity (m²/d) and thickness (m) of the separating aquitard.

2. The drawdown in the quasi-steady flow period in observation wells (Fig. 10.3b), located in the first and second aquifers pumped from two pumping wells (Hantush 1967) can be calculated as:

$$s^{(1)} = \left\{ \begin{aligned} & \frac{Q_1}{4\pi(T_1 + T_2)} \left[\ln \frac{2.25a^*t}{r_1^2} + 2 \frac{T_2}{T_1} K_0 \left(\frac{r_1}{B^*} \right) \right] + \\ & + \frac{Q_2}{4\pi(T_1 + T_2)} \left[\ln \frac{2.25a^*(t-t')}{r_2^2} - 2K_0 \left(\frac{r_2}{B^*} \right) \right] \end{aligned} \right\}, \quad (10.45)$$

$$s^{(2)} = \left\{ \begin{aligned} & \frac{Q_1}{4\pi(T_1 + T_2)} \left[\ln \frac{2.25a^*t}{r_1^2} - 2K_0 \left(\frac{r_1}{B^*} \right) \right] + \\ & + \frac{Q_2}{4\pi(T_1 + T_2)} \left[\ln \frac{2.25a^*(t-t')}{r_2^2} + 2 \frac{T_1}{T_2} K_0 \left(\frac{r_2}{B^*} \right) \right] \end{aligned} \right\}, \quad (10.46)$$

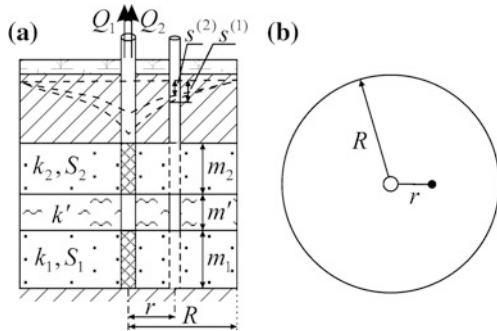
where $K_0(\cdot)$ is modified Bessel function of the second kind of the zero order (see Appendix 7.13); t' is the interval between the start of pumping-well operation in aquifers (1) and (2), d ; r_1 , r_2 are the distances from the observation well located in one of the aquifers to the pumping well located in the first and second aquifers, respectively, m .

10.3.2 Circular Aquifers

The basic assumptions and conditions (Fig. 10.4) are:

- general conditions for a leaky aquifer of infinite lateral extent are considered (see the beginning of Sect. 3.2.1);
- the external contour of the aquifer is a circular boundary of groundwater flow;
- the pumping well is located in the center of the circular aquifer; the pumping is carried out from the two adjacent aquifers simultaneously.

Fig. 10.4 Circular leaky aquifer system with the simultaneous testing of two adjacent aquifers:
a cross-section and **b** planar view



Either of the two boundary conditions: (1) constant head boundary or (2) impermeable boundary is specified on the external contour of the aquifer (see Fig. A3.10a, c).

Basic Analytical Relationships

Transient Flow Equations

1. The external contour of the aquifer is a constant-head boundary. The draw-downs in the first and second aquifers (Hantush 1967) are:

$$\begin{aligned}
 s^{(1)} = & \frac{Q_1}{2\pi(T_1 + T_2)} \left\{ \ln \frac{R}{r} + \frac{T_2}{T_1} \left[\text{K}_0 \left(\frac{r}{B^*} \right) - \text{K}_0 \left(\frac{R}{B^*} \right) \text{I}_0 \left(\frac{r}{B^*} \right) / \text{I}_0 \left(\frac{R}{B^*} \right) \right] - \right. \\
 & - \frac{2a_1 R^2}{a_2 B^{*2}} \sum_{n=1}^{\infty} \left[\frac{1}{\lambda_n} \left(\frac{1}{\varepsilon_n} \exp \left(-\varepsilon_n \frac{a_2 t}{R^2} \right) - \frac{1}{\delta_n} \exp \left(-\delta_n \frac{a_2 t}{R^2} \right) \right) \beta_n \right] - \\
 & - \frac{2a_1 B_2^2}{a_2 B^{*2}} \sum_{n=1}^{\infty} \left[\frac{1}{\lambda_n} \left(\left(1 - \frac{x_n^2}{\delta_n} \right) \exp \left(-\delta_n \frac{a_2 t}{R^2} \right) - \left(1 - \frac{x_n^2}{\varepsilon_n} \right) \exp \left(-\varepsilon_n \frac{a_2 t}{R^2} \right) \right) \beta_n \right] \left. \right\} + \\
 & + \frac{Q_2}{2\pi(T_1 + T_2)} \left\{ \ln \frac{R}{r} - \text{K}_0 \left(\frac{r}{B^*} \right) + \text{K}_0 \left(\frac{R}{B^*} \right) \text{I}_0 \left(\frac{r}{B^*} \right) / \text{I}_0 \left(\frac{R}{B^*} \right) - \right. \\
 & - 2 \frac{a_2 R^2}{a_1 B^{*2}} \sum_{n=1}^{\infty} \left[\frac{1}{\lambda'_n} \left(\frac{1}{\varepsilon'_n} \exp \left(-\varepsilon'_n \frac{a_1 t}{R^2} \right) - \frac{1}{\delta'_n} \exp \left(-\delta'_n \frac{a_1 t}{R^2} \right) \right) \beta_n \right] \left. \right\}, \tag{10.47}
 \end{aligned}$$

$$\begin{aligned}
 s^{(2)} = & \frac{Q_1}{2\pi(T_1 + T_2)} \left\{ \ln \frac{R}{r} - \text{K}_0 \left(\frac{r}{B^*} \right) + \text{K}_0 \left(\frac{R}{B^*} \right) \text{I}_0 \left(\frac{r}{B^*} \right) / \text{I}_0 \left(\frac{R}{B^*} \right) - \right. \\
 & - 2 \frac{a_1 R^2}{a_2 B^{*2}} \sum_{n=1}^{\infty} \left[\frac{1}{\lambda_n} \left(\frac{1}{\varepsilon_n} \exp \left(-\varepsilon_n \frac{a_2 t}{R^2} \right) - \frac{1}{\delta_n} \exp \left(-\delta_n \frac{a_2 t}{R^2} \right) \right) \beta_n \right] \left. \right\} + \\
 & + \frac{Q_2}{2\pi(T_1 + T_2)} \left\{ \ln \frac{R}{r} + \frac{T_1}{T_2} \left[\text{K}_0 \left(\frac{r}{B^*} \right) - \text{K}_0 \left(\frac{R}{B^*} \right) \text{I}_0 \left(\frac{r}{B^*} \right) / \text{I}_0 \left(\frac{R}{B^*} \right) \right] - \right. \\
 & - \frac{2a_2 R^2}{a_1 B^{*2}} \sum_{n=1}^{\infty} \left[\frac{1}{\lambda'_n} \left(\frac{1}{\varepsilon'_n} \exp \left(-\varepsilon'_n \frac{a_1 t}{R^2} \right) - \frac{1}{\delta'_n} \exp \left(-\delta'_n \frac{a_1 t}{R^2} \right) \right) \beta_n \right] - \\
 & - \frac{2a_2 B_1^2}{a_1 B^{*2}} \sum_{n=1}^{\infty} \left[\frac{1}{\lambda'_n} \left(\left(1 - \frac{x_n^2}{\delta'_n} \right) \exp \left(-\delta'_n \frac{a_1 t}{R^2} \right) - \left(1 - \frac{x_n^2}{\varepsilon'_n} \right) \exp \left(-\varepsilon'_n \frac{a_1 t}{R^2} \right) \right) \beta_n \right] \left. \right\}, \tag{10.48}
 \end{aligned}$$

$$\beta_n = \frac{J_0(x_n r/R)}{J_1^2(x_n)}, \tag{10.49}$$

where R is the radius of the circular aquifer, m; x_n are the positive roots of the equation $J_0(x_n) = 0$ (see Appendix 7.15); $J_0(\cdot)$ and $J_1(\cdot)$ are Bessel functions of the first kind of the zero and the first order; $\text{I}_0(\cdot)$ and $\text{K}_0(\cdot)$ are modified Bessel

functions of the first and the second kind of the zero order (see Appendix 7.13); for λ_n , δ_n , ε_n —see formulas (Eqs. 3.60–3.62);

$$\lambda'_n = \sqrt{\left[\left(1 - \frac{a_2}{a_1} \right) x_n^2 + \frac{R^2}{B_1^2} - \frac{a_2 R^2}{a_1 B_2^2} \right]^2 + 4 \frac{a_2 R^4}{a_1 B_2^2 B_1^2}}; \quad (10.50)$$

$$\delta'_n = 0.5 \left[\left(1 + \frac{a_2}{a_1} \right) x_n^2 + \frac{R^2}{B_1^2} + \frac{a_2 R^2}{a_1 B_2^2} + \lambda'_n \right]; \quad (10.51)$$

$$\varepsilon'_n = 0.5 \left[\left(1 + \frac{a_2}{a_1} \right) x_n^2 + \frac{R^2}{B_1^2} + \frac{a_2 R^2}{a_1 B_2^2} - \lambda'_n \right]; \quad (10.52)$$

B^* , B_1 , B_2 are evaluated with Eqs. 3.49–3.53.

2. The external contour of the aquifer is an impermeable boundary. The drawdowns in the first and second aquifers can be evaluated as (Bochever 1968):

$$s = \left\{ \frac{Q_1 + Q_2}{4\pi T} \left[2 \frac{at}{R^2} + \ln \frac{R}{r} - \frac{2}{3} + \frac{r^2}{2R^2} - 2 \sum_{n=1}^{\infty} \frac{J_0(x_{n,1} r/R)}{x_{n,1}^2 J_0^2(x_{n,1})} \exp\left(-x_{n,1}^2 \frac{at}{R^2}\right) \right] \pm \frac{Q_1 - Q_2}{4\pi T} \left[K_0\left(\frac{r}{B}\right) + I_0\left(\frac{r}{B}\right) \frac{K_1(R/B)}{I_1(R/B)} - 2 \frac{B^2}{R^2} \exp\left(-\frac{R^2 at}{B^2 R^2}\right) - 2 \sum_{n=1}^{\infty} \frac{J_0(x_{n,1} r/R)}{(x_{n,1}^2 + R^2/B^2) J_0^2(x_{n,1})} \exp\left(-\left(x_{n,1}^2 + \frac{R^2}{B^2}\right) \frac{at}{R^2}\right) \right] \right\}, \quad (10.53)$$

where $x_{n,1}$ are the positive roots of the equation $J_1(x_{n,1}) = 0$ (see Appendix 7.15); $I_1(\cdot)$ and $K_1(\cdot)$ are modified Bessel functions of the first and the second kind of the first order (see Appendix 7.13); the sign “ \pm ”: the plus sign is used when evaluating the drawdown in the observation well located in the first aquifer ($s = s^{(1)}$), and the minus sign is used for the drawdown in the observation well in the second aquifer ($s = s^{(2)}$).

10.4 Dipole Flow Tests

A dipole flow test is simultaneous pumping out and injection into of two test wells located some distance from one another in the horizontal or vertical plane. The magnitudes of the discharge rate in the wells are the same.

10.4.1 Horizontal Dipole

Two fully penetrating wells are located at a distance (L) from one another in an isotropic aquifer of infinite lateral extent. Three aquifer types (confined, unconfined, and leaky aquifers) are considered (Fig. 10.5). Water is being pumped at a constant rate from one well and injected into the other well at the same rate.

Basic Analytical Relationships

Transient Flow Equations

The drawdown (drawup) in the confined aquifer (Fig. 10.4a) is:

$$s = \frac{Q}{4\pi T} \left[W\left(\frac{r_1^2 S}{4Tt}\right) - W\left(\frac{r_2^2 S}{4Tt}\right) \right], \tag{10.54}$$

in the unconfined aquifer (Fig. 10.4b):

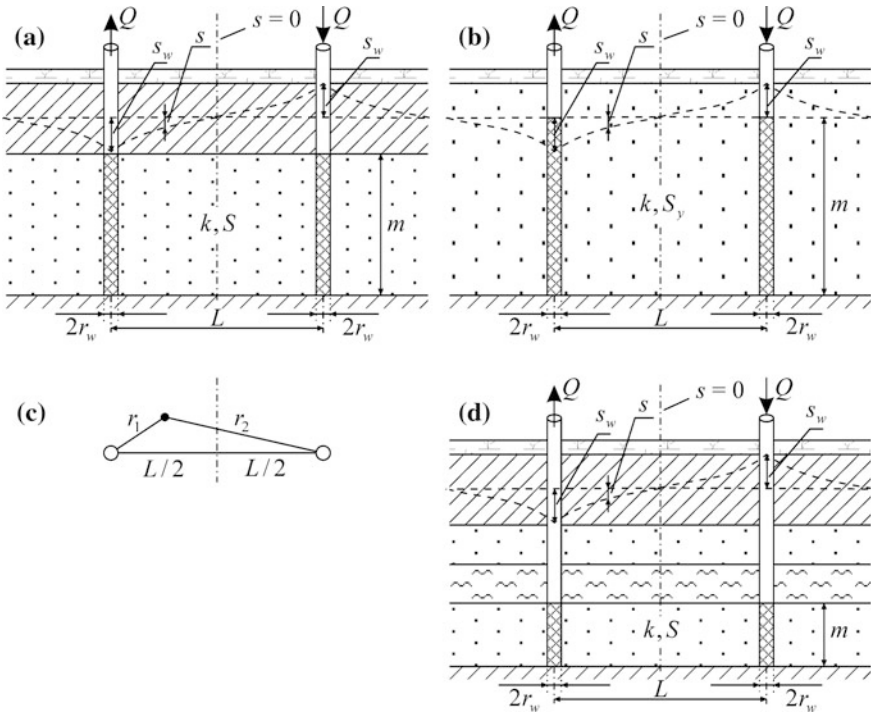


Fig. 10.5 Dipole flow test in **a** confined, **b** unconfined and **d** leaky aquifer. **a, b, d** Cross-sections; **c** planar view with distances from the observation well to the pumping and injection wells

$$s = m - \sqrt{m^2 - \frac{Q}{2\pi k} \left[W\left(\frac{r_1^2 S_y}{4kmt}\right) - W\left(\frac{r_2^2 S_y}{4kmt}\right) \right]} \quad (10.55)$$

and in a leaky aquifer (Fig. 10.4c):

$$s = \frac{Q}{4\pi T} \left[W\left(\frac{r_1^2 S}{4Tt}, \frac{r_1}{B}\right) - W\left(\frac{r_2^2 S}{4Tt}, \frac{r_2}{B}\right) \right], \quad (10.56)$$

where r_1 , r_2 are the distances to the pumping and injection well, respectively, m ; S , S_y are the specific storage of the confined aquifer and the specific yield of the unconfined aquifer, respectively, dimensionless; k , m are the hydraulic conductivity (m/d) and the initial water-saturated thickness (m) of the unconfined aquifer; B is the leakage factor (m), which is determined by the number of adjacent aquifers (see Appendix 1).

If the observation well is located closer to the pumping well ($r_1 < r_2$), then s is the drawdown. If the observation well is located closer to the injection well ($r_1 > r_2$), then s is the drawup (in this case, the value is negative: $s < 0$). On the line where the distances from the test wells are equal ($r_1 = r_2$), the water-level change is zero ($s = 0$).

The Eqs. 10.54–10.56 were constructed based on the superposition principle and appropriate equations for aquifers of infinite lateral extent (Eqs. 1.1, 2.22, and 3.1). Equation 10.55 refers only to the gravity-drainage period. Equation 10.56 refers to an arbitrary configuration of the main and adjacent aquifers shown in Fig. 3.2.

Steady-State Flow Equations

1. The maximal drawdown (drawup) in an observation well located in a confined aquifer (Fig. 10.4a) at a distance r_1 from the pumping well is (Jacob 1949):

$$s_m = \frac{Q}{2\pi T} \ln \frac{r_2}{r_1}. \quad (10.57)$$

The maximal change in the water level in one of the test wells (Jacob 1949) is:

$$s_{mw} = \frac{Q}{2\pi T} \ln \frac{L - r_w}{r_w} \approx \frac{Q}{2\pi T} \ln \frac{L}{r_w}, \quad (10.58)$$

where L is the distance between the test wells, m ; r_w is the radius of the test well, m .

In practical calculations, the wellbore radius under the logarithm in the numerator in Eq. 10.58 can be neglected.

2. In an unconfined aquifer (Fig. 10.4b), the water-level change in the observation well can be described by the solution (Kerkis 1956):

$$s_m(2m - s_m) = \frac{Q}{\pi k} \ln \frac{r_2}{r_1}, \tag{10.59}$$

and, similarly to Eq. 10.58, the water-level change in a test well can be calculated as (Kerkis 1956):

$$s_{mw}(2m - s_{mw}) = \frac{Q}{\pi k} \ln \frac{L - r_w}{r_w} \approx \frac{Q}{\pi k} \ln \frac{L}{r_w}. \tag{10.60}$$

3. Leaky aquifer (Fig. 10.4c). The water-level change in an observation well is:

$$s_m = \frac{Q}{2\pi T} \left[K_0\left(\frac{r_1}{B}\right) - K_0\left(\frac{r_2}{B}\right) \right] \tag{10.61}$$

and in the test well:

$$s_{mw} = \frac{Q}{2\pi T} \left[K_0\left(\frac{r_w}{B}\right) - K_0\left(\frac{L}{B}\right) \right]. \tag{10.62}$$

In practical calculations, when $r_2/B < 0.05$, Eq. 10.61 can be replaced by the solution Eq. 10.57 for a confined aquifer. This follows from an approximation of function $K_0(\cdot)$ for a small argument (see Appendix 7.13).

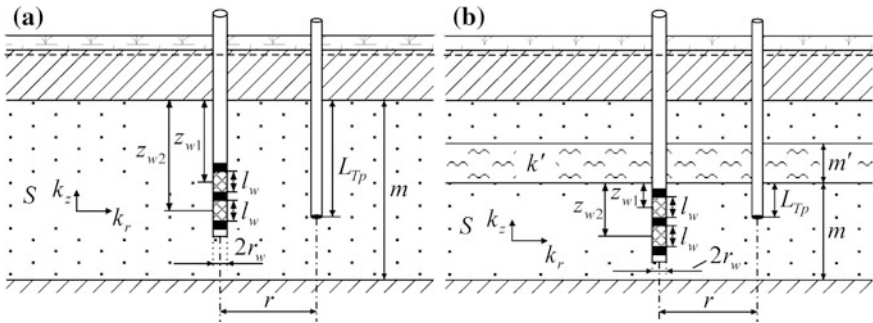


Fig. 10.6 A vertical dipole test in **a** a nonleaky and **b** a leaky aquifer

10.4.2 Vertical Dipole

A partially penetrating test well with dipole chambers is located in a homogeneous, vertically anisotropic nonleaky (Fig. 10.6a) or leaky aquifer (Fig. 10.6b) of infinite lateral extent. Water is withdrawn from the upper chamber at a constant rate and pumped at the same rate into the lower chamber. The drawdown in the upper chamber and the drawup in the lower chamber of the test well, as well as water-level changes in a piezometer, located in any point in the aquifer, are determined.

Basic Analytical Relationships

Transient Flow Equations

1. Water-level changes in a piezometer located in a nonleaky aquifer (Fig. 10.6a) are:

$$s = \frac{Q}{\pi^2 k_r l_w} \sum_{n=1}^{\infty} \left[\frac{1}{n} W \left(\frac{r^2 S}{4k_r m t}, \chi \frac{n\pi r}{m} \right) \times \left(\cos \frac{n\pi z_{w1}}{m} - \cos \frac{n\pi z_{w2}}{m} \right) \sin \frac{n\pi l_w}{2m} \cos \frac{n\pi L_{Tp}}{m} \right] \quad (10.63)$$

and in a leaky aquifer (Fig. 10.6b):

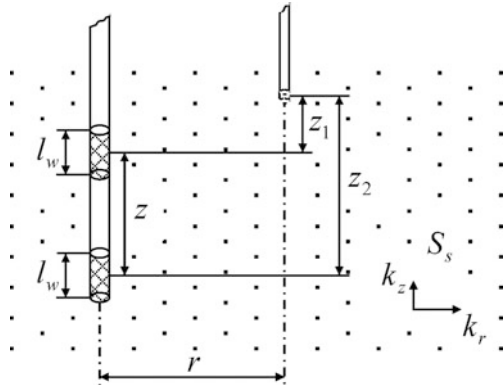
$$s = \frac{Q}{\pi^2 k_r l_w} \sum_{n=1}^{\infty} \left[\frac{1}{n} W \left(\frac{r^2 S}{4k_r m t}, \sqrt{\left(\frac{r}{B_r} \right)^2 + \left(\chi \frac{n\pi r}{m} \right)^2} \right) \times \left(\cos \frac{n\pi z_{w1}}{m} - \cos \frac{n\pi z_{w2}}{m} \right) \sin \frac{n\pi l_w}{2m} \cos \frac{n\pi L_{Tp}}{m} \right], \quad (10.64)$$

where z_{w1} , z_{w2} are the vertical distances from the aquifer top to the centers of the upper and lower chamber, respectively, m; $\chi = \sqrt{k_r/k_z}$ is anisotropy factor, dimensionless; k_r , k_z are horizontal and vertical hydraulic conductivities, respectively, m/d; L_{Tp} is the vertical distance from the aquifer top to the open part of the piezometer, m; l_w is the length of a dipole chamber, m; $B_r = \sqrt{k_r m m' / k'}$ is the leakage factor, m.

Equation 10.63 was derived from Hantush solutions Eqs. 1.104 and 1.105. Equation 10.64 was derived from the Hantush solution Eq. 3.89.

2. Water-level changes in a dipole chamber of the well located in a nonleaky aquifer (Fig. 10.6a) (Kabala 1993) are:

Fig. 10.7 A vertical dipole test in an aquifer infinite in the horizontal plane and thickness



$$s_w = \frac{Q}{\pi k_r m} \sum_{n=1}^{\infty} \left\{ \left(\frac{2m}{n\pi l_w} \sin \frac{n\pi l_w}{2m} \right)^2 \sin \left(n\pi \frac{z_{w2} + z_{w1}}{2m} \right) \sin \left(n\pi \frac{z_{w2} - z_{w1}}{2m} \right) \times \right. \\ \left. \times \cos \left(n\pi \frac{z}{m} \right) W \left(\frac{r_w^2 S}{4k_r m t}, \frac{\chi n\pi r_w}{m} \right) \right\} \quad (10.65)$$

and in a leaky aquifer (Fig. 10.6b):

$$s_w = \frac{Q}{\pi k_r m} \sum_{n=1}^{\infty} \left\{ \left(\frac{2m}{n\pi l_w} \sin \frac{n\pi l_w}{2m} \right)^2 \sin \left(n\pi \frac{z_{w2} + z_{w1}}{2m} \right) \sin \left(n\pi \frac{z_{w2} - z_{w1}}{2m} \right) \times \right. \\ \left. \times \cos \left(n\pi \frac{z}{m} \right) W \left[\frac{r_w^2 S}{4k_r m t}, \sqrt{\left(\frac{r_w}{B_r} \right)^2 + \left(\frac{\chi n\pi r_w}{m} \right)^2} \right] \right\}, \quad (10.66)$$

where $z = z_{w1}$, when the drawdown in the upper chamber is determined; $z = z_{w2}$, when the drawup in the lower chamber is determined.

Equation 10.65 was derived from Eq. 10.66 at $B_r \rightarrow \infty$.

3. Water-level changes in a piezometer during a dipole test in an aquifer infinite in thickness (Fig. 10.7) (Zlotnik and Ledder 1996) are:

$$s = \frac{Q}{8\pi k_r l_w} \left[M \left(\frac{r^2 S_s}{4k_r t}, \frac{0.5l_w + z_1}{\chi r} \right) + M \left(\frac{r^2 S_s}{4k_r t}, \frac{0.5l_w - z_1}{\chi r} \right) - \right. \\ \left. - M \left(\frac{r^2 S_s}{4k_r t}, \frac{0.5l_w + z_2}{\chi r} \right) - M \left(\frac{r^2 S_s}{4k_r t}, \frac{0.5l_w - z_2}{\chi r} \right) \right], \quad (10.67)$$

where S_s is the specific storage, $1/m$; z_1, z_2 are the vertical distances from the centers of the upper and lower chamber to the open part of the piezometer, m .

The relationship (Eq. 10.67), for an aquifer infinite in thickness, follows from Eq. 1.97.

Steady-State Flow Equations

1. Water-level changes in a piezometer located in a nonleaky aquifer (Fig. 10.6a) are:

$$s_m = \frac{2Q}{\pi^2 k_r l_w} \sum_{n=1}^{\infty} \left[\frac{1}{n} K_0 \left(\chi \frac{n\pi r}{m} \right) \times \right. \\ \left. \times \left(\cos \frac{n\pi z_{w1}}{m} - \cos \frac{n\pi z_{w2}}{m} \right) \sin \frac{n\pi l_w}{2m} \cos \frac{n\pi L_{Tp}}{m} \right] \quad (10.68)$$

and in a leaky aquifer (Fig. 10.6b):

$$s_m = \frac{2Q}{\pi^2 k_r l_w} \sum_{n=1}^{\infty} \left[\frac{1}{n} K_0 \left(\sqrt{\left(\frac{r}{B_r} \right)^2 + \left(\chi \frac{n\pi r}{m} \right)^2} \right) \times \right. \\ \left. \times \left(\cos \frac{n\pi z_{w1}}{m} - \cos \frac{n\pi z_{w2}}{m} \right) \sin \frac{n\pi l_w}{2m} \cos \frac{n\pi L_{Tp}}{m} \right] \quad (10.69)$$

2. Water-level changes in a dipole chamber of a well in a nonleaky aquifer (Fig. 10.6a) (Kabala 1993) is:

$$s_{mw} = \frac{2Q}{\pi k_r m} \sum_{n=1}^{\infty} \left\{ \left(\frac{2m}{n\pi l_w} \sin \frac{n\pi l_w}{2m} \right)^2 \sin \left(n\pi \frac{z_{w2} + z_{w1}}{2m} \right) \sin \left(n\pi \frac{z_{w2} - z_{w1}}{2m} \right) \times \right. \\ \left. \times \cos \left(n\pi \frac{z}{m} \right) K_0 \left(\frac{\chi n\pi r_w}{m} \right) \right\} \quad (10.70)$$

and in a leaky aquifer (Fig. 10.6b):

$$s_{mw} = \frac{2Q}{\pi k_r m} \sum_{n=1}^{\infty} \left\{ \left(\frac{2m}{n\pi l_w} \sin \frac{n\pi l_w}{2m} \right)^2 \sin \left(n\pi \frac{z_{w2} + z_{w1}}{2m} \right) \sin \left(n\pi \frac{z_{w2} - z_{w1}}{2m} \right) \times \right. \\ \left. \times \cos \left(n\pi \frac{z}{m} \right) K_0 \left[\sqrt{\left(\frac{r_w}{B_r} \right)^2 + \left(\frac{\chi n\pi r_w}{m} \right)^2} \right] \right\}, \quad (10.71)$$

z —see note to Eqs. 10.65 and 10.66.

Equation 10.70 was derived from Eq. 10.71 at $B_r \rightarrow \infty$.

The time of the beginning of a steady-state period is evaluated by the formula (Kabala 1993):

$$t_s = 5 \frac{mS}{\pi^2 \chi^2 k_r} = 5 \frac{mS}{\pi^2 k_z}. \quad (10.72)$$

3. Water-level changes in a piezometer during a dipole test in an aquifer infinite in thickness (Fig. 10.7) (Zlotnik and Ledder 1996) are:

$$s_m = \frac{Q}{4\pi k_r l_w} \left\{ \begin{array}{l} \operatorname{arcsinh}\left(\frac{z_1 + 0.5l_w}{\chi r}\right) - \operatorname{arcsinh}\left(\frac{z_1 - 0.5l_w}{\chi r}\right) + \\ + \operatorname{arcsinh}\left(\frac{z_2 - 0.5l_w}{\chi r}\right) - \operatorname{arcsinh}\left(\frac{z_2 + 0.5l_w}{\chi r}\right) \end{array} \right\}. \quad (10.73)$$

The steady-state relationship (Eq. 10.73), for an aquifer infinite in thickness, follows from Eq. 1.98.

References

- Babushkin VD, Plotnikov II, Chuyko VM (1974) Methods for flow properties investigation in heterogeneous rocks. Nedra, Moscow (In Russian)
- Bochever FM (1968) Theory and practical methods of groundwater yield evaluation. Nedra, Moscow (In Russian)
- Hantush MS (1967) Flow to wells in aquifers separated by a semipervious layer. *J Geophys Res* 72 (6):1709–1720
- Jacob CE (1949) Flow of ground water. In: Rouse H (ed) *Engineering hydraulics*, chap 5. Wiley, New York and London, pp 321–386
- Kabala ZJ (1993) The dipole flow test: a new single-borehole test for aquifer characterization. *Water Resour Res* 29(1):99–107
- Kerkis EE (1956) Estimation of aquifer transmissivity from combined pumping-injection test data. *Sovetskaya geologia* 56:83–95 (In Russian)
- Zlotnik V, Ledder G (1996) Theory of dipole flow in uniform anisotropic aquifers. *Water Resour Res* 32(4):1119–1128

Chapter 11

Recovery Tests

The analytical solutions for describing water-level recovery after a pumping test were constructed based on the superposition principle (see Sect. 10.2), which, in this case, determines the water-level changes in a well as the sum of drawdown values corresponding to two periods: pumping from the well with some (constant or variable) discharge rate and level recovery at a zero discharge rate.

The methods of processing depend on the moment considered as the beginning of the water-level recovery record: (1) the change in the level is measured from the water elevation at the start of pumping test, i.e., static level; (2) the change in the level is measured from the start of recovery, i.e., the dynamic level at the moment when pumping stopped. Figure 11.1 contains plots of the water-level changes, representing the same recovery data with different reference points. As shown below, such an approach extends the potentialities for evaluating hydraulic parameters by graphic-analytical methods.

The expressions for water-level changes in an observation well are written as the drawdown at pumping with two discharge stages (see Sect. 10.2.1). The solution for the former case (Fig. 11.1a) for an aquifer infinite in the horizontal plane (see Sect. 1.1.1) can be written as:

$$s = \frac{Q_1}{4\pi T} W\left(\frac{r^2}{4a(t_0 + t_r)}\right) + \frac{Q_2 - Q_1}{4\pi T} W\left(\frac{r^2}{4at_r}\right), \quad (11.1)$$

and that for the latter case (Fig. 11.1b), as:

$$s_r = s_0 - s, \quad (11.2)$$

$$s_0 = \frac{Q_1}{4\pi T} W\left(\frac{r^2}{4at_0}\right), \quad (11.3)$$

where s is the drawdown in the observation well after the cessation of pumping at moment t_r (i.e., the water-level recovery measured from the initial static level in the well), m ; s_0 is the drawdown in the observation well at the moment of pumping

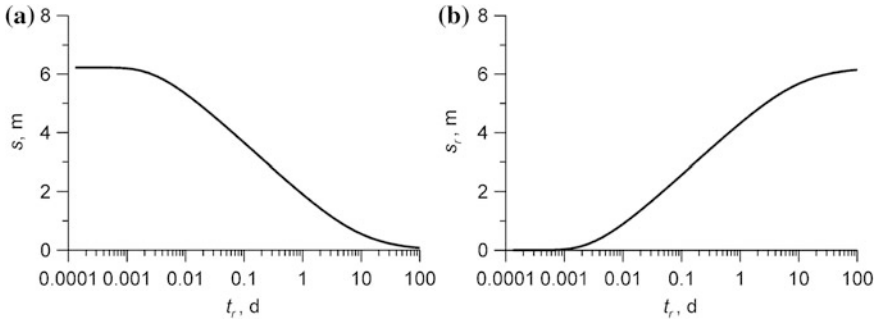


Fig. 11.1 An example of time–drawdown plots, where water-level recovery is measured from **a** the static level at the moment when pumping was started and **b** the dynamic level at the moment of pumping cessation. t_r is the time elapsed from the start of recovery

cessation, m ; s_r is the recovery in the observation well after the cessation of pumping at moment t_r , m ; t_0 is pumping duration, d ; t_r is the time from the start of recovery, d ; $Q_1 = Q$ is the discharge rate during pumping, m^3/d ; $Q_2 = 0$ is zero discharge since the moment of pumping cessation, m^3/d ; T is the transmissivity, m^2/d ; a is the hydraulic diffusivity, m^2/d ; $W(\cdot)$ is well-function (see Appendix 7.1).

Equations 11.1 and 11.2 correspond to Eqs. 11.9 and 11.12. These equations have respective logarithmic approximations:

$$s = \frac{Q}{4\pi T} \ln \frac{2.25a(t_0 + t_r)}{r^2} - \frac{Q}{4\pi T} \frac{2.25at_r}{r^2}, \quad (11.4)$$

$$s_r = \frac{Q}{4\pi T} \ln \frac{2.25at_0}{r^2} - \frac{Q}{4\pi T} \ln \frac{2.25a(t_0 + t_r)}{r^2} + \frac{Q}{4\pi T} \frac{2.25at_r}{r^2}. \quad (11.5)$$

Minor transformations of Eqs. 11.4 and 11.5 lead to basic relationships (Eqs. 11.10 and 11.13) for the level-recovery period, which can be used for graphic-analytical processing of recovery test data.

Any solution, describing water level changes in a well (see Chaps. 1–7), can be written by analogy with Eqs. 11.1 and 11.2, with the well function replaced by a function required for the solution, so:

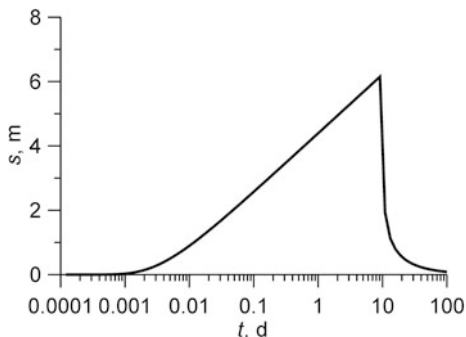
$$s \sim f(t_0 + t_r) - f(t_r), \quad (11.6)$$

$$s_r \sim f(t_0) - f(t_0 + t_r) + f(t_r), \quad (11.7)$$

where f is an arbitrary function of time entering into the flow equation.

Water-level recovery in a well can be treated in the same manner as a constant-discharge pumping test with the use of all appropriate relationships. However, it should be taken into account that such processing (when the pumping period is ignored) may cause errors in transmissivity estimates. Thus, at the duration

Fig. 11.2 An example of a time–drawdown plot ($s-\lg t$), constructed for simultaneous processing of the drawdown and recovery data



of total recovery (t_r) less than 10 % of pumping duration (t_0), i.e., at $t_r \leq 0.1t_0$, the effect of pumping can be ignored in recovery processing, while at the ratio $t_r/t_0 = 2.5$, the error will be a 45 % overestimation (Borevskiy et al. 1973). In the case of areal analysis, on the distance–drawdown plot (see Sect. 12.1.1), the error caused by the neglect of the pumping period will be less.

In addition, a treatment procedure is possible that involves simultaneous processing of the pumping-test and the recovery-test data (Fig. 11.2).

This approach is analogous to processing the data of a variable-discharge pumping test (see Sect. 10.2.1) with the discharge rate for the last stage taken as zero. The solution in this case is written separately for two periods (an example using the Theis solution):

$$s = \begin{cases} \frac{Q}{4\pi T} W\left(\frac{r^2}{4at}\right), & t \leq t_0 \\ \frac{Q}{4\pi T} \left[W\left(\frac{r^2}{4at}\right) - W\left(\frac{r^2}{4a(t-t_0)}\right) \right], & t > t_0. \end{cases} \tag{11.8}$$

The system of equations (Eq. 11.8) can also be written for several pumping wells with the use of Eq. 10.2 and, in the case of variable discharge, Eqs. 10.33 and 10.37. The functional relationships for the water-level recovery after a multi-well pumping at constant discharge rate are given in Sect. 11.2.

Treated below are the analytical relationships underlying graphic-analytical methods for evaluating hydraulic parameters based on data on water-level recovery.

11.1 A Single Pumping Well with a Constant Discharge Rate

11.1.1 Confined Aquifer

This section gives transient, quasi-steady-state, and steady-state relationships describing water-level recovery in an infinite, semi-infinite, and bounded-in-the-

horizontal plane aquifer (see Sect. 1.1). Transient flow equations were constructed with the use of the superposition principle and Theis solution (Eq. 1.3). For strip aquifers, solutions based on Green's function are also given.

Characteristic plots of water-level recovery in an infinite aquifer and their sensitivity to variations of hydraulic parameters are given in Figs. 12.32 and 12.33.

11.1.1.1 Aquifer of Infinite Lateral Extent

Basic Analytical Relationships (recovery is measured from the start of pumping)

Transient Flow Equation (Theis 1935)

$$s = \frac{Q}{4\pi T} \left[W\left(\frac{r^2}{4a(t_0 + t_r)}\right) - W\left(\frac{r^2}{4at_r}\right) \right]. \quad (11.9)$$

Quasi-Steady-State Flow Equation

$$s = \frac{Q}{4\pi T} \ln \frac{t_0 + t_r}{t_r} = \frac{0.183Q}{T} \lg \frac{t_0 + t_r}{t_r}. \quad (11.10)$$

The difference between the storage parameters of an aquifer during pumping and the recovery test is accounted for in the following equation for recovery in the quasi-steady-state flow period (Jacob 1963):

$$s = \frac{Q}{4\pi T} \left(\ln \frac{t_0 + t_r}{t_r} - \ln \frac{S}{S_R} \right), \quad (11.11)$$

where S_R is the storage coefficient at water-level recovery (it may differ from the storage coefficient S at pumping).

Graphic-Analytical Processing

The relationships given in Table 11.1 have been derived from Eqs. 11.10 and 11.11.

The straight line must pass through the origin of coordinates (Fig. 11.3), if the aquifer storage coefficient is the same for the pumping and recovery phases ($S/S_R = 1$) (see the calculation of this ratio in Table 11.1). The straight line may also deviate from the origin because of errors in the measurements of the static level (Shestakov 1973).

Basic Analytical Relationships (recovery is measured from the end of pumping)

Transient Flow Equation

$$s_r = \frac{Q}{4\pi T} \left[W\left(\frac{r^2}{4at_0}\right) - W\left(\frac{r^2}{4a(t_0 + t_r)}\right) + W\left(\frac{r^2}{4at_r}\right) \right]. \quad (11.12)$$

Table 11.1 Graphic-analytical parameter evaluation

Plot	Method	Relationship
$s - \lg \frac{t_0 + t_r}{t_r}$	Straight line ^a	$T = \frac{0.183Q}{C}, \frac{S_R}{S} = 10^{A/C}, \lg a = \lg \frac{r^2}{2.25t_0} + \frac{s_0}{C}$
$(s_1 - s_2) - \lg t_r$	Horizontal straight line	$T = \frac{Q}{2\pi \cdot A} \ln \frac{r_2}{r_1}$
$(s_0 - s) - \lg \frac{t_0 t_r}{t_0 + t_r}$	Straight line ^b	$T = \frac{0.183Q}{C}, \lg a = \frac{A}{C} + \lg \frac{r^2}{2.25}$

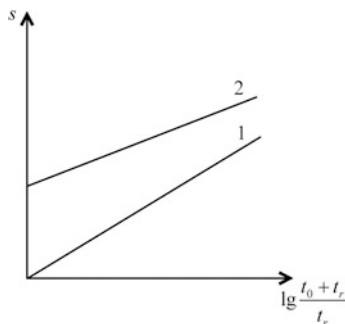
A is the intercept on the ordinate (see Sects. 12.1.1 and 12.1.2); C is the slope of the straight line (see Sect. 12.1.1); s_1, s_2, r_1, r_2 are recovery values (s), measured from the start of pumping, and the distances from the pumping well (r) to the first and second observation wells; s_0 is the drawdown at the end of pumping

^aThe straight line passes through the origin

^b $s_0 - s = s_r$, the treatment procedure is the same as for the plot $s_r - \lg t'$ in Table 11.2

^cThis relationship was taken from Borevskiy et al. (1973)

Fig. 11.3 Schematic plot of water-level recovery with the static level specified (I) correctly and (2) incorrectly



Quasi-Steady-State Flow Equation

$$s_r = \frac{Q}{4\pi T} \ln \frac{2.25at'}{r^2} = \frac{0.183Q}{T} \lg \frac{2.25at'}{r^2}, \tag{11.13}$$

$$t' = \frac{t_0 t_r}{t_0 + t_r}. \tag{11.14}$$

Graphic-Analytical Processing

The relationships in Table 11.2 have been derived from Eq. 11.13.

Table 11.2 Graphic-analytical parameter evaluation

Plot	Method	Relationship
$s_r - \lg r$	Straight line	$T = \frac{0.366Q}{C}, \lg a = 2 \frac{A}{C} - \lg(2.25 \cdot t')$
$s_r - \lg t'$	The same	$T = \frac{0.183Q}{C}, \lg a = \frac{A}{C} + \lg \frac{r^2}{2.25}$
$s_r - \lg \frac{t'}{r^2}$	The same	$T = \frac{0.183Q}{C}, \lg a = \frac{A}{C} - \lg(2.25)$
$(s_{r,1} - s_{r,2}) - \lg t_r$	Horizontal straight line	$T = \frac{Q}{2\pi \cdot A} \ln \frac{r_2}{r_1}$

$s_{r,1}, s_{r,2}$ are water-level recovery values measured from the end of pumping for the first and second observation wells

11.1.1.2 Semi-infinite Aquifer: Constant-Head Boundary

Basic Analytical Relationships (recovery is measured from the start of pumping)

Transient Flow Equation

$$s = \frac{Q}{4\pi T} \left[W\left(\frac{r^2}{4a(t_0 + t_r)}\right) - W\left(\frac{\rho^2}{4a(t_0 + t_r)}\right) - W\left(\frac{r^2}{4at_r}\right) + W\left(\frac{\rho^2}{4at_r}\right) \right], \tag{11.15}$$

where ρ is the distance between the observation and image wells (see Fig. A3.2 and Eq. A3.1), m.

Graphic-Analytical Processing

The relationships in Table 11.3 have been derived from Eq. 11.17. The parameters in this table are determined by the initial measurements of recovery.

Table 11.3 Graphic-analytical parameter evaluation

Plot	Method	Relationship
$s - \lg t_r$	Horizontal straight line	$T = \frac{Q}{2\pi \cdot A} \ln \frac{\rho}{r}$
$s - \lg \frac{\rho}{r}$	Straight line	$T = \frac{0.366Q}{C}$
$(s_1 - s_2) - \lg t_r$	Horizontal straight line	$T = \frac{Q}{2\pi \cdot A} \ln \frac{\rho_1 r_2}{\rho_2 r_1}$

ρ_1, ρ_2 are the distances from the first and second observation wells to the image well, respectively

Table 11.4 Graphic-analytical parameter evaluation

Plot	Method	Relationship
$s_r - \lg t_r$	Horizontal straight line ^a	$T = \frac{Q}{2\pi \cdot A} \ln \frac{\rho}{r}$
$s_{mr} - \lg \frac{\rho}{r}$	Straight line	$T = \frac{0.366Q}{C}$
$(s_{r,1} - s_{r,2}) - \lg t_r$	Horizontal straight line ^a	$T = \frac{Q}{2\pi \cdot A} \ln \frac{\rho_1 r_2}{\rho_2 r_1}$

^aParameters are determined based on the final measurements of level recovery

Basic Analytical Relationships (recovery is measured from the end of pumping)

Transient Flow Equation

$$s_r = \frac{Q}{4\pi T} \left[\begin{aligned} &W\left(\frac{r^2}{4at_0}\right) - W\left(\frac{\rho^2}{4at_0}\right) - W\left(\frac{r^2}{4a(t_0 + t_r)}\right) + \\ &+ W\left(\frac{\rho^2}{4a(t_0 + t_r)}\right) + W\left(\frac{r^2}{4at_r}\right) - W\left(\frac{\rho^2}{4at_r}\right) \end{aligned} \right]. \quad (11.16)$$

Steady-State Flow Equation

$$s_{mr} = \frac{Q}{2\pi T} \ln \frac{\rho}{r} = \frac{0.366Q}{T} \lg \frac{\rho}{r}. \quad (11.17)$$

Graphic-Analytical Processing

The relationships given in Table 11.4 have been derived from Eq. 11.17.

11.1.1.3 Aquifer Semi-infinite in the Horizontal Plane: Impermeable Boundary

Basic Analytical Relationships (recovery is measured from the start of pumping)

Transient Flow Equation

$$s = \frac{Q}{4\pi T} \left[W\left(\frac{r^2}{4a(t_0 + t_r)}\right) + W\left(\frac{\rho^2}{4a(t_0 + t_r)}\right) - W\left(\frac{r^2}{4at_r}\right) - W\left(\frac{\rho^2}{4at_r}\right) \right]. \quad (11.18)$$

Quasi-Steady-State Flow Equation

$$s = \frac{Q}{2\pi T} \ln \frac{t_0 + t_r}{t_r} = \frac{0.366Q}{T} \lg \frac{t_0 + t_r}{t_r}. \quad (11.19)$$

Table 11.5 Graphic-analytical parameter evaluation

Plot	Method	Relationship
$s - \lg \frac{t_0 + t_r}{t_r}$	Straight line ^a	$T = \frac{0.366Q}{C}$
$(s_1 - s_2) - \lg t_r$	Horizontal straight line ^b	$T = \frac{Q}{2\pi \cdot A} \ln \frac{\rho_2 r_2}{\rho_1 r_1}$

^aThe parameters are evaluated for a linear segment passing from the origin of coordinates (the last recovery values); the linear segment, corresponding to the initial recovery values, would yield double transmissivity

^bTransmissivity is evaluated for a linear segment corresponding to the initial values of the water-level recovery

Graphic-Analytical Processing

The relationships given in Table 11.5 have been derived from Eqs. 11.19 and 11.21.

Basic Analytical Relationships (recovery is measured from the end of pumping)

Transient Flow Equation

$$s_r = \frac{Q}{4\pi T} \left[\begin{aligned} &W\left(\frac{r^2}{4at_0}\right) + W\left(\frac{\rho^2}{4at_0}\right) - W\left(\frac{r^2}{4a(t_0 + t_r)}\right) - \\ &- W\left(\frac{\rho^2}{4a(t_0 + t_r)}\right) + W\left(\frac{r^2}{4at_r}\right) + W\left(\frac{\rho^2}{4at_r}\right) \end{aligned} \right]. \tag{11.20}$$

Quasi-Steady-State Flow Equation

$$s_r = \frac{Q}{2\pi T} \ln \frac{2.25at'}{r\rho} = \frac{0.366Q}{T} \lg \frac{2.25at'}{r\rho}, \tag{11.21}$$

where t' is determined from (Eq. 11.14).

Graphic-Analytical Processing

The relationships given in Table 11.6 have been derived from Eq. 11.21.

Table 11.6 Graphic-analytical parameter evaluation

Plot	Method	Relationship
$s_r - \lg t'$	Straight line	$T = \frac{0.366Q}{C}, \lg a = \frac{A}{C} + \lg \frac{r\rho}{2.25}$
$s_r - \lg r\rho$	The same	$T = \frac{0.366Q}{C}, \lg a = \frac{A}{C} - \lg(2.25 \cdot t')$
$s_r - \lg \frac{t'}{r\rho}$	The same	$T = \frac{0.366Q}{C}, \lg a = \frac{A}{C} - \lg(2.25)$
$(s_{r,1} - s_{r,2}) - \lg t_r$	Horizontal straight line	$T = \frac{Q}{2\pi \cdot A} \ln \frac{\rho_2 r_2}{\rho_1 r_1}$

11.1.1.4 Strip Aquifer: Constant-Head Boundary

Basic Analytical Relationships (recovery is measured from the start of pumping)

Transient Flow Equation

$$s = \frac{Q}{4\pi T} \left\{ \begin{aligned} &W\left(\frac{r^2}{4a(t_0 + t_r)}\right) + \sum_{j=1}^n (-1)^j \sum_{i=1}^2 W\left[\frac{(\rho_i^j)^2}{4a(t_0 + t_r)}\right] - \\ &- W\left(\frac{r^2}{4at_r}\right) - \sum_{j=1}^n (-1)^j \sum_{i=1}^2 W\left[\frac{(\rho_i^j)^2}{4at_r}\right] \end{aligned} \right\}, \quad (11.22)$$

where ρ_i^j is the distance from the observation well to the j th image well reflected from the left ($i = 1$) or right ($i = 2$) planar boundaries (see Fig. A3.4); it is determined by Eqs. A3.3 and A3.4, $m; n \rightarrow \infty$ is the number of reflections from a boundary.

Quasi-Steady-State Flow Equation

$$s = \frac{Q}{4\pi T} \ln \frac{t_0 + t_r}{t_r} = \frac{0.183Q}{T} \lg \frac{t_0 + t_r}{t_r}. \quad (11.23)$$

Graphic-Analytical Processing

The relationships given in Table 11.7 have been derived from Eqs. 11.23, 11.25, and 11.26.

Table 11.7 Graphic-analytical parameter evaluation

Plot	Method	Relationship
$s - \lg \frac{t_0 + t_r}{t_r}$	Straight line	$T = \frac{0.183Q}{C}$
$s - \lg t_r$	Horizontal straight line ^a	$T = \frac{Q}{2\pi \cdot A} r'^b, T = \frac{Q}{4\pi \cdot A} r'^c$
$(s_1 - s_2) - \lg t_r$	The same	$T = \frac{Q}{2\pi \cdot A} \ln \frac{r'_1{}^b}{r'_2{}^b}, T = \frac{Q}{4\pi \cdot A} \ln \frac{r'_1{}^c}{r'_2{}^c}$

^aThe parameters are evaluated for a linear segment corresponding to the initial values of water-level recovery

^bFrom solution (Eq. 1.20), r' is evaluated from Eq. 1.21

^cFrom solution (Eq. 1.21), r' is evaluated from Eq. 1.23

r'_1, r'_2 are reduced distances for the first and second observation wells

Basic Analytical Relationships (recovery is measured from the end of pumping)

Transient Flow Equation

$$s_r = \frac{Q}{4\pi T} \left\{ W\left(\frac{r^2}{4at_0}\right) + \sum_{j=1}^n (-1)^j \sum_{i=1}^2 W\left[\frac{(\rho_i^j)^2}{4at_0}\right] - W\left(\frac{r^2}{4a(t_0 + t_r)}\right) - \sum_{j=1}^n (-1)^j \sum_{i=1}^2 W\left[\frac{(\rho_i^j)^2}{4a(t_0 + t_r)}\right] + W\left(\frac{r^2}{4at_r}\right) + \sum_{j=1}^n (-1)^j \sum_{i=1}^2 W\left[\frac{(\rho_i^j)^2}{4at_r}\right] \right\}. \tag{11.24}$$

Steady-State Flow Equations

1. Based on the superposition principle:

$$s_{mr} = \frac{Q}{2\pi T} \ln r' = \frac{0.366Q}{T} \lg r', \tag{11.25}$$

where r' is reduced distance, evaluated from Eq. 1.21.

2. Based on Green's function:

$$s_{mr} = \frac{Q}{4\pi T} \ln r' = \frac{0.183Q}{T} \lg r', \tag{11.26}$$

where r' is determined by Eq. 1.23.

Graphic-Analytical Processing

The relationships given in Table 11.8 have been derived from Eqs. 11.25 and 11.26.

Table 11.8 Graphic-analytical parameter evaluation

Plot	Method	Relationship
$s_r - \lg t_r$	Horizontal straight line ^a	$T = \frac{Q}{2\pi \cdot A} \ln r'^b, T = \frac{Q}{4\pi \cdot A} \ln r'^c$
$s_{mr} - \lg r'$	Straight line	$T = \frac{0.366Q_b}{C}, T = \frac{0.183Q_c}{C}$
$(s_{r,1} - s_{r,2}) - \lg t_r$	Horizontal straight line ^a	$T = \frac{Q}{2\pi \cdot A} \ln \frac{r'_{1b}}{r'_{2}}, T = \frac{Q}{4\pi \cdot A} \ln \frac{r'_{1c}}{r'_{2}}$

^aThe parameters are evaluated for a linear segment corresponding to the final values of water-level recovery

^{b, c}See note to Table 11.7

11.1.1.5 Strip Aquifer: Impermeable Boundaries

Basic Analytical Relationships (recovery is measured from the start of pumping)

Transient Flow Equation

$$s = \frac{Q}{4\pi T} \left\{ W\left(\frac{r^2}{4a(t_0 + t_r)}\right) + \sum_{j=1}^n \sum_{i=1}^2 W\left[\frac{(\rho_i^j)^2}{4a(t_0 + t_r)}\right] - W\left(\frac{r^2}{4at_r}\right) - \sum_{j=1}^n \sum_{i=1}^2 W\left[\frac{(\rho_i^j)^2}{4at_r}\right] \right\}. \tag{11.27}$$

Graphic-Analytical Processing

The relationship in Table 11.9 has been derived with the use of a logarithmic transformation of Eq. 11.27 for the difference of the drawdowns in two observation wells. Here, the reduced distance is defined as:

$$r' = \left(r \prod_{j=1}^n \rho_1^j \rho_2^j \right)^{1/(2n+1)}. \tag{11.28}$$

Basic analytical relationships (recovery is measured from the end of pumping)

Transient Flow Equation

$$s_r = \frac{Q}{4\pi T} \left\{ W\left(\frac{r^2}{4at_0}\right) + \sum_{j=1}^n \sum_{i=1}^2 W\left[\frac{(\rho_i^j)^2}{4at_0}\right] - W\left(\frac{r^2}{4a(t_0 + t_r)}\right) - \sum_{j=1}^n \sum_{i=1}^2 W\left[\frac{(\rho_i^j)^2}{4a(t_0 + t_r)}\right] + W\left(\frac{r^2}{4at_r}\right) + \sum_{j=1}^n \sum_{i=1}^2 W\left[\frac{(\rho_i^j)^2}{4at_r}\right] \right\}. \tag{11.29}$$

Graphic-Analytical Processing

Water-level recovery measurements represented in this form are not processed by the graphic-analytical method in this work.

Table 11.9 Graphic-analytical parameter evaluation

Plot	Method	Relationship
$(s_1 - s_2) - \lg t_r$	Horizontal straight line	$T = \frac{(2n+1)Q}{2\pi \cdot A} \ln \frac{r'_2}{r'_1}$

The parameters are evaluated for a linear segment corresponding to the initial conditions of water-level recovery

11.1.1.6 Strip Aquifer: Constant-Head and Impermeable Boundaries

Basic analytical relationships (recovery is measured from the start of pumping)

Transient Flow Equation

$$\begin{aligned}
 s = \frac{Q}{4\pi T} \left\{ W\left(\frac{r^2}{4a(t_0 + t_r)}\right) + \sum_{j=1,3,\dots}^n \sum_{i=1}^2 (-1)^{(j+2i-1)/2} W\left(\frac{(\rho_i^j)^2}{4a(t_0 + t_r)}\right) + \right. \\
 + \sum_{j=2,4,\dots}^n (-1)^{j/2} \sum_{i=1}^2 W\left(\frac{(\rho_i^j)^2}{4a(t_0 + t_r)}\right) - W\left(\frac{r^2}{4at_r}\right) - \\
 \left. - \sum_{j=1,3,\dots}^n \sum_{i=1}^2 (-1)^{(j+2i-1)/2} W\left(\frac{(\rho_i^j)^2}{4at_r}\right) - \sum_{j=2,4,\dots}^n (-1)^{j/2} \sum_{i=1}^2 W\left(\frac{(\rho_i^j)^2}{4at_r}\right) \right\}. \tag{11.30}
 \end{aligned}$$

Quasi-Steady-State Flow Equation

$$s = \frac{Q}{4\pi T} \ln \frac{t_0 + t_r}{t_r} = \frac{0.183Q}{T} \lg \frac{t_0 + t_r}{t_r}. \tag{11.31}$$

Graphic-Analytical Processing

The relationships in Table 11.10 have been derived from Eqs. 11.31, 11.33, and 11.34

Table 11.10 Graphic-analytical parameter evaluation

Plot	Method	Relationship
$s - \lg \frac{t_0 + t_r}{t_r}$	Straight line	$T = \frac{0.183Q}{C}$
$s - \lg t_r$	Horizontal straight line ^a	$T = \frac{Q}{2\pi \cdot A} r'^b, T = \frac{Q}{4\pi \cdot A} r'^c$
$(s_1 - s_2) - \lg t_r$	The same	$T = \frac{Q}{2\pi \cdot A} \ln \frac{r'_{1b}}{r'_{2b}}, T = \frac{Q}{4\pi \cdot A} \ln \frac{r'_{1c}}{r'_{2c}}$

^aThe parameters are evaluated for a linear segment corresponding to the initial values of water-level recovery

^bFrom solution (Eq. 1.29), r' is determined from Eq. 1.30

^cFrom solution (Eq. 1.31), r' is determined from Eq. 1.32

Basic Analytical Relationships (recovery is measured from the end of pumping)*Transient Flow Equation*

$$\begin{aligned}
s_r = \frac{Q}{4\pi T} \left\{ & \mathbf{W}\left(\frac{r^2}{4at_0}\right) + \sum_{j=1,3,\dots}^n \sum_{i=1}^2 (-1)^{(j+2i-1)/2} \mathbf{W}\left(\frac{(\rho_i^j)^2}{4at_0}\right) + \right. \\
& + \sum_{j=2,4,\dots}^n (-1)^{j/2} \sum_{i=1}^2 \mathbf{W}\left(\frac{(\rho_i^j)^2}{4at_0}\right) - \mathbf{W}\left(\frac{r^2}{4a(t_0+t_r)}\right) - \\
& - \sum_{j=1,3,\dots}^n \sum_{i=1}^2 (-1)^{(j+2i-1)/2} \mathbf{W}\left(\frac{(\rho_i^j)^2}{4a(t_0+t_r)}\right) - \\
& - \sum_{j=2,4,\dots}^n (-1)^{j/2} \sum_{i=1}^2 \mathbf{W}\left(\frac{(\rho_i^j)^2}{4a(t_0+t_r)}\right) + \mathbf{W}\left(\frac{r^2}{4at_r}\right) + \\
& \left. + \sum_{j=1,3,\dots}^n \sum_{i=1}^2 (-1)^{(j+2i-1)/2} \mathbf{W}\left(\frac{(\rho_i^j)^2}{4at_r}\right) + \sum_{j=2,4,\dots}^n (-1)^{j/2} \sum_{i=1}^2 \mathbf{W}\left(\frac{(\rho_i^j)^2}{4at_r}\right) \right\}.
\end{aligned} \tag{11.32}$$

Steady-State Flow Equations

1. Based on the superposition principle:

$$s_{mr} = \frac{Q}{2\pi T} \ln r' = \frac{0.366Q}{T} \lg r', \tag{11.33}$$

where the reduced distance r' is determined by Eq. 1.30.

2. Based on Green's function:

$$s_{mr} = \frac{Q}{4\pi T} \ln r' = \frac{0.183Q}{T} \lg r', \tag{11.34}$$

where the reduced distance r' is determined by Eq. 1.32.

Graphic-Analytical Processing

The relationships given in Table 11.11 have been derived from Eqs. 11.33 and 11.34.

Table 11.11 Graphic-analytical parameter evaluation

Plot	Method	Relationship
$s - \lg t_r$	Horizontal straight line ^a	$T = \frac{Q}{2\pi \cdot A} r'^b, T = \frac{Q}{4\pi \cdot A} r'^c$
$s_{mr} - \lg r'$	Straight line	$T = \frac{0.366Q}{C}$
$(s_{r,1} - s_{r,2}) - \lg t_r$	Horizontal straight line ^a	$T = \frac{Q}{2\pi \cdot A} \ln \frac{r'_{1b}}{r'_2}, T = \frac{Q}{4\pi \cdot A} \ln \frac{r'_{1c}}{r'_2}$

^aThe parameters are evaluated for a linear segment corresponding to the initial values of water-level recovery

^{b, c}See note to Table 11.10

11.1.2 Unconfined Aquifer

The solutions describing water-level recovery are given for a fully penetrating well located in an unconfined isotropic aquifer of infinite lateral extent (see Sect. 2.1), and have been constructed based on the relationship (Eq. 2.22) for drawdown under gravity-drainage conditions.

Basic Analytical Relationships (recovery is measured from the start of pumping)

Transient Flow Equation:

$$s(2m - s) = \frac{Q}{2\pi k} \left[W\left(\frac{r^2}{4a(t_0 + t_r)}\right) - W\left(\frac{r^2}{4at_r}\right) \right], \tag{11.35}$$

where $a = km/S_y$ is the hydraulic diffusivity of the unconfined aquifer, m^2/d ; S_y is the specific yield, dimensionless; k is the hydraulic conductivity, m/d ; m is the initial saturated thickness of an unconfined aquifer, m .

Quasi-Steady-State Flow Equation

$$s(2m - s) = \frac{Q}{2\pi k} \ln \frac{t_0 + t_r}{t_r} = \frac{0.366Q}{k} \lg \frac{t_0 + t_r}{t_r}. \tag{11.36}$$

Graphic-Analytical Processing

The relationship in Table 11.12 has been derived from Eq. 11.36.

Table 11.12 Graphic-analytical parameter evaluation

Plot	Method	Relationship
$s(2m - s) - \lg \frac{t_0 + t_r}{t_r}$	Straight line	$k = \frac{0.366Q}{C}$

Table 11.13 Graphic-analytical parameter evaluation

Plot	Method	Relationship
$s_r(2m - s_r) - \lg t'$	Straight line	$k = \frac{0.366Q}{C}, \lg a = \frac{A}{C} + \lg \frac{r^2}{2.25}$
$s_r(2m - s_r) - \lg \frac{t'}{r^2}$	The same	$k = \frac{0.366Q}{C}, \lg a = \frac{A}{C} - \lg 2.25$
$s_r(2m - s_r) - \lg r$	The same	$k = \frac{0.732Q}{C}, \lg a = 2 \frac{A}{C} - \lg(2.25 \cdot t')$

Basic Analytical Relationships (recovery is measured from the end of pumping)

Transient Flow Equation

$$s_r(2m - s_r) = \frac{Q}{2\pi k} \left[W\left(\frac{r^2}{4at_0}\right) - W\left(\frac{r^2}{4a(t_0 + t_r)}\right) + W\left(\frac{r^2}{4at_r}\right) \right]. \quad (11.37)$$

Quasi-Steady-State Flow Equation

$$s_r(2m - s_r) = \frac{Q}{2\pi k} \ln \frac{2.25at'}{r^2} = \frac{0.366Q}{T} \lg \frac{2.25at'}{r^2}, \quad (11.38)$$

where t' is determined by Eq. 11.14.

Graphic-Analytical Processing

The relationships in Table 11.13 have been derived from Eq. 11.38.

11.2 A System of Pumping Wells with Constant Discharge Rates

Solutions for water-level recovery after multi-well pumping test are considered. It is assumed that all wells are shutdown simultaneously. The solutions are given for a confined aquifer of infinite lateral extent (see Sect. 1.1.1).

In addition, the section gives quasi-steady flow equations for water-level recovery after asynchronous starts of operation of test wells during pumping. Transient relationships for this case can be derived from Eq. 10.6. The construction of calculated curves describing level recovery after a multi-well asynchronous perturbation is convenient to do on a plot $s - \lg(t - t_0)$, similar to the recovery after pumping with variable discharge rates (for details, see Sect. 11.3).

Basic Analytical Relationships (recovery is measured from the start of pumping)

Transient Flow Equations

At the synchronous start of operation of pumping wells:

$$s = \frac{1}{4\pi T} \sum_{i=1}^N Q_i \left[W\left(\frac{r_i^2}{4a(t_0 + t_r)}\right) - W\left(\frac{r_i^2}{4at_r}\right) \right] \quad (11.39)$$

or, after asynchronous start of the operation of pumping wells:

$$s = \frac{1}{4\pi T} \sum_{i=1}^N Q_i \left[W\left(\frac{r_i^2}{4a(t_0 - t_i + t_r)}\right) - W\left(\frac{r_i^2}{4at_r}\right) \right], \quad (11.40)$$

where N is the number of pumping wells; Q_i is the discharge rate of the i th pumping well, m^3/d ; r_i is the distance from the observation well to the i th pumping well, m ; t_i is the start time of operation of the i th pumping well, measured from the start of pumping, d .

Quasi-Steady-State Flow Equation

After simultaneous starting of the operation of pumping wells and their simultaneous shutdown:

$$s = \frac{Q_t}{4\pi T} \ln \frac{t_0 + t_r}{t_r}, \quad (11.41)$$

$$Q_t = \sum_{i=1}^N Q_i. \quad (11.42)$$

For asynchronous starting of the operation of pumping wells and their simultaneous shutdown:

$$s = \frac{1}{4\pi T} \ln t'_A, \quad (11.43)$$

$$\ln t'_A = \sum_{i=1}^N Q_i \ln \frac{t_0 - t_i + t_r}{t_r}. \quad (11.44)$$

Graphic-Analytical Processing

The relationships given in Table 11.14 have been derived from Eqs. 11.41 and 11.43.

Table 11.14 Graphic-analytical parameter evaluation

Plot	Method	Relationship
$s - \lg \frac{t_0 + t_r}{t_r}$	Straight line	$T = \frac{0.183Q_t}{C}$
$(s_1 - s_2) - \lg t_r$	Horizontal straight line ^a	$T = \frac{Q_t}{2\pi \cdot A} \ln \frac{r'_2}{r'_1}$
$s - \lg t'_A$	Straight line ^b	$T = \frac{0.183}{C}$

^aThe parameters are determined for a linear segment corresponding to the initial values of water-level recovery

^bBy the data of level recovery after an asynchronous perturbation

The reduced distances (r'_1, r'_2) are determined by Eq. 11.48

Basic Analytical Relationships (recovery is measured from the end of pumping)

Transient Flow Equations

At the synchronous start of operation of pumping wells:

$$s_r = \frac{1}{4\pi T} \sum_{i=1}^N Q_i \left[W\left(\frac{r_i^2}{4at_0}\right) - W\left(\frac{r_i^2}{4a(t_0 + t_r)}\right) + W\left(\frac{r_i^2}{4at_r}\right) \right] \quad (11.45)$$

or, after an asynchronous start of operation of pumping wells:

$$s_r = \frac{1}{4\pi T} \sum_{i=1}^N Q_i \left[W\left(\frac{r_i^2}{4a(t_0 - t_i)}\right) - W\left(\frac{r_i^2}{4a(t_0 - t_i + t_r)}\right) + W\left(\frac{r_i^2}{4at_r}\right) \right]. \quad (11.46)$$

Quasi-Steady-State Flow Equations

After simultaneous start of the operation of pumping wells and their simultaneous shutdown:

$$s_r = \frac{Q_t}{4\pi T} \ln \frac{2.25at'}{r'^2}, \quad (11.47)$$

$$\ln r' = \frac{1}{Q_t} \sum_{i=1}^N Q_i \ln r_i, \quad (11.48)$$

where Q_t is the sum of the discharge rates of all pumping wells (Eq. 11.42); t' is determined by Eq. 11.14.

For asynchronous start of the operation of pumping wells and their simultaneous shutdown

$$s_r = \frac{Q_t}{4\pi T} \ln \frac{2.25at'_A}{r'^2}, \tag{11.49}$$

$$\ln t'_A = \frac{1}{Q_t} \sum_{i=1}^N Q_i \ln \frac{(t_0 - t_i)t_r}{t_0 - t_i + t_r}, \tag{11.50}$$

where r' is determined from Eq. 11.48.

Graphic-Analytical Processing

The relationships given in Table 11.15, have been derived from Eqs. 11.47 and 11.49.

Table 11.15 Graphic-analytical parameter evaluation

Plot	Method	Relationship
$s_r - \lg t'$	Straight line	$T = \frac{0.183Q_t}{C}, \lg a = \frac{A}{C} + \lg \frac{r'^2}{2.25}$
$s_r - \lg r'$	The same	$T = \frac{0.366Q_t}{C}, \lg a = 2\frac{A}{C} - \lg(2.25 \cdot t')$
$s_r - \lg \frac{t'}{r'^2}$	The same	$T = \frac{0.183Q_t}{C}, \lg a = \frac{A}{C} - \lg(2.25)$
$(s_{r,1} - s_{r,2}) - \lg t_r$	Horizontal straight line ^a	$T = \frac{Q_t}{2\pi \cdot A} \ln \frac{r'_2}{r'_1}$
$s_r - \lg t'_A$	Straight line ^b	$T = \frac{0.183Q_t}{C}, \lg a = \frac{A}{C} + \lg \frac{r'^2}{2.25}$
$s_r - \lg r'$	The same	$T = \frac{0.366Q_t}{C}, \lg a = 2\frac{A}{C} - \lg(2.25 \cdot t'_A)$
$s_r - \lg \frac{t'_A}{r'^2}$	The same	$T = \frac{0.183Q_t}{C}, \lg a = \frac{A}{C} - \lg(2.25)$

^aThe parameters are determined for a linear segment corresponding to the final values of water-level recovery; on the plot of the difference between drawdown values, the formula for determining the transmissivity does not depend on whether the perturbation is synchronous

^bThe parameters are determined from level-recovery data after asynchronous perturbation

11.3 Variable Discharge Rate

A confined aquifer of infinite lateral extent (see Sect. 1.1.1) is used in this section to demonstrate the potentialities of and the problems in the processing of level-recovery data in an observation well after pumping from one or several wells with varying discharge rates.

Basic Analytical Relationships (recovery is measured from the start of pumping)

Transient Flow Equations

Analytical transient relationships for processing the data of pumping tests with variable discharge rates are described by Eqs. 10.33 and 10.37. To evaluate water-level recovery in such an experiment, one more step with a zero discharge is added. The hydraulic parameters are evaluated using a time–drawdown plot for both pumping and recovery phases based on the matching method (see Sect. 12.3).

Recovery data on the time–drawdown plot look uninformative (see Fig. 11.2). Therefore, it is recommended to process this segment of the curve with the use of a plot in coordinates $s - \lg(t - t_0)$, which corresponds to a plot constructed by the measurements of level recovery alone $s - \lg t_r$, where $t_r = t - t_0$ is the time from the start of the test less the duration of pumping (see Fig. 11.1a).

Quasi-Steady-State Flow Equations

Recovery after pumping from a single well is:

$$s = \frac{1}{4\pi T} \sum_{j=1}^{n_1} (Q_1^j - Q_1^{j-1}) \ln(t - t_1^j) - \frac{Q_1^{n_1}}{4\pi T} \ln t_r \tag{11.51}$$

and after a multi-well pumping:

$$s = \frac{1}{4\pi T} \left[\sum_{i=1}^N \sum_{j=1}^{n_i} (Q_i^j - Q_i^{j-1}) \ln(t - t_i^j) \right] - \frac{1}{4\pi T} \sum_{i=1}^N Q_i^{n_i} \ln t_r, \tag{11.52}$$

where n_i is the number of steps of discharge changes in the i th pumping well before the start of level recovery; $Q_i^{n_i}$ is the discharge rate at the last step in the i th pumping well before the end of pumping, m³/day; t_i^j is the time of the start of the j th step in the i th pumping well, d.

Graphic-Analytical Processing

The relationships given in Table 11.16, have been derived from Eqs. 11.51 and 11.52.

Table 11.16 Graphic-analytical parameter evaluation

Plot	Method	Relationship
$s - \lg(t - t_0)$	Straight line	$T = \frac{0.183}{C} \sum_{i=1}^N Q_i^{n_i a}, T = \frac{0.183 Q_1^{n_1}}{C} b$

^aBased on data on level recovery after multi-well pumping

^bBased on data on level recovery after pumping from a single pumping well

References

- Borevskiy BV, Samsonov BG, Yazvin LS (1973) Methods for aquifer parameters estimation from pumping test data. Nedra, Moscow (In Russian)
- Jacob CE (1963) The recovery method for determining the coefficient of transmissibility. In: Bentall R (ed) Methods of determining permeability, transmissibility and drawdown. U.S. Geological Survey Water-Supply, paper 1536-I, pp 283–292
- Shestakov VM (1973) Groundwater dynamics. MSU, Moscow (In Russian)
- Theis CV (1935) The relation between the lowering of the piezometric surface and the rate and duration of discharge of a well using ground-water storage. EOS T Am Geophys Un 16 (2):519–524

Part III

Solution of Hydrogeological Problems Using ANSDIMAT

The third, final part of the book contains algorithms for evaluating hydraulic characteristics by analytical and graphical methods, supplemented by a brief characteristic of ANSDIMAT software, which provides a practical implementation of aquifer-test data processing. Basic groundwater flow equations (see Parts I and II) are used to construct drawdown plots for typical cases. The plots for various types of both aquifers and test scenarios are presented. The effect of hydraulic characteristics and boundary conditions on the behavior of level-variation plots is demonstrated.

The third part describes options provided by the ANSDIMAT computer program. In particular, an alternative approach to well-system simulation is considered, and solutions of some practical engineering-hydrogeological problems are proposed including the assessment of aquifer characteristics by data on groundwater-level monitoring and the evaluation of water inflow into open pits.

Chapter 12

Aquifer-Test Analytical Methods

The methods used to analyze aquifer tests can be conventionally divided into graphical methods and matching methods. Each conceptual model requires special interpretation of the approaches and procedures for choosing treatment methods for optimal and prompt evaluation of the required characteristics. The choice of the method largely depends on the type of flow regime within the analyzed interval of the observation curve, which may be transient, quasi-steady-state, or steady-state. Thus, graphical methods can be applied to quasi-steady-state flow; graphical methods for distance–drawdown analysis can be used for steady-state flow; and data matching and type-curve methods for transient flow.

The duration of the pumping test in complex aquifer systems can determine the choice of the conceptual model. A good and, sometimes the only, method for treating the initial segments of observation curves is the use of solutions for simplified conditions. For example, aquifers bounded in the horizontal plane or thickness can be regarded as analogous models with unbounded flow and multi-aquifer systems can be analyzed as systems with a lower number of layers. When the test time is sufficiently long, additional schematization with the use of averaged or reduced aquifer characteristics can be applied.

Processing methods (Sects. 12.1–12.3) are discussed mostly as applied to a constant-discharge pumping test in a homogeneous, isotropic, confined aquifer (see Sect. 1.1.1).

The last section (Sect. 12.4) gives a set of drawdown plots for different types of aquifers.

12.1 Graphical Methods

Graphical methods are based on transformations of original analytical relationships and the use of drawdown plots. Such methods are most rapid, informative, and convenient for evaluating the hydraulic characteristics.

Most functions used to describe groundwater flow during a definite time period—this commonly refers to quasi-steady-state flow (see Fig. 12.1)—are reduced to simple linear equations. However, their accuracy remains sufficiently high. This approach enables that averaged parameters are obtained, given the drawdown in one or several observation wells for a chosen time interval within the test period. Graphical methods are applied to the conceptual models that have the best-developed solutions.

12.1.1 Straight-Line Method

The straight-line method is based on the approximation of the initial analytical relationship by a linear equation (Theis 1935; Jacob 1946; Cooper and Jacob 1946).

A logarithmic approximation of the Theis solution (Eq. 1.1) with the passage to decimal logarithm yields the following relationship for drawdown after a quasi-steady-state regime has been reached:

$$s = \frac{0.183Q}{T} \lg \frac{2.25Tt}{Sr^2} = \frac{0.183Q}{T} \lg \frac{2.25at}{r^2}, \quad (12.1)$$

where s is the drawdown in an observation well, m; Q is the discharge rate, m³/d; $T = km$ is the transmissivity, m²/d; k , m are the hydraulic conductivity (m/d) and thickness (m) of the aquifer; S is the storage coefficient, dimensionless; $a = T/S$ is the hydraulic diffusivity, m²/d; r is the radial distance from the pumping to the observation well, m; t is the time elapsed from the start of pumping, d.

The linear Eq. 12.1 follows from the property of the well-function for small values of its arguments (see Appendix 7.1):

$$W\left(\frac{r^2}{4at}\right) \approx \ln \frac{2.25at}{r^2} \text{ for } \frac{r^2}{4at} \leq 0.05, \quad (12.2)$$

where $W(\cdot)$ is a well-function.

Representing Eq. 12.1 in different forms (Cooper and Jacob 1946):

$$s = \frac{0.183Q}{T} \left(\lg t + \lg \frac{2.25a}{r^2} \right), \quad (12.3)$$

$$s = \frac{0.366Q}{T} \left(-\lg r + \lg \sqrt{2.25at} \right), \quad (12.4)$$

$$s = \frac{0.183Q}{T} \left(\lg \frac{t}{r^2} + \lg(2.25a) \right), \quad (12.5)$$

we obtain three straight-line-based methods for determining the hydraulic characteristics, corresponding to the three types of plots involved, i.e., time–drawdown

plot, distance–drawdown plot, and time–distance–drawdown plot. The time–drawdown plot (Fig. 12.1a) uses the drawdown measured in a single observation well; the distance–drawdown plot (Fig. 12.1b) is based on the drawdown measured in several observation wells at a specified moment; and the time–distance–drawdown plot (Fig. 12.1c) uses the drawdown measured in several observation wells.

The slope of the straight line (α) and the intercept on the ordinate (A) on a plot are used to evaluate the transmissivity (T) and hydraulic diffusivity (a) of the aquifer.

The methods for evaluating hydraulic characteristics by the straight-line method for different types of plots is summarized in Table 12.1.

Table 12.1 shows independent evaluation of the transmissivity and hydraulic diffusivity. Given these characteristics, the aquifer storage coefficient can be readily calculated: $S = T/a$. In addition, the intercept on the abscissa (Fig. 12.1) can be used to determine the storage coefficient (or hydraulic diffusivity) by formulas given in Table 12.2.

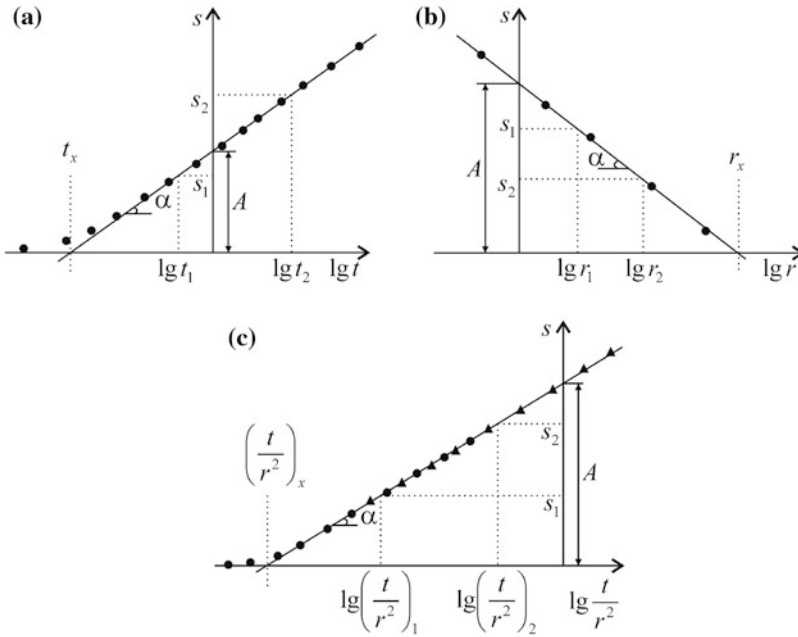


Fig. 12.1 Parameter evaluation by straight-line method on the **a** time–drawdown, **b** distance–drawdown, and **c** time–distance–drawdown plots. The *triangles* and *circles* indicate the measured data

Table 12.1 Parameter evaluation by straight-line method

Time–drawdown plot (Eq. 12.3, Fig. 12.1a)	Distance–drawdown plot (Eq. 12.4, Fig. 12.1b)	Time–distance–drawdown plot (Eq. 12.5, Fig. 12.1c)
$s - \lg t$	$s - \lg r$	$s - \lg \frac{t}{r^2}$
$s = C \lg t + A$	$s = -C \lg r + A$	$s = C \lg \frac{t}{r^2} + A$
$C = \frac{s_2 - s_1}{\lg t_2 - \lg t_1}$	$C = \frac{s_1 - s_2}{\lg r_2 - \lg r_1}$	$C = \frac{s_2 - s_1}{\lg(t/r^2)_2 - \lg(t/r^2)_1}$
$T = \frac{0.183Q}{C}$	$T = \frac{0.366Q}{C}$	$T = \frac{0.183Q}{C}$
$\lg a = \frac{A}{C} + \lg \frac{r^2}{2.25}$	$\lg a = 2 \frac{A}{C} - \lg(2.25t)$	$\lg a = \frac{A}{C} - \lg 2.25$

$C = \tan \alpha$ is the slope of the straight line; A is the intercept on the ordinate

Table 12.2 Parameter evaluation by the straight-line method

Plot	$s - \lg t$	$s - \lg r$	$s - \lg t/r^2$
Storage coefficient, dimensionless	$S = \frac{2.25Tt_x}{r^2}$	$S = \frac{2.25Tr}{r_x^2}$	$S = 2.25T \left(\frac{t}{r^2}\right)_x$
Hydraulic diffusivity, m ² /d	$a = \frac{r^2}{2.25t_x}$	$a = \frac{r_x^2}{2.25t}$	$a = \frac{1}{2.25(t/r^2)_x}$

t_x , r_x , and $(t/r^2)_x$ are the intercepts of the straight line on the abscissa of appropriate plots (see Fig. 12.1)

12.1.2 Horizontal Straight-Line Method

Consider a system of equations for the drawdown in two observation wells with Eq. 12.1 used for quasi-steady-state period:

$$\begin{cases} s_1 = \frac{0.183Q}{T} \lg \frac{2.25at}{r_1^2} \\ s_2 = \frac{0.183Q}{T} \lg \frac{2.25at}{r_2^2} \end{cases} \Rightarrow s_1 - s_2 = \frac{0.366Q}{T} \lg \frac{r_2}{r_1}, \quad (12.6)$$

where s_1 , s_2 are drawdown values in the first and second observation wells, m; r_1 , r_2 are the distances from the first and second observation wells to the pumping well, m.

Equation 12.6 shows that the drawdown difference between two wells does not depend on time once quasi-steady-state flow regime has been reached. Aquifer transmissivity can be readily evaluated by the intercept A (Fig. 12.2a) of the straight line parallel to the abscissa (Sindalovskiy 2014)

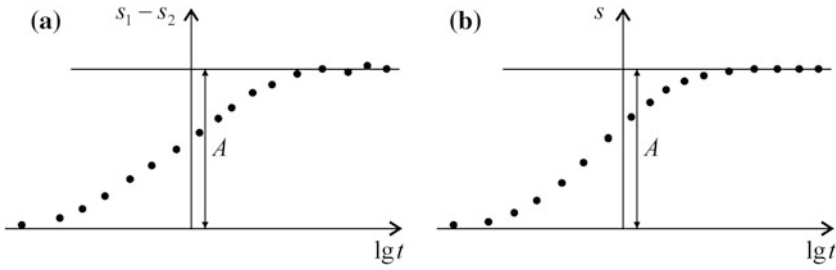


Fig. 12.2 Transmissivity evaluation by the method of *horizontal straight line* based on time-drawdown data. The plots are constructed for **a** the drawdown difference between two wells and **b** the drawdown in a single well located near a constant-head boundary

$$T = \frac{0.366Q}{A} \lg \frac{r_2}{r_1}. \tag{12.7}$$

The same method is used for aquifers with steady-state flow (Fig. 12.2b), for example, in the case of pumping near a constant-head boundary (see Sect. 1.2.1). In such case, the transmissivity can be evaluated by a single observation well for the period of level stabilization (see, e.g., the formula for s — $\lg t$ plot in Table 1.3). Note that the horizontal straight line is also used for the drawdown difference in two wells in the period of steady-state flow (see parameter evaluation on $(s_1 - s_2)$ — $\lg t$ plot in Table 1.3).

12.1.3 Type Curve Method

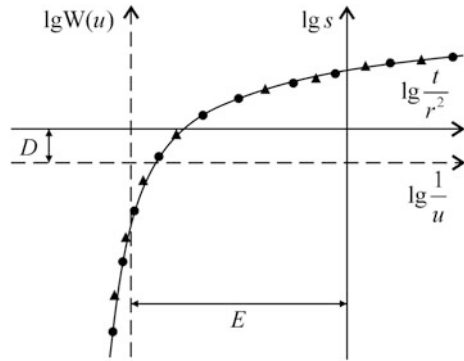
The type curve method is based on taking the logarithm of both the original analytical relationship and an argument of a special function, which enters this relationship (Ferris et al. 1962).

Let us consider a system of equations [for the case of solution (Eq. 1.3)]:

$$\begin{cases} s = \frac{Q}{4\pi T} W(u) \\ u = \frac{r^2}{4at} \end{cases} \Rightarrow \begin{cases} \lg s = \lg \frac{Q}{4\pi T} + \lg W(u) \\ \lg \frac{1}{u} - \lg \frac{t}{r^2} = \lg(4a) \end{cases} \Rightarrow \begin{cases} \lg s - \lg W(u) = \lg \frac{Q}{4\pi T} = D \\ \lg \frac{1}{u} - \lg \frac{t}{r^2} = \lg(4a) = E, \end{cases} \tag{12.8}$$

where $D = \lg \frac{Q}{4\pi T}$, $E = \lg(4a)$ are the shifts of the curve of the measured values and the type curve along the vertical and horizontal, respectively.

Fig. 12.3 Parameter evaluation by type curve on a log–log time–distance–drawdown plot. The *solid curve* is the type curve; *triangles and circles* indicate measured data. The *dashed lines* are the coordinate axes of the type curve



The system (Eq. 12.8) shows that it is convenient to plot the measured values in coordinates $\lg s - \lg(t/r^2)$ and the type curve in coordinates $\lg W(u) - \lg(1/u)$. In this case, the coordinate axes of the factual and type curves will be shifted by D along the vertical and by E along the horizontal (Fig. 12.3). The plot of the factual curve here is a time–distance–drawdown plot. For the conceptual models that ignore the effect of boundaries and leakage, the drawdown plots for different observation wells, ideally, should coincide.

Different representations of the second equation of the system (Eq. 12.8) provide different possible uses of the type curve. For a time–drawdown plot, it can be written as:

$$u = \frac{r^2}{4at} \Rightarrow \lg \frac{1}{u} = \lg t + \lg \frac{4a}{r^2} \Rightarrow \lg \frac{1}{u} - \lg t = \lg \frac{4a}{r^2} = E, \quad (12.9)$$

with which the plot of the factual curve will have the form $\lg s - \lg t$, the plot of the type curve will be $\lg W(u) - \lg(1/u)$, and $E = \lg(4a/r^2)$. In this case, the type curve is associated with a chosen observation well. For the distance–drawdown plot:

$$u = \frac{r^2}{4at} \Rightarrow \lg \sqrt{u} = \lg r - \lg \sqrt{4at} \Rightarrow \lg r - \lg \sqrt{u} = \lg \sqrt{4at} = E, \quad (12.10)$$

and then the factual curve is plotted in coordinates $\lg s - \lg r$, the type curve is plotted in coordinates $\lg W(u) - \lg \sqrt{u}$, and $E = \lg \sqrt{4at}$.

In these two examples (Eqs. 12.9 and 12.10), $D = \lg \frac{Q}{4\pi T}$.

All possible combinations of plotting the type and factual curves and the formulas for evaluating the hydraulic parameters are summarized in Table 12.3.

Table 12.3 Plotting type and factual curves

Processing method	Coordinates of the curve		Shift of axe	
	Factual	Type	Vertical	Horizontal
Time–distance–drawdown	$\lg s - \lg \frac{t}{r^2}$	$\lg W(u) - \lg \frac{1}{u}$	$D = \lg \frac{Q}{4\pi T}$	$E = \lg(4a)$
Time–drawdown	$\lg s - \lg t$	$\lg W(u) - \lg \frac{1}{u}$		$E = \lg \frac{4a}{r^2}$
Distance–drawdown	$\lg s - \lg r$	$\lg W(u) - \lg \sqrt{u}$		$E = \lg \sqrt{4at}$

12.2 Method of Bisecting Line

The method of bisecting line is based on a graphical determination of the agreement between the factual and estimated values at a correct choice of the hydraulic parameter (Sindalovskiy 2006). This is made using a plotted ratio of the actual drawdown in two wells versus the ratio of the calculated drawdown in the same wells (Fig. 12.4).

When data on the drawdown in two observation wells are available, we obtain a system of equations in the first (s_1) and second (s_2) wells (for the case of Eq. 1.3):

$$\begin{cases} s_1 = \frac{Q}{4\pi T} W\left(\frac{r_1^2}{4at}\right) \\ s_2 = \frac{Q}{4\pi T} W\left(\frac{r_2^2}{4at}\right) \end{cases} \Rightarrow \frac{s_1}{s_2} = \frac{W\left(\frac{r_1^2}{4at}\right)}{W\left(\frac{r_2^2}{4at}\right)} \Rightarrow \frac{s_1}{s_2} = \frac{W(u_1)}{W(u_2)}, \quad (12.11)$$

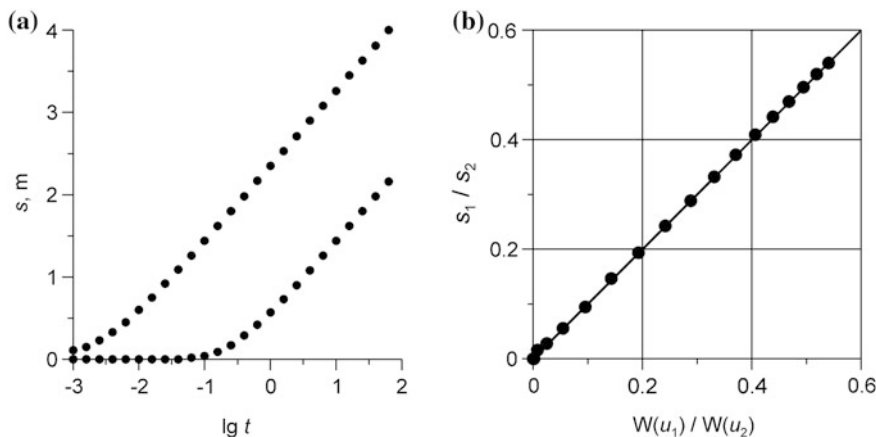


Fig. 12.4 An example of parameter evaluation by the method of bisecting line. **a** Time–drawdown plot for two observation wells; **b** a plot for the method of bisecting line based on the drawdown in these wells. The dots indicate measured data

where u_1, u_2 are arguments of the function for the first and second observation wells.

The choice of hydraulic diffusivity is based on the method of bisecting line on the plot $\frac{s_1}{s_2} - \frac{W(u_1)}{W(u_2)}$. The plot constructed in these coordinates is a straight line passing through the origin at an angle of 45° (Fig. 12.4b). This will be true with the correctly chosen value of hydraulic diffusivity. Otherwise, points on the plot will deviate from the linear segment. An advantage of the method is that the estimate of the hydraulic diffusivity does not depend on aquifer transmissivity and pumping-well discharge.

The method of bisecting line is a graphical analog of the point method for parameter evaluation based on the drawdown ratio in two observation wells.

In the cases where a single observation well is available with measurement data for periods of pumping and recovery, the system of equations (Eq. 12.11) can be replaced by:

$$\begin{cases} s_0 = \frac{Q}{4\pi T} W\left(\frac{r}{4at_0}\right) \\ s = \frac{Q}{4\pi T} \left[W\left(\frac{r}{4a(t_0+t_r)}\right) - W\left(\frac{r}{4at_r}\right) \right] \end{cases} \Rightarrow \frac{s_0}{s} = \frac{W\left(\frac{r}{4at_0}\right)}{W\left(\frac{r}{4a(t_0+t_r)}\right) - W\left(\frac{r}{4at_r}\right)}, \quad (12.12)$$

where s_0 is the drawdown in an observation well at the moment when pumping was stopped, m ; t_0 is pumping duration, d ; t_r is the time elapsed from the start of recovery, d .

In the latter case, the plot is constructed in coordinates $\frac{s_0}{s} - \frac{W(u)}{W'(u)}$, where $W'(u)$ is the expression in square brackets in the second equation of the system (Eq. 12.12). In this case, a plot in log–log coordinates is more demonstrative.

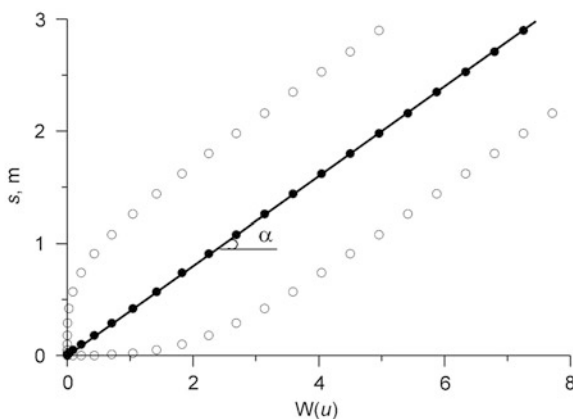
A variant of such an approach to solving the problem is based on a representation of the Theis solution (Eq. 1.3) as a linear equation (Shtengelov 1994):

$$y = Cx, \text{ where } y = s, C = \frac{Q}{4\pi T}, x = W\left(\frac{r^2}{4at}\right).$$

If we construct a plot in coordinates $s - W(u)$, where $u = r^2/(4at)$, then the correctly specified hydraulic diffusivity will give a straight line passing from the origin (Fig. 12.5).

The slope (α) of the straight line is used to determine aquifer transmissivity: $T = 0.08Q/C$, where $C = \tan \alpha$. Ideally, all points from the first measurement series must fall on a single straight line. The construction of a plot with a hydraulic diffusivity that disagrees with the properties of the aquifer under consideration will lead to a deformation of the initial part of the curve and shift the linear segment relative to the origin; however, the slope will remain unchanged.

Fig. 12.5 An example of the use of the straight-line method in $s-W(u)$ plot. The *black dots* are for a correctly specified hydraulic diffusivity, the *hollow dots* are for incorrectly estimated hydraulic diffusivity



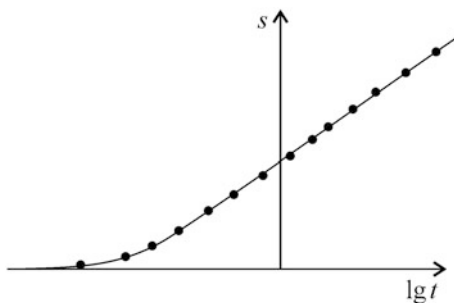
12.3 Matching Methods

Matching methods involve the solving of a direct or inverse problem for the search for the hydraulic parameters of an aquifer. A criterion of solution correctness is the visual agreement between the factual and calculated curves.

12.3.1 Direct Method: Manual Trial and Error

In this method, the direct groundwater flow problem is solved. The required coefficients are chosen here by visual comparison of the plot of factual water-level changes and a theoretical curve (Fig. 12.6), calculated by an appropriate relationships for specified technical characteristics of the test (discharge rate, the distance to the pumping well, time, etc.). The direct method makes it possible to promptly and vividly analyze the sensitivity to various hydraulic and engineering parameters and to compare results obtained with different conceptual models. The manual trial and

Fig. 12.6 Parameter evaluation by curve fitting on a time-drawdown plot. The *solid curve* shows calculation results, the *dots* are measured data



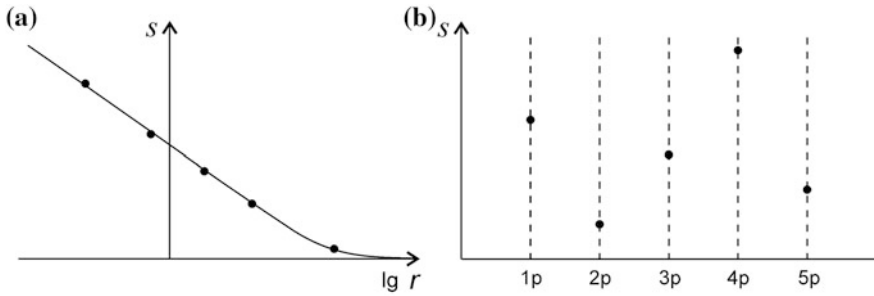


Fig. 12.7 **a** Matching method on a distance–drawdown-plot and **b** one-dimensional plot, constructed by drawdown values in observation wells (well names are given on the abscissa for a specified moment). The *full curve* shows calculation results, and the *dots* are measured values

error becomes an indispensable method for data processing in aquifer tests carried out under the conditions where there are no acceptable graphical methods: complex conditions, multi-well pumping with variable discharge rate, slug tests, etc.

When using such method, one should take into account that in some conceptual models, where fitting involves more than two parameters, the result of estimation may be not unique. This is primarily true for aquifers in which anisotropy is taken into account (see Sects. 1.2 and 1.3) and for leaky aquifers (see Chap. 3).

In addition to evaluating the hydraulic characteristics, the fitting method can predict water-level variation over time at any point in the aquifer (Fig. 12.6) or over space at any moment (Fig. 12.7a). This is of particular importance in the case of likely changes in pumping-well discharge rates, when there are no simple analytical solutions available to promptly evaluate the effect of test perturbation. Parameter fitting for the case of time–distance–drawdown analysis, when a plot contains curves for several observation wells, provides an estimate of the degree of heterogeneity or anisotropy of the analyzed area.

A specific feature of the manual trial-and-error approach for the conditions where the principle of superposition is applied (bounded aquifers or multi-well pumping tests) is that the drawdown at a point in an aquifer, reflected on the plot, depends not only on the distance to a single pumping well, but also on the distances to the flow boundary and/or other pumping wells. Therefore, distance–drawdown analysis can be carried out only for discrete points, in which observation wells are located, and for specified moments in time (Fig. 12.7b).

A variety of manual trial-and-error method is the choice of parameters using water-level measurement in two observation wells. In this case, time plots are constructed for drawdown ratios or differences (Fig. 12.8). The methods of drawdown ratios and differences in this form are analogous to point methods, which were earlier in wide use, with the difference that the researcher obtains parameters averaged over the entire chosen time interval, rather than for one or two measurements (Sindalovskiy 2014).

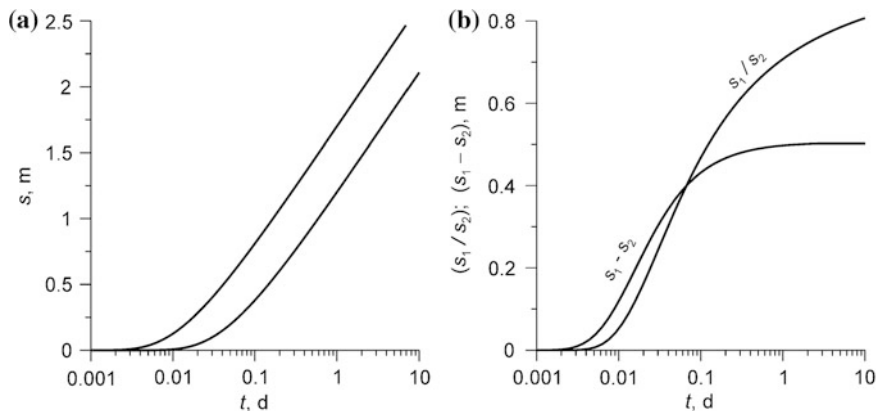


Fig. 12.8 An example of plots constructed by drawdown ratio and drawdown difference in two observation wells. **a** Time–drawdown plot for two observation wells; **b** drawdown ratio and drawdown difference plots based on the values given in the *left plot*

Drawdown-ratio method. A time–drawdown plot is used to construct a plot of the drawdown ratio for two chosen observation wells. The process of choosing parameters is similar to that in the manual trial-and-error method. An advantage of this approach over the previous method is that, in the case of a pumping test with a single constant-discharge well, the original equation transforms into an equation with one unknown (normally, hydraulic diffusivity). Some variables (e.g., discharge rate and transmissivity) are eliminated from the trial-and-error procedure and only one parameter (in some cases, two) is to be determined:

$$\frac{s_1}{s_2} = W\left(\frac{r_1^2}{4at}\right) / W\left(\frac{r_2^2}{4at}\right). \quad (12.13)$$

Equation 12.13 is written for a pumping test in a confined aquifer of infinite lateral extent (see Sect. 1.1.1). This equation is used to evaluate the hydraulic diffusivity. For other types of aquifer tests or other conditions (e.g., aquifer type, the presence of boundary conditions, etc.), this can be another parameter. For example, for a leaky aquifer (see Sect. 3.1.1), an equation written for steady-state-flow period depends only on the leakage factor:

$$\frac{s_1}{s_2} = K_0\left(\frac{r_1}{B}\right) / K_0\left(\frac{r_2}{B}\right). \quad (12.14)$$

In the case of aquifers bounded in the horizontal plane, the drawdown ratio in the steady-state-flow period may depend only on the positions of the wells relative to the boundaries and may not depend on any hydraulic parameters. For example, in the case of a semi-infinite aquifer (constant-head boundary) (see Sect. 1.2.2.1):

$$\frac{s_1}{s_2} = \lg\left(\frac{\rho_1}{r_1}\right) / \lg\left(\frac{\rho_2}{r_2}\right), \quad (12.15)$$

where ρ_1 , ρ_2 are the distances from the first and second observation wells to the image well, respectively, m.

For a constant-drawdown pumping test (see Chap. 8), the drawdown in the pumping well is excluded from the evaluation.

The plot s_1/s_2 — $\lg t$ is more convenient to construct for observation wells lying at distances $r_1 > r_2$, i.e., s_2 is to be the drawdown in the observation point nearest to the pumping well.

Drawdown-difference method. This method is used mostly for graphical processing (see Sect. 12.1.2). However, it can be also used for manual trial-and-error parameter choice:

$$s_1 - s_2 = \frac{Q}{4\pi T} \left[W\left(\frac{r_1^2}{4at}\right) - W\left(\frac{r_2^2}{4at}\right) \right] \approx \frac{Q}{2\pi T} \ln \frac{r_2}{r_1}. \quad (12.16)$$

As seen from Eq. 12.16, the drawdown for a transient flow period depends on the transmissivity and hydraulic diffusivity, while, in the case of quasi-steady-state flow, it depends on the transmissivity alone. The plot for the drawdown-difference method is constructed in coordinates $(s_1 - s_2)$ — $\lg t$, where s_1 is to be the drawdown in the observation point nearest to the pumping well (i.e., $r_1 < r_2$).

12.3.2 Inverse Method for Sensitivity Analysis

Automatic mode for parameter evaluations is based on minimizing the differences between the factual (input) data and the values calculated by one of the basic analytical relationships (see Chaps. 1–11). The input data are the groundwater-level measurements in one or several observation wells.

In the case of relatively simple groundwater flow equations, the inverse problem can be solved with the use of the least-squares method. When flow processes are described by complex functions, special programs, such as UCODE_2005 (Poeter et al. 2005) can be used. Guides for the use of such codes are given in Appendix 6.

The procedure of application of the least-squares method can be considered as applied to an aquifer test in an infinite confined aquifer (see Sect. 1.1.1).

Suppose that the drawdown s_i in an observation well at a distance r from the pumping well at moment t_i can be determined by the Theis solution (Eq. 1.3):

$$s_i = c_k W\left(\frac{r^2}{4at_i}\right), \quad (12.17)$$

where $c_k = Q/(4\pi T)$ is a constant, depending on the discharge rate of the pumping well and aquifer transmissivity.

Consider the sum of squares of differences between the measured and calculated values at some unknown values of parameters a and c_k to be determined:

$$\delta = \sum_{i=1}^n \left[s_i - c_k \mathbf{W} \left(\frac{r^2}{4at_i} \right) \right]^2 = f(a, c_k), \quad (12.18)$$

where n is the number of measurements involved in inverse-problem solution.

The objective is to find the values of parameters a and c_k to minimize the difference (Eq. 12.18). Differentiating function $f(a, c_k)$ by each unknown parameter, and equating the partial derivatives to zero, we obtain a system of two equations with two unknowns a and c_k :

$$\begin{cases} \frac{\partial f}{\partial a} = \left\{ \sum_{i=1}^n \left[s_i - c_k \mathbf{W} \left(\frac{r^2}{4at_i} \right) \right]^2 \right\}'_a = 0, \\ \frac{\partial f}{\partial c_k} = \left\{ \sum_{i=1}^n \left[s_i - c_k \mathbf{W} \left(\frac{r^2}{4at_i} \right) \right]^2 \right\}'_{c_k} = 0. \end{cases} \quad (12.19)$$

Now, we calculate the derivatives:

$$\begin{cases} \frac{\partial f}{\partial a} = 2 \sum_{i=1}^n [s_i - c_k \mathbf{W}(u_i)] (-c_k) \frac{\partial \mathbf{W}(u_i)}{\partial a} = 0, \\ \frac{\partial f}{\partial c_k} = 2 \sum_{i=1}^n [s_i - c_k \mathbf{W}(u_i)] [-\mathbf{W}(u_i)] = 0, \end{cases} \Rightarrow \begin{cases} \sum_{i=1}^n [s_i - c_k \mathbf{W}(u_i)] \frac{e^{-u_i}}{a} = 0, \\ \sum_{i=1}^n [s_i - c_k \mathbf{W}(u_i)] \mathbf{W}(u_i) = 0, \end{cases} \quad (12.20)$$

where $u_i = \frac{r^2}{4at_i}$.

Finally, the system of equations for calculating the hydraulic characteristics becomes:

$$\begin{cases} \sum_{i=1}^n \left[s_i \frac{1}{a} \exp(-u_i) \right] - \frac{\sum_{i=1}^n [s_i \mathbf{W}(u_i)]}{\sum_{i=1}^n [\mathbf{W}(u_i)]^2} \sum_{i=1}^n \left\{ \mathbf{W}(u_i) \frac{1}{a} \exp(-u_i) \right\} = 0, \\ c_k = \frac{\sum_{i=1}^n [s_i \mathbf{W}(u_i)]}{\sum_{i=1}^n [\mathbf{W}(u_i)]^2}, \end{cases} \quad (12.21)$$

where the hydraulic diffusivity a is found from the first equation of the system (Eq. 12.21), for example, by bracketing technique or iterations, and the parameter c_k (and hence, aquifer transmissivity T) can be directly calculated from the second equation of the system (Eq. 12.21). The hydraulic diffusivity can be evaluated to any required accuracy.

In the general form, the system of equations for an arbitrary conceptual model with any number of pumping and observation wells and step-wise variation of discharge rate in each pumping well can be written as:

$$\begin{cases} \sum_{m=1}^{N_0} \sum_{i=1}^n s_i^m \Sigma' - c_k \sum_{m=1}^{N_0} \sum_{i=1}^n \Sigma \times \Sigma' = 0, \\ \sum_{m=1}^{N_0} \sum_{i=1}^n s_i^m \Sigma - c_k \sum_{m=1}^{N_0} \sum_{i=1}^n \Sigma^2 = 0, \end{cases} \quad (12.22)$$

where $\Sigma = \sum_{j=1}^{N+M} \sum_{k=1}^{n_j} \Delta Q_j^k F(a, t_i^k, r_j^m)$; $\Sigma' = \sum_{j=1}^{N+M} \sum_{k=1}^{n_j} \Delta Q_j^k \frac{\partial F(a, t_i^k, r_j^m)}{\partial a}$; c_k is a constant, which depends on the chosen model (normally, it involves the transmissivity or the hydraulic conductivity of the aquifer); $i = 1, 2, 3, \dots, n$ is measurement number; $j = 1, 2, 3, \dots, N + M$ are the numbers of pumping wells (both real and image); $k = 1, 2, 3, \dots, n_j$ is the number of a step in the discharge rate in the j th pumping well (either real or image); $F(a, t_i^k, r_j^m)$ is a function describing the conceptual model; s_i^m is the value of the i th factual measurement in the m th observation well, m ; M is the number of image wells for bounded aquifers (for infinite aquifers $M = 0$); $m = 1, 2, 3, \dots, N_0$ is the number of an observation well (N_0 is the number of the observation wells used in parameter estimation); N is the number of pumping wells; n is the number of factual measurements used in parameter estimation (this number may be different in different observation wells); n_j is the number of discharge steps in the j th real or image pumping well (in each such well, it can be different); ΔQ_j^k is the k th discharge change in the j th pumping (real or image) well, m^3/d ; r_j^m is the distance from the m th observation well to the j th pumping (real or image) well, m ; t_i^k is the moment of the i th measurement to the beginning of the k th step (discharge change), d .

As with the system of equations (Eq. 12.21), the first part of Eq. 12.22 is solved by approximate calculation of the root. This root is used to evaluate the hydraulic diffusivity of the aquifer to any required degree of accuracy. The obtained value is substituted into the second equation of the system (Eq. 12.22), whence the transmissivity or hydraulic conductivity can be evaluated by direct calculation:

$$c_k = \frac{\sum_{m=1}^{N_0} \sum_{i=1}^n s_i^m \Sigma}{\sum_{m=1}^{N_0} \sum_{i=1}^n \Sigma^2}. \quad (12.23)$$

Before starting the procedure of automated matching, it is reasonable to exclude the measurements that are knowingly unacceptable for some reason (technical factors or researcher's mistakes). Otherwise, the final results may be strongly distorted. It is recommended to use the obtained parameters to construct a time–drawdown, distance–drawdown, or distance–drawdown–time curve and compare visually the factual and theoretical data.

The least-squares method is convenient for parameter evaluation by the straight-line method (see Sect. 12.1.1) for automated linear approximation of factual measurements corresponding to a quasi-steady-state period. In this case, the algorithm for solving the inverse problem is similar to the algorithm based on Eqs. 12.17–12.21, where Eq. 12.17 is replaced by

$$s_i = c_k \left(\lg t_i + \lg \frac{2.25a}{r^2} \right). \quad (12.24)$$

Equation 12.24 is given for plot s — $\lg t$. Similar equalities can be readily written for other plots to which the straight-line method can be applied.

12.4 Diagnostic Curve for Aquifer Tests

The plot of data obtained in the course of an aquifer test depends on aquifer type, the presence of boundary conditions, and the type of test (pumping test, recovery test, slug test, etc.). An expert can use the appearance of the plot to derive some conclusions regarding the conditions of the test. The model curves given in this section have been constructed with the use of the ANSDIMAT software package (Sindalovskiy 2014).

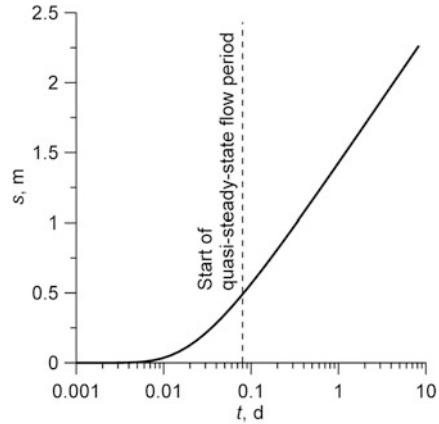
12.4.1 Confined Aquifer

12.4.1.1 Aquifer of Infinite Lateral Extent

Water-level drawdown in an observation well located in a confined aquifer of infinite areal extent (see Sect. 1.1) can be described by the Theis solution (Eq. 1.1). The time–drawdown plot s — $\lg t$ (Fig. 12.9) contains a linear segment corresponding to a quasi-steady-state period. The beginning of the period depends on the distance to the pumping well and the hydraulic diffusivity of the aquifer (Eq. A4.16).

The hydraulic parameters of an aquifer have an effect on the behavior of the drawdown curve: the transmissivity is associated with its slope (Fig. 12.10a, b), and the storage characteristics (storage coefficient or hydraulic diffusivity) shift the curve to the left or to the right (Fig. 12.10c).

Fig. 12.9 Time–drawdown plot for a confined aquifer of infinite lateral extent



The initial segment of the drawdown plot (Fig. 12.11) is largely dependent on the wellbore storage and skin. The further is the observation well from the pumping well, the lesser the manifestation of those effects. The moment after which the effect of storage on the drawdown can be neglected depends on the aquifer transmissivity and the casing radius of the pumping well (Eq. A2.3).

The plots given in Fig. 12.11 have been constructed with the use of Moench solutions (Eqs. 1.4 and 1.5). They show that the wellbore skin has different effect on the drawdown in the pumping and observation wells. In the observation well, the wellbore skin causes a time lag in level drop with subsequent alignment with the Theis curve (Fig. 12.11a). The drawdown curve in the pumping well, after a short delay, passes above the Theis curve (Fig. 12.11b).

Observation well storage has a lesser effect on the test result, though this effect can be appreciable in large-diameter observation wells (Fig. 12.11c).

12.4.1.2 Aquifer Bounded in the Horizontal Plane

This section considers typical plots for confined semi-infinite and strip aquifers (see Sects. 1.1.2 and 1.1.3).

For semi-infinite aquifers, the pattern of the drawdown plot depends on the type of boundary condition. In pumping tests near a constant-head boundary, the curve reaches a steady state after a transient flow period (Fig. 12.12a), whose duration depends on aquifer hydraulic diffusivity and the distances from the pumping and observation wells to the boundary (see Eq. A4.17). In the presence of an impermeable boundary, the drawdown plot (Fig. 12.12b) is similar to the drawdown plot in an aquifer of infinite lateral extent (see Fig. 12.9), with the difference that the slope of the plot is twice as large as in the former case and the quasi-steady-state period sets in later. The onset time of the quasi-steady-state period is evaluated in this case with the use of the same formula (see Eq. A4.17).

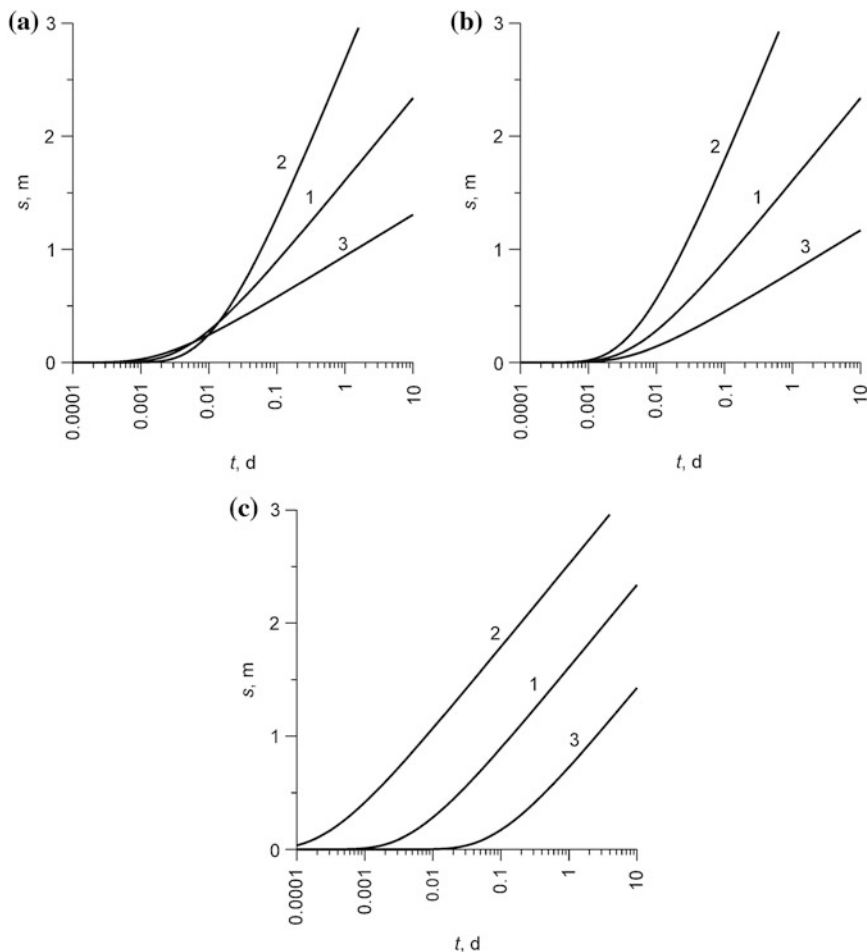


Fig. 12.10 The effect of hydraulic parameters on the drawdown in a confined aquifer: **a** transmissivity ($T_2 < T_1 < T_3$) at constant storage coefficient; **b** transmissivity ($T_2 < T_1 < T_3$) at constant hydraulic diffusivity; **c** storage coefficient ($S_2 < S_1 < S_3$) [or hydraulic diffusivity ($a_3 < a_1 < a_2$)] at constant transmissivity. The numbers at the curves (1, 2, 3) correspond to the subscripts at hydraulic characteristics

In a strip aquifer, the steady-state period forms only if at least one of the boundaries is of the constant-head type (Fig. 12.13).

In the case of two parallel impermeable boundaries, the drawdown plot in coordinates $s - \lg t$ does not contain a linear segment (Fig. 12.14). However, a plot in coordinates $s - \sqrt{t}$ contains a strictly linear segment, enabling the use of this plot to evaluate hydraulic characteristics (see Table 1.6).

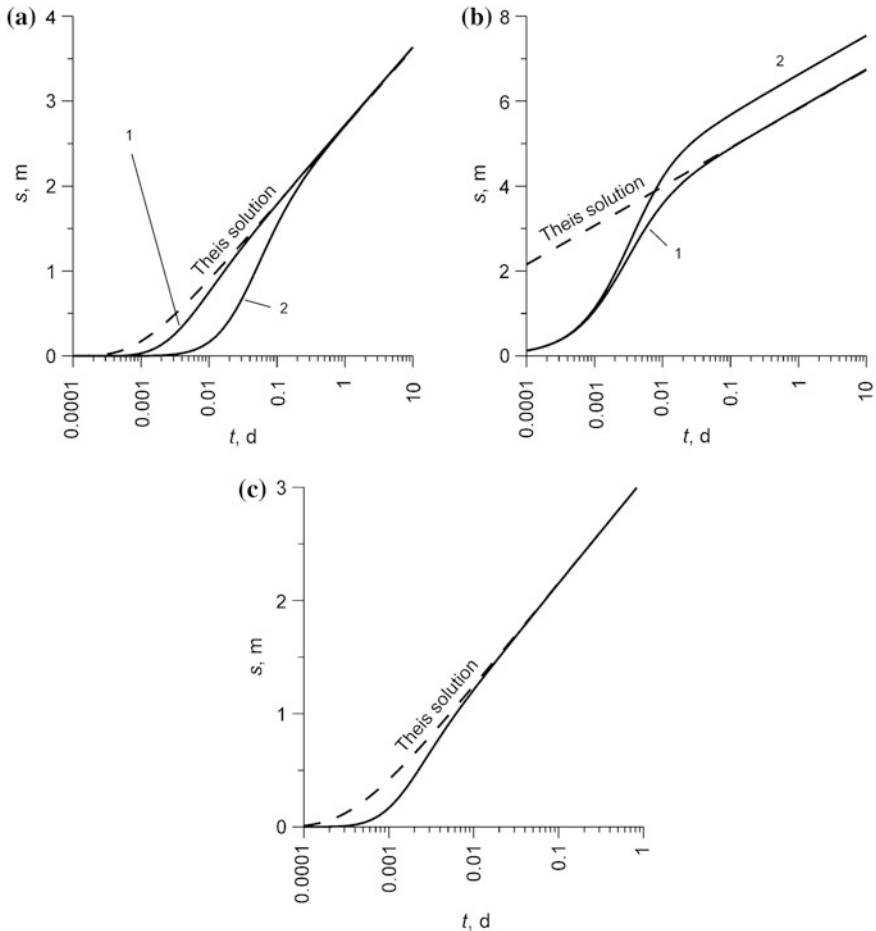


Fig. 12.11 The effect of wellbore storage and skin on the drawdown in **a** observation and **b** pumping wells. The curves show (1) Moench solution with wellbore storage taken into account and (2) the Moench solution with both wellbore storage and wellbore skin taken into account. **c** The effect of observation-well storage on the drawdown in this well

12.4.1.3 Partially Penetrating Wells

Partially penetrating wells (see Sects. 1.2 and 1.3) can be used to determine the vertical anisotropy of an aquifer. The closer the observation well to the pumping well, the greater the effect of its partial penetration on the drawdown. At distances greater than aquifer thickness, the partial penetration of wells and the vertical component of the hydraulic conductivity have but little effect on the drawdown.

A partially penetrating well in the form of a point source (see Sect. 1.2) is rarely used in practical calculations because it generally implies an aquifer infinite in thickness. In the case of point source, the plot of the drawdown comes to

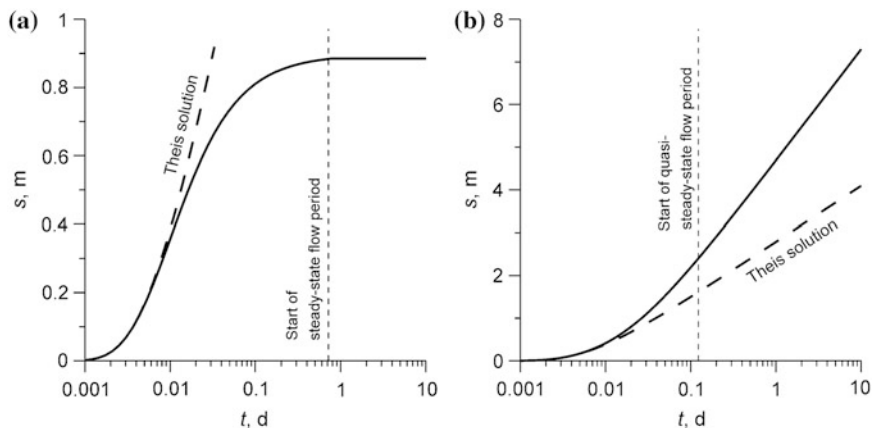


Fig. 12.12 Time–drawdown plot for semi-infinite aquifers: **a** constant-head (Eq. 1.13) and **b** impermeable boundaries (Eq. 1.15)

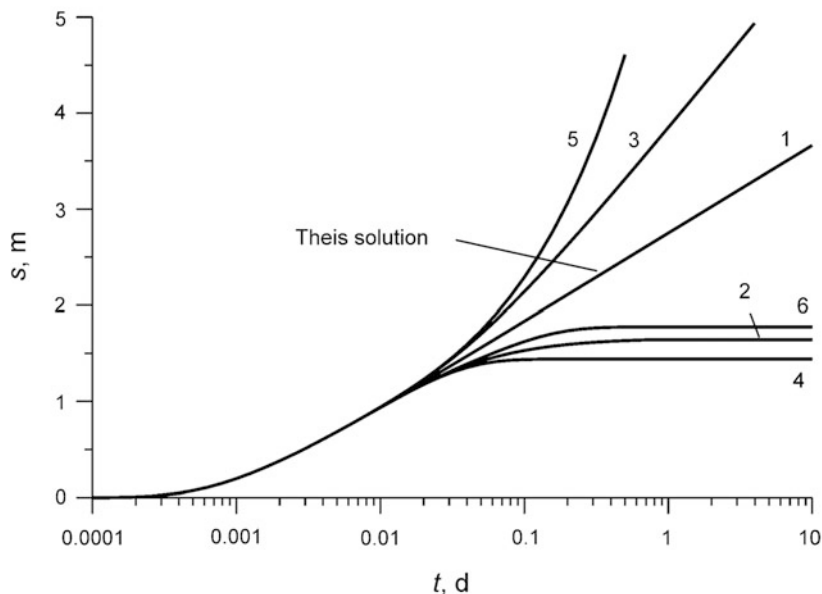


Fig. 12.13 The effect of boundaries and boundary conditions on the drawdown in an observation well: (curve 1) aquifer of infinite lateral extent (Eq. 1.1), (curve 2) semi-infinite aquifer with constant-head boundary (Eq. 1.13), (curve 3) semi-infinite aquifer with impermeable boundary (Eq. 1.15), (curve 4) strip aquifer with constant-head boundaries (Eq. 1.17), (curve 5) strip aquifer with impermeable boundaries (Eq. 1.24), and (curve 6) strip aquifer with constant-head and impermeable boundaries (Eq. 1.27)

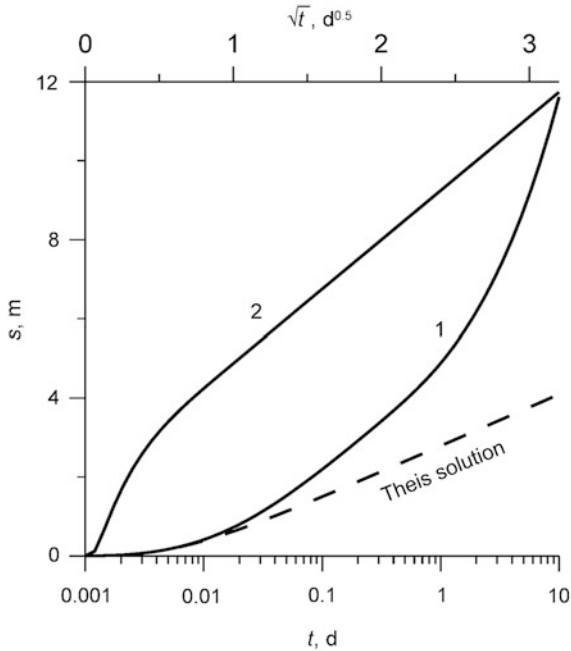


Fig. 12.14 The drawdown in a strip aquifer with impermeable boundaries: (curve 1) in coordinates $s - \lg t$, (curve 2) in coordinates $s - \sqrt{t}$

steady-state when it depends on whether the aquifer is anisotropic (Fig. 12.15a) and what is the position of the observation well. In aquifers where the components of the hydraulic conductivity (k_r and k_z) are different and the effective hydraulic conductivity ($\sqrt{k_r k_z}$) has a constant value, the drawdown curves in the steady-state-flow period coincide (see curves 2 and 3 in Fig. 12.15a). The time–drawdown plot $s - 1/\sqrt{t}$ (Fig. 12.15b) contains a linear segment corresponding to a quasi-steady-state period.

A possible form of the drawdown plot in a partially penetrating well, represented by a linear source (see section “[Aquifer Infinite in the Horizontal Plane](#)” of Chap. 1), is given in Fig. 12.16. In the case of an aquifer with large thickness, the drawdown plot will become a straight line after some delay.

12.4.2 Unconfined Aquifer

Plots (Figs. 12.17 and 12.18) show typical drawdown curves for an unconfined aquifer (see Sect. 2.1). The plots contain three segments (early time response, intermediate, and late time response), which correspond to different flow regimes during pumping tests: (1) a short period, when the storage coefficient reflects the

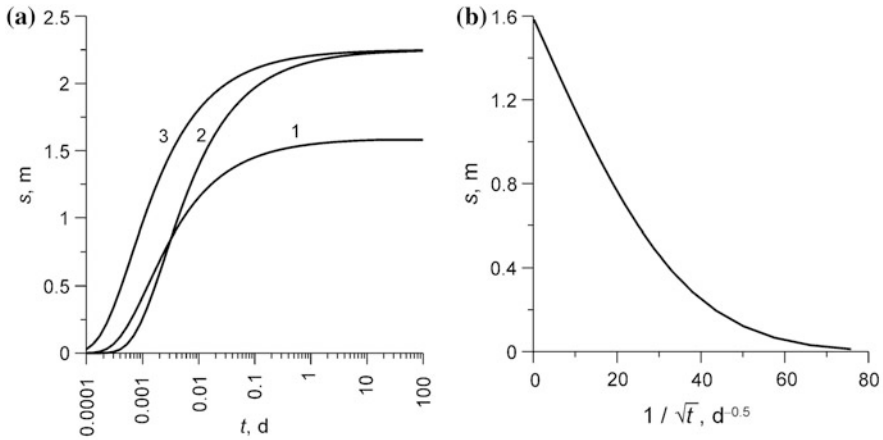
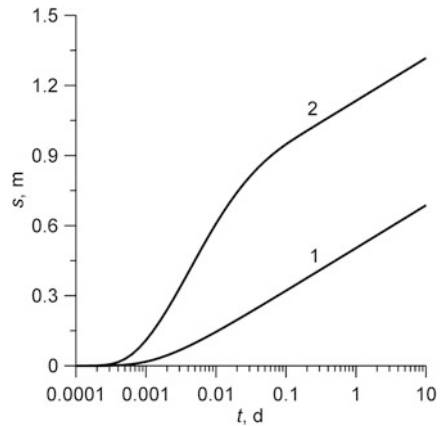


Fig. 12.15 Time-drawdown plots for a point source in a confined aquifer infinite in the horizontal plane and thickness (Eq. 1.79): **a** in coordinates $s\text{--}\lg t$; **b** in coordinates $s\text{--}1/\sqrt{t}$. (curve 1) isotropic aquifer, (curve 2) anisotropic aquifer ($k_r > k_z$), and (curve 3) anisotropic aquifer ($k_r < k_z$)

Fig. 12.16 Comparison of the drawdown plots in a confined aquifer: (curve 1) Theis solution (Eq. 1.1); (curve 2) Hantush solution for a linear source (Eq. 1.104)



elastic compression of the aquifer, (2) this segment of the curve corresponds to pseudo-steady-state flow with a temporary stabilization of the water level, and (3) the gravity-drainage period, which corresponds to the manifestation of aquifer specific yield.

The plots in Figs. 12.17, 12.18, 12.19 and 12.20 were constructed with the use of Boulton solution (Eq. 2.10) for fully penetrating wells.

When the aquifer drainage is considerable (more than 20 % of its initial water-saturated thickness), the accurate treatment of measurement data (Fig. 12.19) requires drawdown correction (Eq. 2.28).

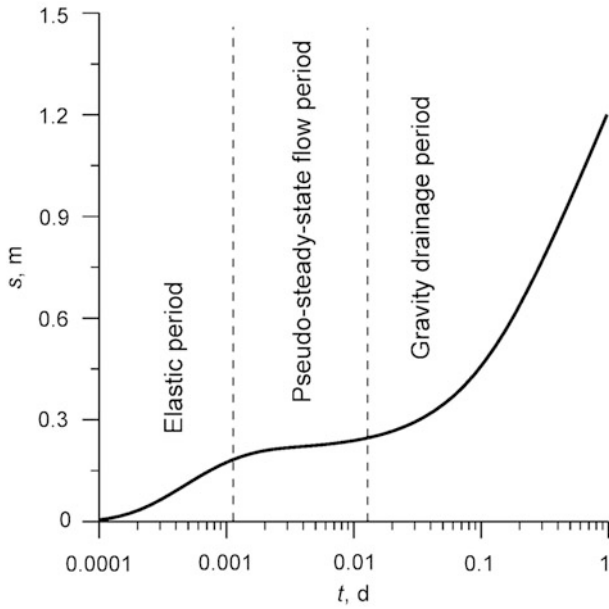


Fig. 12.17 Time–drawdown plot for an unconfined aquifer

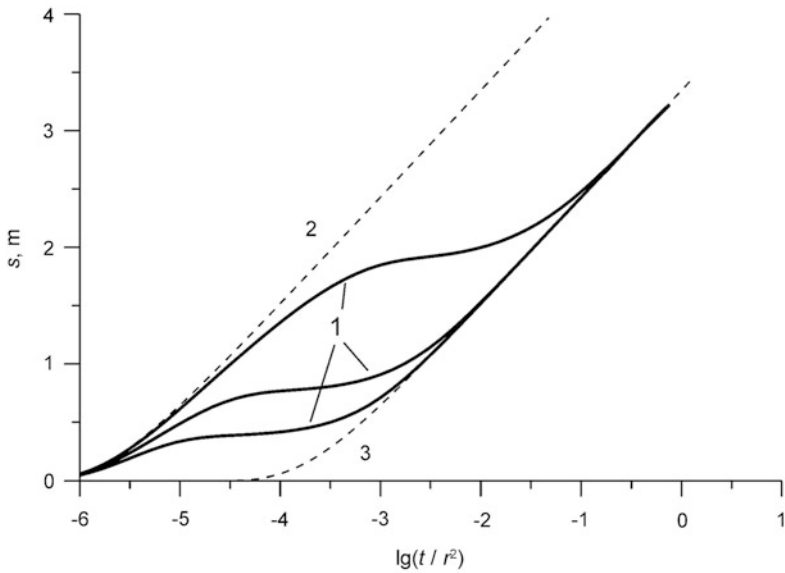


Fig. 12.18 Time–distance–drawdown plot for an unconfined aquifer (*curve 1*). The plot is drawn for three observation wells based on the Boultou solution (Eq. 2.10). The *thin dashed lines* are the Theis solution (Eq. 1.1) assuming an elastic storage coefficient (*curve 2*) and a specific yield of an unconfined aquifer (*curve 3*)

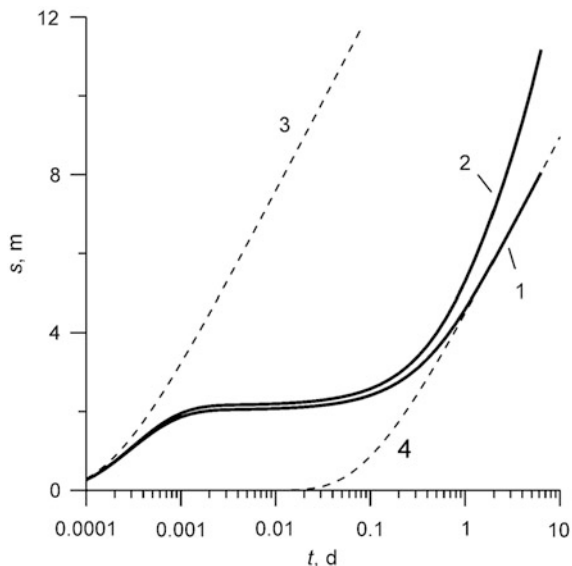


Fig. 12.19 Time–drawdown plot for an unconfined aquifer. Solution without correction (*curve 1*); corrected drawdown (*curve 2*). The *thin dashed lines* are Theis solution (Eq. 1.1) assuming an elastic storage coefficient (*curve 3*) and a specific yield of unconfined aquifer (*curve 4*)

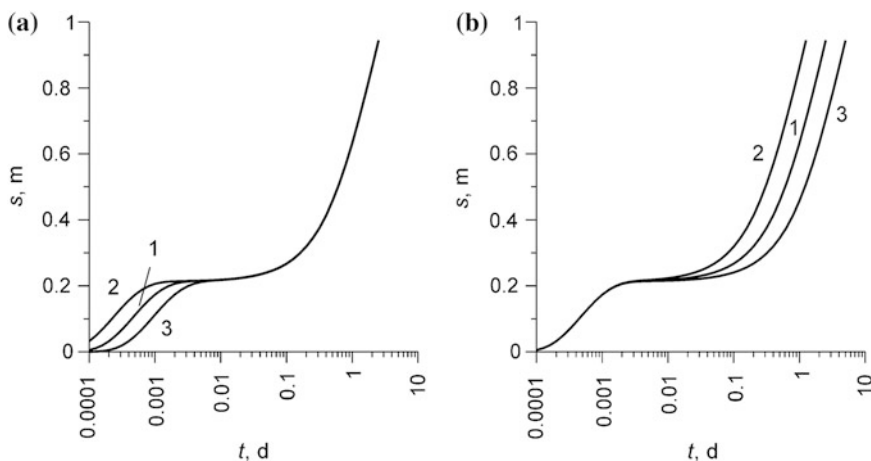


Fig. 12.20 Time–drawdown plot for an unconfined aquifer. The effect of hydraulic characteristics: **a** specific storage ($S_2 < S_1 < S_3$); **b** specific yield ($S_{y2} < S_{y1} < S_{y3}$). The numbers on the *curves* (1, 2, 3) correspond to subscripts at hydraulic characteristics

The effect of storage parameters on the drawdown in an unconfined aquifer is illustrated by Fig. 12.20. The plots show the effect of the elastic storage coefficient (S) on the initial segment of the curve and the effect of specific yield (S_y) on its final

segment. However, this feature can be seen only when the specific yield is much greater than its elastic analog: $S_y \gg S$.

12.4.3 *Leaky Aquifer*

Pumping tests in leaky aquifers are described in Chap. 3. The pattern of the drawdown plot in such aquifers depends on the hydraulic characteristics of adjacent aquifers and aquitards.

At constant water level in the adjacent aquifer (see Sect. 3.1), the drawdown in the main aquifer will stabilize (Fig. 12.21). The moment when the steady-state period begins depends on the leakage factor and the hydraulic diffusivity of the main aquifer (see Eq. A4.19).

The storage characteristics of aquitards and water-level changes in adjacent aquifers may have a considerable effect on the drawdown in leaky aquifers (Fig. 12.22).

In a pumping test in an unconfined two-layer aquifer (see Sect. 3.5.1), the water-level drawdown plot (Fig. 12.23) is similar to that in a single-layer unconfined aquifer (see Fig. 12.17). The difference is that the first segment of the curve corresponds to the storage coefficient (S) of the main confined aquifer; and the third segment, to the specific yield (S_y) of the upper unconfined aquitard (see Fig. 3.12).

In multi-aquifer systems (see Sect. 3.6), the drawdown (Fig. 12.24) depends on the number of adjacent aquifers and aquitards. The Moench solutions (Eq. 3.122), implemented in DP_LAQ code (see Appendix 5.5), were used for plotting.

12.4.4 *Horizontally Heterogeneous Aquifer*

Pumping tests in horizontally heterogeneous aquifers were described in Chap. 4. The drawdown plot (Fig. 12.25) depends on the type of the boundary between heterogeneity zones (linear or radial) and the zone in which the observation well is located (the main or adjacent) (see Fig. 4.1).

In the presence of a linear interface between the two zones, the drawdown plots for observation wells located in the main and adjacent zones have the same slope during the quasi-steady-state flow period (Fig. 12.25a).

The drawdown plot in a radial-heterogeneous aquifer (Fig. 12.25b) is similar to a plot in a homogeneous aquifer with wellbore skin taken into account (see curve 2 in Fig. 12.11a). The wellbore zone here corresponds to the pumping-well skin with the difference that the skin storage coefficient is not taken into account in the homogeneous aquifer.

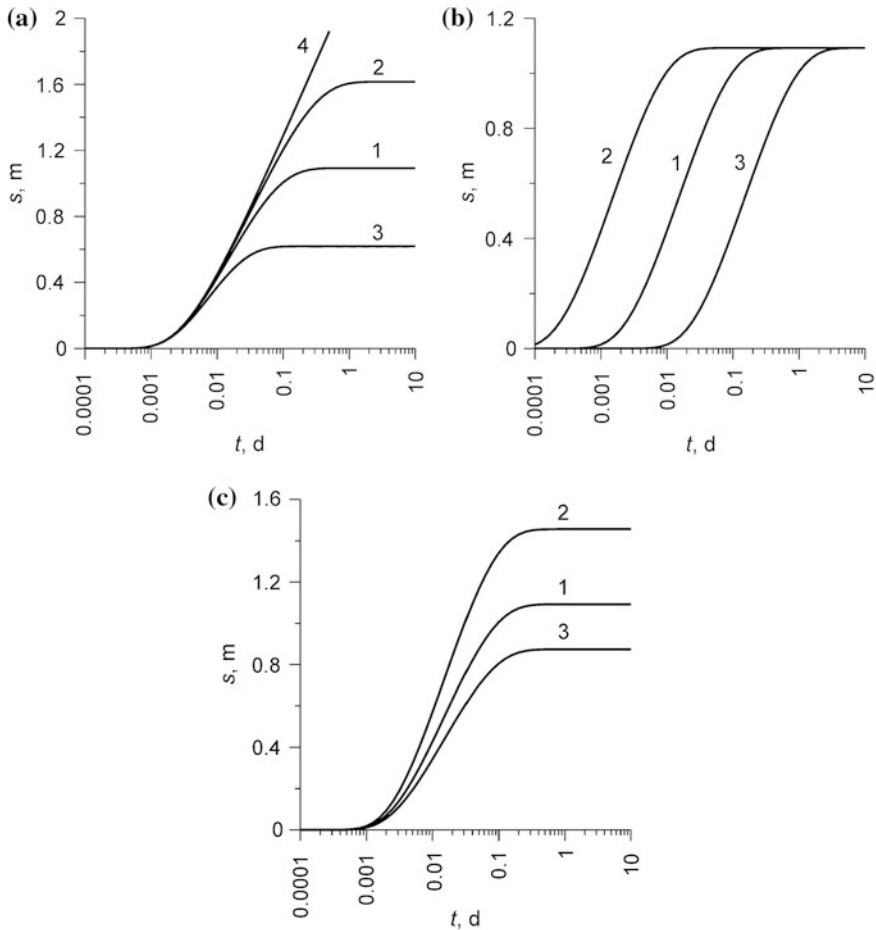


Fig. 12.21 Time–drawdown plots for a leaky aquifer: Hantush–Jacob solution (Eq. 3.1). The effect of hydraulic characteristics: **a** leakage factor ($B_3 < B_1 < B_2$); **b** hydraulic diffusivity ($a_3 < a_1 < a_2$); **c** transmissivity ($T_2 < T_1 < T_3$). As $B_4 \rightarrow \infty$, the Hantush–Jacob solution tends to the Theis solution (Eq. 1.1). The numbers on the curves (1, 2, 3, 4) correspond to subscripts at hydraulic characteristics

12.4.5 Pumping Test near a Stream

In pumping tests near a stream (see Sect. 5.1), the drawdown in an aquifer shows the effect of the hydraulic conductivity and the thickness of the stream bed. The retardation coefficient of the semipervious stream bed (see Eq. 5.12) causes an increase in the drawdown in the steady-state flow period as compared with the drawdown during pumping near a constant-head boundary (Fig. 12.26).

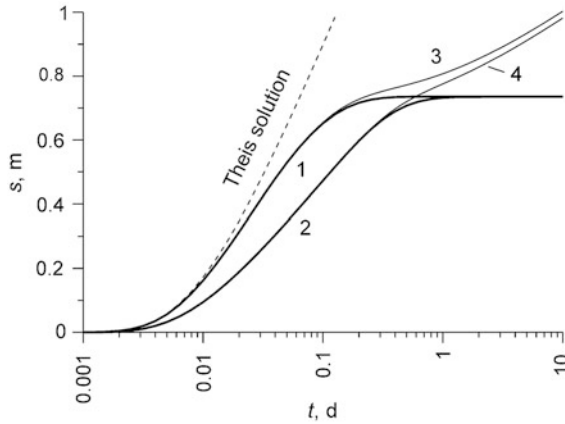
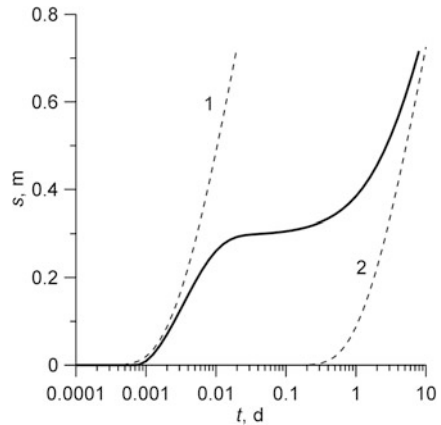


Fig. 12.22 Time–drawdown plots for leaky aquifers: (*curve 1*) the water level in the adjacent aquifer is constant—the Hantush–Jacob solution (Eq. 3.1); (*curve 2*) the water level in the adjacent aquifer is constant, aquitard storage is taken into account (Eq. 3.67); (*curve 3*) the water level in the adjacent aquifer is variable (Eq. 3.40); (*curve 4*) the water level in the adjacent aquifer is variable, aquitard storage is taken into account (Eq. 3.73)

Fig. 12.23 Time–drawdown plot for a two-layer unconfined aquifer (*thick solid line*): the Mironenko solution (Eq. 3.94). The *thin dashed lines* are Theis solutions (Eq. 1.1) assuming (*curve 1*) a storage coefficient of the lower confined aquifer and (*curve 2*) a specific yield of the upper unconfined aquitard



12.4.6 Pumping Test in a Fractured-Porous Reservoir

Figure 12.27 shows a typical plot of the drawdown in a fractured-porous medium (see Sect. 6.1). By its appearance, this plot is similar to the drawdown plot in an unconfined aquifer (Fig. 12.17). The plot was constructed with the use of the Moench solution (Eq. 6.3), implemented in the code DP_LAQ (see Appendix 5.5).

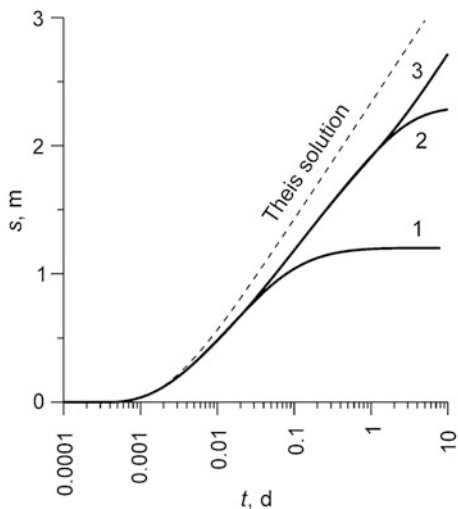


Fig. 12.24 Time-drawdown plot for a three-layer system with different numbers of adjacent aquifers: (curve 1) two adjacent aquifers (see Fig. 3.15a); (curve 2) a single adjacent aquifer (see Fig. 3.15c); (curve 3) no adjacent aquifers (see Fig. 3.15e)

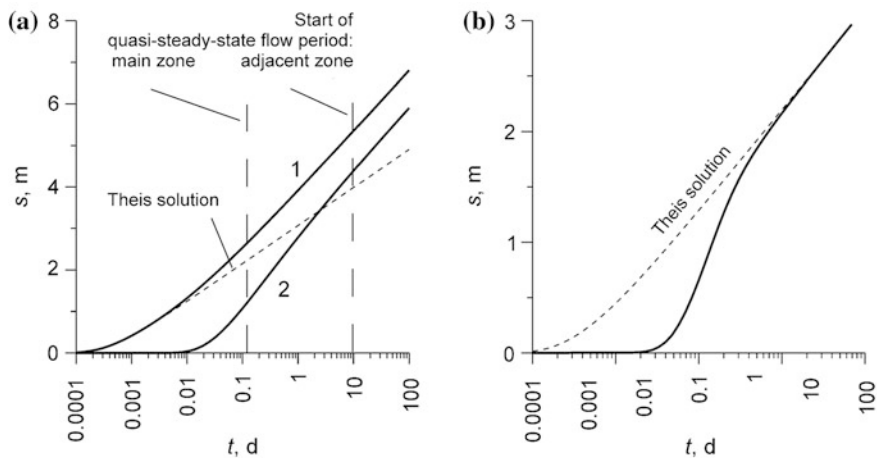


Fig. 12.25 Time-drawdown plots for horizontally heterogeneous aquifers: **a** the drawdown in the main (curve 1) and adjacent zones (curve 2) of a linearly heterogeneous aquifer (Eqs. 4.8 and 4.9); **b** the drawdown in the main zone of a radial-heterogeneous aquifer (Eq. 4.15)

Fig. 12.26 Time–drawdown plots for pumping near a stream. Stream-bed resistance is taken into account (curve 1): Hantush solution (Eq. 5.7); constant-head boundary (curve 2) (Eq. 1.13)

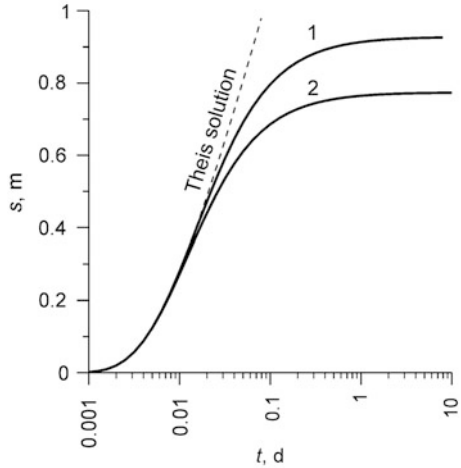
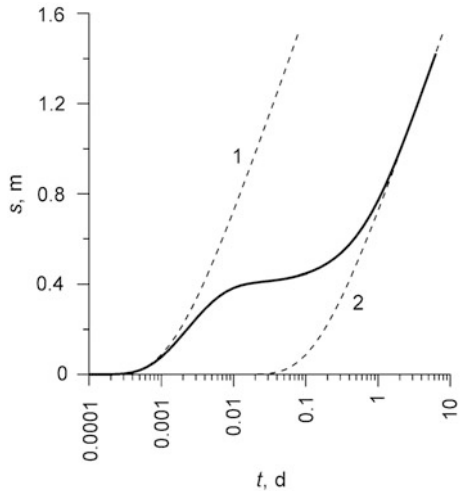


Fig. 12.27 Time–drawdown plot for pumping test in a fractured-porous medium (thick solid line). The thin dashed lines are Theis solution (Eq. 1.1) assuming (curve 1) a specific storage of a fractured system and (curve 2) a specific storage of a block system (the hydraulic diffusivity depends on the specific storage of the block system and the hydraulic conductivity of the fractured system)



12.4.7 Constant-Head Test

In the case of constant-head pumping tests (see Chap. 8), hydraulic characteristics can be evaluated either by the drawdown in observation wells or by changes in the discharge of the pumping well. The drawdown curves in Fig. 12.28a were plotted with the use of Eqs. 8.1 and 8.11; and the plots of discharge (Fig. 12.28b), with the use of Eqs. 8.3 and 8.13.

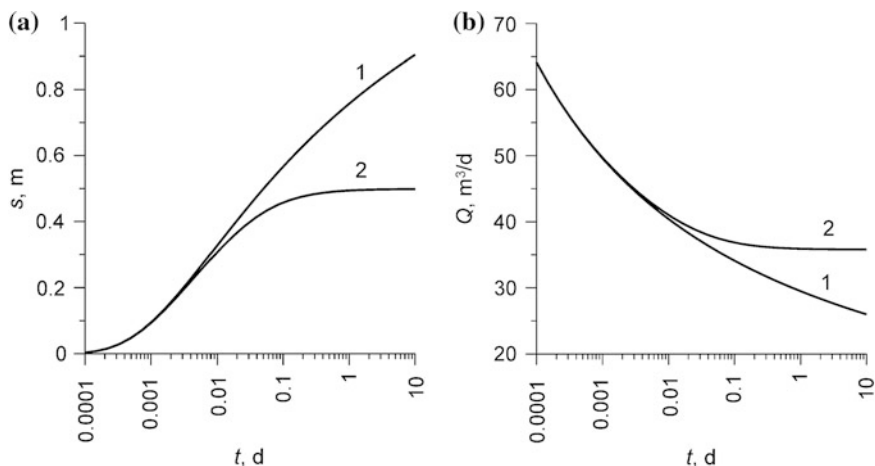


Fig. 12.28 Time plots for a constant-drawdown pumping. Plots of **a** drawdown in an observation well and **b** discharge in the pumping well for a confined aquifer (*curve 1*) and a leaky aquifer (*curve 2*)

The effects of hydraulic characteristics on the drawdown in an observation well and the pumping-well discharge during a constant-head pumping test are shown in Fig. 12.29.

12.4.8 Slug Test

Plots of water-level recovery during slug tests (see Chap. 9) are convenient to construct in normalized coordinates with the ordinate equal to the ratio of level recovery to the initial change of the water level in the tested well (Fig. 12.30). As can be seen from the plot, a noninstantaneous change in the initial level causes a delay in recovery, hence, an underestimation of aquifer specific storage. The plot also gives a typical curve of water-level changes in an observation well. However, in practice, observation wells are rarely used, because of the small radius of influence in slug tests (see Appendix 4).

The effect of the storage coefficient and transmissivity on water-level changes in the tested well during slug tests is shown in Fig. 12.31.

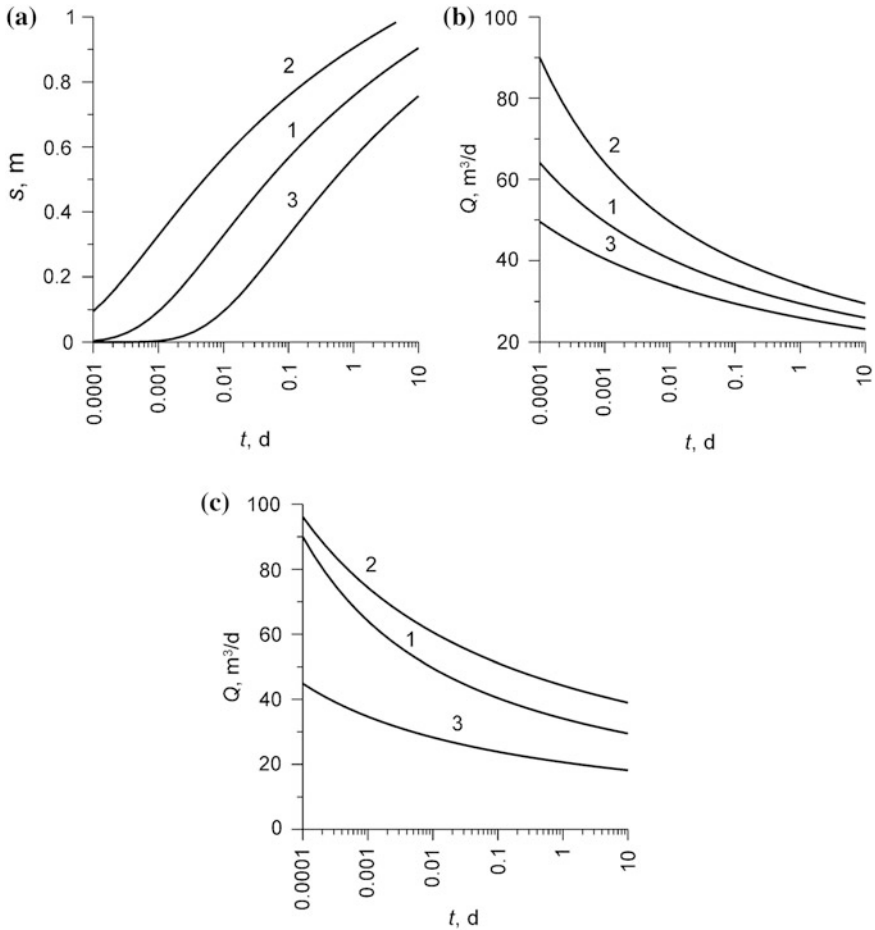


Fig. 12.29 The effect of hydraulic characteristics on the drawdown in an observation well and the discharge in the pumping well during a constant-head pumping test. The effect of hydraulic diffusivity (or specific storage) on **a** the drawdown ($a_3 < a_1 < a_2$ or $S_2 < S_1 < S_3$) and **b** discharge ($a_2 < a_1 < a_3$ or $S_3 < S_1 < S_2$). **c** The effect of transmissivity ($T_3 < T_1 < T_2$) on discharge. The numbers at the curves (1, 2, 3) correspond to the subscripts at hydraulic characteristics

12.4.9 Recovery Test

Observations of water-level recovery after pumping provide data that can be used to evaluate hydraulic characteristics. Their effect on level-recovery dynamics in a confined aquifer (see Sect. 1.1) is shown in Figs. 12.32 and 12.33. The plots

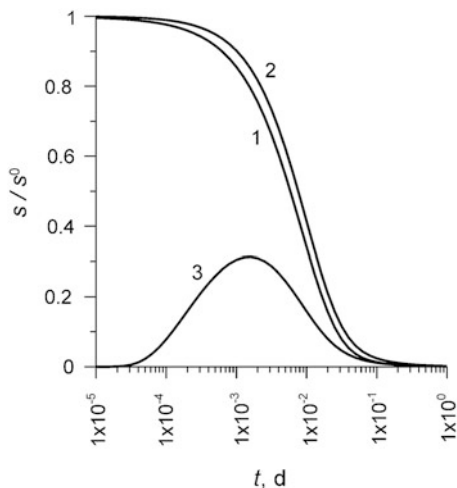


Fig. 12.30 Normalized water-level recovery versus time for a slug test: Cooper solution for the tested well (Eq. 9.1)—an instantaneous change in the initial water level (*curve 1*); Picking solution (Eq. 9.5), taking into account a delay in the change in initial level (*curve 2*); Cooper solution of an observation well (*curve 3*) (Eq. 9.3)

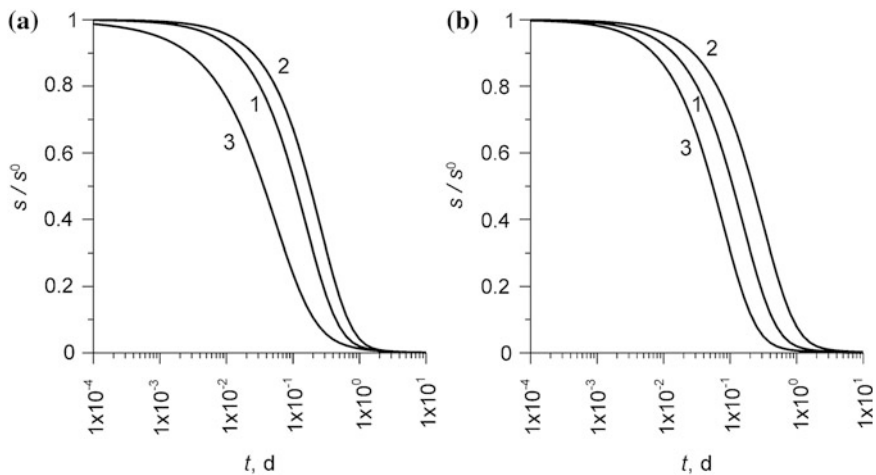


Fig. 12.31 Normalized water-level recovery versus time for slug tests. The effect of hydraulic characteristics: **a** storage coefficient ($S_2 < S_1 < S_3$); **b** transmissivity ($T_2 < T_1 < T_3$). The numbers at the *curves* (1, 2, 3) correspond to the subscripts at hydraulic characteristics

were constructed for different reference points of recovery measurement (see Chap. 11), i.e., from the start of pumping (Fig. 12.32) and from the end of pumping (Fig. 12.33).

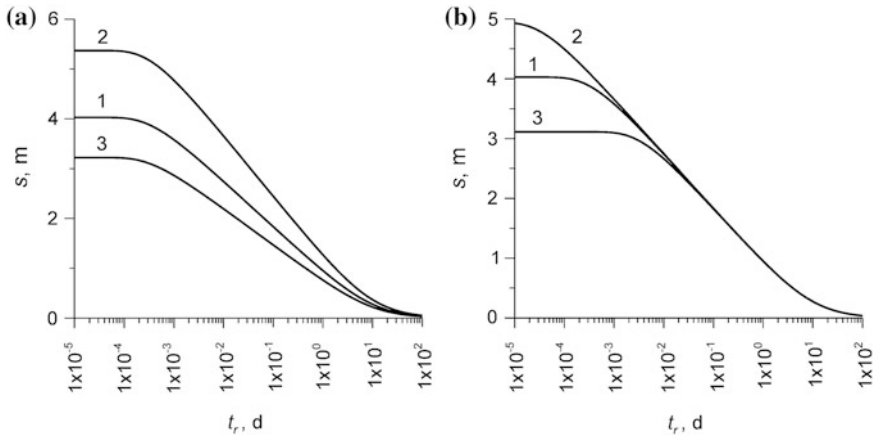


Fig. 12.32 The effect of hydraulic characteristics on recovery (the water level is measured from the start of pumping) (Eq. 11.9): **a** transmissivity ($T_2 < T_1 < T_3$); **b** storage coefficient (or hydraulic diffusivity) ($S_2 < S_1 < S_3$ or $a_3 < a_1 < a_2$). The numbers at the curves (1, 2, 3) correspond to the subscripts at hydraulic characteristics. t_r is time measured from the start of recovery

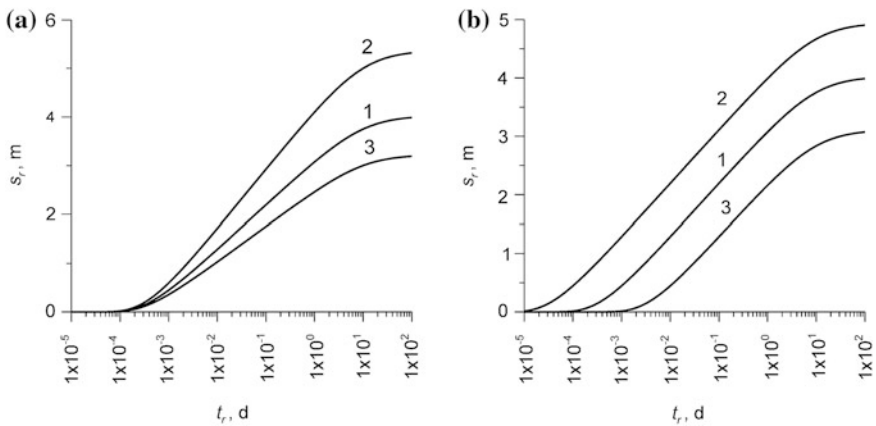


Fig. 12.33 The effect of hydraulic characteristics on recovery (the water level is measured from the end of pumping) (Eq. 11.12): **a** transmissivity ($T_2 < T_1 < T_3$); **b** storage coefficient (or hydraulic diffusivity) ($S_2 < S_1 < S_3$ or $a_3 < a_1 < a_2$). The numbers at the curves (1, 2, 3) correspond to the subscripts at hydraulic characteristics. s_r is level recovery measured from the dynamic level at the moment when pumping was stopped

References

Cooper HH, Jacob CE (1946) A generalized graphical method for evaluating formation constants and summarizing well-field history. EOS T Am Geophys Un 27(4):526–534
 Ferris JG, Knowles DB, Brown RN, Stallman RW (1962) Theory of aquifer test. U.S. Geological Survey Water-Supply, paper 1536-E

- Jacob CE (1946) Effective radius of drawdown test to determine artesian well. *J Hydr Eng Div-ASCE* 72(5):629–646
- Poeter EP, Hill MC, Banta ER, Mehl S, Christensen S (2005) UCODE_2005 and six other computer codes for universal sensitivity analysis, calibration, and uncertainty evaluation. Techniques and methods 6-A11. U.S. Geological Survey, Reston, Virginia
- Shtengelov RS (ed) (1994) Computer hydrodynamic calculations. MSU, Moscow (In Russian)
- Sindalovskiy LN (2006) Handbook of analytical solutions for aquifer test analysis. SpBSU, Sankt-Petersburg (In Russian)
- Sindalovskiy LN (2014) Analytical modeling of aquifer tests and well systems (ANSDIMAT software guide). Nauka, Sankt-Petersburg (In Russian)
- Theis CV (1935) The relation between the lowering of the piezometric surface and the rate and duration of discharge of a well using ground-water storage. *EOS T Am Geophys Un* 16 (2):519–524

Chapter 13

Analytical Solutions for Complex Engineering Problems

The basic analytical relationships and methods proposed in this study for processing aquifer test data were implemented and tested in ANSDIMAT software (**A**nalytical and **N**umerical **S**olutions **D**irect and **I**nverse **M**ethods for **A**quifer **T**est) (Sindalovskiy 2014). The main function of this software is the evaluation of the hydraulic characteristics of aquifers subject to pumpage from wells. An important supplement to this is a function of the software, enabling analytical evaluation of aquifer characteristics based on monitoring data, where the source of perturbation is variations in the surface level of a water body.

In addition, the software provides a number of interesting and useful functions aimed at solving engineering–hydrogeological problems, such as design calculations for a system of interacting wells in the software module of analytical simulations, evaluation of water inflow into open pits, design calculations of well drainage, and wellhead protection areas. The solution of these problems is based on groundwater flow equations describing the water flow toward wells. Taken together with other options of the program (including numerical simulation of axially symmetric problems; prompt calculation of expected drawdown under typical conditions; auxiliary expert calculations; databases on hydraulic characteristics; evaluation of special functions; online unit conversions; and many others), this makes ANSDIMAT a comprehensive and up-to-date instrument indispensable in the everyday work of hydrogeologists.

This book is focused primarily on solutions related for processing aquifer tests, while not intended to give a detail description of the software and the problems it can solve. This chapter considers the analytical solutions incorporated in ANSDIMAT and not discussed in previous chapters. These are solutions for parameter evaluations based on data on aquifer response to fluctuation in the river stage (Sect. 13.1) and for the calculation of water inflow into open pits (Sect. 13.3). The chapter also gives brief information on an alternative approach to simulating well systems (Sect. 13.3), which considerably simplifies the solution of complex engineering problems.

13.1 Evaluation of Groundwater Response to Stream-Stage Variation

The objective is to evaluate the hydraulic characteristics of aquifers based on data on groundwater-level monitoring, reflecting level variations in observation wells caused by variations in the surface level of a water body (e.g., in a river). The conditions considered include an instantaneous rise or drop of water level in a river (Sect. 13.1.1) or step-wise level changes (Sect. 13.1.2).

Here, as well as in the case with common testing, the calculations take into account various factors, including the effect of boundaries, leakage, retardation by semipervious streambeds, etc. Analytical solutions are given for semi-infinite and bounded nonleaky and leaky confined aquifers. For guides for correcting solutions for unconfined aquifers, see Eqs. 13.12 and 13.13. The bounded aquifers include the strip aquifer, which has two boundaries, one of which is a river and the other is an impermeable boundary; and the quadrant aquifer with two perpendicular rivers with the same characteristics and synchronous level variations.

The transient solutions for stream-aquifer interaction make it possible to evaluate aquifer hydraulic diffusivity (a) and, under appropriate conditions, the retardation coefficient of the semipervious streambed (ΔL) and the leakage factor (B).

13.1.1 Instantaneous Level Change Followed by a Steady-State Period

A stream's water level abruptly rises (or drops) by s^0 (Figs. 13.1 and 13.3) and next remains constant. The rate of water-level change in a homogeneous aquifer depends on its hydraulic diffusivity. In the case of leakage through the underlying layer (Fig. 13.3) and/or the retardation because of the semipervious streambed (Figs. 13.1b, d and 13.3b, d), groundwater dynamics experience the effect of the hydraulic properties of the aquitard underlying the aquifer, as well as the properties of the stream bank, which separates the river from the aquifer.

Basic Analytical Relationships

Transient Flow Equations

1. Nonleaky aquifers

1.1. Semi-infinite aquifer with the retardation coefficient of the semipervious streambed is not taken into account (Fig. 13.1a) (Carslow and Jaeger 1959):

$$s = s^0 \operatorname{erfc} \frac{r}{2\sqrt{at}}, \quad (13.1)$$

where s is groundwater-level change in an observation well, m; s^0 is an instantaneous initial change in river's water level, m; r is the distance from the observation

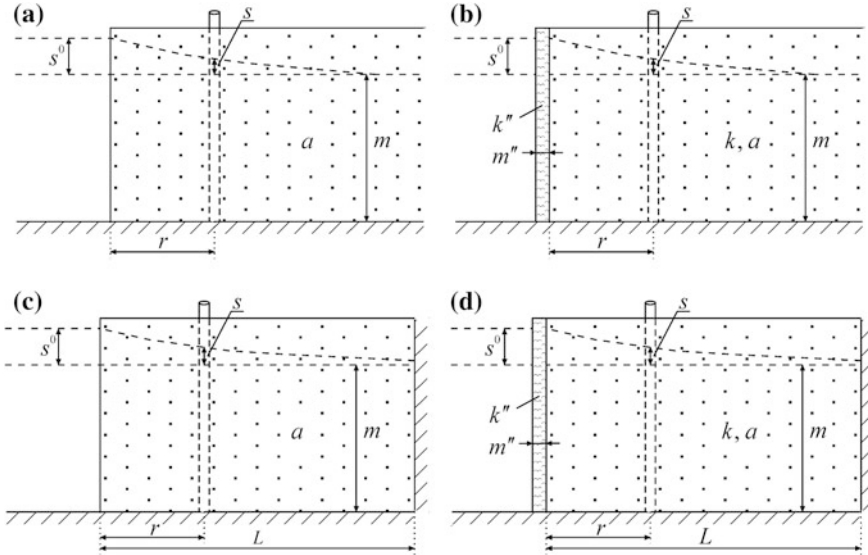


Fig. 13.1 Nonleaky aquifers. **a, b** Semi-infinite aquifers; **c, d** strip aquifers; **a, c** the hydraulic characteristics of the streambed and the aquifer are the same; **b, d** conceptual models taking into account the retardation coefficient of the semipervious streambed

well to the river, m ; a is the hydraulic diffusivity (m^2/d): in the case of a confined aquifer, $a = km/S$; for an unconfined aquifer, $a = km/S_y$; k is the hydraulic conductivity of the aquifer, m/d ; m is confined aquifer thickness or the initial water-saturated thickness of an unconfined aquifer, m ; S is the storage coefficient of a confined aquifer, dimensionless; S_y is the specific yield of an unconfined aquifer, dimensionless; t is the time elapsed since the start of perturbation in the stream, d ; $erfc(\cdot)$ is the complementary error function (see Appendix 7.12).

1.2. Semi-infinite aquifer with the retardation coefficient of the semipervious streambed taken into account (Fig. 13.1b) (Carslow and Jaeger 1959; Hall and Moench 1972):

$$s = s^0 \left[\operatorname{erfc} \frac{r}{2\sqrt{at}} - \exp\left(\frac{r}{\Delta L} + \frac{at}{\Delta L^2}\right) \operatorname{erfc}\left(\frac{r}{2\sqrt{at}} + \frac{\sqrt{at}}{\Delta L}\right) \right], \quad (13.2)$$

where $\Delta L = m''k/k''$ is the retardation coefficient, m ; k'' , m'' is the hydraulic conductivity (m/d) and thickness (m) of the semipervious streambed.

1.3. Strip aquifer with the retardation coefficient of the semipervious streambed not taken into account (Fig. 13.1c) (Cooper and Rorabough 1963; Hall and Moench 1972):

$$s = s^0 \left[1 - \frac{2}{L} \sum_{n=1}^{\infty} \frac{1}{\beta} \sin(\beta r) \exp(-\beta^2 at) \right], \tag{13.3}$$

where $\beta = \pi(2n - 1)/(2L)$; L is the distance between the river and the impermeable boundary, m.

An alternative solution (Pinder et al. 1969) is:

$$s = s^0 \sum_{n=1}^{\infty} (-1)^{n-1} \left[\operatorname{erfc} \frac{2(n-1)L+r}{2\sqrt{at}} + \operatorname{erfc} \frac{2nL-r}{2\sqrt{at}} \right]. \tag{13.4}$$

1.4. Strip aquifer with the retardation coefficient of the semipervious streambed taken into account (Fig. 13.1d) (Carslow and Jaeger 1959; Hall and Moench 1972):

$$s = s^0 \left[1 - \frac{2L}{\Delta L} \sum_{n=1}^{\infty} \frac{\exp(-\gamma_n^2 at/L^2) \cos(\gamma_n[1-r/L])}{\left(\gamma_n^2 + (L/\Delta L)^2 + L/\Delta L\right) \cos \gamma_n} \right], \tag{13.5}$$

where γ_n are positive roots of the equation $\gamma \tan \gamma = L/\Delta L$ (see Appendix 7.15).

1.5. Aquifer–quadrant with the retardation coefficient of the semipervious streambed not taken into account (Figs. 13.1a and 13.2a) (Shestakov 1965):

$$s = s^0 \left[1 - \operatorname{erf} \frac{r}{2\sqrt{at}} \operatorname{erf} \frac{r_2}{2\sqrt{at}} \right], \tag{13.6}$$

where r_2 is the distance from the observation well to the second stream, m; $\operatorname{erf}(\cdot)$ is the error function (see Appendix 7.12).

1.6. Aquifer–quadrant with the retardation coefficient of the semipervious streambed taken into account (Figs. 13.1b and 13.2b):

$$s = s^0 \left[1 - \operatorname{erf} \frac{r}{2\sqrt{at}} \operatorname{erf} \frac{r_2}{2\sqrt{at}} - \exp\left(\frac{r}{\Delta L} + \frac{at}{\Delta L^2}\right) \operatorname{erfc}\left(\frac{r}{2\sqrt{at}} + \frac{\sqrt{at}}{\Delta L}\right) - \exp\left(\frac{r_2}{\Delta L} + \frac{at}{\Delta L^2}\right) \operatorname{erfc}\left(\frac{r_2}{2\sqrt{at}} + \frac{\sqrt{at}}{\Delta L}\right) \right]. \tag{13.7}$$

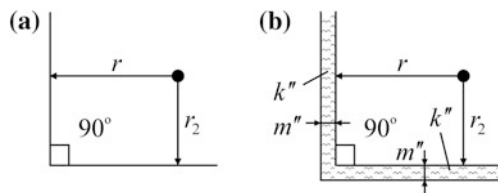


Fig. 13.2 A planar view of an aquifer-quadrant. **a** The hydraulic properties of streambed and the aquifer are the same; **b** a conceptual model with the retardation coefficient of the semipervious streambed taken into account

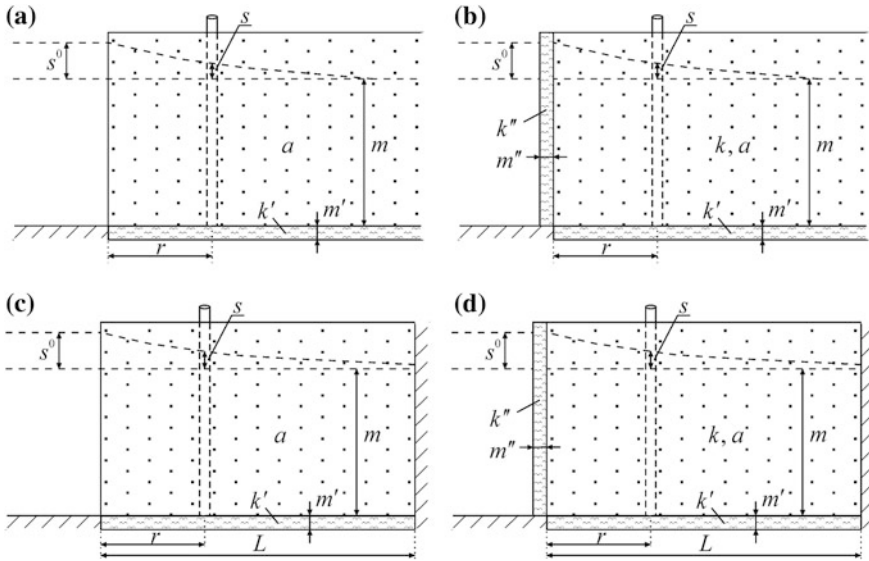


Fig. 13.3 Leaky aquifers. **a, b** Semi-infinite aquifers; **c, d** strip aquifers; **a, c** the hydraulic characteristics of river bed and the aquifer are the same; **b, d** conceptual models with the retardation coefficient of the semipervious streambed taken into account

2. Leaky aquifers (Teloglou and Bansal 2012)

2.1. Semi-infinite aquifer with the retardation coefficient of the semipervious streambed not taken into account (Fig. 13.3a):

$$s = \frac{s^0}{2} \left[\exp(-r/B) \operatorname{erfc} \frac{r - 2at/B}{2\sqrt{at}} + \exp(r/B) \operatorname{erfc} \frac{r + 2at/B}{2\sqrt{at}} \right], \quad (13.8)$$

where $B = \sqrt{kmm'/k'}$ is the leakage factor, m , k' , m' are the hydraulic conductivity (m/d) and thickness (m) of the aquitard.

2.2. Semi-infinite aquifer with the retardation coefficient of the semipervious streambed taken into account (Fig. 13.3b):

$$s = s^0 \left\{ \frac{1}{2} \left[\frac{\exp(-r/B) \operatorname{erfc} \frac{r - 2at/B}{2\sqrt{at}}}{1 + \Delta L/B} + \frac{\exp(r/B) \operatorname{erfc} \frac{r + 2at/B}{2\sqrt{at}}}{1 - \Delta L/B} \right] - \frac{\exp[r/\Delta L + (1 - \Delta L^2/B^2)at/\Delta L^2] \operatorname{erfc} \frac{r + 2at/\Delta L}{2\sqrt{at}}}{1 - \Delta L^2/B^2} \right\}. \quad (13.9)$$

In Eq. 13.9, the retardation coefficient of the semipervious streambed cannot be equal to the leakage factor, i.e., $\Delta L \neq B$.

2.3. Strip aquifer with the retardation coefficient of the semipervious streambed not taken into account (Fig. 13.3c):

$$s = s^0 \left\{ \frac{\cosh \frac{L-r}{B}}{\cosh \frac{L}{B}} - 2 \sum_{n=1}^{\infty} \frac{\gamma_n \cos[\gamma_n(1-r/L)] \exp[-(L^2/B^2 + \gamma_n^2)at/L^2]}{(\gamma_n^2 + L^2/B^2) \sin \gamma_n} \right\}, \tag{13.10}$$

here, γ_n are the positive roots of the equation $\gamma \tan \gamma \rightarrow \infty$ (see Appendix 7.15). These roots are $\gamma_n = \pi/2 \cdot (2n - 1)$.

2.4. Strip aquifer with the retardation coefficient of the semipervious streambed taken into account (Fig. 13.3d):

$$s = s^0 \left\{ \frac{\cosh \frac{L-r}{B}}{\frac{\Delta L}{B} \sinh \frac{L}{B} + \cosh \frac{L}{B}} - \frac{2L}{\Delta L} \sum_{n=1}^{\infty} \frac{\gamma_n^2 \cos[\gamma_n(1-r/L)] \exp[-(L^2/B^2 + \gamma_n^2)at/L^2]}{(\gamma_n^2 + L/\Delta L + L^2/\Delta L^2)(\gamma_n^2 + L^2/B^2) \cos \gamma_n} \right\}, \tag{13.11}$$

3. Unconfined aquifers

Equations 13.1–13.11 are given for confined or unconfined aquifers where groundwater-level changes are insignificant compared with the initial water-saturated thickness. In other cases, the equations are written in the following manner (Marino 1973): for an instantaneous rise in river-water level:

$$s = \sqrt{m^2 + s^0(2m + s^0)f(r, t)} - m \tag{13.12}$$

and for an instantaneous drop in river-water level:

$$s = m - \sqrt{m^2 - s^0(2m - s^0)f(r, t)}, \tag{13.13}$$

where m is the initial water-saturated thickness of the unconfined aquifer, $m; f(r, t)$ is a function describing level variations in the aquifer.

For example, level rise in an observation well located in a semi-infinite unconfined aquifer (Fig. 13.1a) can be calculated as:

$$s = \sqrt{m^2 + s^0(2m + s^0)\text{erfc} \frac{r}{2\sqrt{at}}} - m. \tag{13.14}$$

Equations for a Steady-State Flow Period (for leaky aquifers) (Teloglou and Bansal 2012)

1. Semi-infinite aquifer with the retardation coefficient of the semipervious streambed not taken into account (Fig. 13.3a):

$$s = s^0 \exp(-r/B). \tag{13.15}$$

2. Semi-infinite aquifer with the retardation coefficient of the semipervious streambed taken into account (Fig. 13.3b):

$$s = s^0 \frac{\exp(-r/B)}{1 + \Delta L/B}. \tag{13.16}$$

3. Strip aquifer with the retardation coefficient of the semipervious streambed not taken into account (Fig. 13.3c):

$$s = s^0 \cosh \frac{L-r}{B} / \cosh \frac{L}{B}. \tag{13.17}$$

4. Strip aquifer with the retardation coefficient of the semipervious streambed taken into account (Fig. 13.3d):

$$s = s^0 \frac{\cosh \frac{L-r}{B}}{\frac{\Delta L}{B} \sinh \frac{L}{B} + \cosh \frac{L}{B}}. \tag{13.18}$$

13.1.2 Multi-stage or Gradual Level Changes

The equations proposed in Sect. 13.1.1 imply an instantaneous change in river level by s^0 . In the case of level oscillations (Fig. 13.4a), the interaction between a river and an aquifer can be described by a general equation, which is based on transient relationships for a single perturbation and the principle of superposition:

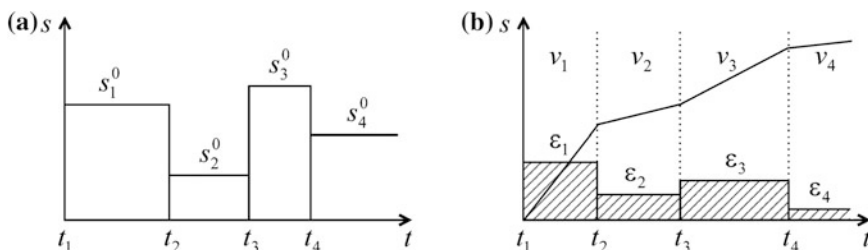


Fig. 13.4 Examples of plots of river-level changes: **a** step-wise; **b** level change with a variable rate (the rate v_j is constant within a time interval). The *hatched rectangles* show the values of recharge (ϵ_j) for time intervals. j is stage number

$$s = \sum_{j=1}^{n_t} (s_j^0 - s_{j-1}^0) \cdot f[r, (t - t_j)], \quad (13.19)$$

where $f(r, t)$ is a function describing level variations in the aquifer (see Sect. 13.1.1); n_t is the number of water level change stages by moment t ; s_j^0 is the height of the j th stage of river level change ($s_0^0 = 0$), m; t is the time elapsed from the first perturbation in the river, d; t_j is the moment of the start of the j th stage ($t_1 = 0$), d.

For example, level change in a semi-infinite aquifer (Fig. 13.1a) at such variations can be calculated as

$$s = \sum_{j=1}^{n_t} (s_j^0 - s_{j-1}^0) \cdot \operatorname{erfc} \frac{r}{2\sqrt{a(t - t_j)}}. \quad (13.20)$$

Equation 13.1 implies instantaneous changes in river level. In the case of a gradual rise (drop) of the level at a constant rate, the water-level change in an aquifer can be calculated as (Bochever et al. 1969)

$$s = vt \cdot 4i^2 \operatorname{erfc} \frac{r}{2\sqrt{at}} \quad (13.21)$$

or, with infiltration recharge taken into account:

$$s = vt \cdot 4i^2 \operatorname{erfc} \frac{r}{2\sqrt{at}} + \frac{\varepsilon t}{S} \left(1 - 4i^2 \operatorname{erfc} \frac{r}{2\sqrt{at}} \right), \quad (13.22)$$

where v is the constant rate of level rise (drop) in the river, m/d; ε is recharge, m/d; $i^2 \operatorname{erfc}(\cdot)$ is an iterated integral of the complementary error function (see Appendix 7.12).

When the rate of level rise is a step function (remaining constant during some time intervals) (Fig. 13.4b), the equation for level variations in the aquifer can be written as:

$$s = \sum_{j=1}^{n_t} \left[(v_j - v_{j-1})(t - t_j) 4i^2 \operatorname{erfc} \frac{r}{2\sqrt{a(t - t_j)}} + \frac{1}{S} (\varepsilon_j - \varepsilon_{j-1})(t - t_j) \left(1 - 4i^2 \operatorname{erfc} \frac{r}{2\sqrt{a(t - t_j)}} \right) \right], \quad (13.23)$$

where v_j is the j th stage of level rise (drop) in the stream ($v_0 = 0$), m/d; ε_j is the j th stage of recharge ($\varepsilon_0 = 0$), m/d.

Equation 13.23 implies synchronous changes in the level rise (drop) rate and the recharge value (Fig. 13.4b).

13.2 Analytical Modeling

The problems of groundwater dynamics in terms of the aquifer system's response to wellfield operation are commonly solved with the use of models based on numerical methods for solving differential equations. The obvious advantages of numerical models and methods in solving various hydrogeological problems are widely known. These include, primarily: the incorporation of various initial and boundary conditions; the description of arbitrary geological heterogeneity and nonlinear boundaries of groundwater flow; the simulation of complex hydrogeological sections with intercalation of aquifers and their wedging out; the inclusion of natural and anthropogenic factors that have their effect on the hydrodynamics; and many others.

The drawbacks of numerical models include, in particular: the dependence of the result on the model domain discretization and the choice of time step; the effect of model domain boundaries on groundwater flow; the difficulties in the validation of the obtained result and its possible ambiguity; and the problems with simulating pumping wells (especially in regional-scale problems). Another disadvantage is the considerable time required to develop a numerical model and the necessary experience in dealing with simulation programs.

In many cases, the lack of data on the study object requires the researcher to schematize and simplify the hydrogeological conditions, neglecting the complexity of the subsurface environment. Under such conditions, the use of full-fledge numerical models can be unjustified and, in some cases, erroneous.

ANSDIMAT software implements an alternative approach to well-systems simulation. This approach is based on the development of simplified hydrodynamic models underlain by the solutions of well-known groundwater flow equations (Theis 1935; Hantush 1964; Neuman 1972; Moench 1993; etc.) and the principle of superposition (see Sect. 10.2). In other words, this approach can be referred to as analytical modeling, i.e., basic analytical solutions are used to simulate the response of aquifers to pumping under standard geological conditions.

The analytical model works within a specified structure: confined aquifer, unconfined aquifer, leaky aquifer, horizontally heterogeneous aquifers, etc. The effect of linear boundaries of groundwater flow can be taken into account (Fig. 13.5). This means that an analytical model can be used in the cases where the natural hydrogeological situation can be schematized to simple standard conditions.

Analytical modeling can be of use for the hydrogeologists involved in assessing groundwater resources, planning and implementing pumping tests, designing large and small-size water supply systems, as well as assessing the mutual interaction of these systems in operation and their environmental effects. Such an approach to simulation provides the researcher with an instrument for prompt and descriptive choice of the optimal number and layout of wells, the evaluation of maximal

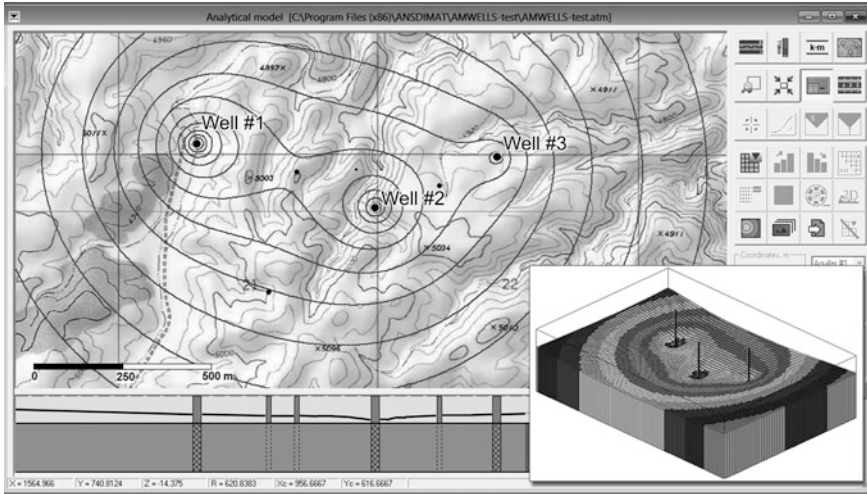


Fig. 13.5 ANSDIMAT software graphical interface window showing the predicted drawdown map and profile

drawdown at likely discharge rates of the pumping wells, and the assessment of the duration of pumping test and its range of influence.

The major advantage of analytical modeling is the absolute accuracy of the estimated level change in either pumping well or any point within the model domain. Also important in this case is the correct simulation of flows in infinite domains, whereas the results of numerical simulation may contain considerable errors because of incorrectly specified model domain boundaries. The analytical models do not require discretization in space or time, thus making the development and use of models much simpler.

The drawbacks of such models are the limited number of standard situations and the impossible specification of complex groundwater-flow boundaries.

As mentioned above, the analytical modeling of well systems is based on the fundamental transient groundwater flow equations and the principle of superposition. Any such equation describes water-level changes in an aquifer under the effect of a single constant-discharge well, while the superposition incorporates the effect of any number of wells, variations of their discharge, and groundwater-flow boundaries (see Figs. 10.1 and 10.2). This reasoning can be expressed by the general Eq. 10.23.

Groundwater flows in different zones of heterogeneous or layered aquifers within one model domain can be described by different analytical equations. For example, in the case of horizontally heterogeneous aquifers (see Sect. 4.1), the drawdown in the main and adjacent zones is described by two different formulas

(Maksimov 1962; Fenske 1984). For a leaky aquifer system with the drawdown in an adjacent aquifer and aquitard storage taken into account (see Sect. 3.3), three formulas are used in the calculations (Neuman and Witherspoon 1969). Each of them separately describes level changes in the pumped aquifer, the unpumped aquifer, and the aquitard.

The development of analytical models in the ANSDIMAT environment is relatively simple, comprising three stages: (1) the choice of a typical conceptual model (including boundary conditions), which will be used by the program to automatically generate a three-dimensional model domain; (2) the specification of the thicknesses and hydraulic characteristics of the aquifers and aquitards; and (3) the location of pumping wells in the model domain and the assignment of their discharges (either constant or variable). This is quite enough for achieving the final result: to visualize water-level variations at any point in the model domain, to find the maximal drawdown, and to construct the time–drawdown plot and a map of the groundwater’s potentiometric surface.

The incorporation in the model of the active porosity of aquifer material, as well as the gradient of natural groundwater flow and its direction, enables analytical simulation models to be used to solve simple solute transport problems: e.g., to calculate the trajectories and travel times of conservative particles, starting from any point of the model domain, and to delineate the wellhead protection areas for arbitrarily distributed groundwater-intake facilities.

With the allocation of a contour of an open pit in the model domain, water inflow into the pit can be evaluated, drainage wells distribution can be designed, and their discharges required for draining the pit can be evaluated.

13.3 Simplified Analytical Relationships for Assessing Water Inflow into an Open Pit

The evaluation of water inflow into open pits requires preliminary schematization of the geological section and, specification of groundwater flow boundaries (if any) with appropriate boundary conditions.

The basic assumptions and conditions (Fig. 13.6) are:

- the aquifer is confined, unconfined, or confined–unconfined; in any of the three cases, the leakage from the underlying layer can also be considered;
- five configurations of flow domain are considered: infinite aquifer, semi-infinite aquifer, strip aquifer, quadrant aquifer, and circular aquifer;
- two variants of boundary conditions are considered: constant-head and impermeable boundaries.

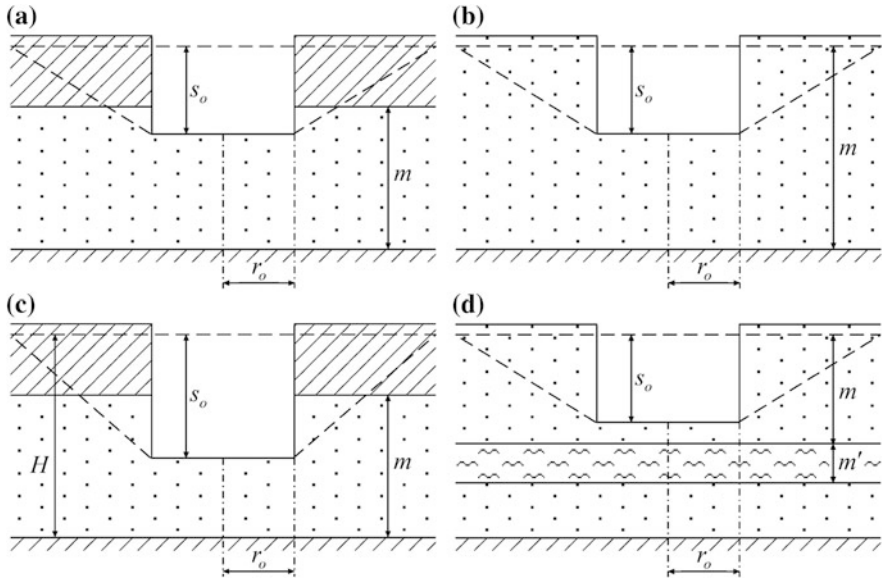


Fig. 13.6 Schematic diagrams for calculating water inflow into an open pit. **a** Confined aquifer; **b** unconfined aquifer; **c** confined–unconfined aquifer; **d** an example of pit location in a leaky unconfined aquifer

13.3.1 Effective Open Pit Radius

Water inflow into a pit depends on its radius, as the pit is assumed circular. In the case of arbitrary shape (Fig. 13.7), an effective pit radius needs to be introduced depending on the configuration of the outer contour of the pit.

There are several formulas for evaluating effective pit radius.

1. Nonelongated pit (Fig. 13.7a), $b/d > 0.5$. An estimate of the effective radius by pit area (Trojanskiy et al. 1956):

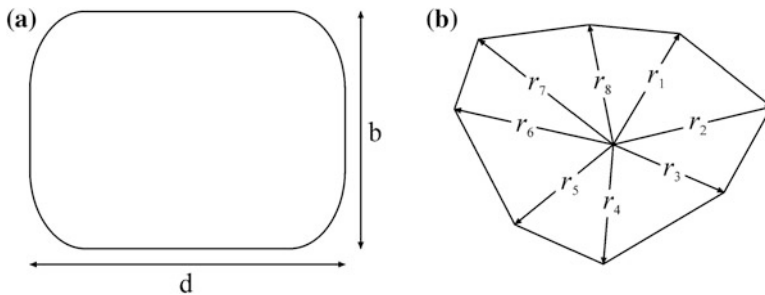


Fig. 13.7 Schematic diagrams for evaluating an effective pit radius: examples of pit contours of **a** simple and **b** complex shape

Table 13.1 The values of function η

b/d	0.05	0.1	0.2	0.3	0.4	0.5
η	1.05	1.08	1.12	1.144	1.16	1.174

$$r_o = \sqrt{F/\pi} \quad (13.24)$$

or by pit perimeter (Mironenko et al. 1965):

$$r_o = P/(2\pi), \quad (13.25)$$

where r_o is the effective pit radius, m; d , b are pit length and width, respectively, m; F is pit area, m^2 ; P is pit perimeter, m.

2. Elongated pit, $b/d \leq 0.5$. An estimate of the effective radius by the formula (Mironenko et al. 1965):

$$r_o = \frac{\eta}{4}(d+b), \quad (13.26)$$

where η is a tabulated function of b/d ratio (Table 13.1).

Function η can be approximated by a polynomial (the author's approximation):

$$\eta = -5.1183 \cdot x^4 + 7.1598 \cdot x^3 - 3.8585 \cdot x^2 + 1.1255 \cdot x + 1.0007, \quad (13.27)$$

where $x = b/d$.

3. A complex-shape pit (Fig. 13.7b). An estimate of effective radius by distances from characteristic points on the pit contour (Mironenko et al. 1965):

$$\lg r_o = \frac{1}{n} \sum_{i=1}^n \lg r_i, \quad (13.28)$$

where r_i is the distance from a chosen point (e.g., pit center) to a characteristic point on the pit perimeter (e.g., an angular point), m; n is the number of characteristic points on the pit contour.

13.3.2 The Radius of Influence for Infinite Nonleaky Aquifers

An important characteristic in the calculation of water inflow into open pits is the radius of influence. The radius of influence for limited aquifers can be evaluated analytically, depending on the type of boundary (linear, circular, etc.) and the boundary condition, while, in the case of an infinite nonleaky aquifer, the estimate of the range is ambiguous.

There are several formulas for evaluating the radius of influence.

1. The radius of pit influence for transient groundwater flow (Mironenko et al. 1965) is:

$$R_o = r_o + \sqrt{\pi at}, \quad (13.29)$$

where R_o is the radius of influence, m; a is hydraulic diffusivity, m^2/d ; t is the time elapsed since the start of drainage system operation, d.

2. An estimate of the radius of influence based on the recharge rate (Mironenko et al. 1965):

$$R_o \sqrt{\lg R_o - \lg r_o - 0.217} = 0.66 \sqrt{\frac{k}{\varepsilon} (2m - s_o) s_o - 0.5r_o}, \quad (13.30)$$

where k is hydraulic conductivity, m/d ; s_o is the drawdown at a pit outline, m; m is the initial water-saturated thickness of the unconfined aquifer, m; ε is recharge rate, m/d .

3. Estimating the radius of influence by the drawdown in an observation well located at some distance from the pit (Trojanskiy et al. 1956):
in the case of a confined aquifer:

$$R_o = \exp \frac{s_o \ln r - s \ln r_o}{s_o - s}, \quad (13.31)$$

in the case of an unconfined aquifer:

$$R_o = \exp \frac{s_o(2m - s_o) \ln r - s(2m - s) \ln r_o}{s_o(2m - s_o) - s(2m - s)}, \quad (13.32)$$

in the case of a confined–unconfined aquifer:

$$R_o = \exp \frac{\left[(2H - m)m - (H - s_o)^2 \right] \ln r - \left[(2H - m)m - (H - s)^2 \right] \ln r_o}{(H - s)^2 - (H - s_o)^2}, \quad (13.33)$$

where r is the distance from the observation well to pit center, m; s is the drawdown in the observation well, m; H is the initial head in the confined–unconfined aquifer, measured from its bottom (Fig. 13.6c), m.

13.3.3 Estimating Water Inflow into an Open Pit

This section gives basic analytical relationships for evaluating water inflow (Q) into open pits and the drawdown (s_o) in a pit given the inflow (Q). The solutions imply the pit to be fully penetrating. The partial penetration of a pit should be taken into account when its radius is less than the aquifer thickness and the penetration depth is less than half the aquifer thickness. The analytical relationships for such cases are derived from equations described in Sects. 1.3.3.1, 2.1, and 3.4.

Given water inflow Q into a pit and the drawdown s_o , a new inflow Q_n at any design drawdown s_{on} can be evaluated (Trojanskiy et al. 1956): for a confined aquifer (Fig. 13.6a):

$$Q_n = Q \frac{s_{on}}{s_o} \quad (13.34)$$

and for an unconfined aquifer (Fig. 13.6b):

$$Q_n = Q \frac{(2m - s_{on})s_{on}}{(2m - s_o)s_o}. \quad (13.35)$$

13.3.3.1 Nonleaky Aquifers

The solutions considered can be used to assess water inflow into a pit and the drawdown at the pit outline in the absence of leakage from adjacent aquifers (Fig. 13.6a, b, c).

Basic Analytical Relationships

Estimating water inflow and drawdown for a pit in a confined aquifer (Fig. 13.6a) (Trojanskiy et al. 1956):

$$Q = 2\pi km \frac{s_o}{\ln R_o - \ln r_o}, \quad (13.36)$$

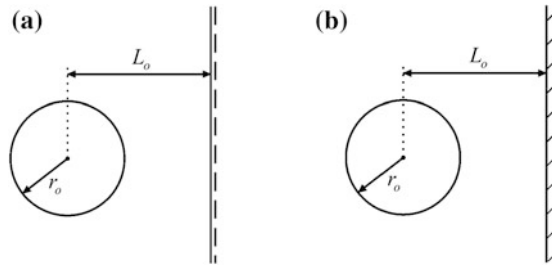
$$s_o = \frac{Q}{2\pi km} \ln \frac{R_o}{r_o}; \quad (13.37)$$

unconfined aquifer (Fig. 13.6b) (Trojanskiy et al. 1956):

$$Q = \pi k \frac{(2m - s_o)s_o}{\ln R_o - \ln r_o}, \quad (13.38)$$

$$s_o = m - \sqrt{m^2 - \frac{Q}{\pi k} \ln \frac{R_o}{r_o}}; \quad (13.39)$$

Fig. 13.8 Semi-infinite aquifer: the pit is located near
a a constant-head and
b impermeable boundary



and confined–unconfined aquifer (Fig. 13.6c) (Mironenko et al. 1965):

$$Q = \pi k \frac{(2H - m)m - (H - s_o)^2}{\ln R_o - \ln r_o}, \quad (13.40)$$

$$s_o = H - \sqrt{(2H - m)m - \frac{Q}{\pi k} \ln \frac{R_o}{r_o}}. \quad (13.41)$$

The radius of influence R_o in Eqs. 13.36–13.41 depends on whether the groundwater flow is bounded and on the boundary conditions.

1. Aquifers of infinite lateral extent: the radius of influence is determined by a formula from Eqs. 13.29–13.33.

2. Semi-infinite aquifers (Fig. 13.8)

2.1. Constant-head boundary (Fig. 13.8a) (Mironenko et al. 1965):

$$R_o = 2L_o, \quad (13.42)$$

where L_o is the distance from the pit center to the boundary, m . A more accurate formula can be derived from Eq. 1.14:

$$R_o = \sqrt{r_o^2 + 4L_o^2}, \quad (13.43)$$

2.2. Impermeable boundary (Fig. 13.8b): Eq. 1.16 yields:

$$R_o = \frac{2.25at}{\sqrt{r_o^2 + 4L_o^2}}, \quad (13.44)$$

3. Strip aquifer (Fig. 13.9)

3.1. Constant-head boundaries (Fig. 13.9a) (Mironenko et al. 1965):

$$R_o = \frac{2}{\pi} L \sin \frac{\pi L_o}{L}, \quad (13.45)$$

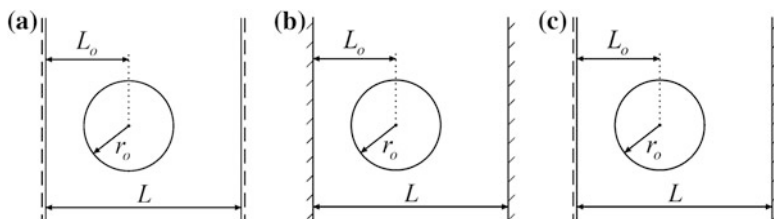


Fig. 13.9 Strip aquifer: the location of a pit between two parallel boundaries. **a** Constant-head boundaries, **b** impermeable boundaries, and **c** constant-head and impermeable boundaries. L is the width of the strip aquifer

where L is strip-aquifer width, m . An alternative formula can be derived from Eq. 1.22:

$$R_o = r_o \sqrt{\frac{\cosh \frac{\pi r_o}{L} - \cos \frac{2\pi L_o}{L}}{\cosh \frac{\pi r_o}{L} - 1}} \tag{13.46}$$

3.2. Impermeable boundaries (Fig. 13.9b): Eq. 1.26 yields

$$R_o = r_o \exp \left\{ \frac{\sqrt{\pi}}{L} \left[\exp \left(-\frac{r_o^2}{4at} \right) \sqrt{4at} - \sqrt{\pi} r_o \operatorname{erfc} \sqrt{\frac{r_o^2}{4at}} \right] + \sum_{n=1}^{\infty} \frac{1}{n} \cos^2 \frac{n\pi L_o}{L} \left[\exp \left(-\frac{n\pi r_o}{L} \right) \operatorname{erfc} \left(\sqrt{\frac{r_o^2}{4at} - \frac{n\pi\sqrt{at}}{L}} \right) - \exp \left(\frac{n\pi r_o}{L} \right) \operatorname{erfc} \left(\sqrt{\frac{r_o^2}{4at} + \frac{n\pi\sqrt{at}}{L}} \right) \right] \right\} \tag{13.47}$$

3.3. Constant-head and impermeable boundaries (Fig. 13.9c) (Mironenko et al. 1965):

$$R_o = \frac{4}{\pi} L \tan \frac{\pi L_o}{2L} \tag{13.48}$$

An alternative formula can be derived from Eq. 1.31:

$$R_o = r_o \sqrt{\frac{\left[\cosh \frac{\pi r_o}{2L} - \cos \frac{\pi L_o}{L} \right] \left[\cosh \frac{\pi r_o}{2L} + 1 \right]}{\left[\cosh \frac{\pi r_o}{2L} + \cos \frac{\pi L_o}{L} \right] \left[\cosh \frac{\pi r_o}{2L} - 1 \right]}}, \tag{13.49}$$

here, L_o is the distance from pit center to the constant-head boundary, m .

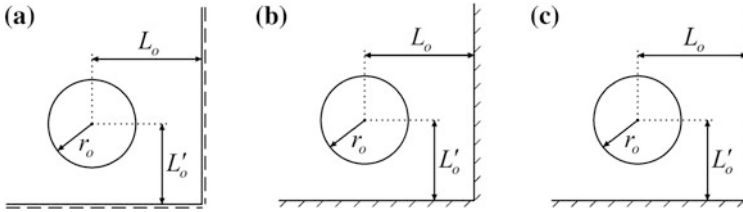


Fig. 13.10 Aquifer-quadrant: a pit located in a corner between perpendicular boundaries. **a** Constant-head boundaries, **b** impermeable boundaries, and **c** constant-head and impermeable boundaries

4. Aquifer-quadrant (Fig. 13.10)

4.1. Constant-head boundaries (Fig. 13.10a) (Mironenko et al. 1965):

$$R_o = \frac{2L_oL'_o}{\sqrt{L_o^2 + L_o'^2}}, \tag{13.50}$$

where L'_o is the distance from the pit center to the second boundary (in the case of mixed boundary conditions, to the impermeable boundary), m. Equation 13.50 was derived from Eq. 1.34.

4.2. Impermeable boundaries (Fig. 13.10b): Eq. 1.37 yields

$$R_o = \frac{(2.25at)^2}{8L'_oL_o\sqrt{L_o^2 + L_o'^2}}, \tag{13.51}$$

4.3. Constant-head and impermeable boundaries (Fig. 13.10c) (Mironenko et al. 1965):

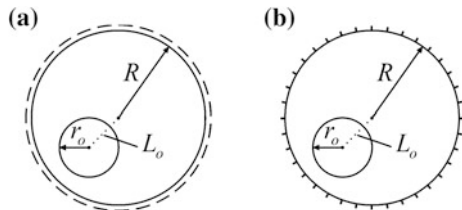
$$R_o = 2L_o\sqrt{L_o^2/L_o'^2 + 1}. \tag{13.52}$$

Formula (Eq. 13.52) was derived from Eq. 1.40.

5. Circular aquifer (Fig. 13.11)

5.1. Constant-head boundary (Fig. 13.11a) (Mironenko et al. 1965):

Fig. 13.11 Circular aquifer: a pit located within a circular aquifer with a **a** constant-head and **b** impermeable boundary. R is the radius of the circle



$$R_o = R - \frac{L_o^2}{R}, \quad (13.53)$$

where R is the radius of circular aquifer, m; L_o is the distance from pit center to circle center, m. Formula (Eq. 13.53) is derived from Eq. 1.78.

5.2. Impermeable boundary (Fig. 13.11b) (Bochever 1968):

$$R_o = \frac{0.47R^3}{\sqrt{(R^2 - L_o^2)^2 + r_o^2 R^2}}. \quad (13.54)$$

In the case of a circular aquifer with an impermeable boundary, Eq. 13.54 is substituted into the following relationships: for a confined aquifer (Fig. 13.6a):

$$Q = 2\pi km \frac{s_o + s'_o}{2at/R^2 + \ln R_o - \ln r_o}, \quad (13.55)$$

$$s_o = \frac{Q}{2\pi km} \left(\ln \frac{R_o}{r_o} + \frac{2at}{R^2} \right) - s'_o; \quad (13.56)$$

for an unconfined aquifer (Fig. 13.6b):

$$Q = \pi k \frac{(2m - s_o)s_o + 2s'_o m}{2at/R^2 + \ln R_o - \ln r_o}, \quad (13.57)$$

$$s_o = m - \sqrt{m^2 - \frac{Q}{\pi k} \left(\ln \frac{R_o}{r_o} + \frac{2at}{R^2} \right) + 2s'_o m}; \quad (13.58)$$

for a confined–unconfined aquifer (Fig. 13.6c):

$$Q = \pi k \frac{(2H - m)m - (H - s_o)^2 + 2s'_o m}{2at/R^2 + \ln R_o - \ln r_o}, \quad (13.59)$$

$$s_o = H - \sqrt{(2H - m)m - \frac{Q}{\pi k} \left(\ln \frac{R_o}{r_o} + \frac{2at}{R^2} \right) + 2s'_o m}; \quad (13.60)$$

$$s'_o = \frac{Q'}{\pi km R^2} at, \quad (13.61)$$

where s'_o is a correction for drawdown in the pit introduced to account for the additional inflow from the outer domain, m; Q' is the rate of additional inflow, m³/d.

13.3.3.2 Leaky Aquifers

Solutions for water inflow into a pit and the drawdown at the pit outline can be considered in the case of leakage from the underlying layer (Fig. 13.6d). Contrary to the nonleaky aquifers (see Sect. 13.3.3.1), formulas for water inflow include a new term, namely, a function of the radius of influence (F_R). This function is an integrated characteristic, depending on the pit radius, leakage factor, and distances to the boundaries.

Basic Analytical Relationships

Confined aquifer:

$$Q = s_o \frac{2\pi km}{F_R}, \quad (13.62)$$

$$s_o = \frac{Q}{2\pi T} F_R; \quad (13.63)$$

unconfined aquifer (Fig. 13.6d):

$$Q = \pi k \frac{(2m - s_o)s_o}{F_R}, \quad (13.64)$$

$$s_o = m - \sqrt{m^2 - \frac{Q}{\pi k} F_R}; \quad (13.65)$$

confined–unconfined aquifer:

$$Q = \pi k \frac{(2H - m)m - (H - s_o)^2}{F_R}, \quad (13.66)$$

$$s_o = H - \sqrt{(2H - m)m - \frac{Q}{\pi k} F_R}, \quad (13.67)$$

where F_R is the function of the radius of influence, dimensionless.

As was the case with a nonleaky aquifer (Sect. 13.3.3.1), solutions for water inflow into and drawdown in the pit (Eqs. 13.62–13.67) depend on whether the flow is bounded and on appropriate boundary conditions.

1. Infinite aquifers: Eq. 3.11 yields

$$F_R = K_0(r_o/B), \quad (13.68)$$

2. Semi-infinite aquifers (Fig. 13.8): Eq. 3.12 yields

$$F_R = K_0(r_o/B) \pm K_0(2L_o/B), \quad (13.69)$$

where the minus sign is for a constant-head boundary, and the plus sign, for an impermeable boundary; $K_0(\cdot)$ is modified Bessel function of the second kind of the zero order (see Appendix 7.13).

3. Strip aquifer (Fig. 13.9)

3.1. Constant-head boundaries: Eq. 3.20 yields

$$F_R = \sum_{n=1}^{\infty} \frac{2}{\beta_n} \exp\left(-\frac{\pi r_o}{L} \beta_n\right) \left(\sin \frac{n\pi L_o}{L}\right)^2, \quad \beta_n = \sqrt{n^2 + \left(\frac{L}{\pi B}\right)^2}. \quad (13.70)$$

3.2. Impermeable boundaries: Eq. 3.22 yields

$$F_R = \frac{\pi B}{L} \exp\left(-\frac{r_0}{B}\right) + \sum_{n=1}^{\infty} \frac{2}{\beta_n} \exp\left(-\frac{\pi r_0}{L}\right) \left(\cos \frac{n\pi L_o}{L}\right)^2, \quad \beta_n = \sqrt{n^2 + \left(\frac{L}{\pi B}\right)^2}. \quad (13.71)$$

3.3. Impermeable and constant-head boundaries: Eq. 3.24 yields

$$F_R = \sum_{n=1}^{\infty} (-1)^n \frac{4}{\beta_n} \exp\left(-\frac{\pi r_0}{2L}\right) \sin \frac{(2n-1)\pi(L_o-2L)}{2L} \cos \frac{(2n-1)\pi(L_o-L)}{2L}, \quad (13.72)$$

$$\beta_n = \sqrt{(2n-1)^2 + \left(\frac{2L}{\pi B}\right)^2}.$$

4. Aquifer-quadrant (Fig. 13.10):

$$F_R = K_0\left(\frac{r_o}{B}\right) \begin{array}{c} - \\ + \end{array} K_0\left(\frac{2L'_o}{B}\right) \begin{array}{c} + \\ - \end{array} K_0\left(\frac{2\sqrt{L_o^2 + L_o'^2}}{B}\right) \begin{array}{c} - \\ + \end{array} K_0\left(\frac{2L_o}{B}\right), \quad (13.73)$$

where the top signs correspond to an aquifer-quadrant with constant-head boundaries; the middle signs to impermeable boundaries; and the bottom signs to mixed boundary conditions. Equation 13.73 was derived from Eq. 3.11 and the principle of superposition.

5. Circular aquifer (Fig. 13.11)

5.1. Constant-head boundary: Eq. 3.37 yields

$$R_o = K_0\left(\frac{r_o}{B}\right) - \frac{K_0\left(\frac{R}{B}\right) I_0^2\left(\frac{L_o}{B}\right)}{I_0\left(\frac{R}{B}\right)} - 2 \sum_{m=1}^{\infty} \frac{K_m\left(\frac{R}{B}\right) I_m^2\left(\frac{L_o}{B}\right)}{I_m\left(\frac{R}{B}\right)}. \quad (13.74)$$

5.2. Impermeable boundary: Eq. 3.39 yields

$$R_o = K_0\left(\frac{r_o}{B}\right) + \frac{K_1\left(\frac{R}{B}\right) I_0^2\left(\frac{L_o}{B}\right)}{I_1\left(\frac{R}{B}\right)} + 2 \sum_{m=1}^{\infty} \frac{K_{m+1}\left(\frac{R}{B}\right) + K_{m-1}\left(\frac{R}{B}\right)}{I_{m+1}\left(\frac{R}{B}\right) + I_{m-1}\left(\frac{R}{B}\right)} I_m^2\left(\frac{L_o}{B}\right), \quad (13.75)$$

where $I_0(\cdot)$ and $I_1(\cdot)$ are modified Bessel functions of the first kind of the zero and the first order; $K_0(\cdot)$ and $K_1(\cdot)$ are modified Bessel functions of the second kind of the zero and the first order; $I_m(\cdot)$ and $K_m(\cdot)$ are modified Bessel functions of the first and the second kind of the m th order) (see Appendix 7.13).

References

- Bochever FM (1968) Theory and practical methods of groundwater yield evaluation. Nedra, Moscow (In Russian)
- Bochever FM, Garmonov IV, Lebedev AV, Shestakov VM (1969) Fundamentals of hydraulic calculations. Nedra, Moscow (In Russian)
- Carslow HS, Jaeger JC (1959) Conduction of heat in solids. Oxford at the Clarendon Press, London
- Cooper HH, Rorabough MI (1963) Ground-water movements and bank storage due to flood stages in surface streams. U.S. Geological Survey Water-Supply, paper 1536-J
- Fenske PR (1984) Unsteady drawdown in the presence of a linear discontinuity. In: Rosenshein JS, Bennett GD (eds) Groundwater hydraulics. Water resources monograph series 9. American Geophysical Union, Washington, pp 125–145
- Hall FR, Moench AF (1972) Application of the convolution equation to stream-aquifer relationship. Water Resour Res 8(2):487–493
- Hantush MS (1964) Hydraulics of wells. In: Chow VT (ed) Advances in hydroscience, vol 1. Academic Press, New York and London, pp 281–432
- Marino MA (1973) Water-table fluctuation in semipervious stream-unconfined aquifer systems. J Hydrol 19(1):43–52
- Maksimov VA (1962) On unsteady-state flow of elastic fluid to a well in heterogeneous media. J Appl Mech Tech Phys (PMTF) 3:109–112 (In Russian)
- Mironenko VA, Norvatov YuA, Bokiyy LL (1965) Groundwater flow design calculation for open pit drainage systems. Part II. VNIMI, Leningrad (In Russian)
- Moench AF (1993) Computation of type curves for flow to partially penetrating wells in water-table aquifers. Groundwater 31(6):966–971

- Neuman SP (1972) Theory of flow in unconfined aquifers considering delayed gravity response. *Water Resour Res* 8(4):1031–1045
- Neuman SP, Witherspoon PA (1969) Theory of flow in a confined two aquifer system. *Water Resour Res* 5(4):803–816
- Pinder GF, Bredehoeft JD, Cooper HH (1969) Determination of aquifer diffusivity from aquifer response to fluctuations in river stage. *Water Resour Res* 3(4):850–855
- Shestakov VM (1965) Theoretical basics of evaluation of stream-aquifer interactions, dewatering, and well drainage. MSU, Moscow (In Russian)
- Sindalovskiy LN (2014) Analytical modeling of aquifer tests and well systems (ANSDIMAT software guide). Nauka, Sankt-Petersburg (In Russian)
- Teloglou IS, Bansal RK (2012) Transient solution for stream-unconfined aquifer interaction due to time varying stream head and in the presence of leakage. *J Hydrol* 428–429:68–79
- Theis CV (1935) The relation between the lowering of the piezometric surface and the rate and duration of discharge of a well using ground-water storage. *EOS T Am Geophys Un* 16 (2):519–524
- Trojanskiy SV, Belitskiy AS, Chekin AI (1956) Groundwater hydrology and dewatering of mine fields. Ugletekhizdat, Moscow (In Russian)

Appendix 1

Hydraulic Characteristics

A major objective of pumping tests is to evaluate the hydraulic characteristics of aquifers based on data on groundwater-level changes.

This appendix describes the main hydraulic characteristics, their denotations, and dimensions, and provides brief definitions.

Hydraulic conductivity, k , m/d: *horizontal* k_r ; *vertical* k_z . This is the rate of fluid flow under unit head gradient; this characteristic depends on pore-space geometry and the fluid's hydrodynamic properties, i.e., the density and viscosity; it characterizes the ability of the soil to pass a fluid.

The hydraulic conductivity is evaluated as:

$$k = \frac{k_0 \rho_w g}{\mu}, \quad (\text{A1.1})$$

where k_0 is the permeability, i.e., the ability of a porous medium to pass a liquid, gas, or fluid mixture under pressure gradient; the permeability depends on the properties of the moving fluid and pore-space geometry, m^2 ; ρ_w is water density, kg/m^3 ; g is the acceleration of gravity, m/s^2 ; μ is fluid dynamic viscosity, $\text{kg}/(\text{m}\cdot\text{s})$.

The hydraulic conductivity is a proportionality coefficient between the Darcy flux and the head gradient. This relationship is expressed by Darcy's law (Darcy 1856):

$$v = k \frac{\Delta H}{L}, \quad (\text{A1.2})$$

where v is specific discharge (Darcy flux), m/d; ΔH is head difference, m; L is flow path length, m.

With the Darcy flux expressed as the ratio of flow rate to flow cross-section area:

$$v = \frac{Q}{w}, \quad (\text{A1.3})$$

Darcy's law becomes:

$$Q = kw \frac{\Delta H}{L}, \quad (\text{A1.4})$$

where Q is the volumetric flow rate, m^3/d ; w is flow cross-section area, m^2 .

In stratified (multilayer) aquifers with hydraulic conductivity values of individual layers varying no more than five–ten-fold, the mean hydraulic conductivity for flow along the bedding can be evaluated as:

$$\bar{k}_r = \frac{\sum_{i=1}^n k_i m_i}{\sum_{i=1}^n m_i}, \quad (\text{A1.5})$$

and for flow perpendicular to the bedding, as:

$$\bar{k}_z = \frac{\sum_{i=1}^n m_i}{\sum_{i=1}^n m_i / k_i}, \quad (\text{A1.6})$$

where n is the number of layers; k_i is the hydraulic conductivity of the i th layer, m/d ; m_i is the thickness of the i th layer, m .

Transmissivity, T , m^2/d . The discharge per cross-section of unit width in an aquifer of given thickness. It is defined as:

$$T = km, \quad (\text{A1.7})$$

where m is aquifer thickness, m .

In the case of a multilayer aquifer comprising n layers, the transmissivity is calculated as:

$$T = \sum_{i=1}^n k_i m_i. \quad (\text{A1.8})$$

In the case of irregular horizontal heterogeneity, the mean transmissivity is defined as:

$$\bar{T} = \frac{\sum_{i=1}^n T_i F_i}{\sum_{i=1}^n F_i}, \quad (\text{A1.9})$$

where T_i is the transmissivity of the i th zone, m^2/d ; F_i is the area of the i th zone, m^2 .

Specific storage, S_s , $1/\text{m}$. This is the change in water volume per unit rock or sediment (aquifer materials) volume per unit head change. The specific storage is defined as:

$$S_s = \rho_w g \left[\frac{n}{E} + (1 - n)a_c \right] = \rho_w g [nC_w + (1 - n)a_c], \quad (\text{A1.10})$$

where n is porosity; a_c is aquifer compressibility coefficient, a characteristic of the rate of pore volume decrease under increasing load, 1/Pa; $E = 1/C_w \approx 2.2 \times 10^9$ Pa is Young's modulus, Pa; C_w is water compressibility, the relative change in water density per unit change of pressure, Pa^{-1} .

For specific storage, the equality (Eq. A1.10) can also be written as

$$S_s = \rho_w g [nC_w + \alpha], \quad (\text{A1.11})$$

where $\alpha = (1 - n)a_c$ is aquifer matrix compressibility, 1/Pa.

Storage coefficient, S , dimensionless. This is a characteristic of changes in aquifer water content under its deformation at changes in the rock-stress state under the effect of hydrodynamic factors, such as head change, water withdrawal, etc. It is defined as:

$$S = S_s m. \quad (\text{A1.12})$$

The storage coefficient can also be expressed in terms of aquifer transmissivity and hydraulic diffusivity:

$$S = T/a = km/a. \quad (\text{A1.13})$$

For a multilayer aquifer, comprising n layers, the storage coefficient is calculated as:

$$S = \sum_{i=1}^n S_{si} m_i, \quad (\text{A1.14})$$

where S_{si} is the specific storage of the i th layer, 1/m.

Specific yield, S_y , dimensionless. The ratio of a change in water volume in the zone of unconfined flow to a change in the volume of this zone.

Hydraulic diffusivity, a , m^2/d . This is a characteristic of the rate of changes in the head (hydrostatic pressure) in an aquifer. It is defined as:

$$a = T/S = km/S = k/S_s, \quad (\text{A1.15})$$

Hydraulic diffusivity for an unconfined aquifer, a , m^2/d . This characteristic reflects the propagation velocity of perturbations in unconfined aquifers. It is defined as:

$$a = k\bar{m}/S_y, \quad (\text{A1.16})$$

where \bar{m} is the mean water-saturated thickness of an unconfined aquifer, m.

Leakage factor, B , m. This is an integral characteristic, depending on the transmissivity of the pumped aquifer as well as the hydraulic conductivity and the thickness of aquitards. The lesser is B , the more intense the leakage, other conditions being the same. The value of the leakage factor is governed by the number of source layers. When there is a single source layer, and water enters through a single aquitard, overlying or underlying the aquifer (see Fig. 3.2b),

$$B = \sqrt{\frac{Tm'}{k'}}, \quad (\text{A1.17})$$

while in the case of two source layers, when water enters through two aquitards, underlying and overlying it (see Fig. 3.2e),

$$B = \sqrt{\frac{Tm'm''}{k'm'' + k''m'}}, \quad (\text{A1.18})$$

where T is pumped aquifer transmissivity, m^2/d ; k' , k'' are the hydraulic conductivities of the aquitards, m/d ; m' , m'' are aquitard thicknesses, m .

Coefficient of vertical anisotropy, χ , dimensionless. The square root of the ratio of the vertical (k_z) to horizontal (k_r) hydraulic conductivities is:

$$\chi = \sqrt{k_z/k_r}. \quad (\text{A1.19})$$

Retardation coefficient, ΔL , m . A generalized hydrogeological characteristic introduced to account for streambed permeability. This can be calculated as:

$$\Delta L = \frac{k}{k'} m'. \quad (\text{A1.20})$$

Here k is aquifer hydraulic conductivity, m/d ; k' , m' are the hydraulic conductivity (m/d) and the thickness (m) of semipervious stream bed.

Appendix 2

Wellbore Storage, Wellbore Skin, and Shape Factor

The change in groundwater level in an aquifer reflects the effect of both the hydraulic characteristics of the aquifer under study and pumping-well design: wellbore radius, the extent of well penetration, and wellbore state (Fig. A2.1). In some analytical solutions (see Parts I and II), this is accounted for by specifying the wellbore storage and skin.

Wellbore storage, which depends on the casing radius and screen radius and length, can be expressed by a dimensionless parameter (Moench 1997):

$$W_D = \frac{r_c^2}{2r_w^2 S_s l_w}, \tag{A2.1}$$

where l_w is the length of the pumping-well screen, m; r_w , r_c are the radiuses of the pumping well and its casing, respectively, m; S_s is specific storage, 1/m.

The duration of the wellbore-storage effect on water-level changes in the pumping well during pumping depends on the aquifer transmissivity and casing radius (see Eq. A4.20).

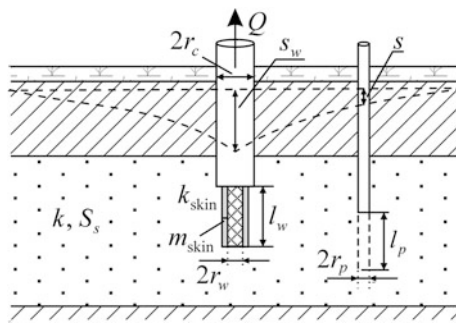
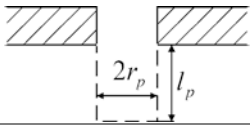
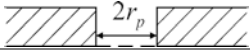

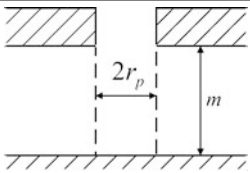
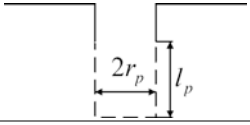
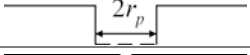
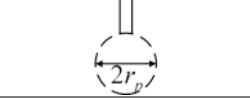
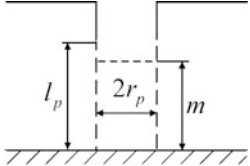


Fig. A2.1 Scheme for calculating wellbore storage and wellbore skin

Table A2.1 Formulas for shape factor

No	Conceptual model	Shape factor, m
1		$F = \frac{2\pi l_p}{\ln\left(l_p/\chi r_p + \sqrt{1 + (l_p/\chi r_p)^2}\right)}$
2		$F = 4r_p$
3		$F = 2\pi r_p$
4		$F = \frac{2\pi m}{\ln\left(2m/\chi r_p + \sqrt{1 + (2m/\chi r_p)^2}\right)}$
5		$F = \frac{2\pi l_p}{\ln\left(l_p/2\chi r_p + \sqrt{1 + (l_p/2\chi r_p)^2}\right)}$
6		$F = 5.5r_p$
7		$F = 4\pi r_p$
8		$F = \frac{\pi(l_p + m)}{\ln\left(m/\chi r_p + \sqrt{1 + (m/\chi r_p)^2}\right)}$

l_p is the screen length of the observation well, m ; m is aquifer thickness or the initial water-saturated thickness of an unconfined aquifer, m ; $\chi = \sqrt{k_z/k_r}$ is anisotropy coefficient

Wellbore skin is determined by wellbore radius, as well as skin hydraulic conductivity and thickness (Moench 1997):

$$W_{\text{skin}} = \frac{km_{\text{skin}}}{r_w k_{\text{skin}}}, \tag{A2.2}$$

where k is aquifer hydraulic conductivity, m/d; k_{skin} , m_{skin} are the hydraulic conductivity (m/d) and thickness (m) of wellbore skin, respectively.

The effect of delayed response of observation well or piezometer on drawdown is lesser (Moench 1997):

$$W'_D = \frac{r_p^2}{2r_w^2 S_s F}, \quad (\text{A2.3})$$

where r_p is observation well radius, m; F is shape factor (see Table A2.1), m.

Formulas for calculating the shape factor were studied by Forchheimer (1914), Hvorslev (1951), Aravin and Numerov (1953), etc. The results of these studies are generalized in Table A2.1(Sunjoto 1994), where the first four conceptual models refer to wells in a confined aquifer, while the others refer to an unconfined aquifer.

Appendix 3

Boundary Conditions and Image Wells

This appendix gives schematic pictures of aquifers with groundwater flow bounded in horizontal or vertical plane. Formulas are given for calculating the distances from the observation well to image wells to be used in drawdown evaluation. In the case of combined boundary conditions, incorporating a constant-head and an impermeable boundary (see, for example, Fig. A3.3c), the distances from wells to the boundary (L_w and L_p) are taken to be those to the constant-head boundary.

1. Semi-infinite Aquifer

In the case of semi-infinite aquifers, two types of boundary conditions are considered: a constant-head boundary and an impermeable boundary (Fig. A3.1).

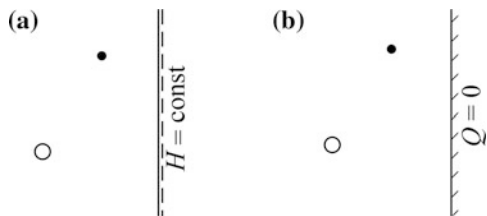
The horizontal distance from the observation to the image well (Fig. A3.2), obtained by reflecting the pumping well about a linear planar boundary is calculated by the following relationship:

$$\rho = \sqrt{(L_w + L_p)^2 + y^2} = \sqrt{r^2 + 4L_wL_p}, \tag{A3.1}$$

where L_p , L_w are the distances from the observation and pumping wells to the planar boundary, m; r is the radial distance from the pumping to the observation well, m; y is the projection of the distance from the observation to the pumping well onto the boundary line (m) and is defined as

$$y = \sqrt{r^2 - (L_w - L_p)^2}. \tag{A3.2}$$

Fig. A3.1 Schematic planar view of a semi-infinite aquifer with **a** a constant-head boundary and **b** an impermeable boundary. Circles are pumping wells, and dots are observation wells



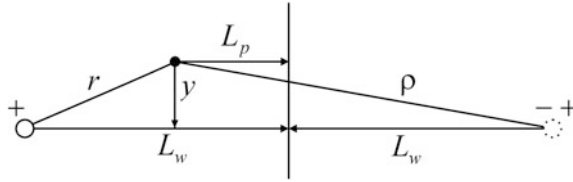


Fig. A3.2 Horizontal distances to the boundary and to an image well. The signs of discharges over the image well: minus is for the constant-head boundary, and plus is for the impermeable boundary

For calculating the drawdown in the pumping well, the distance to the image well is taken equal to twice the distance to the boundary: $\rho = 2L_w$.

2. Strip Aquifer

In the case of aquifers bounded in the horizontal plane by two parallel straight lines, the following variants of boundary conditions are considered: two constant-head boundaries, two impermeable boundaries, and combined boundary conditions (Fig. A3.3).

The number of reflections of the pumping well from the parallel boundaries is infinite (Fig. A3.4). In analytical solutions for a strip aquifer, the number of reflections is replaced by a finite number, such that its further increase has no effect on the calculation accuracy.

The horizontal distances from the observation well to the image wells (Fig. A3.4) obtained by reflecting the pumping well about the left (ρ_1^j) and the right (ρ_2^j) boundaries are evaluated by the following relationships:

$$\rho_1^j = \sqrt{\left(L_p + L_w + \sum_{j_0=2,4,\dots}^j 2L_w + \sum_{j_0=3,5,\dots}^j 2L_w \right)^2 + y^2}, \quad (\text{A3.3})$$

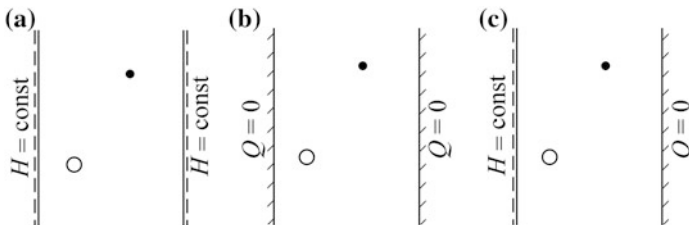


Fig. A3.3 Schematic planar view of a strip aquifer. **a** Two constant-head boundaries; **b** two impermeable boundaries; **c** combined boundary conditions

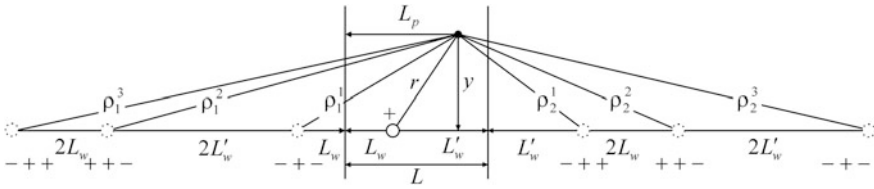


Fig. A3.4 Schematic planar view of a strip aquifer with horizontal distances from the observation well to image wells. The first, second, and third signs of image well discharges under the wells are for a constant-head boundary, impermeable boundary, and combined boundary conditions, respectively

$$\rho_2^j = \sqrt{\left(L'_p + L'_w + \sum_{j_0=2,4,\dots}^j 2L_w + \sum_{j_0=3,5,\dots}^j 2L'_w \right)^2 + y^2}, \quad (A3.4)$$

where j is the number of an image well; j_0 is the number of a reflection in determining the distance to the j th image well; L is the width of the strip aquifer, m ; $L'_p = L - L_p$, $L'_w = L - L_w$ are the distances from the observation and image well to the second boundary of the strip aquifer, m .

3. Wedge-Shaped Aquifer

In the case of a wedge-shaped aquifer (as well as for the strip aquifer), three variants of boundary conditions are considered: two constant-head boundaries, two impermeable boundaries, and combined boundary conditions (Fig. A3.5).

The number of image wells used in drawdown calculation in wedge-shaped aquifers is determined by the angle θ between the two intersecting boundaries (Fig. A3.5). The general rule for determining the number of reflections (i.e., the number of image wells) is formulated as:

$$n = 360/\theta - 1, \quad (A3.5)$$

where θ is the angle between two intersecting boundaries, degrees.

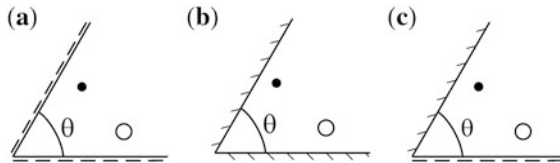


Fig. A3.5 Schematic planar view of a wedge-shaped aquifer. **a** Two constant-head boundaries; **b** two impermeable boundaries; **c** combined boundary conditions

Table A3.1 Determining the number of image wells

θ (degree)	1	2	3	4	5	6	9	10	15	20	30	45	60	90
n	359	179	119	89	71	59	39	35	23	17	11	7	5	3

Before applying Eq. A3.5, one has to check whether the angle is a multiple of 180° (for constant-head boundary or impermeable boundary conditions) or 90° (for combined boundary conditions). Otherwise, the nearest angle satisfying this requirement is used (see Table A3.1).

In the case of combined boundary conditions, the angles of 4° , 20° , and 60° are excluded from those given in Table A3.1.

The positions of wells relative to aquifer boundaries can be characterized by the distance to the vertex of the angle (the intersection point of the two boundaries) and the distance to one of the boundaries (Fig. A3.6a, c). However, for practical calculations, it is handier to use the distances from a well to both boundaries (Fig. A3.6a).

The order and scheme of reflection of imagen wells about two intersecting boundaries are given by Ferris et al. (1962). In that study, the reflected wells are numbered from the pumping well counterclockwise (Fig. A3.6a). The formulas used to evaluate the distances to image wells are as follows:

$$\rho_j = \sqrt{(L_{Aw} \cos \theta_j - L_{Ap} \cos \theta_p)^2 + (L_{Aw} \sin \theta_j - L_{Ap} \sin \theta_p)^2}, \quad (\text{A3.6})$$

$$\theta_j = \theta_w + 2 \sum_{i=1,3,\dots}^j (\theta - \theta_w) + 2 \sum_{i=2,4,\dots}^j \theta_w, \quad (\text{A3.7})$$

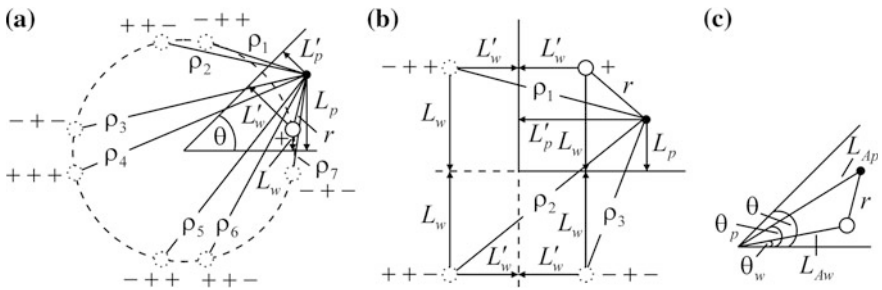


Fig. A3.6 Schematic planar views of a wedge-shaped aquifer. **a, b** Horizontal distances from the observation well to image wells in the case of **a** an arbitrary angle between the boundaries and **b** an aquifer-quadrant; **c** scheme for calculating the distances to image wells. The first, second, and third signs at the image wells are for constant-head, impermeable, and combined boundary conditions, respectively

$$\theta_w = \arcsin(L_w/L_{Aw}), \quad \theta_w = \arctan \frac{\sin \theta}{L'_w/L_w + \cos \theta}, \quad (\text{A3.8})$$

$$\theta_p = \arcsin(L_p/L_{Ap}), \quad \theta_p = \arctan \frac{\sin \theta}{L'_p/L_p + \cos \theta}, \quad (\text{A3.9})$$

$$L_{Aw} = L_w / \sin \theta_w, \quad L_{Ap} = L_p / \sin \theta_p, \quad (\text{A3.10})$$

where L_{Ap} , L_{Aw} are the distances from the observation and pumping wells to the vertex of angle, determined by the equalities (Eq. A3.10), m; L_p , L_w are the distances from the observation and pumping wells to the first boundary, m; L'_p , L'_w are the distances from the observation and pumping wells to the second boundary, m; θ_j is an angle, characterizing the position of the j th image well and determined by Eq. A3.7, degrees; θ_p , θ_w are angles characterizing the position of observation and pumping wells and determined by Eqs. A3.8 and A3.9, degrees.

For an aquifer-quadrant (Fig. A3.6b), the evaluation of distances to the three image wells is simpler:

$$\begin{aligned} \rho_1 &= \sqrt{(L_w - L_p)^2 + (L'_w + L'_p)^2}, \\ \rho_2 &= \sqrt{(L_w + L_p)^2 + (L'_w + L'_p)^2}, \\ \rho_3 &= \sqrt{(L_w + L_p)^2 + (L'_w - L'_p)^2}. \end{aligned} \quad (\text{A3.11})$$

4. U-Shaped Aquifer

A U-shaped aquifer has two parallel semi-infinite linear boundaries and one limited linear boundary, perpendicular to the parallel boundaries. In the case of U-shaped aquifers, the following boundary conditions are considered: all boundaries are constant-head (Fig. A3.7a); parallel constant-head boundaries and impermeable perpendicular boundary (Fig. A3.7b); impermeable parallel boundaries and constant-head perpendicular boundary (Fig. A3.7c); all boundaries are impermeable (Fig. A3.7d); one of the parallel boundaries is constant-head, and the other is impermeable; the perpendicular boundary is constant-head or impermeable (Fig. A3.7e, f).

The calculation of the drawdown in pumping tests in a U-shaped aquifer involves two infinite rows of image wells. The distances from the image wells, obtained by reflection from the parallel boundaries (see the first row of image wells, Fig. A3.8), are evaluated with the use of solutions (Eqs. A3.3 and A3.4) for a strip aquifer, where y is calculated by Eq. A3.2 or by the difference of the distances to the perpendicular boundary:

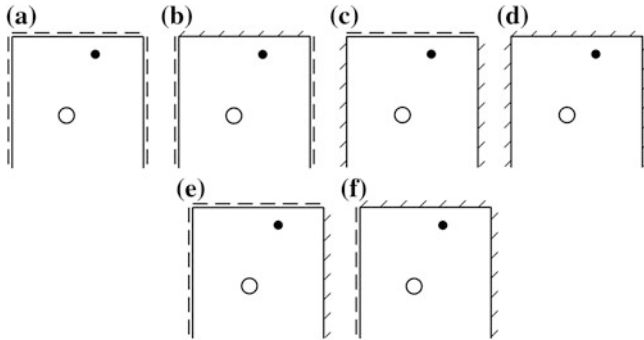


Fig. A3.7 Schematic planar view of a U-shaped aquifer. **a, b** Constant-head parallel boundaries; **c, d** impermeable parallel boundaries; **e, f** mixed boundary conditions on parallel boundaries

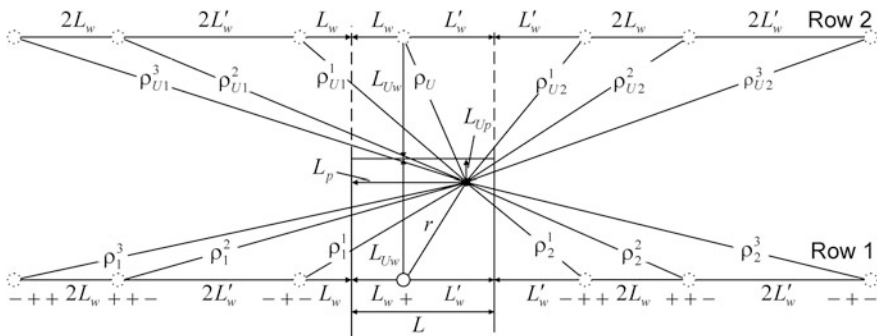


Fig. A3.8 Schematic planar view of a U-shaped aquifer with horizontal distances from the observation well to image wells. The signs under each image well in the first row refer to parallel constant-head boundaries (the first sign), impermeable boundaries (the second sign), and mixed boundary conditions (the third sign). The discharge signs for the second row are the same in the case of an impermeable perpendicular boundary and change to the opposite for a constant-head boundary

$$y = |L_{Uw} - L_{Up}| = \sqrt{r^2 - (L_w - L_p)^2}. \tag{A3.12}$$

The distances to the image wells of the second row (Fig. A3.8), reflected from the left ρ_{U1}^j and right ρ_{U2}^j boundaries, are evaluated as

$$\rho_{U1}^j = \sqrt{\left(L_p + L_w + \sum_{j_0=2,4,\dots}^j 2L'_w + \sum_{j_0=3,5,\dots}^j 2L_w\right)^2 + (L_{Uw} + L_{Up})^2}, \quad (\text{A3.13})$$

$$\rho_{U2}^j = \sqrt{\left(L'_p + L'_w + \sum_{j_0=2,4,\dots}^j 2L_w + \sum_{j_0=2,4,\dots}^j 2L'_w\right)^2 + (L_{Uw} + L_{Up})^2}, \quad (\text{A3.14})$$

where j is the number of the image well to which the distance is evaluated; j_0 is the reflection number in evaluating the distance to the j th image well; L_p, L_w are the distances from the observation and pumping well to the parallel boundary, respectively, m; L'_p, L'_w are the distances from the observation and pumping well to the second parallel boundary, respectively, m; L_{Up}, L_{Uw} are the distances from the observation and pumping well to the perpendicular boundary, respectively, m.

The distance from the pumping well to the image well reflected from the perpendicular boundary can be evaluated as

$$\rho_U = \sqrt{(L_w - L_p)^2 + (L_{Uw} + L_{Up})^2}. \quad (\text{A3.15})$$

5. Rectangular Aquifer

The aquifer is a rectangular domain. In the case of a rectangular aquifer, six variants of boundary conditions are considered (Fig. A3.9).

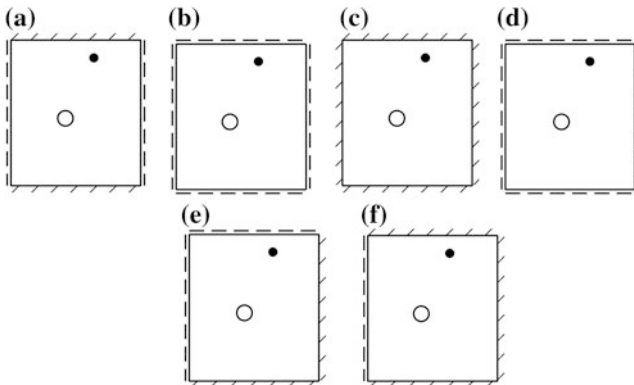


Fig. A3.9 Schematic planar view of a rectangular aquifer. **a** Two pairs of parallel constant-head and impermeable boundaries; **b** all boundaries are constant head; **c** all boundaries are impermeable; **d** three boundaries are constant-head and one is impermeable; **e** two pairs of perpendicular constant-head and impermeable boundaries; **f** one constant-head and three impermeable boundaries

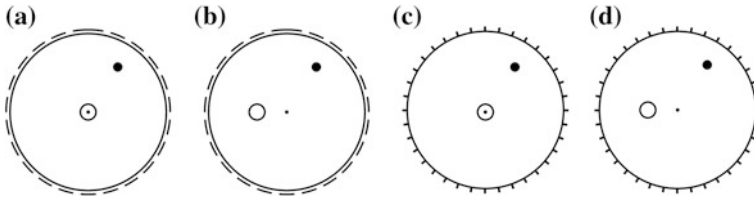


Fig. A3.10 Schematic planar view of a circular aquifer. **a, b** Constant-head boundary; **c, d** impermeable boundary; **a, c** the pumping well coincides with the center of the circular aquifer or **b, d** not coincides with it

The reflection of the pumping well about two pairs of parallel boundaries yields an infinite number of rows, each containing an infinite number of image wells (Ferris et al. 1962). In this book, analytical solutions for calculating the drawdown in a rectangular aquifer based on the effect of image wells are not considered.

6. Circular Aquifer

The circular boundary of an aquifer (Fig. A3.10) implies the presence of one of two boundary conditions—constant-head boundary or impermeable boundary. Analytical solutions for aquifer tests in circular aquifers depend on both the boundary condition and the position of the pumping well relative to aquifer center.

7. Partially Penetrating Well in a Semi-infinite Aquifer

Partially penetrating wells are represented by a point (see Sect. 1.2.2) or linear (see Sect. 1.3.2) source. The groundwater flow boundaries considered for such cases include (1) boundaries in the horizontal plane (constant-head or impermeable) (Fig. A3.11a, b) and (2) an impermeable boundary in the top or bottom of the aquifer (Fig. A3.11c, d).

Under a conceptual model of point source with a planar boundary (Fig. A3.11a, b), the distance to the image well is:

$$\rho = \sqrt{4L_wL_p + d^2}, \tag{A3.16}$$

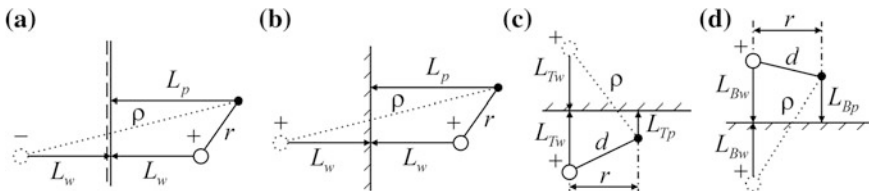


Fig. A3.11 Scheme for a point source in an aquifer semi-infinite in **a, b** plane and **c, d** thickness with distances between the observation and image wells. **a** A constant-head boundary in plane; **b** an impermeable boundary in plane; **c, d** an impermeable boundary in **c** the top and **d** bottom of the aquifer

where $d = \sqrt{r^2 + z^2}$ is the distance between screen centers of the pumping and observation wells (see Fig. 1.10), m ; z is the vertical distance between screen centers of the pumping and observation wells, m .

In the case of a linear source under such conditions, the distance to the image well is evaluated by Eq. A3.1, similarly to the case of a fully penetrating well.

When a partially penetrating well is located near the aquifer top or bottom (Fig. A3.11c, d), then, whatever is the representation of the well (point or linear source), the distance to the image well is:

$$\rho = \sqrt{r^2 + (L_{Tp} + L_{Tw})^2} \text{ or } \rho = \sqrt{r^2 + (L_{Bp} + L_{Bw})^2}, \quad (\text{A3.17})$$

where L_{Tp} , L_{Tw} are vertical distances from the aquifer top to screen centers of the observation and pumping wells, respectively, m ; L_{Bp} , L_{Bw} are the vertical distances from screen centers of the observation and pumping wells to the aquifer bottom, respectively, m .

8. Partially Penetrating Well in an Aquifer Bounded in the Horizontal Plane or Thickness

Partially penetrating wells (linear or point sources) are generally considered in aquifers bounded in the plane or thickness (Fig. A3.12). In the case of planar boundaries (e.g., strip aquifer), all boundary conditions given for fully penetrating wells are taken into account (Fig. A3.3), while in the case of boundaries in thickness, only impermeable boundaries at the aquifer top and bottom are considered.

For a point source in a strip aquifer (Fig. A3.12c), the distances to image wells are:

$$\rho_1^j = \sqrt{\left(L_p + L_w + \sum_{j_0=2,4,\dots}^j 2(L - L_w) + \sum_{j_0=3,5,\dots}^j 2L_w \right)^2 + d^2 - (L_w - L_p)^2}, \quad (\text{A3.18})$$

$$\rho_2^j = \sqrt{\left(2L - (L_p + L_w) + \sum_{j_0=2,4,\dots}^j 2L_w + \sum_{j_0=3,5,\dots}^j 2(L - L_w) \right)^2 + d^2 - (L_w - L_p)^2}. \quad (\text{A3.19})$$

For a point source in an aquifer bounded in thickness and infinite in the plane (Fig. A3.12b), the distances to image wells are:

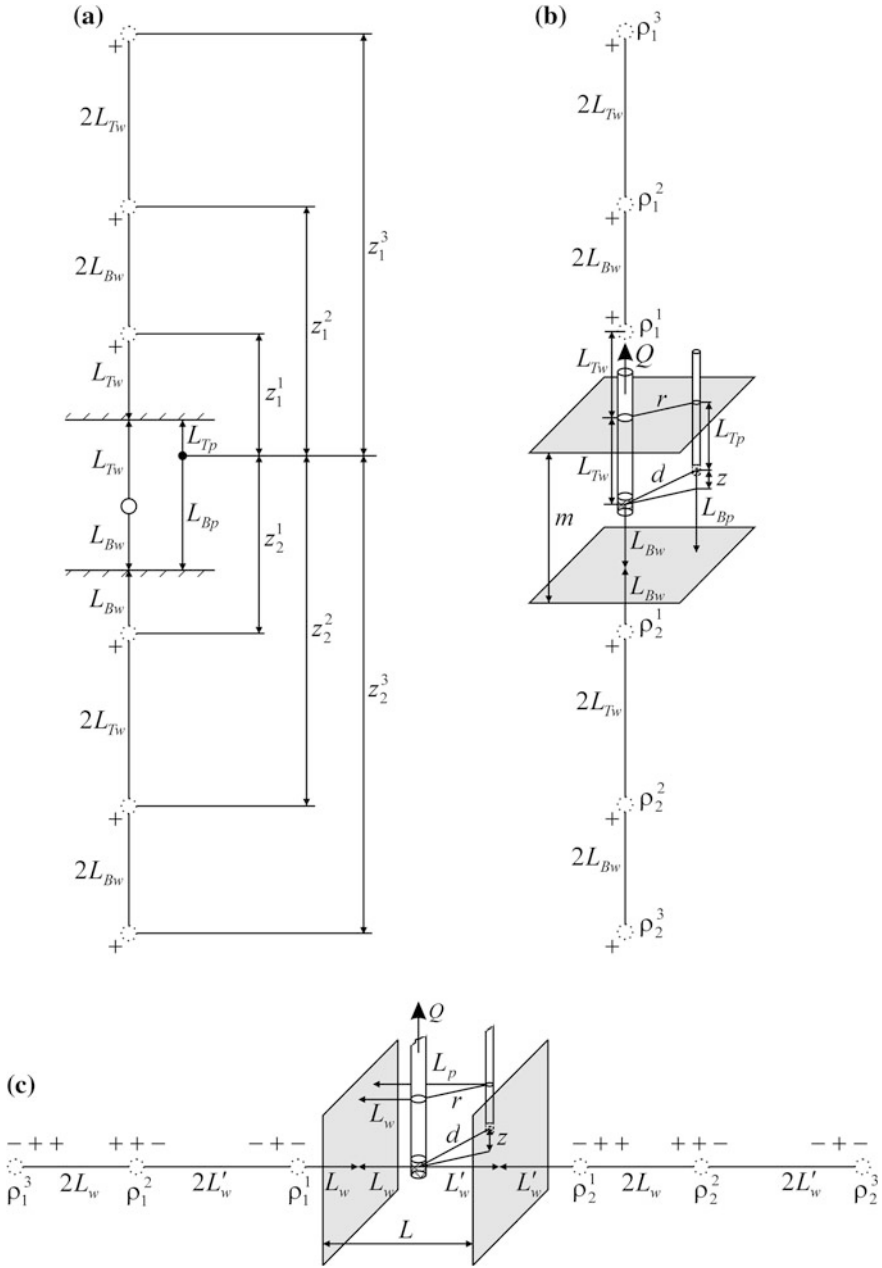


Fig. A3.12 Schemes for evaluating the distances to image wells for point and linear sources. **a** Cross-section for a linear source, the circle, the dot in the section are the centers of the pumping and observation wells, respectively; **b**, **c** three-dimensional schemes for a point source in an aquifer limited in **b** thickness and **c** the plane. For explanations of discharge signs, see in Fig. A3.4

$$\rho_1^j = \sqrt{\left(L_{Tp} + L_{Tw} + \sum_{j_0=2,4,\dots}^j 2L_{Bw} + \sum_{j_0=3,5,\dots}^j 2L_{Tw} \right)^2 + r^2}, \quad (\text{A3.20})$$

$$\rho_2^j = \sqrt{\left(L_{Bp} + L_{Bw} + \sum_{j_0=2,4,\dots}^j 2L_{Tw} + \sum_{j_0=3,5,\dots}^j 2L_{Bw} \right)^2 + r^2}. \quad (\text{A3.21})$$

The distances to image wells for a linear source in a strip aquifer are evaluated similarly to fully penetrating wells by Eqs. A3.3 and A3.4.

The vertical distances from the open part of piezometer or screen center of a partially penetrating observation well (see Fig. 1.22) to screen centers of image wells (Fig. A3.12a), obtained by reflection of the pumping well about the top z_1^j and bottom z_2^j , are:

$$z_1^j = L_{Tp} + L_{Tw} + \sum_{j_0=2,4,\dots}^j 2L_{Bw} + \sum_{j_0=3,5,\dots}^j 2L_{Tw}, \quad (\text{A3.22})$$

$$z_2^j = L_{Bp} + L_{Bw} + \sum_{j_0=2,4,\dots}^j 2L_{Tw} + \sum_{j_0=3,5,\dots}^j 2L_{Bw}. \quad (\text{A3.23})$$

Appendix 4

Equations for Universal Screening Assessments

This appendix gives some simplified relationships that can be helpful for experts in planning aquifer tests and assessing their results.

1. Transmissivity Evaluation

Aquifer transmissivity is evaluated by the drawdown in the pumping well at the moment of the pumping-test end, given the discharge of the pumping well (Logan 1964). In the case of a confined aquifer, the transmissivity is evaluated by an approximate formula:

$$T \approx 1.22Q/s_w, \tag{A4.1}$$

where T is aquifer transmissivity, m^2/d ; Q is the constant discharge rate of the pumping well, m^3/d ; s_w is the drawdown in the pumping well at the end of the pumping test, m .

In the case of an unconfined aquifer, the hydraulic conductivity is evaluated as:

$$k \approx 2.43 \frac{Q}{s_w(2m - s_w)}, \tag{A4.2}$$

where k is the hydraulic conductivity, m/d ; m is the initial water-saturated thickness of the unconfined aquifer, m .

Equations A4.1 and A4.2 refer to fully penetrating pumping wells, located in an aquifer of infinite lateral extent (see Sects. 1.1.1 and 2.1). Such an estimate is rough and does not substitute for the need of the interpretation of the pumping tests by analytical and graphical methods.

When two observation wells are available, the transmissivity is calculated by the Thiem formula (Thiem 1906):

$$T = \frac{Q}{2\pi(s_1 - s_2)} \ln \frac{r_2}{r_1}, \tag{A4.3}$$

where s_1 , s_2 , r_1 , r_2 are the drawdowns (s) and distances to the pumping well (r) for the first and second observation wells, respectively, m .

Equation A4.3 corresponds to a confined aquifer. In an unconfined aquifer, the hydraulic conductivity is calculated as (Dupuit 1863):

$$k = \frac{Q}{\pi \cdot [s_1(2m - s_1) - s_2(2m - s_2)]} \ln \frac{r_2}{r_1}. \quad (\text{A4.4})$$

If drawdown observations are carried out in the pumping well and an observation well, the variables in formulas (Eqs. A4.3 and A4.4) need to be changed: the variables with subscript 1 now refer to the drawdown and radius of the pumping well ($s_1 = s_w$, $r_1 = r_w$); and those with subscript 2 refer to the observation well ($s_2 = s$, $r_2 = r$).

By analogy with Eqs. A4.3 and A4.4, formulas can be constructed for calculating the transmissivity (hydraulic conductivity) by two drawdown values in one observation well. In this case, we obtain for a confined and an unconfined aquifer, respectively:

$$T = \frac{Q}{4\pi(s_1 - s_2)} \ln \frac{t_1}{t_2}, \quad (\text{A4.5})$$

$$k = \frac{Q}{2\pi \cdot [s_1(2m - s_1) - s_2(2m - s_2)]} \ln \frac{t_1}{t_2}, \quad (\text{A4.6})$$

here, s_1 , s_2 , t_1 , t_2 are the drawdowns (s) at two moments (t) in the same observation well.

Equations A4.3–A4.6 are applicable to quasi-steady-state or steady-state flow regimes.

2. Hydraulic Diffusivity Evaluation

If data on the moment of the start of water-level recovery in an observation well after pumping test are available, the hydraulic diffusivity of an aquifer is evaluated by a formula (Maksimov 1979):

$$a = \frac{r^2 t_0}{4t_s(t_0 + t_s) \ln(t_0/t_s + 1)}, \quad (\text{A4.7})$$

where a is the hydraulic diffusivity, m^2/d ; r is the distance from the pumping to the observation well, m ; t_0 is pumping duration, d ; t_s is the time elapsed from the end of pumping to the moment when water level drop changed to level rise, d .

At the common measurement accuracy (1 cm), we will have underestimates of the hydraulic diffusivity.

3. Radius of Influence of a Pumping Test

The effect of pumping tests depends on aquifer hydraulic diffusivity and on the time elapsed since the start of perturbation.

In an aquifer of infinite lateral extent, the radius of influence can be approximately estimated as:

$$R \approx 1.5\sqrt{at}, \quad (\text{A4.7})$$

where t is the time elapsed since the start of pumping test, d.

The radius of influence of a pumping test can also be estimated by the draw-downs in two observation wells in a quasi-steady-state flow period (Maksimov 1959):

$$\lg R = \frac{s_1 \lg r_2 - s_2 \lg r_1}{s_1 - s_2}. \quad (\text{A4.8})$$

Equation A4.8 is applicable to confined aquifers. It was derived from the drawdown ratio in two observation wells (see Eq. 12.13) where the well-function is replaced by its logarithmic approximation (see Eqs. 1.11 and 1.12). By analogy, for an unconfined aquifer:

$$\lg R = \frac{s_1(2m - s_1) \lg r_2 - s_2(2m - s_2) \lg r_1}{s_1(2m - s_1) - s_2(2m - s_2)} \quad (\text{A4.9})$$

and for a confined-unconfined aquifer:

$$\lg R = \frac{\left[(2H - m)m - (H - s_1)^2 \right] \lg r_2 - \left[(2H - m)m - (H - s_2)^2 \right] \lg r_1}{(H - s_2)^2 - (H - s_1)^2}, \quad (\text{A4.10})$$

where H is the initial head, measured from aquifer bottom (see Fig. 2.2b), m.

The radius of the zone of the quasi-steady-state flow regime (R_Q) is calculated using approximations of the well-function $W(u)$ (see Appendix 7.1), for which the function can be assumed linear at $u = \frac{r^2}{4at} < 0.05$. This gives an estimate of the distance from the pumping well to the observation point, within which the flow regime is quasi-steady-state, i.e., the radius of its occurrence is:

$$R_Q \approx 0.45\sqrt{at}. \quad (\text{A4.11})$$

The radius of influence of a slug test (see Sect. 9.1) is insignificant compared with pumping tests. For a slug test in a confined aquifer, the radius of influence can be calculated as (Guyonnet et al. 1993):

$$R \approx Ar_w \left(\frac{Tt}{Sr_w^2} \right)^n; \quad (\text{A4.12})$$

Table A4.1 The values of dimensionless parameters at different calculation accuracies

Parameter	Accuracy		
	1 %	5 %	10 %
A	3.54	2.74	2.36
B	8.37	3.53	2.32
n	0.462	0.434	0.410
m	0.495	0.468	0.440
\bar{t}	2.5	1.3	1.0

it cannot exceed a maximal value:

$$R_{\max} \approx Br_w \left(\frac{r_c^2}{2Sr_w^2} \right)^m, \quad (\text{A4.13})$$

where T , S are the aquifer transmissivity (m^2/d) and storage coefficient (dimensionless); r_w , r_c are the radiuses of the well and its casing, m ; A , B , n , m are dimensionless constants depending on the accuracy of estimating the radius of influence (see Table A4.1).

Slug tests can also provide the time t_{\max} , after which the radius of influence stops increasing. The maximal time is evaluated based on the reduced time:

$$\bar{t} \approx \left(\frac{Tt_{\max}}{Sr_w^2} \right)^n / \left(\frac{r_c^2}{2Sr_w^2} \right)^m. \quad (\text{A4.14})$$

Whence:

$$t_{\max} \approx \bar{t}^{1/n} \left(\frac{r_c^2}{2Sr_w^2} \right)^{m/n} \frac{Sr_w^2}{T}, \quad (\text{A4.15})$$

where \bar{t} is a dimensionless constant (see Table A4.1).

The calculations in (Eqs. A4.12, A4.13, and A1.15) depend on the estimation accuracy of the radius of influence (Table A4.1), i.e., 1, 5, or 10 % of the normalized water-level recovery s_w/s^0 (where s_w , s^0 are level recovery in the tested well and the initial perturbation, respectively, m).

For calculating the radius of influence of a slug test in low-permeability rocks by the pressure-pulse method (see Sect. 9.2), the casing radius is to be replaced by Eq. 9.6.

4. Time Criteria

1. Equation A4.11 readily yields an estimate of the start of the quasi-steady-state period in an aquifer of infinite lateral extent at distance r from the pumping well (see Fig. 12.9):

$$t \approx 5r^2/a. \quad (\text{A4.16})$$

2. The moment of the start of the steady-state period during pumping near a constant-head boundary (see Sect. 1.1.2.1) depends on the hydraulic diffusivity and the distances from the pumping and observation wells to the boundary. For the observation well, it is defined as (see Fig. 12.12a)

$$t \approx 5(r^2 + 4L_w L_p)/a \quad (\text{A4.17})$$

and for the pumping well:

$$t \approx 20L_w^2/a, \quad (\text{A4.18})$$

where L_p , L_w are the distances from the observation and pumping wells to the planar boundary, m; r is the radial distance from the pumping to the observation well, m.

3. In the case of an impermeable boundary, Eq. A4.17 gives the time of the start of quasi-steady-state period (see Sect. 1.1.2.2 and Fig. 12.12b).

Equation A4.17 was obtained by linearization of the well-function $W(u)$ (see Appendix 7.1), which enters the second term in Eqs. 1.13 and 1.15.

4. The time of the onset of steady-state period during pumping in a leaky aquifer (see Sect. 3.1.1) depends on the hydraulic diffusivity and leakage factor. For the ratio $r/B < 2$,

$$t \approx 5B^2/a, \quad (\text{A4.19})$$

where B is the leakage factor (see Eq. A1.17 or Eq. A1.18), m. Such an estimate is based on an approximation of the well-function for leaky aquifers $W(u, \beta)$ (see Table A7.3).

5. Papadopoulos and Cooper (1967) showed that the function describing the drawdown in a large-diameter well $F(u, \beta)$ (see Appendix 7.9) is equal, under some conditions, to the well-function $W(u)$: $u/\beta < 10^{-3}$. This yields the time after which the pumping well storage can be neglected (see Fig. 12.11a):

$$t = 250 \frac{r_c^2}{T}, \quad (\text{A4.20})$$

where r_c is pumping well casing radius, m.

5. Recharge

Recharge can have a contribution (commonly insignificant) to water-level changes in an aquifer during aquifer tests. In the case of constant-rate recharge, water-level change in a confined aquifer during pumping from a single well is (Bochever 1976):

$$s = \frac{Q}{4\pi T} W\left(\frac{r^2 S}{4Tt}\right) - \frac{\varepsilon t}{S}, \quad (\text{A4.21})$$

where ε is recharge rate, m/d.

Equation A4.21 suggests that the drawdown increases to reach a maximum, after which it starts decreasing. The moment of maximal drawdown can be calculated as

$$t_{\max} = \frac{QS}{4\pi\varepsilon T} = \frac{Q}{4\pi\varepsilon a}. \quad (\text{A4.22})$$

Equation A4.21 and the Theis solution (Eq. 1.1) differ by:

$$\Delta s = \frac{\varepsilon t}{S} = \frac{\varepsilon ta}{T}. \quad (\text{A4.23})$$

In the case of unconfined aquifers, the storage coefficient (S) in this formula is to be replaced by the specific yield (S_y). Formula (Eq. A4.23) provides an estimate of the effect of recharge on water-level changes during pumping tests. It also relates the recharge rate, level changes in an observation well, and the hydraulic conductivity of an aquifer without a pumping test (Bochever et al. 1969).

Appendix 5

Application of Computer Programs for Analysis Aquifer Tests

This appendix describes the known numerical–analytical computer programs designed to evaluate the drawdown in aquifers during pumping tests under complex hydrogeological conditions with additional complicating factors such as wellbore storage, wellbore skin, an inclination of the pumping well, etc. The description is supplemented by examples of input files and interpretation of output files. The algorithms of the presented programs are incorporated into the calculations of basic analytical relationships with the ANSDIMAT software system (Sindalovskiy 2014).

All programs calculate the drawdown in aquifers of infinite lateral extent during aquifer tests with a constant pumping discharge rate.

Appendix 5.1 Program DELAY2

The program was developed in 1986 by S.P. Neuman. The description of input parameters (Table A5.1) is based on the code DELAY2.FOR and publications by the program’s author (Neuman 1972–1975).

Program application features (Fig. A5.1) include:

- the aquifer is homogeneous, vertically anisotropic, and unconfined;
- the pumping well is partially penetrating;
- the dimensionless drawdown is evaluated in a partially penetrating observation well or piezometer;
- the wellbore radius is assumed to be infinitely small, i.e., the wellbore storage is neglected.

Input. The general format of input file for calculating a single value:

SIGMA, TS, BETA, PD, DD, ZD, ZD1, ZD2

Input-file format for calculating the average drawdown in observation well:

SIGMA, TS, BETA, PD, DD, , ZD1, ZD2

Input-file format for calculating the drawdown in a piezometer:

SIGMA, TS, BETA, PD, DD, ZD

Fig. A5.1 Schematic diagram to problem solution with DELAY2 program

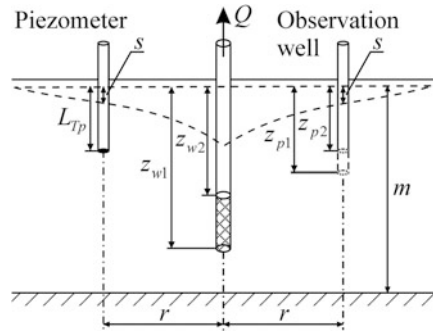


Table A5.1 Dimensionless input parameters of DELAY2 program

Parameter	Formula	Description
SIGMA	S/S_y	Ratio of storage coefficient to specific yield
TS	$\frac{k_r m t}{S r^2}$	Dimensionless time with respect to storage coefficient
BETA	$(\chi r/m)^2$	Dimensionless distance
PD	z_{w1}/m	Ratio of the distance from the initial water table to the bottom of perforations in the pumping well to the initial saturated-aquifer thickness
DD	z_{w2}/m	Ratio of the distance from the initial water table to the top of perforations in the pumping well to the initial saturated-aquifer thickness
ZD	$\frac{m - L_{Tp}}{m}$	Ratio of the vertical distance from the bottom of aquifer to the observation point to the initial saturated-aquifer thickness; leave blank if you want the average drawdown from ZD1 to ZD2
ZD1	$\frac{m - z_{p1}}{m}$	Ratio of the vertical distance from the bottom of aquifer to the bottom of perforations in the observation well to the initial saturated-aquifer thickness; leave blank if you want the drawdown at a point
ZD2	$\frac{m - z_{p2}}{m}$	Ratio of the vertical distance from the bottom of aquifer to the top of perforations in the observation well to the initial saturated-aquifer thickness; leave blank if you want drawdown at a point

In the case of a fully penetrating pumping well ($z_{w1} = m, z_{w2} = 0$): PD = 1, DD = 0

In the case of a fully penetrating observation well ($z_{p1} = m, z_{p2} = 0$): ZD1 = 0, ZD2 = 1

Here, the input file consists of a single line; however, for running the program in this case, a blank line is to be added to the end of the input file.

Output. After execution of the program, the value of the function—an estimate of the integral in Eq. 2.1—will be written in the output file (see parameter AVR in the output file).

Table A5.2 Input data for calculating the drawdown in an unconfined aquifer

Parameter	Value	Description
m	20	Initial water-saturated thickness, m
r	1	Distance from the pumping to the observation well (or piezometer), m
t	1	Time elapsed from the start of pumping, d
z_{w1}, z_{w2}	16, 10	Distance from the initial water table to the bottom and top of pumping-well screen, m
z_{p1}, z_{p2}	9, 5	Distance from the initial water table to the bottom and top of observation-well screen, m
L_{Tp}	7	Distance from the initial water table to the open part of the piezometer, m
k_r, k_z	4, 2	Hydraulic conductivities in the horizontal and vertical direction, respectively, m/d
S	0.0001	Storage coefficient, dimensionless
S_y	0.05	Specific yield, dimensionless

Example. Calculating the average drawdown in a partially penetrating observation well and the drawdown in a piezometer. The input data for this problem are given in Table A5.2.

Table A5.3 gives dimensionless parameters, evaluated by formulas in Table A5.1 with input data in Table A5.2.

An example of input file for calculating the average drawdown in an observation well:

2.0e-3, 8.0e5, 1.25e-3, 0.8, 0.5, , 0.55, 0.75

The output file will contain the dimensionless drawdown AVRG = 5.16310.

An example of input file for calculating the drawdown in a piezometer:

2.0e-3, 8.0e5, 1.25e-3, 0.8, 0.5, 0.65

The output file will contain the dimensionless drawdown AVRG = 4.92693.

The obtained values can be used to evaluate the drawdown so:

$$s = \frac{Q}{4\pi k_r m} \text{AVRG.}$$

Comment. For calculating the drawdown in a piezometer, the 274th line of the source code (DELAY2.FOR)

IF (DZD2 .**LT**. 0 .) DDD=DCOS (B*DZD)

is to be replaced by

IF (DZD2 .**LE**. 0 .) DDD=DCOS (B*DZD)

Table A5.3 Calculating dimensionless parameters for DELAY2 program

SIGMA	TS	BETA	PD	DD	ZD	ZD1	ZD2
2.0e-3	8.0e5	1.25e-3	0.8	0.5	0.65	0.55	0.75

Appendix 5.2 Program WTAQ2

The program was developed in 1995 by A.F. Moench. The description of input parameters (Table A5.4) is based on the code WTAQ2.FOR and publications of the program’s author (Moench 1993, 1996).

Program application features (Fig. A5.2) include:

- the aquifer is homogeneous, vertically anisotropic, unconfined or confined;
- the pumping well is fully or partially penetrating;
- in an unconfined aquifer, gradual drainage at the water table can be taken into account;
- the drawdown (or dimensionless drawdown) is calculated in a fully or partially penetrating observation well or piezometer;
- the wellbore radius is assumed to be infinitely small, i.e., the wellbore storage is neglected.

Input. Input-file format for calculating a single value (the file contains six lines):

```
TDYLAST  NLC  NOX  KT
ALPHA    SIGMA  XKZKR  IWT
XLD      XDD  IPWS
RERRH    RERRNR  RERRSUM  XMAX  NS
AS  AR  AQ  AT  IA
R_OVER_B  ZD  ZD1  ZD2  IOWS
```

Output. After execution of the program, the value of the function, in the case of dimensionless output ($IA = 0$), or the drawdown, in the case of dimensional output ($IA = 1$), will be written into the output file. The denotation of the calculated parameter in the output file depends on aquifer type and on whether the output is dimensional (Table A5.5).

Example. Calculating the average drawdown in a partially penetrating observation well in an unconfined aquifer. The calculation is carried out in dimensionless and dimensional form. For the input data for problem solution, see Table A5.2. In the case of dimensional form, the discharge rate of the pumping well is to be specified— $Q = 100 \text{ m}^3/\text{d}$. Dimensionless parameters based on formulas in Table A5.4 and input data (see Table A5.2) are given in Table A5.6.

Example of input file for dimensionless output:	Input-file format:
1.6e3 0 1 0	TDYLAST NLC NOX KT
1.0e10 2.0e-3 0.5 1	ALPHA SIGMA XKZKR IWT
0.8 0.5 0	XLD XDD IPWS
1.0e-6 1.0e-10 1.0e-15 2000. 8	RERRH RERRNR RERRSUM XMAX NS
0.0 0.0 0.0 0.0 0	AS AR AQ AT IA
0.05 0.0 0.55 0.75 0	R_OVER_B ZD ZD1 ZD2 IOWS

Table A5.4 Input parameters for WTAQ2 program

Parameter	Formula	Description
<i>Line 1</i>		
TDYLAST	$\frac{k_r m t}{S_y r^2}$	Largest value of dimensionless time. For calculating a single value in an unconfined aquifer set TDYLAST = TDY; for a confined aquifer, in this case $TD = k_r m t / (S r^2)$
NLC		Number of log cycles on TD scale; for calculating a single value, NLC = 0
NOX		Number of (equally spaced) points on TD scale; for calculating a single value, NOX = 1
KT		Number of beta type curves, the maximum allowable value of KT is 6; for calculating a single value, KT = 0
<i>Line 2</i>		
ALPHA	$\frac{\alpha m S_y}{k_z}$	Value of dimensionless ALPHA, let ALPHA = 1.0e10 for instantaneous release of water from overlying unsaturated zone; otherwise, ALPHA is to be specified with the use of the presented formula, where α can be found from Eq. 2.15 or Eq. 2.16
SIGMA	S/S_y	Ratio of storage coefficient to specific yield; for a confined aquifer, the value of 1 can be used
XKZKR	k_z/k_r	Ratio of vertical to horizontal hydraulic conductivity
IWT		0 (confined aquifer), 1 (unconfined aquifer)
<i>Line 3</i>		
XLD	z_{w1}/m	Position of the bottom of pumped-well screen; in the case of fully penetrating well (IPWS = 1), the value of 0 can be used
XDD	z_{w2}/m	Position of the top of pumped-well screen; in the case of fully penetrating well (IPWS = 1), the value of 0 can be used
IPWS		0 (partially penetrating pumped well), 1 (fully penetrating pumped well)
<i>Line 4</i>		
RERRH		Relative error criterion for Hantush convergence (1.0e-6)
RERRNR		Relative error for Newton-Raphson iteration and summation (1.0e-10)
RERRSUM		Convergence criterion for the summation (1.0e-15)
XMAX		Maximum number of terms in summation (1000-4000)
NS		Number of terms used in the Stehfest algorithm, this must be an even number, the value of which depends upon computer precision (8); if results are numerically unstable, NS can be reduced to 6 (or even 4); precision will be reduced, however, and results should be checked for accuracy
<i>Line 5</i>		
AS	S	Storage coefficient; for dimensionless output (IA = 0), 0 can be used
AR	r	Radial distance to observation point, L; for dimensionless output (IA = 0), 0 can be used
AQ	Q	Pumping rate, L ³ /T; for dimensionless output (IA = 0), 0 can be used

(continued)

Table A5.4 (continued)

Parameter	Formula	Description
AT	$k_r m$	Transmissivity in radial direction, L^2/T ; for dimensionless output (IA = 0), 0 can be used
IA		0 (dimensional quantities not wanted), 1 (dimensional quantities wanted)
<i>Lines 6+—up to 6 lines; for the calculation of a single value, do not repeat this line</i>		
R_OVER_B	r/m	Radial distance divided by aquifer thickness
ZD	$\frac{m - L_{Tp}}{m}$	Normalized position of piezometer measured from base of aquifer; in the case of an observation well, 0 can be used
ZD1	$\frac{m - z_{p1}}{m}$	Normalized position of the bottom of observation-well screen; in the case of piezometer and for a fully penetrating observation well, 0 can be used
ZD2	$\frac{m - z_{p2}}{m}$	Normalized position of the top of observation-well screen; in the case of piezometer and for a fully penetrating observation well, 0 can be used
IOWS		0 (partially penetrating observation well), 1 (fully penetrating observation well), 2 (piezometer)

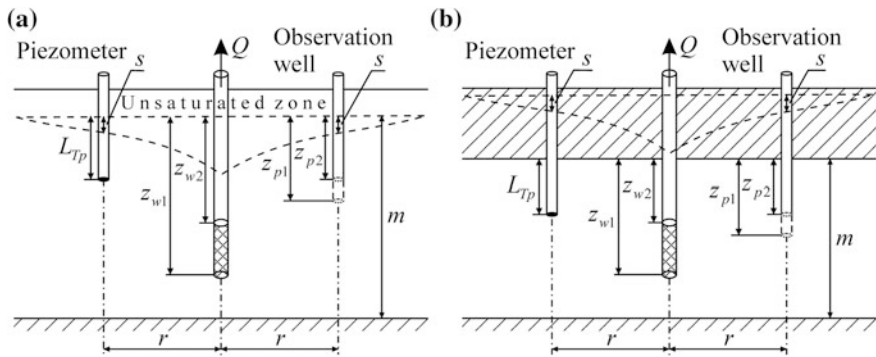


Fig. A5.2 Schematic diagrams to the solution of the problem with WTAQ2 program. **a** Unconfined aquifer with unsaturated zone; **b** confined aquifer

Table A5.5 Denotations of the calculated parameter in the output file of WTAQ2 program

Parameter	Aquifer	Output	Equation
HD	Unconfined	Dimensionless	Evaluating function (Eq. 2.19)
HANTUSH	Confined	Dimensionless	Evaluating function (Eq. 1.107)
DRAWDOWN	Unconfined	Dimensional	Drawdown evaluation (Eq. 2.19)
DRAWDOWN	Confined	Dimensional	Drawdown evaluation (Eq. 1.107)

Table A5.6 Evaluating dimensionless parameters of program WTAQ2

TDYLAST	SIGMA	XKZKR	XLD	XDD	ZD1	ZD2	R_OVER_B
1.6e3	2.0e-3	0.5	0.8	0.5	0.55	0.75	0.05

In the output file, we obtain $HD = 5.214D+00$. From the obtained value, the drawdown can be calculated by:

$$s = \frac{Q}{4\pi k_r m} HD.$$

Example of input file for dimensional output:	Input-file format:
1.6e3 0 1 0	TDYLAST NLC NOX KT
1.0e10 2.0e-3 0.5 1	ALPHA SIGMA XKZKR IWT
0.8 0.5 0	XLD XDD IPWS
1.0e-6 1.0e-10 1.0e-15 2000. 8	RERRH RERRNR RERRSUM XMAX NS
1.0e-4 1.0 100.0 80.0 1	AS AR AQ AT IA
0.05 0.0 0.55 0.75 0	R_OVER_B ZD ZD1 ZD2 IOWS

In the output file, we obtain $DRAWDOWN = 5.187D-01$. This corresponds to the dimensionless value of HD :

$$DRAWDOWN = \frac{Q}{4\pi k_r m} HD.$$

Appendix 5.3 Program WTAQ3

The program was developed in 1997 by A.F Moench. The description of input parameters (Table A5.7) is based on the code WTAQ3. FOR and a publication by the program’s author (Moench 1997).

Program application features (Fig. A5.3) include:

- the aquifer is homogeneous, vertically anisotropic, unconfined or confined;
- the pumping well is fully or partially penetrating;
- wellbore storage and skin are taken into account;
- gradual drainage at the water table in an unconfined aquifer can be taken into account;
- delayed piezometer response can be included in the analysis;
- the drawdown (or dimensionless drawdown) is evaluated in a fully or partially penetrating pumping well, observation well, or piezometer.

Input. Input-file format for calculating a single value (the file consists of six lines):

```

TDYLAST   NLC     NOX     KT
GAMMA     SIGMA   XKD     IWT
RWD   WD   SW   XLD   XDD   IPWS   IPUMP
RERRNR   RERRSUM  XMAX   NS
RATIO_SS  RATIO_B   AS   ARW  AQ   AT   IA
RD   WDPRIME  XZD   XZD1  XZD2  IOWS  IDPR
    
```

Table A5.7 Input parameters of WTAQ3 program

Parameter	Formula	Description
<i>Line 1</i>		
TDYLAST	$\frac{k_r mt}{S_y r_w^2}$	Largest value of dimensionless time. For calculating a single value in an unconfined aquifer, set TDYLAST = TDY; for a confined aquifer, $TD = k_r mt / (S r_w^2)$ is specified here. For dimensionless calculation in an observation well (or piezometer), here $r_w = r$
NLC		Number of log cycles on TD scale; for calculating a single value, NLC = 0
NOX		Number of (equally spaced) points on TD scale; for calculating a single value, NOX = 1
KT		Number of theoretical curves. The maximum allowable value of KT is 6. The first value computes the drawdown in the pumping well: HWD. The subsequent values compute in observation wells (or piezometers): HD. For calculating a single value in the pumping well, KT = 1; for calculating a single value in an observation well (or piezometer), KT = 2
<i>Line 2</i>		
GAMMA	$\frac{\alpha m S_y}{k_z}$	Value of GAMMA. Set GAMMA = 1.D09 for instantaneous release of water from the overlying unsaturated zone; otherwise, to specify GAMMA, use the presented formula, where α can be determined by Eq. 2.15 or Eq. 2.16
SIGMA	S/S_y	Ratio of storage coefficient to specific yield; for a confined aquifer, 1 can be used
XKD	k_z/k_r	Ratio of vertical-to-horizontal hydraulic conductivity
IWT		0 (confined aquifer), 1 (unconfined aquifer)
<i>Line 3</i>		
RWD	r_w/m	Pumped-well radius divided by saturated thickness
WD	$\frac{r_c^2}{2r_w^2 S_s I_w}$	Dimensionless wellbore-storage parameter (see Eq. A2.1)
SW	$\frac{km_{skin}}{r_w k_{skin}}$	Dimensionless wellbore-skin parameter (see Eq. A2.2)
XLD	z_{w1}/m	Depth below initial water table to the bottom of pumped-well screen divided by saturated thickness
XDD	z_{w2}/m	Depth below initial water table to the top of pumped-well screen divided by saturated thickness
IPWS		0 (partially penetrating pumped well), 1 (fully penetrating pumped well)
IPUMP		0 (no computations are made for pumped-well solution), 1 (computations are made for pumped well)
<i>Line 4</i>		
RERRNR		Relative error for Newton–Raphson iteration and summation (1.0e–9 to 1.0e–10)
RERRSUM		Relative error for summation (1.0e–7 to 1.0e–8)
XMAX		Maximum number of terms in summation (3000)

(continued)

Table A5.7 (continued)

Parameter	Formula	Description
NS		Number of terms used in the Stehfest algorithm. This must be an even number, the value of which depends upon computer precision (8) (if the computer holds 16 significant figures in double precision, let NS = 8–12). Note: if results are numerically unstable, NS can be reduced to 6 (or even 4). Precision will be reduced, however, and results should be checked for accuracy
<i>Line 5</i>		
RATIO_SS		Ratio of new value of specific storage to original value in input file. Set RATIO_SS = 1.0 initially
RATIO_B		Ratio of new value of aquifer thickness to initial value. Set RATIO_B = 1.0 initially
AS	S	Value of storage coefficient based on initial estimate of saturated thickness and specific storage; for dimensionless output (IA = 0), 0 can be used
ARW	r_w	Radius of pumped well, L; for dimensionless output (IA = 0), 0 can be used
AQ	Q	Pumping rate, L^3/T ; for dimensionless output (IA = 0), 0 can be used
AT	$k_{r,m}$	Value of transmissivity based on initial estimate of saturated thickness, L^2/T ; for dimensionless output (IA = 0), 0 can be used
IA		0 (dimensional quantities not wanted), 1 (dimensional quantities wanted)
<i>Lines 6 and beyond; for calculating a single value, do not repeat this line</i>		
RD	r/r_w	Radial distance divided by pumped-well radius
WDPRIME	$\frac{r_p^2}{2r_w^2 S_s F}$	Piezometer response-time factor, where F is shape factor (see Eq. A2.3)
XZD	L_{Tp}/m	Depth below initial water table to the center of piezometer divided by saturated thickness
XZD1	z_{p1}/m	Depth below initial water table to the bottom of observation well divided by saturated thickness
XZD2	z_{p2}/m	Depth below initial water table to the top of observation well divided by saturated thickness
IOWS		0 (partially penetrating observation well), 1 (fully penetrating observation well), 2 (piezometer)
IDPR		0 (no delayed piezometer response), 1 (delayed piezometer response included). Note: if IDPR equals 1, it is not necessary that IOWS equals 0

Table A5.8 provides the parameters of the first line of input file for the single output value.

Output. After execution of the program, the value of function, for dimensional output (IA = 0), or the drawdown, for dimensional output (IA = 1), will be written into the output file. The denotation of the calculated parameter in the output file depends on the type of well and on whether the output is dimensional (Table A5.9).

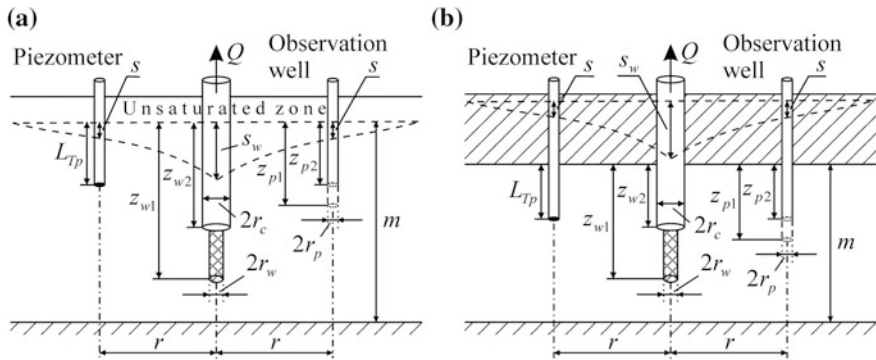


Fig. A5.3 Schematic diagrams for solving the problem in WTAQ3 program. **a** Unconfined aquifer with unsaturated zone; **b** confined aquifer. For the denotations for solving the problem with wellbore skin taken into account, see Fig. A2.1

Table A5.8 Parameters to be specified in the first line of WTAQ3 program input file

Type of well	NLC	NOX	KT
Pumping well: IPUMP=1	0	1	1
Observation well (or piezometer): IPUMP=0	0	1	2
Pumping and observation well (or piezometer): IPUMP=1	0	1	2

Table A5.9 Denotation of the evaluated parameter in the output file of program WTAQ3

Parameter	Type of well	Output	Equation
HD	Observation well (or piezometer)	Dimensionless	Calculating function (Eq. 2.20), (Eq. 1.108)
HWD	Pumping well	Dimensionless	Calculating function (Eq. 2.21), (Eq. 1.109)
DRAWDOWN	Observation well (or piezometer)	Dimensional	Calculating drawdown (Eq. 2.20), (Eq. 1.108)
DRAWDOWN	Pumping well	Dimensional	Calculating drawdown (Eq. 2.21), (Eq. 1.109)

Example. Calculating average drawdown in partially penetrating observation and pumping wells in an unconfined aquifer with wellbore storage taken into account. The calculation is carried out in a dimensionless ($IA = 0$) and dimensional ($IA = 1$) form. For the input data for solving the problem, see Table A5.2. For dimensional form, the discharge rate of the pumping well is to be specified— $Q = 100 \text{ m}^3/\text{d}$. Additionally, to take into account the wellbore storage, the radiuses of its screen and casing are required: $r_w = 0.1 \text{ m}$, $r_c = 0.2 \text{ m}$.

Dimensionless parameters based on formulas in Table A5.7 and input data (see Table A5.2) are given in Table A5.10.

Table A5.10 Calculating dimensionless parameters for WTAQ3 program

TDYLAST	SIGMA	XKD	RWD	WD	XLD	XDD	RD	XZD1	XZD2
1.6e5 ^a /1.6e3 ^b	2e-3	0.5	0.005	66666.7	0.8	0.5	10	0.45	0.25

^aFor dimensional output

^bFor dimensionless output

Example of input file for dimensionless output (for an observation well):	Input-file format:
1.6e3 0 1 2 1.0e9 2.0e-3 0.5 1 0.005 66666.7 0.0 0.8 0.5 0 0 1.0e-10 1.0e-8 3000. 4 1.0 1.0 0.0 0.0 0.0 0.0 0 10.0 0.0 0.0 0.45 0.25 0 0	TDYLAST NLC NOX KT GAMMA SIGMA XKD IWT RWD WD SW XLD XDD IPWS IPUMP RERRNR RERRSUM XMAX NS RATIO_SS RATIO_B AS ARW AQ AT IA RD WDPRIME XZD XZD1 XZD2 IOWS IDPR

In output file, we obtain HD = 5.250D+00. The obtained value yields the drawdown

$$s = \frac{Q}{4\pi k_r m} HD.$$

An example of input file of dimensional output (for an observation well):	Input-file format:
1.6e5 0 1 2 1.0e9 2.0e-3 0.5 1 0.005 66666.7 0.0 0.8 0.5 0 0 1.0e-10 1.0e-8 3000. 4 1.0 1.0 1.0e-4 0.1 100. 80. 1 10.0 0.0 0.0 0.45 0.25 0 0	TDYLAST NLC NOX KT GAMMA SIGMA XKD IWT RWD WD SW XLD XDD IPWS IPUMP RERRNR RERRSUM XMAX NS RATIO_SS RATIO_B AS ARW AQ AT IA RD WDPRIME XZD XZD1 XZD2 IOWS IDPR

In the output file, we will have DRAWDOWN = 5.222D-01. This corresponds to the dimensionless value HD:

$$DRAWDOWN = \frac{Q}{4\pi k_r m} HD.$$

To take into account a piezometer, set IDPR = 1 in the sixth line of the input file and calculate WDPRIME (see Line 6 in Table A5.7).

Example of input file for dimensional output (for the pumping well):	Input-file format:
1.6e5 0 1 1	TDYLAST NLC NOX KT
1.0e9 2.0e-3 0.5 1	GAMMA SIGMA XKD IWT
0.005 66666.7 0.0 0.8 0.5 0 1	RWD WD SW XLD XDD IPWS IPUMP
1.0e-10 1.0e-8 3000. 4	RERRNR RERRSUM XMAX NS
1.0 1.0 1.0e-4 0.1 100. 80. 1	RATIO_SS RATIO_B AS ARW AQ AT IA
10.0 0.0 0.0 0.45 0.25 0 0	RD WDPRIME XZD XZD1 XZD2 IOWS IDPR

In the output file, we obtain DRAWDOWN = 2.926D+00.

To take into account wellbore skin, specify the value SW in the third line of the input file (Table A5.7). If we take $k_{\text{skin}} = 0.5$ m/d, $m_{\text{skin}} = 0.01$ m, we will obtain SW = 0.8 and the drawdown in the pumping well for this problem: DRAWDOWN = 3.456D+00.

Appendix 5.4 Program WTAQ Version 2

The program was developed in 2011 by P.M. Barlow and A.F. Moench. The description of input parameters (Tables A5.12, A5.13, A5.14 and A5.15) is based on a guide written by the program's authors (Barlow and Moench 2011).

The potentialities of the program are the same as those of WTAQ3 (see Appendix 5.3 and Fig. 5.3). Additionally, the program takes into account the effect of drainage with unsaturated-zone characterization on water level changes in an unconfined aquifer. The program also provides an option allowing the effect of wellbore storage to be ignored.

This appendix includes brief information about the input file for the program for the drawdown calculation (in meters)—dimensional format. For the description of the input file for obtaining the dimensionless drawdown, see the guide (Barlow and Moench 2011).

Input. Input-file formats for calculating the drawdown in the pumping and observation wells are different. The first thirteen lines are the same, followed by two lines for calculating the drawdown in a pumping well or five lines for the drawdown in an observation well.

Input-file format for calculating a single value:

```
TITLE
FORMAT
AQTYPE
BB   HKR   HKZ   SS   SY
IDRA  NALPHA
ACC  AKK  AMM  AXMM
ITS  IMEAS
TLAST  NLC  NOX
ISOLN
RERRNR  ERROR  NTMS  NNN  METHOD
IPWS  IPWD  IPUMP
QQ  RW  RC  ZPD  ZPL  SW
NTSPW  IRUN
```

Next, two lines are included for calculating the drawdown in a pumping well:

```
TIMEPW (I)  XMEASPW (I)
```

```
NOBWC
```

or five lines, for the drawdown in an observation well or piezometer:

```
NOBWC
OBNAME  IOWS  IDPR
R  Z1  Z2  ZP  RP  XLL
NTSOB  IRUN
TIMEOB (I)  XMEASOB (I)
```

The number and the values of parameters in the sixth line of the input file depend on the type of drainage at the water table—IDRA (Table A5.11).

Table A5.12 explains the first thirteen lines of the input file for program WTAQ Version 2. Next, Table A5.13 gives explanations for parameters required for calculating the drawdown in the pumping well; and Table A5.14, the same for an observation well or a piezometer.

Parameters in Table A5.15 are given for the solution by the Stehfest algorithm (ISOLN = 1) (see Lines 9 and 10 in Table A5.12): the calculation of the drawdown in a confined aquifer and in an unconfined aquifer at instantaneous drainage or gradual drainage at water table.

Constants for describing functional relationships between the saturation, permeability, and capillary pressure in unsaturated zone enter into the following functions (Gardner 1958; Mathias and Butler 2006):

Table A5.11 Specifying the sixth line’s parameters, depending on IDRA and NALPHA (see Line 5)

IDRA	NALPHA	Line 6	Comment
0	0	1e9	Instantaneous drainage at the water table
1	1	ALPHA	Gradual drainage at the water table. Empirical drainage constants, in units of inverse time; this can be determined by (Eq. 2.15 or Eq. 2.16)
2	0	ACC AKK AMM AXMM	Drainage with unsaturated-zone characterization. Parameter values see in Tables A5.12 and A5.16

Table A5.12 Input parameters for program WTAQ Version 2 for dimensional format

Parameter	Denotation	Description
<i>Line 1</i>		
TITLE		Title of simulation; up to 70 characters in length
<i>Line 2</i>		
FORMAT		Analysis format. Enter DIMENSIONAL
<i>Line 3</i>		
AQTYPE		Type of aquifer being simulated. Two options are provided: AQTYPE = CONFINED or AQTYPE = WATER TABLE
<i>Line 4</i>		
BB	m	Thickness or initial saturated thickness of the aquifer at the beginning of simulation, in units of length
HKR	k_r	Horizontal hydraulic conductivity of aquifer, in units of length per time
HKZ	k_z	Vertical hydraulic conductivity of aquifer, in units of length per time
SS	$S_s = S/m$	Specific storage of aquifer, in units of inverse length
SY	S_y	Specific yield of aquifer, dimensionless. Enter 0.0 if AQTYPE = CONFINED
<i>Line 5</i>		
IDRA		Type of drainage at water table. Enter 0 if AQTYPE = CONFINED. Three options are provided: 0 (instantaneous drainage), 1 (gradual drainage), 2 (drainage with unsaturated-zone characterization)
NALPHA		Enter 0 if IDRA = 0 or 2; enter 1 if IDRA = 1 (see Table A5.11)
<i>Line 6</i> depends on the value of IDRA (see Table A5.11); parameters for IDRA = 2 are given here		
ACC	a_c	Soil-moisture retention exponent, in units of inverse length
AKK	a_k	Relative hydraulic-conductivity exponent, in units of inverse length. The value specified must be greater than or equal to that specified for ACC
AMM		Initial unsaturated-zone thickness above the capillary fringe, in units of length
AXMM		The unsaturated-zone thickness above the capillary fringe above which an assumption of an infinitely thick unsaturated-zone thickness is assumed, in units of length
<i>Line 7</i>		
ITS		Time specification. Here we specify ITS = 1
IMEAS		Specification of measured drawdown data. Here we specify IMEAS = 0
<i>Line 8</i>		
TLAST		Largest value of time. Here we specify TLAST = 0.0
NLC		The number of logarithmic cycles on the time scale for which drawdown will be calculated. For calculating a single value, NLC = 0

(continued)

Table A5.12 (continued)

Parameter	Denotation	Description
NOX		The number of equally spaced times per logarithmic cycle for which drawdown will be calculated. For calculating a single value, NOX = 0
<i>Line 9</i>		
ISOLN		Numerical-inversion solution type: 1 (solution by the Stehfest algorithm—must use this option for confined aquifers), 2 (solution by the de Hoog algorithm—must use this option for IDRA = 2)
<i>Line 10</i> —data are given for calculations in an unconfined aquifer taking into account the drainage with unsaturated-zone characterization: IDRA = 2 (see Line 5), ISOLN = 2 (see Line 9). In other cases, the description of parameters in Line 10 see in Table A5.15		
RERRNR		Relative error for Newton-Raphson iteration and finite summations of drawdown for water-table aquifers. A value of 1.0e-10 is suggested
ERROR		Relative error sought for the accuracy of the numerical inversion. A value of 1.0e-4 is suggested
NTMS		Factor used to determine the number of terms in the finite summation for drawdown for unconfined aquifers. Suggested values are 20 or 30
NNN		Number of terms used in the summation of the Fourier series of the approximation to the inverse Laplace transform. A value of 6 is suggested
METHOD		Indicates which method will be used to accelerate the convergence of the Fourier series. Options are 1, 2, or 3. Only METHOD = 3 has been tested and was found to be satisfactory
<i>Line 11</i>		
IPWS		Type of pumped well: 0 (partially penetrating pumped well), 1 (fully penetrating pumped well)
IPWD		Type of diameter of pumped well: 0 (infinitesimal diameter – line-source theory), 1 (finite diameter)
IPUMP		Option to suppress calculations of drawdown at pumped well: 0 (drawdown is not calculated at pumped well), 1 (drawdown is calculated at pumped well)
<i>Line 12</i>		
QQ	Q	Pumping rate of well, in units of cubic length per time
RW	r_w	Radius of pumped well screen, in units of length
RC	r_c	Inside radius of pumped well in the interval where water levels are changing during pumping, in units of length. Enter 0.0 if IPWD = 0
ZPD	z_{w2}	Depth below the top of aquifer or initial water table to the top of the screened interval of the pumped well, in units of length
ZPL	z_{w1}	Depth below the top of aquifer or initial water table to the bottom of the screened interval of the pumped well, in units of length
SW	$\frac{km_{skin}}{r_w k_{skin}}$	Wellbore skin parameter, dimensionless

(continued)

Table A5.12 (continued)

Parameter	Denotation	Description
<i>Line 13</i>		
NTSPW		Number of user-specified times for which drawdown at the pumped well will be calculated. If NTSPW = 0, no drawdowns are calculated for the pumped well. For calculating a single value in the pumping well, NTSPW = 1, for that in an observation well, NTSPW = 0
IRUN		Option to suppress drawdown calculations for the pumped well. Options are: 0 (drawdowns not calculated), 1 (drawdowns calculated). For calculating a single value in a pumping well, IRUN = 1, for the same in an observation well, IRUN = 0

Table A5.13 Continuation of Table A5.12: input parameters required to calculate the drawdown in the pumping well

Parameter	Description
<i>Line 14</i>	
TIMEPW(I)	To determine a single drawdown in the pumping well, one moment in time for which the calculation is required is to be specified
XMEASPW (I)	Leave blank
<i>Line 15 (or Line 14 for calculation of drawdown in an observation well or piezometer)</i>	
NOBWC	Number of observation wells or piezometers for which drawdown curves will be calculated. For calculating a single drawdown in the pumping well, NOBWC = 0; for a single drawdown in the observation well, NOBWC = 1

(1) effective-saturation function—relationship between capillary forces and porous materials saturation:

$$S_e(h) = \exp(a_c h), \tag{A5.1}$$

(2) relative permeability function—relationship between capillary forces and relative permeability:

$$k_{rel}(h) = \exp(a_k h). \tag{A5.2}$$

From (Eqs. A5.1 and A5.2), we obtain the relative permeability as a function of saturation:

$$k_{rel}(S_e) = S_e^{a_k/a_c}, \tag{A5.3}$$

$$S_e = \frac{S - S_r}{1 - S_r}, \tag{A5.4}$$

Table A5.14 Continuation of Table A5.12: input parameters required to calculate the drawdown in an observation well or piezometer

Parameter	Denotation	Description
<i>Line 15</i>		
OBNAME		Name of observation well or piezometer; up to ten characters in length
IOWS		Type of observation well or piezometer: 0 (partially penetrating observation well), 1 (fully penetrating observation well), 2 (observation piezometer)
IDPR		Options for delayed response of observation well: 0 (no delayed response), 1 (delayed response)
<i>Line 16</i>		
R	r	Radial distance from the axis of pumped well to observation well or piezometer, in units of length
Z1	z_{p2}	Depth below top of aquifer or initial water table to the top of screened interval of observation well, in units of length. Use for IOWS = 0 or 1. Enter 0.0 if IOWS = 2
Z2	z_{p1}	Depth below top of aquifer or initial water table to the bottom of screened interval of observation well, in units of length. Use for IOWS = 0 or 1. Enter 0.0 if IOWS = 2
ZP	L_{Tp}	Depth below top of aquifer or initial water table to center of piezometer, in units of length. Use for IOWS = 2. Enter 0.0 if IOWS = 0 or 1
RP	r_p	Inside radius of the observation well (or piezometer) standpipe in the interval over which water levels are changing during pumping, in units of length. Enter 0.0 if IDPR = 0 (no delayed response)
XLL	l_p	Length of screened interval of observation well, in units of length. Enter 0.0 if IDPR = 0 (no delayed response)
<i>Line 17</i>		
NTSOB		Number of user-specified times for which drawdown at the observation well or piezometer will be calculated. If NTSOB = 0, no drawdowns are calculated for the observation well or piezometer. For calculating a single value, NTSOB = 1
IRUN		Option to suppress drawdown calculations for the observation well or piezometer. Allows user to specify time-drawdown data (Line 17), but those data are ignored during the simulation. Options are: 0 (drawdowns not calculated), 1 (drawdowns calculated). For calculating a single value, IRUN = 1
<i>Line 18</i>		
TIMEOB(I)		To determine a single drawdown in an observation well or piezometer, one moment in time for which the calculation is required is to be specified
XMEASOB(I)		Leave blank

Table A5.15 Parameters for the solution by the Stehfest algorithm (ISOLN = 1)

Parameter	Description
RERRNR	Error for Newton-Raphson iteration and finite summations of drawdown for water-table aquifers. A value of 1.0e-10 is suggested. Enter 0.0 for AQTYPE = CONFINED
RERRSUM	Relative error for finite summations of the drawdown for confined aquifers. Suggested value is 1.0e-7 to 1.0e-8. Enter 0.0 if AQTYPE = WATER TABLE
NMAX	Maximum number of terms permitted in the finite summations of the drawdown for confined aquifers. Suggested value is 200. Enter 0 if AQTYPE = WATER TABLE
NTMS	Factor used to determine the number of terms in the finite summations for the drawdown for water-table aquifers. Suggested values are 20 or 30. Enter 0 if AQTYPE = CONFINED
NS	Number of terms used in the Stehfest algorithm. This must be an even integer, the value of which depends upon computer precision. If the computer holds 16 significant figures in double precision, let NS = 6-12. A value of 8 is recommended

where h is pressure head in the unsaturated zone ($h < 0$), m ; a_c , a_k are empirical parameters characterizing porous materials capillary properties (the soil-moisture retention exponent and the relative hydraulic-conductivity exponent), $1/m$; S_e is the effective saturation, dimensionless; k_{rel} is relative permeability, dimensionless; S , S_r are the saturation and residual saturation, dimensionless.

Since $S = \theta/n$, then (Eq. A5.4):

$$S_e = \frac{\theta - \theta_r}{n - \theta_r}, \quad (\text{A5.5})$$

where dimensionless parameters include θ as volumetric soil-moisture content; θ_r as residual soil-moisture content; and n as sediment porosity.

The relationship A5.3 was first proposed by Averyanov (1949) in the form:

$$k_{rel}(S_e) = S_e^m, \quad (\text{A5.6})$$

where the exponent m , according to different estimates can vary between three and four. Comparing Eqs. A5.3 and A5.6 we obtain $a_k = ma_c$.

Table A5.16 gives parameters for drainage with unsaturated-zone characterization (see Line 6 in Table A5.12) and their effect on the drawdown calculation.

Output. The output file of program WTAQ Version 2 depends on input-file format: type-curve format or dimensional format. Examples for calculating the drawdown in meters (dimensional format) are given below in the form of processing functional relationships (Eqs. 2.20 and 2.21).

Example. Evaluating the average drawdown in partially penetrating observation and pumping wells, located in an unconfined aquifer with wellbore storage taken into account. For the input data, see Table A5.2. Additionally, the solution of this

Table A5.16 Parameters for drainage with unsaturated-zone characterization

AMM >= AXMM	Unsaturated zone is of infinite thickness
AMM < AXMM	Unsaturated zone is of finite thickness
ACC	An increase in this parameter reduces the effect of the unsaturated zone
AKK	A decrease in this parameter reduces the effect of the unsaturated zone
AMM	An increase in this parameter reduces the effect of the unsaturated zone
ACC <= AKK	A necessary condition for problem solution

For a detailed description of parameters, see the guide for program WTAQ version 2 (Barlow and Moench 2011)

problem requires the radiuses of the pumping well and its casing: $r_w = 0.1$ m, $r_c = 0.2$ m. Parameters for drainage with unsaturated-zone characterization are also required (see Line 6 in Table A5.12). The discharge rate of the pumping well is $Q = 100$ m³/d.

Input file for calculating the drawdown in an observation well:	Input-file format:
Example for observation well	TITLE
DIMENSIONAL	FORMAT
WATER TABLE	AQTYPE
20.0 4.0 2.0 5.0e-6 0.05	BB HKR HKZ SS SY
2 0	IDRA NALPHA
5.0 30.0 10.0 1.0	ACC AKK AMM AXMM
1 0	ITS IMEAS
0.0 0 0	TLAST NLC NOX
2	ISOLN
1.0e-10 1.e-4 30 6 3	RERRNR ERROR NTMS NNN METHOD
0 1 0	IPWS IPWD IPUMP
100.0 0.1 0.2 10.0 16.0 0.0	QQ RW RC ZPD ZPL SW
0 0	NTSPW IRUN
1	NOBWC
obs1 0 0	OBNAME IOWS IDPR
1.0 5.0 9.0 0.0 0 0	R Z1 Z2 ZP RP XLL
1 1	NTSOB IRUN
1.0	TIMEOB (I)

In the output file, we obtain CALCULATED DRAWDOWN = 0.5398D+00.

To take into account the delayed piezometer response, Line 15 is to contain IDPR = 1; and Line 16 is to contain the radius (RP) and length (XLL) of the observation well. In solving the problem, the program computes the shape factor for a partially penetrating observation well in an unconfined aquifer (see Table A5.1 and Line 277 of the source program code).

In the preparation of input file for the dimensional format, the program uses the shape factor for a partially penetrating observation well in an unconfined aquifer (see Table A5.1 and Line 277 of the source program code).

An example of input file for calculating the drawdown in the pumping well	Input-file format:
<pre> Example for pumping well DIMENSIONAL WATER TABLE 20.0 4.0 2.0 5.0e-6 0.05 2 0 5.0 30.0 10.0 1.0 1 0 0.0 0 0 2 1.0e-10 1.e-4 30 6 3 0 1 1 100.0 0.1 0.2 10.0 16.0 0.0 1 1 1.0 0 </pre>	<pre> TITLE FORMAT AQTYPE BB HKR HKZ SS SY IDRA NALPHA ACC AKK AMM AXMM ITS IMEAS TLAST NLC NOX ISOLN RERRNR ERROR NTMS NNN METHOD IPWS IPWD IPUMP QQ RW RC ZPD ZPL SW NTSPW IRUN TIMEPW(I) NOBWC </pre>

In the output file, we will have CALCULATED DRAWDOWN = 0.2943D+01.

To take into account the wellbore skin of the pumping well, specify SW in the twelfth line of input file (see Table A5.12). Assuming $k_{\text{skin}} = 0.5$ m/d, $m_{\text{skin}} = 0.01$ m, we will obtain SW=8.0 and the drawdown in the pumping well for this problem: CALCULATED DRAWDOWN = 0.3473D+01.

Appendix 5.5 Program DP_LAQ

The program was developed in 1990 by A.F. Moench. The description of input parameters (Table A5.17) was compiled based on software code DP_LAQ.FOR, program author's publications (Moench 1984, 1985), and a paper devoted to Warren–Root model (Warren and Root 1963).

The program is intended for calculating the drawdown in observation wells in stratified systems (see Sect. 3.6) or fractured–porous media (see Sect. 6.1). The program solves the following problems:

- (1) evaluating the drawdown in the main aquifer and in aquitards in a three-layer system (Fig. A5.4b–d);
- (2) evaluating the drawdown in the main aquifer and in aquitards in a two-layer system (Fig. A5.4e, f);
- (3) evaluating the drawdown in a fracture and a block of fractured–porous medium (see Fig. 6.1).

The program considers wellbore storage and skin. Fracture skin is also taken into account in the case of fractured–porous media.

Table A5.17 Input parameters for DP_LAQ program

Parameter	Formula	Description
<i>Line 1</i>		
N		The no. of terms in the Stehfest algorithm. It must be an even number, usually in the range of 8–12. N = 8 is usual
<i>Line 2</i>		
IMAT		1 (means groundwater format), 2 (means petroleum format)
LD		1 (means large diameter well), 2 (means line source well)
LCASE		Calculation in stratified systems: 1 (Fig. A5.4b, e), 2 (Fig. A5.4c, f), 3 (Fig. A5.4d) Calculation in fractured–porous media: 4 (means fracture—slabs, Fig. 6.1a), 5 (means fracture—spheres, Fig. 6.1b), 6 (means fracture—Warren and Root, Fig. 6.1c)
IQ		0 (means no leakage), 1 (means leakage from both semi-confining layers, Fig. A5.4b–d), 2 (means leakage from overlying bed only, Fig. A5.4e, f, or double-porosity models, Fig. 6.1), 3 (means leakage from underlying bed only—the layout of layers see in Fig. 3.17c, e)
<i>Line 3—parameters for stratified systems</i>		
SIGP	S'/S	
GAMMP	r_w/B_1	where B_1 see formula (Eq. 3.117)
ZDP	z'_p/m	
<i>Line 4—parameters for stratified systems</i>		
SIGPP	S''/S	
GAMMPP	r_w/B_2	where for B_2 see formula (Eq. 3.118)
ZDPP	z''_p/m	
<i>Line 5</i>		
RD	r/r_w	Dimensionless radial distance
WD	$\frac{r_c^2}{2r_w^2 S_s m}$	Dimensionless wellbore storage coefficient
WSKIN	$\frac{km_{skin}}{r_w k_{skin}}$	Dimensionless coefficient of wellbore skin
<i>Line 6—parameters for fractured–porous media</i>		
SIG	S'_s/S_s	where S'_s, S_s are specific storage values for block and fractured systems, 1/m
GAMM	$2 \frac{r_w}{m_b} \sqrt{\frac{k'}{k}}$	where k', k are hydraulic conductivities for block and fracture systems, m/d; m_b is the average thickness of block, m
FSKIN	$2 \frac{k' m_{skin}^f}{k_{skin}^f m_b}$	Dimensionless coefficient of fracture skin, where k_{skin}^f, m_{skin}^f are the hydraulic conductivity (m/d) and the thickness of fracture skin (m) (see Fig. 6.1d). This is used only for fractured systems with slab-shaped blocks and sphere-shaped blocks (see Fig. 6.1a, b)

(continued)

Table A5.17 (continued)

Parameter	Formula	Description
<i>Line 7—parameters for fractured–porous media</i>		
XLAM	$\alpha r_w^2 \frac{k'}{k}$	The parameter governing inter-porosity flow (Warren and Root 1963), dimensionless. $\alpha = 4n(n + 2)/l^2$ —relates to geometry of blocks under assumption of pseudo-steady-state flow, $1/m^2$; $n = 1, 2, 3$ is the number of normal sets of fractures; $l = \frac{3abc}{ab + bc + ca}$ for $n = 3$, $l = \frac{2ab}{a + b}$ for $n = 2$, $l = a$ for $n = 1$ —characteristic dimension of heterogeneous region, m^2 ; a, b, c are block dimensions along three directions (length, width, height), m
<i>Line 8—parameters for fractured–porous media</i>		
ZD	$2z_p/m_b$	Here, z_p is the distance measured from the center of a slab-shaped block to the fracture (see Fig. 6.1a), m; m_b is the average block thickness, m
RHO	$2z_p/m_b$	Here, z_p is the distance measured from the center of a sphere-shaped block to the fracture (see Fig. 6.1b), m; m_b is average block diameter, m
<i>Line 9</i>		
TDLAST	$\frac{kt}{S_s r^2}$	Last value of dimensionless time. For calculating a single value in an unconfined aquifer—TDLAST = TD. Here, S_s is the specific storage of the main aquifer (for stratified systems) or the fracture system (for fractured–porous media)
NLC		Number of log cycles of time; for calculating a single value, NLC = 0
NOX		Number of points to be computed per log cycle of time; for calculating a single value, NOX = 1
<i>Line 10</i>		
XMULT		Factor for calculating distances to the pumping well; for calculating a single value, XMULT = 1.0
KT		Number of points to be computed per log cycle of time; for calculating a single value, KT = 1

Input. Input-file format for calculating a single value (formatted data input, i.e., each parameter occupies a specified position in the line):

N:				
IMAT:	LD:	LCASE:	IQ:	
	SIGP:		GAMMP:	ZDP:
	SIGPP:		GAMPPP:	ZDPP:
	RD:		WD:	WSKIN:
	SIG:		GAMM:	FSKIN:
	XLAM:			
	ZD:		RHO:	
	TDLAST:	NLC:	NOX:	
	XMULT:	KT:		

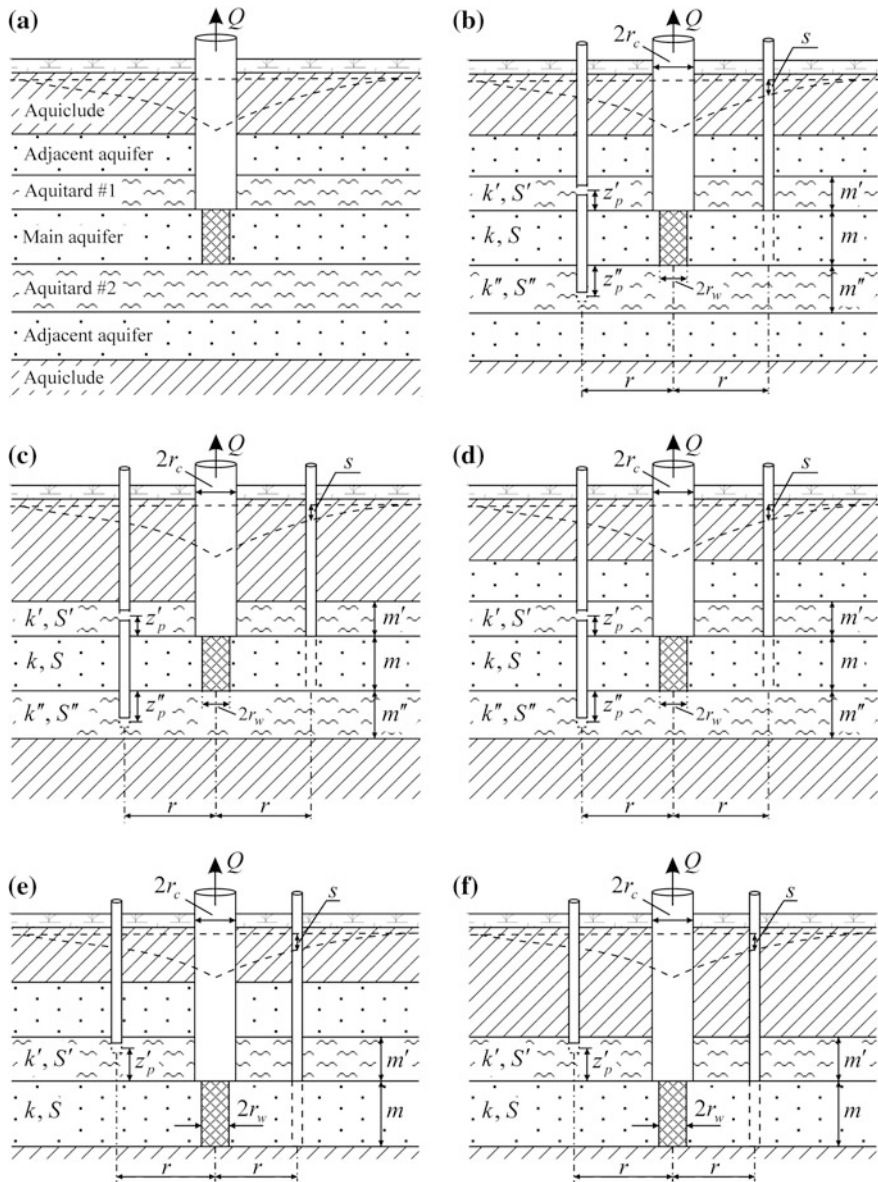


Fig. A5.4 Schematic diagrams for problem solution with DP_LAQ program. **a** The layout and names of geological layers; **b–d** three-layer systems; **e, f** two-layer systems

A short field contains five characters; a long field, ten characters. Parameters N, IMAT, LD, LCASE, IQ, NLC, NOX, and KT are integers, other parameters are real variables to be written with a decimal point.

Table A5.18 The choice of the conceptual model and the denotation of a calculated parameter in the output file

Conceptual model	Fig.	Input (Line 2)		Output		
		LCASE	IQ	HD	HDP	HDPP
Three-flow systems and two adjacent aquifers	A5.4b	1	1	Main aquifer	Aquitard #1	Aquitard #2
Three-flow systems with no adjacent aquifers	A5.4c	2	1	Main aquifer	Aquitard #1	Aquitard #2
Three-flow systems and one adjacent aquifer	A5.4d	3	1	Main aquifer	Aquitard #1	Aquitard #2
Two-flow systems and one adjacent aquifer	A5.4e	1	2 ^a	Main aquifer	Aquitard	
Two-flow systems with no adjacent aquifers	A5.4f	2	2 ^a	Main aquifer	Aquitard	
Fracture—slab-shaped blocks	6.1a	4	2	Fracture	Block	
Fracture—sphere-shaped blocks	6.1b	5	2	Fracture	Block	
Fracture—Warren–Root model	6.1c	6	2	Aquifer		

^aIn the case of leakage through the bottom (Fig. 3.17c, e) of the main aquifer, IQ = 3

The need to fill fields in some lines of the input file depends on the chosen conceptual model: Lines 1, 2, 5, 9, 10 are to be filled for all models; Lines 3, 4, for three-layer systems; Line 3, for two-layer systems; Lines 6, 7, 8, for fractured–porous media. The fields not to be filled may contain arbitrary values or remain empty. The choice of the conceptual model is specified by parameters LCASE and IQ in the second line of the input file (Table A5.18).

Output. After execution of the program, the output file will contain the calculated value of a function that enters one of the relationships for stratified systems (Eqs. 3.122, 3.123, 3.128, or 3.129) or for fractured–porous media (Eqs. 6.1–6.3). The denotation of the calculated parameter in the output file depends on the conceptual model and the position of the observation point in the cross-section (see Table A5.18).

Once started, program DP_LAQ reads the input file DP_LAQ.INP and writes data into DP_LAQ.OUT.

Example 1. Drawdown calculations in observation wells located in the main aquifer of a three-flow system and in adjacent aquifers (Fig. A5.4b). Table A5.19 gives input data for solving the problem. The pumping-well radius is incorporated when evaluating dimensionless parameters, but its value will have no effect on the result, if the wellbore storage is excluded from calculations ($LD = 2$).

Table A5.20 gives dimensionless parameters based on formulas in Table A5.17 and input data in Table A5.19.

Table A5.19 Input data for calculations in three-flow system

Parameter	Value	Description
m, m', m''	20, 5, 10	The thicknesses of the main aquifer and the upper and bottom aquitards, m
r	1	Distances from the observation well to the pumping well, m
t	0.01	The time elapsed from the start of pumping, d
r_w	0.1	Wellbore radius, m
$z'_p (z''_p)$	3 (7)	The vertical distance from the top (bottom) of the main aquifer to the observation point in the top (bottom) aquitard, m
k, k', k''	1, 0.01, 0.005	Hydraulic conductivities of the main aquifer and the top and bottom aquitards, m/d
S, S', S''	1e-5, 1e-4, 2e-4	Storage coefficients of the main aquifer and the top and bottom aquitards, dimensionless
B_1, B_2	100, 200	Leakage factors, m; $B_1 = \sqrt{kmm'/k'}$, $B_2 = \sqrt{kmm''/k''}$

Table A5.20 Calculation of dimensionless parameters of program DP_LAQ for three-flow system

TDLAST	SIGP	GAMMP	ZDP	SIGPP	GAMMPP	ZDPP	RD
2.0e4	10	1.0e-3	0.6	20	5.0e-4	0.7	10

Example of input file for drawdown calculation in a three-flow system with two adjacent aquitards:

8				
1	2	1	1	
10.0		1.0e-3		0.6
20.0		5.0e-4		0.7
10		0.0		0.0
2.0e4	0	1		
1.0	1			

The output file will contain three dimensionless-drawdown values: for the main aquifer (HD = 8.317192D+00), for the top aquitard (HDP = 2.471643D+00), and for the bottom aquitard (HDPP = 8.136826D-03), whence we evaluate drawdowns:

$$s = \frac{Q}{4\pi km}HD, \quad s' = \frac{Q}{4\pi km}HDP, \quad \text{and } s'' = \frac{Q}{4\pi km}HDPP.$$

To take into account the wellbore storage and skin, specify the values WD and WSKIN in the fifth line of the input file and set LD = 1.

Table A5.21 Input data for calculations in a fractured–porous medium

Parameter	Value	Description
r	1	Distance from the observation to pumping well, m
t	0.01	Time elapsed from the start of pumping, d
r_w	0.1	Wellbore radius, m
k, k'	1, 0.1	Hydraulic conductivities of fractured and block system, m/d
S_s, S'_s	1e-5, 1e-3	Specific storages of the nfractured and block system, 1/m
m_b	2	Block dimensions $a = b = c$, m (see comments to XLAM in Table A5.17)

Table A5.22 Calculation of dimensionless parameters of DP_LAQ program for fractured–porous media

TDLAST	SIG	GAMM	XLAM ^a	RD
1.0e3	100	3.16e-2	1.5e-2	10

^aThe parameter was calculated for $n = 3$; $l = 2$; $\alpha = 15 \text{ 1/m}^2$ (see comments to XLAM in Table A5.17)

Example 2. Calculating the drawdown in a fractured–porous medium—Warren–Root model (Fig. 6.1c). Table A5.21 gives the input data for the problem solution.

Table A5.22 gives dimensionless parameters calculated by formulas in Table A5.17 and input data in Table A5.21.

An example of input file for calculations in fractured–porous medium (Warren–Root model):

8				
1	2	6	2	
	10		0.0	0.0
	100.0		3.16e-2	0.0
	1.5e-2			
	1.0e3	0	1	
	1.0	1		

The output file will contain the value of dimensionless drawdown: $HD = 3.128315D+00$, whence we find the drawdown $s = \frac{Q}{4\pi km} HD$.

Comment. In the original code of DP_LAQ program, the calculation and output of HDP and HDPP are commented-out. This refers to the calculations of the drawdown in aquitards and block. To activate these program segments, remove comment signs from Lines 237–246, Line 269 and comment-out Line 268.

Table A5.23 Input parameters of WHI program

Parameter	Denotation	Description
<i>Line 1</i>		
FORMAT		Analysis format, enter 'TYPE CURVE' for dimensionless type-curve analysis; enter 'DIMENSIONAL' for dimensional analysis
<i>Line 2</i>		
D	m	Initial saturated thickness of the aquifer, in units of length
HKX, HKY, HKZ	k_x, k_y, k_z	Principal hydraulic conductivities in the x, y, and z axes, m/d, in units of length per time; $k_x = k_r$
SS, SY	S_s, S_y	Specific storage (1/m) and specific yield (dimensionless)
<i>Line 3</i>		
IDRA		Type of drainage at water table: 0 (instantaneous drainage), 1 (delayed drainage)
<i>Line 3a—only if IDRA = 1</i>		
ALPHA1	α	Empirical drainage index used in Boulton's model, in units of inverse time; this can be determined by relationship Eq. 2.15 or Eq. 2.16
<i>Line 4 for FORMAT = TYPE CURVE</i>		
TDLAST	$\frac{\sqrt[3]{k_x k_y k_z}}{S_y m^2} t$	Largest value of dimensionless time. For calculating a single value—TDLAST = TD
NLC		Number of logarithmic cycles on time scale. Enter 0 to calculate a single value
NOX		Number of equally spaced times per logarithmic cycle for which the drawdown will be calculated. Enter 1 to calculate a single value
<i>Line 4 for FORMAT = DIMENSIONAL</i>		
ITS		Time specification: 0 (log-cycle times), 1 (user-specified times)
IMEAS		Measured drawdown data, enter 0 if ITS = 0; options for ITS = 1: 0 (measured data not specified for each time), 1 (measured data specified for each time)
<i>Line 4a—only for FORMAT = DIMENSIONAL</i>		
TLAST		Largest value of time, enter 0.0 if ITS = 1
NLC		Number of logarithmic cycles on time scale, enter 0 if ITS = 1. Enter 0 to calculate a single value
NOX		Number of equally spaced times per logarithmic cycle for which the drawdown will be calculated, enter 0 if ITS = 1. Enter 1 to calculate a single value
<i>Line 5</i>		
RERRNR		Relative error for Newton–Raphson iteration, a value of $1e-10$ is suggested
NTMS		Factor used to determine the number of terms in the finite summations for water-table aquifers; suggested values are 20 or 30. For partially penetrating wells or a piezometer, increase this value

(continued)

Table A5.23 (continued)

Parameter	Denotation	Description
NS		Number of Stehfest terms; must be an even integer; 8 terms are usually sufficient
<i>Line 6</i>		
IPWS		Type of pumped well: 0 (horizontal well), 1 (inclined well)
<i>Line 7</i>		
Q	Q	Pumping rate of the horizontal or inclined well, in units of cubic length per time. In dimensionless format, this is a fictitious value
ZW	$m - L_{rw}$	Distance from horizontal well to the bottom boundary, or distance from the center of the inclined well to the bottom boundary, in units of length
XLEN	l_w	Horizontal or inclined well-screen length, in units of length
ANGLE	θ	Angle between the inclined well and the x axis, in radians; 0°—horizontal well, 90°—vertical well. Leave blank if IPWS = 0 (horizontal well)
<i>Line 8</i>		
NOBWC		Number of observation wells or piezometers for which type curves will be calculated; must be less than or equal to 25. Enter 1 to calculate a single value
<i>Line 9</i>		
IOWS		Type of observation well or piezometer: 0 (partially penetrating observation well), 1 (fully penetrating observation well), 2 (observation piezometer)
<i>Line 10</i>		
X0, Y0		x and y are the coordinates of the observation well, in units of length. The pumping well is located in coordinate origin (x = 0, y = 0); therefore, the distance from the observation to the pumping well can be calculated as $r = \sqrt{X0^2 + Y0^2}$
Z1	$m - L_{rp} + \frac{l_p}{2}$	z coordinate of the top of screened interval of observation well (only for IOWS = 0 or 2)
Z2	$m - L_{rp} - \frac{l_p}{2}$	z coordinate of the bottom of screened interval of observation well (only for IOWS = 0)
<i>Line 11</i> —only when ITS = 1; only for FORMAT = DIMENSIONAL		
NTSOB		Number of user-specified times at which the drawdown will be calculated. Enter 1 to calculate a single value
<i>Line 12</i> —only when ITS = 1; only for FORMAT = DIMENSIONAL		
TIMEOB (ID)		To determine a single drawdown in an observation well or piezometer, specify a single moment at which the drawdown is to be calculated
XMEASOB (ID)		Measured drawdown for time i. Leave blank if IMEAS = 0

Appendix 5.6 Program WHI

The program was developed in 2001 by H. Zhan and V.A. Zlotnik. The description of input parameters (Table A5.23) is based on the code WHI.FOR, publications by the program’s authors (Zhan and Zlotnik 2002a), and an unpublished reference manual (Zhan and Zlotnik 2002b).

Program application features (see Fig. 7.2) include:

- the aquifer is homogeneous, horizontally and vertically anisotropic, and unconfined;
- the pumping well is horizontal or inclined;
- gradual drainage at water table can be taken into account;
- the drawdown (or dimensionless drawdown) is calculated for a fully penetrating or partially penetrating well, or in a piezometer;
- the wellbore radius is assumed to be infinitely small, i.e., the wellbore storage is neglected.

Input. Input-file format for calculating a single value (the number of lines depends on the output format and the type of drainage at water table):

FORMAT					
D	HKX	HKY	HKZ	SS	SY
IDRA					
ALPHA1				only if IDRA = 1 (delayed drainage)	
TDLAST	NLC	NOX		only if FORMAT = TYPE CURVE	
ITS	IMEAS		only if FORMAT = DIMENSIONAL		
TLAST	NLC	NOX			
RERRNR	NTMS	NS			
IPWS					
Q	ZW	XLEN	ANGLE		
NOBWC					
IOWS					
X0	Y0	Z1	Z2		
NTSOB					
TIMEOB (ID)				XMEASOB (ID)	
				only if FORMAT = DIMENSIONAL	
				only if FORMAT = DIMENSIONAL	

Output. After execution of the program, the values that will be written in the output file will be the calculated function value in the case of dimensionless output (FORMAT = TYPE CURVE) or the drawdown in the case of dimensional output (FORMAT = DIMENSIONAL), see Eq. 7.3.

Program WHI reads the input file named INPUT and writes data into OUTPUT.

Example. Drawdown calculation in a partially penetrating observation well. The calculations are carried out in dimensionless and dimensional form. The input data for problem solution are given in Table A5.24.

Table A5.24 Input data for calculating drawdown in an unconfined aquifer at pumping from a horizontal well

Parameter	Vallue	Description
m	20	Initial water-saturated thickness, m
X0, Y0	1, 1	Coordinates of observation well, m
t	0.01	Pumping start time, d
Q	100	Pumping-well discharge rate, m ³ /d
l_w, l_p	10, 18	Screen lengths of the pumping and observation wells, m
L_{Tw}, L_{Tp}	15, 10	Distances from the initial water table to the screen centers of the pumping and observation wells, m
k_x, k_y, k_z	1, 1, 0.5	Horizontal and vertical hydraulic conductivities, m/d; $k_x = k_r$
S_s	0.00001	Specific storage, 1/m
S_y	0.1	Specific yield, dimensionless

The missing parameters for the input file of WHI program are calculated based on Tables A5.23 and A5.24: $ZW = m - L_{Tw} = 5$ m, $Z1 = m - (L_{Tp} - l_w/2) = 19$ m, $Z2 = m - (L_{Tp} + l_w/2) = 1$ m.

Example of input file for dimensional output:	Input-file format:
DIMENSIONAL	FORMAT
20.0 1.0 1.0 0.5 1.0e-5 0.1	D HKX HKY HKZ SS SY
0	IDRA
1 0	ITS IMEAS
0.0 0 0	TLAST NLC NOX
1.0e-10 30 8	RERRNR NTMS NS
0	IPWS
100.0 5.0 10.0	Q ZW XLEN
1	NOBWC
0	IOWS
1.0 1.0 19.0 1.0	X0 Y0 Z1 Z2
1	NTSOB
0.01	TIMEOB (ID)

In the output file, we will have: CALCULATED DRAWDOWN = 0.1882D+01.

For dimensionless output, specify

$$TDLAST = TD/RDSQ = t(X0^2 S_s/k_x + Y0^2 S_s/k_y)^{-1} = 500.0.$$

An example of input file for dimensionless output:	Input-file format:
TYPE CURVE 20.0 1.0 1.0 1.0 0.5 1.0e-5 0.1 0 500.0 0 1 1.0e-10 30 8 0 100.0 5.0 10.0 1 0 1.0 1.0 19.0 1.0	FORMAT D HKX HKY HKZ SS SY IDRA TDLAST NLC NOX RERRNR NTMS NS IPWS Q ZW XLEN NOBWC IOWS X0 Y0 Z1 Z2

In the output file, we will obtain DIMENSIONLESS DRAWDOWN (HD) = 0.1878D+01. From the obtained value, we calculate the drawdown so:

$$s = \frac{Q}{2\pi m^3 \sqrt{k_x k_y k_z}} HD,$$

which corresponds to the value calculated above.

Appendix 6

Application of UCODE_2005

The operation of computer code UCODE_2005 is illustrated by the solution of inverse problems implemented in ANSDIMAT software with the use of the ATFU module (Sindalovskiy 2014). The ATFU module is intended to solve basic groundwater flow equations (see Parts I and II) that enable calculating groundwater-level variations in an aquifer given the hydraulic characteristics. The minimal data set required for running UCODE_2005 and evaluating aquifer parameters based on groundwater-level measurements during an aquifer test is described. An exhaustive description of UCODE_2005 is given in the manual (Poeter et al. 2005).

Computer program ANSDIMAT creates input files in UCODE_2005 format and starts its execution. In its turn, UCODE_2005 (1) starts the ATFU module with supposed values of hydraulic characteristics, (2) analyzes the calculated water-level variations and appropriate actually measured values, (3) corrects the parameters by special algorithms, and (4) restarts ATFU. In this manner, the program UCODE_2005 iterates the ATFU module until the required convergence is achieved. For solving the problem, UCODE_2005 is to be provided with the formats of the input and output files of the program to be run (in this case, ATFU).

The ATFU module takes input data (discharge rate, distance, time, drawdown, etc.) from the input files of ANSDIMAT program and solves the chosen equation with the specified parameters. The ATFU input file (*input.atu*) contains the values of hydraulic parameters arranged in one column. The parameters and their number depend on the chosen equation. For example, in the case of the Theis solution (Eq. 1.3), these are aquifer transmissivity and hydraulic diffusivity:

200

1e5

while in the case of the Neuman solution (Eq. 2.1), the data include horizontal and vertical hydraulic conductivities, storage coefficient, and specific yield:

1

0.5

1e-4

0.1

ATFU creates an output file (*output.atu*) containing a column of the calculated drawdown values for the chosen observation wells and time moments. For example,

```
0.1348103
0.1809126
0.2345209
0.2944637
0.3597146
0.4298151
```

Before the first run, the input file (*input.atu*) is to contain the starting values of the parameters to be adjusted; this file will be modified by UCODE 2005 in the process of the inverse-problem solution.

To solve the inverse problem requires: (1) to choose the factual water level changes in observation wells to be used in solving the problem and (2) to choose the hydraulic characteristics to be evaluated. For example, in the case of the Theis solution (Eq. 1.3), there are three possibilities: (a) simultaneous evaluation of the transmissivity and hydraulic diffusivity, (b) the evaluation of transmissivity given the hydraulic diffusivity, or (c) the evaluation of hydraulic diffusivity given the transmissivity.

Before running UCODE_2005, three files are to be created: *main input file*, *instruction file*, and *template file*. The command line for running the program is:

```
UCODE_2005.exe input-file fn,
```

where *input-file* is the name of the main input file, *fn* is filename prefix for UCODE_2005 output files.

1. Main input file

In the problem under consideration, the name of main input file is *ucode_atfu.in*. The main input file includes input blocks with the basic structure:

```
Begin Blocklabel [Blockformat]
  Blockbody
End Blocklabel
```

Blocklabel. The variable blocklabel identifies the purpose of the data block and the data it can contain. To solve the problem requires the following nine **Blocklabel**'s: Options, Ucode_Control_Data, Reg_Gn_Controls, Model_Command_Lines, Parameter_Groups, Parameter_Data, Observation_Data, Model_Input_Files, and Model_Output_Files.

Blockbody. Contains data or the names of files from which the data are to be read. The format of the data is determined by **Blockformat**.

Blockformat. Defines the structure of the data presented: KEYWORDS, TABLE.

KEYWORDS. **Blockbody** consists of a series of lines in the form: Keyword=value. For example, Verbose=0. This appendix give only the keywords required to solve the problem under consideration. For the full set of keywords for each input block, see the guide (Poeter et al. 2005).

TABLE. **Blockbody** consists of a table of data that may have labels on the columns and may be read from the main input file. The format of the first line for data input in TABLE format:

```
NROW=nr NCOL=nc [COLUMNLABELS] [GROUPNAME=gpname]
```

Here, NROW and NCOL are required keywords; *nr* is the number of rows in the table; *nc* is the number of columns in the table; COLUMNLABELS are column names used to identify the data in the columns of the table; GROUPNAME=*gpname* can be used to assign a group name to all rows in the table; *gpname* is the group name.

The Main input file (*ucode_atfu.in*) consists of nine successively written input blocks, whose format is described in examples below.

1.1 Options input block

The Options input block can be used to control the information written to the main output file. To solve the problem requires one keyword: *Verbose*.

Verbose. Flag that controls what is written to the UCODE_2005 main output file: **0** (no extraneous output), **1** (warnings), **2** (warnings, notes), **3** (warnings, notes, echo selected input), **4** (warnings, notes, echo all input), **5** (warnings, notes, echo all input, plus some miscellaneous information).

Example:

```
BEGIN Options KEYWORDS
  Verbose=0
END Options
```

1.2 UCODE_Control_Data input block

The UCODE_Control_Data input block defines the operations pursued by UCODE_2005 and defines some labeling for data-exchange files. To solve the problem requires three keywords: *ModelName*, *Optimize*, *DataExchange*.

ModelName. Identifies the model. Up to twelve characters.

Optimize. **yes**: estimate parameters; **no**: do not estimate parameters.

DataExchange. **yes**: generate the data-exchange files containing data for graphical and numerical analysis. **no**: do not produce the files.

Example:

```
BEGIN UCODE_CONTROL_DATA KEYWORDS
  ModelName=ANSDIMAT
  Optimize=yes
  DataExchange=yes
END UCODE_CONTROL_DATA
```

1.3 Reg_GN_Controls input block

The Reg_GN_Controls input block controls the performance of the modified Gauss-Newton regression method of estimating parameter values for the UCODE_2005 parameter-estimation mode. To solve the problem requires six keywords: *TolPar*, *TolSOSC*, *MaxIter*, *MaxChange*, *MaxChangeRealm*, and *Stats_On_Nonconverge*.

TolPar. Tolerance based on parameter values: parameter-estimation iterations stop if the maximum fractional change in parameter values between parameter-estimation iterations is less than the value of **TolPar**. Default = 0.01.

TolSOSC. Tolerance based on changes to model fit: parameter-estimation iterations stop if the fractional decline in the sum-of-squared weighted residuals over three parameter-estimation iterations is less than **TolSOSC**. A value of 0.01 requires the reduction to be less than 1 percent over three parameter-estimation iterations. If **TolSOSC** = 0.0, it is not used. Default = 0.0.

MaxIter. Maximum number of parameter-estimation iterations allowed before stopping. Default = 5.

MaxChange. Maximum fractional amount parameter values are allowed to change between parameter-estimation iterations. The value specified here applies to all parameters; use the **Parameter_Data** input block to define a unique **MaxChange** for each parameter. Default = 2.0, which means that parameter values can change as much as 200 percent.

MaxChangeRealm. **Native:** **MaxChange** applies in native space. **Regression:** **MaxChange** applies in regression space. In regression space, **MaxChange** applies to log-transformed values for log-transformed parameters. Default = Native.

Stats_On_Nonconverge. **yes:** when parameter estimation does not converge in the maximum number of iterations, calculate final sensitivities and calculate and print final statistics. **no:** when parameter estimation does not converge, do not calculate and print final statistics.

Example:

```
BEGIN REG_GN_CONTROLS KEYWORDS
  TolPar=0.01
  TolSOSC=0.00
  MaxIter=5
  MaxChange=2
  MaxChangeRealm=Native
  Stats_On_Nonconverge=yes
END REG_GN_CONTROLS
```

1.4 Model_Command_Lines input block

The **Model_Command_Lines** input block defines the command needed to execute a process model. This block contains three keywords: **Command**, **Purpose**, and **CommandID**.

Command. Operating system command that executes the process model(s).

Purpose. The type of process-model run executed by **Command**. Default = forward (the command makes a model run that generates simulated values).

CommandID. A name for the command. The command name is used at the top of the main output file in a list of the programs run; it does not influence the execution process.

Example:

```
BEGIN MODEL_COMMAND_LINES
  Command=atfu.exe
  Purpose=forward
  CommandId=atfu
END MODEL_COMMAND_LINES
```

1.5 Parameter_Groups input block

Use the `Parameter_Groups` input block to assign data that apply to all or many of the parameters within defined groups. To solve the problem requires five keywords: `GroupName`, `Adjustable`, `Transform`, `PerturbAmt`, and `SenMethod`.

`GroupName`. The name of the group (up to twelve characters; not case sensitive). Default = `ParamDefault`.

`Adjustable`. **yes**: change this value as needed depending on the purpose of the UCODE_2005 run defined in the `UCODE_Control_Data` input file. **no**: leave the value of this parameter unchanged.

`Transform`. **yes**: log-transform the parameter for the regression. **no**: estimate the native value in the regression. If `Transform=yes`, any transformed values printed to files are in log base 10 except that weighted residuals for prior information are in natural log. Within the program, calculations are done using natural logs.

`PerturbAmt`. Fractional amount of the parameter value to perturb to calculate sensitivity. Commonly 0.01–0.10.

`SenMethod`. A flag indicating how sensitivities are obtained. Sensitivities for different parameters can be obtained using different methods. For each parameter, sensitivities for all simulated values are calculated by a single method. Options include: **1** (calculate by forward-difference perturbation) and **2** (calculate by central-difference perturbation—two-point method).

Example:

```
BEGIN PARAMETER_GROUPS KEYWORDS
  GroupName=Default
  Adjustable=yes
  Transform=yes
  PerturbAmt=0.01
  SenMethod= 1
END PARAMETER_GROUPS
```

1.6 Parameter_Data input block

The `Parameter_Data` input block provides information about individual parameters. To solve the problem requires two keywords: `ParamName` and `StartValue`.

`ParamName`. Parameter name (up to 12 characters; not case sensitive)—a character string that is used in a template file. Each parameter name needs to be unique. In this problem, the names assigned to parameters are P1, P2, P3, etc.

`StartValue`. Starting parameter value.

Example (evaluating two parameters P1 and P2, the initial values for the search are 200 and 100000):

```
BEGIN PARAMETER_DATA TABLE
  nrow= 2  ncol=2  columnlabels groupname=default
  ParamName StartValue
  P1      200
  P2     100000
END PARAMETER_DATA
```

1.7 Observation_Data input block

The *Observation_Data* input block provides information about individual observations. To solve the problem requires four keywords: *ObsName*, *ObsValue*, *Statistic*, and *StatFlag*.

ObsName. Observation name (up to 20 characters, not case sensitive). Each observation name needs to be unique. The format of the observation name in this problem is as follows: letter «h» + measurement no. + «.» + observation well no. For example, h3.2 means the third measurement in the second well.

ObsValue. Observation value.

Statistic. Value used to calculate the observation weight.

StatFlag. Character string that defines the corresponding statistic and how it is used to calculate the weight. Options are: **var** (variance— $1/\text{Statistic}$), **sd** (standard deviation— $1/\text{Statistic}^2$), **cv** (coefficient of variation— $1/(\text{Statistic} \times \text{ObsValue}^2)$), **wt** (weight— Statistic), **sqrwt** (square root of the weight— Statistic^2).

Example (measurements in two observation wells; six measurements in the first well and four measurements in the second):

```
BEGIN OBSERVATION_DATA TABLE
  NROW=10  NCOL=4  COLUMNLABELS
  ObsName  ObsValue  Statistic  StatFlag
  h1.1     3.99     1         wt
  h2.1     4.1      1         wt
  h3.1     4.2      1         wt
  h4.1     4.33     1         wt
  h5.1     4.42     1         wt
  h6.1     4.5      1         wt
  h1.2     1.51     1         wt
  h2.2     1.61     1         wt
  h3.2     1.7      1         wt
  h4.2     1.78     1         wt
END OBSERVATION_DATA TABLE
```

1.8 Model_Input_Files input block

The *Model_Input_Files* input block lists each process-model input file that needs to be changed when parameter values change and an associated template file. This block contains two keywords: *ModInFile* and *TemplateFile*.

ModInFile. Name for a process-model input file. In this problem—*input.atu*.

TemplateFile. Name of the template file that UCODE_2005 will use to create the associated process-model input file, ModInFile. In this problem—*atfu.in.tpl*.

Example:

```
BEGIN MODEL_INPUT_FILES KEYWORDS
  ModInFile=input.atu
  TemplateFile=atfu.in.tpl
END MODEL_INPUT_FILES
```

1.9 Model_Output_Files input block

The Model_Output_Files input block defines how UCODE_2005 obtains values from the files produced by the process model. This block contains three keywords: ModOutFile, InstructionFile, and Category.

ModOutFile. Name of the process-model output file from which UCODE_2005 is to extract values. In this problem—*output.atu*.

InstructionFile. Name for the instruction file that UCODE_2005 uses to extract values from ModOutFile. In this problem, this is *ucode_atfu.ins*.

Category. The following options are available: **Obs** (the process-model output file is used to calculate simulated equivalents to observations) and **Pred** (the process-model output file is used to calculate predictions).

Example:

```
BEGIN MODEL_OUTPUT_FILES KEYWORDS
  ModOutFile=output.atu
  InstructionFile=ucode_atfu.ins
  Category=Obs
END MODEL_OUTPUT_FILES
```

6.2 Instruction file

In this problem, the name of the instruction file is *ucode_atfu.ins*. Instruction file is used to read information from the process-model output files (*output.atu*). The first two lines of the instruction file contain:

```
jif @
StandardFile Nskip ReadColumn Nread
```

Given next are the names for each of the Nread values. Place each name on a new line.

jif @. Defines the file delimiter needed in instruction file. It is not used to read standard files.

StandardFile. A keyword that indicates a standard file is being read.

Nskip. The number of lines to skip at the beginning of the file, which can be 0 or any positive integer.

ReadColumn. The column of the file from which values are to be read.

Nread. The number of values, and therefore lines, to be read.

Example (the observation names and their number are to agree with data in Observation_Data input block):

```

jif @
StandardFile 0 1 10
h1.1
h2.1
h3.1
h4.1
h5.1
h6.1
h1.2
h2.2
h3.2
h4.2

```

An example of output file (output.atu):

```

3.999016
4.090797
4.180674
4.274287
4.364491
4.455947
1.445078
1.535643
1.624569
1.717396

```

6.3 Template file

In this problem, the name of template file is *atfu.in.tpl*. Template file is used to create process-model input files (*input.atu*). The format of the template file:

```

jtf !
!name!

```

jtf !. Defines the file delimiter needed in template file.

!name!. Here, given between the exclamation marks is the name of the parameter to be evaluated (in the denotations of the problem under consideration P1, P2). The length of the character variable *!name!* is to be equal to the number of characters in the value of the output parameters of file *input.atu*. The lacking characters are replaced by spaces. That is, if the parameter P1 to be evaluated is to be written in the output file as 200.376696988261 (consisting of sixteen characters), then *!name!* is to be written as *!P1□□□□□□□□□□□□□□!*, where the number of spaces (□) is twelve.

Example (template file for the input file *input.atu* for the problem):

```

jtf !
!P1□□□□□□□□□□□□□□!
!P2□□□□□□□□□□□□□□!

```

Here, □ means a space.

Once the inverse problem is solved, the input file (*input.atu*) will contain the required parameters. For example:

```
200.376696988261  
106200.762282559
```

In this example, the program was required to evaluate two parameters. If the first parameter (transmissivity) is to be found, given the second (the hydraulic diffusivity is $1e5$), the template file becomes

```
jtf !  
!P1□□□□□□□□□□□□□□!  
100000.0
```

Otherwise, if the second parameter (hydraulic diffusivity) is to be found, given the first (the transmissivity is 200):

```
jtf !  
200.0  
!P2□□□□□□□□□□□□□□!
```


Appendix 7

Special Functions: Analytical Representations, Graphs, and Approximations

This appendix gives integral expressions and plots of widely known and special mathematical functions that enter into basic groundwater-flow equations (see Parts I and II). The majority of these functions are given with their approximations. The functions and their approximations were taken from different sources. For some functions, the author's approximations are presented. The functions are plotted based on tabulated values presented in the author's work (Sindalovskiy 2006).

Appendix 7.1 Well-Function $W(u)$

Function (Carslow and Jaeger 1959; Theis 1935) (Fig. A7.1 and Table A7.1):

$$W(u) = \int_u^\infty \frac{\exp(-\tau)}{\tau} d\tau; \quad W(u) = -E_i(-u) = E_1(u),$$

where $-E_i(-u)$ is exponential integral function.

Limits of the function: $W(0) = \infty$, $W(\infty) = 0$.

Function derivative:

$$\frac{\partial W(u)}{\partial u} = -\frac{\exp(-u)}{u}.$$

Expansion in series:

$$W(u) = -\gamma - \ln u - \sum_{n=1}^\infty \frac{(-1)^n u^n}{nn!},$$

where $\gamma = 0.5772156649$ is Euler's constant.

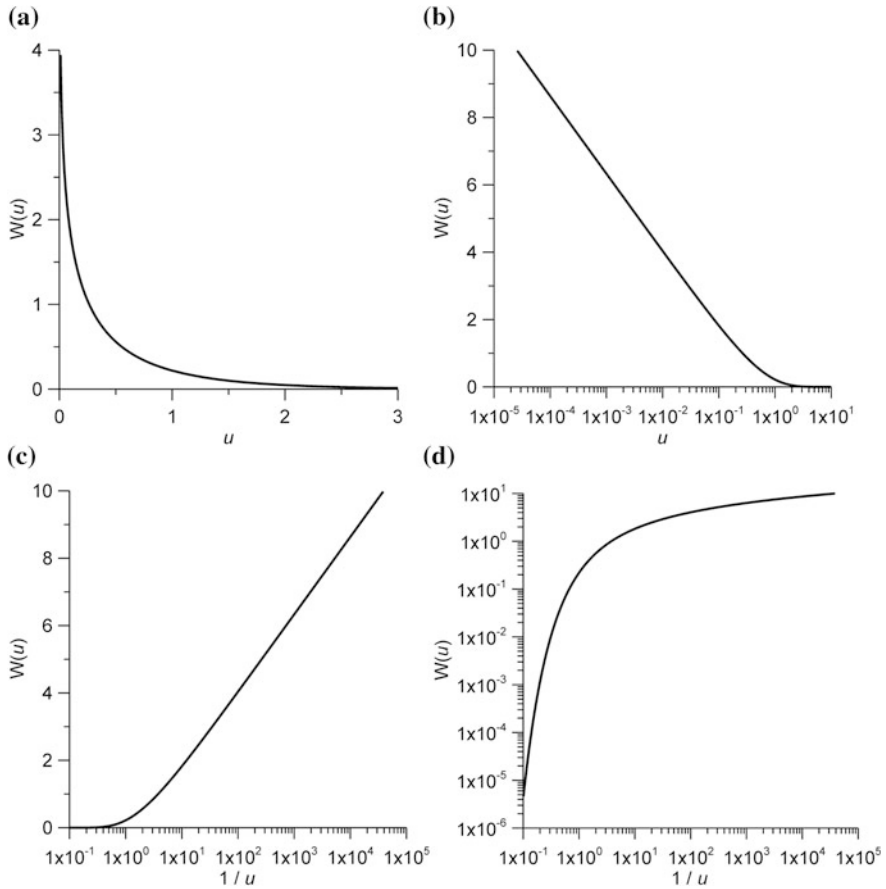


Fig. A7.1 Plots of function $W(u)$: **a** $W(u) - u$, **b** $W(u) - \lg(u)$, **c** $W(u) - \lg(1/u)$, **d** $\lg[W(u)] - \lg(1/u)$

Table A7.1 Approximation of function $W(u)$ (Abramowitz and Stegun 1964)

Range	Representation
$u < 0.05$	$W(u) \approx \ln \frac{0.562}{u}$ —for practical calculations (Hantush 1964)
$u \leq 1$	$W(u) = -\ln u - \gamma + 0.99999193 u - 0.24991055 u^2 + 0.05519968 u^3 - 0.00976004 u^4 + 0.00107857 u^5$
$u \geq 1$	$W(u) = \frac{e^{-x}}{x} \times \frac{u^4 + 8.5733287401 u^3 + 18.059016973 u^2 + 8.6347608925 u + 0.2677737343}{u^4 + 9.5733223454 u^3 + 25.6329561486 u^2 + 21.0996530827 u + 3.9584969228}$

Applications. This function enters into many basic analytical relationships. Its main application is the Theis solution (Eq. 1.1), where $u = \frac{r^2 S}{4Tt} = \frac{r^2}{4at}$.

Appendix 7.2 Well-Function for Leaky Aquifers $W(u, \beta)$

Function (Hantush and Jacob 1955) (Fig. A7.2 and Tables A7.2 and A7.3):

$$W(u, \beta) = \int_u^\infty \frac{1}{\tau} \exp\left(-\tau - \frac{\beta^2}{4\tau}\right) d\tau, \quad W(u, \beta) = 2K_0(\beta) - W\left(\frac{\beta^2}{4u}, \beta\right)$$

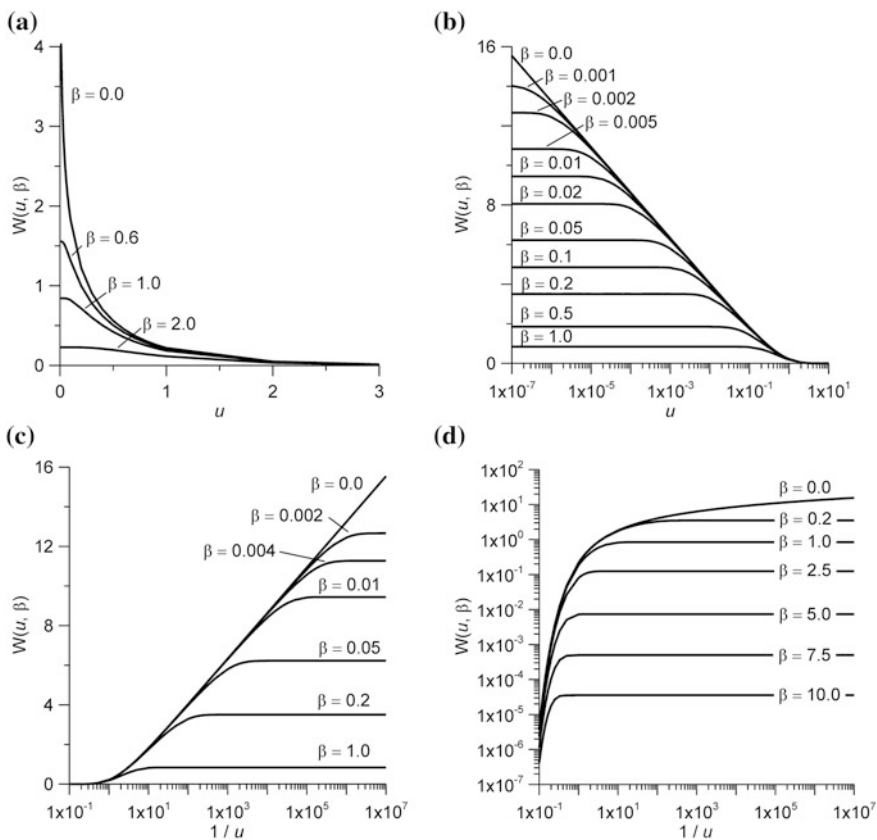


Fig. A7.2 Plots of function $W(u, \beta)$ at different values of its second argument: **a** $W(u, \beta) - u$, **b** $W(u, \beta) - \lg(u)$, **c** $W(u, \beta) - \lg(1/u)$, **d** $\lg[W(u, \beta)] - \lg(1/u)$

Table A7.2 Approximation of function $W(u, \beta)$ (Hantush and Jacob 1955)

Range	Representation
$u \leq 1.0$	$W(u, \beta) = \left(2K_0(\beta) - I_0(\beta)W\left(\frac{\beta^2}{4u}\right) + \exp\left(-\frac{\beta^2}{4u}\right) \left(\gamma + \ln u + W(u) - u + 4u \frac{I_0(\beta) - 1}{\beta^2} \right) - \left(-u^2 \sum_{n=1}^{\infty} \sum_{m=1}^n \frac{(-1)^{n+m}(n-m+1)!}{(n+2)!^2 u^{m-n}} \left(\frac{\beta^2}{4}\right)^m \right) \right)$ <p>For $\beta \leq 2.0$, the infinite series can be replaced by six terms (Walton 1984)</p>
$u \leq 1.0, \beta \leq 0.2$	$W(u, \beta) = 2K_0(\beta) - I_0(\beta)W\left(\frac{\beta^2}{4u}\right) + \exp\left(-\frac{\beta^2}{4u}\right) \left(\gamma + \ln u + W(u) + \frac{u\beta^2}{16} \left(1 - \frac{u}{9}\right) \right)$
$u \leq 0.1, \beta \leq 0.2$	$W(u, \beta) = 2K_0(\beta) - I_0(\beta)W\left(\frac{\beta^2}{4u}\right) + \exp\left(-\frac{\beta^2}{4u}\right) \left(\frac{u\beta^2}{16} \left(1 - \frac{u}{9}\right) + u - \frac{u^2}{2.2!} + \frac{u^3}{3.3!} \right),$ <p>$2.2! = 2.42396548; 3.3! = 8.85534336$</p>
$u \geq 1.0$	$W(u, \beta) = \left(I_0(\beta)W(u) - e^{-u} \left(\gamma + \ln \frac{\beta^2}{4u} + W\left(\frac{\beta^2}{4u}\right) - \frac{\beta^2}{4u} + \frac{I_0(\beta) - 1}{u} \right) + \left(\frac{e^{-u}}{u^2} \sum_{n=1}^{\infty} \left(\frac{\beta^2}{4}\right)^n \sum_{m=1}^n \frac{(-1)^{n+m}(n-m+1)!}{(n+2)!^2 u^{n-m}} \right) \right)$ <p>For $\beta \leq 2.0$, the infinite series can be replaced by six terms (Walton 1984)</p>
$u \geq 1.0, \beta \leq 0.2$	$W(u, \beta) = I_0(\beta)W(u) - \frac{e^{-u}\beta^2}{4u} \left(1 - \frac{1}{36u} + \frac{\beta^2}{16} - \frac{\beta^2}{16u} \right)$

$\gamma = 0.5772156649$ —Euler’s constant

Limits of the function: $W(u, 0) = W(u), W(0, \beta) = 2K_0(\beta)$.

Function derivative:

$$\frac{\partial W(u, \beta)}{\partial u} = - \frac{\exp(-u - 0.25\beta^2/u)}{u}.$$

Expansion in series (Hunt 1977):

$$W(u, \beta) = \sum_{n=0}^{\infty} \left(-\frac{\beta^2}{4u} \right)^n \frac{E_{n+1}(u)}{n!},$$

where $E_n(u) = \int_1^{\infty} \frac{\exp(-u\tau)}{\tau^n} d\tau$ is exponential integral function. The series converges rapidly at $\beta^2/(4u) < 1$.

Applications. This function enters into many basic analytical relationships. The main application is Hantush–Jacob solution (Eq. 3.1), where $u = \frac{r^2 S}{4Tt} = \frac{r^2}{4at}, \beta = \frac{r}{B}$.

Table A7.3 Approximation of function $W(u, \beta)$ for practical applications

Range	Representation
$u > 2\beta$	$W(u, \beta) \approx W(u)$ (Hantush 1964)
$\beta < 0.1, u > 5\beta^2$	$W(u, \beta) \approx W(u)$ (Hantush 1964)
$\beta < 0.01$	$W(u, \beta) \approx W(u)$ (Hantush and Jacob 1955)
$u < 1.0, u < 0.05\beta^2$	$W(u, \beta) \approx 2K_0(\beta) - I_0(\beta)W\left(\frac{\beta^2}{4u}\right)$ (Hantush 1964)
$\beta > 2.0$	$W(u, \beta) = \sqrt{\frac{\pi}{2\beta}} \exp(-\beta) \operatorname{erfc}\left(-\frac{\beta - 2u}{2\sqrt{u}}\right)$ (Walton 2007)
$\beta < 2.0, u < 0.05\beta^2$	$W(u, \beta) = 2K_0(\beta)$ (Walton 2007)

Appendix 7.3 Special Function $M(u, \beta)$

Function (Hantush 1961a, b) (Fig. A7.3 and Table 7.4):

$$M(u, \beta) = \int_u^\infty \frac{\exp(-\tau)}{\tau} \operatorname{erf}(\beta\sqrt{\tau}) d\tau, \quad M(u, \beta) = -M(u, -\beta).$$

Limits of the function: $M(0, \beta) = 2 \operatorname{arcsinh} \beta = 2 \ln(\sqrt{1 + \beta^2} + \beta)$; $M(u, 0) = 0$; $M(u, \infty) = W(u)$.

Applications. This function enters into basic analytical relationships. The main application is in solutions for a linear source (see Sect. 1.3), where $u = \frac{r^2 S}{4Tt} = \frac{r^2}{4at}$; β depends on well location in the aquifer.

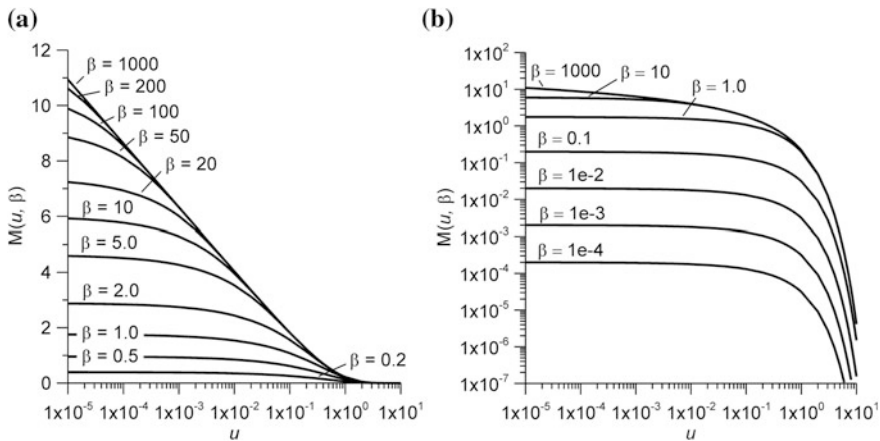


Fig. A7.3 Plots of function $M(u, \beta)$ at different values of its second argument: **a** $M(u, \beta) - \lg(u)$, **b** $\lg[M(u, \beta)] - \lg(u)$

Table A7.4 Approximation of function $M(u, \beta)$ (Hantush 1961b)

Range	Representation
$u < \frac{0.05}{\beta^2} < 0.01$	$M(u, \beta) = 2 \left(\operatorname{arcsinh} \beta - \frac{2}{\sqrt{\pi}} \beta \sqrt{u} \right)$
$u < \frac{0.05}{\beta^2}$	$M(u, \beta) = 2(\operatorname{arcsinh} \beta - \beta \operatorname{erf} \sqrt{u})$
$u > \frac{5}{\beta^2}$	$M(u, \beta) = W(u)$

Appendix 7.4 Special Function $H(u, \beta)$

Function (Hantush 1960) (Fig. A7.4 and Table A7.5):

$$H(u, \beta) = \int_u^\infty \frac{\exp(-\tau)}{\tau} \operatorname{erfc} \left(\frac{\beta \sqrt{u}}{\sqrt{\tau(\tau - u)}} \right) d\tau.$$

Limit of the function: $H(u, 0) = W(u)$.

Applications. This function enters into basic analytical relationships. The main application is in solutions for stratified systems (see Sect. 3.6), where $u = \frac{r^2 S}{4Tt} = \frac{r^2}{4at}$; β depends on the distance, leakage factor and the storage characteristics of the aquifer and aquitards.

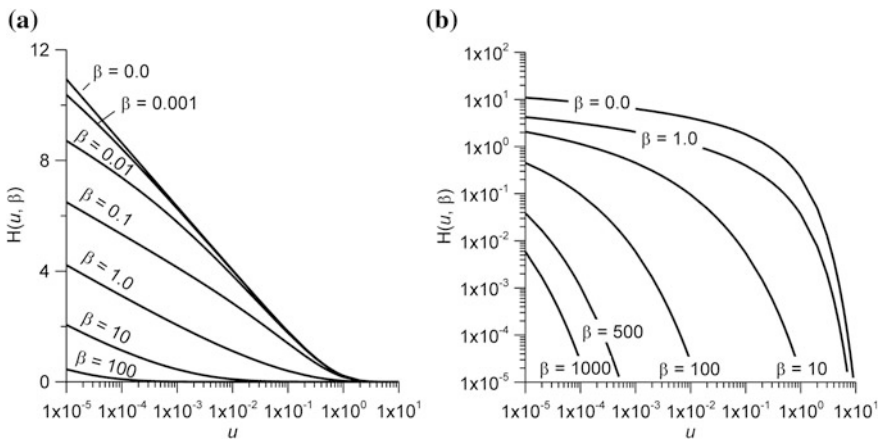


Fig. A7.4 Plots of function $H(u, \beta)$ at different values of its second argument: **a** $H(u, \beta) - \lg(u)$, **b** $\lg[H(u, \beta)] - \lg(u)$

Table A7.5 Approximation of function $H(u, \beta)$ (Hantush 1960)

Range	Representation
$u > 10^4 \beta^2$	$H(u, \beta) \approx W(u) - \frac{4\beta}{\sqrt{\pi u}} \left[0.258 + 0.693 \exp\left(-\frac{u}{2}\right) \right]$
$u < 10^{-5} \beta^{-2}$ and $u < 10^{-4} \beta^2$	$H(u, \beta) \approx \frac{1}{2} \ln \frac{0.044}{u \beta^2}$

Appendix 7.5 Boulton Function

Function (Boulton 1954) (Fig. A7.5 and Table A7.6):

$$F_B(u, \beta) = \int_0^\infty \frac{1}{\tau} J_0(\beta \tau) [1 - \exp(-u \tau \tanh \tau)] d\tau.$$

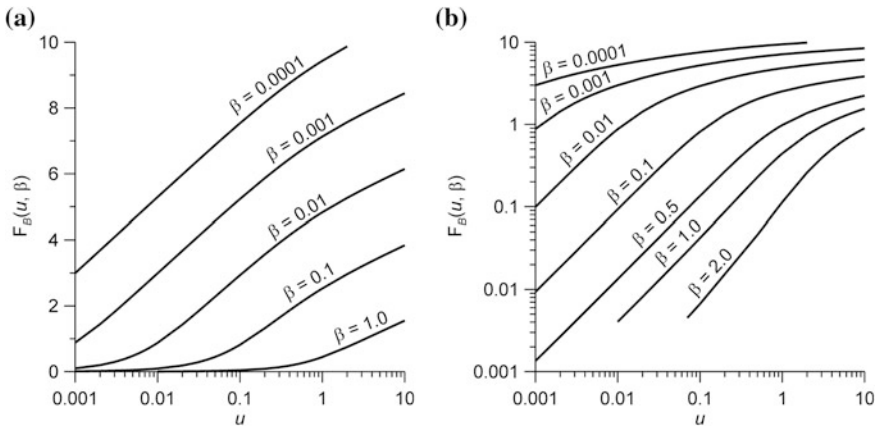


Fig. A7.5 Plots of function $F_B(u, \beta)$ at different values of its second argument: **a** $F_B(u, \beta) - \lg(u)$, **b** $\lg[F_B(u, \beta)] - \lg(u)$

Table A7.6 Approximation of function $F_B(u, \beta)$ for practical applications (Boulton 1954; Hantush 1964)

Range	Representation
$u < 0.05$	$F_B(u, \beta) \approx \operatorname{arcsinh} \frac{1}{\beta} + \operatorname{arcsinh} \frac{u}{\beta} - \operatorname{arcsinh} \frac{1+u}{\beta}$
$u < 0.01$	$F_B(u, \beta) \approx \operatorname{arcsinh} \frac{u}{\beta} - \frac{u}{\sqrt{1+\beta^2}}$
$u < 0.01; u/\beta > 10$	$F_B(u, \beta) \approx \ln(2u/\beta)$
$u > 5$	$F_B(u, \beta) \approx 0.5W\left(\frac{\beta^2}{4u}\right)$

Applications. Function, where $u = \frac{kt}{S_y m}$, $\beta = \frac{r}{m}$, enters into Boulton solution (Eq. 2.17) for unconfined aquifers.

Appendix 7.6 Neuman Function

Function $W_N(u, \beta)$ (Neuman 1973, 1975), where $u = t_s = \frac{k_r m t}{S r^2}$ and $u = t_y = \frac{k_r m t}{S_y r^2}$, $\beta = (\chi r/m)^2$, is defined in the text by Eqs. 2.1, 2.8, and 2.9 (see Sect. 2.1). The plots are given for fully penetrating wells (Figs. A7.6 and A7.7).

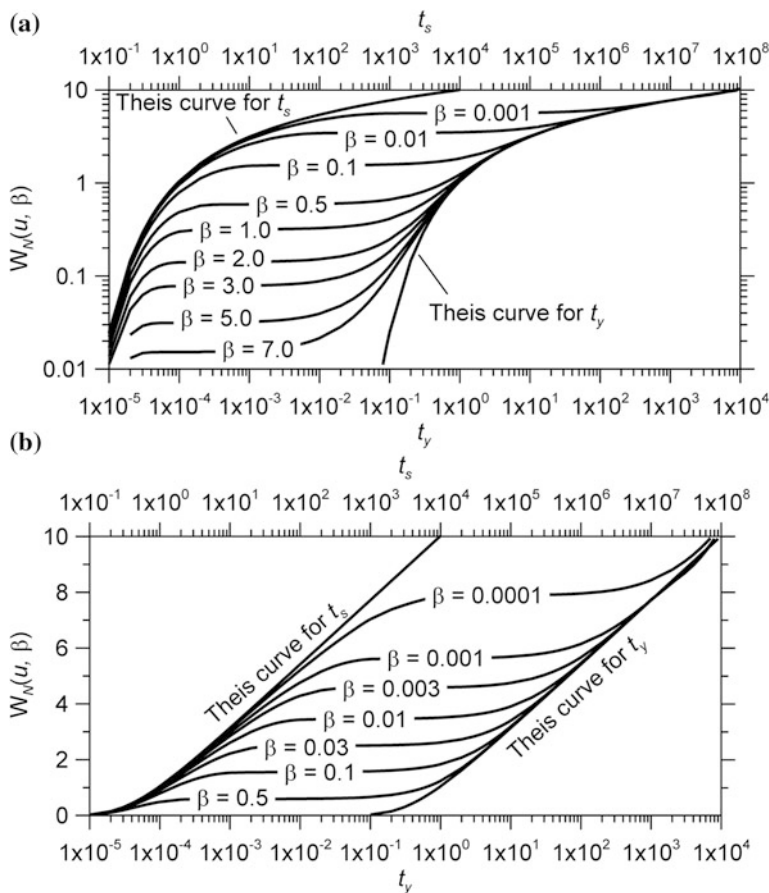


Fig. A7.6 Plots of function $W_N(u, \beta)$ at different values of its second argument: **a** $\lg[W_N(u, \beta)] - \lg(u)$, **b** $W_N(u, \beta) - \lg(u)$. The top scale is for $u = t_s$, the bottom scale, for $u = t_y$

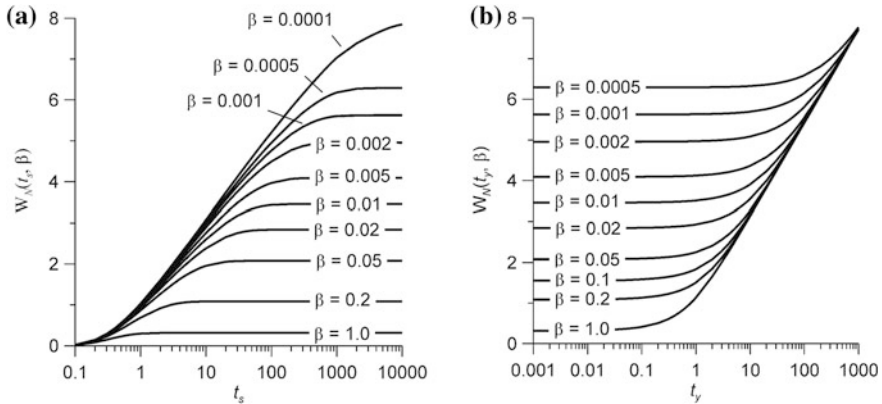


Fig. A7.7 Plots of function $W_N(u, \beta)$ at different values of its second argument: **a** $W_N(t_s, \beta) - \lg(t_s)$, **b** $W_N(t_y, \beta) - \lg(t_y)$

Appendix 7.7 Special Function $J^*(u, \beta_1, \beta_2)$

Function (Hantush 1965) (Fig. A7.8):

$$J^*(u, \beta_1, \beta_2) = 2 \int_1^\infty \exp[-\beta_1(\tau - 1) - u(\tau^2 + \beta_2^2)] \frac{\tau}{\tau^2 + \beta_2^2} d\tau.$$

Limits of the function: $J^*(u, \infty, \beta_2) = J^*(\infty, \beta_1, \beta_2) = J^*(0, \infty, \beta_2) = 0$, $J^*(u, 0, \beta_2) = W(u + u\beta_2^2)$.

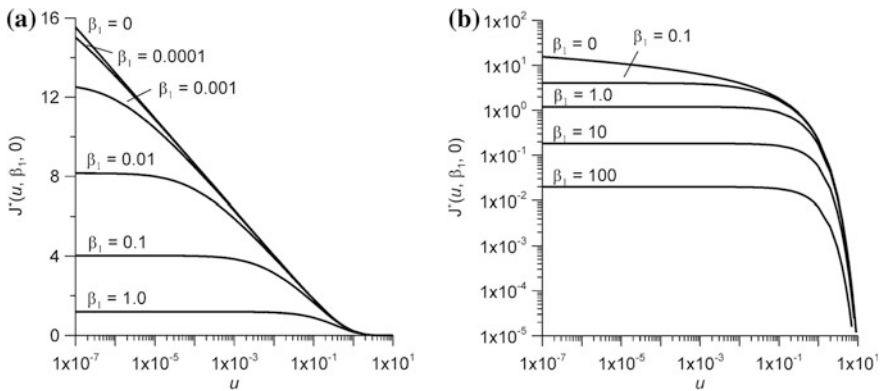


Fig. A7.8 Plots of function $J^*(u, \beta_1, \beta_2)$ for $\beta_2 = 0$: **a** $J^*(u, \beta_1, 0) - \lg(u)$, **b** $\lg[J^*(u, \beta_1, 0)] - \lg(u)$. $\beta_2 = 0$ implies that the pumping and observation wells are located on a perpendicular to the river

Applications. This function enters into Hantush solution for pumping near a stream (Eq. 5.7). The values of arguments are given in equalities (Eqs. 5.9–5.11).

Appendix 7.8 Special Function $W_{NW}(u, \beta)$

Function (Neuman and Witherspoon 1968) (Fig. A7.9 and Table A7.7):

$$W_{NW}(u, \beta) = \frac{2}{\sqrt{\pi}} \int_{\sqrt{\beta}}^{\infty} W\left(\frac{u\tau^2}{\tau^2 - \beta}\right) \exp(-\tau^2) d\tau.$$

Limit of the function: $W_{NW}(u, 0) = W(u)$, $W_{NW}(0, \beta) = \infty$.

Applications. Function, where $u = \frac{r^2}{4at} = \frac{r^2 S}{4Tt}$, $\beta = \frac{z_p^2}{4a't} = \frac{z_p^2 S_s'}{4k't}$, enters into Neuman and Witherspoon solutions (Eq. 3.85) for the drawdown in an aquitard (see Sect. 3.3).

Fig. A7.9 Plots of function $W_{NW}(u, \beta)$ at different values of its second argument: $W_{NW}(u, \beta) - \lg(u)$

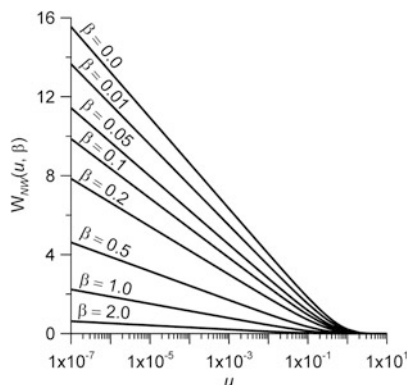


Table A7.7 Approximation of function $W_{NW}(u, \beta)$ (fitted by the author):

Range	Representation ^a
$u < 0.01$ and $10^{-5} \leq \beta \leq 1.0$	$W_{NW}(u, \beta) = -C(\beta) \ln u - A(\beta),$ $C(\beta) = a_0 \exp(b_0 \sqrt{\beta}) + a_1 \exp(b_1 \beta) + a_2 \exp(b_2 \beta^2) + a_3 \exp(b_3 \beta^3) + a_4 \exp(b_4 \beta^4) + a_5 \exp(b_5 \beta^5),$ $A(\beta) = \frac{c_0}{\sqrt{\beta}} + c_1 \exp\left(\frac{d_1}{\sqrt{\beta}}\right) + c_2 \exp\left(\frac{d_2}{\sqrt{\beta}}\right) + c_3 \exp(d_3 \beta^2) + c_4 \exp(d_4 \beta^3) + c_5 \exp(d_5 \beta^4)$

a_0	0.3417002069	b_0	-3.340961289	c_0	-0.00001486338765		
a_1	0.1636688436	b_1	-9.763932273	c_1	0.1263841135	d_1	-0.1362851532
a_2	0.08009713177	b_2	-26.13718737	c_2	0.04322525953	d_2	-0.0275872065
a_3	0.1177404043	b_3	-16.94717556	c_3	0.2984049043	d_3	-4.654639762
a_4	0.152695636	b_4	-3.126743379	c_4	0.02317877338	d_4	-314.2350514
a_5	0.1441917632	b_5	-0.04030147022	c_5	0.2631103306	d_5	-0.6049903099

^a Constant values in equations are given below

Appendix 7.9 Functions for Large-Diameter Wells

1. Function for Large-Diameter Wells for Nonleaky Aquifers

Function (Papadopoulos and Cooper 1967) (Fig. A7.10 and Table A7.8):

$$F(u, \beta) = \frac{32\beta^2}{\pi^2} \int_0^\infty \frac{1 - \exp[-\tau^2/(4u)]}{[\tau J_0(\tau) - 2\beta J_1(\tau)]^2 + [\tau Y_0(\tau) - 2\beta Y_1(\tau)]^2} \tau^3 d\tau$$

Applications. Equation 1.8; $u = \frac{r_w^2 S}{4Tt}$, $\beta = S \frac{r_w^2}{r_c^2}$.

2. Function for the Drawdown in an Observation Well in a Nonleaky Aquifer during Pumping from a Large-Diameter Pumping Well

Function (Carslow and Jaeger 1959; Papadopoulos and Cooper 1967):

$$F(u, \beta_1, \beta_2) = 8 \frac{\beta_2}{\pi} \int_0^\infty \left\{ \frac{\left[1 - \exp\left(-\frac{\tau^2}{4u}\right) \right] \times \left[J_0(\beta_1 \tau) [\tau Y_0(\tau) - 2\beta_2 Y_1(\tau)] - Y_0(\beta_1 \tau) [\tau J_0(\tau) - 2\beta_2 J_1(\tau)] \right]}{[\tau J_0(\tau) - 2\beta_2 J_1(\tau)]^2 + [\tau Y_0(\tau) - 2\beta_2 Y_1(\tau)]^2} \right\} \frac{d\tau}{\tau^2}$$

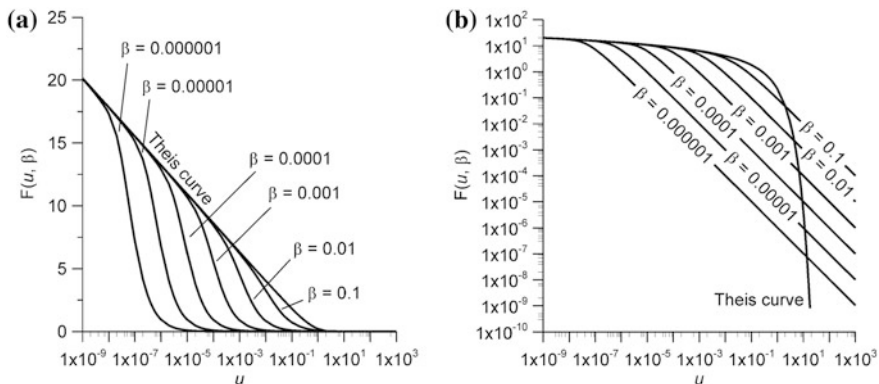


Fig. A7.10 Plots of **a** the function and **b** the logarithm of the function $F(u, \beta)$ versus the logarithm of the first argument at different values of its second argument

Table A7.8 Approximation of function $F(u, \beta)$ (Papadopoulos and Cooper 1967)

Range	Representation
$u/\beta < 0.001$	$F(u, \beta) = W(u)$
For large values of argument u	$F(u, \beta) = \beta/u$

Applications. Equation 1.6; $u = \frac{r_w^2 S}{4Tt}$, $\beta_1 = \frac{r}{r_w}$, $\beta_2 = S \frac{r_w^2}{r_c^2}$.

3. Function for Large-Diameter Wells for a Leaky Aquifer

Function (Lai and Chen-Wu Su 1974):

$$F_L(u, \beta_2, \beta_3) = 32 \frac{\beta_3^2}{\pi^2} \int_0^\infty \left\{ \left[1 - \exp\left(-\frac{\tau^2 + \beta_2^2}{4u}\right) \right] \frac{\tau}{\tau^2 + \beta_2^2} \times \right. \\ \left. \times \frac{1}{\left[(\tau^2 + \beta_2^2) J_0(\tau) - 2\beta_3 \tau J_1(\tau) \right]^2 + \left[(\tau^2 + \beta_2^2) Y_0(\tau) - 2\beta_3 \tau Y_1(\tau) \right]^2} \right\} d\tau.$$

Applications. Equation 3.7; $u = \frac{r_w^2 S}{4Tt}$, $\beta_2 = \frac{r_w}{B}$, $\beta_3 = S \frac{r_w^2}{r_c^2}$.

4. Function for the Drawdown in an Observation Well in a Leaky Aquifer during Pumping from a Large-Diameter Pumping Well

Function (Lai and Chen-Wu Su 1974):

$$F_L(u, \beta_1, \beta_2, \beta_3) = 8 \frac{\beta_3}{\pi} \int_0^\infty \left\{ \left[1 - \exp\left(-\frac{\tau^2 + \beta_2^2}{4u}\right) \right] \frac{\tau}{\tau^2 + \beta_2^2} \times \right. \\ \left. \times \frac{J_0(\beta_1 \tau) \left[(\tau^2 + \beta_2^2) Y_0(\tau) - 2\beta_3 \tau Y_1(\tau) \right] - Y_0(\beta_1 \tau) \left[(\tau^2 + \beta_2^2) J_0(\tau) - 2\beta_3 \tau J_1(\tau) \right]}{\left[(\tau^2 + \beta_2^2) J_0(\tau) - 2\beta_3 \tau J_1(\tau) \right]^2 + \left[(\tau^2 + \beta_2^2) Y_0(\tau) - 2\beta_3 \tau Y_1(\tau) \right]^2} \right\} d\tau.$$

Applications. Equation 3.5; $u = \frac{r_w^2 S}{4Tt}$, $\beta_1 = \frac{r}{r_w}$, $\beta_2 = \frac{r_w}{B}$, $\beta_3 = S \frac{r_w^2}{r_c^2}$.

5. Well-Function $S(u, \beta)$, Taking into Account Pumping-Well Screen Radius

Function (Carslow and Jaeger 1959) (Fig. A7.11 and Table A7.9):

$$S(u, \beta) = \frac{4}{\pi} \int_0^\infty \frac{J_1(\tau) Y_0(\beta \tau) - Y_1(\tau) J_0(\beta \tau)}{J_1^2(\tau) + Y_1^2(\tau)} \cdot \frac{1 - \exp(-u\tau^2)}{\tau^2} d\tau.$$

Limits of the function: $S(u, 1) = F(1/4u, \infty)$ —function $S(u, 1)$ is equal to the function for a large-diameter well at the second argument tending to infinity; $S(u, \beta) = F(1/4u, \beta, \infty)$ —function $S(u, \beta)$ is equal to the function for a large-diameter well for calculating the drawdown in an observation well at the third argument tending to infinity.

Functions $W(u)$, $S(u, \beta)$, $F(u, \beta)$, and $F(u, \beta_1, \beta_2)$ describe water-level changes in a confined aquifer (see Sect. 1.1.1). Their major differences are as follows: $W(u)$ does not take into account the wellbore storage; $S(u, \beta)$ —only the radius of pumping-well screen is taken into account (casing radius tends to zero); $F(u, \beta)$ and $F(u, \beta_1, \beta_2)$ —wellbore storage is taken into account.

Applications. This function is not used in this book. $u = \frac{Tt}{Sr_w^2} = \frac{at}{r_w^2}$, $\beta = \frac{r}{r_w}$.

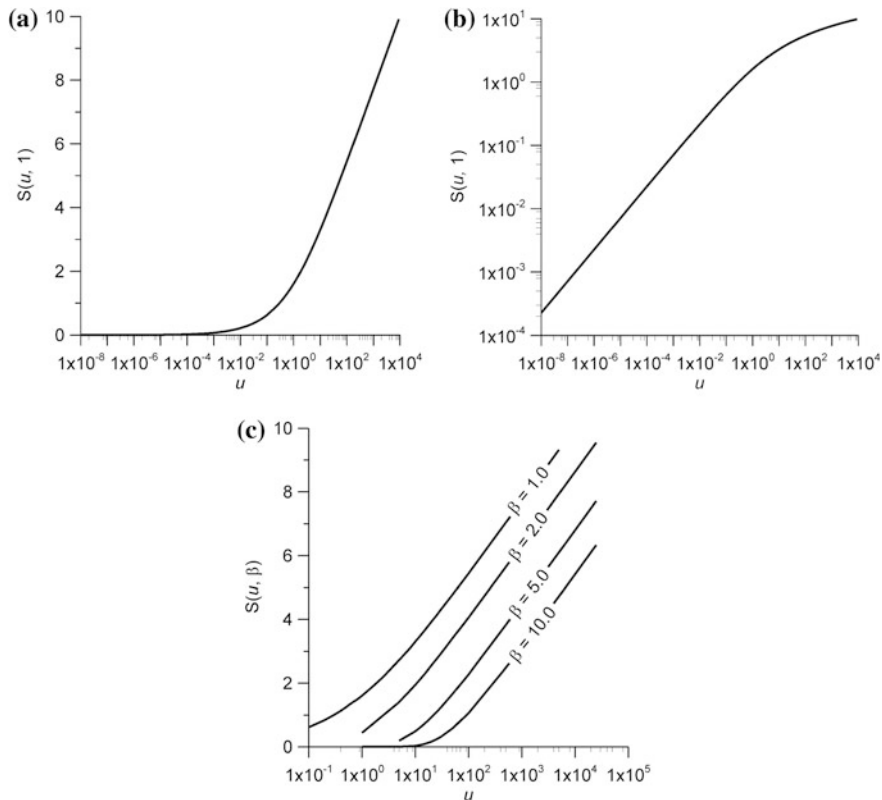


Fig. A7.11 Plots of function $S(u, \beta)$ at $\beta = 1$: **a** $S(u, \beta) - \lg(u)$; **b** $\lg[S(u, \beta)] - \lg(u)$. **c** Plot of function $S(u, \beta) - \lg(u)$ at different values of its second argument

Table A7.9 Approximation of function $S(u, \beta)$

Range	Representation
$u > 20$	$S(u, \beta) \approx W\left(\frac{\beta^2}{4u}\right)$ (Hantush 1964)
$u > 150$ and $\beta = 1$	$S(u, 1) \approx \ln(u) + 0.81$ (fitted by the author)
$u < 0.01$ and $\beta = 1$	$S(u, 1) \approx \exp[0.497 \ln(u) + 0.774]$ (fitted by the author)

Appendix 7.10 Functions for Slug Tests

1. Function $F_s(u, \beta)$ for Water-Level Changes in the Pumping Well during a Slug Test—Slug Test Function

Function (Carslow and Jaeger 1959; Cooper et al. 1967) (Fig. A7.12):

$$F_s(u, \beta) = \frac{8\beta}{\pi^2} \int_0^\infty \frac{\exp(-u\tau^2/\beta)}{[\tau J_0(\tau) - 2\beta J_1(\tau)]^2 + [\tau Y_0(\tau) - 2\beta Y_1(\tau)]^2} \frac{d\tau}{\tau}$$

Applications. Function, where $u = \frac{Tt}{r_c^2}$, $\beta = S \frac{r_w^2}{r_c^2}$, enters into the Cooper solution (Eq. 9.1) for slug tests.

2. Function for Water-Level Changes in an Observation Well during a Slug Test

Function (Carslow and Jaeger 1959; Cooper et al. 1967):

$$F_{sp}(u, \beta_1, \beta_2) = \frac{2}{\pi} \int_0^\infty \exp(-u\tau^2/\beta_1) \times \frac{J_0(\tau\beta_2)[\tau Y_0(\tau) - 2\beta_1 Y_1(\tau)] - Y_0(\tau\beta_2)[\tau J_0(\tau) - 2\beta_1 J_1(\tau)]}{[\tau J_0(\tau) - 2\beta_1 J_1(\tau)]^2 + [\tau Y_0(\tau) - 2\beta_1 Y_1(\tau)]^2} d\tau$$

Applications. Function, where $u = \frac{Tt}{r_c^2}$, $\beta_1 = S \frac{r_w^2}{r_c^2}$, $\beta_2 = \frac{r}{r_w}$, enters into the Cooper solution (Eq. 9.3) for the drawdown in an observation well during slug tests.

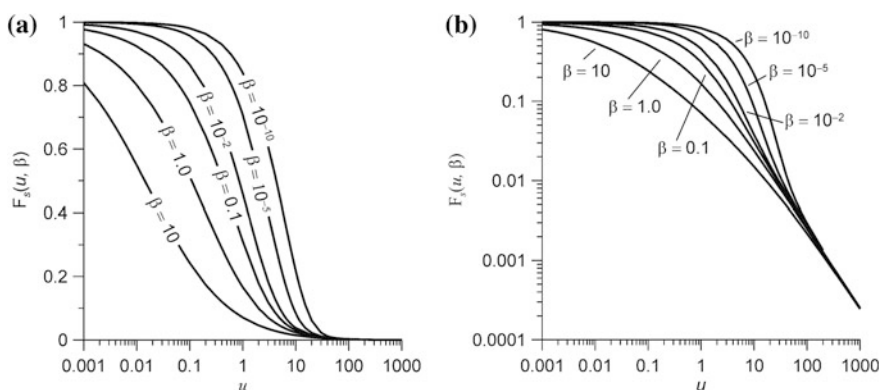


Fig. A7.12 Plots of function $F_s(u, \beta)$ at different values of its second argument: **a** $F_s(u, \beta) - \lg(u)$, **b** $\lg[F_s(u, \beta)] - \lg(u)$

Appendix 7.11 Functions for Constant-Head Tests

1. Flowing Well-Function for Nonleaky Aquifers $A(u, \beta)$

Function (Fig. A7.13 and Table A7.10):

$$A(u, \beta) = 1 - \frac{2}{\pi} \int_0^\infty \frac{J_0(\tau)Y_0(\tau\beta) - Y_0(\tau)J_0(\tau\beta)}{J_0^2(\tau) + Y_0^2(\tau)} \cdot \frac{\exp(-u\tau^2)}{\tau} d\tau.$$

Applications. Equation 8.1; $u = \frac{at}{r_w^2}$, $\beta = \frac{r}{r_w}$.

2. Flowing-Well Function for Leaky Aquifers $Z(u, \beta_1, \beta_2)$

Function (Table A7.11):

$$Z(u, \beta_1, \beta_2) = \frac{K_0(\beta_1\beta_2)}{K_0(\beta_2)} + \exp(-u\beta_2^2) \frac{2}{\pi} \int_0^\infty \frac{J_0(\tau\beta_1)Y_0(\tau) - Y_0(\tau\beta_1)J_0(\tau)}{J_0^2(\tau) + Y_0^2(\tau)} \frac{\exp(-u\tau^2)}{\tau^2 + \beta_2^2} \tau d\tau.$$

Limits of the function: $Z(\infty, \beta_1, \beta_2) = K_0(\beta_1\beta_2)/K_0(\beta_2)$, $Z(u, \beta_1, 0) = A(u, \beta_1)$.

Applications. Equation 8.11; $u = \frac{at}{r_w^2}$, $\beta_1 = \frac{r}{r_w}$, $\beta_2 = \frac{r_w}{B}$.

Fig. A7.13 Plot of function $A(u, \beta)$ versus the logarithm of the first argument at different values of its second argument

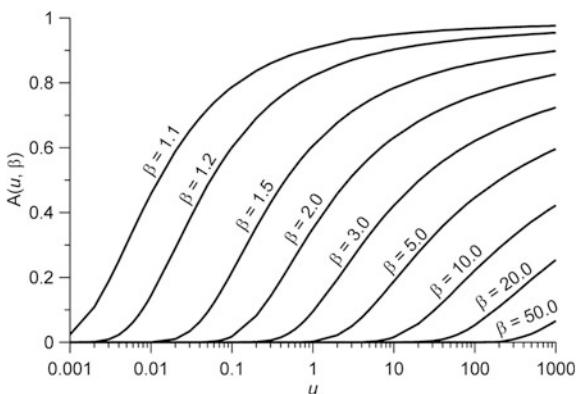


Table A7.10 Approximation of function $A(u, \beta)$ (Hantush 1964)

Range	Representation
$u < 0.05$	$A(u, \beta) \approx \frac{1}{\sqrt{\beta}} \left[\operatorname{erfc} \frac{\beta - 1}{2\sqrt{u}} + \frac{(\beta - 1)\sqrt{u}}{4\beta} i \operatorname{erfc} \frac{\beta - 1}{2\sqrt{u}} \right]$
$u > 500$	$A(u, \beta) \approx \frac{W[\beta^2/(4u)]}{\ln(2.25u)}$

Table A7.11 Approximation of function $Z(u, \beta_1, \beta_2)$ (Hantush 1964)

Range	Representation
$\frac{u}{\beta_1^2} < 0.05$	$Z(u, \beta_1, \beta_2) \approx \frac{1}{2\sqrt{\beta_1}} \left\{ \begin{aligned} &\exp[\beta_2(\beta_1 - 1)]\operatorname{erfc}\left(\beta_2\sqrt{u} + \frac{\beta_1 - 1}{2\sqrt{u}}\right) + \\ &+ \exp[-\beta_2(\beta_1 - 1)]\operatorname{erfc}\left(-\beta_2\sqrt{u} + \frac{\beta_1 - 1}{2\sqrt{u}}\right) \end{aligned} \right\}$
$u\beta_2^2 > 1$	$Z(u, \beta_1, \beta_2) \approx W\left(\frac{\beta_1^2}{4u}, \beta_1\beta_2\right) / W\left(\frac{1}{4u}, \beta_2\right)$

3. Flowing-Well-Discharge Function for Nonleaky Aquifers $G(u)$

Function (Fig. A7.14 and Table A7.12):

$$G(u) = \frac{4u}{\pi} \int_0^\infty \tau \exp(-u\tau^2) \left[\frac{\pi}{2} + \arctan \frac{Y_0(\tau)}{J_0(\tau)} \right] d\tau.$$

Applications. Equation 8.3; $u = \frac{at}{r_w^2}$.

4. Flowing-Well-Discharge Function for Leaky Aquifers $G(u, \beta)$

Function (Fig. A7.15 and Table A7.13):

$$G(u, \beta) = \frac{\beta K_1(\beta)}{K_0(\beta)} + \frac{4}{\pi^2} \exp(-u\beta^2) \int_0^\infty \frac{1}{J_0^2(\tau) + Y_0^2(\tau)} \frac{\tau \exp(-u\tau^2)}{\tau^2 + \beta^2} d\tau.$$

Limit of the function: $G(u, 0) = G(u)$.

Applications. Equation 8.13; $u = \frac{at}{r_w^2}$, $\beta = \frac{r_w}{B}$.

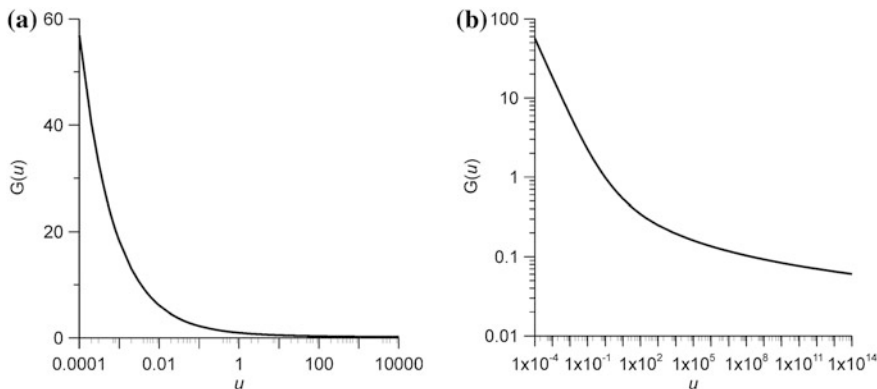


Fig. A7.14 Plots of function $G(u)$: **a** $G(u) - \lg(u)$, **b** $\lg[G(u)] - \lg(u)$

Table A7.12 Approximation of function $G(u)$ (Jacoband Lohman 1952)

Range	Representation
$u < 0.05$	$G(u) \approx 0.5 + \frac{1}{\sqrt{\pi u}}$
$0.05 \leq u \leq 3$	$G(u) = \left[\begin{aligned} &0.985285352 - 0.6990572583(\lg u) + 0.3617096836(\lg u)^2 - \\ &-0.1933285166(\lg u)^3 + 0.02384555597(\lg u)^4 + \\ &+ 0.113819123(\lg u)^5 + 0.1394865128(\lg u)^6 + 0.0400202701(\lg u)^7 \end{aligned} \right]$ (fitted by the author)
$3 \leq u \leq 500$	$G(u) = \left[\begin{aligned} &0.9640284025 - 0.5853545608(\lg u) + 0.1426085197(\lg u)^2 + \\ &+ 0.008430131774(\lg u)^3 + 0.03620076922(\lg u)^4 - \\ &-0.04772201769(\lg u)^5 + 0.01800303964(\lg u)^6 - 0.002262080907(\lg u)^7 \end{aligned} \right]$ (fitted by the author)
$u > 500$	$G(u) \approx 2 / \ln(2.25u); G(u) \approx 2/W[1/(4u)]$
$u \geq 1$	$G(10^n) = \frac{1}{100\pi} \left\{ \begin{aligned} &\frac{2}{100} G_0(10^n, 10^{-2-n/2}) + \\ &+ \frac{1}{100} \sum_{m=1}^9 (2m+1) [G_0(10^n, m10^{-2-n/2}) + G_0(10^n, (m+1)10^{-2-n/2})] + \\ &+ \sum_{m=1}^{\infty} (2m+1) [G_0(10^n, m10^{-1-n/2}) + G_0(10^n, (m+1)10^{-1-n/2})] \end{aligned} \right\},$ $n = \lg u \text{—the power of 10; } G_0(u, \beta) = \exp(-u\beta^2) \left[\frac{\pi}{2} + \arctan \frac{Y_0(\beta)}{J_0(\beta)} \right]$

Fig. A7.15 Plot of function $\lg[G(u, \beta)] - \lg(u)$

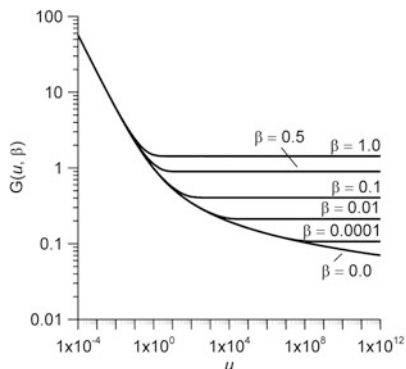


Table A7.13 Approximation of function $G(u, \beta)$ (Hantush 1959, 1964)

Range	Representation
$u < 0.01$	$G(u, \beta) \approx G(u, 0) = G(u)$
$u\beta^2 > 1, \beta < 0.01$	$G(u, \beta) \approx 2/W(0.25u^{-1}, \beta)$
$\beta^2/u > 25$	$G(u, \beta) \approx 0.5 + \exp(-\beta^2 u) / \sqrt{\pi u}$

Appendix 7.12 Error Functions

1. Error Function $\operatorname{erf}(u)$ and Complementary Error Function $\operatorname{erfc}(u)$

Functions (Fig. A7.16 and Table A7.14):

$$\operatorname{erf} u = \frac{2}{\sqrt{\pi}} \int_0^u \exp(-\tau^2) d\tau, \operatorname{erf}(-u) = -\operatorname{erf} u;$$

$$\operatorname{erfc} u = \frac{2}{\sqrt{\pi}} \int_u^\infty \exp(-\tau^2) d\tau$$

Limit values: $\operatorname{erf} 0 = 0, \operatorname{erf} \infty = 1; \operatorname{erfc} 0 = 1, \operatorname{erfc} \infty = 0, \operatorname{erfc}(-\infty) = 2.$

Relationships: $\operatorname{erf} u = 1 - \operatorname{erfc} u, \operatorname{erfc} u = 1 - \operatorname{erf} u, \operatorname{erfc}(-u) = 1 + \operatorname{erf} u.$

Derivatives of the functions:

$$\frac{\partial \operatorname{erf} u}{\partial u} = \frac{2}{\sqrt{\pi}} \exp(-u^2); \frac{\partial \operatorname{erfc} u}{\partial u} = -\frac{2}{\sqrt{\pi}} \exp(-u^2).$$

Expansion in series (Abramowitz and Stegun 1964):

Fig. A7.16 Representation of functions $\operatorname{erf}(u)$ and $\operatorname{erfc}(u)$

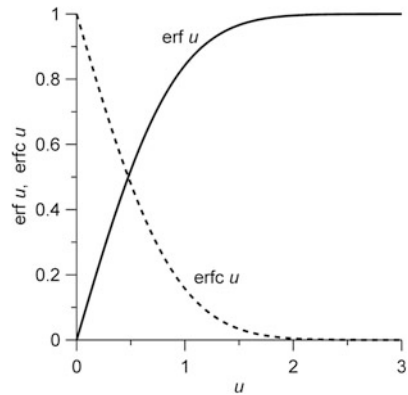


Table A7.14 Approximation of function $\operatorname{erf}(u)$

Range	Representation
$0 < u < \infty$	$\operatorname{erf} u = 1 - \exp(-u^2) \left(\begin{array}{l} 0.254829592t - 0.284496736t^2 + 1.421413741t^3 - \\ -1.453152027t^4 + 1.061405429t^5 \end{array} \right),$ <p>where $t = \frac{1}{1 + 0.3275911u}$ (Abramowitz and Stegun 1964)</p>
$u \leq 0.1$	$\operatorname{erf} u \approx \frac{2u}{\sqrt{\pi}}$ (Hantush 1964)

$$\operatorname{erf} u = \frac{2}{\sqrt{\pi}} \sum_{n=0}^{\infty} \frac{(-1)^n u^{2n+1}}{n!(2n+1)}.$$

2. Iterated Integral of the Complementary Error Function $i^n \operatorname{erfc}(u)$

Function (Fig. A7.17 and Table A7.15):

$$i^n \operatorname{erfc} u = \frac{2}{\sqrt{\pi}} \int_u^{\infty} \frac{(\tau - u)^n}{n!} \exp(-\tau^2) d\tau, \quad i^n \operatorname{erfc} u = \frac{i^{n-2} \operatorname{erfc} u}{2n} - \frac{u i^{n-1} \operatorname{erfc} u}{n}.$$

Limit value: $i^n \operatorname{erfc} 0 = \frac{1}{2^n \Gamma(1 + n/2)}$, where $\Gamma(u)$ is gamma function (see Appendix 7.14).

Function derivative:

$$\frac{\partial(i^n \operatorname{erfc} u)}{\partial u} = -i^{n-1} \operatorname{erfc} u.$$

Fig. A7.17 Representation of iterated error function integrals for different values of n

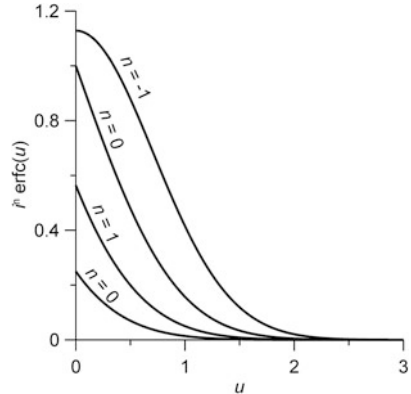


Table A7.15 Iterated integrals of error functions for $n = -1, 0, 1, 2$

n	Equation	$u = 0$
-1	$i^{-1} \operatorname{erfc} u = \frac{2}{\sqrt{\pi}} \exp(-u^2)$	1.128379167
0	$i^0 \operatorname{erfc} u = \operatorname{erfc} u$	1
1	$i^1 \operatorname{erfc} u = i \operatorname{erfc} u = -u \operatorname{erfc} u + \frac{1}{\sqrt{\pi}} \exp(-u^2)$	0.5641895835
2	$i^2 \operatorname{erfc}(u) = \left(\frac{1}{4} + \frac{u^2}{2}\right) \operatorname{erfc}(u) - \frac{u}{2\sqrt{\pi}} \exp(-u^2)$	0.25

Appendix 7.13 Bessel Functions

1. Bessel Functions of the First and Second Kind of the Zero and First Order: $J_0(u)$, $J_1(u)$, $Y_0(u)$, $Y_1(u)$ (Table A7.16 and Fig. A7.18)

- $J_0(u)$ —Bessel function of the first kind of the zero order (Table A7.17);
- $J_1(u)$ —Bessel function of the first kind of the first order (Table A7.18);
- $Y_0(u)$ —Bessel function of the second kind of the zero order (Table A7.19);
- $Y_1(u)$ —Bessel function of the second kind of the first order (Table A7.20).

Table A7.16 Integral representations and derivatives of Bessel functions

Function	Derivative
$J_0(u) = \frac{1}{\pi} \int_0^\pi \cos(u \sin \tau) d\tau$	$-J_1(u)$
$J_1(u) = \frac{1}{\pi} \int_0^\pi \cos(u \sin \tau - \tau) d\tau$	$J_0(u) - \frac{1}{u} J_1(u)$
$Y_0(u) = \frac{4}{\pi^2} \int_0^{\pi/2} \cos(u \cos \tau) [\gamma + \ln(2u \sin^2 \tau)] d\tau$	$-Y_1(u)$
$Y_1(u) = \frac{1}{\pi} \int_0^\pi \sin(u \sin \tau - \tau) d\tau - \frac{1}{\pi} \int_0^\infty (e^\tau + e^{-\tau} \cos \pi) \exp(-u \sinh \tau) d\tau$	$Y_0(u) - \frac{1}{u} Y_1(u)$

$\gamma = 0.5772156649$ —Euler constant

Table A7.17 Approximation of function $J_0(u)$ (Abramowitz and Stegun 1964)

Range	Representation
$u < 0.1$	$J_0(u) \approx 1$ —for practical calculations (Hantush 1964)
$u \leq 3$	$J_0(u) = 1 - 2.2499997\omega^2 + 1.2656208\omega^4 - 0.3163866\omega^6 + 0.0444479\omega^8 - 0.0039444\omega^{10} + 0.00021\omega^{12}$
$u \geq 3$	$J_0(u) = \frac{f_0}{\sqrt{u}} \cos \theta_0, w = u/3,$ $f_0 = 0.79788456 - 0.00000077\omega^{-1} - 0.0055274\omega^{-2} - 0.00009512\omega^{-3} + 0.00137237\omega^{-4} - 0.00072805\omega^{-5} + 0.00014476\omega^{-6},$ $\theta_0 = u - 0.78539816 - 0.04166397\omega^{-1} - 0.00003954\omega^{-2} + 0.00262573\omega^{-3} - 0.00054125\omega^{-4} - 0.00029333\omega^{-5} + 0.00013558\omega^{-6}$
$u > 16$	$J_0(u) \approx \sqrt{\frac{2}{\pi u}} \cos\left(u - \frac{\pi}{4}\right)$ —for practical calculations (Hantush 1964)

Table A7.18 Approximation of function $J_1(u)$ (Abramowitz and Stegun 1964)

Range	Representation
$u < 0.1$	$J_1(u) \approx 0.5u$ —for practical calculations (Hantush 1964)
$u \leq 3$	$w = u/3,$ $J_1(u) = u \left(0.5 - 0.56249985\omega^2 + 0.21093573\omega^4 - 0.03954289\omega^6 + 0.00443319\omega^8 - \right.$ $\left. - 0.00031761\omega^{10} + 0.00001109\omega^{12} \right)$
$u \geq 3$	$J_1(u) = \frac{f_1}{\sqrt{u}} \cos \theta_1, w = u/3,$ $f_1 = 0.79788456 + 0.00000156\omega^{-1} + 0.01659667\omega^{-2} + 0.00017105\omega^{-3} -$ $- 0.00249511\omega^{-4} + 0.00113653\omega^{-5} - 0.00020033\omega^{-6},$ $\theta_1 = u - 2.35619449 + 0.12499612\omega^{-1} + 0.0000565\omega^{-2} - 0.00637879\omega^{-3} +$ $+ 0.00074348\omega^{-4} + 0.00079824\omega^{-5} - 0.00029166\omega^{-6}$
$u > 16$	$J_1(u) \approx \sqrt{\frac{2}{\pi u}} \sin\left(u - \frac{\pi}{4}\right)$ —for practical calculations (Hantush 1964)

Table A7.19 Approximation of function $Y_0(u)$ (Abramowitz and Stegun 1964)

Range	Representation
$u < 0.01$	$Y_0(u) \approx \frac{2}{\pi} \left(0.5772 + \ln \frac{u}{2} \right)$ —for practical calculations (Hantush 1964)
$u \leq 3$	$w = u/3,$ $Y_0(u) = \frac{2}{\pi} \ln \frac{u}{2} J_0(u) + 0.36746691 + 0.60559366\omega^2 - 0.74350384\omega^4 + 0.25300117\omega^6 -$ $- 0.04261214\omega^8 + 0.00427916\omega^{10} - 0.00024846\omega^{12}$
$u \geq 3$	$Y_0(u) = \frac{f_0}{\sqrt{u}} \sin \theta_0, w = u/3,$ $f_0 = 0.79788456 - 0.00000077\omega^{-1} - 0.0055274\omega^{-2} - 0.00009512\omega^{-3} +$ $+ 0.00137237\omega^{-4} - 0.00072805\omega^{-5} + 0.00014476\omega^{-6},$ $\theta_0 = u - 0.78539816 - 0.04166397\omega^{-1} - 0.00003954\omega^{-2} + 0.00262573\omega^{-3} -$ $- 0.00054125\omega^{-4} - 0.00029333\omega^{-5} + 0.00013558\omega^{-6}$
$u > 16$	$Y_0(u) \approx \sqrt{\frac{2}{\pi u}} \sin\left(u - \frac{\pi}{4}\right)$ —for practical calculations (Hantush 1964)

Table A7.20 Approximation of function $Y_1(u)$ (Abramowitz and Stegun 1964)

Range	Representation
$u < 0.01$	$Y_1(u) \approx -\frac{2}{\pi u}$ —for practical calculations (Hantush 1964)
$u \leq 3$	$w = u/3,$ $Y_1(u) = \frac{1}{u} \left(\frac{2u}{\pi} \ln \frac{u}{2} J_1(u) - 0.6366198 + 0.2212091\omega^2 + 2.1682709\omega^4 - 1.3164827\omega^6 + \right.$ $\left. + 0.3123951\omega^8 - 0.0400976\omega^{10} + 0.0027873\omega^{12} \right)$
$u \geq 3$	$Y_1(u) = \frac{f_1}{\sqrt{u}} \sin \theta_1, w = u/3,$ $f_1 = 0.79788456 + 0.00000156\omega^{-1} + 0.01659667\omega^{-2} + 0.00017105\omega^{-3} -$ $- 0.00249511\omega^{-4} + 0.00113653\omega^{-5} - 0.00020033\omega^{-6},$ $\theta_1 = u - 2.35619449 + 0.12499612\omega^{-1} + 0.0000565\omega^{-2} - 0.00637879\omega^{-3} +$ $+ 0.00074348\omega^{-4} + 0.00079824\omega^{-5} - 0.00029166\omega^{-6}$
$u > 16$	$Y_1(u) \approx -\sqrt{\frac{2}{\pi u}} \cos\left(u - \frac{\pi}{4}\right)$ —for practical calculations (Hantush 1964)

Fig. A7.18 Plots of Bessel functions: $J_0(u)$, $J_1(u)$, $Y_0(u)$, $Y_1(u)$

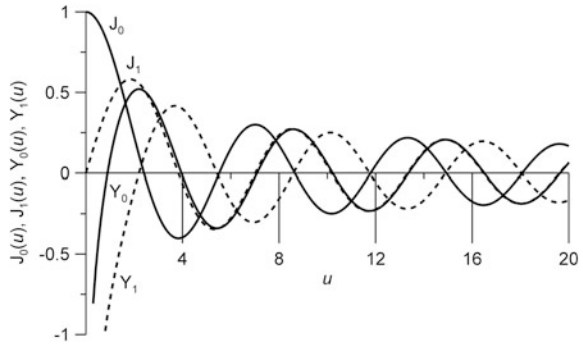
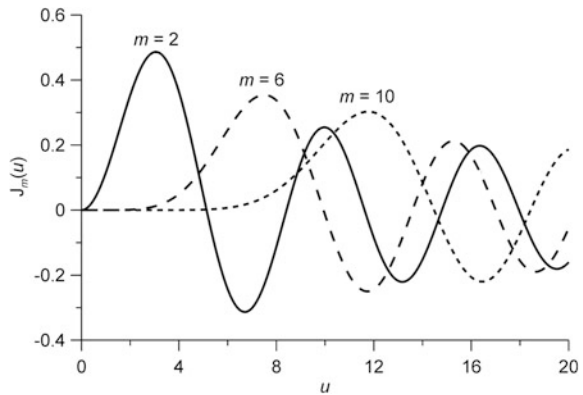


Fig. A7.19 Plot of function $J_m(u)$ versus its argument for different orders



2. Bessel Function of the First Kind of the mth Order $J_m(u)$

Function (Fig. A7.19):

$$J_m(u) = \frac{1}{\pi} \int_0^\pi \cos(u \sin \tau - m\tau) d\tau.$$

Expansion in series (Abramowitz and Stegun 1964)

$$J_m(u) = \left(\frac{u}{2}\right)^m \sum_{n=0}^\infty \frac{(-u^2/4)^n}{n! \Gamma(m+n+1)!}.$$

3. Modified Bessel Functions of the First and Second Kind of the Zero and First Order: $I_0(u)$, $I_1(u)$, $K_0(u)$, $K_1(u)$ (Table A7.21 and Fig. A7.20):

$I_0(u)$ —modified Bessel function of the first kind of the zero order (Table A7.22);

$I_1(u)$ —modified Bessel function of the first kind of the first order (Table A7.23);

$K_0(u)$ —modified Bessel function of the second kind of the zero order (Table A7.24);

$K_1(u)$ —modified Bessel function of the second kind of the first order (Table A7.25).

Table A7.21 Integral representations and derivatives of modified Bessel functions

Function	Derivative
$I_0(u) = \frac{1}{\pi} \int_0^\pi \exp(u \cos \tau) d\tau$	$I_1(u)$
$I_1(u) = \frac{1}{\pi} \int_0^\pi \exp(u \cos \tau) \cos \tau d\tau$	$I_0(u) - \frac{1}{u} I_1(u)$
$K_0(u) = \int_0^\infty \exp(-u \cosh \tau) d\tau$	$-K_1(u)$
$K_1(u) = \int_0^\infty \exp(-u \cosh \tau) \cosh \tau d\tau$	$-K_0(u) - \frac{1}{u} K_1(u)$

Table A7.22 Approximation of function $I_0(u)$ (Abramowitz and Stegun 1964)

Range	Representation
$u < 0.1$	$I_0(u) \approx 1$ —for practical calculations (Hantush 1964)
$u \leq 3.75$	$\omega = u/3.75,$ $I_0(u) = 1 + 3.5156229\omega^2 + 3.0899424\omega^4 + 1.2067492\omega^6 + 0.2659732\omega^8 + 0.0360768\omega^{10} + 0.0045813\omega^{12}$
$u \geq 3.75$	$\omega = u/3.75,$ $I_0(u) = \frac{e^u}{\sqrt{u}} \left(0.39894228 + 0.01328592\omega^{-1} + 0.00225319\omega^{-2} - 0.00157565\omega^{-3} + 0.00916281\omega^{-4} - 0.02057706\omega^{-5} + 0.02635537\omega^{-6} - 0.01647633\omega^{-7} + 0.00392377\omega^{-8} \right)$
$u > 5$	$I_0(u) \approx \left(1 + \frac{1}{8u} \right) \frac{e^u}{\sqrt{2\pi u}}$ —for practical calculations (Hantush 1964)

Table A7.23 Approximation of function $I_1(u)$ (Abramowitz and Stegun 1964)

Range	Representation
$u < 0.1$	$I_1(u) \approx 0.5u$ —for practical calculations (Hantush 1964)
$u \leq 3.75$	$\omega = u/3.75,$ $I_1(u) = u \left(0.5 + 0.87890594\omega^2 + 0.51498869\omega^4 + 0.15084934\omega^6 + 0.02658733\omega^8 + 0.00301532\omega^{10} + 0.00032411\omega^{12} \right)$
$u \geq 3.75$	$\omega = u/3.75,$ $I_1(u) = \frac{e^u}{\sqrt{u}} \left(0.39894228 - 0.03988024\omega^{-1} - 0.00362018\omega^{-2} + 0.00163801\omega^{-3} - 0.01031555\omega^{-4} + 0.02282967\omega^{-5} - 0.02895312\omega^{-6} + 0.01787654\omega^{-7} - 0.00420059\omega^{-8} \right)$
$u > 5$	$I_1(u) \approx \left(1 - \frac{3}{8u} \right) \frac{e^u}{\sqrt{2\pi u}}$ —for practical calculations (Hantush 1964)

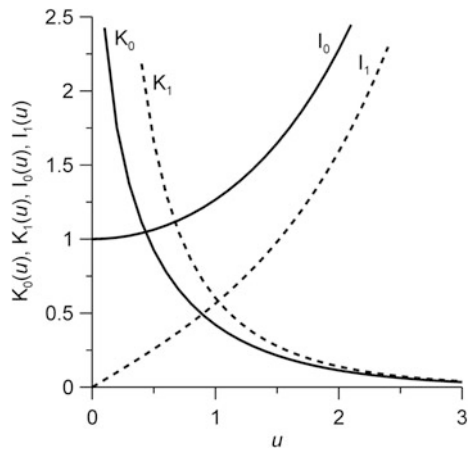
Table A7.24 Approximation of function $K_0(u)$ (Abramowitz and Stegun 1964)

Range	Representation
$u < 0.05$	$K_0(u) \approx \ln \frac{1.12}{u}$ —for practical calculations (Hantush 1964)
$u \leq 2$	$\omega = u/2,$ $K_0(u) = -\ln \omega I_0(u) - 0.57721566 + 0.4227842\omega^2 + 0.23069756\omega^4 + 0.0348859\omega^6 +$ $+ 0.00262698\omega^8 + 0.0001075\omega^{10} + 0.0000074\omega^{12}$
$u \geq 2$	$\omega = u/2,$ $K_0(u) = \frac{e^{-u}}{\sqrt{u}} \left(1.25331414 - 0.07832358\omega^{-1} + 0.02189568\omega^{-2} - 0.01062446\omega^{-3} + \right)$ $\left(+ 0.00587872\omega^{-4} - 0.0025154\omega^{-5} + 0.00053208\omega^{-6} \right)$
$u > 5$	$K_0(u) \approx \sqrt{\frac{\pi}{2u}} \left(1 - \frac{1}{8u} \right) e^{-u}$ —for practical calculations (Hantush 1964)

Table A7.25 Approximation of function $K_1(u)$ (Abramowitz and Stegun 1964)

Range	Representation
$u < 0.05$	$K_1(u) \approx \frac{1}{u}$ —for practical calculations (Hantush 1964)
$u \leq 2$	$\omega = u/2,$ $K_1(u) = \frac{1}{u} \left(u \ln \omega I_1(u) + 1 + 0.15443144\omega^2 - 0.67278579\omega^4 - 0.18156897\omega^6 - \right)$ $\left(- 0.01919402\omega^8 - 0.00110404\omega^{10} - 0.00004686\omega^{12} \right)$
$u \geq 2$	$\omega = u/2,$ $K_1(u) = \frac{e^{-u}}{\sqrt{u}} \left(1.25331414 + 0.23498619\omega^{-1} - 0.0365562\omega^{-2} + 0.01504268\omega^{-3} - \right)$ $\left(- 0.00780353\omega^{-4} + 0.00325614\omega^{-5} - 0.00068245\omega^{-6} \right)$
$u > 5$	$K_1(u) \approx \sqrt{\frac{\pi}{2u}} \left(1 + \frac{3}{8u} \right) e^{-u}$ —for practical calculations (Hantush 1964)

Fig. A7.20 Plots of modified Bessel functions: $I_0(u), I_1(u), K_0(u), K_1(u)$



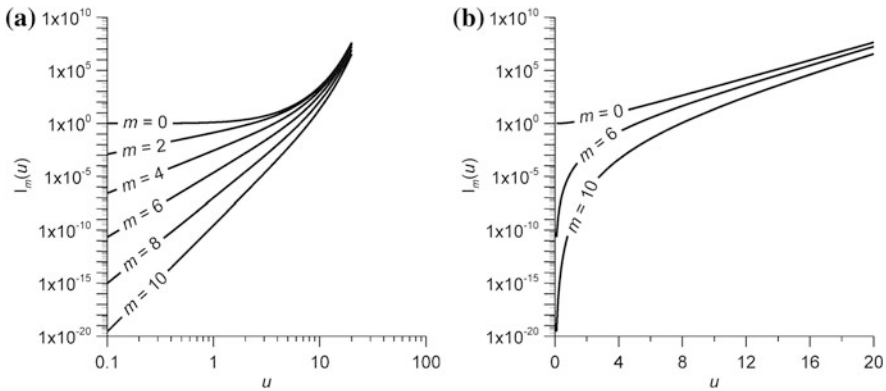


Fig. A7.21 Plot of the logarithm of function $I_m(u)$ versus **a** the logarithm of the argument and **b** its argument for different orders of function

4. Modified Bessel Function of the First Kind of the mth Order $I_m(u)$

Function (Fig. A7.21):

$$I_m(u) = \frac{1}{\pi} \int_0^\pi \exp(u \cos \tau) \cos(m\tau) d\tau.$$

Expansion in series (Abramowitz and Stegun 1964)

$$I_m(u) = \left(\frac{u}{2}\right)^m \sum_{n=0}^\infty \frac{(u^2/4)^n}{n! \Gamma(m+n+1)!}.$$

5. Modified Bessel Function of the Second Kind of the mth Order $K_m(u)$

Function (Fig. A7.22):

$$K_m(u) = \int_0^\infty \exp(-u \cosh \tau) \cosh(m\tau) d\tau.$$

Expansion in series (Abramowitz and Stegun 1964):

$$K_m(u) = \left\{ \begin{aligned} &\frac{1}{2} \left(\frac{u}{2}\right)^{-m} \sum_{n=0}^{m-1} \left[\frac{(m-n-1)!}{n!} \left(-\frac{u^2}{4}\right)^n \right] + (-1)^{m+1} \ln\left(\frac{u}{2}\right) I_m(u) + \\ &+ \frac{(-1)^m}{2} \left(\frac{u}{2}\right)^m \sum_{n=0}^\infty \left[[\psi(n+1) + \psi(m+n+1)] \frac{(u^2/4)^n}{n!(m+n)!} \right] \end{aligned} \right\},$$

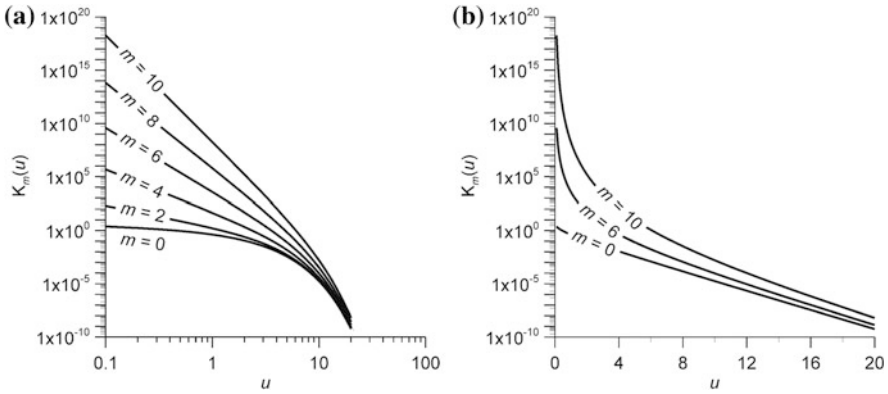


Fig. A7.22 Plot of the logarithm of function $K_m(u)$ versus **a** the logarithm of its argument and **b** its argument for different orders of the function

where $\psi(i) = -\gamma + \sum_{j=1}^{i-1} j^{-1}$ is psi-function; $\psi(1) = -\gamma$; $\gamma = 0.5772156649$ is Euler constant.

Appendix 7.14 Gamma Function $\Gamma(u)$

Functions (Fig. A7.23 and Table A7.27):

$$\Gamma(u) = \int_0^\infty \tau^{u-1} \exp(-\tau) d\tau; \Gamma(u + 1) = u!; \Gamma(u) = (u - 1)!$$

Expansion in series (Abramowitz and Stegun 1964): $\frac{1}{\Gamma(u)} = \sum_{n=1}^\infty c_n u^n$, where values of c_n are given in Table A7.26.

Table A7.26 Values of c_n

n	c_n	n	c_n	n	c_n
1	1.00000 00000 000000	10	-0.00021 52416 741149	19	0.00000 00001 043427
2	0.57721 56649 015329	11	0.00012 80502 823882	20	0.00000 00000 077823
3	-0.65587 80715 202538	12	-0.00002 01348 547807	21	-0.00000 00000 036968
4	-0.04200 26350 340952	13	-0.00000 12504 934821	22	0.00000 00000 005100
5	0.16653 86113 822915	14	0.00000 11330 272320	23	-0.00000 00000 000206
6	-0.04219 77345 555443	15	-0.00000 02056 338417	24	-0.00000 00000 000054
7	-0.00962 19715 278770	16	0.00000 00061 160950	25	0.00000 00000 000014
8	0.00721 89432 466630	17	0.00000 00050 020075	26	0.00000 00000 000001
9	-0.00116 51675 918591	18	-0.00000 00011 812746		

Fig. A7.23 Plots of function $\Gamma(u)$; $\Gamma(u) - u$ and $1/\Gamma(u) - u$

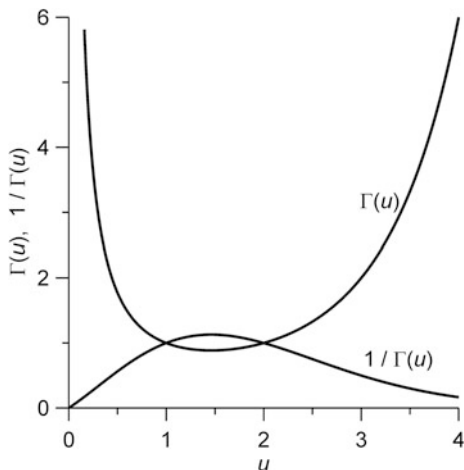


Table A7.27 Approximation of function $\Gamma(u)$ (Abramowitz and Stegun 1964)

Range	Representation
$0 \leq u \leq 1$	$\Gamma(u + 1) = \left(1 - 0.577191652u + 0.988205891u^2 - 0.897056937u^3 + 0.918206857u^4 - \right. \\ \left. - 0.756704078u^5 + 0.482199394u^6 - 0.193527818u^7 + 0.035868343u^8 \right)$

Appendix 7.15 Roots of Some Transcendent Equations

1. Roots of Equation $\alpha_n \tan(\alpha_n) = c$

See Fig. A7.24 and Table A7.28

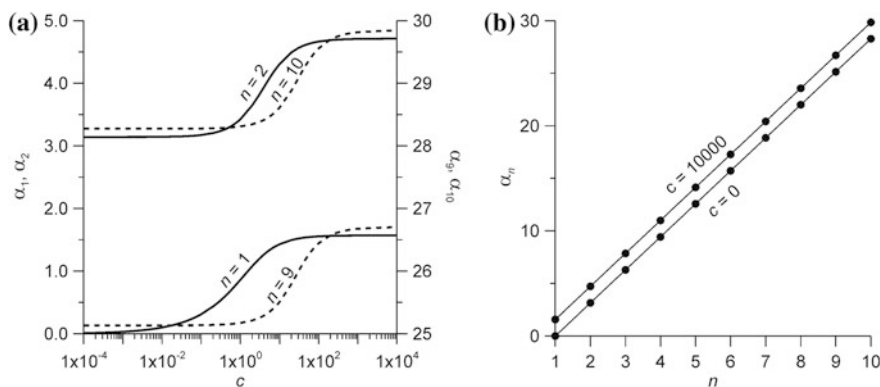


Fig. A7.24 Roots of equation $\alpha_n \tan(\alpha_n) = c$. Dependence of the root (1st, 2nd, 9th, and 10th) on **a** c and **b** its number n at different values of c (0 and 10000). c is a constant; n is the root's number

Table A7.28 Approximations of transcendent equation (Hantush 1967)

Range	Representation
$n > 6$	$\alpha_n = \alpha_6 + (n - 6)\pi$
$c \leq 0.2; n = 2, 3, 4, \dots$	$\alpha_1 = \left(1 - \frac{c}{6}\right)\sqrt{c}; \alpha_n = (n - 1)\pi + \frac{c}{(n - 1)^2\pi^2} - \frac{c^2}{(n - 1)^3\pi^3}$
$c \leq 0.01; n = 2, 3, 4, \dots$	$\alpha_1 = \sqrt{c}; \alpha_n = (n - 1)\pi$
$c \rightarrow \infty$	$\alpha_n = (2n - 1)\frac{\pi}{2}$ (from the properties of tangent)

2. Roots of Equations $J_0(x_n) = 0, J_1(x_{n,1}) = 0$

See Fig. A7.25 and Table A7.29.

3. Roots of Equation $J_m(x_{n,m}) = 0$

See Fig. A7.26.

4. Roots of Equation $J'_m(y_{n,m}) = 0$

See Fig. A7.27.

$$J'_m(\beta) = \frac{m}{\beta}J_m(\beta) - J_{m+1}(\beta) = J_{m-1}(\beta) - \frac{m}{\beta}J_m(\beta).$$

Fig. A7.25 Roots of equations $J_0(x_n) = 0, J_1(x_{n,1}) = 0$. Dependence of the root values of two equations on the root's number (first ten roots). n is the root's number

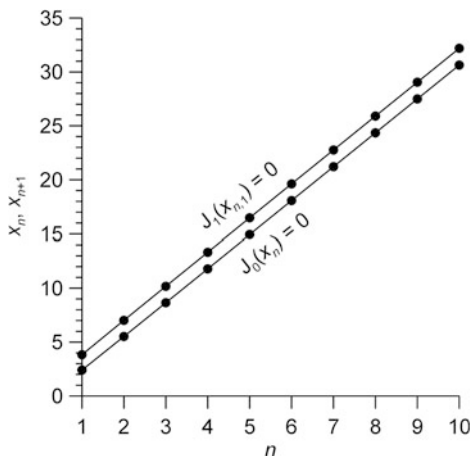


Table A7.29 Approximation of transcendent equations (for large root's numbers)

Equation	Representation
$J_0(x_n) = 0$	$x_n = \pi n - \pi/4$
$J_1(x_{n,1}) = 0$	$x_{n,1} = \pi n + \pi/4$

Fig. A7.26 Roots of equation $J_m(x_{n,m}) = 0$. Dependence of equation root on the root's number (first ten roots) for different orders of the function. n is the root's number

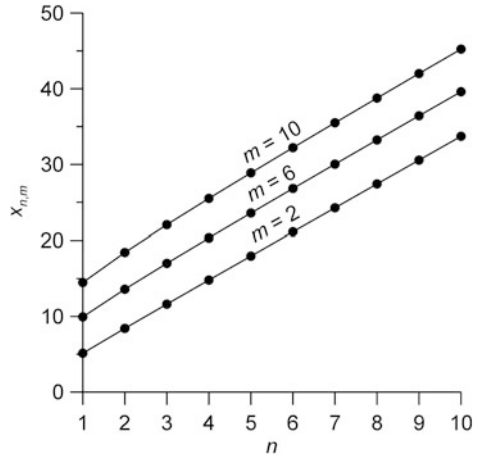
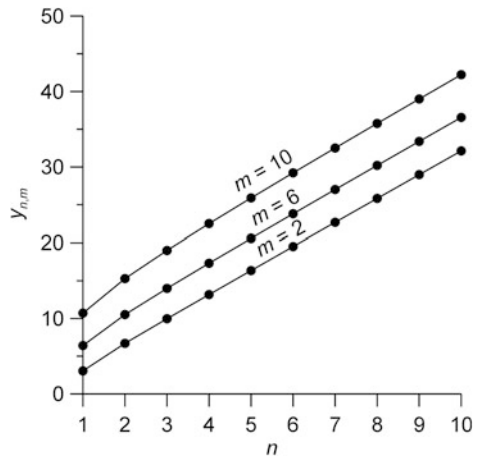


Fig. A7.27 Roots of equation $J'_m(y_{n,m}) = 0$. Dependence of equation root on the root's number (first ten roots) for different orders of function derivative. n is the root's number



5. Roots of Equation $J_0(\alpha_n) Y_0(c\alpha_n) - Y_0(\alpha_n) J_0(c\alpha_n) = 0$

See Fig. A7.28.

6. Roots of Equation $J_0(\alpha_n) Y_1(c\alpha_n) - Y_0(\alpha_n) J_1(c\alpha_n) = 0$

See Fig. A7.29.

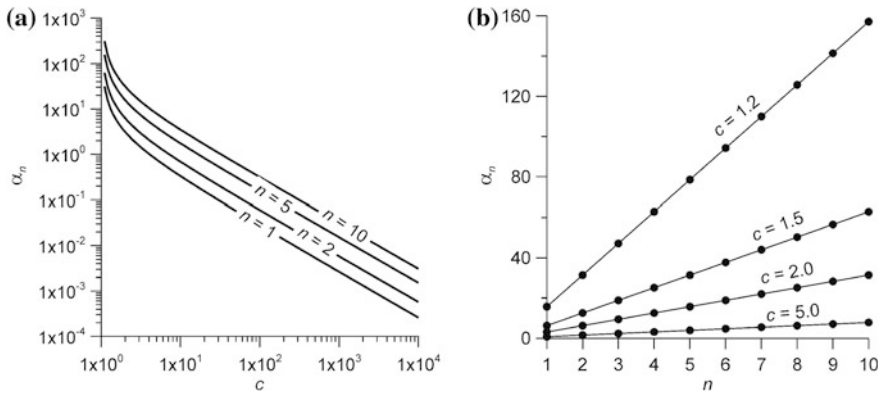


Fig. A7.28 Roots of equation $J_0(\alpha_n) Y_0(c\alpha_n) - Y_0(\alpha_n) J_0(c\alpha_n) = 0$. **a** Dependence of the logarithm of the root (1st, 2nd, 5th, and 10th) on the logarithm of c and **b** dependences of the root on its number at different c (1.2, 1.5, 2.0, and 5.0). c is a constant; n is the root's number

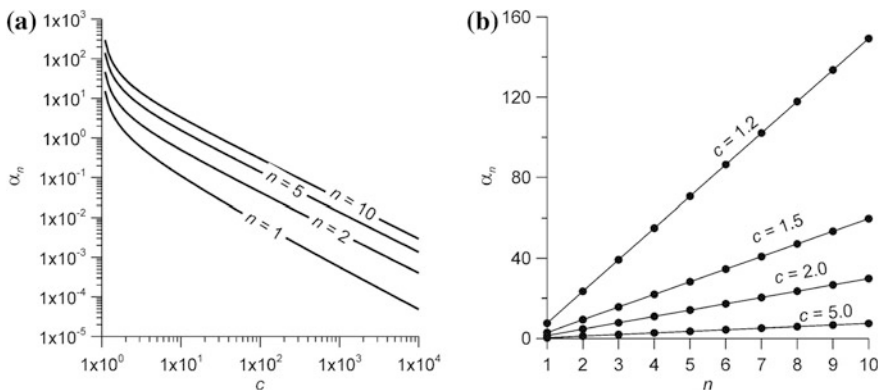


Fig. A7.29 Roots of equation $J_0(\alpha_n) Y_1(c\alpha_n) - Y_0(\alpha_n) J_1(c\alpha_n) = 0$. **a** Dependence of the logarithm of the root (1st, 2nd, 5th, and 10th) on the logarithm of c and **b** dependences of the root on its number at different c (1.2, 1.5, 2.0, and 5.0). c is a constant; n is the root's number

Appendix 7.16 Useful Mathematical Functions

This appendix mostly gives trigonometric functions mentioned in the book. The list of their denotations, equivalent representations, and derivatives is given here (Table A7.30).

Table A7.30 Useful mathematical functions

Function	Denotation	Equals	Equivalent	Derivative	$u = 0$	$u = -u$
Sine	$\sin u$			$\cos u$	0	$-\sin u$
Cosine	$\cos u$			$-\sin u$	1	$\cos u$
Tangent	$\tan u$	$\frac{\sin u}{\cos u}$		$\sec^2 u$	0	$-\tan u$
Cotangent	$\cotan u$	$\frac{1}{\tan u} = \frac{\cos u}{\sin u}$		$-\operatorname{cosec}^2 u$	∞	$-\cotan u$
Secant	$\sec u$	$\frac{1}{\cos u}$		$\sec u \tan u$	1	$\sec u$
Cosecant	$\operatorname{cosec} u$	$\frac{1}{\sin u}$		$-\operatorname{cosec} u \times \cotan u$	∞	$-\operatorname{cosec} u$
Inverse sine	$\arcsin u$		$\arctan \frac{u}{\sqrt{-u^2+1}}$	$\frac{1}{\sqrt{1-u^2}}$	0	$-\arcsin u$
Inverse cosine	$\arccos u$		$\arctan \frac{-u}{\sqrt{-u^2+1}} + 2\arctan 1$	$-\frac{1}{\sqrt{1-u^2}}$	$\pi/2$	$\pi - \arccos u$
Inverse tangent	$\arctan u$			$\frac{1}{1+u^2}$	0	$-\arctan u$
Inverse cotangent	$\operatorname{arccotan} u$	$\arctan \frac{1}{u}$		$-\frac{1}{1+u^2}$	$\pi/2$	$\pi - \operatorname{arccotan} u$
Inverse secant	$\operatorname{arcsec} u$	$\arccos \frac{1}{u}$		$\frac{1}{u\sqrt{u^2-1}}$	∞	$\pi - \operatorname{arcsec} u$
Inverse cosecant	$\operatorname{arccosec} u$	$\arcsin \frac{1}{u}$		$-\frac{1}{u\sqrt{u^2-1}}$		$-\operatorname{arccosec} u$
Hyperbolic sine	$\sinh u$		$\frac{e^u - e^{-u}}{2}$	$\cosh u$	0	$-\sinh u$

(continued)

Table A7.30 (continued)

Function	Denotation	Equals	Equivalent	Derivative	$u = 0$	$u = -u$
Hyperbolic cosine	$\cosh u$		$\frac{e^u + e^{-u}}{2}$	$\sinh u$	1	$\cosh u$
Hyperbolic tangent	$\tanh u$	$\frac{\sinh u}{\cosh u}$	$\frac{e^u - e^{-u}}{e^u + e^{-u}}$	$1 - \tanh^2 u$	0	$-\tanh u$
Hyperbolic cotangent	$\operatorname{cotanh} u$	$\frac{\cosh u}{\sinh u}$	$\frac{e^u + e^{-u}}{e^u - e^{-u}}$	$-\operatorname{cosech}^2 u$	∞	$-\operatorname{cotanh} u$
Hyperbolic secant	$\operatorname{sech} u$	$\frac{1}{\cosh u}$		$-\operatorname{sech} u \times \tanh u$	1	$\operatorname{sech} u$
Hyperbolic cosecant	$\operatorname{cosech} u$	$\frac{1}{\sinh u}$		$-\operatorname{cosech} u \times \operatorname{cotanh} u$	∞	$-\operatorname{cosech} u$
Inverse hyperbolic sine	$\operatorname{arsinh} u$		$\ln(u + \sqrt{u^2 + 1})$	$\frac{1}{\sqrt{1 + u^2}}$	0	$-\operatorname{arsinh} u$
Inverse hyperbolic cosine	$\operatorname{arcosh} u$		$\ln(u + \sqrt{u^2 - 1}), u \geq 1$	$\frac{1}{\sqrt{u^2 - 1}}$		$\operatorname{arcosh} u$
Inverse hyperbolic tangent	$\operatorname{artanh} u$		$\frac{1}{2} \ln \frac{1+u}{1-u}, 0 \leq u^2 < 1$	$\frac{1}{1 - u^2}$	0	$-\operatorname{artanh} u$
Inverse hyperbolic cotangent	$\operatorname{arccotanh} u$	$\operatorname{artanh} \frac{1}{u}$	$\frac{1}{2} \ln \frac{u+1}{u-1}, u^2 > 1$	$\frac{1}{1 - u^2}$		$-\operatorname{arccotanh} u$
Inverse hyperbolic secant	$\operatorname{arsech} u$	$\operatorname{arcosh} \frac{1}{u}$	$\ln\left(\frac{1}{u} + \sqrt{\frac{1}{u^2} - 1}\right), 0 < u \leq 1$	$\mp \frac{1}{u\sqrt{1 - u^2}}$	∞	
Inverse hyperbolic cosecant	$\operatorname{arcosech} u$	$\operatorname{arcsinh} \frac{1}{u}$	$\ln\left(\frac{1}{u} + \sqrt{\frac{1}{u^2} + 1}\right)$	$\mp \frac{1}{u\sqrt{1 + u^2}}$	∞	$-\operatorname{arcosech} u$
Base logarithm	$\ln u$	$\ln 10 \cdot \lg u \approx 2.3026 \lg u$		$\frac{1}{u}$		

(continued)

Table A7.30 (continued)

Function	Denotation	Equals	Equivalent	Derivative	$u = 0$	$u = -u$
Decimal logarithm	$\lg u$	$\lg e \cdot \ln u \approx$ $\approx 0.43429 \ln u$		$\frac{1}{u \ln 10}$		
Exponential function	$\exp u; e^u$			e^u	1	$\frac{1}{e^u}$
Power function	10^u	$\exp(u \ln 10)$		$10^u \ln 10$	1	$\frac{1}{10^u}$

^{a)}The minus sign is for $u > 0$, the plus sign, for $u < 0$

References

- Abramowitz M, Stegun IA (ed) (1964) Handbook of mathematical functions with formulas, graphs, and mathematical tables. National Bureau of Standards Applied Mathematics Series-55
- Averyanov SF (1949) Dependence of soil permeability from air saturation. *Doclady AN SSSR* 69 (2):141–144 (In Russian)
- Aravin VI, Numerov SN (1953) Theory of fluid and gas flow in the porous media. Gostehizdat, Moscow (In Russian)
- Barlow PM, Moench AF (2011) WTAQ version 2—a computer program for analysis of aquifer tests in confined and water-table aquifers with alternative representations of drainage from the unsaturated zone. U.S. Geological Survey. Techniques and Methods 3-B9
- Bochever FM (ed) (1976) Design of groundwater supply system. Strojizdat, Moscow (In Russian)
- Bochever FM, Garmonov IV, Lebedev AV, Shestakov VM (1969) Fundamentals of hydraulic calculations. Nedra, Moscow (In Russian)
- Boulton NS (1954) The drawdown of the water-table under non-steady conditions near a pumped well in an unconfined formation. *P I Civil Eng* 3(4):564–579
- Carslow HS, Jaeger JC (1959) Conduction of heat in solids. Oxford at the Clarendon Press, London
- Cooper HH, Bredehoeft JD, Papadopoulos IS (1967) Response of a finite diameter well to an instantaneous charge of water. *Water Resour Res* 3(1):263–269
- Darcy H (1856) *Les fontaines publiques de la ville Dijon*. Paris
- Dupuit J (1863) *Etudes theoriques et pratiques sur le mouvement des eaux dans les canaux decouverts et a travers les terrains permeables*. Paris
- Ferris JG, Knowles DB, Brown RN, Stallman RW (1962) Theory of aquifer test. U.S. Geological Survey Water-Supply, paper 1536-E
- Forchheimer P (1914) *Hydraulik*. Teubner, Leipzig und Berlin
- Gardner WR (1958) Some steady-state solutions of the unsaturated moisture flow equation with application to evaporation from a water table. *Soil Sci* 85:228–232
- Guyonnet D, Mishra S, Mccord J (1993) Evaluating the volume of porous medium investigated during slug tests. *Ground Water* 31(4):627–633
- Hantush MS (1959) Nonsteady flow to flowing wells of leaky aquifers. *J Geophys Res* 64 (8):1043–1052
- Hantush MS (1960) Modification of the theory of leaky aquifers. *J Geophys Res* 65(11):3713–3725
- Hantush MS (1961) Aquifer tests on partially penetrating wells. *J Hydr Eng Div-ASCE* 87 (HY5):171–195
- Hantush MS (1961) Drawdown around a partially penetrating well. *J Hydr Eng Div-ASCE* 87 (HY4):83–98
- Hantush MS (1964) Hydraulics of wells. In: Te Chow Ven (ed) *Advances in hydroscience*, vol 1. Academic Press, New York and London, pp 281–432
- Hantush MS (1965) Wells near streams with semipervious beds. *J Geophys Res* 70(12):2829–2838

- Hantush MS (1967) Flow of groundwater in relatively thick leaky aquifers. *Water Resour Res* 3 (2):583–590
- Hantush MS, Jacob CE (1955) Non-steady radial flow in an infinite leaky aquifer. *EOS T Am Geophys Un* 36(1):95–100
- Hunt B (1977) Calculation of the leaky aquifer function. *J Hydrol* 33(1/2):179–183
- Hvorslev MJ (1951) Time lag and soil permeability in groundwater observations. U.S. Army Corps Engineers, Waterways Experiment Station, Bulletin 36, Vicksburg, MS
- Jacob CE, Lohman SW (1952) Nonsteady flow to a well of constant drawdown in an extensive aquifer. *EOS T Am Geophys Un* 33(4):559–569
- Lai RYS, Cheh-Wu Su (1974) Nonsteady flow to a large well in a leaky aquifer. *J Hydrol* 22 (3/4):333–345
- Logan J (1964) Estimating transmissibility from routine production tests of water wells. *Ground Water* 2(1):35–37
- Maksimov VM (ed) (1959) Hydrogeologist reference guide. Gostoptekhizdat, Leningrad (In Russian)
- Maksimov VM (ed) (1979) Hydrogeologist reference guide, vol 1. Nedra, Leningrad (In Russian)
- Mathias SA, Butler AP (2006) Linearized Richards' equation approach to pumping test analysis in compressible aquifers. *Water Resour Res* 42(6). doi:[10.1029/2005WR004680](https://doi.org/10.1029/2005WR004680)
- Moench AF (1984) Double-porosity models for a fissured groundwater reservoir with fracture skin. *Water Resour Res* 20(7):831–846
- Moench AF (1985) Transient flow to a large-diameter well in an aquifer with storative semiconfining layers. *Water Resour Res* 21(8):1121–1131
- Moench AF (1993) Computation of type curves for flow to partially penetrating wells in water-table aquifers. *Ground Water* 31(6):966–971
- Moench AF (1996) Flow to a well in a water-table aquifer: an improved Laplace transform solution. *Ground Water* 34(4):593–596
- Moench AF (1997) Flow to a well of finite diameter in a homogeneous, anisotropic water table aquifer. *Water Resour Res* 33(6):1397–1407
- Neuman SP (1972) Theory of flow in unconfined aquifers considering delayed gravity response. *Water Resour Res* 8(4):1031–1045
- Neuman SP (1973) Supplementary comments on "Theory of flow in unconfined aquifers considering delayed gravity response". *Water Resour Res* 9(4):1102–1103
- Neuman SP (1974) Effect of partial penetration on flow in unconfined aquifers considering delayed gravity response. *Water Resour Res* 10(2):303–312
- Neuman SP (1975) Analysis of pumping test data from anisotropic unconfined aquifers. *Water Resour Res* 11(2):329–345
- Neuman SP, Witherspoon PA (1968) Theory of flow in aquicludes adjacent to slightly leaky aquifers. *Water Resour Res* 4(1):103–112
- Papadopoulos IS, Cooper HH (1967) Drawdown in a well of large diameter. *Water Resour Res* 3 (1):241–244
- Poeter EP, Hill MC, Banta ER, Mehl S, Christensen S (2005) UCODE_2005 and six other computer codes for universal sensitivity analysis, calibration, and uncertainty evaluation. Techniques and Methods 6-A11. U.S. Geological Survey, Reston, Virginia
- Sindalovskiy LN (2006) Handbook of analytical solutions for aquifer test analysis. SpBSU, Sankt-Petersburg (In Russian)
- Sindalovskiy LN (2014) Analytical modeling of aquifer tests and well systems (ANSDIMAT software guide). Nauka, Sankt-Petersburg (In Russian)
- Sunjoto S (1994) Infiltration well and urban drainage concept. Future groundwater at risk. In: Proceedings of the Helsinki conference, pp 527–532
- Theis CV (1935) The relation between the lowering of the piezometric surface and the rate and duration of discharge of a well using ground-water storage. *EOS T Am Geophys Un* 16 (2):519–524
- Thiem G (1906) Hydrologische methoden. Leipzig

- Walton WC (1984) Analytical groundwater modeling with programmable calculators and hand-held computers. In: Rosenshein JS, Bennett GD (eds) Groundwater hydraulics. Water Resources Monograph Series 9. American Geophysical Union, Washington, pp 298–312.
- Walton WC (2007) Aquifer test modeling. CRC Press, Taylor & Francis Group, Boca Raton, London, New York
- Warren JE, Root PJ (1963) The behavior of naturally fractured reservoirs. Soc Petrol Eng J 3 (3):245–255
- Zhan H, Zlotnik VA (2002a) Groundwater flow to a horizontal or slanted well in an unconfined aquifer. Water Resour Res 38(7):2001W. doi:[10.1029/2001WR000401](https://doi.org/10.1029/2001WR000401)
- Zhan H, Zlotnik VA (2002b) User's manual for program WHI (unpublished)

Index

A

Abramowitz M, 354, 370, 372–379
Aravin VI, 291
Averyanov SF, 328

B

Babushkin VD, 40, 136, 194
Bansal RK, 265, 266
Barlow P, 60, 322, 329
Bindeman NN, 137
Bochever FM, 12, 14, 15, 27, 28, 85, 91, 121, 122, 124, 134, 197, 268, 279, 309, 310
Borevskiy BV, 14, 63, 207, 209
Boulton NS, 58–60, 65, 247, 248, 337, 359, 360
Bouwer H, 172, 173
Bredehoeft JD, 169, 170
Butler AP, 323

C

Carslow HS, 5, 7, 31, 167, 168, 262–264, 353, 363, 364, 366
Case CM, 101, 102
Chan YK, 24
Cheh-Wu Su, 74, 75
Cooley RL, 101, 102
Cooper HH, 6, 7, 167–170, 176, 228, 257, 263, 309, 363, 364, 366

D

Darcy H, 285, 286
De Glee GJ, 76
De Smedt F, 141
Dupuit J, 306

F

Fenske PR, 117, 118, 271
Ferris JG, 231, 296, 300
Forchheimer P, 10, 291

G

Gardner WR, 323
Girinskiy NK, 40
Gringarten AC, 143, 144
Guyonnet D, 157, 307
Gylybov, 134

H

Hall FR, 263, 264
Hantush MS, 6, 12, 14, 16, 27–29, 39, 40, 46–49, 52, 66–68, 74, 75, 79–87, 89, 90, 92, 98, 104–106, 108, 110, 129–131, 134, 156–159, 162, 163, 194, 196, 201, 247, 251, 252, 254, 269, 354–359, 361, 362, 365, 367–370, 372, 373, 375, 376, 380
Hunt B, 132, 356
Hvorslev MJ, 175, 176, 291

I

Isayev RG, 125

J

Jacob CE, 7, 12, 14, 16, 27–29, 61, 63, 74, 76, 79–86, 104, 105, 156, 199, 208, 228, 251, 252, 355–357, 369
Jaeger JC, 5, 7, 31, 156, 167, 168, 262–264, 353, 363, 364, 366
Jenkins DN, 143

K

Kabala ZJ, 201, 203
Kerkis EE, 199, 200
Kipp KL, 176

L

Lai RYS, 74, 75, 364
Lapuk BB, 29, 105, 126
Latinopoulos P, 24
Ledder G, 202, 204

Logan J, 305

Lohman SW, 156, 369

M

Maksimov VA, 117, 118, 271

Maksimov VM, 306, 307

Marino MA, 266

Mathias SA, 323

Mironenko VA, 40, 101, 128, 252, 273, 274, 276–278

Mishra S, 157

Moench AF, 3, 5, 38, 47–49, 56, 60–62, 106, 109, 112, 113, 139, 141, 242, 244, 250, 252, 263, 264, 269, 289, 290, 314, 317, 322, 329, 330

Muskat M, 13, 21, 29

N

Neuman SP, 56–59, 93, 94, 97, 269, 271, 311, 343, 360, 362

Numerov SN, 291

P

Papadopoulos IS, 6, 169, 170, 309, 363, 364

Park E, 152

Picking LW, 167–169, 257

Pinder GF, 264

Poeter EP, 238, 343, 344

Prentice JK, 143

Prickett TA, 61, 62

Pykhachov GB, 125

R

Ramey HJ Jr, 144

Rice RC, 172, 173

Root PJ, 139, 140, 330–332, 334, 336

Rorabough MI, 263

S

Serdyukov LI, 101

Shchelkachev VN, 29, 105, 126

Shestakov VM, 40, 127–129, 131, 208, 264

Shtengelov RS, 234

Stegun IA, 354, 370, 372–379

Sternberg YM, 157, 158

Sunjoto S, 291

T

Tartakovsky DM, 133, 134

Teloglou IS, 265, 266

Theis CV, 5, 207, 208, 228, 234, 238, 241, 242, 247–249, 251, 252, 254, 269, 310, 343, 344, 353, 355

Thiem G, 305

Thomas RG, 6, 75

Trojanskiy SV, 272, 274, 275

V

Van der Kamp G, 176

Verigin NN, 27

W

Walton WC, 356, 357

Warren JE, 139, 140, 330–332, 334, 336

Witherspoon PA, 93, 94, 97, 271

Y

Yang SY, 164, 171

Yeh HD, 120, 164, 171

Z

Zeegofer YuO, 127, 129

Zhan H, 150, 152, 339

Zlotnik VA, 133, 134, 150, 202, 204, 339